TARGETING PROTEIN POST-TRANSLATIONAL MODIFICATIONS (PTMS) FOR DIAGNOSIS AND TREATMENT OF SEPSIS

EDITED BY: Yongqing Li, Venkat Magupalli, Erxi Wu and Wei Chong
PUBLISHED IN: Frontiers in Immunology

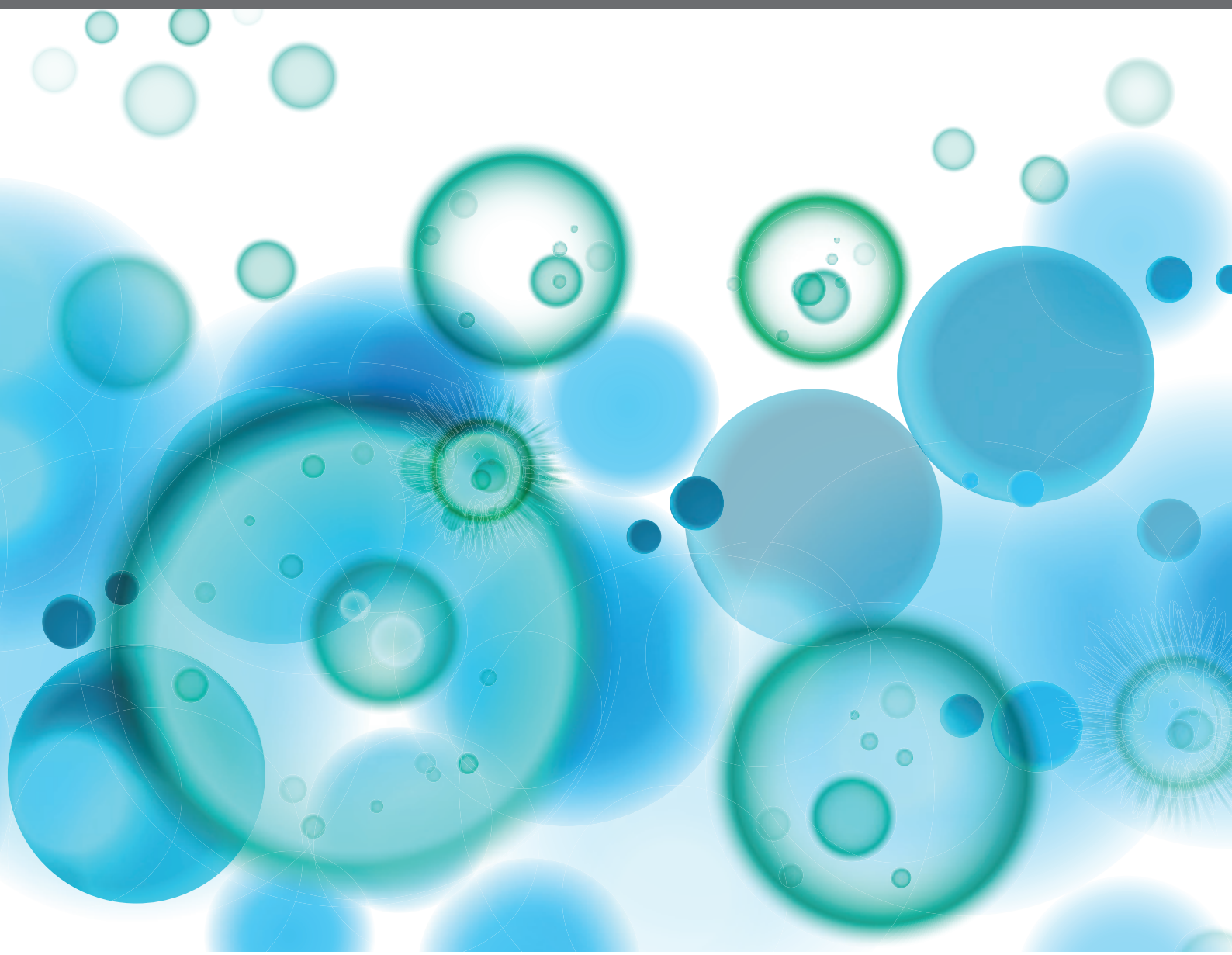

frontiers Research Topics

ISSN 1664-8714
ISBN 978-2-88974-582-1
DOI 10.3389/978-2-88974-582-1

About Frontiers

Frontiers is more than just an open-access publisher of scholarly articles: it is a pioneering approach to the world of academia, radically improving the way scholarly research is managed. The grand vision of Frontiers is a world where all people have an equal opportunity to seek, share and generate knowledge. Frontiers provides immediate and permanent online open access to all its publications, but this alone is not enough to realize our grand goals.

Frontiers Journal Series

The Frontiers Journal Series is a multi-tier and interdisciplinary set of open-access, online journals, promising a paradigm shift from the current review, selection and dissemination processes in academic publishing. All Frontiers journals are driven by researchers for researchers; therefore, they constitute a service to the scholarly community. At the same time, the Frontiers Journal Series operates on a revolutionary invention, the tiered publishing system, initially addressing specific communities of scholars, and gradually climbing up to broader public understanding, thus serving the interests of the lay society, too.

Dedication to Quality

Each Frontiers article is a landmark of the highest quality, thanks to genuinely collaborative interactions between authors and review editors, who include some of the world's best academicians. Research must be certified by peers before entering a stream of knowledge that may eventually reach the public - and shape society; therefore, Frontiers only applies the most rigorous and unbiased reviews.
Frontiers revolutionizes research publishing by freely delivering the most outstanding research, evaluated with no bias from both the academic and social point of view. By applying the most advanced information technologies, Frontiers is catapulting scholarly publishing into a new generation.

What are Frontiers Research Topics?

Frontiers Research Topics are very popular trademarks of the Frontiers Journals Series: they are collections of at least ten articles, all centered on a particular subject. With their unique mix of varied contributions from Original Research to Review Articles, Frontiers Research Topics unify the most influential researchers, the latest key findings and historical advances in a hot research area! Find out more on how to host your own Frontiers Research Topic or contribute to one as an author by contacting the Frontiers Editorial Office: frontiersin.org/about/contact

TARGETING PROTEIN POST-TRANSLATIONAL MODIFICATIONS (PTMS) FOR DIAGNOSIS AND TREATMENT OF SEPSIS

Topic Editors:
Yongqing Li, University of Michigan, United States
Venkat Magupalli, Harvard Medical School, United States
Erxi Wu, Baylor Scott and White Health, United States
Wei Chong, The First Affiliated Hospital of China Medical University, China

Citation: Li, Y., Magupalli, V., Wu, E., Chong, W., eds. (2022). Targeting Protein Post-Translational Modifications (PTMs) for Diagnosis and Treatment of Sepsis. Lausanne: Frontiers Media SA. doi: 10.3389/978-2-88974-582-1

Table of Contents

05 ***Editorial: Targeting Protein Post-Translational Modifications (PTMs) for Diagnosis and Treatment of Sepsis***
Panpan Chang and Yongqing Li

09 ***p53 Deacetylation Alleviates Sepsis-Induced Acute Kidney Injury by Promoting Autophagy***
Maomao Sun, Jiaxin Li, Liangfeng Mao, Jie Wu, Zhiya Deng, Man He, Sheng An, Zhenhua Zeng, Qiaobing Huang and Zhongqing Chen

26 ***Roles of RAGE/ROCK1 Pathway in HMGB1-Induced Early Changes in Barrier Permeability of Human Pulmonary Microvascular Endothelial Cell***
Meng-jiao Zhao, Hao-ran Jiang, Jing-wen Sun, Zi-ang Wang, Bo Hu, Cheng-rui Zhu, Xiao-han Yin, Ming-ming Chen, Xiao-chun Ma, Wei-dong Zhao and Zheng-gang Luan

38 ***Evaluation of the Molecular Mechanisms of Sepsis Using Proteomics***
He Miao, Song Chen and Renyu Ding

56 ***Diagnostic Value of sIL-2R, TNF-α and PCT for Sepsis Infection in Patients With Closed Abdominal Injury Complicated With Severe Multiple Abdominal Injuries***
Guang-hua Zhai, Wei Zhang, Ze Xiang, Li-Zhen He, Wei-wei Wang, Jian Wu and An-quan Shang

67 ***The Role of HDAC6 in Autophagy and NLRP3 Inflammasome***
Panpan Chang, Hao Li, Hui Hu, Yongqing Li and Tianbing Wang

80 ***Peptidylarginine Deiminase 2 in Host Immunity: Current Insights and Perspectives***
Zhenyu Wu, Patrick Li, Yuzi Tian, Wenlu Ouyang, Jessie Wai-Yan Ho, Hasan B. Alam and Yongqing Li

93 ***Circulating CitH3 Is a Reliable Diagnostic and Prognostic Biomarker of Septic Patients in Acute Pancreatitis***
Baihong Pan, Yaozhen Li, Yu Liu, Wei Wang, Gengwen Huang and Yang Ouyang

103 ***miR-221-5p-Mediated Downregulation of JNK2 Aggravates Acute Lung Injury***
Jing Yang, Hanh Chi Do-Umehara, Qiao Zhang, Huashan Wang, Changchun Hou, Huali Dong, Edith A. Perez, Marc A. Sala, Kishore R. Anekalla, James M. Walter, Shuwen Liu, Richard G. Wunderink, G.R. Scott Budinger and Jing Liu

117 ***Citrullinated Histone H3 Mediates Sepsis-Induced Lung Injury Through Activating Caspase-1 Dependent Inflammasome Pathway***
Yuzi Tian, Patrick Li, Zhenyu Wu, Qiufang Deng, Baihong Pan, Kathleen A. Stringer, Hasan B. Alam, Theodore J. Standiford and Yongqing Li

128 ***Lactylated Histone H3K18 as a Potential Biomarker for the Diagnosis and Predicting the Severity of Septic Shock***
Xin Chu, Chenyi Di, Panpan Chang, Lina Li, Zhe Feng, Shirou Xiao, Xiaoyu Yan, Xiaodong Xu, Hexin Li, Ruomei Qi, Huan Gong, Yanyang Zhao, Fei Xiao and Zhigang Chang

141 **GPR174 *mRNA Acts as a Novel Prognostic Biomarker for Patients With Sepsis* via *Regulating the Inflammatory Response***
Jianli Wang, Yanyan Hu, Zhongshu Kuang, Yao Chen, Lingyu Xing, Wei Wei, Mingming Xue, Sucheng Mu, Chaoyang Tong, Yilin Yang and Zhenju Song

frontiers in Immunology

EDITORIAL
published: 03 February 2022
doi: 10.3389/fimmu.2022.856146

Editorial: Targeting Protein Post-Translational Modifications (PTMs) for Diagnosis and Treatment of Sepsis

Panpan Chang[1,2,3] *and Yongqing Li*[4]*

[1] Trauma Medicine Center, Peking University People's Hospital, Beijing, China, [2] Key Laboratory of Trauma and Neural Regeneration, Peking University, Beijing, China, [3] National Center for Trauma Medicine of China, Beijing, China, [4] Department of Surgery, University of Michigan Medical School, Ann Arbor, MI, United States

Keywords: protein posttranslational modifications (PTMs), sepsis, biomarker, treatment, diagnosis

Editorial on the Research Topic

Targeting Protein Post-Translational Modifications (PTMs) for Diagnosis and Treatment of Sepsis

Sepsis is a serious clinical problem that is associated with unacceptably high mortality and for many of those who survive long-term morbidity (1). Although accumulating evidence and studies have increased understanding of this problem in the past 10 years, it remains lack of effective diagnosis and treatment to improve the outcome due to its complicated pathophysiological mechanisms. Growing evidence suggests that post-translational modifications (PTMs) could be a cornerstone in regulating cell functions and multiples diseases, including sepsis. It is unclear exactly how infection induces specific protein PTMs, and how the protein PTMs consequently lead to inflammatory disorder, cytokine storm, disseminated intravascular coagulation, organ dysfunction, *etc.* This Research Topic of *Frontiers in Immunology* introduced latest progress in modulation of PTMs in infection and immune response, PTMs-induced transcriptional reprogramming of immune cells in severe inflammation and/or infection, and proteins derived from PTMs as sepsis diagnostic biomarkers and therapeutic targets (**Figure 1**).

OPEN ACCESS

Edited and reviewed by:
Pietro Ghezzi,
Brighton and Sussex Medical School, United Kingdom

***Correspondence:**
Yongqing Li
yqli@med.umich.edu

Specialty section:
This article was submitted to Inflammation, a section of the journal Frontiers in Immunology

Received: *16 January 2022*
Accepted: *17 January 2022*
Published: *03 February 2022*

Citation:
Chang P and Li Y (2022) Editorial: Targeting Protein Post-Translational Modifications (PTMs) for Diagnosis and Treatment of Sepsis. Front. Immunol. 13:856146. doi: 10.3389/fimmu.2022.856146

MODULATION OF PTMs IN INFECTION AND IMMUNE RESPONSE

The findings by Sun et al. described that deacetylation of p53 promotes autophagy of renal tubular epithelia cells (RTEC) to alleviate sepsis-induced acute kidney injury (AKI). The p53 could be regulated by various PTMs such as phosphorylation, acetylation, methylation, glycosylation (2). Emerging evidence indicates that autophagy plays protective roles in various types of AKI (3), and upregulation of p53 could mediate the attenuation of autophagy in AKI (4). The study by Sun et al. emphasizes the potential of deacetylated p53-mediated RTEC autophagy for future sepsis-induces AKI treatments. Zhao et al. updated the role of high mobility group box protein 1 (HMGB1) in disrupting the endothelial barrier integrity during acute lung injury (ALI) in sepsis. This study demonstrates that HMGB1 induced F-actin rearrangement, adherens junction and tight junction rupture lead to increase of the endothelial barrier permeability through the RAGE/ROCK1 pathway, which phosphorylates myosin light chain in the early stage. As increased vascular permeability is essential to pulmonary edema during sepsis-induced ALI (5), this finding confirmed a potential

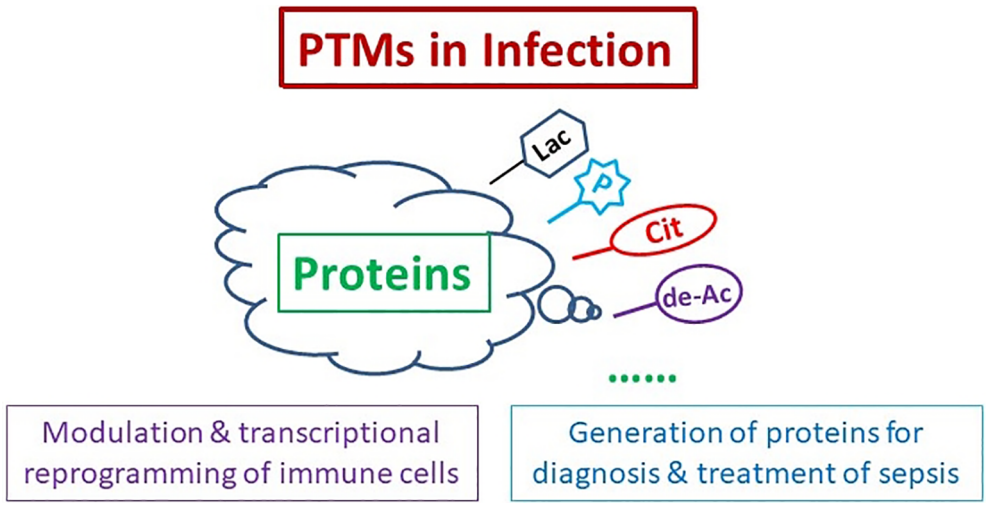

FIGURE 1 | Protein Post-translational Modifications (PTMs) for Diagnosis and Treatment of Sepsis. PTMs of proteins participate in modulation and transcriptional reprogramming of immune cells, and generation of the proteins for sepsis diagnosis and treatment. Cit, citrullination; de-Ac, deacetylation; Lac, lactylation; P, phosphorylation.

therapeutic target for the endothelial cell (EC) barrier dysfunction following sepsis. Yang et al. revealed that miR-221-5p downregulated c-Jun N-terminal protein kinase 2 (JNK2) to aggravate sepsis-induced ALI. This team has previously demonstrated that JNK2 promotes stress-induced mitophagy by targeting small mitochondrial alternative reading frame (smARF) for ubiquitin-mediated proteasomal degradation, thereby preventing mitochondrial dysfunction and restraining inflammasome activation (6). The present study has advanced the field further by providing a potential mechanism for the association between mitochondrial dysfunction and sepsis. Chang et al. summarized histone deacetylase 6 (HDAC6) regulating autophagy and NLRP3 inflammasomes *via* multiple mechanisms. HDAC6 has two functional deacetylase domains and a ubiquitin-binding zinc finger domain (ZnF-BUZ) (7). Due to its unique structure, HDAC6 regulates various physiological processes, including autophagy and NLRP3 inflammasome. With the development of small molecules inhibiting HDAC6, some clinical trials have shown that selective HDAC6 inhibitors are effective in tumor treatment (8–10). Considering the function of HDAC6 in autophagy and NLRP3 inflammasome and broad role of HDAC6 inhibitors, further studies should be pursued in future research.

PTMs-INDUCED TRANSCRIPTIONAL REPROGRAMMING OF IMMUNE CELLS IN SEVERE INFLAMMATION AND/OR INFECTION

Wu et al. discussed the role of peptidylarginine deiminase 2 (PAD2) in host immunity. PAD family enzymes catalyze the conversion of arginine residues to citrulline, regulating activity of host immunity. PAD2 mediates protein citrullination to regulate multiple cellular processes including gene transcription (11), antigen generation (12), extracellular trap formation (13), and pyroptosis (14). Dysregulated activity of PAD2 is associated with a series of immune disorders including sepsis, rheumatoid arthritis, multiple sclerosis, and tumor formation. Recently, Li's group found that PAD2 mediates pyroptosis and neutrophil extracellular traps (NETs) during sepsis (15, 16). Accumulating evidence suggests that PAD2 may be a promising novel biomarker and therapeutic target for a broad spectrum of diseases such as sepsis, autoimmune and inflammatory diseases. Miao et al. discussed the development of proteomics in sepsis. They summarize the application of proteomics in elucidating the molecular mechanism and potential therapeutic targets of sepsis and the research progress of protein PTMs in sepsis.

PROTEINS DERIVED FROM PTMS FOR SEPSIS DIAGNOSIS AND TREATMENT

In 2011, Li's group first identified citrullinated histone H3 (CitH3) as a biomarker for early diagnosis and prognosis of endotoxic shock in a mouse model (17). In next series of studies, they developed a novel CitH3 monoclonal antibody to target PAD2 and PAD4 generated CitH3 (18) and confirmed that CitH3 is more effective than existing biomarkers such as procalcitonin (PCT), interleukin (IL) 1β, and IL-6 in a mouse model of endotoxic shock and human patients with sepsis (19, 20). However, the mechanisms involved are unveiled. In this Research Topic, CitH3 is further discussed in three manuscripts. Wu et al. showed that activation of PAD enzymes by microbial infection induces formation of NETs and pyroptosis, leading to CitH3 released from immune cells such as neutrophils and microphages.

Tian et al. further revealed that CitH3 activates caspase-1 dependent inflammasome pathway. Their studies illustrate a novel mechanism, suggesting that CitH3 is an important self-mediator that triggers formation a "*vicious circle*" during sepsis and sepsis-induced ALI. Another study from Pan et al. explored the diagnostic potential of CitH3 in septic patients with acute pancreatitis (AP). Their findings indicate that CitH3 concentration is increased in septic AP patients and is closely correlated with disease severity and clinical outcomes. These two groups' data suggest that CitH3 could be a promising therapeutic target and biomarker in sepsis. Interestingly, Chu et al. reported lactylation of histone H3 lysine 18 (H3K18) in patients with septic shock. H3K9 lactylation has been recently studied in macrophage following hypoxia, lipopolysaccharides, or bacterial infection (21). The data presented by Chu et al. indicate that H3K18 lactylation may be a potential biomarker to reflect the severity of critical illness and the presence of infection. The studies with a large sample size are needed to confirm the conclusion.

Zhai et al. reported that combination of soluble interleukin-2 receptor (sIL-2R), tumor necrosis factor-a (TNF-a) and PCT has good value in the diagnosis of sepsis infection in patients with closed abdominal injury complicated with severe multiple abdominal injuries. Additionally, Wang et al. showed G-protein coupled receptor 174 (GPR174) mRNA acts as a novel prognostic biomarker for patients with sepsis. GPR174 is involved in the dysregulated immune response of sepsis, however, the clinical value and effects of GPR174 in septic patients are still unknown. Wang et al.'s study indicates the role of GPR174 regulating inflammation following sepsis and suggest the potential of GPR174 as a prognosis biomarker for sepsis.

An important goal of this Research Topic was to highlight the scientific community of advances made on the discovery of new mechanisms from PTMs, to solve the clinical problem, sepsis. The contributed papers serve to illustrate a significant underlying message that various PTMs mediate infection and immune response, regulate transcriptional reprogramming of immune cells in severe inflammation, and work as potential biomarkers for diagnosis and prognosis of sepsis. Further studies are still needed to explore underlying mechanisms and clinical application using a plethora of technologies including bioinformatics, molecular biology studies and rigorous statistical methods.

AUTHOR CONTRIBUTIONS

PC and YL wrote the manuscript. YL made critical revision. All authors contributed to the article and approved the submitted version.

FUNDING

This work was funded by grants from the National Institute of Health R01 (R01HL155116) to YL, the Joint-of- Institute (Grant# U068874) to YL, National Natural Science Foundation of China (82102315) to PC, and Beijing Natural Science Foundation (7214265) to PC.

REFERENCES

1. Cecconi M, Evans L, Levy M, Rhodes A. Sepsis and Septic Shock. *Lancet* (2018) 392(10141):75–87. doi: 10.1016/S0140-6736(18)30696-2
2. Kruiswijk F, Labuschagne CF, Vousden KH. P53 in Survival, Death and Metabolic Health: A Lifeguard With a Licence to Kill. *Nat Rev Mol Cell Biol* (2015) 16(7):393–405. doi: 10.1038/nrm4007
3. Zhao W, Zhang L, Chen R, Lu H, Sui M, Zhu Y, et al. SIRT3 Protects Against Acute Kidney Injury *via* AMPK/mTOR-Regulated Autophagy. *Front Physiol* (2018) 9:1526. doi: 10.3389/fphys.2018.01526
4. Tang C, Ma Z, Zhu J, Liu Z, Liu Y, Liu Y, et al. P53 in Kidney Injury and Repair: Mechanism and Therapeutic Potentials. *Pharmacol Ther* (2019) 195:5–12. doi: 10.1016/j.pharmthera.2018.10.013
5. Gill SE, Rohan M, Mehta S. Role of Pulmonary Microvascular Endothelial Cell Apoptosis in Murine Sepsis-Induced Lung Injury *In Vivo*. *Respir Res* (2015) 16:109. doi: 10.1186/s12931-015-0266-7
6. Zhang Q, Kuang H, Chen C, Yan J, Do-Umehara HC, Liu XY, et al. The Kinase Jnk2 Promotes Stress-Induced Mitophagy by Targeting the Small Mitochondrial Form of the Tumor Suppressor ARF for Degradation. *Nat Immunol* (2015) 16(5):458–66. doi: 10.1038/ni.3130
7. Micelli C, Rastelli G. Histone Deacetylases: Structural Determinants of Inhibitor Selectivity. *Drug Discov Today* (2015) 20(6):718–35. doi: 10.1016/j.drudis.2015.01.007
8. Tu Y, Hershman DL, Bhalla K, Fiskus W, Pellegrino CM, Andreopoulou E, et al. A Phase I-II Study of the Histone Deacetylase Inhibitor Vorinostat Plus Sequential Weekly Paclitaxel and Doxorubicin-Cyclophosphamide in Locally Advanced Breast Cancer. *Breast Cancer Res Treat* (2014) 146(1):145–52. doi: 10.1007/s10549-014-3008-5
9. Yee AJ, Bensinger WI, Supko JG, Voorhees PM, Berdeja JG, Richardson PG, et al. Ricolinostat Plus Lenalidomide, and Dexamethasone in Relapsed or Refractory Multiple Myeloma: A Multicentre Phase 1b Trial. *Lancet Oncol* (2016) 17(11):1569–78. doi: 10.1016/S1470-2045(16)30375-8
10. Vogl DT, Raje N, Jagannath S, Richardson P, Hari P, Orlowski R, et al. Ricolinostat, the First Selective Histone Deacetylase 6 Inhibitor, in Combination With Bortezomib and Dexamethasone for Relapsed or Refractory Multiple Myeloma. *Clin Cancer Res* (2017) 23(13):3307–15. doi: 10.1158/1078-0432.CCR-16-2526.Citedin:Pubmed
11. Sun B, Chang HH, Salinger A, Tomita B, Bawadekar M, Holmes CL, et al. Reciprocal Regulation of Th2 and Th17 Cells by PAD2-Mediated Citrullination. *JCI Insight* (2019) 4(22):e129687. doi: 10.1172/jci.insight.129687.Citedin:Pubmed
12. Arnoux F, Mariot C, Peen E, Lambert NC, Balandraud N, Roudier J, et al. Peptidyl Arginine Deiminase Immunization Induces Anticitrullinated Protein Antibodies in Mice With Particular MHC Types. *Proc Natl Acad Sci USA* (2017) 114(47):E10169–77. doi: 10.1073/pnas.1713112114
13. Mohanan S, Horibata S, McElwee JL, Dannenberg AJ, Coonrod SA. Identification of Macrophage Extracellular Trap-Like Structures in Mammary Gland Adipose Tissue: A Preliminary Study. *Front Immunol* (2013) 4:67. doi: 10.3389/fimmu.2013.00067
14. Mishra N, Schwerdtner L, Sams K, Mondal S, Ahmad F, Schmidt RE, et al. Cutting Edge: Protein Arginine Deiminase 2 and 4 Regulate NLRP3 Inflammasome-Dependent IL-1beta Maturation and ASC Speck Formation in Macrophages. *J Immunol* (2019) 203(4):795–800. doi: 10.4049/jimmunol.1800720
15. Wu Z, Tian Y, Alam HB, Li P, Duan X, Williams AM, et al. Peptidylarginine Deiminases 2 Mediates Caspase-1-Associated Lethality in Pseudomonas Aeruginosa Pneumonia-Induced Sepsis. *J Infect Dis* (2021) 223(6):1093–102. doi: 10.1093/infdis/jiaa475
16. Wu Z, Deng Q, Pan B, Alam HB, Tian Y, Bhatti UF, et al. Inhibition of PAD2 Improves Survival in a Mouse Model of Lethal LPS-Induced Endotoxic Shock. *Inflammation* (2020) 43(4):1436–45. doi: 10.1007/s10753-020-01221-0

17. Li Y, Liu B, Fukudome EY, Lu J, Chong W, Jin G, et al. Identification of Citrullinated Histone H3 as a Potential Serum Protein Biomarker in a Lethal Model of Lipopolysaccharide-Induced Shock. *Surgery* (2011) 150(3):442–51. doi: 10.1016/j.surg.2011.07.003
18. Deng Q, Pan B, Alam HB, Liang Y, Wu Z, Liu B, et al. Citrullinated Histone H3 as a Therapeutic Target for Endotoxic Shock in Mice. *Front Immunol* (2019) 10:2957. doi: 10.3389/fimmu.2019.02957
19. Pan B, Alam HB, Chong W, Mobley J, Liu B, Deng Q, et al. CitH3: A Reliable Blood Biomarker for Diagnosis and Treatment of Endotoxic Shock. *Sci Rep* (2017) 7(1):8972. doi: 10.1038/s41598-017-09337-4
20. Tian Y, Russo RM, Li Y, Karmakar M, Liu B, Puskarich MA, et al. Serum Citrullinated Histone H3 Concentrations Differentiate Patients With Septic Verses non-Septic Shock and Correlate With Disease Severity. *Infection* (2021) 49(1):83–93. doi: 10.1007/s15010-020-01528-y
21. Zhang D, Tang Z, Huang H, Zhou G, Cui C, Weng Y, et al. Metabolic Regulation of Gene Expression by Histone Lactylation. *Nature* (2019) 574 (7779):575–80. doi: 10.1038/s41586-019-1678-1

Conflict of Interest: The authors declare that the research was conducted in the absence of any commercial or financial relationships that could be construed as a potential conflict of interest.

Publisher's Note: All claims expressed in this article are solely those of the authors and do not necessarily represent those of their affiliated organizations, or those of the publisher, the editors and the reviewers. Any product that may be evaluated in this article, or claim that may be made by its manufacturer, is not guaranteed or endorsed by the publisher.

frontiers in Immunology

ORIGINAL RESEARCH
published: 14 July 2021
doi: 10.3389/fimmu.2021.685523

p53 Deacetylation Alleviates Sepsis-Induced Acute Kidney Injury by Promoting Autophagy

Maomao Sun[1,2†], Jiaxin Li[1,2†], Liangfeng Mao[1,2], Jie Wu[1], Zhiya Deng[1], Man He[1], Sheng An[1], Zhenhua Zeng[1,2], Qiaobing Huang[1,2*] and Zhongqing Chen[1,2*]*

[1] Department of Critical Care Medicine, Nanfang Hospital, Southern Medical University, Guangzhou, China, [2] Guangdong Provincial Key Laboratory of Shock and Microcirculation, School of Basic Medical Sciences, Southern Medical University, Guangzhou, China

OPEN ACCESS

Edited by:
Erxi Wu,
Baylor Scott and White Health,
United States

Reviewed by:
Thomas Griffith,
University of Minnesota Twin Cities,
United States
Erika M. Palmieri,
National Cancer Institute at Frederick,
United States

***Correspondence:**
Zhenhua Zeng
zhenhuazeng.2008@163.com
Qiaobing Huang
bing@smu.edu.cn
Zhongqing Chen
zhongqingchen2008@163.com

[†]*These authors have contributed equally to this work*

Specialty section:
This article was submitted to Inflammation, a section of the journal Frontiers in Immunology

Received: *25 March 2021*
Accepted: *29 June 2021*
Published: *14 July 2021*

Citation:
Sun M, Li J, Mao L, Wu J, Deng Z, He M, An S, Zeng Z, Huang Q and Chen Z (2021) p53 Deacetylation Alleviates Sepsis-Induced Acute Kidney Injury by Promoting Autophagy. Front. Immunol. 12:685523. doi: 10.3389/fimmu.2021.685523

Recent studies have shown that autophagy upregulation can attenuate sepsis-induced acute kidney injury (SAKI). The tumor suppressor p53 has emerged as an autophagy regulator in various forms of acute kidney injury (AKI). Our previous studies showed that p53 acetylation exacerbated hemorrhagic shock-induced AKI and lipopolysaccharide (LPS)-induced endothelial barrier dysfunction. However, the role of p53-regulated autophagy in SAKI has not been examined and requires clarification. In this study, we observed the dynamic changes of autophagy in renal tubular epithelial cells (RTECs) and verified the protective effects of autophagy activation on SAKI. We also examined the changes in the protein expression, intracellular distribution (nuclear and cytoplasmic), and acetylation/deacetylation levels of p53 during SAKI following cecal ligation and puncture (CLP) or LPS treatment in mice and in a LPS-challenged human RTEC cell line (HK-2 cells). After sepsis stimulation, the autophagy levels of RTECs increased temporarily, followed by a sharp decrease. Autophagy inhibition was accompanied by an increased renal tubular injury score. By contrast, autophagy agonists could reduce renal tubular damage following sepsis. Surprisingly, the expression of p53 protein in both the renal cortex and HK-2 cells did not significantly change following sepsis stimulation. However, the translocation of p53 from the nucleus to the cytoplasm increased, and the acetylation of p53 was enhanced. In the mechanistic study, we found that the induction of p53 deacetylation, due to either the resveratrol/quercetin -induced activation of the deacetylase Sirtuin 1 (Sirt1) or the mutation of the acetylated lysine site in p53, promoted RTEC autophagy and alleviated SAKI. In addition, we found that acetylated p53 was easier to bind with Beclin1 and accelerated its ubiquitination-mediated degradation. Our study underscores the importance of deacetylated p53-mediated RTEC autophagy in future SAKI treatments.

Keywords: sepsis, acute kidney injury, autophagy, p53, deacetylation

INTRODUCTION

Sepsis is defined as organ dysfunction that results from the host's deleterious response to infection (1). The kidney is one of the most common organs affected by sepsis, resulting in a condition known as sepsis-associated acute kidney injury (also known as sepsis-induced AKI or SAKI), which increased the morbidity and mortality caused by sepsis (2). The accurate estimation of the incidence and trends associated with AKI secondary to sepsis has been challenging. Several cohort studies have described the frequency of AKI among patients with sepsis, and the incidence of SAKI among sepsis patients has been reported between 22% to 53% (3). Even if SAKI patients survive, the possibility of developing chronic kidney disease is greatly increased (2, 3). Our previous studies have shown that damage to renal tubular epithelial cells (RTECs) is an important underlying cause of SAKI (4). However, the exact mechanism of RTEC damage in SAKI is not completely understood.

The tumor suppressor p53 has emerged as an important player in various forms of AKI (5, 6). This transcription factor primarily responds to cellular stress and DNA damage by halting the cell cycle and promoting apoptosis in extreme cases of cell stress including AKI (7). Although the primary role of p53 activation is to safeguard the genome and prevent malignant transformation, its role in AKI appears to be less straightforward and can be detrimental inasmuch as it can trigger cell death in sublethal injured tubular cells (8). Recent evidence indicates that autophagy inhibition is an important cause of various types of AKI (9). The upregulation of p53 could mediate the attenuation of autophagy and aggravate AKI induced by ischemia-reperfusion conditions and cisplatin treatment (6). However, the role of p53 in SAKI has not been reported and the underlying mechanism remains unknown. p53 is subject to a wide range of post-translational modifications (PTM), including phosphorylation, acetylation, methylation, glycosylation, farnesylation, hydroxylation, ADP ribosylation, and PIN1-mediated prolyl isomerization, in addition to modification with ubiquitin and other ubiquitin-like proteins (5). Our previous studies showed that p53 acetylation exacerbated hemorrhagic shock-induced AKI (10) and lipopolysaccharide (LPS)-induced endothelial barrier dysfunction (11).

In this study, we examined the changes in the protein expression, intracellular distribution (nuclear and cytoplasmic), and acetylation/deacetylation state of p53 in cecal ligation and puncture (CLP) or LPS-induced animal model of SAKI and in a LPS-challenged human RTEC cell line (HK-2 cells). Surprisingly, the expression of p53 protein both in renal cortex and HK-2 cell did not significantly change after sepsis stimulation. However, the translocation of p53 from the nucleus to the cytoplasm increased, and the acetylation of p53 was enhanced. In the mechanistic study, we found that the induction of p53 deacetylation, by the activation of deacetylase Sirtuin 1 (Sirt1) through resveratrol/quercetin or the mutation of acetylated lysine site in p53, promoted RTEC autophagy, which alleviated SAKI. In addition, we also found that acetylated p53 was easier to bind with Beclin1 and accelerated its ubiquitination-mediated degradation. Our study underscores the importance of deacetylated p53-mediated RTEC autophagy in future SAKI treatments.

MATERIAL AND METHODS

Reagents and Antibodies

Rapamycin (Rapa, S1039), 3-methyladenine (3-MA, S2767), tenovin-6 (S4900), resveratrol (RSV, S1396), chloroquine (CHQ, S6999), quercetin (QCT, S2391), MG132 (S2619) and protease inhibitor cocktail were purchased from Selleck (Houston, Texas, USA). Lipopolysaccharide (LPS, L2630) and pentobarbital (P010) were purchased from Sigma (St. Louis, MO, USA). TUNEL Apoptosis Assay Kit (C1088), deacetylase inhibitor cocktail (P1112), Nuclear and Cytoplasmic Protein Extraction Kit (P0027), and protein A+G agarose beads (P2012) were purchased from Beyotime (Shanghai, China). Immunoprecipitation kit and anti-Beclin1 (11306-1) antibodies were purchased from Proteintech Co. (Chicago, IL, USA). Anti-autophagy-related 5 (Atg5, A0203), anti-p53 (A5761), anti-p62 (A7353), pan-acetylated lysine (A2391), anti-Sirt1 (A0127) and goat anti-mouse lgG (H+L; AS008) antibodies were purchased from Abclonal, China. Anti-microtubule-associated protein 1A/1B-light chain 3 (LC3A/B, 12741S), acetyl-p53 (Lys379; #2570) and Ubiquitin (Ub, P4D1, 3936S) antibodies were purchased from Cell Signaling Technology (Beverly, MA, USA). Anti-glyceraldehyde 3-phosphate dehydrogenase (GAPDH, RM2002), anti-proliferating cell nuclear antigen (PCNA, RM2009), horseradish peroxidase (HRP)-labeled goat anti-mouse secondary antibodies (RM3001), HRP-labeled goat anti-rabbit secondary antibodies (RM3002), and anti-Flag-tag (RM1002) antibodies were purchased from Beijing Ruikang, China. Anti-LC3A/B (SAB1305552) antibody was purchased from Sigma (St. Louis, MO, USA). Anti-p53 (PAb 240) antibody was purchased from Abcam, USA. Antibody against kidney injury molecule-1 (KIM-1, NBP1-76701) was purchased from Novus, USA. TRIzol reagent (#D1105) was purchased from GBCBIO Technologies, China. HiScript® III RT SuperMix (#R323) and SYBR® qPCR Master Mix (#Q331) were purchased from Vazyme, China.

SAKI Animal Model Study

The experimental animals C57/BL6 mice, weighed between 20–22 g and aged 6–8 weeks, were obtained from the Animal Center of Southern Medical University, Guangzhou, China. The animal experiments were conducted in strict accordance with the recommendations of the Guide for the Care and Use of Laboratory Animals (US National Institutes of Health, Bethesda, MD, USA), and the study protocol was approved by the Committee on Ethics in Animal Experiments of Southern Medical University. Two septic animal models, CLP- and LPS-induced septic mouse models, were used in present study. The chemical reagents with doses of 4 mg/kg Rapa, 20 mg/kg 3-MA, 25 mg/kg tenovin-6, 50 mg/kg CHQ, 30 mg/kg RSV and 25 mg/kg QCT were intraperitoneally injected 2 h before CLP as required, respectively (12–15). All these chemical reagents were

first dissolved in DMSO, and then diluted with saline to reach the working concentration.

The CLP procedure was performed as described in previous studies (16). Specifically, the experimental mice were weighed and anesthetized by the intraperitoneal injection of 2% pentobarbital at a dose of 23 mL/kg. A midline laparotomy was performed using mini-midsection, and the cecum was ligated just below the ileocecal valve by using 4–0 silk ligatures to maintain intestinal continuity. The cecum was perforated at 2 locations 1 cm apart by using a 21-gauge needle and gently compressed until feces were extruded. The bowel was then returned to the abdomen, and the incision was closed. Control mice (sham group) underwent the same surgical procedures without ligating and puncturing the cecum. At the end of the operation, all mice received fluid resuscitation with normal saline (50 mL/kg) by subcutaneous injection. After the CLP model was created, the mice were executed for the observation of renal pathological changes. The autophagy in RETCs, the expression level of p53 protein in kidney and serum creatinine (sCr) levels were also detected. Some other animals (20 in each group) were remained for survival analyses.

LPS-induced septic mouse model was created with 15 mg/kg LPS *via* intraperitoneal injection as described in previous study (17). The mice were then executed for the observation of the autophagy in RETCs and the expression level of p53 protein in kidney.

Cell Culture, Transfection, and Adenovirus Transduction

The experimental RTEC HK-2 cells were purchased from Kunming Cell Bank, China (numbered KCB200815YJ). HK-2 cells were cultured in Dulbecco's modified Eagle's medium (DMEM) supplemented with 10% (v/v) heat-inactivated fetal bovine serum (FBS) at 37°C in a humidified atmosphere containing 5% CO_2. A recent mycoplasma contamination test on HK-2 cells was negative.

HK-2 cells were stimulated with 10 μg/ml LPS to construct a cellular sepsis model. According to the requirements of different experiments, cells were transfected with control small interfering RNA (siRNA), Sirt1 siRNA, empty plasmid vectors, HA-Sirt1 plasmid and His-Ub plasmid vectors for 6 h by using Opti-MEM® I reduced serum media and Lipofectamine 2000. The siRNA, HA-SIRT1 and His-Ub plasmid were synthesized by GenePharma (Shanghai, China). The siRNA-targeted sequences were as follows: control siRNA, sense 5'-UUCUCCGAACGUGUCACGUTT-3' and antisense 5'-ACGUGACACGUUCGGAGAATT-3'; SIRT1 siRNA, sense 5'-GCUGUACGAGGAGAUAUUUTT-3' and antisense 5'-AAAUAUCUCCUCGUACAGCTT-3'. After the cells were transfected for 36 h, follow-up experiments were performed. The adenoviral vector expressing Flag- and GFP-tagged wild-type and lysine-mutated p53 (Ad-p53 and Ad-p53K382R, respectively) were packaged by GeneChem Co. Ltd (Shanghai, China). The adenoviral vector expressing Flag- and GFP-tagged wild-type Beclin1 (Ad-Beclin1) was also packaged by GeneChem Co. Ltd. Cells were transduced with 10^9 plaque-forming units (PFU)/mL of adenoviruses for 48 h, followed by corresponding experiments.

Histology and Immunohistochemistry

The histology of mouse kidneys was observed by hematoxylin-eosin (HE) staining and periodic acid-Schiff (PAS) staining. Briefly, fresh renal cortical tissues were sliced into sections, fixed with 10% formalin for approximately 24 h, and then stained and observed under an optical microscope (Zeiss, LSM780, Thuringia Germany). Two professional pathologists, who were blinded to the experimental protocol and the experimental group of this subject, scored the damage to the renal cortex. Five sections were selected for each group, and 10 random fields of view were selected from each section. The histological assessment of renal damage included the observed loss of the tubule brush border, renal tubule hemorrhage, tubular casts, inflammatory infiltration, and obvious necrosis in the cortex (18, 19). The scoring principle was as follows: 0, no damage; 1, ≤10% damage; 2, 11%–25% damage; 3, 26%–45% damage; 4, 46%–75% damage, and 5, ≥76% damage. Finally, statistical analysis and graphing were performed, according to the scoring results.

For immunohistochemical staining, renal tissues were obtained, fixed with 4% formaldehyde solution overnight, dehydrated using an alcohol gradient, cleared using xylene, and embedded in paraffin. Subsequently, the paraffin-embedded tissue blocks were sliced into 4–6 μm sections, which were then mounted onto glass slides. The slides were baked in an oven at 55°C for 2 h, followed by deparaffinization and rehydration, prior to antigen retrieval using sodium citrate. KIM-1 has been used as an useful biomarker for renal proximal tubule damage to facilitate the early diagnosis of renal tubule dysfunction (20). In this study, kidney sections were probed with antibodies against KIM-1 at a dilution of 1:100 at room temperature for 1 h. Then the sections were incubated for 15 min at room temperature with biotinylated secondary antibody. A streptavidin-peroxidase enzyme conjugate was added to each section for 10 min, and the peroxidase activity of KIM-1 was visualized. The density of KIM-1 staining was quantified by Image software (Media Cybernetics, Inc., Rockville, MD, USA)

TUNEL Assay

Terminal deoxynucleotidyl transferase dUTP mediated nick-end labeling (TUNEL) assay was performed to evaluate apoptosis in renal tissues, as described in our previously published literature (16). Briefly, the renal tissues (4 μm) were fixed, paraffin-embedded, and labeled with a TUNEL reaction mixture containing terminal deoxynucleotidyl transferase and nucleotides including tetramethylrhodamine-labeled dUTP. After the reactions were terminated, the slides were examined by fluorescence microscopy. Blue dots, generated by 4', 6-diamidino-2-phenylindole (DAPI) staining, identified the nucleus, whereas green dots were generated by the TUNEL assay, indicating the presence of degraded DNA. The overlap between the blue dots and green dots represented apoptotic cells. A total of 30 fields of view from 5 samples were used to evaluate

the number of TUNEL-positive cells in the kidney. Data are expressed as the number of apoptotic cells in each 200× magnification field of view.

Renal Function Assessment

Blood samples were collected at 12 h after CLP and then centrifuged at 3,000 rpm for 15 min at room temperature to separate the serum. The levels of sCr were analyzed using an automatic biochemical analyzer (Chemray 240, Shenzhen, China).

Ultrastructure Observation With Transmission Electron Microscopy

Kidney tissues were cryosectioned in 2% formaldehyde and 2.5% glutaraldehyde in 0.1 M sodium cacodylate buffer for 1 h and then washed in phosphate-buffered saline (PBS) for 2 days. The samples were then fixed in 1% osmic acid, dehydrated with ethanol and acetone gradients, embedded in epoxy resin, and cut into ultrathin sections. The tissue sections were stained with uranyl acetate and lead citrate and then observed under an H-7500 transmission electron microscope (Hitachi, Tokyo, Japan). The number of autophagosomes and autophagolysosomes was counted in 30 randomly selected fields in each group at 8000× magnification, and representative fields at 40,000× magnification were selected for display.

Western Blotting Analysis

The kidney tissues and cells were homogenized by ultrasound and lysed in radioimmunoprecipitation assay (RIPA) lysis buffer containing 1× protease inhibitor cocktail. To detect the acetylation level of the target protein, 1× deacetylase inhibitor cocktail was added to the RIPA lysis buffer. The samples were then centrifuged at 12,000 rpm for 15 min to obtain the supernatants. The proteins in the supernatants were separated using sodium dodecyl sulfate (SDS)-polyacrylamide gel and transferred to polyvinylidene difluoride (PVDF) membranes. The PVDF membrane was blocked in 5% bovine serum albumin (BSA) for 1 h to remove the specific binding and then incubated with primary antibodies overnight at 4°C and secondary antibodies at room temperature for 1 h, and finally, the target protein was visualized with enhanced chemiluminescence reagents. The primary antibodies used were anti-Atg5, anti-LC3A/B, anti-p53, pan-acetylated lysine, acetyl-p53 (Lys379), anti-Sirt1, anti-p62, anti-Beclin1, Anti-GAPDH, anti-PCNA, anti-Flag-tag antibodies. The secondary antibodies used were HRP-labeled goat anti-mouse and anti-rabbit antibodies. The band intensities were quantified using ImageJ software. The protein expression levels were standardized relative to the level of GAPDH or PCNA or p53.

Autophagic Flux Detection by mRFP-GFP-LC3 Adenovirus Transfection

mRFP-GFP-LC3 adenovirus (Hanbio Co. Ltd., Shanghai, China) was transfected to HK-2 cells in each confocal cuvette at a titer of 10^{10} PFU/mL for 48 h, then the cells were harvested and fixed in 4% paraformaldehyde. The expression of both monomeric red fluorescent protein (mRFP) and green fluorescent protein (GFP) in the mRFP-GFP-LC3 tandem fluorescent proteins were used to track LC3 under a confocal laser microscope. Generally, when autophagosomes form in the cells, LC3 will converge into dots, and the LC3 dots will be tagged with both mRFP, resulting in red fluorescence and GFP, resulting in green fluorescence, simultaneously appearing yellow due to superimposition. However, GFP is sensitive to acidity. When autophagosomes fuse with acidic lysosomes, forming autophagolysosomes, the GFP protein becomes quenched, and the LC3 spots only appear red. Therefore, autophagy in HK-2 cells can be recognized by counting the yellow and red dots. In this study, the numbers of spots of each color were obtained from at least three independent experiments in each group.

Immunoprecipitation and Co-Immunoprecipitation Assays

The enriched protein was incubated with 2 μg anti-p53 or anti-Beclin1 antibody overnight at 4°C. Then 40 μl of protein A+G agarose beads were added and spined at 4°C for 3 h. After centrifugation, the supernatant was discarded, and 1× loading buffer was added for western blotting analysis to determine protein expression. The primary antibodies used were pan-acetylated lysine, anti-Beclin1 and Ubiquitin antibodies. The protein expression levels were standardized relative to the level of p53 or IgG-H.

Nucleus and Cytoplasm Protein Isolation

A Nuclear and Cytoplasmic Protein Extraction Kit was used to isolate the nuclear and cytoplasmic p53 proteins from HK-2 cells. According to the manufacturer's recommendations, adherent cells were scraped, and the cell pellet was obtained by centrifugation. Then, 200 μl cytoplasmic protein extraction reagent A containing PMSF was added for every 20 μl of cell pellet volume. After the cell pellet was completely dispersed by vortexing at the highest speed for 5 s, the sample was placed in an ice bath for 10–15 min. Then, 10 μl of cytoplasmic protein extraction reagent B was added to the cell pellet. The mixture was vortexed at the highest speed for 5 s again and placed in an ice bath for another 1 min, followed by centrifugation at 14,000 × *g* at 4°C for 5 min to obtain the supernatant, which was retained as the cytoplasmic protein fraction. Then, 50 μl of nuclear protein extraction reagent containing PMSF was added to the remaining cell pellet. The mixture was subjected to an ice bath and vortexed at high speed for 30 s every 1–2 min for a total of 30 min. Finally, the cell pellet was centrifuged at 14,000 × *g* at 4°C for 10 min to obtain the nuclear protein. The nuclear and cytoplasmic proteins can be used immediately or stored at −70°C.

Immunofluorescence Assays

HK-2 cells were inoculated onto Petri dishes. After discarding the original medium, the cells were rinsed three times with PBS, fixed with 4% paraformaldehyde for 15 min, punched with 0.5% Triton-100 for 15 min, blocked with 5% BSA for 1 h, and then incubated overnight at 4°C with primary antibodies for p53 or LC3 at a dilution of 1:100. The next day, fluorescent secondary antibodies were added and incubated at room temperature for 1 h, and then the nucleus was stained with DAPI after 3 washes with PBS.

Survival Study

Sepsis was induced by CLP, as described above. After awakening from anesthesia, the mice were returned to their cages, and food and water were provided. For survival analysis, 20 mice were included in each group (sham group, vehicle + CLP group and RSV + CLP group), and mice were monitored daily over a 5-day period, and the survival rate was recorded. Survival after surgery was assessed every 6 h during the first 48 h and then every 8 h for 3 days. Apnea for >1 min was considered to indicate death. Mice that survived for > 5 d were sacrificed by cervical dislocation.

Real-Time Quantitative Reverse Transcription Polymerase Chain Reaction (RT-qPCR) Assays

Total RNA was isolated from cells with TRIzol reagent. The RNA concentration was determined by using a BioDrop spectrophotometer (Biochrom Ltd, Cambridge, UK). Complementary DNA was reverse transcribed with HiScript® III RT SuperMix according to the manufacturer's protocol. RT-PCR was performed using SYBR® qPCR Master Mix with specific primers (**Table 1**) in a 7500 Real-Time PCR System (Applied Biosystems, Foster City, CA). β-actin was used as the internal control. The 2−ΔΔCt method was employed to evaluate mRNA expression.

Ubiquitination Assay

For detection of ubiquitinated proteins, cells were transfected with Ad-Beclin1 along with Ad-p53 or Ad-p53K382R. After 12 h, 4 μg of His-Ub expression plasmid was transfected into the cells. After 36 h of transfection, 5 μM MG132, the proteasome inhibitor, was added along with LPS and the cells were further incubated for 12 h. Cells were then harvested for immunoprecipitation.

Statistical Analysis

Survival analysis was performed using Kaplan-Meier plots and compared using the log-rank test. Other results were expressed as the mean ± standard deviation and analyzed by one-way analysis of variance (ANOVA) with SPSS 20.0 (IBM, Armonk, NY, USA). Variance in groups was evaluated using the homogeneity of variance test (the Levene test). When the Levene test indicated homogeneity of variance ($P > 0.1$), the least-significant difference multiple comparison test was used. When equal variance was not assumed (the Levene test; $P < 0.1$), the Welch method was applied, followed by Dunnett's T3 *post hoc* comparisons. All tests were performed using SPSS software (Chicago, IL). P values < *0.05* were considered significant.

RESULTS

Autophagy Inhibition Precedes Apoptosis in RTECs Following Sepsis

We first dynamically observed damage in kidney tissues in the CLP-induced AKI model. Both HE staining and PAS staining showed that some renal tubules expanded and swelled within 4 h after CLP, and some RTECs fell off into the lumen. These pathological changes were gradually aggravated over the next 12 h post-CLP, and the renal tubular injury scores were correspondingly elevated (**Figures 1A–C**). Interestingly, the apoptosis level, as assessed by TUNEL staining, only increased significantly after 12 h of CLP (**Figures 1D, E**). Transmission electron microscopy observation and the quantitative analysis of autophagosomes and autolysosomes revealed that autophagy in RTECs increased progressively and then sharply decreased within 8 h after CLP. The decline in autophagy levels preceded the occurrence of apoptosis (**Figures 1F, G**). Subsequently, we also measured the dynamic changes of autophagy in LPS-induced septic mouse model. We found that the expression of autophagy-related protein LC3II increased gradually and peaked at 8 h, returned to baseline by 24 h. In contrast, p62 (SQSTM1, a mediator of cargo selection and an autophagic substrate) expression reached the lowest levels at 8 h with LPS treatment (**Supplementary Figures 1A–C**), which was consistent with the autophagosomes analysis in CLP-induced septic mouse model. Similar changes of LC3II and p62 have been reported in CLP model in our previous study (15).

Based on the findings of animal experiments, we further detected autophagy in LPS-challenged human RTECS (HK-2 cells). The expression of autophagy-related protein Atg5 and LC3II gradually increased and reached a peak at 8 h and then sharply decreased and dropped at 24 h (**Figures 2A–C**). Considering that the hindrance of autophagic flux would cause the failure of autophagosomes to fuse with lysosomes to form autophagolysosomes, which would result in the increased expression of autophagy-related proteins; therefore, we detected autophagic flux using laser confocal microscopy. We transfected HK-2 cells with the autophagy double-labeled adenovirus mRFP-GFP-LC3 to detect autophagic flux. According

TABLE 1 | Sequences of primers for RT-qPCR.

Gene name	Forward primer	Reverse primer
ATG2A	5'-CCTCTGTGAGACCAAGGATGAG-3'	5'-CCAGACAGAAGTAGCCAAGTCC-3'
ATG2B	5'-CTTCAGATGGAGTTGGAGGAGAC-3'	5'-AGTGGCTCCTTTCAGTCCTACG-3'
ATG4B	5'-ATGGGAGTTGGCGAAGGCAAGT-3'	5'-AGCTCCACGTATCGAAGACAGC-3'
TSC2	5'-GCCACTACTGTGCCTTTGAGTC-3'	5'-CCCTCAGAGAATCGCCAGTACT-3'
UVRAG	5'-TCTACACCGACAACTCCATCCG-3'	5'-TCTGGCATTTTGGAGAGGAAGTG-3'
DRAM1	5'-ATCTTCAAGCCATCCTGTGTG-3'	5'-GAGGTTTGATCCGCATAATCTG-3'
BAX	5'-TCAGGATGCGTCCACCAAGAAG-3'	5'-TGTGTCCACGGCGGCAATCATC-3'
PIG3	5'-CACCAGTTTGCTGAGGTCTAGG-3'	5'-CCTGGATTTCGGTCACTGGGTA-3'
NOXA1	5'-CTCGATGCAGAGACAGAGGTCG-3'	5'-AGGAGCCTGTTTGCCAACTTGC-3'
β-Actin	5'-AAATCGTGCGTGACATCAAAGA-3'	5'-GCCATCTCCTGCTCGAAGTC -3'

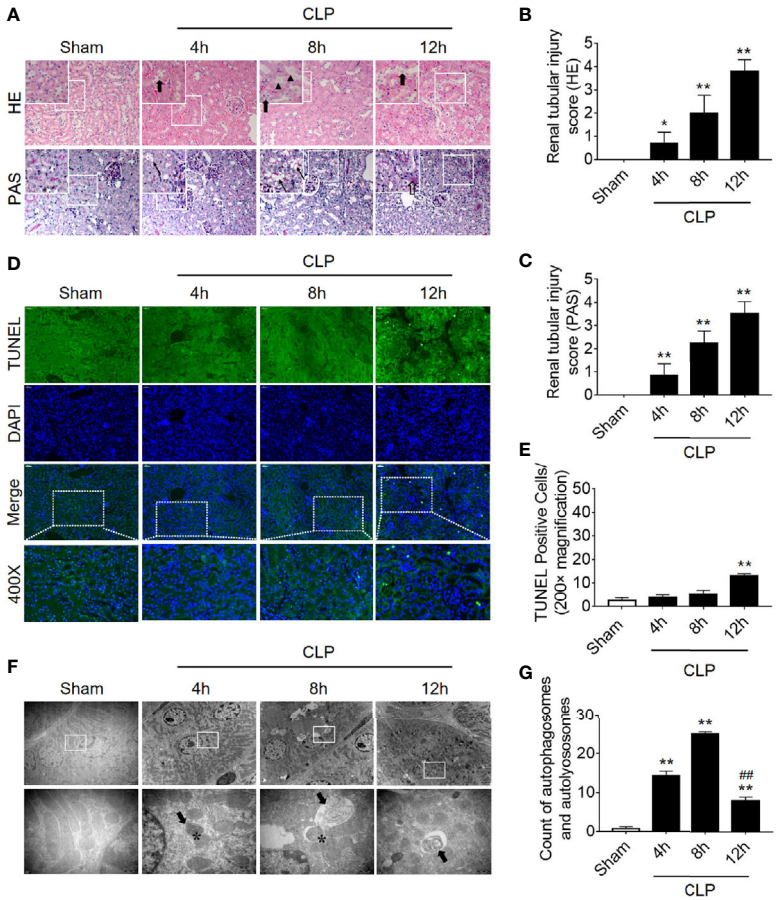

FIGURE 1 | Renal pathology score, apoptosis, and autophagy following CLP-induced sepsis. **(A)** Hematoxylin-eosin (HE) staining (upper panel: 200×; inset: 400×) and periodic acid-Schiff (PAS) staining (lower panel: 200×; inset: 400×) of the renal cortex following CLP-induced sepsis. Black thick arrows: Nuclei of RTECs shed to lumen; Long black arrows: tubular dilation; Black triangles: renal tubular casts; White thick arrows: severe tubular damage. **(B, C)** The tubular damage score was evaluated based on pathological observations from HE and PAS staining. $^{*}p < 0.05$, $^{**}p < 0.01$ *vs.* sham group; n = 5. **(D)** Cell apoptosis of the renal cortex, as assessed by TUNEL-positive cell staining following CLP-induced sepsis. Upper panel: 200×; lower panel: 400×. **(E)** Semi-quantitative analysis of TUNEL-positive cells. $^{**}p < 0.01$ *vs.* sham group; n = 5. **(F)** Observation of autophagy in the renal cortex under transmission electron microscope following CLP-induced sepsis. Black thick arrows: autophagosomes or autolysosomes; Asterisk: mitochondrial autophagy; upper panel: magnified ×7000; lower panel: magnified ×40000. **(G)** Semi-quantitatively analysis of autophagy. The numbers of autophagosomes and autolysosomes in renal epithelial cells were calculated in 20 randomly selected fields. $^{**}p < 0.01$ *vs.* sham group; $^{\#\#}p < 0.01$ *vs.* 8 h group; n = 20. CLP, cecal ligation and puncture; RTEC, renal tubular epithelial cell; TUNEL, terminal deoxynucleotidyl transferase dUTP nick-end labeling.

to the manufacturer's recommendations, free red dots [red dots (mRFP) minus the overlap of red and green dots (GFP)] represented autolysosomes, and the yellow dots with overlapping red dots and green dots represented autophagosomes. As expected, the number of both autophagosomes and autophagolysosomes showed a trend of increasing first and then decreasing (**Figures 2D–F**), indicating that the autophagy flux has not been blocked, which is the same as the observed trend of autophagy-related protein expression.

Autophagy Activation Alleviates Renal Injury

Next, we verified the protective effects of autophagy activation on kidney after sepsis. The autophagy agonist Rapa and the autophagy inhibitor 3-MA were used for this experiment. Using transmission electron microscopy, we found that Rapa pretreatment significantly promoted the level of autophagy in RTECs at 12 h after CLP (**Figures 3A, B**) and alleviated renal tubular injury (**Figures 3C–E**). Correspondingly, 3-MA inhibited the formation of autophagosomes in RTECs, which further aggravated renal tubular injury after CLP (**Figure 3**). A more specific autophagy inhibitor CHQ was applied to further confirm the effect of autophagy inhibition. The result showed that CHQ blocked autophagy with significant increase of p62 expression (**Supplementary Figures 2A–C**), accompanied by aggravated renal tubular injury (**Supplementary Figures 2D, E**).

Translocation of p53 From Nucleus to Cytoplasm Increases Following Sepsis

Because the level of apoptosis was increased while autophagy started to be inhibited (**Figure 1**), it is speculated that autophagy inhibition

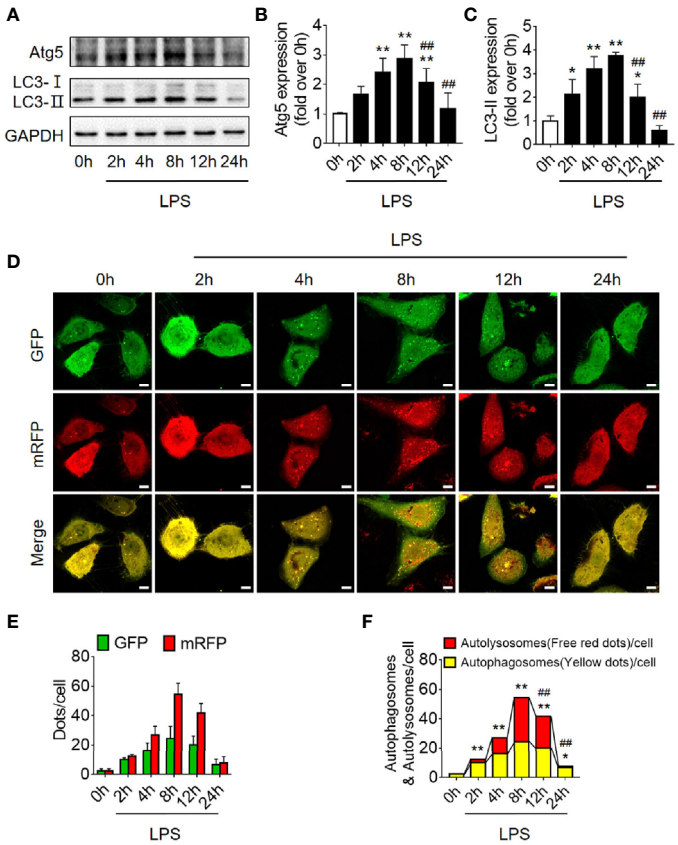

FIGURE 2 | Autophagy determination in LPS-induced HK-2 cells. **(A)** Representative western blot showing the Atg 5 and LC3II protein expression levels in HK-2 cells following LPS stimulation at various time-points. GAPDH was used as an internal reference. **(B, C)** densitometric analyses of Atg5 and LC3II protein expression. n = 4-5. **(D)** The autophagic flux in HK-2 cells was determined by cellular immunoassay following LPS stimulation at various time-points. The autophagy double-labeled adenovirus mRFP-GFP-LC3 was used to detect autophagic flux (magnification ×630 and scale bar = 10 μm). **(E)** The mean number of GFP and mRFP dots per cell. **(F)** The mean numbers of autophagosomes and autolysosomes per cell. $^{*}p < 0.05$, $^{**}p < 0.01$ *vs.* the 0 h group, $^{\#\#}p < 0.01$ *vs.* the 8 h group. The results are representative of at least three independent experiments. LPS, lipopolysaccharide; Atg5, autophagy-related protein 5; LC3II, Microtubule-associated protein 1A/1B-light chain 3; GAPDH, glyceraldehyde 3-phosphate dehydrogenase; mRFP, monomeric red fluorescence protein; GFP, Green fluorescent protein.

might be induced by signaling changes in apoptosis pathway. p53, an important molecule in crosstalk of autophagy and apoptosis, was emerged. First, we found that the expression level of p53 protein in renal cortical tissue was not elevated (**Figures 4A, B**). The pro-autophagic role of p53 on renal tubular cells has been shown to depend on the intracellular distribution of p53 (6). We then measured the protein abundance of p53 in the nucleus and cytoplasm of HK-2 cells stimulated by LPS. We found that although the total p53 protein level was not changed significantly, the nuclear p53 protein level was progressively reduced, and correspondingly, the cytoplasmic level of p53 progressively increased, suggesting an increase in p53 nuclear to cytoplasmic translocation after 4–12 h of LPS stimulation (**Figures 4C–F**). These phenomena were further confirmed in cellular immunofluorescence experiments (**Figures 4G, H**). Since p53 works as a transcription factor while it locates in nucleus, the expression of p53 target genes, selectively those autophagy and apoptosis pathway-related genes were detected. The results revealed that, as p53 translocated out of nucleus, autophagy-related ATG2A mRNA was decreased continuously. ATG2B and ATG4B mRNA level were transiently increased at LPS stimulation but then decreased, while DRAM1, UVRAG and TSC2 did not change (**Supplementary Figures 3A–F**). The mRNA expression of pro-apoptotic BAX, PIG3, and NOXA1 were decreased 8 h after LPS stimulation (**Supplementary Figures 3G–I**). These results were mostly coincidence with the timing of p53 translocation out of nucleus.

Increased p53 Acetylation Inhibits Autophagy in RTECs

It is known that p53 acetylation modification is critical in its activity, we then explored the level of p53 acetylation during SAKI and examined the effects of promoting p53 acetylation on autophagy. As expected, the acetylation of p53 in renal cortical tissue was considerably increased (**Figure 5A**) at 12 h following CLP. According to previous reports (5, 6) and our published data (10, 11), p53 acetylation may increase p53 activity. Tenovin-6 acts as an enhancer of endogenous acetylation of p53 by inhibiting the protein-deacetylating activities of Sirt1 and Sirt2 (21, 22). It is

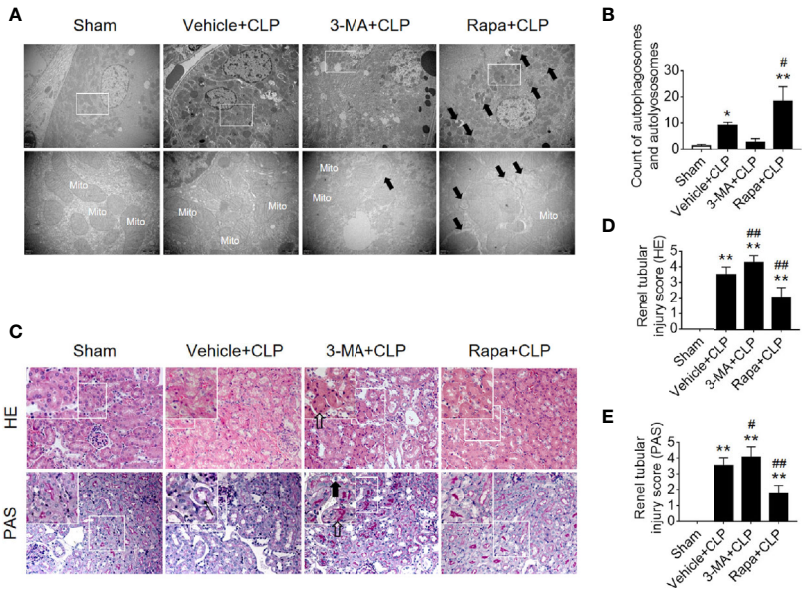

FIGURE 3 | Effects of autophagy regulation on renal pathology score and autophagy in CLP-induced sepsis. **(A)** Observation of autophagic structures in the renal cortex under a transmission electron microscope following autophagy regulation in septic mice. Black thick arrows: autophagosomes or autolysosomes; Mito, mitochondria; upper panel: magnified ×7,000; lower panel: magnified ×40,000. **(B)** Semi-quantitatively analysis of autophagy. The numbers of autophagosomes and autolysosomes in renal epithelial cells were calculated in 20 randomly selected fields. $^{**}p < 0.05$, $^{**}p < 0.01$ *vs.* sham group; $^{\#}p < 0.05$ *vs.* the vehicle + CLP group; n = 20. **(C)** Autophagy regulation on Hematoxylin-Eosin (HE) staining (upper panel: 200×; inset: 400×) and periodic acid-Schiff (PAS) staining (lower panel: 200×; inset: 400×) of the renal cortex following CLP-induced sepsis. Black thick arrows: Nuclei of RTECs shed to lumen; Long black arrows: tubular dilation; White thick arrows: severe tubular damage. **(D, E)** The tubular damage score was evaluated based on pathological observations from HE and PAS staining. $^{*}p < 0.01$ *vs.* sham group; $^{\#}p < 0.05$, $^{\#\#}p < 0.01$ *vs.* the vehicle + CLP group; n = 5. CLP, cecal ligation and puncture; RTEC, renal tubular epithelial cell.

used in this study to induce p53 acetylation in CLP septic model. As expected, tenovin-6 treatment significantly increased p53 acetylation at 12 h after CLP (**Supplementary Figures 1G–H**), reduced the number of autophagosomes in RTECs and exacerbated kidney damage (**Figures 5B, C**). Since the acetylation of p53 (acetyl-p53) aggravated the autophagy in RTECs after sepsis were confirmed, the specific acetylation site deserves further clarification. According to a previous report (20), the acetylation site of p53 is K379 in mice and K382 in humans. Our study showed that the acetyl-p53 (K379) was significantly increased in the renal cortical tissues at 12 h after CLP/LPS compared with the level in the control group (**Figures 5D–F** and **Supplementary Figures 1D–F**). Consistent with the animal model, the acetyl-p53 (K382) level in HK-2 cells was also considerably increased 12 h following the LPS challenge (**Figures 5G–I**). In our study, the translocation of p53 from nucleus to cytoplasm increased after 4–12 h of LPS stimulation, so we also measured the acetylation levels of cytoplasmic p53 and nuclear p53 respectively. There was an increasing trend in acetylation of cytoplasmic p53 8 h after LPS exposure (**Supplementary Figures 4A–C**).

Mutation of Lysine (K) of p53 to Arginine (R) With Loss of PTM Site Promotes Autophagy

Since the K382 lysine is the main acetylation site of p53 in human cells, we mutated this site to explore the effects of p53 deacetylation on autophagy promotion. We used p53 overexpression virus (Ad-p53) and p53 K382R mutant virus (Ad-p53K382R) with both GFP and Flag tags. The transfection efficiency of the virus was verified by examining the expression levels of GFP and p53 (**Figures 6A, B**). Compared with the Ad-p53+LPS group, no elevated acetyl-p53 was observed in the Ad-p53K382R+LPS group after LPS stimulation due to the site mutation, whereas the level of p62 protein significantly decreased (**Figures 6C–G**), and LC3II protein increased, as assessed by western blotting (**Figures 6C–G**) and immunofluorescence analysis (**Figure 6H**). These results collectively suggested that the deacetylation of p53 *via* a point mutation at the lysine K382 could promote autophagy. These data confirmed the influence of p53 acetylation/deacetylation on autophagy regulation. Therefore, the identification of a drug capable of regulating p53 deacetylation could be useful for promoting autophagy in SAKI.

Activation of Deacetylase Sirt1 Promotes Autophagy and Reduces SAKI

Sirt1 is a NAD^+-dependent deacetylase that is known to directly deacetylate p53 (K382) to regulate the function of p53 (23). To investigate the effects of Sirt1-mediated deacetylation of p53 on autophagy, HA-tagged Sirt1 overexpression plasmid (**Figure 7A**) and Sirt1 siRNA (**Figure 8A**) were applied in RTECs. As expected, Sirt1 overexpression did not decrease

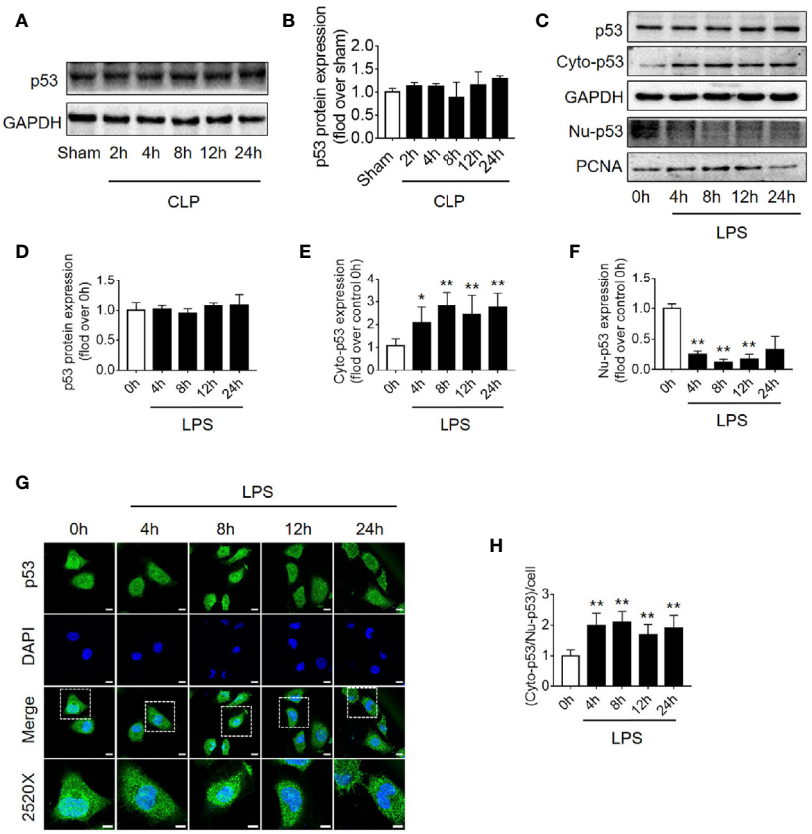

FIGURE 4 | p53 protein expression and intracellular distribution. **(A)** Representative western blot showing p53 protein levels in the renal cortex following CLP-induced sepsis. GAPDH was used as an internal reference. **(B)** Densitometric analyses of p53 protein expression. n = 3. **(C)** Representative western blot showing p53 protein levels in HK-2 cells following LPS treatment. GAPDH was used as an internal control of p53 total protein and cytoplasmic protein levels, and PCNA was used as an internal control for nuclear proteins. **(D–F)** Densitometric analyses of p53 total protein level, cytoplasmic protein level (cyto-p53), and nuclear protein level (Nu-p53). n = 3-5. $^{*}p < 0.05$, $^{**}p < 0.01$ *vs.* the 0 h group. **(G)** Representative cellular immunofluorescence observation of p53 in the nucleus and cytoplasm after LPS stimulation. p53 was labeled with green fluorescence using FITC, and the nucleus was labeled with blue fluorescence by DAPI. The magnification of the upper panel is 630×, and the magnification of the bottom panel is 2520×. Scale bar, 10 μm. **(H)** The ratio of the fluorescence intensity of cytoplasm p53 to nucleus p53 in each cell. $^{**}p < 0.01$ *vs.* the 0 h group. Results represent at least three independent experiments. CLP, cecal ligation and puncture; GAPDH, glyceraldehyde 3-phosphate dehydrogenase; LPS, lipopolysaccharide; PCNA, proliferating cell nuclear antigen; FITC, fluorescein isothiocyanate; DAPI, 4',6-diamadino-2-phenylindole.

the expression of total p53 and the translocation of p53 from nucleus to cytoplasm, but significantly reduced the level of acetyl-p53 (K382) in HK-2 cells challenged with LPS for 12 h (**Figures 7B–D** and **Supplementary Figures 4D–F**). By contrast, siRNA-mediated Sirt1 knockout aggravated p53 acetylation but did not affect p53 protein expression (**Figures 8B–D**). Moreover, Sirt1 overexpression elevated the numbers of both autophagosomes and autolysosomes (**Figures 7E–G**), whereas Sirt1 knockout attenuated the formation of autophagosomes and autolysosomes (**Figures 8E–G**). These results indicated that Sirt1-induced deacetylation of p53 was able to enhance RTEC autophagy.

Two Sirt1 chemical agonists, RSV and QCT, were then applied to clarify the effects of Sirt1 activation on acetylation of p53 and RTEC autophagy (24). First, we verified that both RSV and QCT could reduce the acetylation level of p53 at lysine 379 (**Supplementary Figures 5A–F**). Then we found that RSV administration promoted the autophagy of RTECs, as determined by an observed increase in autophagosomes (**Figures 9A, B**). Consistently, QCT administration increased the protein expression of LC3II, but decreased the protein expression of p62 (**Supplementary Figures 5G–I**). Moreover, RSV attenuated pathological renal damage (**Figure 9C**), resulted in a reduced renal tubular damage score (**Figures 9D, E**), and partially reduced the levels of KIM-1 (**Figures 9C, F**) and sCr (**Figure 9G**). QCT also attenuated pathological kidney damage (**Supplementary Figures 2D–F**). In addition, RSV administration prolonged the survival times of CLP mice (**Figure 9H**).

p53 Interacted With Beclin1 and Acetylated p53 Promoted Ubiquitination of Beclin1

Beclin1 is a well-known key regulator of autophagy. Our previous studies have shown that the protein level of Beclin1 is reduced in the late stage of SAKI (15), so we supposed that

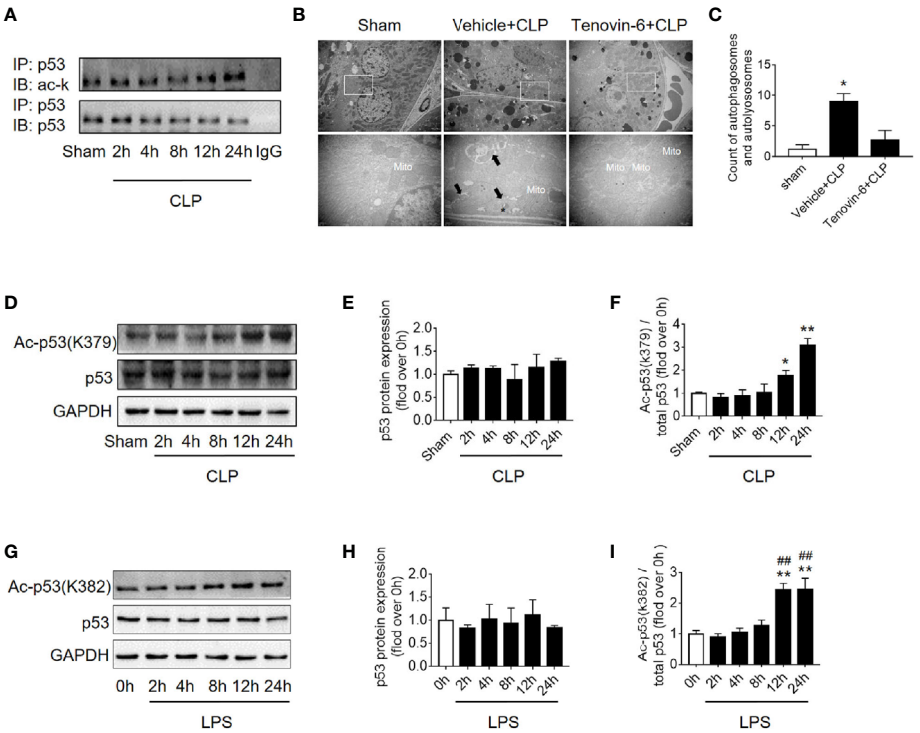

FIGURE 5 | p53 acetylation following CLP/LPS-induced sepsis. **(A)** Protein expression and acetylation levels of p53 based on p53 immunoprecipitation (IP) from the kidney cortex of CLP-induced septic mice. IB, immunoblotting; ac, acetylation. **(B)** p53 activation of autophagy in the renal cortex of CLP-induced septic mice. Tenovin-6 was used to upregulate p53 acetylation. Black thick arrows: autophagosomes or autolysosomes; Mito: mitochondria; upper panel: magnified ×7,000; lower panel: magnified ×40,000. **(C)** Semi-quantitative analysis of autophagy. The numbers of autophagosomes and autolysosomes in renal epithelial cells were calculated in 20 randomly selected fields. $^{*}p < 0.05$ *vs.* sham group. **(D)** Levels of total protein expression and acetylated p53 (ac-p53) at lysine site K379 in the kidney cortex of CLP-induced septic mice. **(E, F)** Densitometric analyses of the levels of p53 protein expression and acetylation (ac-p53) at lysine site of K379 in the kidney cortex of CLP-induced septic mice. $^{*}p < 0.05$, $^{**}p < 0.01$ *vs.* sham group; n = 3-4. **(G)** Levels of total protein expression and acetylated p53 (ac-p53) at lysine site K382 in LPS-induced HK-2 cells. **(H, I)** Densitometric analyses of the levels of p53 protein expression and acetylation at lysine site K382 in LPS-induced HK-2 cells. $^{**}p < 0.01$ *vs.* the 0 h group; $^{\#\#}p < 0.01$ *vs.* the 8 h group; n = 4. CLP, cecal ligation and puncture; LPS, lipopolysaccharide.

acetylated p53 might regulate autophagy through Beclin1. The interaction of p53 and Beclin1 was first confirmed in our study (**Figure 10A**) and then we found that transfection of p53 K382R mutant virus significantly reduced the ubiquitination of Beclin1 in HK-2 cells (**Figure 10B**). These results suggested that acetylated p53 suppressed the autophagy by promoting the ubiquitination-mediated degradation of Beclin1.

DISCUSSION

In this study, we found that increased levels of p53 acetylation suppressed RTEC autophagy after sepsis. The activation of autophagy, which was induced by p53 following deacetylation by Sirt1, was able to reduce SAKI (**Figure 11**). Our study provides a new perspective for elucidating the underlying mechanisms of SAKI, indicating a possible avenue for intervention and identifying a future drug target.

Autophagy, another type of programmed cell death different from apoptosis, occurs in all eukaryotic cells and contributes to the renewal and reuse of cellular components and energy homeostasis (25). The process of autophagy is complex, and its hallmark is the formation of autophagosomes and autophagolysosomes. During this process, autophagy-related proteins such as Beclin1 and LC3 both increase, while the autophagy cargo receptor protein p62 decreases (26). A previous study demonstrated that the LIR domain enables p62 to combine with LC3II, and the UBA domain enables p62 to bind to ubiquitin; consequently, ubiquitinated proteins may be degraded by autophagy. In SAKI, excessive accumulation of p62 is able to promote apoptosis, to enhance the release of the toxic substance LDH, and to inhibit the proliferation of RTECs (21). Different from the final result of cell death caused by apoptosis, activated autophagy plays a renal protective role by preventing apoptosis, preserving the mitochondrial functions, and maintaining the balance between the productions of pro- and anti-inflammatory cytokines (22). Our previous research has confirmed the above phenomena and verified that autophagy activation could reduce SAKI (15). The role of p53 in SAKI is rarely reported, although previous studies have explored the damaging role of p53 in bilateral renal ischemia-reperfusion induced AKI and cisplatin nephrotoxic AKI (27, 28).

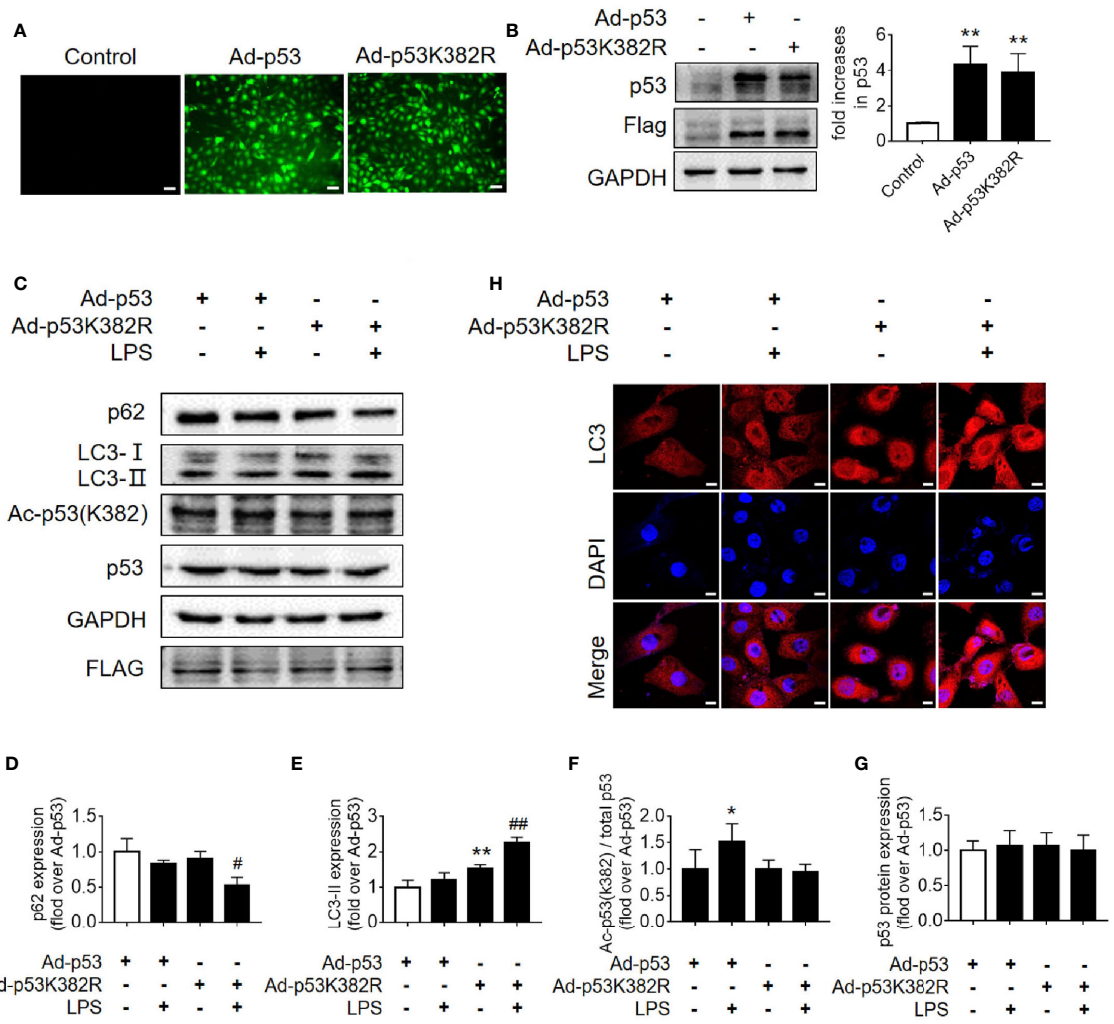

FIGURE 6 | Mutation of p53 (K382 lysine site) mediated-p53 deacetylation promotes autophagy. **(A)** Confirmation of the effect of p53 virus transfection. HK-2 cells were transfected with either p53 adenovirus (Ad-p53) or p53K382R adenovirus (Ad-p53K382R). Deacetylation of p53 was induced by the mutation of lysine (K) at 382 to arginine (R). **(B)** Representative western blot and densitometric analyses of p53 protein expression. n = 3. $^{**}p < 0.01$ *vs.* Control group. **(C)** Representative western blot of p62, LC3-I, LC3-II, acetylated p53 (Ac-p53), and p53. GAPDH was used as an internal reference. **(D–G)** Densitometric analyses of p62, LC3-I, LC3-II, acetylated p53 (Ac-p53), and p53. n = 3-4. $^{*}p < 0.05$, $^{**}p < 0.01$ *vs.* the Ad-p53 group; $^{\#}p < 0.05$, $^{\#\#}p < 0.01$ *vs.* the Ad-p53 + LPS group. **(H)** Effects of the p53 point mutation on autophagy protein LC3 under cellular immunofluorescence (magnification ×630 and scale bar = 10 μm). LC3 is labeled with red fluorescence of GRF, and the nucleus is labeled with the blue fluorescence of DAPI. The brightness of red represents the abundance of LC3 protein. LC3II, Microtubule-associated protein 1A/1B-light chain 3; GAPDH, glyceraldehyde 3-phosphate dehydrogenase; LPS, lipopolysaccharide; DAPI, 4', 6-diamadino-2-phenylindole.

Other literature has suggested that acetylated p53 may cause damage to myocardial cells (29), liver cells (30), and neurons (31) under septic conditions by promoting apoptosis. Garrison et al. (32) suggested that p53 mediates apoptosis to optimize the neutrophil lifespan and ensure the proper clearance of bacteria, presenting a counter-balance between the innate immune response to infection and survival following DNA damage. Our research confirmed that the acetylation of p53 in RTECs aggravated SAKI. Histological examination found that RTEC is less likely to undergo apoptosis and necrosis during the development of SAKI (33, 34). In consistent with this finding, we found that p53 might not act through the apoptotic pathway but rather acts through the inhibition of autophagy during the pathogenesis of SAKI. Our results revealed particularly significant inhibition of autophagy 12 h after CLP, indicating that the influence of p53 on the development of SAKI might rely on the regulation of autophagy rather than the promotion of apoptosis, which represents the largest innovation of this research to the understanding of the mechanisms that drive SAKI.

Interestingly, a large body of previous literature (30, 35, 36) and our own previous studies (4, 10, 11) have shown that an increase in p53 activity may be related to the modification of its acetylation swfi 2tatus. Acetylated p53 can be deacetylated by various deacetylases, such as histone deacetylase-1 (HDAC1),

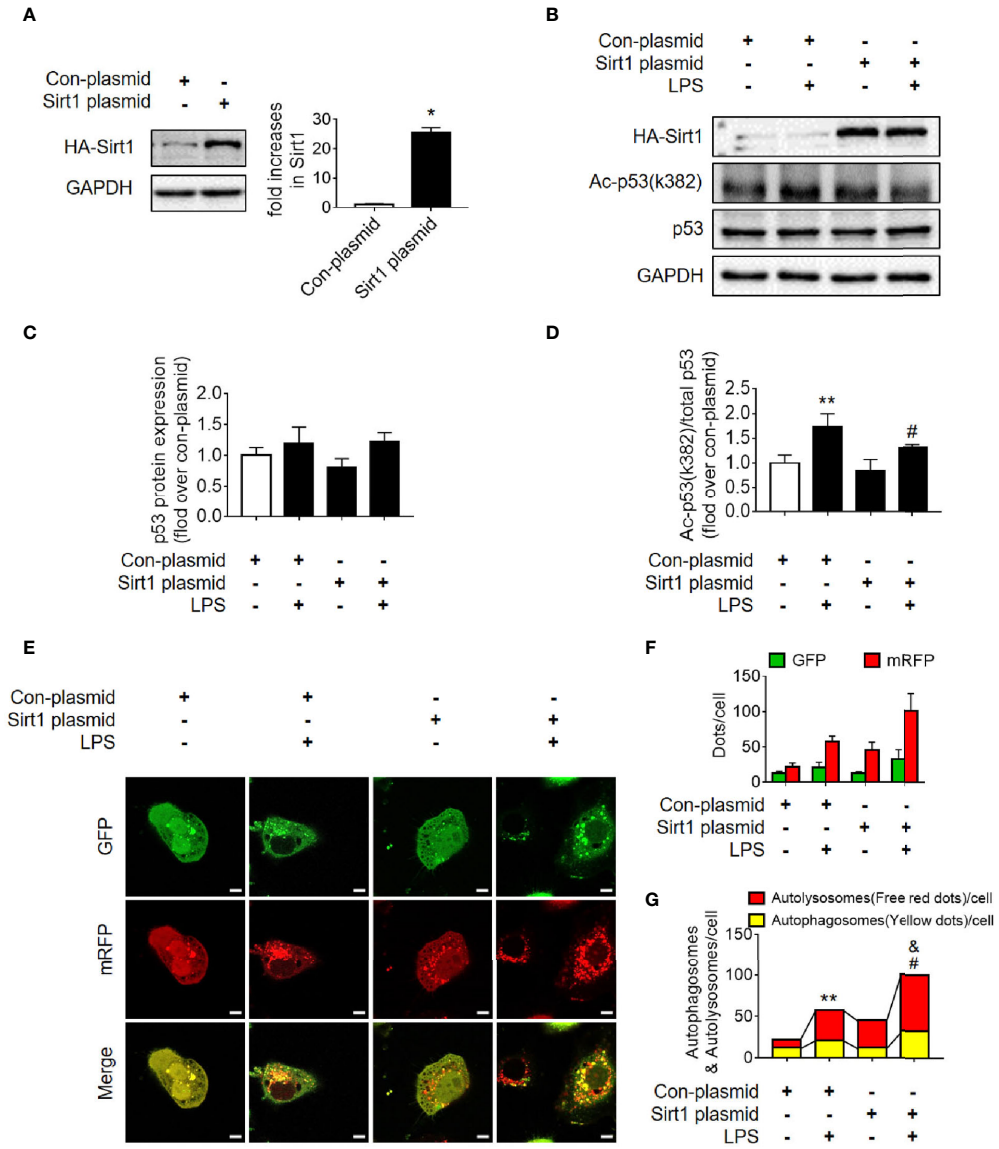

FIGURE 7 | Determination of the effects of Sirt1 plasmid transfection. **(A)** Confirmation of plasmid-induced Sirt1 overexpression using western blot. Con-plasmid, control plasmid. **(B)** Representative western blot of HA-Sirt1, acetylated-p53 (Ac-p53), and p53 in LPS-treated HK-2 cells. **(C, D)** Densitometric analyses of p53 protein expression and acetylated-p53 (Ac-p53). n = 3-4. **(E)** Effects of Sirt1 overexpression on autophagic flux based on the cellular immunoassay following LPS stimulation at different groups (magnification ×630 and scale bar = 10 μm). **(F)** Effects of Sirt1 overexpression on GFP and mRFP counts per cell. **(G)** Effects of Sirt1 overexpression on autophagosomes and autolysosomes per cell. $^{*}p < 0.05$, $^{**}p < 0.01$ *vs.* con-plasmid group; $^{\#}p < 0.05$ *vs.* con-plasmid + LPS group; $^{\&}p < 0.05$ *vs.* the Sirt1 plasmid group. The results are representative of at least three independent experiments. LPS, lipopolysaccharide; GFP, green fluorescent protein; mRFP, monomeric red fluorescent protein.

HDAC6 and Sirt1. In research mainly related to tumors, it has been reported that HDAC1 and HDAC6 could deacetylate p53, leading to the repression of p53-dependent transcriptional activation, cell growth arrest, as well as apoptosis (37–39). The role of p53 in sepsis depends on its acetylation/deacetylation modifications, which is primarily regulated by the newly identified deacetylation modification enzyme Sirt1. Sirt1 is a nicotinamide adenine dinucleotide (NAD+) dependent protein deacetylase, which was originally found to regulate apoptosis and DNA repair, which affects longevity (40). Sirt1 deacetylates both histones and other non-histone proteins (10). Our previous studies have demonstrated that Sirt1 can improve SAKI by deacetylating Beclin1, which mediates autophagy activation (15). The first non-histone target that was identified for Sirt1 activity was p53. Our previous study revealed that Sirt1 protein expression also decreased gradually following sepsis (41), which should be the cause of p53 acetylation in this study. Present study further emphasized the role of p53 deacetylation in autophagy

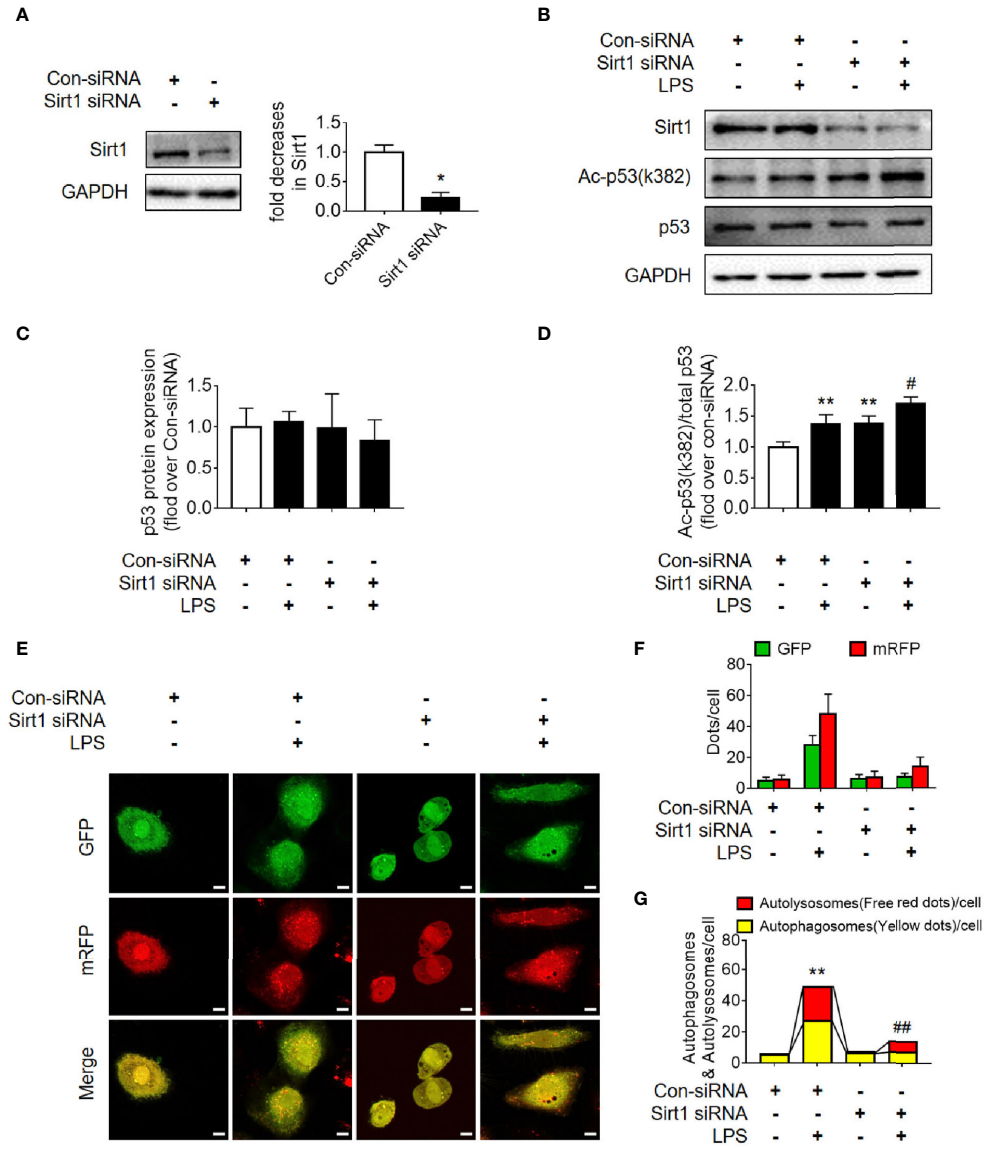

FIGURE 8 | Determination of the effects of Sirt1 small interfering RNA (siRNA) transfection. **(A)** Confirmation of siRNA-mediated Sirt1 knockdown using western blot. Con-siRNA, control siRNA. **(B)** Representative Western blot of Sirt1, acetylated-p53 (Ac-p53), and p53 in LPS-treated HK-2 cells. **(C, D)** Densitometric analyses of p53 protein expression and acetylated-p53 (Ac-p53). n = 3. **(E)** Effects of Sirt1 knockdown on autophagic flux assessed by cellular immunoassay following LPS stimulation in different groups (magnification ×630 and scale bar = 10 μm). **(F)** Effect of Sirt1 knockdown on the numbers of GFP and mRFP counts per cell. **(G)** Effect of Sirt1 knockdown on autophagosomes and autolysosomes per cell. $^{*}p < 0.05$, $^{**}p < 0.01$ *vs.* con-siRNA group; $^{\#}p < 0.05$, $^{\#\#}p < 0.01$ *vs.* con-siRNA + LPS group. Results represent at least three independent experiments. LPS, lipopolysaccharide; GFP, green fluorescent protein; mRFP, monomeric red fluorescent protein.

activation and provided an experimental basis for the more precise exploration of p53 deacetylation modifications (the non-Sirt1-mediated broad-spectrum deacetylation) as potential future treatments for SAKI.

Previous studies have shown that the regulatory effects of p53 on autophagy are closely related to the intracellular distribution of p53. Nuclear p53 transactivates a large set of target genes involved in the autophagic process, including AMP-activated protein kinase (AMPK) (6, 42). In a rat AKI model, induced by ischemia-reperfusion injury, the nuclear p53 localization in renal tubular cells was demonstrated to promote autophagy (43). However, cytosolic p53 may have an anti-autophagic function (44). In many studies (45–47), cytosolic p53 inhibited mitophagy (a common form of autophagy) by disturbing the mitochondrial translocation of Parkin. In this study, we found that although the total protein expression level of p53 did not change significantly during the early stages of SAKI, the nuclear to cytoplasmic translocation of p53 increased prior to the observed inhibition of autophagy. We also found that, coincident with the translocation of p53 out of nucleus, the mRNA levels of p53

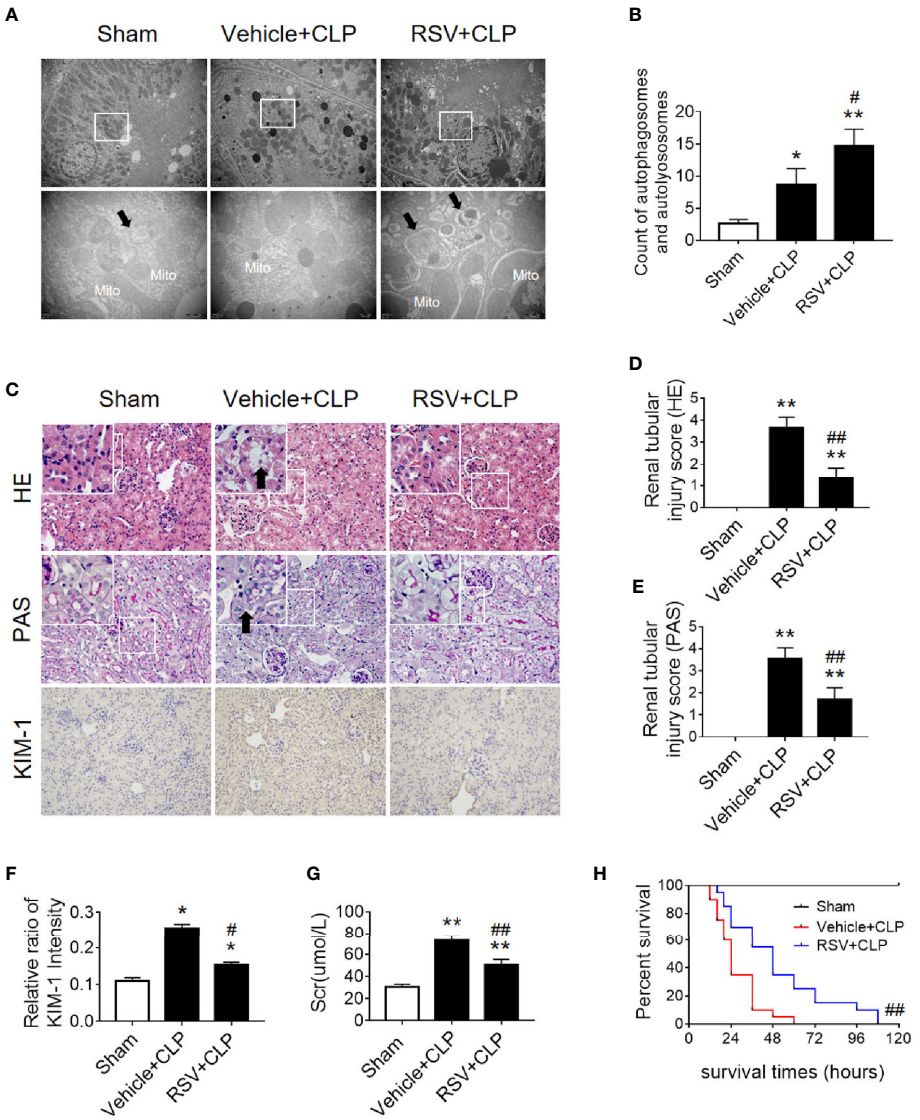

FIGURE 9 | Activation of the deacetylase Sirt1 by RSV promotes autophagy and reduces SAKI. **(A)** Effect of Sirt1 activation by RSV on autophagy in the renal cortex of CLP-induced septic mice. Black thick arrows: autophagosomes or autolysosomes; Mito, mitochondria. Upper panel: magnified ×7,000; lower panel: magnified ×40,000. **(B)** Semi-quantitative analysis of autophagy. The number of autophagosomes and autolysosomes in renal epithelial cells was calculated in 20 randomly selected fields. **(C)** Effects of Sirt1 activation by RSV on kidney pathology, as evidenced by HE staining, PAS staining, and KIM-1 immunohistochemistry. Upper Panel: Hematoxylin-Eosin (HE) staining (200×; inset: 400×); Middle panel: periodic acid-Schiff (PAS) staining (200×; inset: 400×). Black thick arrows: Nucleus of RTECs shed to lumen; Lower panel: KIM-1 immunohistochemistry (200×). **(D, E)** The tubular damage score was evaluated based on pathological observations from HE and PAS staining. These scores are based on the data obtained from the observation of 5 specimens in each group with 10 randomly selected fields of view from a 200× microscope for each specimen. **(F)** Relative ratio of kidney injury molecule-1 (KIM-1). The data were obtained from at least three independent experiments. **(G)** Effect of Sirt1 activation by RSV on the level of sCr. **(H)** Effects of Sirt1 activation by RSV on the survival times in CLP-induced septic mice. The survival rates were estimated by the Kaplan-Meier method and compared by the log-rank test. n = 20. $^{*}p < 0.05$, $^{**}p < 0.01$ *vs.* sham group; $^{\#}p < 0.05$, $^{\#\#}p < 0.01$ *vs.* the vehicle + CLP group. CLP, cecal ligation and puncture; RTEC, renal tubule epithelial cell.

target genes ATG2A, ATG4B, BAX, PIG3A and NOXA1 decreased, while the mRNA levels of ATG2B, DRAM1, UVRAG and TSC2 did not change significantly. In addition, the interaction of p53 and Beclin1 has also been confirmed in this study. In HK-2 cells stimulated by LPS for 12 h, wild-type p53 virus significantly ubiquitinated Beclin1, while p53K382R mutant virus reduced the ubiquitination of Beclin1. Therefore we speculated that acetylated p53 promoted the proteasomal degradation of Beclin1, leading to the suppression of autophagy in HK-2 cells. This result also provides another pathway or mechanism for the effect of Sirt1, showing that the Sirt1-induced alteration of p53 acetylation status might also in turn affect the activity of Beclin1 and then autophagy. In fact, previous studies have proved that p53 and beclin-1 interact through the BH3 domain of

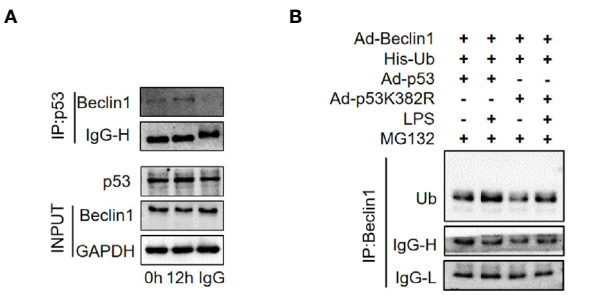

FIGURE 10 | The interaction of p53 and Beclin1 in HK-2 cells. **(A)** Association of Beclin1 with p53 in the HK-2 cells. The interaction between p53 and Beclin1 was determined by Co- immunoprecipitation assays. **(B)** Determination of the ubiquitination of Beclin1. Ad-Beclin1 and His-tagged ubiquitin protein and Ad-p53 or Ad-p53K382R were individually transfected into HK-2 cells with or without LPS stimulation. LPS, lipopolysaccharide.

beclin-1, and the cytoplasm is the main site of interaction (48). However, the mechanism underlying the translocation of p53 from nuclear to cytoplasmic remains unclear, and this will also be an important direction for future research.

In this study, we applied RSV and QCT to activate Sirt1 to deacetylate p53. The administration of RSV and QCT both promoted the autophagy of RTECs and attenuated pathological renal damage in septic model. It is noticed that because of the persistent presence of CLP-induced infection in mice (feces in the abdominal cavity were not cleared or the intestinal contents may continue to drain into the abdominal cavity), the mice eventually die. Therefore, the administration of RSV only prolonged the survival time of CLP mice, which is consistent with other studies (49, 50).

Our research has some limitations. First, the regulatory mechanism underlying the p53 nuclear to cytoplasmic translocation process has not yet been studied. Second, the index in this study did not involve apoptosis, especially the p53-related apoptosis pathways. Instead, we focused on the mechanism through which p53 acetylation/deacetylation regulates autophagy. Third, a more precise study of the effect of p53 acetylation on autophagy by transfection of adenovirus will help increase the depth and credibility of our research and the observation time could be extended (such as more than 24 h or even longer). Moreover, we also need to consider the use of p53 virus or recombinant protein in septic mice model.

In conclusion, our study found that p53 acetylation-mediated autophagy inhibition underlies the pathogenesis of SAKI. We demonstrated that Sirt1 upregulation could reduce SAKI by deacetylating p53 to activate autophagy, and Sirt1 activators, such as resveratrol or quercetin, might have potential to be developed into a SAKI treatment in the future.

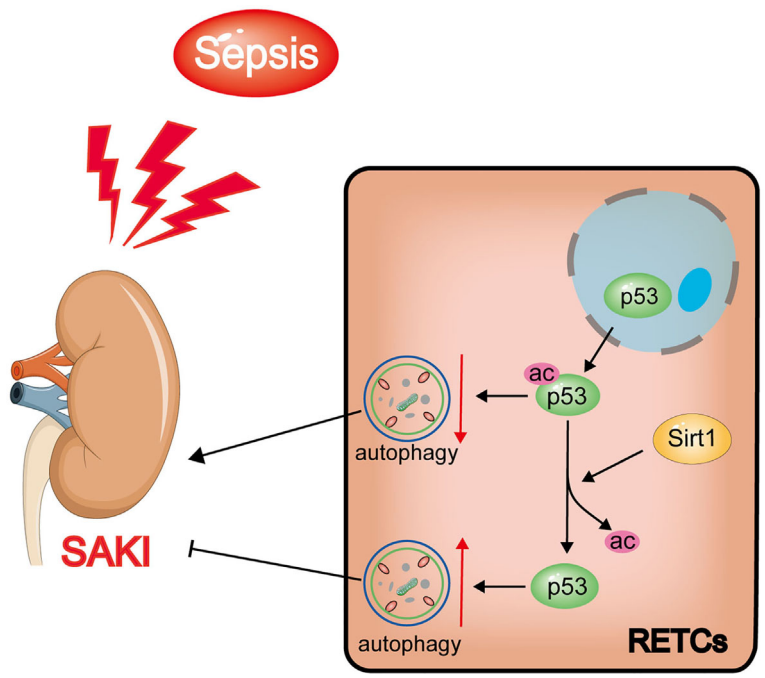

FIGURE 11 | Schematic diagram showing the effects of Sirt1-induced p53 deacetylation on autophagy activation in septic-associated acute kidney injury (SAKI). The p53 total protein expression does not change significantly, but the nuclear to cytoplasmic translocation and acetylation increased in renal tubular epithelial cells (RTECs) following sepsis. The elevated acetylation of p53 promotes autophagy inhibition and aggravates SAKI. The deacetylation of p53 induced by Sirt1 can attenuate this process to a certain extent.

DATA AVAILABILITY STATEMENT

The original contributions presented in the study are included in the article/**Supplementary Material**. Further inquiries can be directed to the corresponding authors.

ETHICS STATEMENT

The animal study was reviewed and approved by Committee on Ethics in Animal Experiments of Southern Medical University.

AUTHOR CONTRIBUTIONS

ZC, QH, and ZZ prepared the concept and designed the research. MS, JL, LM, JW, ZD, MH, and SA performed the experiments. ZC, ZZ, and MS analyzed data. MS and JL prepared the figures. MS, LM, ZZ, and QH interpreted the results of experiments. MS and JL drafted the paper. ZC, QH, and ZZ edited and revised the paper. MS and JL contributed equally to this paper. All authors contributed to the article and approved the submitted version.

FUNDING

This work was supported by the National Natural Science Foundation of China [grant numbers 81701955, 81871604 and 81870210], the Natural Science Foundation of Guangdong Province, China [grant numbers 2020A151501361 and 2017A030313590], and the Guangdong Basic and Applied Basic Research Foundation [grant number 2019A1515012022].

SUPPLEMENTARY MATERIAL

The Supplementary Material for this article can be found online at: https://www.frontiersin.org/articles/10.3389/fimmu.2021.685523/full#supplementary-material

REFERENCES

1. Singer M, Deutschman CS, Seymour CW, Shankar-Hari M, Annane D, Bauer M, et al. The Third International Consensus Definitions for Sepsis and Septic Shock (Sepsis-3). *Jama* (2016) 315:801–10. doi: 10.1001/jama.2016.0287
2. Poston JT, Koyner JL. Sepsis Associated Acute Kidney Injury. *BMJ (Clinical Res ed)* (2019) 364:k4891. doi: 10.1136/bmj.k4891
3. Bellomo R, Kellum JA, Ronco C, Wald R, Martensson J, Maiden M, et al. Acute Kidney Injury in Sepsis. *Intensive Care Med* (2017) 43:816–28. doi: 10.1007/s00134-017-4755-7
4. Xu S, Gao Y, Zhang Q, Wei S, Chen Z, Dai X, et al. SIRT1/3 Activation by Resveratrol Attenuates Acute Kidney Injury in a Septic Rat Model. *Oxid Med And Cell Longevity* (2016) 2016:7296092. doi: 10.1155/2016/7296092
5. Kruiswijk F, Labuschagne CF, Vousden KH. P53 in Survival, Death and Metabolic Health: A Lifeguard With a Licence to Kill. *Nat Rev Mol Cell Biol* (2015) 16:393–405. doi: 10.1038/nrm4007
6. Tang C, Ma Z, Zhu J, Liu Z, Liu Y, Liu Y, et al. P53 in Kidney Injury and Repair: Mechanism and Therapeutic Potentials. *Pharmacol Ther* (2019) 195:5–12. doi: 10.1016/j.pharmthera.2018.10.013
7. Molitoris BA, Dagher PC, Sandoval RM, Campos SB, Ashush H, Fridman E, et al. siRNA Targeted to P53 Attenuates Ischemic and Cisplatin-Induced Acute Kidney Injury. *J Am Soc Nephrol JASN* (2009) 20:1754–64. doi: 10.1681/ASN.2008111204
8. Sutton TA, Hato T, Mai E, Yoshimoto M, Kuehl S, Anderson M, et al. P53 Is Renoprotective After Ischemic Kidney Injury by Reducing Inflammation. *J Am Soc Nephrol JASN* (2013) 24:113–24. doi: 10.1681/ASN.2012050469
9. Zhao W, Zhang L, Chen R, Lu H, Sui M, Zhu Y, et al. SIRT3 Protects Against Acute Kidney Injury via AMPK/mTOR-Regulated Autophagy. *Front Physiol* (2018) 9:1526. doi: 10.3389/fphys.2018.01526
10. Zeng Z, Chen Z, Xu S, Zhang Q, Wang X, Gao Y, et al. Polydatin Protecting Kidneys Against Hemorrhagic Shock-Induced Mitochondrial Dysfunction via SIRT1 Activation and P53 Deacetylation. *Oxid Med Cell Longevity* (2016) 2016:1737185. doi: 10.1155/2016/1737185
11. Zhang W, Zhang Y, Guo X, Zeng Z, Wu J, Liu Y, et al. Sirt1 Protects Endothelial Cells Against LPS-Induced Barrier Dysfunction. *Oxid Med Cell Longevity* (2017) 2017:4082102. doi: 10.1155/2017/4082102
12. Wang Y, Quan F, Cao Q, Lin Y, Yue C, Bi R, et al. Quercetin Alleviates Acute Kidney Injury by Inhibiting Ferroptosis. *J Advanced Res* (2021) 28:231–43. doi: 10.1016/j.jare.2020.07.007
13. Yang M, Cao L, Xie M, Yu Y, Kang R, Yang L, et al. Chloroquine Inhibits HMGB1 Inflammatory Signaling and Protects Mice From Lethal Sepsis. *Biochem Pharmacol* (2013) 86:410–8. doi: 10.1016/j.bcp.2013.05.013
14. Singh D, Chander V, Chopra K. The Effect of Quercetin, a Bioflavonoid on Ischemia/Reperfusion Induced Renal Injury in Rats. *Arch Med Res* (2004) 35:484–94. doi: 10.1016/j.arcmed.2004.10.004
15. Deng Z, Sun M, Wu J, Fang H, Cai S, An S, et al. SIRT1 Attenuates Sepsis-Induced Acute Kidney Injury via Beclin1 Deacetylation-Mediated Autophagy Activation. *Cell Death Dis* (2021) 12:217. doi: 10.1038/s41419-021-03508-y
16. Wei S, Gao Y, Dai X, Fu W, Cai S, Fang H, et al. SIRT1-Mediated HMGB1 Deacetylation Suppresses Sepsis-Associated Acute Kidney Injury. *Am J Physiol Renal Physiol* (2019) 316:F20–f31. doi: 10.1152/ajprenal.00119.2018
17. Wu J, Deng Z, Sun M, Zhang W, Yang Y, Zeng Z, et al. Polydatin Protects Against Lipopolysaccharide-Induced Endothelial Barrier Disruption via SIRT3 Activation. *Lab Investigation; A J Tech Methods Pathol* (2020) 100:643–56. doi: 10.1038/s41374-019-0332-8
18. Zhao X, Qiu X, Zhang Y, Zhang S, Gu X, Guo H. Three-Dimensional Aggregates Enhance the Therapeutic Effects of Adipose Mesenchymal Stem Cells for Ischemia-Reperfusion Induced Kidney Injury in Rats. *Stem Cells Int* (2016) 2016:9062638. doi: 10.1155/2016/9062638
19. Jiang Y, Zeng Y, Huang X, Qin Y, Luo W, Xiang S, et al. Nur77 Attenuates Endothelin-1 Expression via Downregulation of NF-κb and P38 MAPK in A549 Cells and in an ARDS Rat Model. *Am J Of Physiol Lung Cell Mol Physiol* (2016) 311:L1023–l1035. doi: 10.1152/ajplung.00043.2016
20. Krummel KA, Lee CJ, Toledo and G.M. Wahl F. The C-Terminal Lysines Fine-Tune P53 Stress Responses in a Mouse Model But Are Not Required for Stability Control or Transactivation. *Proc Natl Acad Sci USA* (2005) 102:10188–93. doi: 10.1073/pnas.0503068102
21. Li T, Zhao J, Miao S, Xu Y, Xiao X, Liu Y. Dynamic Expression and Roles of Sequestome−1/P62 in LPS−induced Acute Kidney Injury in Mice. *Mol Med Rep* (2018) 17:7618–26. doi: 10.3892/mmr.2018.8809
22. Dai XG, Xu W, Li T, Lu JY, Yang Y, Li Q, et al. Involvement of Phosphatase and Tensin Homolog-Induced Putative Kinase 1-Parkin-Mediated Mitophagy in Septic Acute Kidney Injury. *Chin Med J* (2019) 132:2340–7. doi: 10.1097/CM9.0000000000000448
23. Vaziri H, Dessain SK, Ng Eaton E, Imai SI, Frye RA, Pandita TK, et al. Hsir2 (SIRT1) Functions as an NAD-Dependent P53 Deacetylase. *Cell* (2001) 107:149–59. doi: 10.1016/S0092-8674(01)00527-X
24. Wang D, He X, Wang D, Peng P, Xu X, Gao B, et al. Quercetin Suppresses Apoptosis and Attenuates Intervertebral Disc Degeneration via the SIRT1-Autophagy Pathway. *Front In Cell Dev Biol* (2020) 8:613006. doi: 10.3389/fcell.2020.613006

25. Cuervo AM, Bergamini E, Brunk UT, Dröge W, Ffrench M, Terman A. Autophagy and Aging: The Importance of Maintaining "Clean" Cells. *Autophagy* (2005) 1:131–40. doi: 10.4161/auto.1.3.2017
26. Kaushal GP, Shah SV. Autophagy in Acute Kidney Injury. *Kidney Int* (2016) 89:779–91. doi: 10.1016/j.kint.2015.11.021
27. Cao JY, Wang B, Tang TT, Wen Y, Li ZL, Feng ST, et al. Exosomal miR-125b-5p Deriving From Mesenchymal Stem Cells Promotes Tubular Repair by Suppression of P53 in Ischemic Acute Kidney Injury. *Theranostics* (2021) 11:5248–66. doi: 10.7150/thno.54550
28. Yang A, Liu F, Guan B, Luo Z, Lin J, Fang W, et al. P53 Induces miR-199a-3p to Suppress Mechanistic Target of Rapamycin Activation in Cisplatin-Induced Acute Kidney Injury. *J Cell Biochem* (2019) 120:17625–34. doi: 10.1002/jcb.29030
29. Han D, Li X, Li S, Su T, Fan L, Fan WS, et al. Reduced Silent Information Regulator 1 Signaling Exacerbates Sepsis-Induced Myocardial Injury and Mitigates the Protective Effect of a Liver X Receptor Agonist. *Free Radical Biol Med* (2017) 113:291–303. doi: 10.1016/j.freeradbiomed.2017.10.005
30. Lee Y, Jeong GS, Kim KM, Lee W, Bae JS. Cudratricusxanthone A Attenuates Sepsis-Induced Liver Injury via SIRT1 Signaling. *J Cell Physiol* (2018) 233:5441–6. doi: 10.1002/jcp.26390
31. Zhao L, An R, Yang Y, Yang X, Liu H, Yue L, et al. Melatonin Alleviates Brain Injury in Mice Subjected to Cecal Ligation and Puncture via Attenuating Inflammation, Apoptosis, and Oxidative Stress: The Role of SIRT1 Signaling. *J Pineal Res* (2015) 59:230–9. doi: 10.1111/jpi.12254
32. Garrison SP, Thornton JA, Häcker H, Webby R, Rehg JE, Parganas E, et al. The P53-Target Gene Puma Drives Neutrophil-Mediated Protection Against Lethal Bacterial Sepsis. *PloS Pathog* (2010) 6:e1001240. doi: 10.1371/journal.ppat.1001240
33. Gomez H, Ince C, De Backer D, Pickkers P, Payen D, Hotchkiss J, et al. A Unified Theory of Sepsis-Induced Acute Kidney Injury: Inflammation, Microcirculatory Dysfunction, Bioenergetics, and the Tubular Cell Adaptation to Injury. *Shock (Augusta Ga)* (2014) 41:3–11. doi: 10.1097/SHK.0000000000000052
34. Hotchkiss RS, Karl IE. The Pathophysiology and Treatment of Sepsis. *New Engl J Med* (2003) 348:138–50. doi: 10.1056/NEJMra021333
35. Ma H, Wang X, Ha T, Gao M, Liu L, Wang R, et al. MicroRNA-125b Prevents Cardiac Dysfunction in Polymicrobial Sepsis by Targeting TRAF6-Mediated Nuclear Factor κb Activation and P53-Mediated Apoptotic Signaling. *J Infect Dis* (2016) 214:1773–83. doi: 10.1093/infdis/jiw449
36. Zhang H, Xu CF, Ren C, Wu TT, Dong N, Yao YM. Novel Role of P53 in Septic Immunosuppression: Involvement in Loss and Dysfunction of CD4+ T Lymphocytes. *Cell Physiol Biochem Int J Exp Cell Physiol Biochem Pharmacol* (2018) 51:452–69. doi: 10.1159/000495241
37. Ryu HW, Shin DH, Lee DH, Choi J, Han G, Lee KY, et al. HDAC6 Deacetylates P53 at Lysines 381/382 and Differentially Coordinates P53-Induced Apoptosis. *Cancer Lett* (2017) 391:162–71. doi: 10.1016/j.canlet.2017.01.033
38. Liu Y, Tavana O, Gu W. P53 Modifications: Exquisite Decorations of the Powerful Guardian. *J Mol Cell Biol* (2019) 11:564–77. doi: 10.1093/jmcb/mjz060
39. Yoshida M, Furumai R, Nishiyama M, Komatsu Y, Nishino N, Horinouchi S. Histone Deacetylase as a New Target for Cancer Chemotherapy. *Cancer Chemother Pharmacol* (2001) 48 Suppl 1:S20–6. doi: 10.1007/s002800100300
40. van Leeuwen I, Lain S. Sirtuins and P53. *Adv Cancer Res* (2009) 102:171–95. doi: 10.1016/S0065-230X(09)02005-3
41. Xu SQ, lI LL, Wu J, An S, Fang HH, Han YY, et al. Melatonin Attenuates Sepsis-Induced Small-Intestine Injury by Upregulating SIRT3-Mediated Oxidative-Stress Inhibition, Mitochondrial Protection, and Autophagy Induction. *Front Immunol* (2021) 12:625627. doi: 10.3389/fimmu.2021.625627
42. Li H, Peng X, Wang Y, Cao S, Xiong L, Fan J, et al. Atg5-Mediated Autophagy Deficiency in Proximal Tubules Promotes Cell Cycle G2/M Arrest and Renal Fibrosis. *Autophagy* (2016) 12:1472–86. doi: 10.1080/15548627.2016.1190071
43. Ishihara M, Urushido M, Hamada K, Matsumoto T, Shimamura Y, Ogata K, et al. Sestrin-2 and BNIP3 Regulate Autophagy and Mitophagy in Renal Tubular Cells in Acute Kidney Injury. *Am J Physiol Renal Physiol* (2013) 305:F495–509. doi: 10.1152/ajprenal.00642.2012
44. Tasdemir E, Maiuri MC, Galluzzi L, Vitale I, Djavaheri-Mergny M, D'Amelio M, et al. Regulation of Autophagy by Cytoplasmic P53. *Nat Cell Biol* (2008) 10:676–87. doi: 10.1038/ncb1730
45. Hoshino A, Ariyoshi M, Okawa Y, Kaimoto S, Uchihashi M, Fukai K, et al. Inhibition of P53 Preserves Parkin-Mediated Mitophagy and Pancreatic β-Cell Function in Diabetes. *Proc Natl Acad Sci USA* (2014) 111:3116–21. doi: 10.1073/pnas.1318951111
46. Song YM, Lee WK, Lee YH, Kang ES, Cha BS, Lee BW. Metformin Restores Parkin-Mediated Mitophagy, Suppressed by Cytosolic P53. *Int J Mol Sci* (2016) 17(1):122. doi: 10.3390/ijms17010122
47. Hoshino A, Mita Y, Okawa Y, Ariyoshi M, Iwai-Kanai E, Ueyama T, et al. Cytosolic P53 Inhibits Parkin-Mediated Mitophagy and Promotes Mitochondrial Dysfunction in the Mouse Heart. *Nat Commun* (2013) 4:2308. doi: 10.1038/ncomms3308
48. Tripathi R, Ash D, Shaha C. Beclin-1-P53 Interaction Is Crucial for Cell Fate Determination in Embryonal Carcinoma Cells. *J Cell And Mol Med* (2014) 18:2275–86. doi: 10.1111/jcmm.12386
49. Holthoff JH, Wang Z, Seely KA, Gokden N, Mayeux PR. Resveratrol Improves Renal Microcirculation, Protects the Tubular Epithelium, and Prolongs Survival in a Mouse Model of Sepsis-Induced Acute Kidney Injury. *Kidney Int* (2012) 81:370–8. doi: 10.1038/ki.2011.347
50. Zhang ZS, Zhao HL, Yang GM, Zang JT, Zheng DY, Duan CY, et al. Role of Resveratrol in Protecting Vasodilatation Function in Septic Shock Rats and its Mechanism. *J Trauma Acute Care Surg* (2019) 87:1336–45. doi: 10.1097/TA.0000000000002466

Conflict of Interest: The authors declare that the research was conducted in the absence of any commercial or financial relationships that could be construed as a potential conflict of interest.

frontiers in Immunology

ORIGINAL RESEARCH
published: 20 October 2021
doi: 10.3389/fimmu.2021.697071

Roles of RAGE/ROCK1 Pathway in HMGB1-Induced Early Changes in Barrier Permeability of Human Pulmonary Microvascular Endothelial Cell

Meng-jiao Zhao[1†], Hao-ran Jiang[2†], Jing-wen Sun[3], Zi-ang Wang[1], Bo Hu[1], Cheng-rui Zhu[1], Xiao-han Yin[1], Ming-ming Chen[1], Xiao-chun Ma[1], Wei-dong Zhao[3†] and Zheng-gang Luan[1*†]*

[1] Department of Critical Care Medicine, The First Affiliated Hospital of China Medical University, Shenyang, China, [2] Department of Breast Oncology, The First Affiliated Hospital of China Medical University, Shenyang, China, [3] Department of Developmental Cell Biology, Key Laboratory of Cell Biology, Ministry of Public Health, and Key Laboratory of Medical Cell Biology, Ministry of Education, China Medical University, Shenyang, China

OPEN ACCESS

Edited by:
Venkat Magupalli,
Harvard Medical School, United States

Reviewed by:
Katsuya Hirano,
Kagawa University, Japan
Ritu Mishra,
National Institute of Immunology (NII), India
Felice D'Agnillo,
United States Food and Drug Administration, United States

***Correspondence:**
Zheng-gang Luan
luanzhenggang@sina.com
Wei-dong Zhao
wdzhao@cmu.edu.cn

[†]These authors have contributed equally to this work

Specialty section:
This article was submitted to Inflammation, a section of the journal Frontiers in Immunology

Received: 18 April 2021
Accepted: 01 October 2021
Published: 20 October 2021

Citation:
Zhao M-j, Jiang H-r, Sun J-w, Wang Z-a, Hu B, Zhu C-r, Yin X-h, Chen M-m, Ma X-c, Zhao W-d and Luan Z-g (2021) Roles of RAGE/ROCK1 Pathway in HMGB1-Induced Early Changes in Barrier Permeability of Human Pulmonary Microvascular Endothelial Cell. Front. Immunol. 12:697071. doi: 10.3389/fimmu.2021.697071

Background: High mobility group box 1 (HMGB1) causes microvascular endothelial cell barrier dysfunction during acute lung injury (ALI) in sepsis, but the mechanisms have not been well understood. We studied the roles of RAGE and Rho kinase 1 (ROCK1) in HMGB1-induced human pulmonary endothelial barrier disruption.

Methods: In the present study, the recombinant human high mobility group box 1 (rhHMGB1) was used to stimulate human pulmonary microvascular endothelial cells (HPMECs). The endothelial cell (EC) barrier permeability was examined by detecting FITC-dextran flux. CCK-8 assay was used to detect cell viability under rhHMGB1 treatments. The expression of related molecules involved in RhoA/ROCK1 pathway, phosphorylation of myosin light chain (MLC), F-actin, VE-cadherin and ZO-1 of different treated groups were measured by pull-down assay, western blot and immunofluorescence. Furthermore, we studied the effects of Rho kinase inhibitor (Y-27632), ROCK1/2 siRNA, RAGE-specific blocker (FPS-ZM1) and RAGE siRNA on endothelial barrier properties to elucidate the related mechanisms.

Results: In the present study, we demonstrated that rhHMGB1 induced EC barrier hyperpermeability in a dose-dependent and time-dependent manner by measuring FITC-dextran flux, a reflection of the loss of EC barrier integrity. Moreover, rhHMGB1 induced a dose-dependent and time-dependent increases in paracellular gap formation accompanied by the development of stress fiber rearrangement and disruption of VE-cadherin and ZO-1, a phenotypic change related to increased endothelial contractility and endothelial barrier permeability. Using inhibitors and siRNAs directed against RAGE and ROCK1/2, we systematically determined that RAGE mediated the rhHMGB1-induced stress fiber reorganization *via* RhoA/ROCK1 signaling activation and the subsequent MLC phosphorylation in ECs.

Conclusion: HMGB1 is capable of disrupting the endothelial barrier integrity. This study demonstrates that HMGB1 activates RhoA/ROCK1 pathway *via* RAGE, which phosphorylates MLC inducing stress fiber formation at short time, and HMGB1/RAGE reduces AJ/TJ expression at long term independently of RhoA/ROCK1 signaling pathway.

Keywords: endothelium, high mobility group box 1, barrier permeability, signaling, inflammation

INTRODUCTION

A hallmark of acute lung injury (ALI) is pulmonary edema caused by increased vascular permeability during septic inflammation (1, 2). The pulmonary microvascular endothelial cells play a key effect on maintaining the endothelial barrier integrity between the microvascular lumen and the lung interstitium. EC barrier function depends on the integrity of endothelial cell (EC), the coordinate expression and interplay of proteins in cellular junction complexes, including the F-actin cytoskeleton, adherens junction (AJ) and tight junction (TJ) (3, 4). The barrier hyperpermeability is always related to the cytoskeleton rearrangement of EC and the disruption of AJ and TJ, resulting in EC contraction and intercellular gap formation (5, 6). High mobility group box 1 (HMGB1), a potent proinflammatory cytokine, can disrupt intercellular junctions, increasing endothelial barrier permeability (7, 8). Our previous investigation shows that HMGB1 is involved in the progression of ALI, which has been demonstrated to be associated with microvascular barrier dysfunction elicited by the AJ and TJ disruption (7, 9). Recent studies have indicated that HMGB1 and the receptor for advanced glycation end products (RAGE) conduce to endothelial barrier dysfunction, and RAGE is the primary receptor mediating HMGB1-induced hyperpermeability and paracellular gap formation (10–12). HMGB1 also elicits activation of Rho small GTPases which play important effects on rearranging the F-actin cytoskeleton and the intercellular junctional proteins (13, 14). Rho kinase (ROCK) is a downstream target of RhoA and exists in two similar isoforms: ROCK1 and ROCK2 (15, 16). ROCK activated by the GTP-bound form of Rho can directly phosphorylate myosin light chain (MLC) and reduce the dephosphorylation of phosphorylated MLC (pMLC) (17, 18). ROCK1 and ROCK2 play different functional roles in regulating cytoskeleton arrangement by phosphorylating different downstream proteins (16). The previous studies have demonstrated that ROCK1 was involved in TNFα-induced early endothelial hyperpermeability and ROCK1 induced actin cytoskeletal instability by regulating actomyosin contraction, whereas ROCK2 stabilized the actin cytoskeleton by regulating cofilin phosphorylation (15, 16). To verify the hypothesis that ROCK-dependent cell contraction plays a key role in HMGB1-induced increases in pulmonary microvascular endothelial barrier permeability, we investigated the effects of HMGB1 on the structure and function of endothelial barrier and elucidated the roles of RAGE and ROCK in HMGB1-induced human pulmonary endothelial barrier disruption. Our findings indicated that HMGB1 induced F-actin rearrangement, AJ/TJ rupture, and then enhanced the EC barrier permeability through the RAGE/ROCK1 pathway in the early stage.

Abbreviations: HPMEC, human pulmonary microvascular endothelial cell; HMGB1, high mobility group box 1; ALI, acute lung injury; AJ, adherens junction; TJ, tight junction; VE-cadherin, vascular endothelial cadherin; ZO-1, zonula occludens 1; RAGE, receptor for advanced glycation end products; ROCK, Rho kinase; MLC, myosin light chain; pMLC, phosphorylated MLC; EC, endothelial cell.

METHODS

Reagents

Human pulmonary microvascular endothelial cell (HPMEC) was obtained from Tongpai Biotechnology Co., Ltd (Shanghai, China). Recombinant human HMGB1 (rhHMGB1) was obtained from Shanghai Primegene Bio-Tech Co., Ltd (Shanghai, China). FPS-ZM1 (a high-affinity RAGE-specific inhibitor) was from Sigma-Aldrich (St. Louis, MO, USA). Y-27632 (ROCK inhibitor) was from Selleck Chemicals (Houston, Texas, USA). CCK-8 kit was from Beyotime Technology (Shanghai, China). Fluorescein isothiocyanate-dextran was from Sigma-Aldrich (St. Louis, MO, USA). Phalloidin-iFluor 594 Conjugate was obtained from Absin Bioscience (Shanghai, China). ROCK1/2 siRNA (SC-29473/SC-29474), RAGE siRNA (SC-36374) and negative control siRNA were from Santa Cruz Biotechnology Co., Ltd (Shanghai, China). Lipofectamine® Reagent was employed for siRNA transfection (Paisley, UK). ZO-1 (monoclonal rabbit anti-human, CST 13663S), VE-cadherin (monoclonal rabbit anti-human, CST 2500T), MLC (monoclonal rabbit anti-human, CST 3672), p-MLC (Ser-19, monoclonal rabbit anti-human, CST 3674T) and ROCK1/2 (monoclonal rabbit anti-human, CST 4035/9029) antibodies were obtained from Cell Signaling Technology (CST, Boston, USA). RAGE (polyclonal rabbit anti-human, Cat No. 16346-1-AP) and Tubblin (monoclonal mouse anti-human, Cat No. 66240-1-Ig) antibodies were from Proteintech (North America). RhoA antibody (monoclonal rabbit anti-human, Catalog # 17-294 Lot # DAM1764537) was from Millipore Corporation (Temecula, CA). Rho activation kit was purchased from Upstate Biotechnology (Millipore, Dundee, UK). Anti-mouse and anti-rabbit secondary antibodies conjugated to horse radish peroxidase were purchased from Proteintech (North America). Donkey anti-Rabbit IgG (H+L) Alexa Fluor 488 Highly Cross-Adsorbed Secondary Antibody was from Invitrogen (Carlsbad, USA). Regular Range Prestained Protein Marker was from Proteintech (North America). Enhanced chemiluminescence (ECL) was from Tanon Science & Technology Co. (Shanghai, China).

Cell Culture and Treatments

HPMECs were inoculated in Dulbecco's modified Eagle's culture medium with 10% fetal bovine serum at 37°C and in 5% CO_2. The medium was replaced every 1-2 days. All experiments were conducted in confluent monolayers on the 3rd or 4th day after seeding (passages 5-7). After 24 hours of serum-free culture, the cells were treated with rhHMGB1. rhHMGB1 was trypsinized to abolish the micro-amounts of endotoxin (7). HPMECs were then stimulated with rhHMGB1 at 600 ng/ml for 10 min, 30 min, 1 h, 6 h and 24 h, or treated with rhHMGB1 at 100, 200 and 600 ng/ml for 24 h. In order to detect the toxicity of Y-27632 and FPS-ZM1 to ECs, HPMECs were treated with Y-27632 (5, 10, 15 uM) and FPS-ZM1 (0.01, 0.05, 0.1 uM) for 24 h respectively.

Transfection of siRNA

HPMECs were grown on dishes precoated with 4 g/ml fibronectin. To prepare siRNA-lipofectamine complexes, siRNAs were mixed with lipofectamine reagent diluted in OptiMEM® medium for 5 min at room temperature. ECs at 60-80% confluence were treated for 4 h with 10 nM ROCK1/2 siRNA, 100 nM RAGE siRNA or the corresponding negative control siRNA through adding the siRNA lipofectamine complexes to the ECs in serum-free medium. The transfected cells were then incubated with normal medium at 37°C with 5% CO2 for 48 h.

Cell Viability Assay

Cell viability was examined by CCK-8 measurement. HPMECs were inoculated in 96-well plates. CCK-8 solution (10 μl/well) was added, followed by culture at 37°C for 4 h. The absorbance at 450 nm was detected with a microplate reader (Thermo Labsystems, IL, USA). Cell viability was calculated as a percentage of that of control group.

Measurement of Endothelial Permeability

HPMECs were inoculated on 0.4-um pore Transwell filters. FITC-dextran (MR 40,000; Sigma–Aldrich) was added into the upper chamber at a concentration of 1 mg/ml and equalized for 1h, then the culture medium sample was collected from the lower chamber to detect base permeability. After indicated treatment, the media were taken from the lower chamber. The FITC fluorescence intensity was detected by a fluorescence spectrometer (MV06744, MoleCular Devices, Shanghai). The excitation wavelength was 482 nm and the detection wavelength was 525 nm.

Immunofluorescence

For VE-cadherin and ZO-1 localization, ECs were fixed with ice-cold methanol on chamber slides. Cells were blockaded with serum and treated with primary antibodies (VE-cadherin and ZO-1, 1:200) and Alexa Fluor 488 donkey anti-rabbit antibody (1:200). For F-actin localization, ECs were fixed in 4% paraformaldehyde, permeabilized with 0.1% Triton X-100, blockaded with 5% BSA, and treated with 5 mg/ml of fluorescein isothiocyanate conjugated phalloidin. Confocal laser scanning microscope was used for image acquisition (Zeiss, Germany). The fluorescence intensity of F-actin, VE-cadherin and ZO-1 was quantitatively analyzed by the Image J software (National Institutes of Health, Bethesda, MD, USA).

Western Blot

Protein concentration was measured by the BCA method, and then the samples were titrated to the same concentration. Protein samples (10 μl) were subjected to 10% SDS-PAGE, transferred to a polyvinylidene fluoride membrane, blockaded by 5% BSA at room temperature for 1 h, then treated with primary antibodies (4°C, overnight) followed by incubation with HRP-coupled anti-mouse/rabbit IgG antibody (1:8000 dilution, room temperature, 1 h). Bands were developed with SuperSignalWest Pico Chemiluminescent Substrate and images were captured by Tanon 5200 System (Tanon, Shanghai). Primary antibodies and their dilution ratios applied in this present study were as follows: anti-RhoA (1:2000), anti-ROCK1/2 (1:1000), anti-MLC (1:1000), anti-pMLC (Ser-19, 1:1000), anti-VE-cadherin (1:1000), anti-ZO-1 (1:1000), anti-RAGE (1:800) and anti-tubblin (1:8000). Anti-tubblin protein was determined as an endogenous control for other proteins. At least three different repeats were performed for quantification. Band intensity was normalized by its own endogenous control.

Assessment of Activated RhoA

RhoA activation was determined with a pull-down assay kit in line with the manufacturer's instructions. ECs were lysed with a Triton X-100 lysis buffer. EC lysates were centrifuged at 13,000g at 4°C for 3 min, and equal volumes of lysates were treated with rhotekin-Rho-binding domain-coated agarose beads at 4°C for 1 h, then the beads were washed three times. The content of GTP-RhoA (RhoA associated with the beads) and total RhoA in cell lysates were measured by immunoblot. The activity of RhoA was examined by normalizing the amount of rhotekin-Rho-binding domain-bound RhoA to the total amount of RhoA in cell lysates.

Statistical Analysis

Experiments were performed in a minimum of triplicate replications. All values were expressed as means ± standard deviation (SD). SPSS 17 for Windows was used for statistical analysis. The one-way ANOVA test followed by Dunnett's post-test was applied for comparisons between groups. P value < 0.05 was considered to indicate statistical significance.

RESULTS

HMGB1-Mediated the Formation of Stress Filaments and Disruption of AJ/TJ Proteins

The changes of cell viability in HPMECs treated with different concentrations of rhHMGB1, Y-27632 and FPS-ZM1 were examined by CCK-8 method (**Figures 1A**, **2A** and **4A**). As indicated in **Figures 1B, C**, rhHMGB1 stimulation upregulated FITC-dextran flux in a dose-dependent and time-dependent manner. rhHMGB1 at a dose of 600 ng/ml showed a significant

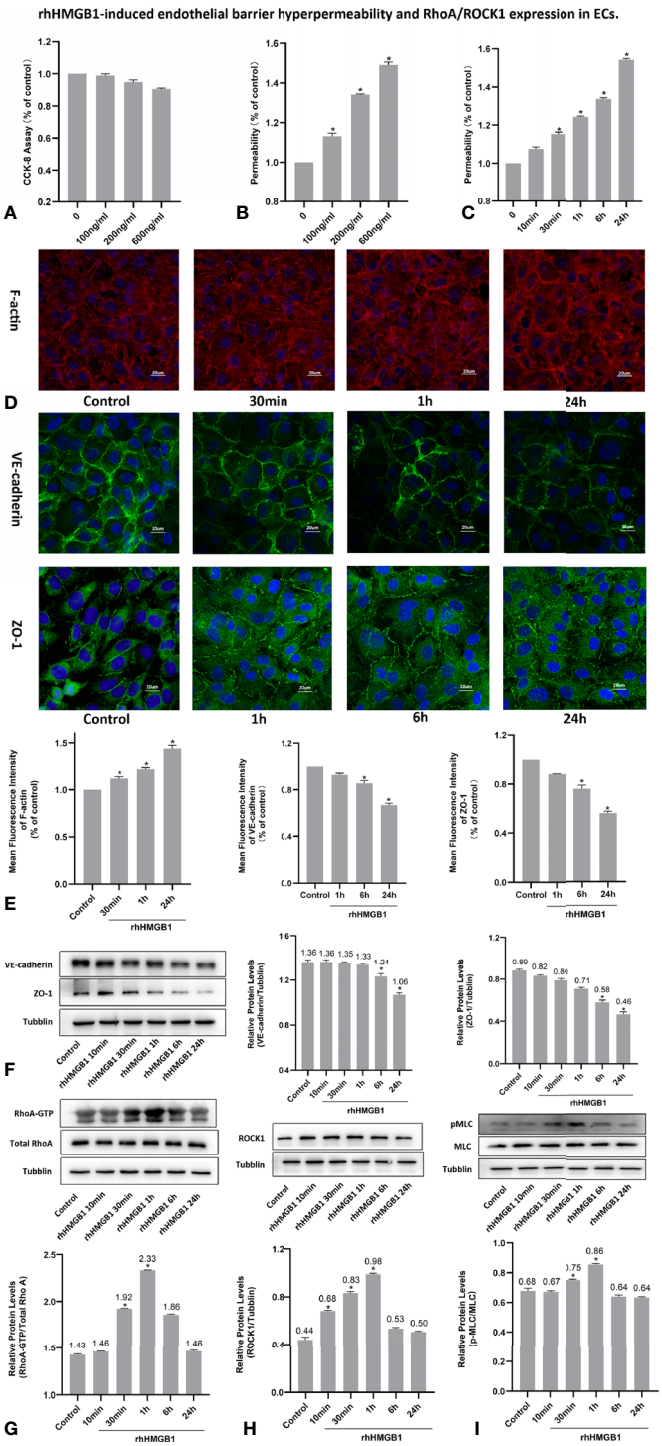

FIGURE 1 | rhHMGB1-induced endothelial barrier hyperpermeability and RhoA/ROCK1 expression in ECs. **(A)** Cell viability of HPMEC was evaluated by CCK-8 measurement after stimulated with different concentration of rhHMGB1 for 24 h. **(B)** HPMECs were stimulated with the indicated concentrations of rhHMGB1 for 24 h. **(C)** HPMECs were stimulated with 600 ng/ml rhHMGB1 for the indicated times. **(D, E)** Immunofluorescence location of F-actin, VE-cadherin and ZO-1 in HPMECs was detected after 600 ng/ml rhHMGB1 stimulation for the indicated times. The fluorescence intensity of F-actin, VE-cadherin and ZO-1 was quantitatively analyzed using the Image J software. **(F)** The concentration of 600 ng/ml rhHMGB1 could selectively downregulate the expression level of VE-cadherin and ZO-1 at 24 h. **(G)** Time course of rhHMGB1-mediated increase in RhoA activity. Western blots showed the content of GTP-bound RhoA and total RhoA in cell lysate. **(H)** rhHMGB1 (600 ng/ml) treatment significantly upregulated ROCK1 expression in HPMECs at 60 min. **(I)** Treatment with 600 ng/ml rhHMGB1 could transiently promote the expression of pMLC. Values were shown as mean ± SD of 3 independent trials. *$p < 0.05$ *vs*. control.

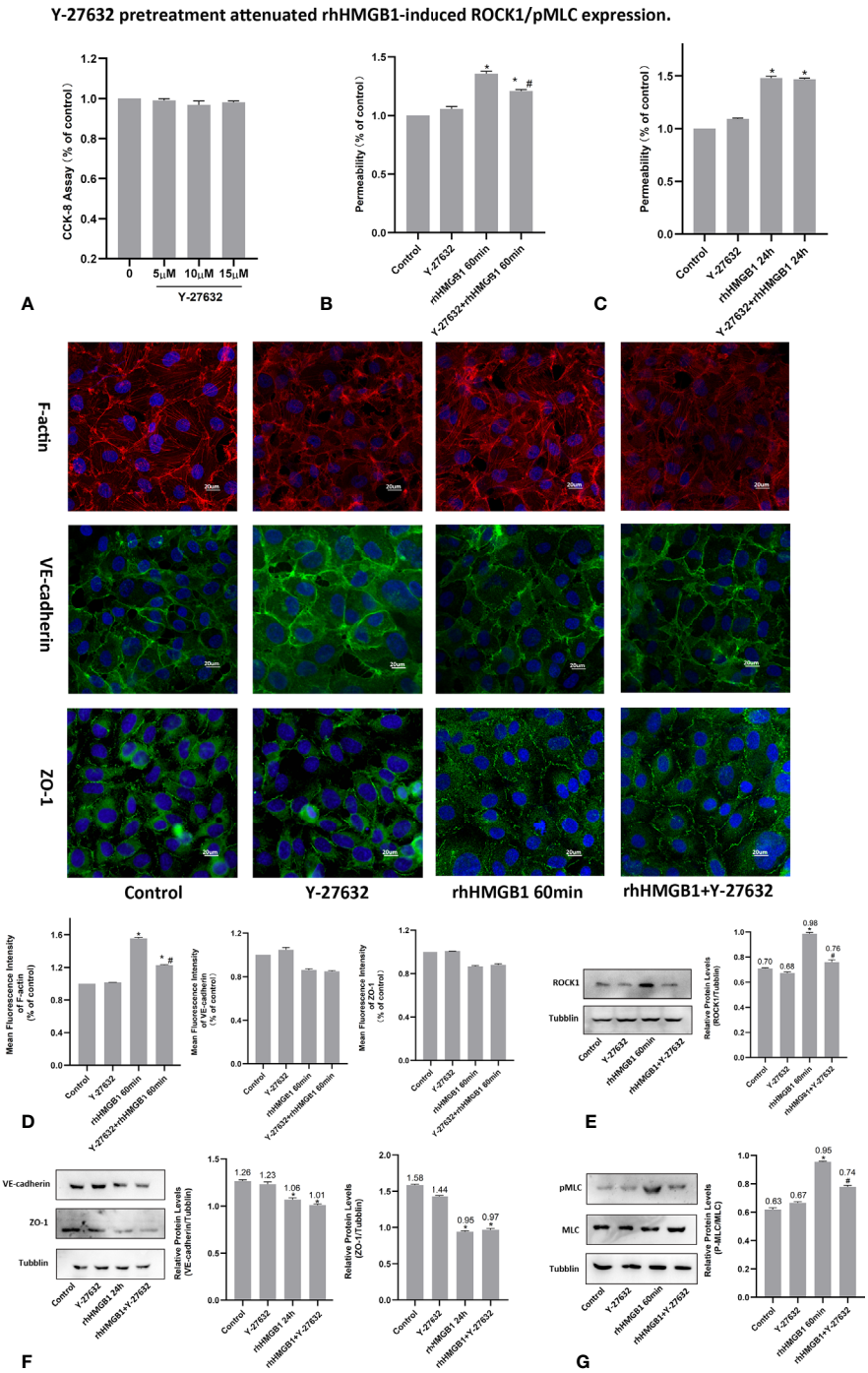

FIGURE 2 | Y-27632 pretreatment attenuated rhHMGB1-induced ROCK1/pMLC expression. **(A)** CCK-8 assay was performed with HPMECs for 24 h with different dosages of Y-27632 as indicated. **(B)** Effects of Y-27632 on changes in FITC-dextran flux in HPMECs. HPMECs were pretreated with Y-27632 and then treated with 600 ng/ml rhHMGB1 for 60 min. **(C)** Role of Y-27632 pretreatment in increased barrier permeability induced by rhHMGB1 at 24 h. **(D)** Effects of Y-27632 on rhHMGB1-mediated morphological change in endothelial F-actin, VE-cadherin and ZO-1. HPMECs were pretreated with Y-27632 for 1 h before rhHMGB1 (600 ng/ml) stimulation for 60 minutes to examine morphology of endothelial F-actin, VE-cadherin and ZO-1 by immunofluorescence. Fluorescence intensity of F-actin, VE-cadherin and ZO-1 was measured in ECs. **(E)** Y-27632 pretreatment downregulated the ROCK1 expression induced by rhHMGB1 at 60 min. **(F)** Effects of Y-27632 treatment on rhHMGB1-induced changes in the protein expression levels of VE-cadherin and ZO-1 at 24 h. Y-27632 were added for the last 4 h of the 24 h rhHMGB1 treatment. **(G)** Pretreatment with Y-27632 attenuated rhHMGB1-induced MLC phosphorylation at 60 min. ECs were pretreated with Y-27632 for 1 h and then stimulated with rhHMGB1 (600 ng/ml) for 1 h. Values were indicated as mean ± SD of 3 separate trials. $^{*}p < 0.05$ *vs*. control. $^{\#}p < 0.05$ *vs*. rhHMGB1 60-min group.

effect on EC barrier permeability (**Figure 1B**). The barrier permeability of HPMEC was markedly increased 30 min after rhHMGB1 treatment, and progressively increased to 24 h (**Figure 1C**). Therefore, the selected concentration of rhHMGB1 was 600 ng/ml in the following experiments. ECs were also treated with Y-27632 (10 uM) and FPS-ZM1 (0.05 uM) for 1 h prior to stimulation with rhHMGB1 and for the last 4 h of the 24 h rhHMGB1 stimulation respectively. Immunofluorescence microscopy revealed that rhHMGB1 also induced progressive cytoskeletal changes in cultured HPMECs that were apparent after 30 min of rhHMGB1 treatment (**Figure 1D**). The 24 h exposure of rhHMGB1 elicited the formation of stress filaments and paracellular gaps (**Figures 1D, E**). After rhHMGB1 treatment for 60 min, membrane localization of VE-cadherin and ZO-1 was also significantly ruptured, indicating that AJ/TJ integrity was disrupted (**Figure 1E**). To investigate the molecular mechanisms for the rhHMGB1-mediated endothelial barrier disruption, we checked whether changes in endothelial cell barrier permeability were paralleled with changes in the expression levels of intercellular junction proteins. As shown in **Figure 1F**, western blot revealed that treatment with rhHMGB1 elicited a time-dependent decrease in the expressions of VE-cadherin and ZO-1, which were measurable at 6 h of rhHMGB1 stimulation in ECs, and a more significant decrease was measured at 24 h.

Effects of ROCK1 on HMGB1-Mediated HPMEC Hyperpermeability

To investigate the effects of ROCK activation played on the rhHMGB1-mediated EC barrier hyperpermeability, the ECs were pretreated with Y-27632 or transfected with ROCK1/2 siRNA before rhHMGB1 stimulation. Western blot was used to assess the protein expression of ROCK1/2 in HPMECs after transfection with ROCK1/2 siRNA and there was no evidence of cytotoxicity found in ROCK1/2 siRNA transfected cells (**Figures 3B, C**). As shown in **Figures 1G, H**, the time-dependent increases in RhoA activity and ROCK1 expression by rhHMGB1 treatment were measured. The activity of RhoA/ROCK1 was significantly upregulated at 30 min and 60 min of rhHMGB1 treatment, but the activity of RhoA/ROCK1 returned to baseline by 24 h. The rhHMGB1-induced EC hyperpermeability at 60min was significantly inhibited by Y-27632 pretreatment and ROCK1 knockdown (**Figures 2B**, **3D**). However, transfection with ROCK2 siRNA alone did not reduce rhHMGB1-induced early permeability increases at 60 min (**Figure 3D**). In addition, transfection with ROCK1/2 siRNA had no significant inhibitory role in rhHMGB1-induced late permeability increases at 24 h (**Figure 3D**). When ECs were treated with Y-27632 for the last 4 h of the 24 h rhHMGB1 stimulation, the results indicated that suppression of ROCK had no marked inhibitory role in rhHMGB1-induced hyperpermeability at 24 h (**Figure 2C**), in accordance with the presence of stress filaments and intercellular gaps at 24h (**Figures 1D, E**). These data indicated that ROCK1 activation was necessary for rhHMGB1-mediated early increase in endothelial barrier permeability. Furthermore, the results of western blot showed that treatment with Y-27632 and ROCK1 siRNA had no significant effects on the expressions of VE-cadherin and ZO-1 in HPMECs after 24 h of rhHMGB1 stimulation (**Figures 2F**, **3E**).

HMGB1 Induced MLC Activation in HPMECs

It was demonstrated that Rho/ROCK signaling pathway played a key influence on increasing the level of MLC phosphorylation (19). Thus, pMLC is an important initial event for the increased paracellular flow of endothelial cell leakage (18). In the present study, some modest morphological changes occurred in the actin cytoskeleton after treatment with rhHMGB1 for 30 min (**Figure 1D**), which could reflect the enhanced Rho/ROCK activity and MLC phosphorylation. As shown in **Figure 1I**, rhHMGB1 stimulation (600 ng/ml) for 60 minutes obviously increased the expression level of pMLC, which was consistent with a time-dependent increase in RhoA activity and ROCK1 expression (**Figures 1G, H**). Results showed that rhHMGB1 induced an increase in Ser-19 phosphorylation at 30 min and 1 h and the expression level of Ser-19 phosphorylated MLC returned to baseline by 24 h, as shown on immunoblot (**Figure 1I**). The inhibition of ROCK1 expression with Y-27632 and ROCK1 siRNA could downregulate the phosphorylation of MLC after 60 min of rhHMGB1 treatment (**Figures 2G**, **3H**), which was accompanied by decreases in the fluorescence intensity of F-actin at 60 min (**Figures 2D**, **3F**). Pretreatment with FPS-ZM1 and RAGE siRNA could result in a marked downregulation of the activity of RhoA/ROCK1 and phosphorylation of MLC in HPMECs treated with rhHMGB1 for 60 minutes (**Figures 4C, F** and **5E, F**), and then reduce the fluorescence intensity of stress fibers in the cell center at 60 min (**Figures 4D**, **5D**).

RhoA/ROCK1 Pathway Mediates HMGB1-Induced EC Barrier Disruption in HPMECs

As shown in **Figures 1G, H**, the time-dependent increases in RhoA activity and ROCK1 expression by rhHMGB1 treatment were measured. The results showed that the peak activity of RhoA appeared at 60 min and rhHMGB1 treatment also significantly up-regulated the expression of ROCK1 at 60min. Thus, binding of active GTP-bound RhoA caused unfolding and activation of ROCK1, which was accompanied by rhHMGB1-mediated MLC phosphorylation, stress filament formation, VE-cadherin and ZO-1 disruption, and the early increase in EC barrier permeability (**Figure 1**). Pretreatment with Y-27632 and ROCK1 knockdown could partially inhibit rhHMGB1-mediated EC leakage and restore FITC-dextran flux of the endothelial barrier after 60 min of rhHMGB1 stimulation (**Figures 2B**, **3D**). After pretreatment with Y-27632 and ROCK1 siRNA, the expression of ROCK1 protein at 60 min was significantly downregulated (**Figures 2E**, **3G**), and the membrane location of VE-cadherin and ZO-1 in intercellular junctions was partially restored after 60 min of rhHMGB1 stimulation (**Figures 2D**, **3F**). The 60 min exposure of rhHMGB1 increased the fluorescence intensity of F-actin in the cell center, and pretreatment with Y-27632 and ROCK1 siRNA decreased the fluorescence intensity of central stress filaments after 60 min of rhHMGB1 exposure (**Figures 2D**, **3F**). These findings

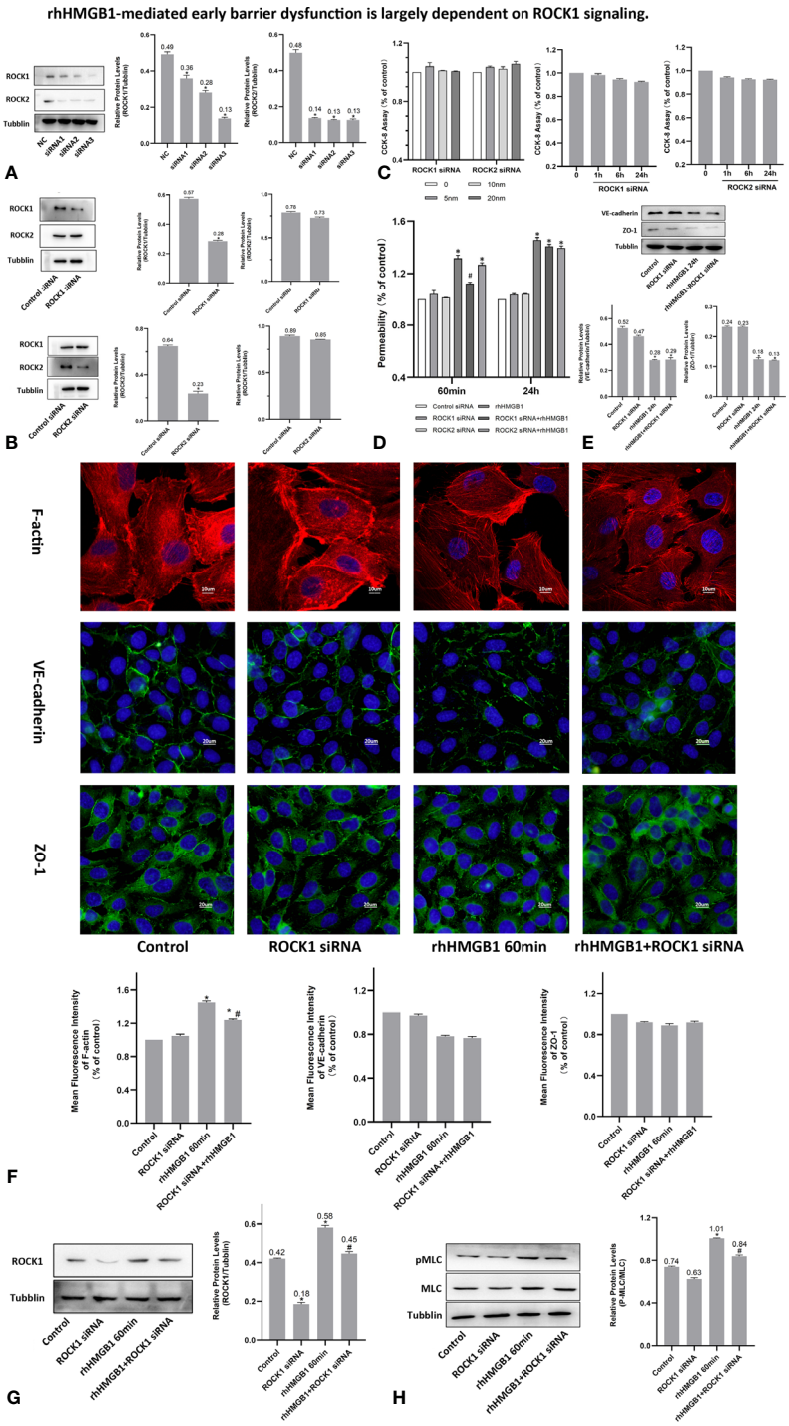

FIGURE 3 | rhHMGB1-mediated early barrier dysfunction is largely dependent on ROCK1 signaling. **(A, B)** ECs were transfected with ROCK1/2 siRNA. Western blot was used to assess the protein expression of ROCK1/2 in HPMECs. **(C)** Cell viability was assessed by the CCK-8 assay after transfection with different concentration of ROCK1/2 siRNA for 24 h or transfection with 10 nM ROCK1/2 siRNA for the indicated times. There was no evidence of cytotoxicity found in ROCK1/2 siRNA transfected cells. **(D)** Examination of FITC-dextran flux of HPMECs. ROCK1 knockdown ameliorated rhHMGB1-induced early permeability increases (at 60 min). **(E)** Effects of ROCK1 siRNA on the expression of VE-cadherin and ZO-1 induced by rhHMGB1 at 24 h. **(F)** ECs were transfected with ROCK1 siRNA and then stimulated with rhHMGB1 for 60 min. Immunofluorescence staining of F-actin, VE-cadherin and ZO-1 was detected by fluorescence microscopy. Image J software was used to analyze the fluorescence intensity of F-actin, VE-cadherin and ZO-1. **(G)** ROCK1 knockdown attenuated the ROCK1 expression induced by rhHMGB1 at 60 min. **(H)** ROCK1 knockdown downregulated the rhHMGB1-induced pMLC expression in cells at 60 min. Mean ± SD of 3 independent trials was shown. *$p < 0.05$ *vs*. corresponding control group. $^{\#}p < 0.05$ *vs*. rhHMGB1 60-min group. NC, negative control.

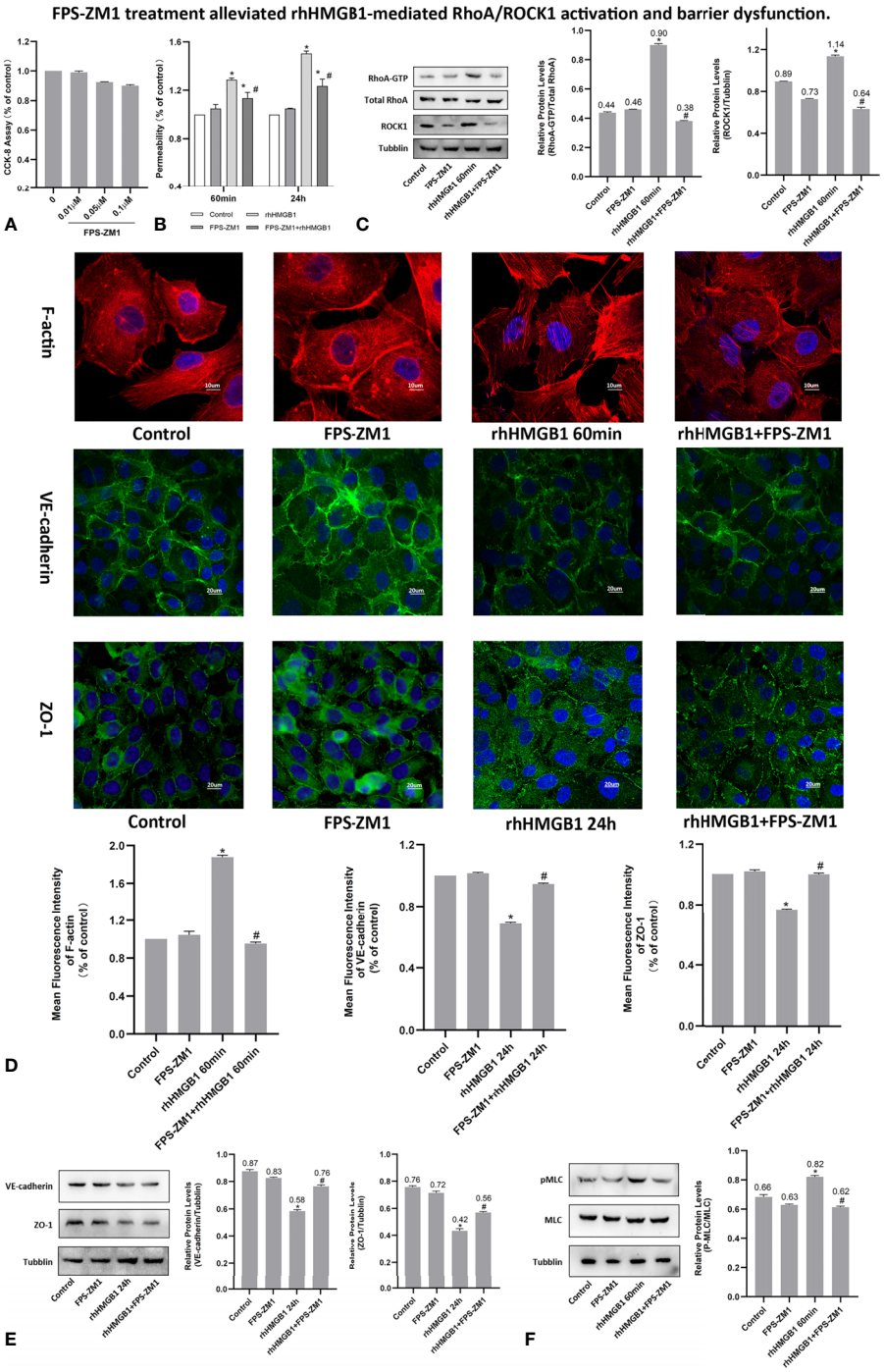

FIGURE 4 | FPS-ZM1 treatment alleviated rhHMGB1-mediated RhoA/ROCK1 activation and barrier dysfunction. **(A)** Cell viability was determined by CCK-8 assay after treated with different dosage of FPS-ZM1 for 24 h. **(B)** FPS-ZM1 improved lung endothelial permeability at 60 min and 24 h after rhHMGB1 stimulation. **(C)** FPS-ZM1 significantly downregulated RhoA and ROCK1 expression in HPMECs at 60 min after rhHMGB1 stimulation. **(D)** Effects of FPS-ZM1 on rhHMGB1-mediated morphological changes in endothelial F-actin, VE-cadherin and ZO-1. ECs were treated with FPS-ZM1 for 1 h prior to stimulation with rhHMGB1 to evaluate morphology of endothelial cytoskeleton F-actin or for the last 4 h of the 24 h rhHMGB1 stimulation to assess morphology of endothelial VE-cadherin and ZO-1 by immunofluorescence microscopy. Image J software was used to analyze the fluorescence intensity of F-actin, VE-cadherin and ZO-1. **(E)** FPS-ZM1 significantly increased VE-cadherin and ZO-1 expression levels in HPMECs at 24 h after rhHMGB1 stimulation. ECs were treated with FPS-ZM1 for the last 4 h of the 24 h rhHMGB1 stimulation. **(F)** Effects of FPS-ZM1 on rhHMGB1-mediated pMLC expression in cells. ECs were pretreated with FPS-ZM1 for 1 h and then treated with rhHMGB1 for 60 minutes. Mean ± SD of 3 independent trials was shown. $^{*}p < 0.05$ *vs*. control. $^{\#}p < 0.05$ *vs*. rhHMGB1 60-min group or rhHMGB1 24-h group.

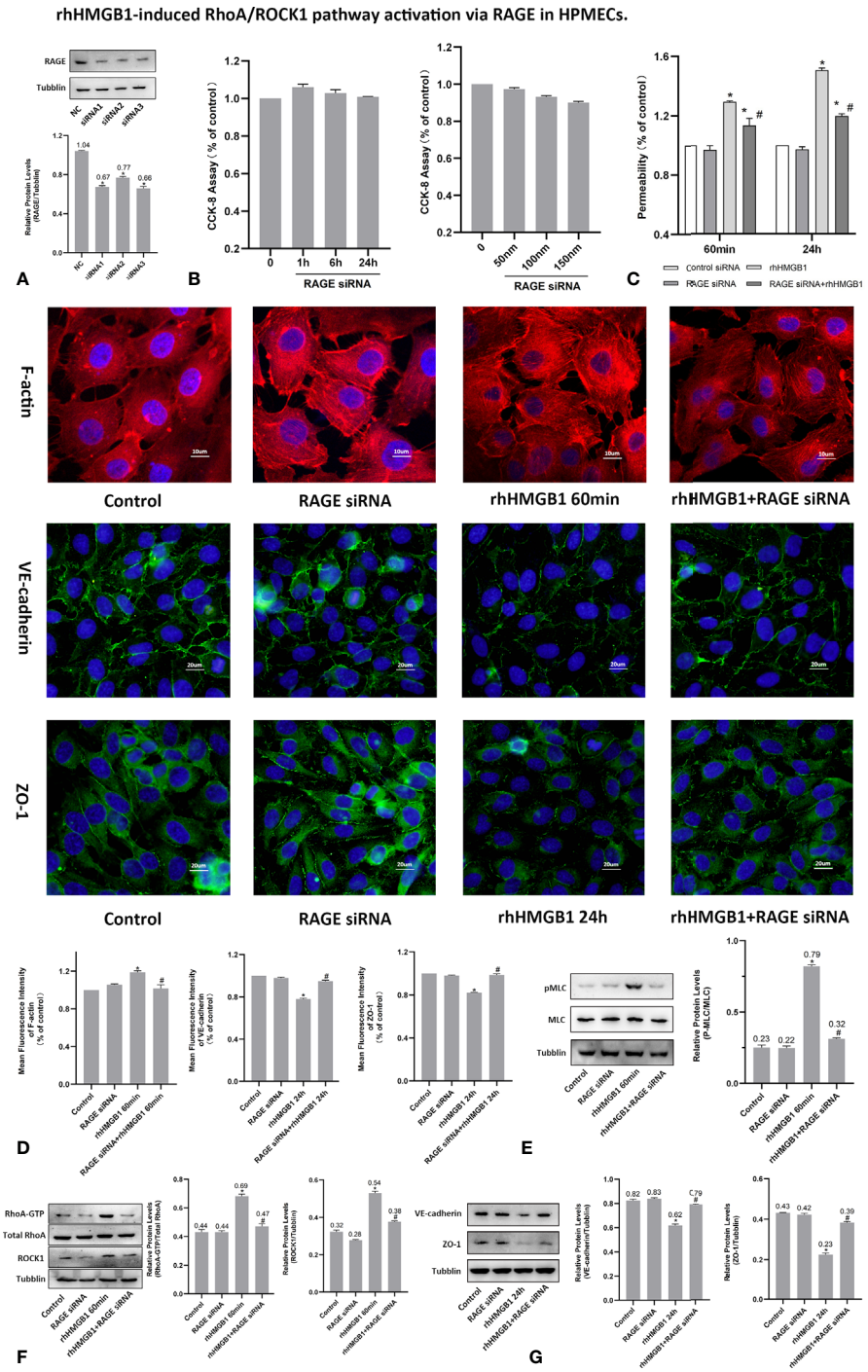

FIGURE 5 | rhHMGB1-induced RhoA/ROCK1 pathway activation *via* RAGE in HPMECs. **(A)** ECs were transfected with RAGE siRNA. Western blots were used to determine the expression of RAGE in endothelial cells. **(B)** Cytotoxicity of RAGE siRNA was assessed by CCK-8 assay after transfected with different concentration of RAGE siRNA for 24 h or transfected with 100 nM RAGE siRNA for the different times. No evidence of cytotoxicity was found in RAGE siRNA transfected cells. **(C)** Treatment with RAGE siRNA ameliorated endothelial barrier dysfunction induced by rhHMGB1 at 60 min and 24 h. **(D)** ECs were transfected with RAGE siRNA and then stimulated with rhHMGB1 for 60 min and 24 h. Immunofluorescence staining of F-actin, VE-cadherin and ZO-1 was determined by fluorescence microscopy. Fluorescence intensity of F-actin, VE-cadherin and ZO-1 was measured in ECs. **(E)** Knockdown of RAGE by siRNA reduced the rhHMGB1-induced MLC phosphorylation at 60 min as detected by western blot. **(F)** Effects of inhibition of RAGE with siRNA on increased expression of RhoA and ROCK1 induced by rhHMGB1 at 60 min in HPMECs. **(G)** Role of RAGE siRNA in the VE-cadherin and ZO-1 protein expression levels in ECs at 24 h after rhHMGB1 treatment. Mean ± SD of 3 independent trials was shown. $^{*}p < 0.05$ *vs*. corresponding control group. $^{\#}p < 0.05$ *vs*. rhHMGB1 60-min group or rhHMGB1 24-h group. NC, negative control.

suggest that RhoA and ROCK1 may be implicated in rhHMGB1-mediated early increase in EC permeability and stress filament formation in HPMECs.

RAGE Mediates the EC Barrier Leakage Induced by HMGB1

To investigate whether RAGE is implicated in the rhHMGB1-mediated increases in EC barrier permeability, the expression of RAGE was silenced by siRNA in HPMECs. In addition, HPMECs were also treated with the specific RAGE inhibitor FPS-ZM1 (20) for 60 min prior to stimulation with rhHMGB1 or for the last 4 h of the 24 h rhHMGB1 stimulation. As indicated in **Figures 4B**, **5C**, FPS-ZM1 and RAGE knockdown significantly decreased endothelial permeability by comparison with the rhHMGB1 treatment group at 60 min and 24 h. Inhibition of RAGE with FPS-ZM1 and RAGE siRNA could also downregulate the activity of RhoA/ROCK1 and phosphorylation of MLC at 60 min (**Figures 4C, F** and **5E, F**), and then partly prevent the rhHMGB1-mediated formation of stress fibers in the cell center (**Figures 4D**, **5D**). Furthermore, inhibition of ROCK1 could also reduce the expression of pMLC (**Figures 2G**, **3H**), and partly recover the membrane localization of VE-cadherin and ZO-1 after 60 min of rhHMGB1 stimulation (**Figures 2D**, **3F**). Therefore, it seems likely that a signaling pathway proceeds from RAGE to RhoA/ROCK1 through the F-actin reorganization and disruption of AJ/TJ related proteins, which finally destroys the early EC barrier function in the present study. In addition, FPS-ZM1 and RAGE siRNA could upregulate the expression levels of VE-cadherin and ZO-1 at 24 h (**Figures 4E**, **5G**). Similarly, inhibition of RAGE could also partially restore the cytomembrane location of VE-cadherin and ZO-1 after 24 h of rhHMGB1 stimulation (**Figures 4D**, **5D**).

DISCUSSION

HMGB1 is released in late endotoxemia and it is closely associated with the severity and prognosis of sepsis (21, 22). It is demonstrated that HMGB1 could elicit microvascular EC cytoskeletal rearrangement and barrier dysfunction (12). EC cytoskeleton, especially F-actin rearrangement, is main histological basis in enhanced EC barrier permeability, which elicits the increase in cell contractility and intercellular gap formation (23, 24). To our best knowledge, this study demonstrates here that HMGB1 elicits progressive changes to the filamentous actin, intercellular junctions and increases HPMEC barrier permeability in a time-dependent and dose-dependent manner. Furthermore, RAGE and RhoA/ROCK1 were implicated in the HMGB1-mediated EC cytoskeletal reorganization and early endothelial barrier dysfunction. This present study showed that HMGB1 disrupted the microvascular endothelial cell barrier, which might be implicated in the pathogenesis of ALI in sepsis.

Phosphorylation of MLC has been reported to involve in the regulation of EC barrier permeability after treatment with thrombin, histamine, and other inflammatory cytokines and so on (18, 19). In the present study, the early rhHMGB1-induced MLC phosphorylation and subsequent formation of actin stress fibers indicated that changes in EC contractility was occurring. RhoA plays a key role in control of endothelial cellular actin cytoskeletal rearrangement and cell morphology. ROCK (a downstream target of RhoA) mediates stress filament formation by upregulating the levels of MLC phosphorylation (25–27). Then, phosphorylated MLC contributes to actomyosin interaction, causing EC contraction and an increased permeability (28, 29). Furthermore, ROCK1 activation has been reported to influence cell-cell adhesion by modulating interactions between stress fibers and intercellular binding molecules (TJ and AJ) (30). It was demonstrated that ROCK1 activation induced by high glucose caused endothelial-to-mesenchymal transition with loss of CD31 and VE-cadherin, resulting in increased endothelial permeability (31). Previous study also shows that anthrax lethal toxin causes EC barrier dysfunction through actin filament formation and disruption of adherens junctions (32). This study indicated that the changes of VE-cadherin expression associated temporally with the formation of stress fibers and activation of ROCK1 (32).

In this study, our findings showed that RhoA/ROCK1 was activated rapidly by rhHMGB1 in cultured HPMECs and rhHMGB1 stimulation induced rapid aggregation of actin stress filaments, intercellular gap formation and a significant increase in endothelial cell permeability by 60 minutes, indicating that the early cytoskeletal reorganization could affect permeability. To confirm the role of ROCK played in rhHMGB1-mediated EC barrier dysfunction, Y-27632 was added for 1 h prior to treatment with rhHMGB1 or for the last 4 h of the 24 h rhHMGB1 stimulation. Moreover, the ECs were transfected with ROCK1/2 siRNA before rhHMGB1 treatment. The results showed that Y-27632 and ROCK1 knockdown were able to significantly suppress ROCK1 activation, subsequent MLC Phosphorylation and the rhHMGB1-induced hyperpermeability at 60 min. In addition, Y-27632 and ROCK1 knockdown decreased the number of central stress filaments and partially restored cortical localization of F-actin and membrane location of VE-cadherin and ZO-1 at 60 min of rhHMGB1 stimulation in HPMECs. Increased endothelial barrier permeability is often related to lack or disruption of AJ/TJ proteins (7, 33) and indeed VE-cadherin and ZO-1 expressions were downregulated following a long-term rhHMGB1 stimulation in this study. The results of western blot showed that inhibition of ROCK with Y-27632 had no influence on the expression of VE-cadherin and ZO-1 at 24 h of rhHMGB1 stimulation in HPMECs, suggesting that rhHMGB1 induced the disruption of EC barrier at 24 h independent of its effect on the RhoA/ROCK signaling. In addition, our previous study indicated that HMGB1 downregulated AJ/TJ components at 24 h through activation of the RAGE/p38 signaling pathway (7). Other study showed that HMGB1 elicited the activation of the RAGE/ERK1/2 pathway at 24 h, which correlated with barrier dysfunction in the human bronchial epithelial cells (34).

So far, many evidences show that HMGB1 interacts with endothelial cell through RAGE. To study the role of RAGE in EC barrier dysfunction, we inhibited the RAGE activity using RAGE siRNA and its specific inhibitor FPS-ZM1 (20, 35). Recent

studies indicated that the inhibition of RAGE functions *via* FPS-ZM1 might be a meaningful therapeutic strategy for a variety of diseases, such as diabetes-related glomerular filtration barrier damage and irradiation-induced EC barrier disruption (10, 36). Our study also demonstrated that the blockage of RAGE with FPS-ZM1 and RAGE siRNA attenuated the EC barrier hyperpermeability mediated by rhHMGB1 and blocked the rhHMGB1-induced RhoA/ROCK1 activation and MLC phosphorylation. Furthermore, our findings also confirmed FPS-ZM1 as a potential therapeutic drug for treating rhHMGB1-induced EC barrier dysfunction.

In conclusion, our findings demonstrate that rhHMGB1 could induce the early EC barrier disruption, and the potential molecular mechanism may be that rhHMGB1 activates the RhoA/ROCK1 signaling pathway through RAGE, which mediates the phosphorylation of MLC inducing stress fiber formation at short time (up to 60 min), and HMGB1/RAGE disrupts the integrity of AJ/TJ at long term (up to 24 h) independently of RhoA/ROCK1 signaling pathway. These new findings will help to understand the signaling pathways of rhHMGB1-mediated increase in EC barrier permeability and contribute to establish potential therapeutic targets in the treatment of sepsis.

DATA AVAILABILITY STATEMENT

The original contributions presented in the study are included in the article/supplementary material. Further inquiries can be directed to the corresponding authors.

AUTHOR CONTRIBUTIONS

M-JZ, H-RJ, J-WS, Z-AW, BH, C-RZ, X-HY, M-MC and X-CM participated in experimental design, research, data analysis and draft writing. M-JZ, H-RJ and Z-GL wrote and revised the manuscript. Z-GL and W-DZ contributed to the research concept, study design, data analysis and finalization. All authors contributed to the article and approved the submitted version.

FUNDING

The present study was supported by grants from the Natural Science Foundation of Liaoning Province, China (No. 2019-MS-09) and the Liaoning Xingliao Talent Plan Project (No. XLYC2005015).

REFERENCES

1. Gill SE, Rohan M, Mehta S. Role of Pulmonary Microvascular Endothelial Cell Apoptosis in Murine Sepsis-Induced Lung Injury *In Vivo*. *Respir Res* (2015) 16:109. doi: 10.1186/s12931-015-0266-7
2. Belvitch P, Htwe YM, Brown ME, Dudek S. Cortical Actin Dynamics in Endothelial Permeability. *Curr Top Membr* (2018) 82:141–95. doi: 10.1016/bs.ctm.2018.09.003
3. Vandenbroucke E, Mehta D, Minshall R, Malik AB. Regulation of Endothelial Junctional Permeability. *Ann N Y Acad Sci* (2008) 1123:134–45. doi: 10.1196/annals.1420.016
4. Tornavaca O, Chia M, Dufton N, Almagro LO, Conway DE, Randi AM, et al. ZO-1 Controls Endothelial Adherens Junctions, Cell-Cell Tension, Angiogenesis, and Barrier Formation. *J Cell Biol* (2015) 208(6):821–38. doi: 10.1083/jcb.201404140
5. Dudek SM, Garcia JG. Cytoskeletal Regulation of Pulmonary Vascular Permeability. *J Appl Physiol (1985)* (2001) 91(4):1487–500. doi: 10.1152/jappl.2001.91.4.1487
6. Hirase T, Kawashima S, Wong EY, Ueyama T, Rikitake Y, Tsukita S, et al. Regulation of Tight Junction Permeability and Occludin Phosphorylation by Rhoa-P160rock-Dependent and -Independent Mechanisms. *J Biol Chem* (2001) 276(13):10423–31. doi: 10.1074/jbc.M007136200
7. Luan Z, Hu B, Wu L, Jin S, Ma X, Zhang J, et al. Unfractionated Heparin Alleviates Human Lung Endothelial Barrier Dysfunction Induced by High Mobility Group Box 1 Through Regulation of P38-GSK3β-Snail Signaling Pathway. *Cell PhysiolBiochem* (2018) 46(5):1907–18. doi: 10.1159/00048937
8. Zheng YJ, Xu WP, Ding G, Gao YH, Wang HR, Pan SM. Expression of HMGB1 in Septic Serum Induces Vascular Endothelial Hyperpermeability. *Mol Med Rep* (2016) 13(1):513–21. doi: 10.3892/mmr.2015.4536
9. Luan ZG, Zhang J, Yin XH, Ma XC, Guo RX. Ethyl Pyruvate Significantly Inhibits Tumour Necrosis Factor-Alpha, Interleukin-1beta and High Mobility Group Box 1 Releasing and Attenuates Sodium Taurocholate-Induced Severe Acute Pancreatitis Associated With Acute Lung Injury. *Clin Exp Immunol* (2013) 172(3):417–26. doi: 10.1111/cei.12062
10. Zhou H, Jin C, Cui L, Xing H, Liu J, Liao W, et al. HMGB1 Contributes to the Irradiation-Induced Endothelial Barrier Injury Through Receptor for Advanced Glycation End Products (RAGE). *J Cell Physiol* (2018) 233 (9):6714–21. doi: 10.1002/jcp.26341
11. Jeong J, Lee J, Lim J, Cho S, An S, Lee M, et al. Soluble RAGE Attenuates Angii-Induced Endothelial Hyperpermeability by Disrupting HMGB1-Mediated Crosstalk Between AT1R and RAGE. *Exp Mol Med* (2019) 51 (9):113. doi: 10.1038/s12276-019-0312-5
12. Wolfson RK, Chiang ET, Garcia JG. HMGB1 Induces Human Lung Endothelial Cell Cytoskeletal Rearrangement and Barrier Disruption. *Microvasc Res* (2011) 81(2):189–97. doi: 10.1016/j.mvr.2010.11.010
13. Watts B A3rd, George T, Badalamenti A, Good DW. High-Mobility Group Box 1 Inhibits HCO3- Absorption in the Medullary Thick Ascending Limb Through RAGE-Rho-ROCK-Mediated Inhibition of Basolateral Na+/H+ Exchange. *Am J Physiol Renal Physiol* (2016) 311(3):F600–13. doi: 10.1152/ajprenal.00185.2016
14. Duluc L, Wojciak-Stothard B. Rho Gtpases in the Regulation of Pulmonary Vascular Barrier Function. *Cell Tissue Res* (2014) 355(3):675–85. doi: 10.1007/s00441-014-1805-0
15. Mong PY, Wang Q. Activation of Rho Kinase Isoforms in Lung Endothelial Cells During Inflammation. *J Immunol* (2009) 182(4):2385–94. doi: 10.4049/jimmunol.0802811
16. Shi J, Wu X, Surma M, Vemula S, Zhang L, Yang Y, et al. Distinct Roles for ROCK1 and ROCK2 in the Regulation of Cell Detachment. *Cell Death Dis* (2013) 4(2):e483. doi: 10.1038/cddis.2013.10
17. Shi J, Wei L. Rho Kinases in Cardiovascular Physiology and Pathophysiology: The Effect of Fasudil. *J Cardiovasc Pharmacol* (2013) 62(4):341–54. doi: 10.1097/FJC.0b013e3182a3718f
18. Srinivas SP, Satpathy M, Guo Y, Anandan V. Histamine-Induced Phosphorylation of the Regulatory Light Chain of Myosin II Disrupts the Barrier Integrity of Corneal Endothelial Cells. *Invest Ophthalmol Vis Sci* (2006) 47(9):4011–8. doi: 10.1167/iovs.05-1127
19. Ruiz-Loredo AY, López E, López-Colomé AM. Thrombin Promotes Actin Stress Fiber Formation in RPE Through Rho/ROCK-Mediated MLC Phosphorylation. *J Cell Physiol* (2011) 226(2):414–23. doi: 10.1002/jcp.22347
20. Deane R, Singh I, Sagare AP, Bell RD, Ross NT, LaRue B, et al. A Multimodal RAGE-Specific Inhibitor Reduces Amyloid β-Mediated Brain Disorder in a Mouse Model of Alzheimer Disease. *J Clin Invest* (2012) 122(4):1377–92. doi: 10.1172/JCI58642
21. Karlsson S, Pettilä V, Tenhunen J, Laru-Sompa R, Hynninen M, Ruokonen E. HMGB1 as a Predictor of Organ Dysfunction and Outcome in Patients With

Severe Sepsis. *Intensive Care Med* (2008) 34(6):1046–53. doi: 10.1007/s00134-008-1032-9
22. Gil M, Kim YK, Hong SB, Lee KJ. Naringin Decreases Tnf-α and HMGB1 Release From LPS-Stimulated Macrophages and Improves Survival in a CLP-Induced Sepsis Mice. *PLoS One* (2016) 11(10):e0164186. doi: 10.1371/journal.pone.0164186
23. Cong X, Kong W. Endothelial Tight Junctions and Their Regulatory Signaling Pathways in Vascular Homeostasis and Disease. *Cell Signal* (2019) 66:109485. doi: 10.1016/j.cellsig.2019.109485
24. Srinivas SP. Cell Signaling in Regulation of the Barrier Integrity of the Corneal Endothelium. *Exp Eye Res* (2012) 95(1):8–15. doi: 10.1016/j.exer.2011.09.009
25. Abedi F, Hayes AW, Reiter R, Karimi G. Acute Lung Injury: The Therapeutic Role of Rho Kinase Inhibitors. *Pharmacol Res* (2020) 155:104736. doi: 10.1016/j.phrs.2020.104736
26. Garcia JG, Davis HW, Patterson CE. Regulation of Endothelial Cell Gap Formation and Barrier Dysfunction: Role of Myosin Light Chain Phosphorylation. *J Cell Physiol* (1995) 163(3):510–22. doi: 10.1002/jcp.1041630311
27. Mikelis CM, Simaan M, Ando K, Fukuhara S, Sakurai A, Amornphimoltham P, et al. Rhoa and ROCK Mediate Histamine-Induced Vascular Leakage and Anaphylactic Shock. *Nat Commun* (2015) 6:6725. doi: 10.1038/ncomms7725
28. Wang P, Verin AD, Birukova A, Gilbert-McClain LI, Jacobs K, Garcia JG. Mechanisms of Sodium Fluoride-Induced Endothelial Cell Barrier Dysfunction: Role of MLC Phosphorylation. *Am J Physiol Lung Cell Mol Physiol* (2001) 281(6):L1472–83. doi: 10.1152/ajplung.2001.281.6.L1472
29. Verin AD, Birukova A, Wang P, Liu F, Becker P, Birukov K, et al. Microtubule Disassembly Increases Endothelial Cell Barrier Dysfunction: Role of MLC Phosphorylation. *Am J Physiol Lung Cell Mol Physiol* (2001) 281(3):L565–74. doi: 10.1152/ajplung.2001.281.3.L565
30. Riento K, Ridley AJ. Rocks: Multifunctional Kinases in Cell Behaviour. *Nat Rev Mol Cell Biol* (2003) 4(6):446–56. doi: 10.1038/nrm1128
31. Peng H, Li Y, Wang C, Zhang J, Chen Y, Chen W, et al. ROCK1 Induces Endothelial-to-Mesenchymal Transition in Glomeruli to Aggravate Albuminuria in Diabetic Nephropathy. *Sci Rep* (2016) 6:20304. doi: 10.1038/srep20304
32. Warfel JM, D'Agnillo F. Anthrax Lethal Toxin-Mediated Disruption of Endothelial VE-Cadherin Is Attenuated by Inhibition of the Rho-Associated Kinase Pathway. *Toxins (Basel)* (2011) 3(10):1278–93. doi: 10.3390/toxins3101278
33. Wang W, Dentler WL, Borchardt RT. VEGF Increases BMEC Monolayer Permeability by Affecting Occludin Expression and Tight Junction Assembly. *Am J Physiol Heart Circ Physiol* (2001) 280(1):H434–40. doi: 10.1152/ajpheart.2001.280.1.H434
34. Huang W, Zhao H, Dong H, Wu Y, Yao L, Zou F, et al. High-Mobility Group Box 1 Impairs Airway Epithelial Barrier Function Through the Activation of the RAGE/ERK Pathway. *Int J Mol Med* (2016) 37(5):1189–98. doi: 10.3892/ijmm.2016.2537
35. Hong Y, Shen C, Yin Q, Sun M, Ma Y, Liu X. Effects of RAGE-Specific Inhibitor FPS-ZM1 on Amyloid-β Metabolism and Ages-Induced Inflammation and Oxidative Stress in Rat Hippocampus. *Neurochem Res* (2016) 41(5):1192–9. doi: 10.1007/s11064-015-1814-8
36. Sanajou D, Ghorbani Haghjo A, Argani H, Roshangar L, Ahmad SNS, Jigheh ZA, et al. FPS-ZM1 and Valsartan Combination Protects Better Against Glomerular Filtration Barrier Damage in Streptozotocin-Induced Diabetic Rats. *J Physiol Biochem* (2018) 74(3):467–78. doi: 10.1007/s13105-018-0640-2

Conflict of Interest: The authors declare that the research was conducted in the absence of any commercial or financial relationships that could be construed as a potential conflict of interest.

Publisher's Note: All claims expressed in this article are solely those of the authors and do not necessarily represent those of their affiliated organizations, or those of the publisher, the editors and the reviewers. Any product that may be evaluated in this article, or claim that may be made by its manufacturer, is not guaranteed or endorsed by the publisher.

frontiers in Immunology

REVIEW
published: 21 October 2021
doi: 10.3389/fimmu.2021.733537

Evaluation of the Molecular Mechanisms of Sepsis Using Proteomics

He Miao[1], *Song Chen*[2,3]* *and Renyu Ding*[1]*

[1] Department of Intensive Care Unit, The First Hospital of China Medical University, Shenyang, China, [2] Department of Trauma Intensive Care Unit, The First Affiliated Hospital of Hainan Medical University, Haikou, China, [3] Key Laboratory of Emergency and Trauma of Ministry of Education, Hainan Medical University, Haikou, China

Sepsis is a complex syndrome promoted by pathogenic and host factors; it is characterized by dysregulated host responses and multiple organ dysfunction, which can lead to death. However, its underlying molecular mechanisms remain unknown. Proteomics, as a biotechnology research area in the post-genomic era, paves the way for large-scale protein characterization. With the rapid development of proteomics technology, various approaches can be used to monitor proteome changes and identify differentially expressed proteins in sepsis, which may help to understand the pathophysiological process of sepsis. Although previous reports have summarized proteomics-related data on the diagnosis of sepsis and sepsis-related biomarkers, the present review aims to comprehensively summarize the available literature concerning "sepsis", "proteomics", "cecal ligation and puncture", "lipopolysaccharide", and "post-translational modifications" in relation to proteomics research to provide novel insights into the molecular mechanisms of sepsis.

Keywords: sepsis, proteomics, cecal ligation and puncture, lipopolysaccharide, post-translational modifications

OPEN ACCESS

Edited by:
Erxi Wu,
Baylor Scott and White Health, United States

Reviewed by:
Jose Soto,
Baylor Scott and White Health, United States
Ajay Dixit,
University of Minnesota Twin Cities, United States

***Correspondence:**
Song Chen
chensongcmu@126.com
Renyu Ding
renyuding@126.com

Specialty section:
This article was submitted to Inflammation, a section of the journal Frontiers in Immunology

Received: *30 June 2021*
Accepted: *08 October 2021*
Published: *21 October 2021*

Citation:
Miao H, Chen S and Ding R (2021) Evaluation of the Molecular Mechanisms of Sepsis Using Proteomics. Front. Immunol. 12:733537. doi: 10.3389/fimmu.2021.733537

INTRODUCTION

Sepsis is a life-threatening multiple organ dysfunction resulting from a dysregulated host response to infection, including acute respiratory distress syndrome (ARDS), acute kidney injury (AKI), or disseminated intravascular coagulation (DIC) (1, 2). Sepsis is characterized by high morbidity and mortality. The Global Burden of Disease study identified 48.9 million cases of sepsis worldwide in 2017 (3). However, it is difficult to accurately estimate the incidence of sepsis because of the underreporting of cases in medically underdeveloped countries. Furthermore, because of an increasingly aging society in many countries, the occurrence of sepsis is likely to be on the rise (4). Although the guidelines for the diagnosis and treatment of sepsis have made great progress in the past decade and the prognosis has been improved, the mortality rate remains high. More than 25%–30% of patients with sepsis die of the disease, and the in-hospital mortality rate of septic shock is close to 40%–60% (4, 5). Therefore, a deep understanding of the biological mechanism, early and accurate diagnosis, and effective treatment of sepsis is essential.

In the last decade, various omics techniques have been used for the study of sepsis, including genomics (6, 7), transcriptomics (8–10), proteomics (7), and metabolomics (7, 11). Since the completion of the Human Genome Project and accumulation of extensive genomic data, proteomics has become an integral component of the post-genomic era (12). The essence of proteomics is to study the characteristics of proteins on a large scale, including protein identification, post-translational modifications (PTMs; glycosylation, phosphorylation, etc.), and protein function determination (13). There are many research methods for proteomics, such as chromatography-based techniques (traditional techniques) (14) and protein chips (advanced technologies) (14, 15). However, each technology has its advantages and limitations. The following are the two most common approaches for proteomics in sepsis. The first is to search for biomarkers, which helps in the early diagnosis of sepsis and organ function damage caused by sepsis through proteomics (16). The second is to explore the molecular mechanism of sepsis and sepsis-related organ function damage by comparing the differences or dynamic changes in protein expression between sepsis and control patients to identify therapeutic targets, thereby achieving precision medicine. Herein, we reviewed proteomics studies published in the past two decades using the keywords "sepsis," "proteomics," "cecal ligation and puncture" (CLP), "lipopolysaccharide" (LPS), and "post-translational modifications." We summarize the application of proteomics in elucidating the molecular mechanism and potential therapeutic targets of sepsis and the research progress of protein PTMs in sepsis. In addition, we discuss the potential problems and development prospects of proteomics.

PATHOPHYSIOLOGICAL MECHANISMS OF SEPSIS

The detailed complex pathophysiological mechanisms underlying sepsis remain elusive; however, inflammatory and immune responses appear to play key roles in this process. Pathogens activate immune cells by interacting with pattern-recognition receptors (e.g., Toll-like receptors [TLRs]) and regulate the expression of proinflammatory factors *via* signaling pathways such as the TLR/MyD88/NF-κB and TLR/Trif/IRF3 pathways. These receptors recognize the structures of pathogenic microorganisms, known as pathogen-associated molecular patterns (PAMPs). The same receptors also recognize endogenous molecules released from injured cells, known as damage-associated molecular patterns (DAMPs), such as histones, extracellular DNA, and heat shock proteins (HSPs) (17–19). In general, proinflammatory reactions are directed at eliminating invading pathogens, whereas anti-inflammatory responses help to limit the degree of local and systemic tissue injury (20). Therefore, an imbalance between proinflammatory reactions and anti-inflammatory responses results in a series of uncontrolled host responses, including systemic inflammatory response syndrome, coagulation abnormalities, immunosuppression, neuroendocrine disorders, and metabolic disorders (17, 21–23).

Coagulation abnormalities are common in sepsis (24). Proinflammatory mediators induce the expression of tissue factors and promote the cascade of coagulation pathways. Activity of the anticoagulant system (e.g., protein C and antithrombin) is reduced, and the increase in anti-fibrinolytic plasminogen activator inhibitor-1 levels inhibits the activation of the fibrinolytic system (20). These changes cause the formation of microthrombi, resulting in sepsis-induced coagulopathy (SIC) and even DIC (18). Neutrophil extracellular traps (NETs) (19), endothelial cell injury (25), and platelet activation (26) are all involved in the pathophysiological process of SIC.

The apoptosis of lymphocytes and antigen-presenting cells is the main pathogenic event that contributes to immunosuppression in sepsis (27). Immune checkpoints, represented by programmed death (PD)-ligand 1/PD-1, play an important role in the regulation of immune cell apoptosis (19, 28). Myeloid-derived suppressor cells, which are produced in high quantities during sepsis, secrete anti-inflammatory cytokines, such as interleukin (IL)-10 and transforming growth factor-β, which aggravate immunosuppression (18). Impaired phagocytic function of macrophages and neutrophils and decreased expression of HLA-DR on the surface of monocytes also contribute to immunosuppression in sepsis (18).

In sepsis, the sympathetic adrenomedullary system is excited and produces large amounts of catecholamine neurotransmitters, which further increase the expression and release of proinflammatory factors, thereby aggravating endothelial cell injury (17). The cholinergic anti-inflammatory pathway associated with the vagus nerve plays a role in antagonizing the inflammatory response (20). The hypothalamus is the regulatory center of the neuroendocrine and autonomic nervous systems. The function of the hypothalamic–pituitary–adrenal axis is impaired during sepsis, resulting in relative adrenal insufficiency (29). Similarly, sepsis disturbs thyroid hormone synthesis and secretion, which causes low T3 syndrome (27).

Changes in hormone levels during sepsis can also cause metabolic disorders. The classical hormone-induced metabolic disorder is stress-induced hyperglycemia, which is associated with insulin resistance and increased glucocorticoid and glucagon levels (30). Other sepsis-related metabolic disorders include fatty acid/amino acid metabolism disorders, anaerobic metabolism, oxidative stress, and abnormalities in energy metabolism. Mitochondria are the power plants of cells that produce adenosine triphosphate (ATP) *via* the tricarboxylic acid (TCA) cycle and maintain cellular function (31). Mitochondrial dysfunction leads to the generation of large amounts of reactive oxygen species (ROS) and can induce cell death (e.g., mitoptosis), which plays an important role in the mechanism underlying the pathogenesis of sepsis (31). Notably, glucose metabolism pathways, including glycolysis, the TCA cycle, and oxidative phosphorylation (OXPHOS), are closely related to the function of immune cells (i.e., immune metabolism) (32). For example, in sepsis, macrophages are divided into two subtypes: M1 and M2. M1 macrophages generally exert proinflammatory effects by secreting proinflammatory factors (33, 34) with a cellular metabolism mode dominated by glycolysis, relatively low OXPHOS activity, and high inducible nitric oxide synthase

(iNOS) activity (35). By contrast, M2 macrophages dominate during the resolution of inflammation by secreting anti-inflammatory factors and participating in processes linked to immunosuppression and tissue repair (34). M2 macrophages rely on enhanced OXPHOS and the intact TCA cycle to support their metabolic program (36). Thus, these uncontrolled host responses are interrelated and collectively contribute to the pathophysiological process of sepsis.

Such uncontrolled host responses and the accompanying production of inflammatory mediators can damage endothelial cells present in diverse tissues and organs, causing organ dysfunction or even failure (37, 38) (**Figure 1**). The main processes contributing to organ dysfunction in sepsis are as follows (20, 22, 39). First, endothelial cells play an essential role in maintaining organ homeostasis, including vasoregulation, selective vascular permeability, and formation of an anticoagulant surface (40, 41). Therefore, damage to intercellular tight junctions of endothelial cells increases their permeability; pro-inflammatory factors also induce the expression of adhesion factors on the cell and disrupt the glycocalyx to promote the adhesion and aggregation of leukocytes and platelets (40). In addition, inflammatory mediators trigger apoptotic pathways, and the apoptosis of endothelial cells exposes collagen and further induces platelet adhesion (40). The second mechanism involves shock, hypoperfusion, and microcirculatory microthrombosis, which aggravate ischemia and generate a hypoxic environment for the affected organs and tissues. Under such hypoxic conditions or in response to ischemia/reperfusion injury, damaged cells and mitochondria produce large amounts of ROS and reactive nitrogen species (RNS) (17), which can cause lipid peroxidation, destroy the cell structure, and induce cell death (17, 42). Moreover, ROS/RNS can modify the post-transcriptional regulation of proteins, such as nitrosylation and acetylation, resulting in protein dysfunction, which further affects the function of cells and organs (43). In addition to these common effects, other pathophysiological mechanisms contribute to organ dysfunction in sepsis that vary depending on the cellular composition, tissue structure, and organ function (44).

As shown in **Figure 1**, the existing pattern of clinical presentation as a diagnostic criterion is challenged owing to the heterogeneity of sepsis (45). With the rapid development of molecular biology techniques, the analysis of biological subtypes or endogenous phenotypes of sepsis may be helpful for precise sepsis diagnosis and treatment (46, 47).

DIFFERENT BIOLOGICAL SAMPLES IN SEPSIS PROTEOMICS

Biological samples used in sepsis proteomics are varied and can include body fluids (such as plasma, serum, and urine), tissues or organs (such as the liver, heart, and muscle), cells (such as platelets, lymphocytes, monocytes, neutrophils, and endothelial cells), organelles (mitochondria), and exosomes. Each biological sample has its advantages and disadvantages (48). Plasma and serum are readily available samples in the clinic (49); however, plasma proteomics is the most complex form of proteomics. Plasma proteins include both proteins produced under physiological conditions and proteins secreted and shed by cells or tissues under pathological conditions. There are a wide variety of proteins in plasma, a wide range of sources, and large differences in protein content (49, 50). Among them, the

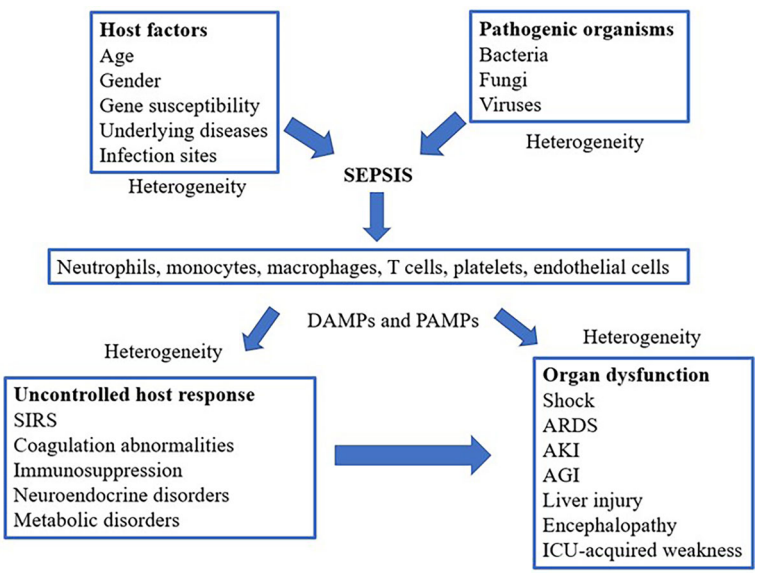

FIGURE 1 | Schematic mechanism of sepsis, including cell types involved and the pathophysiological processes leading to organ dysfunction. SIRS, systemic inflammatory response syndrome; ARDS, acute respiratory distress syndrome; AKI, acute kidney injury; AGI, acute gastrointestinal injury; DAMPs, damage-associated molecular patterns; PAMPs, pathogen-associated molecular patterns; ICU, Intensive Care Unit.

proportion of high-abundance proteins reached approximately 99%, including albumin, IgG, IgA, fibrinogen, transferrin, haptoglobin (HP), and antitrypsin (51, 52). Therefore, during sample preparation, thoroughly removing high-abundant proteins that interfere with the detection and enrichment of low-abundant proteins is key to identifying specific biomarkers for diseases and exploring the potential molecular mechanisms underlying diseases. Currently, there is an increasing number of technologies for the removal of high-abundance proteins from plasma. The classical methods include organic solvent solubilization or precipitation methods and affinity methods. Solvent solubilization and precipitation are consumption methods that reduce the complexity of proteomic samples by removing high-abundance proteins from proteomic samples using organic solvents, such as acetonitrile, ammonium sulfate, and ethanol. Affinity methods include those based on ligands of broad selectivity (e.g., heparin affinity and dye affinity) and those based on antibodies (e.g., immunoaffinity). Among them, the immunoaffinity approaches, which utilize immobilized antibodies for capturing one or more of the high-abundance proteins from biological samples, are the most widely used (51, 53–55). However, there is still no technology that can solve the purification problem for all proteins (56, 57). The current strategy is to use a combination of several different separation and purification techniques for the removal of high-abundance proteins (49, 58, 59). The protein composition in urine is relatively stable compared to that in other body fluids. Although the amount of urinary protein is much lower than that of plasma, more than half of the protein comes from the kidney and urinary tract; therefore, urine proteomics can be used to study the pathophysiological process of kidney disease (60–62). There are proteins secreted in plasma by organs, such as the liver; however, they do not reflect the degree of organ injury (63). Direct analysis of protein expression in organs is therefore beneficial for further understanding the mechanism of organ injury in sepsis. Nonetheless, organs and tissues can only be obtained through animal experiments or autopsies (64). Cytoproteomics is a proteomics technique that uses cells as samples. The cells most closely related to the occurrence and development of sepsis include neutrophils, endothelial cells, platelets, and monocytes. In addition, these cells usually do not include high-abundance proteins (64). The exosome is a bilayer vesicle secreted by cells into the extracellular space that contains proteins, non-coding RNAs, mRNAs, and lipids. It is involved in biological processes, such as immune response, tumor cell migration and invasion, and cell signaling (65–67). Exosomes are present in most body fluids (blood, urine, saliva) and cell culture media (68, 69); additionally, exosomes are one of the sources for screening protein biomarkers (48). Nevertheless, the preparation of exosomes is a complex and time-consuming process (48).

PROTEOMICS IN BASIC RESEARCH

Because sepsis can easily cause cardiovascular, lung, kidney, liver, and other organ dysfunction—leading to a poor prognosis—in recent years, researchers have begun to focus on the changes in protein expression in various organs in sepsis models and devoted themselves to exploring the molecular mechanism of multiple organ injuries in sepsis. Various animal models of sepsis can currently be induced by surgical (e.g., CLP, cecal ligation and incision, colon ascendant stent peritonitis) or non-surgical means (injection of bacteria or exogenous molecules) to mimic the hemodynamic and immunological changes in human sepsis. The most common of these is the CLP procedure in rodents (48, 64, 70, 71). The results of proteomic studies performed in animal models are summarized in **Table 1**.

Renal Proteomics

The kidney is one of the most vulnerable organs in sepsis patients. A total of 22%–51% of sepsis patients admitted in intensive care units experience AKI (87, 88). Understanding the mechanism of AKI in sepsis is therefore essential for the treatment of sepsis patients. The pathophysiological mechanism of AKI in sepsis is unknown. Microvascular dysfunction, inflammation, and metabolic reprogramming are currently considered basic mechanisms of septic AKI (89). Septic AKI still occurs without hemodynamic instability and marked hypoperfusion, even with increased renal blood flow. Inflammatory mediators, including PAMPs and DAMPs released after pathogen invasion, bind to TLRs expressed on immune cells, endothelial cells, and tubular epithelial cells, resulting in endothelial activation, tissue injury, and oxidative stress (89). This series of events ultimately leads to microvascular thrombosis and altered flow continuity (intermittent or no flow) (89). Furthermore, during septic AKI, energy is re-prioritized in the quest to meet vital metabolic needs, prioritizing survival at the expense of cellular function (87, 89, 90). Kellum and Prowle (91) summarized the pathogenesis of AKI caused by various factors. They stated that the main mechanism of AKI in sepsis is an excessive inflammatory response. Róka et al. (72) studied the renal proteome in sepsis and found that renal proteome change was milder in the early phases (1.5 and 6 h) than in the late phases (24 and 48 h). Changes in acute phase proteins (APPs) were the most evident. Of these, lipocalin-2, complement C3, fibrinogen, haptoglobin, and hemopexin were the most upregulated APPs. To further study the molecular mechanism of sepsis-related renal injury, Matejovic et al. (73) selected pigs injected with *Pseudomonas aeruginosa* for kidney biopsy and dynamic proteomics analysis. Twenty differentially expressed proteins were distinguished between the sepsis and control groups. Their study showed that endoplasmic reticulum stress (78 kDa glucose-regulated protein), oxidative stress (peroxiredoxin-6), mitochondrial energy metabolism (enoyl-CoA hydratase), tubular transport (chloride intracellular channel protein 4), and immune/inflammatory signaling (annexin A1, and laminin subunit gamma-1) are activation pathways of AKI in sepsis. Hinkelbein et al. (74) performed proteomic analysis in renal tissues from healthy rats and rats with CLP sepsis (24 and 48 h following CLP). The expression of cytochrome c oxidase subunit B (COX5B) was lower in the 48-h sepsis group than in the control and 24-h groups. Cytochrome oxidase (Complex IV) is an enzyme located at the end of the electron transport chain in the inner mitochondrial membrane

TABLE 1 | Summary of proteomics studies of sepsis infection using animal models.

Species	Sample	Sepsis Model	Altered Pathways	Proteins	Ref.
Mouse	Kidney	Injected with LPS	Acute phase response	**Upregulated:** Lipocalin-2, Complement C3, Fibrinogen, Haptoglobin and Hemopexin	(72)
Pig	Kidney	Injected with pseudomonas aeruginosa	Endoplasmic reticulum (ER) stress, oxidative stress, mitochondrial energy metabolism, tubular transport, and immune/inflammatory signaling	**Downregulated:** Enoyl-CoA hydratase (cellular energetics), and Chloride intracellular channel protein 4 (transporter) **Upregulated:** 78 kDa glucose-regulated protein (ER stress), Peroxiredoxin-6 (oxidative stress protein), Annexin A1(signal transduction), and Laminin subunit gamma-1(cytoskeleton)	(73)
Rat	Kidney	CLP	Mitochondrial energy production	**Downregulated:** COX5B (48 hours after CLP compared to 24 hours)	(74)
Rat	Brain	CLP	Stress, glycolysis, and mitochondrial energy production	**Downregulated:** Chaperone proteins, Enolase and Glucose-6-phosphate dehydrogenase, Creatine kinase isoenzyme and Aconitase 2, Glutamate oxaloacetate transaminase 1, HSP60 (24 h) Glyceraldehyde-3-phosphate dehydrogenase, Aldolase A (48 h) **Upregulated:** G protein beta 1 subunit and COP9 signalosome complex subunit 4 (48 h)	(75)
Rat	Cerebral cortex	CLP	Coagulation, signaling, immune response, and energy metabolism	**Downregulated:** Glandular kallikrein-10, and Succinate dehydrogenase, **Upregulated:** Alpha-2 macroglobulin, Prolyl endopeptidase, Serine protease inhibitor A3N, Kininogen 2, and Alpha-1-acid glycoprotein	(76)
Mouse	Brain	CLP	Immune and coagulation	**Downregulated:** SMAD4, DPYS, PTGDS **Upregulated:** CUL4A	(77)
Cat	Liver mitochondria	Injected with LPS	Reactive oxygen species production and lipid metabolism	**Downregulated:** HSP70, F1-ATPase and key enzymes regulating lipid metabolism (Acyl-CoA dehydrogenase and HMG-CoA synthase) **Upregulated:** Urea cycle enzymes (Carbamoyl phosphate synthetase-1, Ornithine transcarbamylase), HSP 60 and Manganese superoxide dismutase	(78)
Rat	Hepatic mitochondria	CLP	Mitochondrial functions	**Downregulated:** MP1 and MP2 **Upregulated:** MP3	(79)
Mouse	Liver	CLP	Acute phase proteins, oxidative stress, apoptosis, and nitric oxide metabolism	**Downregulated:** Fibrinogen β precursor (6 h), Carbamoyl phosphate synthetase (24 h) **Upregulated:** Calgranulin B, Cyclophilin A (6 h), and Amyloid formation (12 h)	(80)
Mouse	Lung	CLP	Muscle contraction, oxygen transport, protein synthesis, collagen barrier membranes, cell adhesion, and coagulation function	**Downregulated:** Transferrin **Upregulated:** Myosin light chain 4, Cardiomyopathy associated protein 5, Myoglobin, Hemoglobin subunit, 60S ribosomal protein L6,28,34, Fibrinogen alpha chain, Matrix metalloproteinase-9, Tissue-type plasminogen activator, Semaphorin-7A, OTULIN and MAP3K1	(81)
Rat	Heart	CLP	Mitochondrial function	**Downregulated:** Acyl-CoA synthetase 2-like, 2-oxoglutarate dehydrogenase E1 component, Oxoglutarate dehydrogenase, 2-oxoglutarate dehydrogenase complex, and Succinate Coenzyme A ligase (members of the Krebs cycle)	(82)
Rat	Skeletal muscle	CLP	Oxidative stress and mitochondrial dysfunction	**Downregulated:** HSP60, HSP27, HSP β6, and ATP synthase β-chain **Upregulated:** SOD-1, and Ubiquitin-conjugated proteins	(83)
Pig	Plasma	Peritonitis-induced sepsis was initiated by intraperitoneal injection of autologous feces	Oxidative stress, inflammatory, and cytoskeletal assembly	**Upregulated:** CD14, HP, Hemopexin, Microfilament, Actin filament cross-linker protein isoforms 3/4 and Plectin 1	(84)
Mouse	Plasma	CLP	Inflammation, immunity, and coagulation	**Downregulated:** α-2 HS glycoprotein and Zinca-glycoprotein (metabolism) **Upregulated:** Transferrin, Hemopexin, HP, Serum amyloid protein P, and Kininogen	(85)
Rat	Platelet	CLP	Platelet activation, acute phase proteins, cytoskeleton structure, and energy production	**Downregulated:** Protein disulfide-isomerase associated 3, Glucose-6-phosphate dehydrogenase, and Myosin regulatory light polypeptide 9 **Upregulated:** Fibrinogen gamma chain, Growth factor receptor-bound protein 2, Thrombospondin 1, Alpha-1-antitrypsin precursor, Tubulin alpha 6, ATP synthase beta subunit, and succinate dehydrogenase complex subunit B	(86)

HSP, Heat shock protein; LPS, Lipopolysaccharide; CLP, Cecal ligation and puncture; COX5B, Cytochrome c oxidase subunit B;SMAD4, Mothers against decapentaplegic protein 4; DPYS Dihydropyrimidinase; PTGDS, Prostaglandin-H2 D-isomerase; CUL4A, Upregulating the expression of cullin 4A; OTULIN, Ubiquitin thioesterase; MAP3K1, Mitogen-activated protein kinase kinase kinase 1;Hp, Haptoglobin; SOD-1, Superoxide dismutase-1.

and functions as a proton pump (92). Therefore, it is speculated that the occurrence of renal injury in sepsis is closely related to mitochondrial dysfunction. It should be mentioned that different studies yielded different results, possibly resulting from different experimental models, experimental animals, and timing (early and late phases in sepsis).

Cerebral Proteomics

Sepsis-associated encephalopathy (SAE) is defined as diffuse brain dysfunction secondary to systemic infection (93). The manifestations are varied but lack specificity. SAE can present as delirium, agitation, and changes in consciousness (94). More than half of sepsis patients will show features of SAE (93); it can often be the first symptom of sepsis and may lead to long-term impairment (94, 95). Hinkelbein et al. (75) investigated the changes in brain protein expression over time in rats after sepsis induction. Twenty-four proteins were downregulated—including those involved in stress (chaperone proteins), glycolysis (enolase and glucose-6-phosphate dehydrogenase), and mitochondrial energy production (creatine kinase isoenzyme and aconitase 2)—24 h after sepsis induction. After 48 h, 2 proteins were upregulated (G protein beta 1 subunit and COP9 signalosome complex subunit 4), and 3 metabolism-related proteins were downregulated (glutamate oxaloacetate transaminase 1, glyceraldehyde-3-phosphate dehydrogenase, and aldolase A). Glycolysis-related enzyme production is reduced and mitochondrial function impaired, ultimately leading to impaired energy production in brain cells. In addition, chaperonin 60 (HSP60) was found to be downregulated in their study. HSP is a protein generated by cells in response to the induction of stressors (e.g., heat, infection, poisoning, trauma, etc.), and it improves the stress capacity of cells to protect them from the deleterious effects of an imbalance in proteostasis (96, 97). It has been shown that HSP60 also has a neuroprotective effect (98). Therefore, Hinkelbein et al. (75) suggested that the downregulation of HSP60—one of the mechanisms causing brain dysfunction in sepsis—makes brain cells more vulnerable to stress. Yang et al. (76) used isobaric tags for relative and absolute quantification (iTRAQ) technology to study the cerebral cortex of sepsis rat models and identified 91 differentially expressed proteins. These proteins are related to signaling (e.g., succinate dehydrogenase), energy metabolism (e.g., serine protease inhibitor A3N), coagulation (e.g., kininogen 2), and immune response (e.g., alpha-1-acid glycoprotein). Among them, alpha-2 macroglobulin and kininogen, the expression of which was upregulated, act on the complement and coagulation systems, inhibit coagulation, and enhance immunity. The upregulation of prolyl endopeptidase, which hydrolyzes multiple polypeptide neurotransmitters and hormones, may lead to cognitive dysfunction in patients with SAE. The expression of glandular kallikrein-10, involved in the formation of the kallikrein-kinin system, was substantially downregulated, which may be responsible for insufficient blood supply to the brain and increased apoptosis of brain cells in patients with sepsis (76). Xie et al. (77) applied quantitative proteomics based on iTRAQ to analyze the therapeutic mechanism of 2% hydrogen inhalation on brain injury in a sepsis mouse model. A total of 39 differentially expressed proteins were identified in the study, and the functions and pathways of all proteins were analyzed using Gene Ontology (GO) functions and the Kyoto Encyclopedia of Genes and Genomes (KEGG). It was found that H_2 played a role in regulating the immune system and coagulation system. Thus, the protective mechanism of H_2 on SAE was revealed. H_2 decreased SAE in septic mice by downregulating the protein expression of *Drosophila* mothers against decapentaplegic protein 4 (SMAD4), dihydropyrimidinase (DPYS), and prostaglandin-H_2 D-isomerase (PTGDS), and upregulating the expression of cullin4A (CUL4A) (77).

Liver Proteomics

Wang et al. (78) demonstrated that exosomes released from LPS-induced macrophages contain several proinflammatory factors involved in the process of sepsis-induced acute liver injury by regulating the activation of multiple inflammatory pathways (e.g., the NLRP3 inflammasome pathway). It has also been reported that heat shock-induced exosomes from hepatocytes promote liver injury by activating NOD-like receptor signaling pathways (99). Liver mitochondrial proteomics analysis showed altered protein patterns associated with important metabolic pathways, such as regulating ROS production and lipid metabolism, during acute endotoxemia (100). The expression of urea cycle enzymes (carbamoyl phosphate synthetase-1 and ornithine transcarbamylase), HSP 60, and manganese superoxide dismutase increased, whereas the expression of HSP70, F1-ATPase, and key enzymes regulating lipid metabolism (acyl-CoA dehydrogenase and HMG-CoA synthase) was decreased. Chen et al. (79) investigated the changes in liver mitochondrial proteome during sepsis and the role of heat shock treatment. The heat-shock treatment model requires to heat the whole body 24 h before CLP surgery after anesthetizing the rats. Rectal temperature was maintained between 41°C and 42°C for 15 min. After heat shock treatment, HSP-72 was increased in the cytoplasm of rat livers. Three variants (MP1, MP2, and MP3) of aldehyde dehydrogenase 2 (ALDH2) were detected in rat liver mitochondria using two-dimensional gel electrophoresis (2D-GE) separation and liquid chromatography with tandem mass spectrometry (LC-MS/MS) analysis. The expression of MP1 and MP2 was downregulated, whereas that of MP3 was upregulated in the early (9 h after CLP) and late (18 h after CLP) phases of sepsis. However, heat shock treatment reversed this effect. In addition, ALDH2 activity was reduced during sepsis, especially in the late phase of sepsis, as shown by an enzyme activity assay. In contrast, heat shock treatment contributed to the retention of ALDH2 activity. ALDH2 is an important oxidative stress factor *in vivo*. Studies have shown that its overexpression or increased activity can effectively promote the metabolism of toxic aldehydes, inhibit mitochondrial damage, and play an important role in various diseases (101–103). Dear et al. applied the 2D difference in gel electrophoresis (2D-DIGE) technique to study sepsis-induced early (6 h after CLP vs 6 h after sham) and late (24 h after CLP vs 6 h after CLP) proteomic changes in the liver and verified their abundance changes using western blotting. At 6 h after CLP, the protein with the greatest increase in abundance was calgranulin B and that with the greatest decrease was fibrinogen β precursor. At 24 h after surgery, the protein with the greatest increase was associated with amyloid formation, and the greatest decrease was observed in carbamoyl phosphate synthetase. These and other proteins

with altered abundance are involved in processes such as acute phase response, oxidative stress, apoptosis, and nitric oxide (NO) metabolism. One of these proteins, cyclophilin A, increased significantly at 6 h after CLP. Cyclophilin, one of the most abundant proteins in the cytoplasm, is involved in various cellular pathways, including immune regulation, cell signaling, transcriptional regulation, and protein folding and trafficking (104, 105). Notably, cyclophilin interacts with the extracellular receptor CD147 and plays an important role in the regulation of inflammatory responses in a variety of diseases (106). This group found that sepsis-induced renal injury was reduced when CD147 was inhibited, along with a significant reduction in serum cytokine production. Notably, however, the inhibition of CD147 did not significantly reduce sepsis-induced liver injury, as determined by measuring AST and ALT levels to indicate the degree of liver injury. The authors speculated that this may be owing to different pathways of liver and kidney injury in sepsis (80).

Lung Proteomics

ARDS is a clinical syndrome caused by intrapulmonary or extrapulmonary sources characterized by refractory hypoxemia. In ARDS, the common intrapulmonary and extrapulmonary causes are pneumonia and sepsis, respectively (107–109). It has been shown that 2% hydrogen can effectively ameliorate multiple organ damage and increase the survival rate of sepsis mice (110–112). Bian et al. (81) identified differentially expressed proteins, and then elucidated the molecular mechanism of H_2 in treating acute lung injury in sepsis using iTRAQ-based quantitative proteomics analysis. In this study, through functional enrichment analysis, the identified differentially expressed proteins were classified according to their functions, which included muscle contraction (myosin light chain 4, cardiomyopathy associated protein 5), oxygen transport (myoglobin and hemoglobin subunit), protein synthesis (60S ribosomal protein L6,28,34), collagen barrier membrane (matrix metalloproteinase-9), cell adhesion (Semaphorin-7A), and coagulation (fibrinogen alpha chain and tissue-type plasminogen activator). In addition, the expression of Semaphorin-7A, OTULIN, and MAP3K1 increased in sepsis, whereas that of transferrin decreased. H_2 alleviated acute lung injury in septic mice by downregulating Semaphorin-7A, OTULIN, and MAP3K1 expression and upregulating transferrin expression. Thus, it was demonstrated that the protective effect of H_2 on sepsis-related lung injury may be due to an improvement in the oxygen transport capacity of sepsis mice by alleviating mitochondrial injury and the abnormal metabolism of skeletal muscle. This leads to the strengthened contraction of the diaphragm and limb skeletal muscles, improving respiration and circulation.

Heart Proteomics

In patients with septic shock, the incidence of hypofunction is approximately 60% (113), with a high mortality rate. Some studies have applied 2D-GE, MS, and ingenuity pathway analysis to determine the changes in protein levels between sepsis and non-sepsis states (82). They found that 12 proteins were significantly altered in the heart. Among the cardiac-related differentially expressed proteins, five (acyl-CoA synthetase 2-like, 2-oxoglutarate dehydrogenase E1 component, oxoglutarate dehydrogenase, 2-oxoglutarate dehydrogenase complex, and succinate coenzyme A ligase) are members of the Krebs cycle and their expression was downregulated 48 h after sepsis induction. These proteins were associated with impaired energy production in the heart. Numerous studies have shown that mitochondrial reduction can cause a decrease in cardiac function in sepsis (114). Therefore, in sepsis, energy failure is an important pathophysiological mechanism leading to septic cardiomyopathy (115).

Skeletal Muscle Proteomics

In sepsis, proteins are in a hypercatabolic state (decreased synthesis and increased degradation), leading to substantial muscle atrophy. Using a model of burn-related sepsis, Duan et al. (83) identified differentially expressed proteins for muscle atrophy in sepsis. The burn-related sepsis model was established by performing CLP surgery 2 days later in animals with full-thickness skin burns reaching 20% of the total surface area. In their study, some chaperone proteins (HSP60, HSP27, and HSP β6) and metabolic enzymes (ATP synthase β-chain) were downregulated, while SOD-1 expression was upregulated. HSPs have a role in preventing oxidative stress, assisting protein synthesis, and repairing misfolded proteins. Thus, the downregulation of HPS exacerbates oxidative stress-induced proteolysis. The downregulation of metabolic enzyme expression may reduce cellular energy production, which may hinder protein translation (a process that requires ATP). These results suggest that oxidative stress and mitochondrial dysfunction play an essential role in sepsis-induced skeletal muscle atrophy. Duan et al. (83) also reported increased levels of ubiquitin-conjugated proteins (E2) in the muscle of rats with burn-related sepsis, suggesting that the ubiquitin-proteasome pathway is pivotal to protein metabolism in skeletal muscle. Proteins targeted for degradation *via* this pathway are first labeled by ubiquitin molecules mediated by ubiquitin-related enzymes (E1, E2, and E3), that is, ubiquitination of proteins, and later proteolyzed by the proteasome (116). Mass spectrometry can be used for the ubiquitination analysis of biological samples, which suggests the research prospect of proteomics in this direction.

Plasma Proteomics

Most current research techniques in plasma proteomics can remove highly abundant proteins. Nonetheless, there is no efficient method for the removal of moderately abundant proteins, and this is the key to the detection and quantification of low-abundant proteins (117). Thongboonkerd et al. (84) first used a large animal model to study the changes in the plasma proteome of sepsis. In this study, differential proteomics indicated altered plasma levels of 36 proteins (30 upregulated and 6 downregulated) representing 27 unique proteins. Among them, plasma CD14, HP (acute-phase reaction proteins and involved in oxidative stress pathways), and hemopexin (an anti-inflammatory molecule and an oxidative scavenger) were increased in early sepsis. In addition, levels of microfilament, actin filament cross-linker protein isoforms 3 and 4, and plectin

1, which are involved in cytoskeletal assembly, were also increased. Ren et al. (85) compared differentially expressed proteins in the plasma of CLP-operated and sham-operated mice using MS and western blotting after isolating plasma proteins. Plasma protein changes were observed at 4 h (early phase) and 24 h (late phase) after CLP. They demonstrated that significant changes in plasma proteins occurred at 24 h, but not at 4 h after surgery. The identified differentially expressed proteins were associated with inflammation, immunity, and coagulation. The findings suggest that the plasma abundance of fibrinogen and several plasma protease inhibitors (serine/cysteine proteinase inhibitor) change in sepsis, emphasizing the interaction between the inflammatory response and altered coagulability. In addition, the upregulated levels of proteins involved in heme and iron metabolism (e.g., transferrin, hemopexin, HP) confirmed that iron treatment played an important role in innate immune activation. They also found downregulation of two proteins involved in metabolism, the a-2 HS glycoprotein (Fetuin A) and zinc-α glycoprotein.

In summary, in the proteomics of various organs during sepsis, the main pathway affected is the energy generation pathway, especially mitochondrial disorders. The downregulation of mitochondria-related proteins was found in almost all organ dysfunctions. This conclusion is consistent with that of Hohn et al. (118). In their study, differentially expressed proteins were obtained *via* dynamic studies (12, 24, and 48 h) of the organ proteomes and serum proteomes. Separate network analysis of these proteins revealed that changes in the sepsis organ proteome were related to redox activity, cellular energy production and metabolism, and nucleotide or nucleoside metabolism, while those in the plasma proteome were related to lipoprotein metabolism, coagulation, and inflammation.

ADVANTAGES AND DISADVANTAGES OF ANIMAL MODELS

Laboratory animals have a similar genetic inheritance and can be easily controlled for body weight and age. These factors increase the comparability of experiments but do not reflect the heterogeneity of humans (48). At the same time, this allows researchers to avoid the risks caused by experiments on humans, and researchers can obtain different samples according to the purpose of the study and even sacrifice animals. However, animal models cannot fully reproduce the complexity of human sepsis (119). Furthermore, there is no physiological monitoring in animal models, and the severity of sepsis can only be roughly estimated based on the time of death and mortality (120). The above limitations make the experimental results obtained from animal models not fully applicable in clinical practice.

PROTEOMICS IN CLINICAL STUDIES

Although sepsis can occur at all ages, sepsis in the elderly and neonates is characterized by a high incidence and high mortality (121–123). Neonates (especially premature infants) have an immature immune system, poor immune function, and reduced immune function with age (124). Sixty percent of patients with sepsis are elderly (aged ≥65 years), and this proportion may increase with an aging population (125). It has been shown that there are differences in the proteomes of sepsis patients of different ages (126). Cao et al. (126) collected plasma from community-acquired pneumonia (CAP) patients aged 50–65 years and 70–85 years, with and without sepsis, as samples for semi-quantitative plasma proteomics. Fifty-eight proteins were identified, whose expression correlated with age. These proteins were involved in acute phase response (e.g., C-reactive protein, lipopolysaccharide binding-protein, α-1-antichymotrypsin, and transthyretin [TTR]), coagulation pathway (e.g., fibrinogen α chain, fibrinogen β chain, fibrinogen γ chain, and VWF), lipid metabolism (e.g., apolipoprotein B-100 [Apo B100], Apo C, and Apo E), atherosclerosis signaling (e.g., Apo B-100, Apo C, Apo E), and NO and ROS production (e.g., lysozyme C, and clusterin). Therefore, we next discuss the research progress of proteomics in neonatal and adult sepsis. The proteomics results in these clinical studies are summarized in **Table 2**.

Neonatal Sepsis Proteomics

Neonatal sepsis is divided into early and late-onset according to the time of symptom onset. Early-onset often appears within 72 h of birth and usually results from vertical transmission from mother to child. The late-onset form appears 3–7 days after birth and is usually caused by surrounding environmental factors (137–139). At different gestational weeks, the composition of amniotic fluid has few similarities and can be categorized into maternal serum dialysis fluid (early pregnancy), fetal urine (mid pregnancy), and pulmonary secretions (late pregnancy). The fetus swallows amniotic fluid throughout the pregnancy and is therefore directly involved in changes in amniotic fluid material (140). In addition, neutrophils in amniotic fluid are partially derived from the fetus, and assessment of the amniotic fluid reflects the fetal inflammatory response to infection (141, 142). Therefore, proteome analysis in amniotic fluid provides new hints for the diagnosis and prevention of neonatal sepsis. Surface-enhanced laser desorption/ionization time-of-flight MS (SELDI-TOF-MS) is a proteomics technology that combines chromatography with MS, and the analysis is based on a specific algorithm developed for retrieving information on clinically and biologically relevant biomarkers from proteomic SELDI tracing (143). First, samples to be examined are added to a protein array on the chip surface. The protein molecules bind to the chip according to their specific biological or physicochemical properties (hydrophilicity, hydrophobicity, ion exchange, and metal binding), which also facilitate their capture, retention, and purification. Unbound or non-specifically bound proteins are washed out to obtain only specific bound molecules. Finally, a chromatogram is generated using TOF-MS for identification (144, 145). SELDI-TOF-MS enables the use of extremely small amounts of raw biological fluids and rapid screening of numerous biological samples simultaneously (146). Buhimschi et al. (127) performed amniocentesis in 169 women with a singleton pregnancy who gave birth prematurely or with fetal

TABLE 2 | Summary of proteomics of sepsis infection in clinical studies.

Experimental Plan	Sample	Altered Pathways	Proteins	Ref
39 CAP patients (50–65 and 70–85 years old) who did or did not develop severe sepsis	Plasma	Acute phase response, coagulation pathway, lipid metabolism, atherosclerosis signaling, and production of nitric oxide and reactive oxygen species	**Downregulated:** TTR, Apo C III, and Clusterin, **Upregulated:** CRP, LBP, A1ACT, A1AG, Fibrinogen α/β/γ chain, VWF, Apo B-100, Apo E, and Lysozyme C	(126)
Patients who delivered preterm and had intra-amniotic inflammation in response to infection *versus* patients who had symptoms of preterm labor but delivered at term	Amniotic fluid	——	MR score: Neutrophil defensins-1 and-2, Calgranulins A and C	(127)
Newborns with culture-confirmed EONS *versus* gestational age -matched controls	Cord blood	Transfer/carrier, immunity/defense, and protease/extracellular matrix	**Downregulated:** Albumin, Apo A4, Apo E and Apo H **Upregulated:** HP, HpRP, AFP and VDBP	(128)
Survivors *versus* non-survivors on day 28 in patients with sepsis and septic shock	Serum	Complement replacement pathway and acute phase response	Complement factor B subunit Bb, HP, and Clusterin were more significantly upregulated in survivors α-1-B-Glycoprotein was upregulated to a greater extent in non-survivors than in survivors	(129)
Adult male patients diagnosed with sepsis (non-survivors and survivors = 6 each)	Serum	α1 globulins, α2 globulins, and danger–associated molecular patterns/Alarmins	Hp, TTR, ORM1, A1AT, SAA and S100A9 exhibited differential expression patterns between survivors and non-survivors	(130)
Septic patients secondary to CAP *versus* age- and gender-matched healthy volunteers	Peripheral blood mononuclear cells (PBMC) and polymorphonuclear cells (PMN)	Alterations in cytoskeleton, cellular assembly, movement, lipid metabolism, and immune responses in septic patients	**Downregulated:** Apolipoprotein family proteins; F2, GSN and PON1 (inflammation, and coagulation); PLEC, GCC2(cytoskeleton and cell motility) **Upregulated:** HP, FGG, ATM, SERPINA1, SERPINA3, CRP and LBP (inflammation, and coagulation); KIF27, NF1, MYH9, MYO5B, ALMS1, SYNE1, ASPN (cytoskeleton and cell motility)	(131)
Sepsis secondary to HAP *versus* healthy volunteers	Plasma	Lipid metabolism	**Downregulated:** PON1, Apo A1, Apo C, and Apo E **Upregulated:** HP, and SAA1/SAA2	(132)
15 sepsis and 15 SIRS patients	Urine	Inflammation, immunity, and structural or cytoskeletal processes	**Downregulated:** Complement 3, SERPINA1, and Ceruloplasmin **Upregulated:** Cadherin 1, and HP	(133)
Survivors *versus* non-survivors on day 28 in patients with sepsis	Urine	Biological processes of lipid homeostasis, cartilage development, iron ion transport, and certain metabolic processes	**Downregulated:** LAMP-1 and DPP-4 (non-survival) **Upregulated:** SELENBP-1, HSPG-2, A-1-BG, HPR, and LCN (non-survival)	(134)
Septic patients and matched healthy controls	Platelets	Inflammatory response and coagulation activation	**Upregulated:** EFCAB7 (calcium ion binding), Actin (cytoskeleton), IL-1β (cytokine), GPIX (membrane receptor), and GPIIb (integrin)	(135)
Patients with septic shock	Monocytes	Immune response and energy metabolism	**Downregulated:** Oxidative phosphorylation and the Krebs cycle, β-oxidation of fatty acids, the related interferon signaling pathway, MHC II antigen presentation pathway **Upregulated:** Glycolytic metabolism	(136)

CAP, Community-acquired pneumonia; TTR, Transthyretin; Apo, Apolipoprotein;LBP, Lipopolysaccharide binding protein; A1ACT, a-1-antichymotrypsin; A1AG a-1-acid glycoprotein; MR, Mass Restricted; CRP, C-reactive protein; EONS early-onset neonatal sepsis; HpRP, Haptoglobin-related protein; AFP, a-fetoprotein; VDBP,Vitamin-D binding-protein; GSN, a1-antitrypsin, A1T1/SERPINA; serum amyloid A, SAA; orosomucoid 1/a1 acid glycoprotein, ORM1; Prothrombin, F2; Gelsolin; PON1, Paraoxonase 1; PLEC, Plectin; GCC2, GRIP and coiledcoil domain-containing protein 2; FGG, Fibrinogen gamma chain; KIF27, Kinesin-like protein KIF27; NFl, Neurofibromin; MYH9, Myosin-9;MYO5B, Unconventional myosin-Vb; ALMS1, Alstrom syndrome protein 1;SYNE1, Nesprin-1;DPP-4, Dipeptidyl peptidase-4; HPR/HP, Haptoglobin; EFCAB7, EF-hand calcium-binding domain-containing protein 7; IL, Interleukin; GPIX, Glycoprotein IX; GPIIb, Glycoprotein IIB; MHC, Major histocompatibility complex; HLA, Human leukocyte antigen.

membranes. The protein fingerprint of amniotic fluid was obtained using SELDI-TOF-MS and quantified using the mass restricted (MR) score. The MR score includes the expression of four proteins: neutrophil defensin-1 and-2 and calgranulin A and C (64, 147). It is used to identify amniotic inflammation and is associated with tissue chorioamnionitis and early-onset neonatal sepsis(EONS) (148). Abnormal MR scores strongly correlate with early-onset sepsis, as demonstrated by Buhimschi et al. Calgranulin A and C in amniotic fluid are associated with early-onset sepsis and neurodysplasia in neonates (148). Despite the many advantages of MR scoring, amniotic fluid is not readily available, and the functional protein network associated with early-onset sepsis cannot be directly observed (128). Proteomic analysis of cord blood was therefore performed by Buhimschi et al. (128). In their study, 19 differentially expressed proteins were identified in the cord blood of EONS cases using 2D-DIGE and MS. These proteins were classified as transfer/carrier, immunity/defense, and

protease/extracellular matrix according to Ontological classifications. HP, haptoglobin-related protein (HpRP), a-fetoprotein (AFP) and vitamin-D binding-protein (VDBP) (upregulated) and albumin, Apo A4, Apo E, and Apo H (downregulated) are synthesized by hepatic parenchymal cells. Thus, the liver is an important organ mediating inflammatory and immune responses in EONS. In addition, Buhimschi et al. (128) confirmed using western blotting that the Hp and HpRP lanes were evident in cord blood of EONS ("switch-on") but not in neonates with non-early-onset sepsis ("switch-off"). Therefore, the HP "switch-on" pattern may become a biomarker of early sepsis in preterm infants.

Adult Sepsis Proteomics

Kalenka et al. (129) also compared the serum protein of survivors and non-survivors of sepsis or septic shock and identified six differentially expressed proteins (Complement factor B subunit Bb, α-1-B-glycoprotein, HP, and clusterin). These proteins are involved in the complement replacement pathway and acute phase response; they are part of the inflammatory and cytoprotective signaling pathways. To the best of our knowledge, this is the first serum proteomic analysis of patients with sepsis and septic shock to discover several proteins differentially expressed in survivors and non-survivors. Kalenka et al. (129) also demonstrated that proteomics is a feasible tool to identify early alterations in protein expression in patients with sepsis. In a prospective observational study, serum proteome changes from early to late stages were analyzed in sepsis survivors *versus* non-survivors (130). The study identified differences in the levels of HP (acute phase protein), TTR (negative acute phase protein), orosomucoid 1/α1 acid glycoprotein (ORM1, acute phase protein), α1 antitrypsin (A1AT, complement and coagulation pathways), serum amyloid A (SAA), and S100A9 (regulation of inflammatory processes and immune response) between survivors and non-survivors, especially in the early stages of sepsis. Thus, in non–survivors, a dysregulated inflammatory response may be responsible for the death. Sharma et al. (131) selected sepsis patients secondary to CAP as the study subjects to avoid patient heterogeneity and previous interventions. Proteins from sepsis patients were compared with those from age- and sex-matched healthy volunteers. Bioinformatics analysis of the differentially expressed proteins showed that proteins related to the cytoskeleton and cell motility, lipid metabolism and immune response, and other related processes were altered in patients with sepsis. Proteins related to the cytoskeleton and cell motility include those of cell assembly, such as KIF27, NF1, MYH9, MYO5B, ALMS1, SYNE1, and ASPN (upregulated); GSN, PLEC, PON1, F2, and GCC2 (downregulated); and a dynein heavy chain family member (a microtubule-dependent motor ATPase). The apolipoprotein family proteins are downregulated, such as Apo A1, Apo A2, Apo A4, Apo B, Apo C1, Apo C2, Apo C3, and Apo E. Proteins related to inflammation and coagulation include HP, FGG, ATM, SERPINA1, SERPINA3, CRP, and LBP (upregulated) and F2, GSN, and paraoxonase 1 (PON1) (downregulated). In addition, a higher expression of gelsolin and depletion of actin was observed in surviving patients. In a further assessment of lipids and lipoproteins in plasma, it was found that the total cholesterol, HDL-C, and Apo A-I levels were remarkably reduced in septic plasma (131). These results reveal that alterations in cellular structure and lipid metabolism in patients with may be the target for future interventions (131). Another study on plasma proteomics in sepsis patients secondary to hospital-acquired pneumonia (HAP) showed that impaired lipid metabolism was an important alteration in sepsis patients (132). Decreased expression of PON1 and apolipoproteins (Apo A1, Apo C, and Apo E) associated with HDL and increased expression of HP and SAA1/SAA2 were observed. The validation trial indicated that the total plasma cholesterol, HDL-C, LDL-C, non-HDL cholesterol, apolipoproteins ApoA1 and ApoB100, and PON1 levels were downregulated in patients with HAP. These results are similar to the changes in septic patients secondary to CAP and are consistent with the literature emphasizing the important role of lipid metabolism in the pathogenesis of sepsis (132).

Su et al. (133) identified 34 differentially expressed proteins using iTRAQ labeling and 2D-LC-MS analysis of urine from patients with sepsis and systemic inflammatory response syndrome. GO and KEGG analyses indicated that these differentially expressed proteins were involved in inflammatory, immune, and cytoskeletal processes. Among them, five specific proteins were selected by a protein-protein interaction network, which are cadherin 1 (involved in actin cytoskeletal alterations), HP (an anti-inflammatory agent), complement 3, SERPINA1 (inflammatory), and ceruloplasmin (antioxidant and anti-inflammatory defense). The same group also published another article (134), in which proteomic and bioinformatic analyses of urine from sepsis patients with different prognoses (non-survival and survival) revealed that 5 proteins were upregulated (SELENBP-1, HSPG-2, A-1-BG, HPR, and LCN) and 2 proteins were downregulated (LAMP-1 and DPP-4) in the non-survival sepsis group. Three differentially expressed proteins (LAMP-1, SBP-1, and HSPG-2) that had not been reported were validated using western immunoblotting. In non-survivors, LAMP-1 expression was significantly reduced, whereas SBP-1 and HSPG-2 expression did not differ between the survivor and non-survivor groups; thus, urinary LAMP-1 level may be considered to evaluate sepsis prognosis (134). The inflammatory response and activation of coagulation are two important responses of the host defense system in sepsis (149). The coagulation response generated by inflammation induction, in turn, promotes inflammation, and the two interact to form a positive feedback network that promotes the exacerbation of sepsis (149, 150). Neutrophils, monocytes, macrophages, platelets, and other cells play an important role in the development of sepsis. Platelets are enucleated cells, and proteomics can therefore be applied to identify changes in platelet proteins in sepsis. Liu et al. (135) applied 2-DE and MALDI-TOF-MS to identify platelet-derived differentially expressed proteins between sepsis patients and matched healthy controls. This study showed that sepsis patients have increased expression of five platelet proteins: EFCAB7 (calcium ion binding), actin (cytoskeleton), IL-1β (cytokine), GPIX (membrane receptor), and GPIIb (integrin) (135). These five

proteins are involved in inflammatory response and coagulation activation, emphasizing the important role of platelets in sepsis-induced inflammation and coagulation. In contrast, in rats, Hu et al. measured the changes in platelet protein expression 12–24 h after the onset of sepsis to document the response of the platelet proteome to sepsis (86). In this study, the expression of eight proteins increased and the expression of four proteins decreased in platelets from the sepsis group compared with those from the control group. These 12 proteins were divided into the following four categories based on the biological system: 1) platelet activation (fibrinogen gamma chain, growth factor receptor-bound protein 2, and thrombospondin 1); 2) acute phase proteins (protein disulfide-isomerase associated 3, alpha-1-antitrypsin precursor, and thioredoxin); 3) cytoskeletal structure (myosin regulatory light polypeptide 9 and tubulin alpha 6); and 4) energy production (ATP synthase beta subunit, glucose-6-phosphate dehydrogenase, and succinate dehydrogenase complex subunit B). Zhang et al. (151) applied iTRAQ quantitative proteomics to study changes in the proteome of monocyte membranes before and after LPS treatment. A total of 1651 proteins were identified, and subcellular analysis of these proteins indicated that more than 90% of mitochondrial membrane proteins were significantly downregulated. This result demonstrates that the mitochondria may be the main target of bacterial infection in sepsis. Zhang observed that the antigen presentation molecules MHC I and MHC II responded differently to LPS treatment. MHC II molecules (CD74 and HLA-DR) were downregulated, whereas MHC I molecules (HLA-A, -B, and -C) were upregulated. De Azambuja Rodrigues et al. (136) applied LC-MS/MS to identify monocyte proteins from patients with septic shock. The downregulated proteins in sepsis have been implicated in oxidative phosphorylation and the Krebs cycle (ATP5C1, DLST, ETFB, NDUFA11 NDUFA2, NDUFS7, NDUFS8, PDK3, PDP1, PDPR, RXRA, SUCLG2, TACO1, and UQCRQ), β-oxidation of fatty acids (ACADM, DECR1, PCCA, and PCCB), the related interferon signaling pathway (EIF2AK2, EIF4A3, EIF4E2, HLA-DPA1, HLA-DQA2, HLA-DRA, HLA-DRB1, IFIT1, MX1, NUP35, OAS3, PSMB8, and UBE2L6), and MHC II antigen presentation pathway (CD74, CTSH, DCTN3, DYNC1LI2, HLA-DMA, HLA-DMB, HLA- DPA1, HLA-DQA2, HLA-DRA, HLA-DRB1, KIF2A, and OSBPL1A). The upregulated proteins were related to glycolytic metabolism (canonical enzymes PGK1, ALDOA, ALDOC, GADPH, PKLR GPI, and LDHA). The above proteomic results suggest that patients with septic shock show disturbances in monocyte immune response and energy metabolism. The studies by Zhang and De Azambuja Rodrigues suggest impaired monocyte antigen presentation in sepsis.

DISADVANTAGES OF HUMAN SAMPLES

Human samples are remarkably heterogeneous. The clinical symptoms and rate of progression of sepsis can vary widely among people; thus, sample collection may occur at various stages of disease progression. Secondly, proteomics studies of human tissues must be performed on post-mortem or biopsy samples. Therefore, many studies prefer to use animal experiments as the first step (64).

IMPORTANT PTMs OF PROTEINS

PTM refers to the chemical modification of proteins after translation, regulating the activity, localization, folding, and interaction between proteins and other biological macromolecules (including nucleic acids, proteins, and lipids) (152). Several studies have found that many important life activities and disease occurrence are not only correlated with the abundance of proteins but, more importantly, regulated by PTMs of various types of proteins. Through an in-depth study of the differences in the changes in PTMs, it is important to reveal the pathogenesis of diseases, screen clinical markers of diseases, and identify the targets of drugs. These typically include phosphorylation, glycosylation, ubiquitination, nitrosylation, methylation, acetylation, lipidation, and proteolysis. There are increasing studies on various protein modification omics to elucidate these PTMs. These PTM omics are often combined with proteomics to facilitate more in-depth studies of pathophysiological mechanisms or the development of new biomarkers. For example, the combined application of proteomics and phosphoproteomics can more truly reflect the relationship between protein kinases and substrates. Phosphorylation modification can be different in these proteins whose expression is not different (153). The studies of PTMs in sepsis are summarized in **Table 3**.

In a study conducted by Chen et al. (79), liver mitochondrial proteins in CLP rats were isolated and evaluated using two-dimensional gel electrophoresis, and the protein spots were visualized using silver staining and analyzed with Bio-2D software. Three spots of the same molecular weight (MP1, MP2, and MP3) were significantly altered (79). All three spots are the same enzyme, ALDH2. During sepsis, MP1 and MP2 are downregulated, whereas MP3 is upregulated concomitantly (MP1 and MP2 shift to MP3), leading to a decrease in the ALDH2 activity. In addition, MP1 and MP2 presented a higher degree of protein phosphorylation than MP3. Thus, it is speculated that protein phosphorylation may affect ALDH2 enzymatic activity; that is, MP1 and MP2 with higher phosphorylation have a higher enzymatic activity than MP3 with lower phosphorylation (79). This study demonstrated that a PTM, phosphorylation of ALDH2, may play a role in the pathogenesis of sepsis and provide a new target for the therapy (79).

Wang et al. (163) found that mouse macrophage-like RAW 264.7 cells stimulated with LPS began to release a nuclear protein, high mobility group box 1 (HMGB1), after the peak release of early inflammatory factors, such as TNF and IL-1. HMGB1 plays a role in inflammatory regulation and stress response; it is an important inflammatory mediator in the late phase of sepsis and a late predictor of mortality in sepsis patients (164, 165). HMGB1 is a non-histone DNA-binding protein, and its function is closely related to its cellular location. Under stimulation conditions such as hypoxia and oxidative stresses, protein post-translationally modified HMGB1 translocates from

TABLE 3 | Summary of post-translational modifications in sepsis.

Protein	Type of PTM	Main Conclusions	Ref.
ALDH2	Phosphorylation	MP1 and MP2 with higher phosphorylation have a higher enzymatic activity than MP3 with lower phosphorylation (MP1, MP2 and MP3 are the subtypes of ALDH2).	(79)
HMGB1	Redox modification	ROS partially oxidize HMGB1 to form disulfate-type HMGB1, inducing inflammatory cells to produce a range of cytokines to promote the inflammatory response.	(43, 154, 155)
	Acetylation/ deacetylation	Lys acetylation after stimulation with LPS and TNF-α, leads to conformational changes in HMGB1, separation from SIRT1 and transport to the cytoplasm, followed by the release into the extracellular space, which would subsequently activate downstream inflammatory signaling.	
Histone H3	Citrullination	CitH3 was significantly increased in the CLP-induced mice sepsis model. Inhibitors of PAD4 modulate citrullination and reduce CitH3 levels, thereby improving survival in sepsis mice.	(156, 157)
NLRP3	Phosphorylation	Phosphorylation of serine 5 in the PYD inhibits the activation of NLRP3.	(158, 159)
	Ubiquitylation	Sequential ubiquitination of NLRP3 by RNF125 and Cbl-b inhibits the activation of NLRP3 and prevents the development of sepsis in mice.	
Cysteine residues of various signaling proteins	Nitrosylation	SIRT1 activity decreases with increasing S-nitrosylation of SIRT1, resulting in extracellular HMGB1 release. Increased levels of iNOS, leading to enhanced production of NO, induces S-nitrosylation of SIRT1. During the transformation of LPS-stimulated macrophages from the resting state to the M1 type, the expression levels of iNOS and NO were increased, and mitochondrial complexes I and IV were modified by nitrosylation, resulting in the destruction of the mitochondrial electron transfer chain and inhibition of OXPHOS.	(160–162)

ALDH2, Aldehyde dehydrogenase; HMGB 1, High mobility group box 1; ROS, Reactive oxygen species; LPS, Lipopolysaccharide;TNF, Tumor necrosis factor, SIRT1, Sirtuin1; CitH3, Citrullinated Histone H3; CLP, Cecal ligation and puncture; PAD4, Protein-arginine deiminase type-4; NLRP3, NOD-like receptor protein 3; PYD, Pyrin domain;iNOS, inducible nitric oxide synthase; NO, Nitric oxide; OXPHOS, Oxidative phosphorylation.

the nucleus to the cytoplasm or is released into the extracellular space. Acetylation, glycosylation, phosphorylation, ADP-ribosylation, methylation, and redox are the main PTMs of HMGB l. Cys 23, Cys 45, and Cys l06 are key sites for their redox modification, and acetylation and phosphorylation mainly act on HMGB l nuclear localization sequences (NLSs) (164). Under physiological conditions, nuclear HMGBl is a perthiol-type HMGBl in the reduced state. The Cys23, Cys45, and Cysl06 sites connect the thiol side chains (166). ROS generation increases in the perivascular endothelium and tubules of the kidney in an LPS-induced sepsis model. ROS partially oxidize HMGBl to form disulfate-type HMGBl, which confers its cytokine activity and induces inflammatory cells to produce a range of cytokines to promote the inflammatory response (43). In murine macrophage RAW264.7 cells, SIRTl interacts with multiple Lys28-30 on HMGBl to form a complex (154). Lys acetylation after stimulation with LPS and TNF-α leads to conformational changes in HMGBl, separation from SIRTl, and transport to the cytoplasm, followed by the release into the extracellular space, which would subsequently activate downstream inflammatory signaling. In a mouse model of endotoxemia, deacetylation-mediated interaction of SIRT1-HMGB1 improves survival (155).

Histones are highly conserved basic cationic proteins in the cellular chromatin of eukaryotic organisms and are mainly divided into core histones (H2A, H2B, H3, and H4) and linker histones (H1 and H5). The important function of histones is PTMs, including acetylation, methylation, phosphorylation, ubiquitinylation, citrullination, acylation, or glycosylation of ADP. When histones are released into the extracellular space, they are called extracellular histones. The production pathways of extracellular histones include passive necrosis (the membrane is damaged by mechanical trauma or charge- or detergent-related toxicity), NETosis/ETosis (neutrophils/macrophages), necroptosis, pyroptosis, and ferroptosis (167–169). Xu et al. (170) demonstrated that extracellular histones have cytotoxic effects *in vivo* and *in vitro*. In addition, extracellular histones are an endogenous DAMP. By acting on the TLR, they activate various downstream pathways, release many proinflammatory factors (e.g., IL-6, IL-10, TNF-α), and induce platelet aggregation (171, 172). It has been shown that in sepsis patients, circulating histone levels are increased and can cause multiple organ damage (173). This may be caused by a combination of the above mechanisms. There is a close link between the citrullination of histone H3 and sepsis (174). Circulating citrullinated histone H3 (CitH3, a component of NETs) was significantly increased in the CLP-induced mouse sepsis model (156). Inhibitors of protein-arginine deiminase type-4 (PAD4, an enzyme that promotes CitH3 production) modulate this citrullination and reduce CitH3 levels, thereby improving survival in sepsis mice (157). Thus, extracellular histones are involved in the development of sepsis; however, the pathogenic mechanism of their PTMs in sepsis needs further study.

Inflammasomes are protein complexes that promote the maturation and secretion of the cytokines pro-IL-1β and pro-IL-18 by activating caspase-1 (175). There are five inflammasomes, of which the NLRP3 inflammasome plays a key role in sepsis and multiple organ dysfunction as an important component of innate immunity (176). Lee et al. (177) found that NLRP3 deficiency suppressed inflammatory response and improved survival in sepsis mice. Zhong et al. (178) showed that the inhibition of the NLRP3/caspase-1/IL-1β pathway in macrophages attenuated the inflammatory response and microvascular leakage resulting from sepsis. NLRP3 is regulated by a variety of PTMs, including phosphorylation, ubiquitination, alkylation, S-nitrosylation, and ADP-ribosylation (179, 180). Using quantitative proteomics, Stutz et al. (158) found three phosphorylation sites for NLRP3. Among them, they found that the phosphorylation of serine 5 in the pyrin domain inhibits the activation of NLRP3 inflammasome. Phosphatase 2A (PP2A) inhibitors were confirmed using MS to cause increased phosphorylation of serine 5 in LPS-induced macrophages, thereby inhibiting NLRP3 activation. Tang et al. (159) found that RNF125 and Cbl-b (two E3 ubiquitin ligases)

sequentially ubiquitinate NLRP3 to inhibit its activation and prevent the development of sepsis in mice. Thus, PTMs of NLRP3, particularly phosphorylation and ubiquitination, regulate its activation and play an important role in sepsis (181).

In sepsis, inflammatory mediators and cytokines induce iNOS production in various cells. NO generated by iNOS combines with the superoxide anion O_2^- to generate peroxynitrite. NO and peroxynitrite can affect the PTM, especially nitrosylation, of cysteine residues in various signaling proteins, such as those involved in excitation-contraction coupling, contraction, energy supply, anti-apoptosis, and anti-oxidative stress (182). S-Nitrosylation refers to the oxidative modification of cysteine by NO to form protein S-nitrosothiols (183). As mentioned above, acetylation of the lysine residues of HMGB1 leads to the release of HMGB1 into the extracellular space (155). SIRT1 activity decreases with increasing S-nitrosylation of SIRT1, resulting in extracellular HMGB1 release (160). Increased levels of iNOS, leading to enhanced production of NO, induce S-nitrosylation of SIRT1 (161). S-Nitroso-N-acetylpenicillamine, as a donor of NO, can increase both S-nitrosylated-SIRT1 levels and the consequent release of HMGB1 (160). NO and NO-mediated PTM can also regulate macrophage immunometabolism (184). Bailey et al. (185) showed that NO modulates the levels of essential TCA cycle-associated metabolites (e.g., citrate and succinate), the inflammatory mediator itaconate, and the complex I subunit in the respiratory chain in inflammatory murine macrophages. NO can also regulate mitochondrial fatty acid metabolism through reversible protein S-nitrosylation (186). During the transformation of LPS-stimulated macrophages from the resting state to the M1 type, the expression of iNOS and NO was increased, and mitochondrial complexes I and IV were modified by nitrosylation, resulting in the destruction of the mitochondrial electron transfer chain and inhibition of OXPHOS (162). Knockdown of iNOS ameliorated LPS-induced mitochondrial respiratory function impairment in M1 macrophages and promoted enhanced OXPHOS. However, treatment of exogenous NO caused mitochondrial dysfunction and promoted macrophage proinflammatory responses (187).

In summary, protein PTMs can affect the development of sepsis by regulating various signaling pathways. At present, proteins with PTMs in sepsis samples can be identified, and the modified amino acid sites can be located using MS combined with bioinformatics analysis.

CONCLUSIONS

Proteomics is a product of the post-genomic era and can be used to study the characteristics of proteins on a large scale. It is mainly used in medicine in the following aspects: 1) to identify markers for the diagnosis or prognosis of a disease, 2) to elucidate the mechanism of the disease and find potential therapeutic targets, and 3) for the classification of diseases. In this review, we have shown that proteomics has made a great contribution to the elucidation of the molecular mechanisms of sepsis; however, it still has some limitations. First, being a molecular technique, there are some inherent challenges. For example, the identification of low-abundance proteins is difficult. The development of protein isolation and identification techniques has provided many effective methods for identifying low-abundance proteins, but they are still not very satisfactory (188, 189). In addition, proteomics cannot be used to detect and identify unknown proteins. Second, biomarkers discovered using proteomics are rarely applied in the clinic, which may be because the number of samples studied is small, and there is high individual heterogeneity. The widespread clinical application of biomarkers requires population-scale validation of their effectiveness. The high cost and time-consuming nature of proteomics is also one of the reasons why most candidate markers are not applied in the clinic. Proteomics is usually employed as the first step in screening biomarkers, but it cannot determine the absolute concentration of proteins present in a sample. Large-scale screening of differentially expressed proteins is performed using high-throughput proteomics, and the sample size then needs to be expanded for the validation of potential biomarkers. Subsequently, western blotting or an enzyme-linked immunoassay is required to determine the expression of candidate biomarkers. Finally, the biomarkers are translated into targets with clinical application value (58). However, there is still a lack of standard techniques and methods for the evaluation and confirmation of the obtained biomarkers to determine their clinical value (58). At present, proteomics research on PTMs mainly focuses on tumors and cardiovascular diseases, and there are few studies on sepsis. In addition, post-translationally modified proteins are low in content in samples and have a wide dynamic range; therefore, enrichment is required to improve the abundance of modified proteins before mass spectrometry (190, 191). In summary, proteomics as a clinical application technology requires much improvement.

Despite the many limitations of proteomics, it is still used to revolutionize our insights into the complex biological processes of sepsis. Moreover, using proteomics in combination with genomics and metabolomics may help comprehensively understand the pathophysiological mechanisms underlying sepsis, determine potential biomarkers, and improve our approach to precision medicine (192).

AUTHOR CONTRIBUTIONS

HM designed the review and drafted the manuscript. RD and SC reviewed and revised the article. All authors contributed to the article and approved the submitted version.

FUNDING

This study was supported by the grant from LiaoNing Revitalization Talents Program (Grant No. XLYC2007001) and the grant from Changjiang Scholars Program of Ministry of Education of China (TG2019081) and the Natural Science Foundation of Hainan Province (Grant No. 819QN222) and the National Natural Science Foundation of China (Grant No. 81960346, No. 82172174).

REFERENCES

1. Coopersmith CM, De Backer D, Deutschman CS, Ferrer R, Lat I, Machado FR, et al. Surviving Sepsis Campaign: Research Priorities for Sepsis and Septic Shock. *Intensive Care Med* (2018) 44(9):1400–26. doi: 10.1007/s00134-018-5175-z
2. Singer M, Deutschman CS, Seymour CW, Shankar-Hari M, Annane D, Bauer M, et al. The Third International Consensus Definitions for Sepsis and Septic Shock (Sepsis-3). *JAMA* (2016) 315(8):801–10. doi: 10.1001/jama.2016.0287
3. Rudd KE, Johnson SC, Agesa KM, Shackelford KA, Tsoi D, Kievlan DR, et al. Global, Regional, and National Sepsis Incidence and Mortality, 1990–2017: Analysis for the Global Burden of Disease Study. *Lancet* (2020) 395 (10219):200–11. doi: 10.1016/s0140-6736(19)32989-7
4. Cecconi M, Evans L, Levy M, Rhodes A. Sepsis and Septic Shock. *Lancet (London England)* (2018) 392(10141):75–87. doi: 10.1016/S0140-6736(18)30696-2
5. Jawad I, Luksic I, Rafnsson SB. Assessing Available Information on the Burden of Sepsis: Global Estimates of Incidence, Prevalence and Mortality. *J Glob Health* (2012) 2(1):010404. doi: 10.7189/jogh.02.010404
6. Maslove DM, Wong HR. Gene Expression Profiling in Sepsis: Timing, Tissue, and Translational Considerations. *Trends Mol Med* (2014) 20 (4):204–13. doi: 10.1016/j.molmed.2014.01.006
7. Skibsted S, Bhasin MK, Aird WC, Shapiro NI. Bench-To-Bedside Review: Future Novel Diagnostics for Sepsis - a Systems Biology Approach. *Crit Care (London England)* (2013) 17(5):231. doi: 10.1186/cc12693
8. Mommert M, Tabone O, Guichard A, Oriol G, Cerrato E, Denizot M, et al. Dynamic LTR Retrotransposon Transcriptome Landscape in Septic Shock Patients. *Crit Care (London England)* (2020) 24(1):96. doi: 10.1186/s13054-020-2788-8
9. Burnham KL, Davenport EE, Radhakrishnan J, Humburg P, Gordon AC, Hutton P, et al. Shared and Distinct Aspects of the Sepsis Transcriptomic Response to Fecal Peritonitis and Pneumonia. *Am J Respir Crit Care Med* (2017) 196(3):328–39. doi: 10.1164/rccm.201608-1685OC
10. Tang BM, Huang SJ, McLean AS. Genome-Wide Transcription Profiling of Human Sepsis: A Systematic Review. *Crit Care (London England)* (2010) 14 (6):R237. doi: 10.1186/cc9392
11. Lee J, Banerjee D. Metabolomics and the Microbiome as Biomarkers in Sepsis. *Crit Care Clinics* (2020) 36(1):105–13. doi: 10.1016/j.ccc.2019.08.008
12. Mocellin S, Rossi CR, Traldi P, Nitti D, Lise M. Molecular Oncology in the Post-Genomic Era: The Challenge of Proteomics. *Trends Mol Med* (2004) 10 (1):24–32. doi: 10.1016/j.molmed.2003.11.001
13. Petricoin EF, Zoon KC, Kohn EC, Barrett JC, Liotta LA. Clinical Proteomics: Translating Benchside Promise Into Bedside Reality. *Nat Rev Drug Discov* (2002) 1(9):683–95. doi: 10.1038/nrd891
14. Aslam B, Basit M, Nisar MA, Khurshid M, Rasool MH. Proteomics: Technologies and Their Applications. *J Chromatogr Sci* (2017) 55(2):182–96. doi: 10.1093/chromsci/bmw167
15. Yu X, Schneiderhan-Marra N, Joos TO. Protein Microarrays for Personalized Medicine. *Clin Chem* (2010) 56(3):376–87. doi: 10.1373/clinchem.2009.137158
16. Ludwig KR, Hummon AB. Mass Spectrometry for the Discovery of Biomarkers of Sepsis. *Mol Biosyst* (2017) 13(4):648–64. doi: 10.1039/c6mb00656f
17. Arina P, Singer M. Pathophysiology of Sepsis. *Curr Opin Anaesthesiol* (2021) 34(2):77–84. doi: 10.1097/aco.0000000000000963
18. Jarczak D, Kluge S, Nierhaus A. Sepsis-Pathophysiology and Therapeutic Concepts. *Front Med (Lausanne)* (2021) 8:628302. doi: 10.3389/fmed.2021.628302
19. Cheng Z, Abrams ST, Toh J, Wang SS, Wang Z, Yu Q, et al. The Critical Roles and Mechanisms of Immune Cell Death in Sepsis. *Front Immunol* (2020) 11:1918. doi: 10.3389/fimmu.2020.01918
20. Angus DC, van der Poll T. Severe Sepsis and Septic Shock. *N Engl J Med* (2013) 369(9):840–51. doi: 10.1056/NEJMra1208623
21. Gotts JE, Matthay MA. Sepsis: Pathophysiology and Clinical Management. *Bmj* (2016) 353:i1585. doi: 10.1136/bmj.i1585
22. Ling-ling S, Yan-qiu H, Hui-juan R, Yang L, Jing Z. Research Advance of Pathology and Physiology of Sepsis. *Chin J Nosocomiol* (2016) 26(08):1914–6. doi: 10.11816/cn.ni.2016-152123
23. Denning NL, Aziz M, Gurien SD, Wang P. DAMPs and NETs in Sepsis. *Front Immunol* (2019) 10:2536. doi: 10.3389/fimmu.2019.02536
24. Wu R, Wang N, Comish PB, Tang D, Kang R. Inflammasome-Dependent Coagulation Activation in Sepsis. *Front Immunol* (2021) 12:641750. doi: 10.3389/fimmu.2021.641750
25. Okamoto T, Suzuki K. The Role of Gap Junction-Mediated Endothelial Cell-Cell Interaction in the Crosstalk Between Inflammation and Blood Coagulation. *Int J Mol Sci* (2017) 18(11):2254. doi: 10.3390/ijms18112254
26. Levi M, van der Poll T. Inflammation and Coagulation. *Crit Care Med* (2010) 38(2 Suppl):S26–34. doi: 10.1097/CCM.0b013e3181c98d21
27. Ding R, Meng Y, Ma X. The Central Role of the Inflammatory Response in Understanding the Heterogeneity of Sepsis-3. *BioMed Res Int* (2018) 2018:5086516. doi: 10.1155/2018/5086516
28. McBride MA, Patil TK, Bohannon JK, Hernandez A, Sherwood ER, Patil NK. Immune Checkpoints: Novel Therapeutic Targets to Attenuate Sepsis-Induced Immunosuppression. *Front Immunol* (2020) 11:624272. doi: 10.3389/fimmu.2020.624272
29. Schurr JW, Szumita PM, DeGrado JR. Neuroendocrine Derangements in Early Septic Shock: Pharmacotherapy for Relative Adrenal and Vasopressin Insufficiency. *Shock* (2017) 48(3):284–93. doi: 10.1097/shk.0000000000000864
30. Appiah MG, Park EJ, Akama Y, Nakamori Y, Kawamoto E, Gaowa A, et al. Cellular and Exosomal Regulations of Sepsis-Induced Metabolic Alterations. *Int J Mol Sci* (2021) 22(15):8295. doi: 10.3390/ijms22158295
31. Preau S, Vodovar D, Jung B, Lancel S, Zafrani L, Flatres A, et al. Energetic Dysfunction in Sepsis: A Narrative Review. *Ann Intensive Care* (2021) 11 (1):104. doi: 10.1186/s13613-021-00893-7
32. Wang X, Buechler NL, Woodruff AG, Long DL, Zabalawi M, Yoza BK, et al. Sirtuins and Immuno-Metabolism of Sepsis. *Int J Mol Sci* (2018) 19(9):2738. doi: 10.3390/ijms19092738
33. Liu YC, Zou XB, Chai YF, Yao YM. Macrophage Polarization in Inflammatory Diseases. *Int J Biol Sci* (2014) 10(5):520–9. doi: 10.7150/ijbs.8879
34. Shen Y, Song J, Wang Y, Chen Z, Zhang L, Yu J, et al. M2 Macrophages Promote Pulmonary Endothelial Cells Regeneration in Sepsis-Induced Acute Lung Injury. *Ann Transl Med* (2019) 7(7):142. doi: 10.21037/atm.2019.02.47
35. Kumar V. Targeting Macrophage Immunometabolism: Dawn in the Darkness of Sepsis. *Int Immunopharmacol* (2018) 58:173–85. doi: 10.1016/j.intimp.2018.03.005
36. Viola A, Munari F, Sánchez-Rodríguez R, Scolaro T, Castegna A. The Metabolic Signature of Macrophage Responses. *Front Immunol* (2019) 10:1462. doi: 10.3389/fimmu.2019.01462
37. Huang M, Cai S, Su J. The Pathogenesis of Sepsis and Potential Therapeutic Targets. *Int J Mol Sci* (2019) 20(21):5376. doi: 10.3390/ijms20215376
38. van der Poll T, van de Veerdonk FL, Scicluna BP, Netea MG. The Immunopathology of Sepsis and Potential Therapeutic Targets. *Nat Rev Immunol* (2017) 17(7):407–20. doi: 10.1038/nri.2017.36
39. Lelubre C, Vincent JL. Mechanisms and Treatment of Organ Failure in Sepsis. *Nat Rev Nephrol* (2018) 14(7):417–27. doi: 10.1038/s41581-018-0005-7
40. Joffre J, Hellman J, Ince C, Ait-Oufella H. Endothelial Responses in Sepsis. *Am J Respir Crit Care Med* (2020) 202(3):361–70. doi: 10.1164/rccm.201910-1911TR
41. Dauphinee SM, Karsan A. Lipopolysaccharide Signaling in Endothelial Cells. *Lab Invest* (2006) 86(1):9–22. doi: 10.1038/labinvest.3700366
42. Berg RM, Møller K, Bailey DM. Neuro-Oxidative-Nitrosative Stress in Sepsis. *J Cereb Blood Flow Metab* (2011) 31(7):1532–44. doi: 10.1038/jcbfm.2011.48
43. Abdulmahdi W, Patel D, Rabadi MM, Azar T, Jules E, Lipphardt M, et al. HMGB1 Redox During Sepsis. *Redox Biol* (2017) 13:600–7. doi: 10.1016/j.redox.2017.08.001
44. Yan L, Qian L. Clinical Research Progress on the Mechanism of Multiple Organ Damage Caused by Sepsis. *J Jinzhou Med Univ* (2020) 41(04):108–12. doi: 10.13847/j.cnki.lnmu.2020.04.026
45. Seymour CW, Kennedy JN, Wang S, Chang CH, Elliott CF, Xu Z, et al. Derivation, Validation, and Potential Treatment Implications of Novel Clinical Phenotypes for Sepsis. *Jama* (2019) 321(20):2003–17. doi: 10.1001/jama.2019.5791
46. Stanski NL, Wong HR. Prognostic and Predictive Enrichment in Sepsis. *Nat Rev Nephrol* (2020) 16(1):20–31. doi: 10.1038/s41581-019-0199-3

47. Leligdowicz A, Matthay MA. Heterogeneity in Sepsis: New Biological Evidence With Clinical Applications. *Crit Care* (2019) 23(1):80. doi: 10.1186/s13054-019-2372-2
48. Blangy-Letheule A, Persello A, Rozec B, Waard M, Lauzier B. New Approaches to Identify Sepsis Biomarkers: The Importance of Model and Sample Source for Mass Spectrometry. *Oxid Med Cell Longev* (2020) 2020:6681073. doi: 10.1155/2020/6681073
49. Lin L, Zheng J, Yu Q, Chen W, Xing J, Chen C, et al. High Throughput and Accurate Serum Proteome Profiling by Integrated Sample Preparation Technology and Single-Run Data Independent Mass Spectrometry Analysis. *J Proteomics* (2018) 174:9–16. doi: 10.1016/j.jprot.2017.12.014
50. Anderson NL, Anderson NG. The Human Plasma Proteome: History, Character, and Diagnostic Prospects. *Mol Cell Proteomics MCP* (2002) 1 (11):845–67. doi: 10.1074/mcp.R200007-MCP200
51. Lee PY, Osman J, Low TY, Jamal R. Plasma/serum Proteomics: Depletion Strategies for Reducing High-Abundance Proteins for Biomarker Discovery. *Bioanalysis* (2019) 11(19):1799–812. doi: 10.4155/bio-2019-0145
52. Issaq HJ, Xiao Z, Veenstra TD. Serum and Plasma Proteomics. *Chem Rev* (2007) 107(8):3601–20. doi: 10.1021/cr068287r
53. Selvaraju S, Rassi ZE. Liquid-Phase-Based Separation Systems for Depletion, Prefractionation and Enrichment of Proteins in Biological Fluids and Matrices for in-Depth Proteomics Analysis–an Update Covering the Period 2008-2011. *Electrophoresis* (2012) 33(1):74–88. doi: 10.1002/elps.201100431
54. Puangpila C, Mayadunne E, El Rassi Z. Liquid Phase Based Separation Systems for Depletion, Prefractionation, and Enrichment of Proteins in Biological Fluids and Matrices for in-Depth Proteomics Analysis-An Update Covering the Period 2011-2014. *Electrophoresis* (2015) 36(1):238–52. doi: 10.1002/elps.201400434
55. El Rassi Z, Puangpila C. Liquid-Phase Based Separation Systems for Depletion, Prefractionation, and Enrichment of Proteins in Biological Fluids and Matrices for in-Depth Proteomics Analysis-An Update Covering the Period 2014-2016. *Electrophoresis* (2017) 38(1):150–61. doi: 10.1002/elps.201600413
56. Linke T, Doraiswamy S, Harrison EH. Rat Plasma Proteomics: Effects of Abundant Protein Depletion on Proteomic Analysis. *J chromatogr B Anal Technol Biomed Life Sci* (2007) 849(1-2):273–81. doi: 10.1016/j.jchromb.2006.11.051
57. Tu C, Rudnick PA, Martinez MY, Cheek KL, Stein SE, Slebos RJC, et al. Depletion of Abundant Plasma Proteins and Limitations of Plasma Proteomics. *J Proteome Res* (2010) 9(10):4982–91. doi: 10.1021/pr100646w
58. Geyer PE, Holdt LM, Teupser D, Mann M. Revisiting Biomarker Discovery by Plasma Proteomics. *Mol Syst Biol* (2017) 13(9):942. doi: 10.15252/msb.20156297
59. Lee H-J, Lee E-Y, Kwon M-S, Paik Y-K. Biomarker Discovery From the Plasma Proteome Using Multidimensional Fractionation Proteomics. *Curr Opin Chem Biol* (2006) 10(1):42–9. doi: 10.1016/j.cbpa.2006.01.007
60. Fliser D, Novak J, Thongboonkerd V, Argilés A, Jankowski V, Girolami MA, et al. Advances in Urinary Proteome Analysis and Biomarker Discovery. *J Am Soc Nephrol JASN* (2007) 18(4):1057–71. doi: 10.1681/ASN.2006090956
61. Jiang S, Wang Y, Liu Z. The Application of Urinary Proteomics for the Detection of Biomarkers of Kidney Diseases. *Adv Exp Med Biol* (2015) 845:151–65. doi: 10.1007/978-94-017-9523-4_15
62. Caubet C, Lacroix C, Decramer S, Drube J, Ehrich JHH, Mischak H, et al. Advances in Urinary Proteome Analysis and Biomarker Discovery in Pediatric Renal Disease. *Pediatr Nephrol (Berlin Germany)* (2010) 25 (1):27–35. doi: 10.1007/s00467-009-1251-5
63. Malmström E, Kilsgård O, Hauri S, Smeds E, Herwald H, Malmström L, et al. Large-Scale Inference of Protein Tissue Origin in Gram-Positive Sepsis Plasma Using Quantitative Targeted Proteomics. *Nat Commun* (2016) 7:10261. doi: 10.1038/ncomms10261
64. Cao Z, Robinson RAS. The Role of Proteomics in Understanding Biological Mechanisms of Sepsis. *Proteomics Clin Appl* (2014) 8(1-2):35–52. doi: 10.1002/prca.201300101
65. Lässer C, Eldh M and Lötvall J. Isolation and Characterization of RNA-Containing Exosomes. *J Visualized Exp JoVE* (2012) 59):e3037. doi: 10.3791/3037
66. Simpson RJ, Jensen SS and Lim JWE. Proteomic Profiling of Exosomes: Current Perspectives. *Proteomics* (2008) 8(19):4083–99. doi: 10.1002/pmic.200800109
67. Xu Y, Ku X, Wu C, Cai C, Tang J and Yan W. Exosomal Proteome Analysis of Human Plasma to Monitor Sepsis Progression. *Biochem Biophys Res Commun* (2018) 499(4):856–61. doi: 10.1016/j.bbrc.2018.04.006
68. Lässer C, Alikhani VS, Ekström K, Eldh M, Paredes PT, Bossios A, et al. Human Saliva, Plasma and Breast Milk Exosomes Contain RNA: Uptake by Macrophages. *J Trans Med* (2011) 9:9. doi: 10.1186/1479-5876-9-9
69. Simpson RJ, Lim JW, Moritz RL, Mathivanan S. Exosomes: Proteomic Insights and Diagnostic Potential. *Expert Rev Proteomics* (2009) 6(3):267–83. doi: 10.1586/epr.09.17
70. Buras JA, Holzmann B, Sitkovsky M. Animal Models of Sepsis: Setting the Stage. *Nat Rev Drug Discovery* (2005) 4(10):854–65. doi: 10.1038/nrd1854
71. Rittirsch D, Huber-Lang MS, Flierl MA, Ward PA. Immunodesign of Experimental Sepsis by Cecal Ligation and Puncture. *Nat Protoc* (2009) 4 (1):31–6. doi: 10.1038/nprot.2008.214
72. Róka B, Tod P, Kaucsár T, Vizovišek M, Vidmar R, Turk B, et al. The Acute Phase Response Is a Prominent Renal Proteome Change in Sepsis in Mice. *Int J Mol Sci* (2019) 21(1):200. doi: 10.3390/ijms21010200
73. Matejovic M, Tuma Z, Moravec J, Valesova L, Sykora R, Chvojka J, et al. Renal Proteomic Responses to Severe Sepsis and Surgical Trauma: Dynamic Analysis of Porcine Tissue Biopsies. *Shock* (2016) 46(4):453–64. doi: 10.1097/SHK.0000000000000613
74. Hinkelbein J, Bohm L, Braunecker S, Adler C, De Robertis E, Cirillo F. Decreased Tissue COX5B Expression and Mitochondrial Dysfunction During Sepsis-Induced Kidney Injury in Rats. *Oxid Med Cell Longev* (2017) 2017:8498510. doi: 10.1155/2017/8498510
75. Hinkelbein J, Feldmann RE, Peterka A, Schubert C, Schelshorn D, Maurer MH, et al. Alterations in Cerebral Metabolomics and Proteomic Expression During Sepsis. *Curr Neurovascular Res* (2007) 4(4):280–8. doi: 10.2174/156720207782446388
76. Yang Q, Chen Q, Yang G, Cao Y, Lu W. Proteomic Study of Septic Encephalopathy Based on iTRAQ Technology. *Chin J Clin Pharmacol Ther* (2019) 24(11):1269–74. doi: 10.12092/j.issn.1009-2501.2019.11.009
77. Xie K, Lian N, Kan Y, Yang M, Pan J, Yu Y, et al. iTRAQ-Based Quantitative Proteomic Analysis of the Therapeutic Effects of 2% Hydrogen Gas Inhalation on Brain Injury in Septic Mice. *Brain Res* (2020) 1746:147003. doi: 10.1016/j.brainres.2020.147003
78. Wang G, Jin S, Ling X, Li Y, Hu Y, Zhang Y, et al. Proteomic Profiling of LPS-Induced Macrophage-Derived Exosomes Indicates Their Involvement in Acute Liver Injury. *Proteomics* (2018) 19(3):e1800274. doi: 10.1002/pmic.201800274
79. Chen HW, Kuo HT, Hwang LC, Kuo MF, Yang RC. Proteomic Alteration of Mitochondrial Aldehyde Dehydrogenase 2 in Sepsis Regulated by Heat Shock Response. *Shock* (2007) 28(6):710–6. doi: 10.1097/shk.0b013e318050c8c2
80. Dear JW, Leelahavanichkul A, Aponte A, Hu X, Constant SL, Hewitt SM, et al. Liver Proteomics for Therapeutic Drug Discovery: Inhibition of the Cyclophilin Receptor CD147 Attenuates Sepsis-Induced Acute Renal Failure. *Crit Care Med* (2007) 35(10):2319–28. doi: 10.1097/01.CCM.0000281858.44387.A2
81. Bian Y, Qin C, Xin Y, Yu Y, Chen H, Wang G, et al. Itraq-Based Quantitative Proteomic Analysis of Lungs in Murine Polymicrobial Sepsis With Hydrogen Gas Treatment. *Shock* (2018) 49(2):187–95. doi: 10.1097/SHK.0000000000000927
82. Hinkelbein J, Kalenka A, Schubert C, Peterka A, Feldmann RE. Proteome and Metabolome Alterations in Heart and Liver Indicate Compromised Energy Production During Sepsis. *Protein Pept Lett* (2010) 17(1):18–31. doi: 10.2174/092986610789909520
83. Duan X, Berthiaume F, Yarmush D, Yarmush ML. Proteomic Analysis of Altered Protein Expression in Skeletal Muscle of Rats in a Hypermetabolic State Induced by Burn Sepsis. *Biochem J* (2006) 397(1):149–58. doi: 10.1042/BJ20051710
84. Thongboonkerd V, Chiangjong W, Mares J, Moravec J, Tuma Z, Karvunidis T, et al. Altered Plasma Proteome During an Early Phase of Peritonitis-Induced Sepsis. *Clin Sci (Lond)* (2009) 116(9):721–30. doi: 10.1042/CS20080478

85. Ren Y, Wang J, Xia J, Jiang C, Zhao K, Li R, et al. The Alterations of Mouse Plasma Proteins During Septic Development. *J Proteome Res* (2007) 6 (7):2812–21. doi: 10.1021/pr070047k
86. Hu JY, Li CL, Wang YW. Altered Proteomic Pattern in Platelets of Rats With Sepsis. *Blood Cells Mol Dis* (2012) 48(1):30–5. doi: 10.1016/j.bcmd.2011.09.010
87. Bellomo R, Kellum JA, Ronco C, Wald R, Martensson J, Maiden M, et al. Acute Kidney Injury in Sepsis. *Intensive Care Med* (2017) 43(6):816–28. doi: 10.1007/s00134-017-4755-7
88. Vincent JL, Sakr Y, Sprung CL, Ranieri VM, Reinhart K, Gerlach H, et al. Sepsis in European Intensive Care Units: Results of the SOAP Study. *Crit Care Med* (2006) 34(2):344–53. doi: 10.1097/01.ccm.0000194725.48928.3a
89. Peerapornratana S, Manrique-Caballero CL, Gómez H, Kellum JA. Acute Kidney Injury From Sepsis: Current Concepts, Epidemiology, Pathophysiology, Prevention and Treatment. *Kidney Int* (2019) 96 (5):1083–99. doi: 10.1016/j.kint.2019.05.026
90. Poston JT, Koyner JL. Sepsis Associated Acute Kidney Injury. *Bmj* (2019) 364:k4891. doi: 10.1136/bmj.k4891
91. Kellum JA, Prowle JR. Paradigms of Acute Kidney Injury in the Intensive Care Setting. *Nat Rev Nephrol* (2018) 14(4):217–30. doi: 10.1038/nrneph.2017.184
92. Kadenbach B, Hüttemann M, Arnold S, Lee I, Bender E. Mitochondrial Energy Metabolism is Regulated *via* Nuclear-Coded Subunits of Cytochrome C Oxidase. *Free Radical Biol Med* (2000) 29(3-4):211–21. doi: 10.1016/S0891-5849(00)00305-1
93. Gofton TE, Young GB. Sepsis-Associated Encephalopathy. *Nat Rev Neurol* (2012) 8(10):557–66. doi: 10.1038/nrneurol.2012.183
94. Chung H-Y, Wickel J, Brunkhorst FM, Geis C. Sepsis-Associated Encephalopathy: From Delirium to Dementia? *J Clin Med* (2020) 9 (3):703. doi: 10.3390/jcm9030703
95. Helbing D-L, Böhm L, Witte OW. Sepsis-Associated Encephalopathy. *CMAJ Can Med Assoc J = J l'Assoc Med Can* (2018) 190(36):E1083. doi: 10.1503/cmaj.180454
96. Lindquist S, Craig EA. The Heat-Shock Proteins. *Annu Rev Genet* (1988) 22:631–77. doi: 10.1146/annurev.ge.22.120188.003215
97. Morimoto RI, Santoro MG. Stress-Inducible Responses and Heat Shock Proteins: New Pharmacologic Targets for Cytoprotection. *Nat Biotechnol* (1998) 16(9):833–8. doi: 10.1038/nbt0998-833
98. Chan JYH, Cheng HL, Chou JLJ, Li FCH, Dai KY, Chan SHH, et al. Heat Shock Protein 60 or 70 Activates Nitric-Oxide Synthase (NOS) I- and Inhibits NOS II-Associated Signaling and Depresses the Mitochondrial Apoptotic Cascade During Brain Stem Death. *J Biol Chem* (2007) 282 (7):4585–600. doi: 10.1074/jbc.M603394200
99. Li Y, Zhu X, Zhang M, Tong H, Su L. Heatstroke-Induced Hepatocyte Exosomes Promote Liver Injury by Activating the NOD-Like Receptor Signaling Pathway in Mice. *PeerJ* (2019) 7:e8216. doi: 10.7717/peerj.8216
100. Crouser ED, Julian MW, Huff JE, Mandich DV, Green-Church KB. A Proteomic Analysis of Liver Mitochondria During Acute Endotoxemia. *Intensive Care Med* (2006) 32(8):1252–62. doi: 10.1007/s00134-006-0224-4
101. Zhao Y, Wang B, Zhang J, He D, Zhang Q, Pan C, et al. ALDH2 (Aldehyde Dehydrogenase 2) Protects Against Hypoxia-Induced Pulmonary Hypertension. *Arteriosclerosis Thrombosis Vasc Biol* (2019) 39(11):2303–19. doi: 10.1161/ATVBAHA.119.312946
102. Kang P, Wang J, Fang D, Fang T, Yu Y, Zhang W, et al. Activation of ALDH2 Attenuates High Glucose Induced Rat Cardiomyocyte Fibrosis and Necroptosis. *Free Radical Biol Med* (2020) 146:198–210. doi: 10.1016/j.freeradbiomed.2019.10.416
103. Long P, He M, Yan W, Chen W, Wei D, Wang S, et al. ALDH2 Protects Naturally Aged Mouse Retina Inhibiting Oxidative Stress-Related Apoptosis and Enhancing Unfolded Protein Response in Endoplasmic Reticulum. *Aging* (2020) 13(2):2750–67. doi: 10.18632/aging.202325
104. Dawar FU, Xiong Y, Khattak MNK, Li J, Lin L and Mei J. Potential Role of Cyclophilin A in Regulating Cytokine Secretion. *J Leukoc Biol* (2017) 102 (4):989–92. doi: 10.1189/jlb.3RU0317-090RR
105. Nigro P, Pompilio G, Capogrossi MC. Cyclophilin A: A Key Player for Human Disease. *Cell Death Dis* (2013) 4:e888. doi: 10.1038/cddis.2013.410
106. Yurchenko V, Constant S, Eisenmesser E, Bukrinsky M. Cyclophilin-CD147 Interactions: A New Target for Anti-Inflammatory Therapeutics. *Clin Exp Immunol* (2010) 160(3):305–17. doi: 10.1111/j.1365-2249.2010.04115.x
107. Pelosi P, D'Onofrio D, Chiumello D, Paolo S, Chiara G, Capelozzi VL, et al. Pulmonary and Extrapulmonary Acute Respiratory Distress Syndrome are Different. *Eur Respir J Suppl* (2003) 42:48s–56s. doi: 10.1183/09031936.03.00420803
108. Thompson BT, Chambers RC, Liu KD. Acute Respiratory Distress Syndrome. *New Engl J Med* (2017) 377(6):562–72. doi: 10.1056/NEJMra1608077
109. Gajic O, Dabbagh O, Park PK, Adesanya A, Chang SY, Hou P, et al. Early Identification of Patients at Risk of Acute Lung Injury: Evaluation of Lung Injury Prediction Score in a Multicenter Cohort Study. *Am J Respir Crit Care Med* (2011) 183(4):462–70. doi: 10.1164/rccm.201004-0549OC
110. Yu Y, Yang Y, Bian Y, Li Y, Liu L, Zhang H, et al. Hydrogen Gas Protects Against Intestinal Injury in Wild Type But Not NRF2 Knockout Mice With Severe Sepsis by Regulating HO-1 and HMGB1 Release. *Shock (Augusta Ga.)* (2017) 48(3):364–70. doi: 10.1097/SHK.0000000000000856
111. Li Y, Xie K, Chen H, Wang G, Yu Y. Hydrogen Gas Inhibits High-Mobility Group Box 1 Release in Septic Mice by Upregulation of Heme Oxygenase 1. *J Surg Res* (2015) 196(1):136–48. doi: 10.1016/j.jss.2015.02.042
112. Jiang Y, Bian Y, Lian N, Wang Y, Xie K, Qin C, et al. iTRAQ-Based Quantitative Proteomic Analysis of Intestines in Murine Polymicrobial Sepsis With Hydrogen Gas Treatment. *Drug Des Devel Ther* (2020) 14:4885–900. doi: 10.2147/DDDT.S271191
113. Vieillard-Baron A, Caille V, Charron C, Belliard G, Page B, Jardin F. Actual Incidence of Global Left Ventricular Hypokinesia in Adult Septic Shock. *Crit Care Med* (2008) 36(6):1701–6. doi: 10.1097/CCM.0b013e318174db05
114. Watts JA, Kline JA, Thornton LR, Grattan RM, Brar SS. Metabolic Dysfunction and Depletion of Mitochondria in Hearts of Septic Rats. *J Mol Cell Cardiol* (2004) 36(1):141–50. doi: 10.1016/j.yjmcc.2003.10.015
115. Brealey D, Brand M, Hargreaves I, Heales S, Land J, Smolenski R, et al. Association Between Mitochondrial Dysfunction and Severity and Outcome of Septic Shock. *Lancet (London England)* (2002) 360(9328):219–23. doi: 10.1016/S0140-6736(02)09459-X
116. Hanna J, Guerra-Moreno A, Ang J, Micoogullari Y. Protein Degradation and the Pathologic Basis of Disease. *Am J Pathol* (2019) 189(1):94–103. doi: 10.1016/j.ajpath.2018.09.004
117. Pernemalm M, Lehtiö J. Mass Spectrometry-Based Plasma Proteomics: State of the Art and Future Outlook. *Expert Rev Proteomics* (2014) 11(4):431–48. doi: 10.1586/14789450.2014.901157
118. Hohn A, Iovino I, Cirillo F, Drinhaus H, Kleinbrahm K, Boehm L, et al. Bioinformatical Analysis of Organ-Related (Heart, Brain, Liver, and Kidney) and Serum Proteomic Data to Identify Protein Regulation Patterns and Potential Sepsis Biomarkers. *BioMed Res Int* (2018) 2018:3576157. doi: 10.1155/2018/3576157
119. Dyson A, Singer M. Animal Models of Sepsis: Why Does Preclinical Efficacy Fail to Translate to the Clinical Setting? *Crit Care Med* (2009) 37(1 Suppl): S30–7. doi: 10.1097/CCM.0b013e3181922bd3
120. Kingsley SM, Bhat BV. Differential Paradigms in Animal Models of Sepsis. *Curr Infect Dis Rep* (2016) 18(9):26. doi: 10.1007/s11908-016-0535-8
121. Shah BA, Padbury JF. Neonatal Sepsis: An Old Problem With New Insights. *Virulence* (2014) 5(1):170–8. doi: 10.4161/viru.26906
122. Mankowski RT, Anton SD, Ghita GL, Brumback B, Cox MC, Mohr AM, et al. Older Sepsis Survivors Suffer Persistent Disability Burden and Poor Long-Term Survival. *J Am Geriatrics Soc* (2020) 68(9):1962–9. doi: 10.1111/jgs.16435
123. Ganatra HA, Stoll BJ, Zaidi AKM. International Perspective on Early-Onset Neonatal Sepsis. *Clinics Perinatol* (2010) 37(2):501–23. doi: 10.1016/j.clp.2010.02.004
124. Zea-Vera A, Ochoa TJ. Challenges in the Diagnosis and Management of Neonatal Sepsis. *J Trop Paediatrics* (2015) 61(1):1–13. doi: 10.1093/tropej/fmu079
125. Rowe TA, McKoy JM. Sepsis in Older Adults. *Infect Dis Clinics North Am* (2017) 31(4):731–42. doi: 10.1016/j.idc.2017.07.010
126. Cao Z, Yende S, Kellum JA, Angus DC, Robinson RA. Proteomics Reveals Age-Related Differences in the Host Immune Response to Sepsis. *J Proteome Res* (2014) 13(2):422–32. doi: 10.1021/pr400814s
127. Buhimschi CS, Bhandari V, Hamar BD, Bahtiyar M-O, Zhao G, Sfakianaki AK, et al. Proteomic Profiling of the Amniotic Fluid to Detect Inflammation, Infection, and Neonatal Sepsis. *PloS Med* (2007) 4(1):e18. doi: 10.1371/journal.pmed.0040018

128. Buhimschi CS, Bhandari V, Dulay AT, Nayeri UA, Abdel-Razeq SS, Pettker CM, et al. Proteomics Mapping of Cord Blood Identifies Haptoglobin "Switch-on" Pattern as Biomarker of Early-Onset Neonatal Sepsis in Preterm Newborns. *PloS One* (2011) 6(10):e26111. doi: 10.1371/journal.pone.0026111
129. Kalenka A, Feldmann REJ, Otero K, Maurer MH, Waschke KF, Fiedler F. Changes in the Serum Proteome of Patients With Sepsis and Septic Shock. *Anesthesia Analg* (2006) 103(6):1522–6. doi: 10.1213/01.ane.0000242533.59457.70
130. Raju MS VJ, Kamaraju RS, Sritharan V, Rajkumar K, Natarajan S, Kumar AD, et al. Continuous Evaluation of Changes in the Serum Proteome From Early to Late Stages of Sepsis Caused by Klebsiella Pneumoniae. *Mol Med Rep* (2016) 13(6):4835–44. doi: 10.3892/mmr.2016.5112
131. Sharma NK, Tashima AK, Brunialti MKC, Ferreira ER, Torquato RJS, Mortara RA, et al. Proteomic Study Revealed Cellular Assembly and Lipid Metabolism Dysregulation in Sepsis Secondary to Community-Acquired Pneumonia. *Sci Rep* (2017) 7(1):15606. doi: 10.1038/s41598-017-15755-1
132. Sharma NK, Ferreira BL, Tashima AK, Brunialti MKC, Torquato RJS, Bafi A, et al. Lipid Metabolism Impairment in Patients With Sepsis Secondary to Hospital Acquired Pneumonia, a Proteomic Analysis. *Clin Proteomics* (2019) 16:29. doi: 10.1186/s12014-019-9252-2
133. Su L, Zhou R, Liu C, Wen B, Xiao K, Kong W, et al. Urinary Proteomics Analysis for Sepsis Biomarkers With iTRAQ Labeling and Two-Dimensional Liquid Chromatography-Tandem Mass Spectrometry. *J Trauma Acute Care Surg* (2013) 74(3):940–5. doi: 10.1097/TA.0b013e31828272c5
134. Su L, Cao L, Zhou R, Jiang Z, Xiao K, Kong W, et al. Identification of Novel Biomarkers for Sepsis Prognosis via Urinary Proteomic Analysis Using iTRAQ Labeling and 2D-LC-MS/MS. *PloS One* (2013) 8(1):e54237. doi: 10.1371/journal.pone.0054237
135. Liu J, Li J, Deng X. Proteomic Analysis of Differential Protein Expression in Platelets of Septic Patients. *Mol Biol Rep* (2014) 41(5):3179–85. doi: 10.1007/s11033-014-3177-7
136. de Azambuja Rodrigues PM, Valente RH, Brunoro GVF, Nakaya HTI, Araújo-Pereira M, Bozza PT, et al. Proteomics Reveals Disturbances in the Immune Response and Energy Metabolism of Monocytes From Patients With Septic Shock. *Sci Rep* (2021) 11(1):15149. doi: 10.1038/s41598-021-94474-0
137. Shane AL, Sánchez PJ, Stoll BJ. Neonatal Sepsis. *Lancet (London England)* (2017) 390(10104):1770–80. doi: 10.1016/S0140-6736(17)31002-4
138. Cortese F, Scicchitano P, Gesualdo M, Filaninno A, De Giorgi E, Schettini F, et al. Early and Late Infections in Newborns: Where Do We Stand? A Review. *Pediatr neonatol* (2016) 57(4):265–73. doi: 10.1016/j.pedneo.2015.09.007
139. Wynn JL, Wong HR. Pathophysiology and Treatment of Septic Shock in Neonates. *Clin Perinatol* (2010) 37(2):439–79. doi: 10.1016/j.clp.2010.04.002
140. Buhimschi IA. Using SELDI-TOF Mass Spectrometry on Amniotic Fluid and for Clinical Proteomics and Theranostics in Disorders of Pregnancy. *Methods Mol Biol (Clifton N.J.)* (2012) 818:171–97. doi: 10.1007/978-1-61779-418-6_13
141. Sampson JE, Theve RP, Blatman RN, Shipp TD, Bianchi DW, Ward BE, et al. Fetal Origin of Amniotic Fluid Polymorphonuclear Leukocytes. *Am J Obstetrics Gynecol* (1997) 176(1 Pt 1):77–81. doi: 10.1016/S0002-9378(97)80015-4
142. Gomez-Lopez N, Romero R, Xu Y, Leng Y, Garcia-Flores V, Miller D, et al. Are Amniotic Fluid Neutrophils in Women With Intraamniotic Infection and/or Inflammation of Fetal or Maternal Origin? *Am J Obstetrics Gynecol* (2017) 217(6):693.e1–92.e16. doi: 10.1016/j.ajog.2017.09.013
143. Kiehntopf M, Melcher F, Hänel I, Eladawy H, Tomaso H. Differentiation of Campylobacter Species by Surface-Enhanced Laser Desorption/Ionization-Time-of-Flight Mass Spectrometry. *Foodborne Pathog Dis* (2011) 8(8):875–85. doi: 10.1089/fpd.2010.0775
144. Aivado M, Spentzos D, Alterovitz G, Otu HH, Grall F, Giagounidis AA, et al. Optimization and Evaluation of Surface-Enhanced Laser Desorption/Ionization Time-of-Flight Mass Spectrometry (SELDI-TOF MS) With Reversed-Phase Protein Arrays for Protein Profiling. *Clin Chem Lab Med* (2005) 43(2):133–40. doi: 10.1515/cclm.2005.022
145. Marcos B, Gou P, Guàrdia MD, Hortós M, Colleo M, Mach N, et al. Surface-Enhanced Laser Desorption/Ionisation Time-of-Flight Mass Spectrometry: A Tool to Predict Pork Quality. *Meat Sci* (2013) 95(3):688–93. doi: 10.1016/j.meatsci.2012.10.014
146. Buhimschi IA, Buhimschi CS. The Role of Proteomics in the Diagnosis of Chorioamnionitis and Early-Onset Neonatal Sepsis. *Clin Perinatol* (2010) 37(2):355–74. doi: 10.1016/j.clp.2010.03.002
147. Buhimschi IA, Christner R, Buhimschi CS. Proteomic Biomarker Analysis of Amniotic Fluid for Identification of Intra-Amniotic Inflammation. *BJOG an Int J Obstetrics Gynaecol* (2005) 112(2):173–81. doi: 10.1111/j.1471-0528.2004.00340.x
148. Buhimschi CS, Bhandari V, Han YW, Dulay AT, Baumbusch MA, Madri JA, et al. Using Proteomics in Perinatal and Neonatal Sepsis: Hopes and Challenges for the Future. *Curr Opin Infect Dis* (2009) 22(3):235–43. doi: 10.1097/QCO.0b013e32832a5963
149. Iba T, Levy JH. Inflammation and Thrombosis: Roles of Neutrophils, Platelets and Endothelial Cells and Their Interactions in Thrombus Formation During Sepsis. *J Thromb Haemostasis JTH* (2018) 16(2):231–41. doi: 10.1111/jth.13911
150. Jacobi J. Pathophysiology of Sepsis. *Am J health-syst Pharm AJHP Off J Am Soc Health-Syst Pharm* (2002) 59(Suppl 1):S3–8. doi: 10.1093/ajhp/59.suppl_1.S3
151. Zhang H, Zhao C, Li X, Zhu Y, Gan CS, Wang Y, et al. Study of Monocyte Membrane Proteome Perturbation During Lipopolysaccharide-Induced Tolerance Using iTRAQ-Based Quantitative Proteomic Approach. *Proteomics* (2010) 10(15):2780–9. doi: 10.1002/pmic.201000066
152. Mann M, Jensen ON. Proteomic Analysis of Post-Translational Modifications. *Nat Biotechnol* (2003) 21(3):255–61. doi: 10.1038/nbt0303-255
153. Li J, Paulo JA, Nusinow DP, Huttlin EL, Gygi SP. Investigation of Proteomic and Phosphoproteomic Responses to Signaling Network Perturbations Reveals Functional Pathway Organizations in Yeast. *Cell Rep* (2019) 29(7):2092–104.e4. doi: 10.1016/j.celrep.2019.10.034
154. Yan-chen L, Xin L, Dan W, Cai-bin H. Advances on the Effect of Post-Translational Modification on HMGBl Localization. *J Med Postgraduates* (2018) 31(02):193–7. doi: 10.16571/j.cnki.1008-8199.2018.02.017
155. Hwang JS, Choi HS, Ham SA, Yoo T, Lee WJ, Paek KS, et al. Deacetylation-Mediated Interaction of SIRT1-HMGB1 Improves Survival in a Mouse Model of Endotoxemia. *Sci Rep* (2015) 5:15971. doi: 10.1038/srep15971
156. Biron BM, Chung CS, O'Brien XM, Chen Y, Reichner JS, Ayala A. Cl-Amidine Prevents Histone 3 Citrullination and Neutrophil Extracellular Trap Formation, and Improves Survival in a Murine Sepsis Model. *J Innate Immun* (2017) 9(1):22–32. doi: 10.1159/000448808
157. Li Y, Liu Z, Liu B, Zhao T, Chong W, Wang Y, et al. Citrullinated Histone H3: A Novel Target for the Treatment of Sepsis. *Surgery* (2014) 156(2):229–34. doi: 10.1016/j.surg.2014.04.009
158. Stutz A, Kolbe CC, Stahl R, Horvath GL, Franklin BS, van Ray O, et al. NLRP3 Inflammasome Assembly is Regulated by Phosphorylation of the Pyrin Domain. *J Exp Med* (2017) 214(6):1725–36. doi: 10.1084/jem.20160933
159. Tang J, Tu S, Lin G, Guo H, Yan C, Liu Q, et al. Sequential Ubiquitination of NLRP3 by RNF125 and Cbl-B Limits Inflammasome Activation and Endotoxemia. *J Exp Med* (2020) 217(4):e20182091. doi: 10.1084/jem.20182091
160. Kim YM, Park EJ, Kim HJ, Chang KC. Sirt1 S-Nitrosylation Induces Acetylation of HMGB1 in LPS-Activated RAW264.7 Cells and Endotoxemic Mice. *Biochem Biophys Res Commun* (2018) 501(1):73–9. doi: 10.1016/j.bbrc.2018.04.155
161. Nakazawa H, Chang K, Shinozaki S, Yasukawa T, Ishimaru K, Yasuhara S, et al. iNOS as a Driver of Inflammation and Apoptosis in Mouse Skeletal Muscle After Burn Injury: Possible Involvement of Sirt1 S-Nitrosylation-Mediated Acetylation of P65 NF-κb and P53. *PloS One* (2017) 12(1):e0170391. doi: 10.1371/journal.pone.0170391
162. Clementi E, Brown GC, Feelisch M, Moncada S. Persistent Inhibition of Cell Respiration by Nitric Oxide: Crucial Role of S-Nitrosylation of Mitochondrial Complex I and Protective Action of Glutathione. *Proc Natl Acad Sci USA* (1998) 95(13):7631–6. doi: 10.1073/pnas.95.13.7631
163. Wang H, Bloom O, Zhang M, Vishnubhakat JM, Ombrellino M, Che J, et al. HMG-1 as a Late Mediator of Endotoxin Lethality in Mice. *Sci (New York N.Y.)* (1999) 285(5425):248–51. doi: 10.1126/science.285.5425.248
164. Deng M, Scott MJ, Fan J, Billiar TR. Location is the Key to Function: HMGB1 in Sepsis and Trauma-Induced Inflammation. *J Leukoc Biol* (2019) 106(1):161–9. doi: 10.1002/JLB.3MIR1218-497R

165. Wang H, Ward MF, Sama AE. Targeting HMGB1 in the Treatment of Sepsis. *Expert Opin Ther Targets* (2014) 18(3):257–68. doi: 10.1517/14728222.2014.863876
166. Kang R, Chen R, Zhang Q, Hou W, Wu S, Cao L, et al. HMGB1 in Health and Disease. *Mol Aspects Med* (2014) 40:1–116. doi: 10.1016/j.mam.2014.05.001
167. Chen R, Kang R, Fan XG, Tang D. Release and Activity of Histone in Diseases. *Cell Death Dis* (2014) 5(8):e1370. doi: 10.1038/cddis.2014.337
168. Meng S, Zongmei W. Role and Mechanism of Extracellular Histones in Pulmonary Ischemia/Reperfusion Injury. *Int J Anesthesiol Resuscitation* (2019) 03):251–5. doi: 10.3760/cma.j.issn.1673-4378.2019.03
169. Allam R, Kumar SV, Darisipudi MN, Anders HJ. Extracellular Histones in Tissue Injury and Inflammation. *J Mol Med (Berl)* (2014) 92(5):465–72. doi: 10.1007/s00109-014-1148-z
170. Xu J, Zhang X, Pelayo R, Monestier M, Ammollo CT, Semeraro F, et al. Extracellular Histones are Major Mediators of Death in Sepsis. *Nat Med* (2009) 15(11):1318–21. doi: 10.1038/nm.2053
171. Xu J, Zhang X, Monestier M, Esmon NL, Esmon CT. Extracellular Histones are Mediators of Death Through TLR2 and TLR4 in Mouse Fatal Liver Injury. *J Immunol* (2011) 187(5):2626–31. doi: 10.4049/jimmunol.1003930
172. Silk E, Zhao H, Weng H, Ma D. The Role of Extracellular Histone in Organ Injury. *Cell Death Dis* (2017) 8(5):e2812. doi: 10.1038/cddis.2017.52
173. Cheng Z, Abrams ST, Alhamdi Y, Toh J, Yu W, Wang G, et al. Circulating Histones Are Major Mediators of Multiple Organ Dysfunction Syndrome in Acute Critical Illnesses. *Crit Care Med* (2019) 47(8):e677–84. doi: 10.1097/ccm.0000000000003839
174. Li Y, Liu B, Fukudome EY, Lu J, Chong W, Jin G, et al. Identification of Citrullinated Histone H3 as a Potential Serum Protein Biomarker in a Lethal Model of Lipopolysaccharide-Induced Shock. *Surgery* (2011) 150(3):442–51. doi: 10.1016/j.surg.2011.07.003
175. Mangan MSJ, Olhava EJ, Roush WR, Seidel HM, Glick GD, Latz E. Targeting the NLRP3 Inflammasome in Inflammatory Diseases. *Nat Rev Drug Discov* (2018) 17(8):588–606. doi: 10.1038/nrd.2018.97
176. Danielski LG, Giustina AD, Bonfante S, Barichello T, Petronilho F. The NLRP3 Inflammasome and Its Role in Sepsis Development. *Inflammation* (2020) 43(1):24–31. doi: 10.1007/s10753-019-01124-9
177. Lee S, Nakahira K, Dalli J, Siempos II, Norris PC, Colas RA, et al. NLRP3 Inflammasome Deficiency Protects Against Microbial Sepsis *via* Increased Lipoxin B(4) Synthesis. *Am J Respir Crit Care Med* (2017) 196(6):713–26. doi: 10.1164/rccm.201604-0892OC
178. Zhong M, Wu W, Wang Y, Mao H, Song J, Chen S, et al. Inhibition of Sphingosine Kinase 1 Attenuates Sepsis-Induced Microvascular Leakage *via* Inhibiting Macrophage NLRP3 Inflammasome Activation in Mice. *Anesthesiology* (2020) 132(6):1503–15. doi: 10.1097/aln.0000000000003192
179. Zhu Y, Zhengyu J, Xiaoming D. Post-Translational Modification of the NOD-Like Receptors Family Pyrin Domain Containing 3 Inflammasome and its Role in the Pathogenesis of Sepsis. *Int J Anesth Resus* (2021) 03):329–33. doi: 10.3760/cma.j.cn321761-20200928-00249
180. Shim DW, Lee KH. Posttranslational Regulation of the NLR Family Pyrin Domain-Containing 3 Inflammasome. *Front Immunol* (2018) 9:1054. doi: 10.3389/fimmu.2018.01054
181. Ren G, Zhang X, Xiao Y, Zhang W, Wang Y, Ma W, et al. ABRO1 Promotes NLRP3 Inflammasome Activation Through Regulation of NLRP3 Deubiquitination. *EMBO J* (2019) 38(6):e100376. doi: 10.15252/embj.2018100376
182. Sharawy N, Lehmann C. Molecular Mechanisms by Which iNOS Uncoupling can Induce Cardiovascular Dysfunction During Sepsis: Role of Posttranslational Modifications (PTMs). *Life Sci* (2020) 255:117821. doi: 10.1016/j.lfs.2020.117821
183. Stomberski CT, Hess DT, Stamler JS. Protein S-Nitrosylation: Determinants of Specificity and Enzymatic Regulation of S-Nitrosothiol-Based Signaling. *Antioxid Redox Signal* (2019) 30(10):1331–51. doi: 10.1089/ars.2017.7403
184. Palmieri EM, McGinity C, Wink DA, McVicar DW. Nitric Oxide in Macrophage Immunometabolism: Hiding in Plain Sight. *Metabolites* (2020) 10(11):429. doi: 10.3390/metabo10110429
185. Bailey JD, Diotallevi M, Nicol T, McNeill E, Shaw A, Chuaiphichai S, et al. Nitric Oxide Modulates Metabolic Remodeling in Inflammatory Macrophages Through TCA Cycle Regulation and Itaconate Accumulation. *Cell Rep* (2019) 28(1):218–30.e7. doi: 10.1016/j.celrep.2019.06.018
186. Doulias PT, Tenopoulou M, Greene JL, Raju K, Ischiropoulos H. Nitric Oxide Regulates Mitochondrial Fatty Acid Metabolism Through Reversible Protein S-Nitrosylation. *Sci Signal* (2013) 6(256):rs1. doi: 10.1126/scisignal.2003252
187. Everts B, Amiel E, van der Windt GJ, Freitas TC, Chott R, Yarasheski KE, et al. Commitment to Glycolysis Sustains Survival of NO-Producing Inflammatory Dendritic Cells. *Blood* (2012) 120(7):1422–31. doi: 10.1182/blood-2012-03-419747
188. de Jesus JR, da Silva Fernandes R, de Souza Pessôa G, Raimundo IM and Arruda MAZ. Depleting High-Abundant and Enriching Low-Abundant Proteins in Human Serum: An Evaluation of Sample Preparation Methods Using Magnetic Nanoparticle, Chemical Depletion and Immunoaffinity Techniques. *Talanta* (2017) 170:199–209. doi: 10.1016/j.talanta.2017.03.091
189. Palstrøm NB, Rasmussen LM, Beck HC. Affinity Capture Enrichment Versus Affinity Depletion: A Comparison of Strategies for Increasing Coverage of Low-Abundant Human Plasma Proteins. *Int J Mol Sci* (2020) 21(16):5903. doi: 10.3390/ijms21165903
190. Ke M, Shen H, Wang L, Luo S, Lin L, Yang J, et al. Identification, Quantification, and Site Localization of Protein Posttranslational Modifications via Mass Spectrometry-Based Proteomics. *Adv Exp Med Biol* (2016) 919:345–82. doi: 10.1007/978-3-319-41448-5_17
191. Černý M, Skalák J, Cerna H, Brzobohatý B. Advances in Purification and Separation of Posttranslationally Modified Proteins. *J Proteomics* (2013) 92:2–27. doi: 10.1016/j.jprot.2013.05.040
192. Wozniak JM, Mills RH, Olson J, Caldera JR, Sepich-Poore GD, Carrillo-Terrazas M, et al. Mortality Risk Profiling of Staphylococcus Aureus Bacteremia by Multi-Omic Serum Analysis Reveals Early Predictive and Pathogenic Signatures. *Cell* (2020) 182(5):1311–27.e14. doi: 10.1016/j.cell.2020.07.040

Conflict of Interest: The authors declare that the research was conducted in the absence of any commercial or financial relationships that could be construed as a potential conflict of interest.

frontiers in Immunology

ORIGINAL RESEARCH
published: 22 October 2021
doi: 10.3389/fimmu.2021.741268

Diagnostic Value of sIL-2R, TNF-α and PCT for Sepsis Infection in Patients With Closed Abdominal Injury Complicated With Severe Multiple Abdominal Injuries

Guang-hua Zhai[1†], Wei Zhang[2†], Ze Xiang[3†], Li-Zhen He[4,5], Wei-wei Wang[6], Jian Wu[1*] and An-quan Shang[7*]*

[1] Department of Clinical Laboratory, The Affiliated Suzhou Hospital of Nanjing Medical University, Suzhou Municipal Hospital, Gusu School, Nanjing Medical University, Suzhou, China, [2] Department of Laboratory Medicine, Jiaozuo Fifth People's Hospital, Jiaozuo, China, [3] Zhejiang University School of Medicine, Hangzhou, China, [4] Department of Laboratory, Jiaozuo Second People's Hospital, Jiaozuo, China, [5] Department of Laboratory Medicine, The First Affiliated Hospital of Henan Polytechnic University, Henan, China, [6] Department of Pathology, Tinghu People's Hospital of Yancheng City, Yancheng, China, [7] Department of Laboratory Medicine, Shanghai Tongji Hospital, School of Medicine, Tongji University, Shanghai, China

Objective: We aimed to evaluate the diagnostic value of soluble interleukin-2 receptor (sIL-2R), tumor necrosis factor-α (TNF-α), procalcitonin (PCT), and combined detection for sepsis infection in patients with closed abdominal injury complicated with severe multiple abdominal injuries.

Patients and Methods: One hundred forty patients with closed abdominal injury complicated with severe multiple abdominal injuries who were diagnosed and treated from 2015 to 2020 were divided into a sepsis group ($n = 70$) and an infection group ($n = 70$).

Results: The levels of sIL-2R, TNF-α, and PCT in the sepsis group were higher than those in the infection group ($p < 0.05$). The receiver operating characteristic (ROC) curve showed that the areas under the ROC curve (AUCs) of sIL-2R, TNF-α, PCT and sIL-2R+TNF-a +PCT were 0.827, 0.781, 0.821, and 0.846, respectively, which were higher than those of white blood cells (WBC, 0.712), C-reactive protein (CRP, 0.766), serum amyloid A (SAA, 0.666), and IL-6 (0.735). The AUC of the three combined tests was higher than that of TNF-α, and the difference was statistically significant ($p < 0.05$). There was no significant difference in the AUCs of sIL-2R and TNF-α, sIL-2R and PCT, TNF-α and PCT, the three combined tests and sIL-2R, and the three combined tests and PCT ($p > 0.05$). When the median was used as the cut point, the corrected sIL-2R, TNF-α, and PCT of the high-level group were not better than those of the low-level group ($p > 0.05$). When the four groups were classified by using quantile as the cut point, the OR risk values of high levels of TNF-α and PCT (Q4) and the low level of PCT (Q1) after correction were 7.991 and 21.76, respectively, with statistical significance ($p < 0.05$).

OPEN ACCESS

Edited by:
Wei Chong,
The First Affiliated Hospital of China Medical University, China

Reviewed by:
Dong Li,
Jilin University, China
Xing Li,
Changsha Hospital of Traditional Chinese Medicine, China

***Correspondence:**
An-quan Shang
shanganquan@tongji.edu.cn
Jian Wu
wujianglinxing@163.com
Wei-wei Wang
lydia_wangweiwei@sina.com

†These authors have contributed equally to this work

Specialty section:
This article was submitted to Inflammation, a section of the journal Frontiers in Immunology

Received: *14 July 2021*
Accepted: *04 October 2021*
Published: *22 October 2021*

Citation:
Zhai G-h, Zhang W, Xiang Z, He L-Z, Wang W-w, Wu J and Shang A-q (2021) Diagnostic Value of sIL-2R, TNF-α and PCT for Sepsis Infection in Patients With Closed Abdominal Injury Complicated With Severe Multiple Abdominal Injuries. Front. Immunol. 12:741268. doi: 10.3389/fimmu.2021.741268

Conclusions: The detection of sIL-2R, TNF-α, and PCT has good value in the diagnosis of sepsis infection in patients with closed abdominal injury complicated with severe multiple abdominal injuries. The high concentrations of PCT and TNF-α can be used as predictors of the risk of septic infection.

Keywords: sIL-2R, TNF-α, PCT, sepsis, closed abdominal injury complicated with severe multiple abdominal injuries, diagnostic value

INTRODUCTION

Closed abdominal injury with severe multiple traumas is characterized by complex and hidden conditions, and most patients are accompanied by injuries to the brain, chest, and limbs (1). The prognosis of closed abdominal injury depends on the presence or absence of visceral injury, which is characterized by persistent vomiting, nausea, abdominal pain, internal bleeding, and peritoneal irritation in terms of clinical symptoms (2). For patients with closed abdominal injuries accompanied by severe multiple injuries, besides abdominal injuries, fractures, brain injuries, etc., are also present (3). The accompanying multiple injuries may conceal the actual physical signs of patients, thus increasing the difficulty of clinical diagnosis. In the case of closed abdominal injury combined with multiple systemic injuries, the patients' injuries are severe and complex, including shock, sepsis, coma, dyspnea, and other symptoms in the early stage, which makes the diagnosis and treatment more difficult and leads to higher mortality (4).

Sepsis is a systemic inflammatory response syndrome caused by severe infection. The main pathogens of sepsis are bacteria, followed by fungi, viruses, and parasites (5). Sepsis is a major cause of death worldwide, with a high incidence, which can cause damage to important organs such as the heart, lung, and kidney. Sepsis has been reported to cause about 25%–50% of deaths in the United States, Europe, and South America (6). Blood culture is considered as the "golden criteria" for diagnosing septic infection (7), but it has been reported (8) that only half of patients suspected of sepsis were found to be infected by pathogenic bacteria; there were also problems such as contamination of normal skin bacteria and long culture times, leading to the inability to obtain results in time (9). Therefore, the early diagnosis of sepsis and targeted treatment within a few hours of the first diagnosis are extremely important (10). Sepsis is a potentially fatal disease defined as an infection-related syndrome exacerbated by acute organ failure. Organ dysfunction is caused by an acute change in the Sequential Organ Failure Assessment (SOFA) score of ≥2 points, i.e., sepsis = infection + SOFA score ≥2 points (11). Although the diagnostic criteria for sepsis have been established, the early diagnosis of sepsis is still difficult due to the unclear primary infectious focus and the vague definition of sepsis syndrome (12). Several scholars believe that there is a lag in the SOFA score, and most patients are in the late stage of sepsis when they are diagnosed using the SOFA score (13). Therefore, a simple diagnostic index with high diagnostic performance in the early stage of sepsis remains to be studied.

Soluble interleukin 2 receptor (sIL-2R) is a nonspecific indicator produced by lymphocytes under conditions such as malignant tumors and infection, which can reflect diseases related to lymphocyte activation and is also a marker of the activation of the immune system (14). Tumor necrosis factor-α (TNF-α) is a major pro-inflammatory cytokine that plays a key role in antimicrobial and anti-inflammatory responses through mechanisms such as the activation of white blood cells, cell proliferation, differentiation, and apoptosis of lymphocytes (15, 16). A large number of cytokines are produced in the process of infection, among which TNF-a plays a powerful immune regulatory role in host immune response (17). Serum procalcitonin (PCT) is a type of calcitonin propeptide that is elevated during inflammation and infection, and it is also considered as a diagnostic marker for early infection (18). One of the recognized mechanisms of sepsis is that its occurrence and the development process are caused by an imbalance in the anti-inflammatory response. Sepsis can promote the secretion of inflammatory factors in the early stage. At present, there are no reports on the diagnostic value of sIL-2R, TNF-α, and PCT in sepsis patients with closed abdominal injury. Based on the Third International Consensus Definitions for Sepsis and Septic Shock diagnostic criteria (11), this study intended to evaluate the diagnostic value of sIL-2R, TNF-α, PCT, and their combined detection in sepsis patients with closed abdominal injury complicated with severe multiple abdominal injuries. The optimal threshold value of infection in patients with sepsis was determined in this study, and the influence of sIL-2R, TNF-α, and PCT was evaluated, which also provides reference for the early diagnosis of sepsis in patients with closed abdominal injury complicated with severe multiple abdominal injuries.

Abbreviations: sIL-2R, soluble interleukin-2 receptor; TNF-α, tumor necrosis factor-α; PCT, procalcitonin; APACHE II, Acute Physiology and Chronic Health Assessment; NPV, negative predictive value; PPV, positive predictive value; AUC, area under the curve; AOR, adjusted odds ratios; CI, confidence intervals.

MATERIALS AND METHODS

Patients and Clinical Information

We retrospectively analyzed 140 patients with closed abdominal injury complicated with severe multiple abdominal injuries treated in the Fifth People's Hospital of Jiaozuo City, The First Affiliated Hospital of Henan University of Technology, the First People's Hospital of Yancheng City, and the Tinghu People's Hospital of Yancheng City from 2015 to 2020, including 70 patients with sepsis (sepsis group from intensive care units) and

70 patients without sepsis but with local inflammatory infection (infection group from general surgery). All the medical records were confirmed by clinical symptoms, B-ultrasound, X-ray films, and laboratory, among others. The locations of abdominal injuries were the pancreas in 13 cases, the duodenum in 15 cases, colon in 32 cases, liver in 13 cases, small intestine in 19 cases, and the spleen in 48 cases; 98 cases had multiple organ injuries and 42 cases had single organ injuries. The diagnosis of sepsis was based on the Third International Consensus Diagnostic Criteria for Sepsis and Septic Shock 3.0, published in 2016.

The infection group showed two or more of the following signs: body temperature, >38°C or <36°C; heart rate, >90 bpm; respiratory rate of >20 times/min or arterial blood carbon dioxide partial pressure of <32 mmHg; and peripheral blood leukocytes, $>12 \times 10^9$/L or $<4 \times 10^9$/L. The criteria for the sepsis group were in accordance with the signs in the infection group and a SOFA score ≥2.

The exclusion criteria were as follows: patients with solid cancer, hematologic disease, organ transplantation, with missing clinical and laboratory data, treated with antibiotics, and patients with immune deficiency.

The baseline clinical data of 140 enrolled patients were collected from medical records, which included age, gender, sIL-2R, TNF-α, PCT, white blood cells (WBC), C-reactive protein (CRP), and serum amyloid A (SAA), IL-6, as well as Acute Physiology and Chronic Health Assessment (APACHE II). The included detection indexes were based on the serum samples collected for the first time within 24 h of a patient's visit. SAA was detected by kinetics nephelometry. sIL-2R, TNF-α, and IL-6 were detected with ELISA. PCT was detected using immunofluorescence chromatography. All specimens were enrolled after obtaining informed consent from the patients or their family. Written informed consent from the participants was obtained. The study was approved by the ethics committees of the Fifth People's Hospital of Jiaozuo City (approval no. 20160518).

Statistical Analysis

Statistical analyses were performed with SPSS 25.0 software (IBM Corp., Armonk, NY, USA). Continuous data were presented as means ± standard deviations. Measurement data between the two groups were conducted using independent samples *t*-test. Numeration data were analyzed using the χ^2 test. Variables with a non-normal distribution were expressed as median (P25 and P75) and were compared using the non-parametric Mann–Whitney *U* test. GraphPad Prism software was used to generate the receiver operating characteristic (ROC) curves of each index and its combined index in order to determine the sensitivity, specificity, optimal cutoff value, Youden index, negative predictive value (NPV), and the positive predictive value (PPV) of each index in patients infected with sepsis. The area under the ROC curve (AUC) was used to judge the accuracy of the test. The combined predictors of sIL-2R, TNF-α, and PCT were calculated with binary logistic regression analysis. The AUCs were compared between each index using *Z*-test. Spearman's rank correlation coefficient was used to analyze the correlation between the levels of IL-2R, TNF-α, PCT and other laboratory parameters and APACHE II. Binary logistic regression analysis was applied to evaluate the risk predictive value of the levels of sIL-2R, TNF-α, and PCT for sepsis using median (P50) and quartiles (P25, P50, P75) as cut points, respectively. It was also used to calculate the values of the single-factor and multifactor adjusted odds ratios (AORs) and 95% confidence intervals (CI) based on maximum likelihood estimates. A $p < 0.05$ was considered statistically significant.

RESULTS

Clinical Baseline of the Enrolled Subjects in Both Infection and Sepsis Groups

Table 1 shows the clinical baseline of the 140 enrolled patients with closed abdominal injury complicated with severe multiple abdominal injuries. There was no statistical significance in the gender and age distribution between the infection group and the sepsis group ($p > 0.05$). The scores for WBC, CRP, SAA, IL-6, APACHE II, and SOFA in the sepsis group were all higher than those in the infection group, with statistical significance ($p < 0.05$).

Expression Levels of sIL-2R, TNF-α, and PCT in the Two Groups of Subjects

The levels of sIL-2R in the sepsis group were higher than those in the infection group, and the difference was statistically significant ($Z = -6.668$, $p < 0.001$), as shown in **Figure 1A**. The levels of TNF-α in the sepsis group were higher than those in the infection group, and the difference was statistically significant ($Z = -5.728$, $p < 0.001$), as shown in **Figure 1B**. The levels of PCT in the sepsis group were higher than those in the infection group, and the difference was also statistically significant ($Z = -6.560$, $p < 0.001$), as shown in **Figure 1C**.

Correlation Between sIL-2R, TNF-α, PCT, and Other Commonly Used Laboratory Infection Indicators in the Two Groups

The level of sIL-2R was positively correlated with CRP, SAA, IL-6, APACHE II, and the SOFA score in the infection group ($r = 0.396$, $p < 0.001$; $r = 0.314$, $p < 0.008$; $r = 0.262$, $p = 0.028$; $r = 0.302$, $p = 0.011$; and $r = 0.348$, $p = 0.003$, respectively). There was no correlation between the level of sIL-2R and WBC ($r = 0.207$, $p < 0.085$). The levels of sIL-2R in the sepsis group were positively correlated with WBC, CRP, SAA, IL-6, and APACHE II ($r = 0.387$, $p = 0.001$; $r = 0.248$, $p = 0.038$; $r = 0.402$, $p = 0.001$; $r = 0.532$, $p < 0.001$; and $r = 0.244$, $p = 0.042$, respectively). No significant correlation between the level of sIL-2R and the SOFA score was observed for patients with sepsis ($r = 0.019$, $p = 0.876$, which is shown in **Figure 2**.

The TNF-α level in the infected group was positively correlated with IL-6 ($r = 0.247$, $p = 0.039$), while it was not correlated with WBC, CRP, SAA, APACHE II, and the SOFA score ($r = 0.026$, $p = 0.832$; $r = 0.208$, $p = 0.083$; $r = 0.215$, $p = 0.074$; $r = 0.130$, $p = 0.285$; and $r = 0.143$, $p = 0.237$, respectively).

TABLE 1 | Characteristics of the enrolled patients.

Variables	Infection group (*n* = 70)	Sepsis group (*n* = 70)	*p*-value
Gender F/M)	38/32	41/29	0.609
Age (years)	72 (63,80)	78 (65,85)	0.099
Location of abdominal injury			0.994
Pancreas	6	7	
Duodenum	6	9	
Colon	13	19	
Liver	5	8	
Small intestine	9	10	
Spleen	20	28	
WBC ($\times 10^9$/L)	12.22 (9.44–15.88)	17.50 (12.93–19.74)	<0.001
CRP (mg/L)	55.28 (25.23–91.31)	133.59 (85.20–225.50)	<0.001
SAA (mg/L)	76.54 (31.18–102.62)	124.61 (53.78–187.47)	0.001
IL-6 (pg/ml)	10.50 (4.34–29.93)	31.75 (17.93–113.20)	<0.001
sIL-2R	835.50 (658.25–1057.25)	1879.00 (1216.00–2872.50)	<0.001
TNF-α	11.45 (8.54–21.70)	31.20 (16.38–49.10)	<0.001
PCT	0.72 (0.47–1.87)	6.56 (1.75–8.62)	<0.001
SOFA score	0 (0–1)	10 (7–12)	<0.001
PaO_2/FiO_2 (mmHg)	452 (426–469)	287 (264–376)	<0.001
GCS	15 (15–15)	12 (11–14)	<0.001
MAP (mmHg)	90 (85–96)	66 (62–69)	<0.001
TBIL (μmol/L)	11.4 (9.2–15.3)	38.1 (27.8–68.6)	<0.001
PLT ($\times 10^9$/L)	200 (176–232)	95 (83–126)	<0.001
CREA (μmol/L)	78.5 (67–97)	215 (134–319)	<0.001
APACHE II	10 (8–13)	18 (15–23)	<0.001

WBC, white blood cells; CRP, C-reactive protein; SAA, serum amyloid A; IL-6, interleukin 6; sIL-2R, soluble interleukin-2 receptor; TNF-α, tumor necrosis factor alpha; PCT, procalcitonin; SOFA, Sequential Organ Failure Assessment; GCS, Glasgow Coma Scale; MAP, mean arterial pressure; TBIL, total bilirubin; PLT, platelet; CREA, creatinine; APACHE II, Acute Physiology and Chronic Health Assessment.

The TNF-α level was positively correlated with WBC, SAA, and IL-6 in the sepsis group ($r = 0.320$, $p = 0.007$; $r = 0.379$, $p = 0.001$; and $r = 0.401$, $p = 0.001$, respectively), but there was no correlation between the level of TNF-α and CRP, APACHE II, and the SOFA score ($r = 0.103$, $p = 0.395$; $r = 0.152$, $p = 0.209$; and $r = 0.009$, $p = 0.942$, respectively), as shown in **Figure 3**.

The PCT level in the infected group was positively correlated with CRP ($r = 0.360$, $p = 0.002$), while it was not correlated with WBC, SAA, IL-6, APACHE II, and the SOFA score ($r = 0.031$, $p = 0.802$; $r = 0.113$, $p = 0.350$; $r = 0.147$, $p = 0.223$; $r = 0.109$, $p = 0.371$; and $r = 0.165$, $p = 0.172$, respectively). The PCT level in the sepsis group was positively correlated with IL-6 ($r = 0.289$, $p = 0.015$), while it was not correlated with WBC, CRP, SAA, APACHE II, and the SOFA score ($r = 0.225$, $p = 0.061$; $r = 0.163$, $p = 0.178$; $r = 0.220$, $p = 0.067$; $r = 0.203$, $p = 0.093$; and $r = 0.009$, $p = 0.944$, respectively), which is shown in **Figure 4**.

Diagnostic Performance of the Laboratory Infection Indicators in Subjects With Sepsis and Infection

Infection group Y (sepsis group = 1, infection group = 0) was used as the dependent variable; sIL-2R(X1), TNF-α(X2), and PCT(X3) were used as the independent variables. The joint predictors of sIL-2R, TNF-α, and PCT were calculated using binary logistic regression analysis, and the regression equation was $Y = -2.343 + 0.000X1 + 0.026X2 + 0.364X3$. The joint

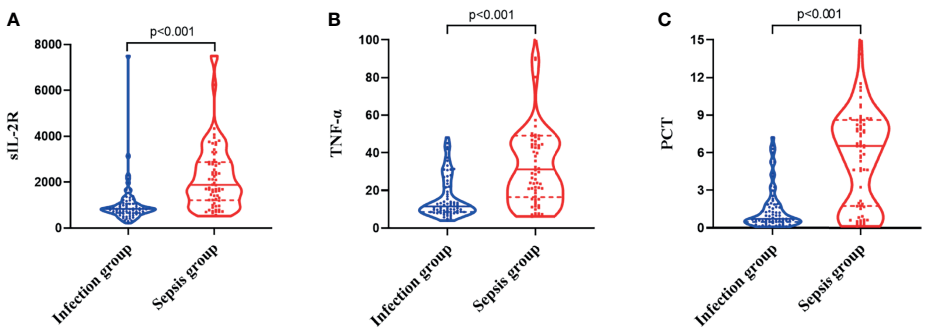

FIGURE 1 | Differences in the expression levels of soluble interleukin-2 receptor (sIL-2R) **(A)**, tumor necrosis factor alpha (TNF-α) **(B)**, and procalcitonin (PCT) **(C)** between the infection group and the sepsis group.

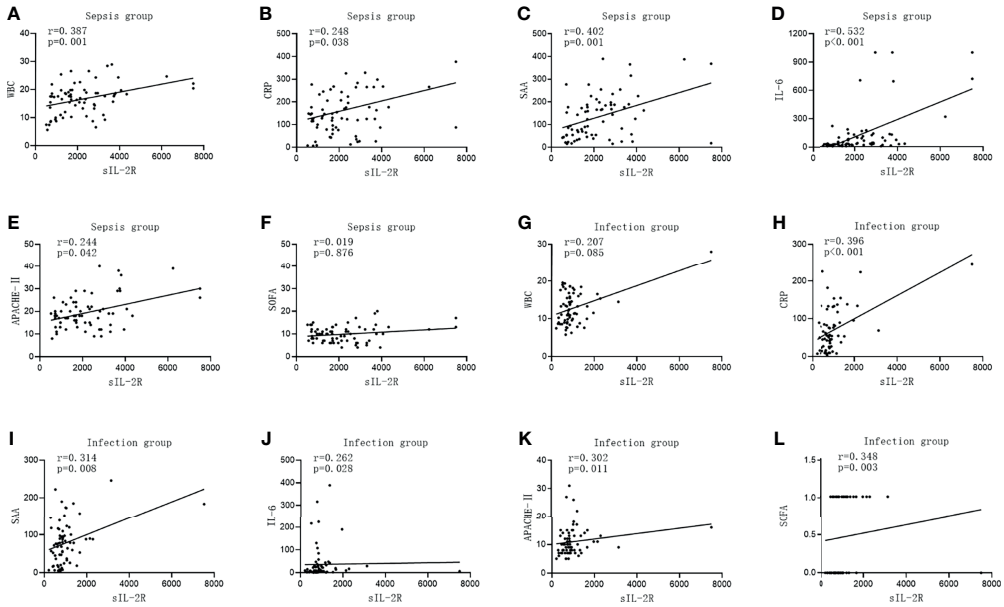

FIGURE 2 | Correlations of soluble interleukin-2 receptor (sIL-2R) with the commonly used infection markers—white blood cells (WBC), C-reactive protein (CRP), serum amyloid A (SAA), interleukin 6 (IL-6), Acute Physiology and Chronic Health Assessment (APACHE II), and the Sequential Organ Failure Assessment (SOFA) score—in patients in the infection group and the sepsis group. **(A–F)** Correlations of sIL-2R with WBC **(A)**, CRP **(B)**, SAA **(C)**, IL-6 **(D)**, APACHE II **(E)**, and with the SOFA score **(F)** in patients in the sepsis group. **(G–L)** Correlations of sIL-2R with WBC **(G)**, CRP **(H)**, SAA **(I)**, IL-6 **(J)**, APACHE II **(K)**, and with the SOFA score **(L)** in patients in the infection group.

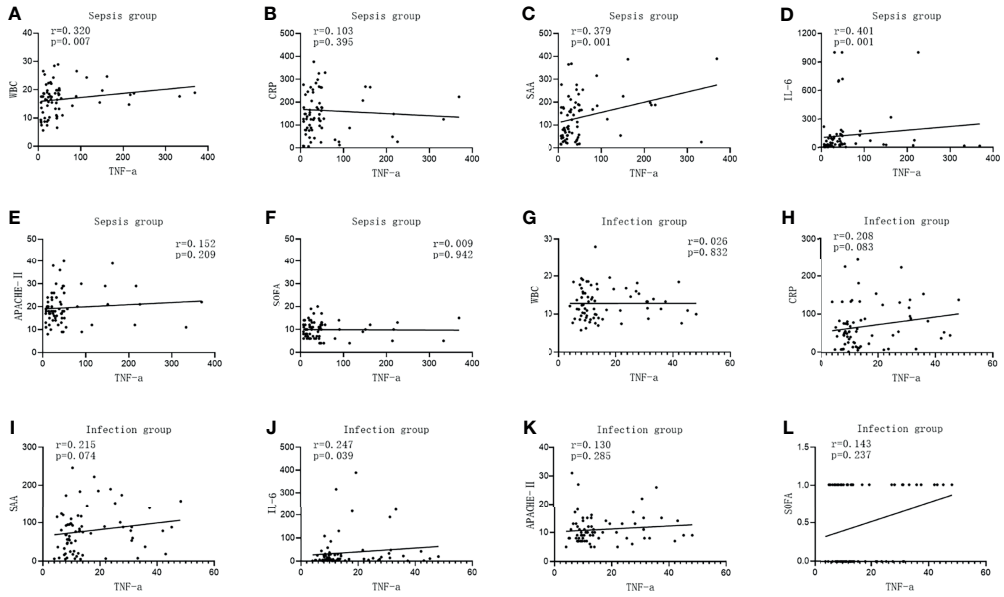

FIGURE 3 | Correlations of tumor necrosis factor alpha (TNF-α) with the commonly used infection markers—white blood cells (WBC), C-reactive protein (CRP), serum amyloid A (SAA), interleukin 6 (IL-6), Acute Physiology and Chronic Health Assessment (APACHE II), and the Sequential Organ Failure Assessment (SOFA) score—in patients in the infection group and the sepsis group. **(A–G)** Correlations of TNF-α with WBC **(A)**, CRP **(B)**, SAA **(C)**, IL-6 **(D)**, APACHE II **(E)**, and with the SOFA score **(F)** in patients in the sepsis group. **(G–L)** Correlations of TNF-α with WBC **(G)**, CRP **(H)**, SAA **(I)**, IL-6 **(J)**, APACHE II **(K)**, and with the SOFA score **(K)** in patients in the infection group.

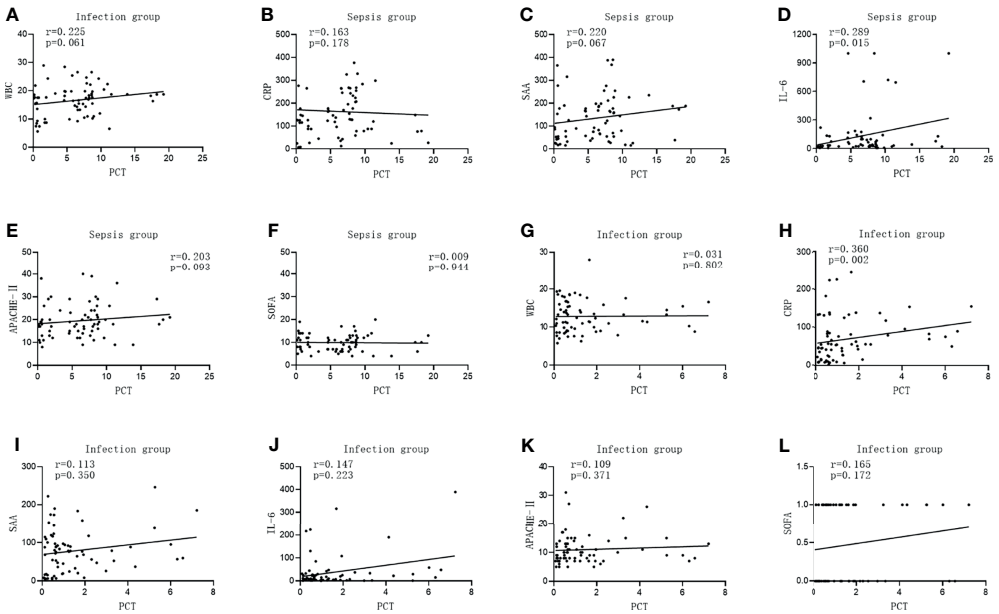

FIGURE 4 | Correlations of procalcitonin (PCT) with the commonly used infection markers—white blood cells (WBC), C-reactive protein (CRP), serum amyloid A (SAA), interleukin 6 (IL-6), Acute Physiology and Chronic Health Assessment (APACHE II), and the Sequential Organ Failure Assessment (SOFA) score in patients in the infection group and sepsis group. **(A–G)** Correlations of PCT with WBC **(A)**, CRP **(B)**, SAA **(C)**, IL-6 **(D)**, APACHE II **(E)**, and with the SOFA score **(F)** in patients in the sepsis group. **(G–L)** Correlation of PCT with WBC **(G)**, CRP **(H)**, SAA **(I)**, IL-6 **(J)**, APACHE II, **(K)** and with the SOFA score **(L)** in patients in the infection group.

predictors were used as three joint test indexes to analyze the results.

GraphPad Prism was used to plot the ROC curves of each index and the combined test, as shown in **Figures 5A–I**. When the AUC of WBC is 0.712 and the cutoff value is 15.46×10^9/L, the sensitivity and specificity were 65.71% and 74.29% and the NPV and PPV were 68.4% and 71.9%, respectively. For CRP detection, when the AUC is 0.766 and the cutoff value is 85.47 mg/L, the sensitivity and specificity were 75.71% and 72.86% and NPV and PPV are 75.0% and 73.6%, respectively. When the AUC is 0.666 and the cutoff value is 123.21 mg/L, the sensitivity and specificity were 51.43% and 84.29% and the NPV and PPV are 63.4% and 76.6%, respectively. IL-6 detection with an AUC of 0.735 and a cutoff value of 9.9 pg/ml showed sensitivity and specificity values of 88.57% and 50.00% and NPV and PPV of 81.4% and 63.9%, respectively. When the AUC of the SOFA score is 1.000 and the cutoff value is 1, the sensitivity and specificity were 100% and 100% and the NPV and PPV were 100% and 100%, respectively. For sIL-2R detection, an AUC of 0.827 and a cutoff value of 1384 U/ml produced sensitivity and specificity values of 70.00% and 88.57% and NPV and PPV of 74.7% and 86.0%, respectively. When the AUC of TNF-α detection is 0.781 and the cutoff value is 14.00 pg/ml, the sensitivity and specificity were 80.00% and 68.57% and the NPV and PPV were 77.4% and 71.8%, respectively. For PCT, when the AUC is 0.821 and the cutoff value is 4.35 ng/ml, the sensitivity and specificity were 68.57% and 91.43% and the NPV and PPV were 74.4% and 88.9%, respectively. The sensitivity and specificity were 70.00% and 95.71% and the NPV and PPV were 76.1% and 94.2%, respectively, for sIL-2R+TNF-α+PCT when the AUC is 0.846 and the cutoff value is 0.70, which are shown in **Table 2**.

According to the data in **Table 2**, the combination of sIL-2R, TNF-α, PCT, and sIL-2R+TNF-a+PCT had higher AUCs and better diagnostic performance. MedCalc software was used to compare the AUCs of sIL-2R, TNF-a, PCT, and sIL-2R+TNF-α+PCT. The AUCs of sIL-2R and TNF-α, sIL-2R and PCT, and TNF-α and PCT were also compared. There was no statistically significant difference in the AUCs between sIL-2R and PCT ($p > 0.05$). The AUC of the combined test was greater than that of TNF-α, and the difference was statistically significant ($p < 0.05$), as shown in **Table 3**.

Risk Assessment of sIL-2R, TNF-α, and PCT in Predicting Sepsis in Patients With Closed Abdominal Injury Complicated With Severe Multiple Abdominal Injuries

Binary logistic regression analysis was used to evaluate the risk predictive value of the levels of sIL-2R, TNF-α, and PCT in the sepsis group. The median cutoff point (two classifications) and the quartiles (P25, P50, and P75) were evaluated as cutoff points (four classifications). Firstly, patients were divided into a low-level group and a high-level group according to the median values of sIL-2R (1,087 U/ml), TNF-α (18.95 pg/ml), and PCT (1.815 ng/ml). Compared with low sIL-2R, the risk of sepsis in patients with high sIL-2R was 11.391 (95%CI = 5.175–25.072, $p < 0.05$), and the adjusted OR was 0.489 (95%CI = 0.103–2.321, $p > 0.05$). Compared with low TNF-α, the risk of sepsis in patients with high TNF-α levels was 7.205 (95%CI = 3.420–15.177, $p <$

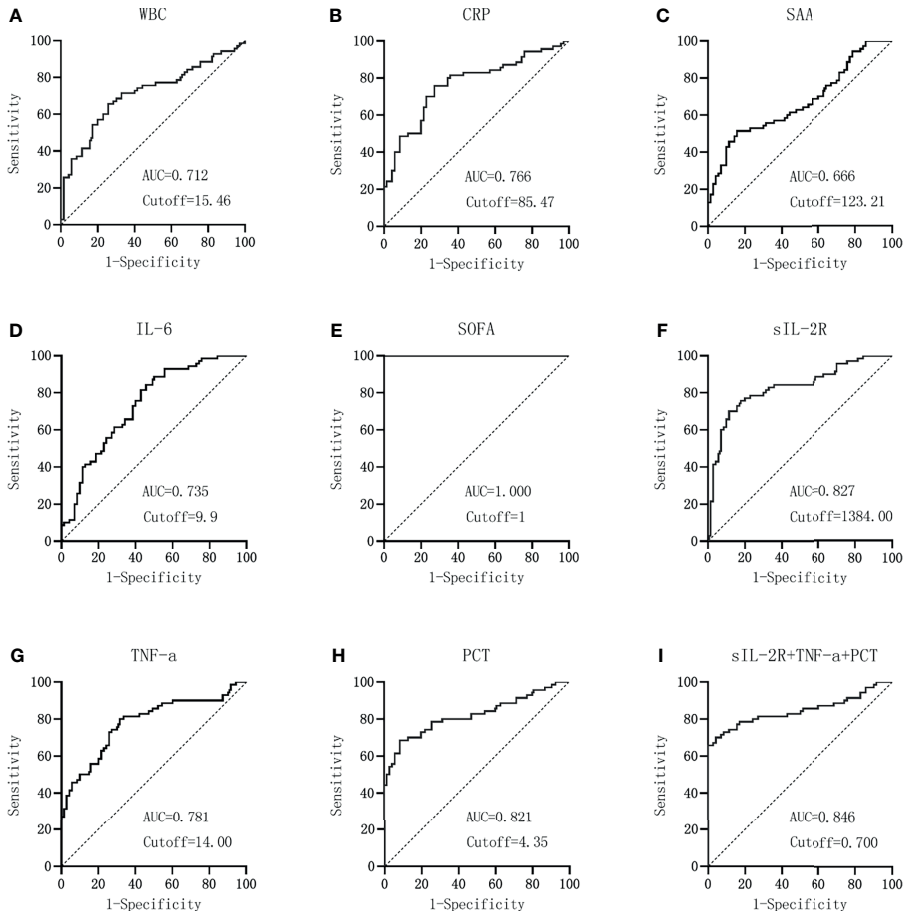

FIGURE 5 | Diagnostic value of the laboratory infection markers in patients in the sepsis group *versus* the infection group. **(A–I)** Diagnostic value of white blood cells (WBC) **(A)**, C-reactive protein (CRP) **(B)**, serum amyloid A (SAA) **(C)**, interleukin 6 (IL-6) **(D)**, Sequential Organ Failure Assessment (SOFA) score **(E)**, soluble interleukin-2 receptor (sIL-2R) **(F)**, tumor necrosis factor alpha (TNF-α) **(G)**, procalcitonin (PCT) **(H)**, and the combined sIL-2R+TNF-a+PCT **(I)** in patients in the sepsis group *versus* the infection group.

0.05), and the adjusted OR was 1.624 (95%CI = 0.531–4.970, $p > 0.05$). Compared with low PCT, the risk of sepsis in patients with high PCT was 8.346 (95%CI = 3.911–17.810, $p < 0.05$), and the adjusted OR was 2.300 (95%CI = 0.812–6.516, $p > 0.05$), which can be seen in **Figures 6** and **7**.

Secondly, according to the quartile values of sIL-2R (Q1 < 740, 740 ≤ Q2 < 1,087, 1,087 ≤ Q3 < 2,124, and 2,124 ≤ Q4), TNF-α (Q1 < 9.8725, 9.8725 ≤ Q2 < 18.95, 18.95 ≤ Q3 < 39.4, and 39.4 ≤ Q4), PCT (Q1 < 0.5925, 0.5925 ≤ Q2 < 1.815, 1.815 ≤ Q3 < 6.67, and 6.67 ≤ Q4), the patients were divided into the Q1,

TABLE 2 | Diagnostic performance of the laboratory infection indicators in subjects with sepsis and infection.

Variables	Youden index	Cutoff	AUC	Sensitivity (%)	Specificity (%)	AUC 95%CI	NPV (%)	PPV (%)
WBC	0.400	15.46	0.712	65.71	74.29	0.629–0.785	68.4	71.9
CRP	0.486	85.47	0.766	75.71	72.86	0.687–0.833	75.0	73.6
SAA	0.357	123.21	0.666	51.43	84.29	0.581–0.743	63.4	76.6
IL-6	0.386	9.90	0.735	88.57	50.00	0.654–0.806	81.4	63.9
SOFA	1.000	1.00	1.000	100	100	0.974–1.000	100.0	100.0
sIL-2R	0.586	1,384.00	0.827	70.00	88.57	0.753–0.885	74.7	86.0
TNF-α	0.486	14.00	0.781	80.00	68.57	0.703–0.846	77.4	71.8
PCT	0.600	4.35	0.821	68.57	91.43	0.748–0.881	74.4	88.9
sIL-2R+TNF-α+PCT	0.657	0.70	0.846	70.00	95.71	0.775–0.901	76.1	94.2

WBC, white blood cells; CRP, C-reactive protein; SAA, serum amyloid A; IL-6, interleukin 6; SOFA, Sequential Organ Failure Assessment; sIL-2R, soluble interleukin-2 receptor; TNF-α, tumor necrosis factor alpha; PCT, procalcitonin; AUC, area under the ROC curve; NPV, negative predictive value; PPV, positive predictive value.

TABLE 3 | Comparison of AUC areas for sIL-2R, TNF-α, PCT and sIL-2R+TNF-α+PCT combined assays.

Variables	*Z*-value	*p*-value
Three combined assays compared with sIL-2R	0.851	0.395
Three combined assays compared with TNF-α	2.355	0.019
Three combined assays compared with PCT	1.160	0.246
sIL-2R and TNF-α	1.386	0.166
sIL-2R and PCT	0.162	0.871
TNF-α and PCT	1.021	0.307

AUC, area under the ROC curve; sIL-2R, soluble interleukin-2 receptor; TNF-α, tumor necrosis factor alpha; PCT, procalcitonin.

Q2, Q3, and Q4 groups from low to high levels. Compared to the group with the lowest sIL-2R levels (Q1), the ORs of sepsis risk in the Q2, Q3, and Q4 groups were 1.000 (0.328–3.052), 6.469 (2.256–18.548), and 26.156 (7.083–96.593), respectively. The ORs after correction were 0.854 (0.224–3.253), 0.403 (0.070–2.335), and 0.681 (0.074–6.262), respectively. Compared to the group with the lowest TNF-α levels (Q1), the ORs of sepsis risk in the Q2, Q3, and Q4 groups were 2.087 (0.707–6.165), 5.333 (1.839–15.471), and 31.000 (8.195–117.272), respectively. The ORs after correction were 1.098 (0.275–4.387), 0.836 (0.193–3.617), and 7.991 (1.274–50.108), respectively. Compared to the group with the lowest PCT levels (Q1), the ORs of sepsis risk in the Q2, Q3, and Q4 groups were 1.000 (0.342–2.921), 3.059 (1.117–8.373), and 98.222 (11.694–824.999), respectively. The corrected ORs were 1.013 (0.260–3.949), 0.916 (0.213–3.942), and 21.760 (2.095–226.008), as shown in **Figures 8** and **9**.

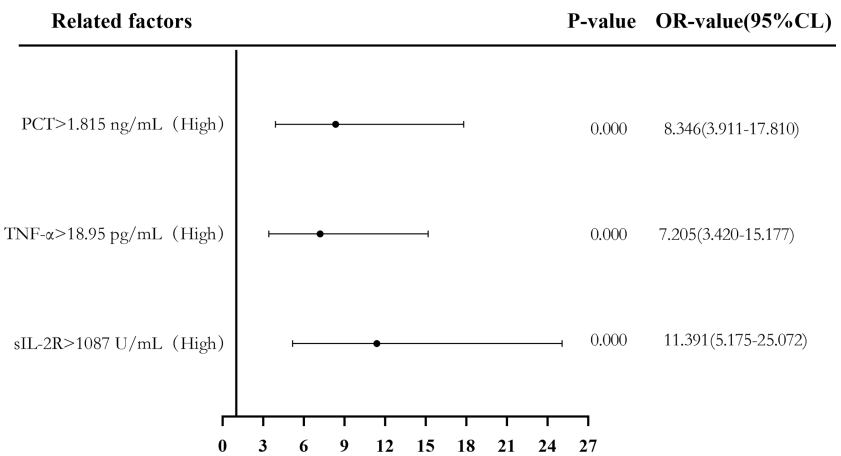

FIGURE 6 | Forest plot of the univariate logistic regression analysis of soluble interleukin-2 receptor (sIL-2R), tumor necrosis factor alpha (TNF-α), procalcitonin (PCT), and infection in patients with sepsis.

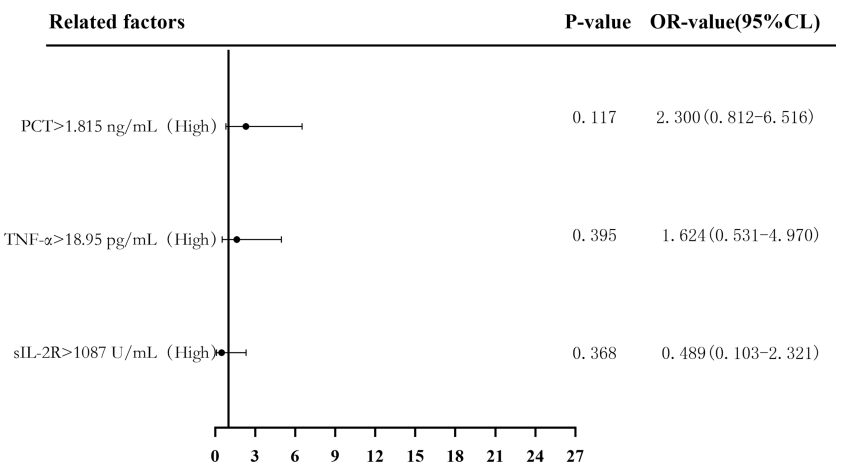

FIGURE 7 | Forest plot of the multifactorial logistic regression analysis of soluble interleukin-2 receptor (sIL-2R), tumor necrosis factor alpha (TNF-α), procalcitonin (PCT) and infection in patients with sepsis. Multifactorial correction included the following variables: sIL-2R, TNF-α, PCT, white blood cells (WBC), C-reactive protein (CRP), serum amyloid A (SAA), interleukin 6 (IL-6), and Acute Physiology and Chronic Health Assessment (APACHE II).

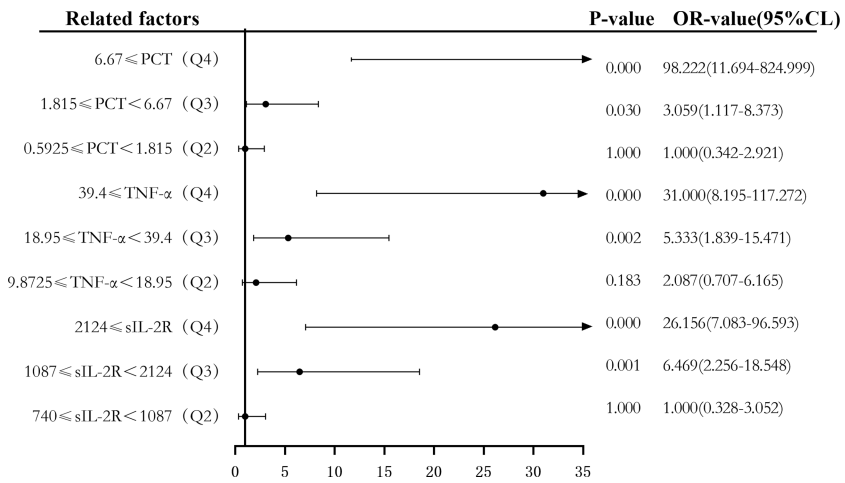

FIGURE 8 | Forest plot of the univariate logistic regression analysis of soluble interleukin-2 receptor (sIL-2R), tumor necrosis factor alpha (TNF-α), procalcitonin (PCT) and infection in patients with sepsis.

DISCUSSION

As an important complication of closed abdominal injury and severe multiple abdominal injuries, sepsis is a complex disease caused by the body's dysfunctional response to infection and is associated with acute organ dysfunction and a high risk of death (19, 20). Sepsis can lead to a global public health emergency, affecting millions of people worldwide and being one of the largest causes of death in the world (21). What plays an essential role in the treatment of sepsis is the early removal of infected lesions and the use of antibiotics as quickly and accurately as possible (22). Mortality is significantly increased for each hour of delay in antibiotic administration (23, 24), and the delay in antibiotic administration was associated with prolonged length of hospital stay, severity of organ dysfunction, and adverse clinical outcomes (25). However, for all patients with suspected sepsis, antibiotics given within 1 h will lead to its unreasonable use and to increased bacterial resistance (26–28). Therefore, early identification and diagnosis of sepsis patients have become particularly important (29).

In this study, we analyzed the diagnostic value of sIL-2R, TNF-α, and PCT in sepsis patients. The results showed that sIL-2R, TNF-α, and PCT in the sepsis group were significantly higher than those in the infection group, which was consistent

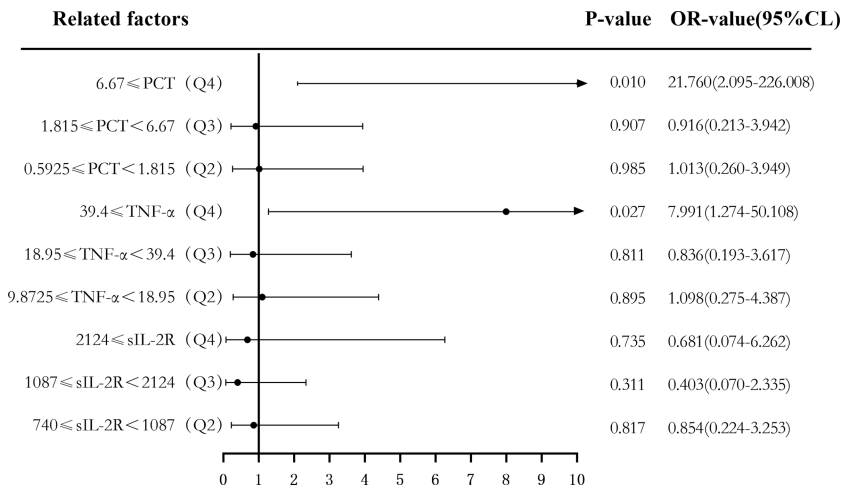

FIGURE 9 | Forest plot of the multifactor logistic regression analysis of soluble interleukin-2 receptor (sIL-2R), tumor necrosis factor alpha (TNF-α), procalcitonin (PCT), and infection in patients with sepsis. Multifactor-corrected variables included: sIL-2R, TNF-α, PCT, white blood cells (WBC), C-reactive protein (CRP), serum amyloid A (SAA), interleukin 6 (IL-6), Acute Physiology and Chronic Health Assessment (APACHE II).

with previous studies (8–10, 12, 13) on infectious diseases. It also showed a certain diagnostic value in the degree of infection in patients with closed abdominal injury combined with severe multiple injuries.

The level of sIL-2R in sepsis patients was positively correlated with WBC, CRP, SAA, IL-6, and APACHE II, and it was also positively correlated with CRP, SAA, IL-6, APACHE II, and the SOFA score in the infection group, indicating that the level of sIL-2R could better reflect the indicators related to inflammation. Similarly, studies have shown that interleukin is an important cytokine released by immune cells *in vivo*, which can regulate immune response and call immune cells to the site of infection, and interleukin presents an inflammatory response after activation of the complement pathway (30). The level of TNF-a was positively correlated with WBC, SAA, and IL-6 in the sepsis group and was also positively correlated with IL-6 in the infection group, which also indicated that the level of TNF-α could better reflect the progression of inflammation; the correlation between the TNF-α level of the sepsis group was better than that of the infection group. TNF-α plays a central role in systemic inflammatory response due to its ability to release other cytokines in the early stage of infection and its direct influence on septic shock, and the plasma levels of TNF-α are associated with sepsis-induced death (31). The level of PCT was positively correlated with IL-6 only in the sepsis group and CRP only in the infection group. The results showed that the levels of sIL-2R, TNF-α, and PCT were correlated with other laboratory indicators of infection in the two groups of patients. Only sIL-2R and TNF-α in patients with sepsis related to other laboratory indicators were higher than PCT, which may be related to differences in the sensitivity and specificity between projects.

The ROC curve of each index and the combined test generated by GraphPad Prism software showed that the AUCs of sIL-2R, TNF-α, PCT, and sIL-2R+TNF-α+PCT were higher than those of WBC, CRP, SAA, and IL-6, which is basically consistent with the study by Spiegel et al. (28), indicating that the sIL-2R, TNF-α, and PCT indexes are better than the routine laboratory infection monitoring indexes in terms of diagnostic value in infectious diseases, despite lower than the SOFA score. Comparison of the AUCs of sIL-2R, TNF-α, PCT, and sIL-2R +TNF-α+PCT showed that there was no difference between the AUCs of the three combined tests and those of sIL-2R and PCT, indicating that the three combined tests were not better than sIL-2R and PCT alone in terms of diagnostic performance. PCT still had good sensitivity and specificity in the diagnosis of sepsis caused by closed abdominal injury combined with severe multiple abdominal injury, and sIL-2R detection also had good diagnostic ability. It should be noted that the PPV of the three joint tests reached 94.2%, so these joint tests can be carried out to increase the positive predictive ability, if conditions permit.

The risk predictive value of the levels of sIL-2R, TNF-α, and PCT for sepsis was assessed using binary logistic regression analysis, with median cutoff points (two classifications) and quartiles (P25, P50, and P75) as cutoff points (four classifications). The results showed that the corrected sIL-2R, TNF-α, and PCT in the high-level group was not superior to those in the low-level group when the median cut point was used for the classification of the two groups. When the four groups were classified using quantiles as cut points, the OR risk values of the high levels of TNF-α and PCT (Q4) and the low level of PCT (Q1) after correction were 7.991 and 21.76, respectively, the difference being statistically significant. There was no significant difference between the other groups and the low-level group (Q1). The results showed that when PCT ≥ 6.67 and TNF-α ≥ 39.4, they could be used as predictors of the risk of sepsis.

CONCLUSIONS

The detection of sIL-2R, TNF-α, and PCT in patients with sepsis has good value for the diagnosis of sepsis infection in patients with closed abdominal injury complicated with severe multiple abdominal injuries. High concentrations of PCT and TNF-α can be used as predictors of the risk of septic infection.

DATA AVAILABILITY STATEMENT

The original contributions presented in the study are included in the article/supplementary material. Further inquiries can be directed to the corresponding authors.

ETHICS STATEMENT

The studies involving human participants were reviewed and approved by the ethics committees of the Fifth People's Hospital of Jiaozuo City (approval no. 20160518). Written informed consent to participate in this study was provided by the participants' legal guardian/next of kin.

AUTHOR CONTRIBUTIONS

JW, WZ, and ZX contributed to the study concept and design, acquisition of data, analysis and interpretation of data, and drafting of the manuscript. W-wW and G-hZ contributed to statistical analysis. L-zH contributed to sample collections. A-qS and G-hZ contributed to the study concept and design, study supervision, and critical revision of the manuscript. All authors contributed to the article and approved the submitted version.

FUNDING

This work was supported by the National Natural Science Foundation of China (no. 81802084) and Jiaozuo science and technology project (no. 2020162).

REFERENCES

1. Chughtai T, Parchani A, Strandvik G, Verma V, Arumugam S, El-Menyar A, et al. Trauma Intensive Care Unit (TICU) at Hamad General Hospital. *Qatar Med J* (2020) 2019(2):5. doi: 10.5339/qmj.2019.qccc.5
2. Khalifa A, Avraham JB, Kramer KZ, Bajani F, Fu CY, Pires-Menard A, et al. Surviving Traumatic Cardiac Arrest: Identification of Factors Associated With Survival. *Am J Emerg Med* (2021) 43:83–7. doi: 10.1016/j.ajem.2021.01.020
3. Pantoja Pachajoa DA, Palacios Huatuco RM, Bruera N, Llahi F, Doniquian AM, Alvarez FA. Minimally Invasive Splenectomy in Grade IV Splenic Trauma: A Case Report Associated With High-Grade Renal Trauma. *Int J Surg Case Rep* (2021) 79:28–33. doi: 10.1016/j.ijscr.2020.12.077
4. Fu C-Y, Bajani F, Bokhari M, Starr F, Messer T, Kaminsky M, et al. Age Itself or Age-Associated Comorbidities? A Nationwide Analysis of Outcomes of Geriatric Trauma. *Eur J Trauma Emerg Surg* (2021) 1–8. doi: 10.1007/s00068-020-01595-8
5. Mustafić S, Brkić S, Prnjavorac B, Sinanović A, Porobić Jahić H, Salkić S. Diagnostic and Prognostic Value of Procalcitonin in Patients With Sepsis. *Med Glas (Zenica)* (2018) 15(2):93–100. doi: 10.17392/963-18
6. De Oro N, Gauthreaux ME, Lamoureux J, Scott J. The Use of Procalcitonin as a Sepsis Marker in a Community Hospital. *J Appl Lab Med* (2019) 3(4):545–52. doi: 10.1373/jalm.2018.026955
7. Sakyi SA, Enimil A, Adu DK, Ephraim RD, Danquah KO, Fondjo L, et al. Individual and Combined Bioscore Model of Presepsin, Procalcitonin, and High Sensitive C - Reactive Protein as Biomarkers for Early Diagnosis of Paediatric Sepsis. *Heliyon* (2020) 6(9):e04841. doi: 10.1016/j.heliyon.2020.e04841
8. Naderpour Z, Momeni M, Vahidi E, Safavi J, Saeedi M. Procalcitonin and D-Dimer for Predicting 28-Day-Mortality Rate and Sepsis Severity Based on SOFA Score; A Cross-Sectional Study. *Bull Emerg Trauma* (2019) 7(4):361–5. doi: 10.29252/beat-070404
9. Downes KJ, Fitzgerald JC, Weiss SL. Utility of Procalcitonin as a Biomarker for Sepsis in Children. *J Clin Microbiol* (2020) 58(7):e01851-19. doi: 10.1128/JCM.01851-19
10. Gregoriano C, Heilmann E, Molitor A, Schuetz P. Role of Procalcitonin Use in the Management of Sepsis. *J Thorac Dis* (2020) 12(Suppl 1):S5–S15. doi: 10.21037/jtd.2019.11.63
11. Singer M, Deutschman CS, Seymour CW, Shankar-Hari M, Annane D, Bauer M, et al. The Third International Consensus Definitions for Sepsis and Septic Shock (Sepsis-3). *JAMA* (2016) 315(8):801–10. doi: 10.1001/jama.2016.0287
12. Song J, Park DW, Moon S, Cho HJ, Park JH, Seok H, et al. Diagnostic and Prognostic Value of Interleukin-6, Pentraxin 3, and Procalcitonin Levels Among Sepsis and Septic Shock Patients: A Prospective Controlled Study According to the Sepsis-3 Definitions. *BMC Infect Dis* (2019) 19(1):968. doi: 10.1186/s12879-019-4618-7
13. Prasad PA, Fang MC, Abe-Jones Y, Calfee CS, Matthay MA, Kangelaris KN. Time to Recognition of Sepsis in the Emergency Department Using Electronic Health Record Data: A Comparative Analysis of Systemic Inflammatory Response Syndrome, Sequential Organ Failure Assessment, and Quick Sequential Organ Failure Assessment. *Crit Care Med* (2020) 48(2):200–9. doi: 10.1097/CCM.0000000000004132
14. Hosomi S, Yamagami H, Itani S, Yukawa T, Otani K, Nagami Y, et al. Sepsis Markers Soluble IL-2 Receptor and Soluble CD14 Subtype as Potential Biomarkers for Complete Mucosal Healing in Patients With Inflammatory Bowel Disease. *J Crohns Colitis* (2018) 12(1):87–95. doi: 10.1093/ecco-jcc/jjx124
15. Nguyen T, Nguyen HT, Wang PC, Chen SC. Identification and Expression Analysis of Two Pro-Inflammatory Cytokines, TNF-α and IL-8, in Cobia (Rachycentron Canadum L.) in Response to Streptococcus Dysgalactiae Infection. *Fish Shellfish Immunol* (2017) 67:159–71. doi: 10.1016/j.fsi.2017.06.014
16. Das CR, Tiwari D, Dongre A, Khan MA, Husain SA, Sarma A, et al. Deregulated TNF-Alpha Levels Along With HPV Genotype 16 Infection Are Associated With Pathogenesis of Cervical Neoplasia in Northeast Indian Patients. *Viral Immunol* (2018) 31(4):282–91. doi: 10.1089/vim.2017.0151
17. Popescu M, Cabrera-Martinez B, Winslow GM. TNF-α Contributes to Lymphoid Tissue Disorganization and Germinal Center B Cell Suppression During Intracellular Bacterial Infection. *J Immunol* (2019) 203(9):2415–24. doi: 10.4049/jimmunol.1900484
18. Schmidt de Oliveira-Netto AC, Morello LG, Dalla-Costa LM, Petterle RR, Fontana RM, Conte D, et al. Procalcitonin, C-Reactive Protein, Albumin, and Blood Cultures as Early Markers of Sepsis Diagnosis or Predictors of Outcome: A Prospective Analysis. *Clin Pathol* (2019) 12:2632010X19847673. doi: 10.1177/2632010X19847673
19. Cecconi M, Evans L, Levy M, Rhodes A. Sepsis and Septic Shock. *Lancet* (2018) 392(10141):75–87. doi: 10.1016/S0140-6736(18)30696-2
20. Rhodes A, Evans LE, Alhazzani W, Levy MM, Antonelli M, Ferrer R, et al. Surviving Sepsis Campaign: International Guidelines for Management of Sepsis and Septic Shock: 2016. *Crit Care Med* (2017) 45(3):486–552. doi: 10.1097/CCM.0000000000002255
21. Coopersmith CM, De Backer D, Deutschman CS, Ferrer R, Lat I, Machado FR, et al. Surviving Sepsis Campaign: Research Priorities for Sepsis and Septic Shock. *Intensive Care Med* (2018) 44(9):1400–26. doi: 10.1007/s00134-018-5175-z
22. Bracht H, Hafner S, Weiß M. [Sepsis Update: Definition and Epidemiology]. *Anasthesiol Intensivmed Notfallmed Schmerzther* (2019) 54(1):10–20. doi: 10.1055/a-0625-5492
23. Seymour CW, Gesten F, Prescott HC, Friedrich ME, Iwashyna TJ, Phillips GS, et al. Time to Treatment and Mortality During Mandated Emergency Care for Sepsis. *N Engl J Med* (2017) 376(23):2235–44. doi: 10.1056/NEJMoa1703058
24. Levy MM, Evans LE, Rhodes A. The Surviving Sepsis Campaign Bundle: 2018 Update. *Intensive Care Med* (2018) 44(6):925–8. doi: 10.1007/s00134-018-5085-0
25. Moss SR, Prescott HC. Current Controversies in Sepsis Management. *Semin Respir Crit Care Med* (2019) 40(5):594–603. doi: 10.1055/s-0039-1696981
26. Singer M. Antibiotics for Sepsis: Does Each Hour Really Count, or Is It Incestuous Amplification. *Am J Respir Crit Care Med* (2017) 196(7):800–2. doi: 10.1164/rccm.201703-0621ED
27. Chen AX, Simpson SQ, Pallin DJ. Sepsis Guidelines. *N Engl J Med* (2019) 380(14):1369–71. doi: 10.1056/NEJMclde1815472
28. Spiegel R, Farkas JD, Rola P, Kenny JE, Olusanya S, Marik PE, et al. The 2018 Surviving Sepsis Campaign's Treatment Bundle: When Guidelines Outpace the Evidence Supporting Their Use. *Ann Emerg Med* (2019) 73(4):356–8. doi: 10.1016/j.annemergmed.2018.06.046
29. Napolitano LM. Sepsis 2018: Definitions and Guideline Changes. *Surg Infect (Larchmt)* (2018) 19(2):117–25. doi: 10.1089/sur.2017.278
30. Palmer J, Pandit V, Zeeshan M, Kulvatunyou N, Hamidi M, Hanna K, et al. The Acute Inflammatory Response After Trauma is Heightened by Frailty: A Prospective Evaluation of Inflammatory and Endocrine System Alterations in Frailty. *J Trauma Acute Care Surg* (2019) 87(1):54–60. doi: 10.1097/TA.0000000000002229
31. Georgescu AM, Banescu C, Azamfirei R, Hutanu A, Moldovan V, Badea I, et al. Evaluation of TNF-α Genetic Polymorphisms as Predictors for Sepsis Susceptibility and Progression. *BMC Infect Dis* (2020) 20(1):221. doi: 10.1186/s12879-020-4910-6

Conflict of Interest: The authors declare that the research was conducted in the absence of any commercial or financial relationships that could be construed as a potential conflict of interest.

frontiers in Immunology

REVIEW
published: 27 October 2021
doi: 10.3389/fimmu.2021.763831

The Role of HDAC6 in Autophagy and NLRP3 Inflammasome

Panpan Chang[1†], Hao Li[2†], Hui Hu[3], Yongqing Li[4] and Tianbing Wang[1*]*

[1] Trauma Medicine Center, Peking University People's Hospital, Key Laboratory of Trauma and Neural Regeneration (Peking University), National Center for Trauma Medicine of China, Beijing, China, [2] Department of Emergency, First Hospital of China Medical University, Shenyang, China, [3] Department of Traumatology, Central Hospital of Chongqing University, Chongqing Emergency Medical Center, Chongqing, China, [4] Department of Surgery, University of Michigan, Ann Arbor, MI, United States

Autophagy fights against harmful stimuli and degrades cytosolic macromolecules, organelles, and intracellular pathogens. Autophagy dysfunction is associated with many diseases, including infectious and inflammatory diseases. Recent studies have identified the critical role of the NACHT, LRR, and PYD domain-containing protein 3 (NLRP3) inflammasomes activation in the innate immune system, which mediates the secretion of proinflammatory cytokines IL-1β/IL-18 and cleaves Gasdermin D to induce pyroptosis in response to pathogenic and sterile stimuli. Accumulating evidence has highlighted the crosstalk between autophagy and NLRP3 inflammasome in multifaceted ways to influence host defense and inflammation. However, the underlying mechanisms require further clarification. Histone deacetylase 6 (HDAC6) is a class IIb deacetylase among the 18 mammalian HDACs, which mainly localizes in the cytoplasm. It is involved in two functional deacetylase domains and a ubiquitin-binding zinc finger domain (ZnF-BUZ). Due to its unique structure, HDAC6 regulates various physiological processes, including autophagy and NLRP3 inflammasome, and may play a role in the crosstalk between them. In this review, we provide insight into the mechanisms by which HDAC6 regulates autophagy and NLRP3 inflammasome and we explored the possibility and challenges of HDAC6 in the crosstalk between autophagy and NLRP3 inflammasome. Finally, we discuss HDAC6 inhibitors as a potential therapeutic approach targeting either autophagy or NLRP3 inflammasome as an anti-inflammatory strategy, although further clarification is required regarding their crosstalk.

Keywords: HDAC6, autophagy, NLRP3 inflammasome, inflammation, post-translational modification

OPEN ACCESS

Edited by:
Rui Li,
University of Pennsylvania, United States

Reviewed by:
Chunying Pei,
Harbin Medical University, China
Jie Xu,
University of Michigan, United States

****Correspondence:***
Tianbing Wang
wangtianbing@pkuph.edu.cn
Panpan Chang
changpanpan@bjmu.edu.cn

[†]These authors have contributed equally to this work and share first authorship

Specialty section:
This article was submitted to Inflammation, a section of the journal Frontiers in Immunology

Received: *24 August 2021*
Accepted: *28 September 2021*
Published: *27 October 2021*

Citation:
Chang P, Li H, Hu H, Li Y and Wang T (2021) The Role of HDAC6 in Autophagy and NLRP3 Inflammasome. Front. Immunol. 12:763831. doi: 10.3389/fimmu.2021.763831

INTRODUCTION

Autophagy is a conservative mechanism for maintaining homeostasis in cells, which degrades misfolded proteins, damaged organelles, and intracellular pathogens (1). It is associated with many diseases, including infectious and inflammatory diseases (2). The NACHT, LRR, and PYD domain-containing protein 3 (NLRP3) inflammasomes are oligomeric complexes activated by invading pathogens, endogenous danger signals, and stress signals (3). The activation of NLRP3 inflammasome induces interleukin-1β (IL-1β) and interleukin-18 (IL-18) release and pyroptosis,

which is a caspase-1-dependent form of programmed cell death (4). NLRP3 inflammasome is essential for defense against infectious and inflammatory diseases, and its aberrant activation aggravates inflammation and tissue damage (5, 6). Recent studies have suggested that autophagy eliminates the overaction of NLRP3 inflammasome and maintains homeostasis (7–9). Additionally, NLRP3 inflammasome activation can upregulate autophagy to suppress excessive responses and protect the host (10, 11). There is emerging evidence highlighting the importance of crosstalk between autophagy and NLRP3 inflammasome in various inflammatory diseases (12–16).

Histone deacetylase 6 (HDAC6) is a class IIb deacetylase found in 18 mammalian HDACs. It harbors two functional deacetylase catalytic domains and a ubiquitin-binding zinc finger domain (ZnF-BUZ) (17). HDAC6 is a structurally and functionally unique cytoplasmic deacetylase that can deacetylate multiple non-histone proteins such as α-tubulin, cortactin, heat shock protein (HSP90), heat shock transcription factor-1 (HSF-1), peroxiredoxin I (Prx I), and peroxiredoxin II (Prx II) (18–21). In addition, HDAC6 binds to ubiquitinated misfolded proteins through the ZnF-BUZ (22). Therefore, it is essential for multiple physiological and pathological processes. Recent studies have demonstrated that HDAC6 regulates autophagy and NLRP3 inflammasome activation through various mechanisms (14, 23–27). It is suggested that HDAC6 plays a possible role in the crosstalk between autophagy and NLRP3 inflammasome, although there is little direct evidence to date. In this review, we present the distinct roles of HDAC6 in the regulation of autophagy and NLRP3 inflammasome. We then focus on exploring the possibility and challenges of HDAC6 involvement in the crosstalk between autophagy and NLRP3 inflammasome. Finally, we discuss HDAC6 inhibitors as a promising therapeutic target for various diseases and its prospect in the crosstalk between autophagy and NLRP3 inflammasome.

THE ROLE OF HDAC6 IN AUTOPHAGY

Autophagy, specifically macroautophagy, is a conserved self-eating process that is vital for cellular homeostasis and delivery intracellular components, including soluble proteins, aggregated proteins, organelles, macromolecular complexes, and foreign bodies for degradation (28). This process begins with the sequestration of organelles or portions of the cytoplasm into a double-membrane structure, the autophagosome (29). Autophagosomes fuse with lysosomes to form hybrid organelles called autophagolysosomes (30). Autophagolysosomes degrade the contents to achieve cell homeostasis and organelle renewal (31). HDAC6 is involved in the regulation of autophagy at multiple levels, including participation in post-translational modifications (PTM) of autophagy-related transcription factors (32, 33), the formation of aggresomes that are routinely cleaned through the autophagy pathway (22, 34, 35), and the transportation and degradation of autophagosomes (**Figure 1**) (23, 25).

The Role of HDAC6 in PTM of Autophagy-Related Transcription Factors

PTM of autophagy-related transcription factors (36), such as transcription factor EB (TFEB) and Forkhead Box 1 (FOXO1) affect their activities, which regulate the autophagy-lysosome pathway (37–39). Recently, it was reported that HDAC6 deacetylates TFEB and FOXO1 to decrease their activity and inhibit autophagy (32, 33, 40, 41).

TFEB is a major regulator of the autophagy-lysosomal pathway (42). Acetylation of TFEB causes translocation to the nucleus and enhancement of autophagy and lysosomal gene transcription (32, 40). It was reported that acetylated TFEB accumulates in the nuclei, which is associated with increased transcriptional activity and lysosomal function following treatment with a pan-HDAC inhibitor, SAHA (40). Similarly, in subtotally nephrectomized rats, the HDAC6 inhibitor Tubastatin A (Tub-A) promotes the acetylation of TFEB, which translocates into the nucleus and enhances the expression of autophagy-related protein Beclin 1 (32), a known direct target of TFEB (43). However, Jung et at. showed that HDAC6 overexpression activated c-Jun NH2-terminal kinase (JNK) and increased the phosphorylation of c-Jun, which activated Beclin 1 dependent autophagy in liver cancer (44).

Besides TFEB, HDAC6 also deacetylates the transcription factor FOXO1 (33), which is a conserved transcription factor that modulates autophagy (45). It has been reported that HDAC6 binds to and deacetylates cytosolic FOXO1, which is required for nuclear translocation and stabilization of interleukin-17 (IL-17)-producing helper T cells (46). Zhang et al. found that trichostatin A (TSA), an HDAC inhibitor, enhances the transcriptional activity of FOXO1 by increasing its acetylation, which enhances the process of autophagy (41). Recently, another study reported that HDAC6 was suppressed by the calcium binding protein S100 calcium binding protein A11 (S100A11) in hepatocytes, which leads to the upregulation of FOXO1 acetylation to enhance its transactional activity and activate autophagy (33).

The Role of HDAC6 in Aggresome Degradation Mediated by Autophagy

Under physiological conditions, misfolded and aggregated proteins are cleaned through ubiquitylation and proteasome-mediated degradation (47, 48). When the degrading capacity is overwhelmed (47), misfolded or aggregated proteins are generally transported along microtubules towards the microtubule-organizing center (MTOC) through motor protein dynein (49). Once at the MTOC, they are packaged into a single aggresome (49), which is eventually degraded by autophagy (50). Aggresomes are crucial for the clearance of accumulated misfolded proteins and cellular death (51). HDAC6 is a component of aggresomes induced by misfolded proteins. In the process of forming aggresomes containing ubiquitinated proteins, HDAC6 works as a bridge between ubiquitinated-misfolded proteins and the dynein motor (22). It binds to polyubiquitinated misfolded CFTR-ΔF508 *via* its C-terminus ubiquitin binding ZnF-BUZ domain, and it binds to the

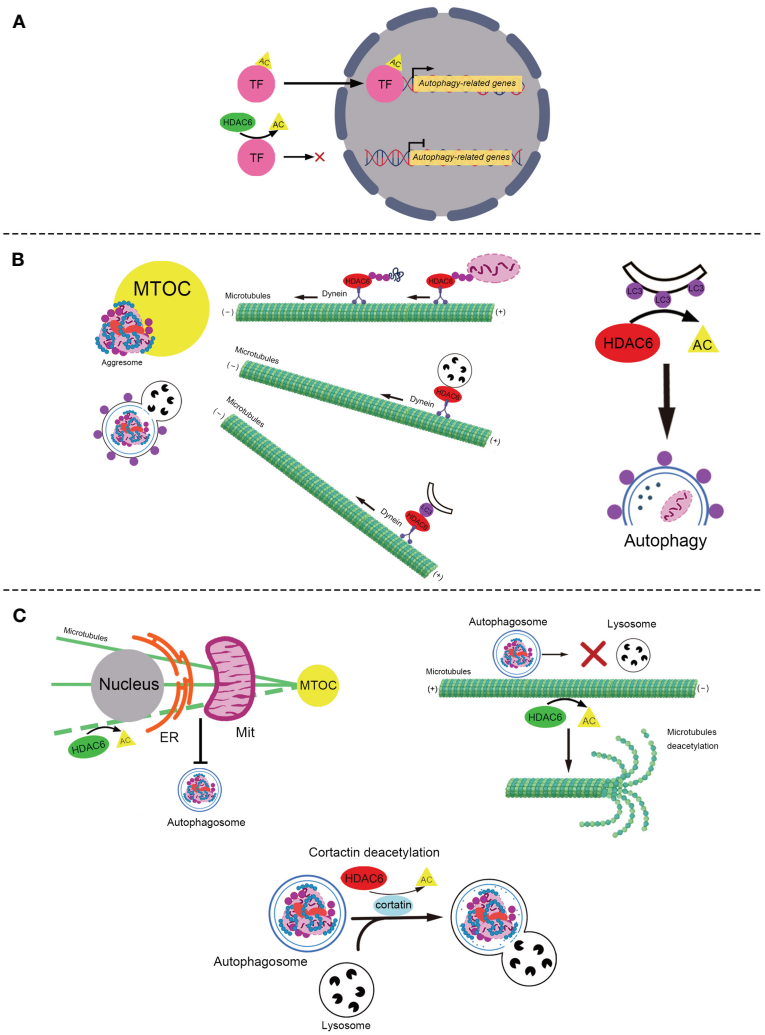

FIGURE 1 | The role of HDAC6 in autophagy. **(A)** The role of HDAC6 in PTM of autophagy-related transcription factors. HDAC6 deacetylates transcription factors, TFEB and FOXO1, to reduce their transcriptional activity and inhibit autophagy. **(B)** HDAC6 promotes the autophagic degradation of aggresome in various ways. Left: HDAC6 interacts with the microtubule motor protein dynein to escort the ubiquitinated misfolded protein or ubiquitinated damaged mitochondria to form the aggresome, to transport the lysosome for the degardaion of aggresome, and to deliver LC3-II (the purple point) to promote the formation of the autophagosome containing aggresome. Right: HDAC6 deacetylates LC3-II to promote the formation of the autophagosome. **(C)** HDAC6 plays various roles in the regulation of autophagy *via* deacetylating α-tubulin and cortactin (positive and negative roles are marked with red and green respectively). Top-left: HDAC6 deacetylates microtubules to block the ER–Mit contact where autophagosome generates. Top-right: HDAC6 suppresses the transport of autophagosomes through deacetylating and reducing the stability of the microtubules. Bottom: HDAC6 blocks the fusion of the autophagosome that contains the misfolded protein or mitochondria and the lysosome by deacetylating cortactin. HDAC6, Histone deacetylase 6; TF, Transcription factor; PTM, Post-translational modifications; AC, Acetylation; FOXO1, Forkhead Box 1; TFEB, Transcription factor EB; MTOC, Microtubule-organizing center; LC3, Microtubule-associated protein 1 light chain 3; ER, Endoplasmic Reticulum; Mit, Mitochondria.

dynein motor through a separate domain, dynein motor domain (DMB) (22). However, HDAC6 may not recognize protein aggregates and may not bind directly to polyubiquitinated proteins. A recent study indicated that the ZnF-UBP domain of HDAC6 binds to unconjugated C-terminal diglycine motifs of ubiquitin, and this interaction is important for the binding and transport of polyubiquitinated protein aggregates (35). In addition, small-molecule inhibition of HDAC6 has been shown to inhibit the formation of aggresomes in multiple myeloma and lymphoma models (52–54). Recently, HDAC6 was found to be involved in the formation of aggresomes of α-synuclein, TAR DNA-binding protein 43, and Tau (34, 55, 56). It has been suggested that HDAC6 acts as a scaffold for a variety of ubiquitinated proteins. Strikingly, although HDAC6 was initially concentrated at the aggresome as previously reported (22), it was no longer detectable in the ubiquitin-positive

structures once aggresomes were cleared by autophagy (57). As the HDAC6 protein levels remained stable during the biological process of aggresome formation and clearance, HDAC6 is not degraded together with aggresomes (57). HDAC6 seems recycled during aggresome-autophagy.

Other studies have shown that HDAC6 is required for lysosomes to form aggregates. Lysosomes are generated in the cell periphery and transported to MTOC to degrade aggresomes (58). HDAC6 and dynein transport lysosomes along microtubules to promote autophagic degradation of aggresomes (59, 60). Lee et al. found that lysosomes in HDAC6 knockout mouse embryonic fibroblasts were dispersed to the cell periphery and not concentrated to protein aggregates (59). Similarly, Iwata et al. also showed that HDAC6 knockdown leads to the periplasmic dispersion of lysosomes (60). This indicates that the targeting of lysosomes to autophagic substrates is regulated by HDAC6.

Microtubule-associated protein 1 light chain 3 (LC3) is a well-known regulator of autophagy (61). LC3-I is conjugated to phosphatidylethanolamine to form LC3-PE conjugate (LC3-II), which is recruited to autophagosomal membranes to promote its formation (62, 63). HDAC6 transports LC3 to the MTOC to promote autophagosome formation (60). The knockdown of HDAC6 attenuates the recruitment of LC3 to aggregated Huntingtin protein for degradation in Neuro2a cells and HeLa cells (60). However, the mechanism by which HDAC6 regulates LC3 needs to be further elucidated. In addition, the deacetylation of LC3 influences autophagy in starvation-induced cells (64). Liu et al. reported that the deacetylation of LC3-II modulated by HDAC6 promotes autophagic flux in starvation-induced HeLa cells (65). The acetylation of LC3-II increases in HDAC6 siRNA Hela cells, which blocks autophagy flux (65). These studies suggested HDAC6 works as a scaffold protein or deacetylase to regulate LC3, which promotes autophagy.

HDAC6 Deacetylates α-Tubulin and Cortactin to Mediate Autophagy

HDAC6 associates with microtubules and filamentous actin (F-actin) by deacetylating α-tubulin (66–68), and cortactin (19), both of which play important roles in autophagy (69–71). As the first reported and most studied physiological substrate of HADC6, α-tubulin is deacetylated by HDAC6 at lysine 40 (72). Additionally, acetylation of cortactin following inhibition of HDAC6 reduces its interaction with F-actin (19).

Microtubules, composed of α- and β-tubulin heterodimers (73), are essential for cell division, shaping, motility, and intracellular transport (74). Accumulating evidence indicates that microtubules participate in the mediation of autophagosome formation (75, 76), autophagosome transport across the cytoplasm (77, 78), and the formation of autolysosomes (79, 80). Lei et al. demonstrated that HDAC6 decreases the acetylation of microtubules to inhibit the formation of autophagosomes in acidic pH-mediated rat cardiomyocytes (81). The possible underlying mechanism is that acetylation of α-tubulin enhances the endoplasmic reticulum-mitochondria contact, which promotes the formation of autophagosomes (82, 83). Additionally, other studies have reported that HDAC6 mediates α-tubulin deacetylation to suppress autophagy in podocytes and human embryonic kidney 293 cells (84, 85). However, the underlying mechanisms remain unclear. It has been suggested that HDAC6 impairs stable acetylated microtubules *via* deacetylating α-tubulin, which leads to the blockade of autophagosome-lysosome fusion and accumulation of autophagosomes (86). In mouse embryonic fibroblasts, bpV(phen), an insulin mimic and a PTEN inhibitor, blocked autophagosomal degradation by reducing the stability of p62 to activate HDAC6 to impair the fusion of autophagosomes and lysosomes, followed by acetylation of microtubules (86). Furthermore, Li et at. found that HDAC6 inhibited the transportation of autophagosomes to fuse with lysosomes through the deacetylation of α-tubulin, resulting in the depolymerization of microtubules (25). In conclusion, HDAC6 suppresses the formation and degradation of autophagosome *via* deacetylation the microtubules.

As an important part of the cytoskeleton, the F-actin network plays an important role in cell movement, adhesion, morphology, and intracellular material transport (87). Additionally, the F-actin network is essential for the fusion of autophagosomes and lysosomes (70). Lee et al. found that HDAC6 promotes autophagy by recruiting a cortactin-dependent, actin-remodeling machinery, which in turn assembles an F-actin network that stimulates autophagosome-lysosome fusion and substrate degradation (23). However, this mechanism has been demonstrated in quality control autophagy but not in starvation-induced autophagy (23). It is possible that substrates of starvation-induced autophagy are widely distributed in the cell and encounter lysosomes more easily (23). Recently, another study reported that HDAC6 was recruited by ATP13A2, whose mutations are associated with Kufor-Rakeb syndrome (KRS), an autosomal recessive form of juvenile-onset atypical Parkinson's disease (PD), which is known as Parkinson's disease-9, to deacetylate cortactin and promote autophagosome-lysosome fusion and autophagy (88). Impaired ATP13A2/HDAC6/cortactin signaling likely contributes to KRS and PD pathogenesis by disrupting the clearance of protein aggregates and damaged mitochondria (88). These results indicate HDAC6 deacetylates cortactin which enhances the activity of the F-actin network to promote the fusion of autophagosomes and lysosomes.

The Role of HDAC6 in Mitophagy

Mitophagy is an autophagic response that specifically targets damaged and potentially cytotoxic mitochondria (89, 90). HDAC6 has also been reported to mediate mitophagy (88, 91, 92). The underlying mechanisms may include the formation of mitochondrial aggregates (mito-aggresomes) (91–94), and degradation of mitophagosomes through cortactin or α-tubulin action (88, 92, 93, 95). Parkin, a ubiquitin ligase, promotes mitophagy by catalyzing mitochondrial ubiquitination, which in turn recruits ubiquitin-binding autophagic components, HDAC6 and p62, leading to mitochondrial clearance (91, 92). Similar to the aggresome, the formation of mito-aggresomes depends on the transportation of microtubule dynein motors mediated by HDAC6 to MTOC (91, 92). HDAC6 deacetylates

cortactin to promote the fusion of mitophagosomes and lysosomes (91, 93). Mito-aggresomes are then degraded by the conventional autophagy pathway (88, 91, 93). Conversely, Pedro et al. found that pharmacological inhibition of the HDAC6 deacetylase activity with Tub-A, did not block striatal neuronal autophagosome-lysosome fusion, suggesting no impairment in mitophagy (95). Interestingly, that HDAC6 inhibition increased acetylated α-tubulin levels, and induced mitophagy in striatal neurons (95). Overall, the effects and mechanisms of HDAC6 in mitophagy remain to be elucidated.

The Relationship of HDAC6 and p62 in Autophagy

P62 is the first selective autophagy adaptor protein discovered in mammals (96, 97), and plays multiple roles in autophagy, including participating in the formation of aggresomes (98, 99), anchoring the aggresomes to the autophagosome (100), and the degradation of aggresomes in selective autophagy (101, 102). Accumulating evidence indicates that the interaction between HDAC6 and p62 is curial for autophagy (23, 39, 86, 91, 103–108). As mentioned above, HDAC6 and p62 work as two ubiquitin-binding proteins required for efficient autophagy that target protein aggregates and damaged mitochondria (23, 91). Cyclin-dependent kinase 1 (CDK1) in human breast cancer is degraded by p62- and HDAC6- mediated selective autophagy (104). Additionally, interferon-stimulated gene 15 (ISG15) interacts with HDAC6 and p62 independently to be degraded through autophagy (105). These studies suggest that HDAC6 and p62 may mediate autophagy in parallel. However, other studies have indicated that HDAC6 and p62 may regulate autophagy synergistically. Yan et al. reported that HDAC6 regulates lipid droplet turnover in response to nutrient deprivation *via* p62-mediated aggresome formation (107). Interestingly, some studies have indicated that p62 inhibits the deacetylase activity of HDAC6 to enhance the acetylation of microtubules or cortactin, promoting autophagic flux (86, 103, 108). In contrast, Jiang et al. showed that p62 promotes the expression of HDAC6, reducing the acetylation level of microtubules and inhibiting autophagy in hormone-independent prostate adenocarcinoma cell lines (109). However, the mechanisms by which p62 regulates HDAC6 remain to be clarified. The relationship between HDAC6 and p62 is complicated. Thus, further research is required to elucidate the underlying mechanisms.

It is interesting that HDAC6 differentially regulates autophagy *via* multiple mechanisms. It may depend on the specific cell type, disease, and autophagy inducer/inhibitor. The mechanisms of HDAC6 regulation in autophagy require further investigation.

THE ROLE OF HDAC6 IN NLRP3 INFLAMMASOME

The canonical NLRP3 inflammasome consists of NLRP3 (the sensors), apoptosis-associated speck-like protein containing a caspase recruitment domain (ASC) (the adaptor), and protein-caspase-1 (the effector) (4). It is critical for the innate immune system to mediate caspase-1 activation to release proinflammatory cytokines IL-1β/IL-18 and cleave Gasdermin D to induce pyroptosis in response to microbial infection and cellular damage (110–112). The mechanism of the canonical NLRP3 inflammasome is currently considered to include the following: priming, activation, and PTM- interacting components. The primary signal induces the activation of Toll-like-receptors (TLRs) and nuclear factor-kappa B (NF-κB), leading to transcriptional upregulation of NLRP3, pro-IL-1β, and pro-IL-18 (112). The secondary signal is provided by multiple molecular or cellular events, including ionic flux, mitochondrial dysfunction, and reactive oxygen species (ROS) generation (113). The aberrant activation of NLRP3 inflammasome is responsible for a wide range of inflammatory diseases such as sepsis, trauma and gout (3, 114–116). HDAC6 plays various roles in the priming, activation and PTM of NLRP3 inflammasome (**Figure 2**) (14, 26, 27, 117).

The Role of HDAC6 in the Priming of NLRP3 Inflammasome

NF-κB, activated by the primary signal, promotes the transcription of NLRP3, pro-IL-1β, and pro-IL-18 (112). The NF-κB transcription factor complex plays a central role in regulating the inducible expression of inflammatory genes in response to immune and inflammatory stimuli. Acetylation of p65, a subunit of NF-κB, has been found to regulate its translocation (118, 119). Jia et al. found that HDAC6 inhibition induces the acetylation of p65 to inhibit its nuclear translocation in diffuse large B-cell lymphoma (120). Xu et al. showed that HDAC6 inhibition upregulated p65 expression in the cytoplasm and reduced p65 expression in the macrophage nucleus to attenuate the transcription of NLRP3 and reduce pyroptosis (27). The inhibition of HDAC6 also reduces p65 expression levels in the nucleus after high glucose stimulation of human retinal pigment epithelium cells, thereby inhibiting the expression of NLRP3 protein and attenuating inflammation (121). These studies suggest HDAC6 deacetylates p65 to upregulate the priming of NLRP3 inflammasome.

Additionally, HDAC6 has been reported to promote the expression of NF-κB to enhance the transcription of pro-IL-1β, increase the release of IL-1β, and aggravate inflammation *via* the interaction of upstream activators of NF-κB, including myeloid differentiation primary response protein 88 (Myd88), α-tubulin, and ROS (93, 122, 123). Gonzalo et al. found that HDAC6 interacts with the TLR adaptor molecule Myd88 (93). The absence of HDAC6 appears to diminish NF-κB induction by TLR4 stimulation and decrease the release of inflammatory factors, including IL-1β (93). Inhibition of HDAC6 upregulates the acetylation of α-tubulin, which decreases the depolymerization of microtubules, to attenuate the activation of NF-κB by blocking IκBα phosphorylation and IL-1β release in mouse lung tissues challenged with lipopolysaccharide (LPS) (122). ROS are mainly produced by NADPH oxidases (124, 125), which are composed of two membrane-bound subunits (p22phox and gp91phox/

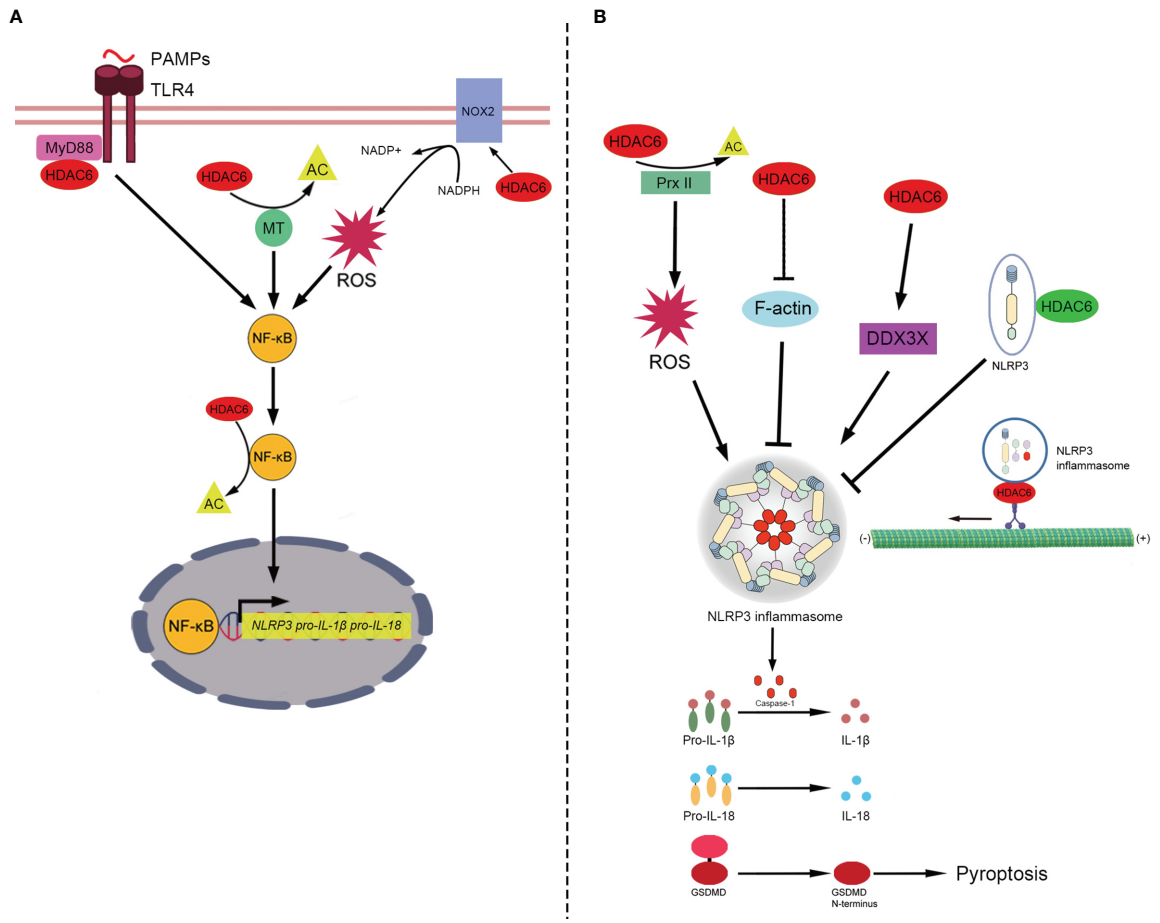

FIGURE 2 | The role of HDAC6 in NLRP3 inflammasome. **(A)** In the priming of NLRP3 inflammasome, HDAC6 promotes NF-κB to enhance the transcription of NLRP3, pro-IL-1β and pro-IL-18. HDAC6 promotes NF-κB in a number of mechanisms. (1) TLR4 senses PAMPs and recruits the downstream adapter proteins MyD88. HDAC6 interacts with MyD88 to enhance the activation of NF-κB. (2) HDAC6 deacetylates microtubules to promote the activity of NF-κB. (3) HDAC6 elevates the expression of NOX2, the component of NADPH oxidase, to promote the level of ROS which upregulates NF-κB activity. (4) HDAC6 directly deacetylates NF-κB. Then, NF-κB upregulates the transcription of NLRP3, pro-IL-1β, and pro-IL-18. **(B)** The role of HDAC6 in the activation and PTM of NLRP3 inflammasome includes a variety of signaling mechanisms (positive and negative roles are marked with red and green respectively). HDAC6 regulates the activation of NLRP3 inflammasome in different ways. (1) HDAC6 suppresses the activity of Prx II *via* deacetylation and increase the level of ROS which is vital for the activation of NLRP3 inflammasome. (2) HDAC6 promotes the activation of NLRP3 inflammasome *via* suppressing F-actin, a negative factor of NLRP3 assembly. (3) HDAC6 enhances the expression of DDX3X. And DDX3X facilitates NLRP3 assembly. In addition, HDAC6 plays both the negative and positive roles in the PTM of NLRP3 inflammasome. The negative one: HDAC6 interacts with ubquitinated NLRP3 protein directly to prevents the activation of NLRP3 inflammasome. The positive one: In an aggresome-like way, HDAC6 works as a dynein adapter to facilitate retrograde transport of NLRP3 inflammasome for activation. Finally, NLRP3 inflammasome releases active caspase-1, which can promote pro-IL-1β/IL-18 to IL-1β/IL-18 and cleave GSDMD to induce pyroptosis. HDAC6, Histone deacetylase 6; NF-κB, Nuclear factor-kappaB; NLRP3, NACHT, LRR, and PYD domains-containing protein 3; Pro-IL-1β, Pro-interleukin-1β; Pro-IL-18, Pro-interleukin-18; PAMPs, Pathogen-associated molecular patterns; TLR4, Toll-like-receptor 4; MyD88, Myeloid differentiation primary response protein 88; AC, Acetylation; MT, microtubule; NADPH, nicotinamide adenine dinucleotide phosphate; NOX2, NADPH oxidase 2; ROS, Reactive oxygen species; Prx II, Peroxiredoxin II; DDX3X, DEAD-Box Helicase 3 X-Linked; F-actin, Filamentous actin; GSDMD, Gasdermin D.

Nox2), three cytosolic subunits (p67phox, p47phox, and p40phox), and a small G-protein Rac (Rac1 and Rac2) (126). HDAC6 upregulates the expression of Nox2-based NADPH oxidase subunits to increase the production of ROS (123, 127–129), which promotes NF-κB activation and IL-1β release (123, 127). Given that the maturation and release of pro-IL-1β are mainly mediated through inflammasome-activating caspase-1 (130, 131), it is possible that HDAC6 stimulates NF-κB activation *via* Myd88, microtubules or ROS to activate NLRP3 inflammasomes. However, the underlying mechanisms remain to be elucidated.

The Role of HDAC6 in the Activation of NLRP3 Inflammasome

Following the primary signal that licenses the cell, the secondary signal occurs following the recognition of an NLRP3 activator and induces full activation and inflammasome formation (113). NLRP3 is activated by a wide variety of stimuli including ROS (132–134).

The crystal structure of NLRP3 contains a highly conserved disulfide bond connecting the PYD domain and the nucleotide-binding site domain, which is highly sensitive to altered redox states (135). Redox regulatory proteins, Prx I and Prx II, are highly homologous 2-cysteine members of the Prx protein family that function as antioxidants at low resting levels of H2O2, an ROS (136). Prx I and Prx II are specific targets of HDAC6 deacetylases. Inhibition of HDAC6 increases the levels of acetylated Prx I and Prx II (20, 137). Recently, Yan et al. reported that pharmacological inhibition of HDAC6 attenuates the expression of NLRP3 and mature caspase-1 and IL-1β, and protects dopaminergic neurons *via* Prx II acetylation, which reduces ROS production (26). These studies suggest that HDAC6 also mediates the activation of NLRP3 inflammasome, probably through Prx I and Prx II deacetylation which upregulates ROS production. However, with the treatment of LPS, ZnF-BUZ but not deacetylase domains facilitates the activation of NLRP3 inflammasome in mouse bone marrow-derived macrophages (iBMDM) (14). Hence, the role of deacetylase domains in the activation of NLRP3 inflammasome remain to be elucidated.

Additionally, HDAC6 inhibitor ACY1215 downregulates the activation of NLRP3 inflammasome *via* modulating F-actin and DEAD-Box Helicase 3 X-Linked (DDX3X) (138, 139). F-actin acts as a negative regulator by interacting directly with NLRP3 and ASC, following the activation of NLRP3 inflammasome (140). Flightless-I (FliI) and leucine-rich repeat FliI-interaction protein 2 (LRRFIP2) are required for the co-localization of NLRP3, ASC, and F-actin (140). Recently, Chen et al. reported that the HDAC6 inhibitor ACY1215 decreases the activation of NLRP3 inflammasome in acute liver failure (ALF) by increasing the expression of F-actin (138). However, the mechanism underlying HDAC6 inhibition that upregulates the expression of F-actin still needs to be elucidated. Interestingly, another study also found similar results that ACY1215 inhibits the activation of M1 macrophages by regulating NLRP3 inflammasome in ALF, but by a different mechanism (141). In LPS-stimulated ALF mice, ACY1215 decreased the expression of NLRP3 and increased the expression of DEAD-Box Helicase 3 X-Linked (DDX3X) (141), a critical factor for NLRP3 inflammasome assembly (139). It is suggested that the DDX3X/NLRP3 pathway is involved in the protective effects of the HDAC6 inhibitor ALF, but the interaction of HDAC6 and DDX3X needs to be further studied.

The Role of HDAC6 in the PTM of NLRP3 Inflammasome

PTM, including ubiquitination, deubiquitination, phosphorylation, and degradation, occurs in almost every aspect of inflammasome activity, and can either lead to the activation of the inflammasome or suppression of inflammasome activation (142). Recently, Magupalli et al. proved that NLRP3 inflammasome activation depends on regulated ubiquitination (143, 144) and engagement of the dynein adaptor HDAC6 to transport NLRP3 inflammasome to the MTOC for activation in a ubiquitin-misfolded protein-like manner (14). However, it is unknown which inflammasome components need to be ubiquitinated. Hwang et al. previously reported that HDAC6 negatively regulates NLRP3 inflammasome activation through its interaction with ubiquitinated NLRP3 (117). Co-immunoprecipitation data revealed a specific association between HDAC6 and NLRP3 (117). PR619 treatment (deubiquitinase inhibitor) resulted in an increase in the interaction of NLRP3 with HDAC6 and a decrease in NLRP3-dependent caspase-1 activation (117). This indicates that the Zn-BUZ domain of HDAC6 might interact with ubiquitinated NLRP3 (117). The effect of HDAC6 on the PTM of NLRP3 inflammasome is controversial, although previous studies indicated that the HDAC6 ubiquitin-binding domain but not deacetylase activity, is required for NLRP3 activation.

DISCUSSION

The association between autophagy and inflammasomes was discovered more than ten years ago. Satioh et al. first reported the interplay between autophagy and the endotoxin-induced inflammatory immune response through activation of the inflammasome and release of cytokines (145). In LPS-stimulated macrophages, autophagy-related protein Atg16L1 (autophagy-related 16-like 1) deficiency resulted in increased caspase-1 activation, leading to increased IL-1β production (145). Since then, Nakahira *et al.* indicated that autophagic proteins regulate NLRP3-dependent inflammation by preserving mitochondrial integrity (146). LC3B-deficient mice produced more caspase-1-dependent cytokines in sepsis models and were susceptible to LPS-induced mortality than controls (146). In the last decade, numerous studies have further indicated that autophagy can affect NLRP3 inflammasome activation through various mechanisms (147). Autophagy can suppress NLRP3 inflammasome activation by removing endogenous inflammasome activators, such as ROS-producing damaged mitochondria (148) and removing inflammasome components (149) and cytokines (150). Additionally, NLRP3 inflammasome activation regulates autophagosome formation through various mechanisms. Silencing NLRP3 downregulated autophagy (151, 152). Interestingly, caspase-1 also regulates the autophagic process through cleavage of other substrates (153, 154). Interplay between autophagy and NLRP3 inflammasomes is essential for the balance between the required host defense inflammatory response and prevention of excessive inflammation. As mentioned above, previous studies have shown that HDAC6 mediates the process of autophagy and the functioning of NLRP3 inflammasomes *via* multiple mechanisms. However, the role of HDAC6 in the crosstalk between autophagy and NLRP3 inflammasome is poorly understood. In the following sections, we will discuss the possible link between HDAC6 and the interplay between autophagy and inflammasomes, considering the current evidence (**Figure 3**).

The Possible Role of HDAC6 in the Autophagic Degradation of the Component of NLRP3 Inflammasomes and Endogenous Inflammasome Activators

Components of NLRP3 inflammasome, including NLRP3 and ASC, are recognized by p62, a ubiquitin-binding protein, that

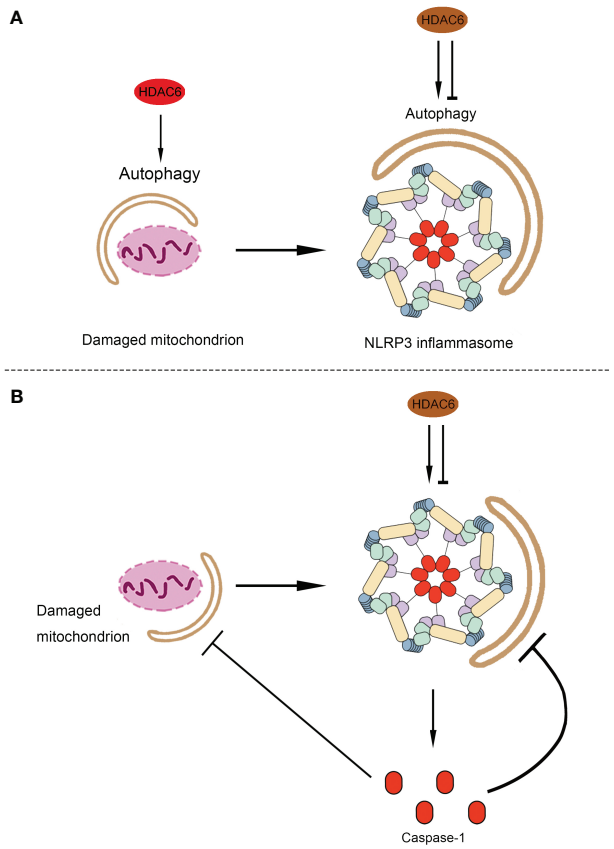

FIGURE 3 | The possible role of HDAC6 in the crosstalk between autophagy and NLRP3 inflammasome. **(A)** The possible role of HDAC6 in the autophagic degradation of the component of NLRP3 inflammasomes and endogenous inflammasome activators. As a source of endogenous inflammasome activators, damaged mitochondrion promotes the activation of NLRP3 inflammasome. Both the damaged mitochondrion and the component of NLRP3 inflammasome can be limited by autophagy. HDAC6 may promote the mitophagy and then inhibit the activation of NLRP3 inflammasome indirectly. Moreover, it is possible that the HDAC6 upregulate or downregulate autophagy to affect NLRP3 inflammasome. **(B)** The possible role of HDAC6 in the regulation of autophagy by NLRP3 inflammasome. HDAC6 plays a dual role in the activation of NLRP3 inflammasome, which release the caspase-1. Caspase-1 inhibits the autophagic degradation of the damaged mitochondrion or the component of NLRP3 inflammasome. Hence, HDAC6 may regulate autophagy *via* the activation of NLRP3 inflammasome. HDAC6, Histone deacetylase 6; NLRP3, NACHT, LRR, and PYD domain-containing protein 3.

forms aggresomes and is degraded by autophagy (149). Similarly, a recent study by Han et al. showed that small molecules (kaempferol-Ka) induced autophagy to promote the degradation of inflammasome components and reduce inflammasome activation in an LPS-induced Parkinson disease mouse model (155). As described previously, HDAC6 can also function as a ubiquitin-binding protein to participate in aggresome formation (22). Additionally, HDAC6 can also mediate the acetylation of cortactin and microtubules to regulate autophagy *via* autophagosome-lysosome fusion and autophagosome transportation (23, 86, 156). Furthermore, HDAC6 interacts with p62 to regulate autophagy *via* various mechanisms (23, 91, 104, 107). Although, there are no studies indicating that HDAC6 promotes autophagy to reduce the activation of NLRP3 inflammasomes directly, according to the current evidence, it is possible that HDAC6 participates in the autophagic degradation of the components of NLRP3 inflammasomes to regulate its activation.

On the other hand, autophagy removes damaged organelles, such as mitochondria, leading to a reduction in the release of mitochondrial-derived damage-associated molecular patterns (DAMPs), mitochondrial ROS (mtROS), and mitochondrial DNA (mtDNA) (148, 157). Numerous studies have shown that Parkin-mediated mitochondrial autophagy suppresses the production of mtROS and mtDNA, which inhibits the activation of NLRP3 inflammasomes (158–162). As mentioned above, following the decoration of mitochondria with ubiquitin by Parkin, HDAC6 is recruited as a ubiquitin-binding autophagic component that causes mitochondrial clearance (91–93). This evidence suggests that HDAC6 may mediate the functioning of NLRP3 inflammasome *via* mitophagy eliminating mtROS and mtDNA.

The Possible Role of HDAC6 in the Regulation of Autophagy by NLRP3 Inflammasome

Following the activation of the NLPR3 inflammasome, caspase-1 cleaves some components of autophagy to block this process (153, 154). Yu et al. showed that caspase-1 triggers mitochondrial damage *via* cleavage of Parkin inhibiting mitophagy, following its activation by NLRP3 and melanoma 2 (AIM2) inflammasomes (153). Furthermore, caspase-1 mediated cleavage of the signaling intermediate Toll-interleukin-1 receptor (TIR)-domain-containing adaptor-inducing interferon-β (TRIF), an essential part of the TLR4-mediated signaling pathway, leading to the promotion of autophagy (154). As HDAC6 regulates the priming, activation, and PTM of NLRP3 inflammasome (14, 26, 27, 117), it is possible that HDAC6 may regulate autophagy through the activation of NLRP3 inflammasomes. The regulation of the crosstalk between autophagy and NLRP3 inflammasome machinery by HDAC6 is obviously complex and requires further investigation, and may be dependent on specific conditions such as cell type, model of disease, inflammasome activator, and autophagy inducer/inhibitor.

CONCLUSION AND PERSPECTIVE

An increasing number of studies have reported the crosstalk between NLRP3 inflammasome and autophagy in various models and diseases in the last ten years. Numerous studies have indicated that autophagy suppresses NLRP3 inflammasome activation, through various mechanisms. In addition, NLRP3 inflammasome activation regulates autophagosome formation *via* multiple mechanisms. The crosstalk between autophagy and NLRP3 inflammasome is essential for host defense and the inflammatory response. On the other hand, accumulating evidence indicates that HDAC6 plays important roles in the mediation of autophagy and functioning of NLRP3 inflammasome *via* differential mechanisms. However, the role of HDAC6 in the crosstalk between autophagy

and NLRP3 inflammasome remains poorly understood. In this review, we explored the possible link between HDAC6 and the interplay between autophagy and inflammasomes, considering the current evidence. HDAC6 is a promising therapeutic target in multiple diseases including inflammatory diseases, cancer, and autoimmune diseases. With the development of small molecules inhibiting HDAC6, some clinical trials have shown that selective HDAC6 inhibitors are effective in tumor treatment (163–166). It is worth noting that the effects of HDAC6 differ in specific cell types and conditions. Considering the role of HDAC6 in autophagy and NLRP3 inflammasome, HDAC6 inhibitors have broad prospects and should be studied further deserves to pursue in future research.

AUTHOR CONTRIBUTIONS

Conception and design – PC and TW. Manuscript preparation – PC and HL. Critical revisions – PC, HL, HH, YL, and TW. All authors contributed to the article and approved the submitted version.

FUNDING

This work is supported by National Natural Science Foundation of China, 82102315 (PC), Beijing Natural Science Foundation, 7214265 (PC), National Natural Science Foundation of China, 31771326 (TW), and UMHS-PUHSC Joint Institute for Translational and Clinical Research, BMU2020JI007 (TW).

ACKNOWLEDGMENTS

We thank Dr. Yao Yongming for the suggestions and help of this manuscript.

REFERENCES

1. Glick D, Barth S, Macleod KF. Autophagy: Cellular and Molecular Mechanisms. *J Pathol* (2010) 221(1):3–12. doi: 10.1002/path.2697
2. Matsuzawa-Ishimoto Y, Hwang S, Cadwell K. Autophagy and Inflammation. *Annu Rev Immunol* (2018) 36:73–101. doi: 10.1146/annurev-immunol-042617-053253
3. Wang L, Hauenstein AV. NLRP3 Inflammasome: Mechanism of Action, Role in Disease and Therapies. *Mol Aspects Med* (2020) 76:100889. doi: 10.1016/j.mam.2020.100889
4. Malik A, Kanneganti TD. Inflammasome Activation and Assembly at a Glance. *J Cell Sci* (2017) 130(23):3955–63. doi: 10.1242/jcs.207365
5. Fusco R, Siracusa R, Genovese T, Cuzzocrea S, Di Paola R. Focus on the Role of NLRP3 Inflammasome in Diseases. *Int J Mol Sci* (2020) 21(12):4223. doi: 10.3390/ijms21124223
6. Zhao C, Zhao W. NLRP3 Inflammasome-A Key Player in Antiviral Responses. *Front Immunol* (2020) 11:211. doi: 10.3389/fimmu.2020.00211
7. Su S-H, Wu Y-F, Lin Q, Wang D-P, Hai J. URB597 Protects Against NLRP3 Inflammasome Activation by Inhibiting Autophagy Dysfunction in a Rat Model of Chronic Cerebral Hypoperfusion. *J Neuroinflamm* (2019) 16 (1):260. doi: 10.1186/s12974-019-1668-0
8. Ou Z, Zhou Y, Wang L, Xue L, Zheng J, Chen L, et al. NLRP3 Inflammasome Inhibition Prevents α-Synuclein Pathology by Relieving Autophagy Dysfunction in Chronic MPTP-Treated NLRP3 Knockout Mice. *Mol Neurobiol* (2021) 58(4):1303–11. doi: 10.1007/s12035-020-02198-5
9. Peng W, Peng F, Lou Y, Li Y, Zhao N, Shao Q, et al. Autophagy Alleviates Mitochondrial DAMP-Induced Acute Lung Injury by Inhibiting NLRP3 Inflammasome. *Life Sci* (2021) 265:118833. doi: 10.1016/j.lfs.2020.118833
10. Sun Q, Fan J, Billiar TR, Scott MJ. Inflammasome and Autophagy Regulation - A Two-Way Street. *Mol Med* (2017) 23:188–95. doi: 10.2119/molmed.2017.00077
11. Cadwell K. Crosstalk Between Autophagy and Inflammatory Signalling Pathways: Balancing Defence and Homeostasis. *Nat Rev Immunol* (2016) 16(11):661–75. doi: 10.1038/nri.2016.100
12. Xue Z, Zhang Z, Liu H, Li W, Guo X, Zhang Z, et al. lincRNA-Cox2 Regulates NLRP3 Inflammasome and Autophagy Mediated Neuroinflammation. *Cell Death Differ* (2019) 26(1):130–45. doi: 10.1038/s41418-018-0105-8
13. Wang H, Guo Y, Qiao Y, Zhang J, Jiang P. Nobiletin Ameliorates NLRP3 Inflammasome-Mediated Inflammation Through Promoting Autophagy via the AMPK Pathway. *Mol Neurobiol* (2020) 57(12):5056–68. doi: 10.1007/s12035-020-02071-5
14. Magupalli VG, Negro R, Tian Y, Hauenstein AV, Di Caprio G, Skillern W, et al. HDAC6 Mediates an Aggresome-Like Mechanism for NLRP3 and Pyrin Inflammasome Activation. *Science* (2020) 369(6510):eaas8995. doi: 10.1126/science.aas8995
15. Seveau S, Turner J, Gavrilin MA, Torrelles JB, Hall-Stoodley L, Yount JS, et al. Checks and Balances Between Autophagy and Inflammasomes During Infection. *J Mol Biol* (2018) 430(2):174–92. doi: 10.1016/j.jmb.2017.11.006
16. Harris J, Lang T, Thomas JPW, Sukkar MB, Nabar NR, Kehrl JH. Autophagy and Inflammasomes. *Mol Immunol* (2017) 86:10–5. doi: 10.1016/j.molimm.2017.02.013
17. Micelli C, Rastelli G. Histone Deacetylases: Structural Determinants of Inhibitor Selectivity. *Drug Discov Today* (2015) 20(6):718–35. doi: 10.1016/j.drudis.2015.01.007
18. Haggarty SJ, Koeller KM, Wong JC, Grozinger CM, Schreiber SL. Domain-Selective Small-Molecule Inhibitor of Histone Deacetylase 6 (HDAC6)-Mediated Tubulin Deacetylation. *Proc Natl Acad Sci USA* (2003) 100 (8):4389–94. doi: 10.1073/pnas.0430973100
19. Zhang X, Yuan Z, Zhang Y, Yong S, Salas-Burgos A, Koomen J, et al. HDAC6 Modulates Cell Motility by Altering the Acetylation Level of Cortactin. *Mol Cell* (2007) 27(2):197–213. doi: 10.1016/j.molcel.2007.05.033
20. Parmigiani RB, Xu WS, Venta-Perez G, Erdjument-Bromage H, Yaneva M, Tempst P, et al. HDAC6 is a Specific Deacetylase of Peroxiredoxins and Is Involved in Redox Regulation. *P Natl Acad Sci USA* (2008) 105(28):9633–8. doi: 10.1073/pnas.0803749105
21. Li Y, Shin D, Kwon SH. Histone Deacetylase 6 Plays a Role as a Distinct Regulator of Diverse Cellular Processes. *FEBS J* (2013) 280(3):775–93. doi: 10.1111/febs.12079
22. Kawaguchi Y, Kovacs JJ, McLaurin A, Vance JM, Ito A, Yao TP. The Deacetylase HDAC6 Regulates Aggresome Formation and Cell Viability in Response to Misfolded Protein Stress. *Cell* (2003) 115(6):727–38. doi: 10.1016/s0092-8674(03)00939-5
23. Lee JY, Koga H, Kawaguchi Y, Tang W, Wong E, Gao YS, et al. HDAC6 Controls Autophagosome Maturation Essential for Ubiquitin-Selective Quality-Control Autophagy. *EMBO J* (2010) 29(5):969–80. doi: 10.1038/emboj.2009.405
24. Nanduri P, Hao R, Fitzpatrick T, Yao TP. Chaperone-Mediated 26S Proteasome Remodeling Facilitates Free K63 Ubiquitin Chain Production and Aggresome Clearance. *J Biol Chem* (2015) 290(15):9455–64. doi: 10.1074/jbc.M114.627950
25. Li Z, Liu S, Fu T, Peng Y, Zhang J. Microtubule Destabilization Caused by Silicate via HDAC6 Activation Contributes to Autophagic Dysfunction in Bone Mesenchymal Stem Cells. *Stem Cell Res Ther* (2019) 10(1):351. doi: 10.1186/s13287-019-1441-4
26. Yan S, Wei X, Jian W, Qin Y, Liu J, Zhu S, et al. Pharmacological Inhibition of HDAC6 Attenuates NLRP3 Inflammatory Response and Protects Dopaminergic Neurons in Experimental Models of Parkinson's Disease. *Front Aging Neurosci* (2020) 12:78. doi: 10.3389/fnagi.2020.00078
27. Xu S, Chen H, Ni H, Dai Q. Targeting HDAC6 Attenuates Nicotine-Induced Macrophage Pyroptosis via NF-Kappab/NLRP3 Pathway. *Atherosclerosis* (2021) 317:1–9. doi: 10.1016/j.atherosclerosis.2020.11.021

28. Yu L, Chen Y, Tooze SA. Autophagy Pathway: Cellular and Molecular Mechanisms. *Autophagy* (2018) 14(2):207–15. doi: 10.1080/15548627.2017.1378838
29. Cao W, Li J, Yang K, Cao D. An Overview of Autophagy: Mechanism, Regulation and Research Progress. *Bull Cancer* (2021) 108(3):304–22. doi: 10.1016/j.bulcan.2020.11.004
30. Parzych KR, Klionsky DJ. An Overview of Autophagy: Morphology, Mechanism, and Regulation. *Antioxid Redox Signal* (2014) 20(3):460–73. doi: 10.1089/ars.2013.5371
31. Dikic I, Elazar Z. Mechanism and Medical Implications of Mammalian Autophagy. *Nat Rev Mol Cell Biol* (2018) 19(6):349–64. doi: 10.1038/s41580-018-0003-4
32. Brijmohan AS, Batchu SN, Majumder S, Alghamdi TA, Thieme K, McGaugh S, et al. HDAC6 Inhibition Promotes Transcription Factor EB Activation and Is Protective in Experimental Kidney Disease. *Front Pharmacol* (2018) 9:34. doi: 10.3389/fphar.2018.00034
33. Zhang L, Zhang Z, Li C, Zhu T, Gao J, Zhou H, et al. S100A11 Promotes Liver Steatosis via FOXO1-Mediated Autophagy and Lipogenesis. *Cell Mol Gastroenterol Hepatol* (2021) 11(3):697–724. doi: 10.1016/j.jcmgh.2020.10.006
34. Su M, Shi JJ, Yang YP, Li J, Zhang YL, Chen J, et al. HDAC6 Regulates Aggresome-Autophagy Degradation Pathway of Alpha-Synuclein in Response to MPP+-Induced Stress. *J Neurochem* (2011) 117(1):112–20. doi: 10.1111/j.1471-4159.2011.07180.x
35. Ouyang H, Ali YO, Ravichandran M, Dong A, Qiu W, MacKenzie F, et al. Protein Aggregates are Recruited to Aggresome by Histone Deacetylase 6 via Unanchored Ubiquitin C Termini. *J Biol Chem* (2012) 287(4):2317–27. doi: 10.1074/jbc.M111.273730
36. Filtz TM, Vogel WK, Leid M. Regulation of Transcription Factor Activity by Interconnected Post-Translational Modifications. *Trends Pharmacol Sci* (2014) 35(2):76–85. doi: 10.1016/j.tips.2013.11.005
37. Zhu L, Duan W, Wu G, Zhang D, Wang L, Chen D, et al. Protective Effect of Hydrogen Sulfide on Endothelial Cells Through Sirt1-FoxO1-Mediated Autophagy. *Ann Transl Med* (2020) 8(23):1586. doi: 10.21037/atm-20-3647
38. Li C, Wang X, Li X, Qiu K, Jiao F, Liu Y, et al. Proteasome Inhibition Activates Autophagy-Lysosome Pathway Associated With TFEB Dephosphorylation and Nuclear Translocation. *Front Cell Dev Biol* (2019) 7:170. doi: 10.3389/fcell.2019.00170
39. Shen M, Cao Y, Jiang Y, Wei Y, Liu H. Melatonin Protects Mouse Granulosa Cells Against Oxidative Damage by Inhibiting FOXO1-Mediated Autophagy: Implication of an Antioxidation-Independent Mechanism. *Redox Biol* (2018) 18:138–57. doi: 10.1016/j.redox.2018.07.004
40. Zhang J, Wang J, Zhou Z, Park JE, Wang L, Wu S, et al. Importance of TFEB Acetylation in Control of Its Transcriptional Activity and Lysosomal Function in Response to Histone Deacetylase Inhibitors. *Autophagy* (2018) 14(6):1043–59. doi: 10.1080/15548627.2018.1447290
41. Zhang J, Ng S, Wang J, Zhou J, Tan SH, Yang N, et al. Histone Deacetylase Inhibitors Induce Autophagy Through FOXO1-Dependent Pathways. *Autophagy* (2015) 11(4):629–42. doi: 10.1080/15548627.2015.1023981
42. Song JX, Liu J, Jiang Y, Wang ZY, Li M. Transcription Factor EB: An Emerging Drug Target for Neurodegenerative Disorders. *Drug Discov Today* (2021) 26(1):164–72. doi: 10.1016/j.drudis.2020.10.013
43. Palmieri M, Impey S, Kang H, di Ronza A, Pelz C, Sardiello M, et al. Characterization of the CLEAR Network Reveals an Integrated Control of Cellular Clearance Pathways. *Hum Mol Genet* (2011) 20(19):3852–66. doi: 10.1093/hmg/ddr306
44. Jung KH, Noh JH, Kim JK, Eun JW, Bae HJ, Chang YG, et al. Histone Deacetylase 6 Functions as a Tumor Suppressor by Activating C-Jun NH2-Terminal Kinase-Mediated Beclin 1-Dependent Autophagic Cell Death in Liver Cancer. *Hepatology* (2012) 56(2):644–57. doi: 10.1002/hep.25699
45. Xing YQ, Li A, Yang Y, Li XX, Zhang LN, Guo HC. The Regulation of FOXO1 and its Role in Disease Progression. *Life Sci* (2018) 193:124–31. doi: 10.1016/j.lfs.2017.11.030
46. Qiu W, Wang B, Gao Y, Tian Y, Tian M, Chen Y, et al. Targeting Histone Deacetylase 6 Reprograms Interleukin-17-Producing Helper T Cell Pathogenicity and Facilitates Immunotherapies for Hepatocellular Carcinoma. *Hepatology* (2020) 71(6):1967–87. doi: 10.1002/hep.30960
47. Johnston HE, Samant RS. Alternative Systems for Misfolded Protein Clearance: Life Beyond the Proteasome. *FEBS J* (2021) 288(15):4464–87. doi: 10.1111/febs.15617
48. Hyttinen JM, Amadio M, Viiri J, Pascale A, Salminen A, Kaarniranta K. Clearance of Misfolded and Aggregated Proteins by Aggrephagy and Implications for Aggregation Diseases. *Ageing Res Rev* (2014) 18:16–28. doi: 10.1016/j.arr.2014.07.002
49. Garcia-Mata R, Gao YS, Sztul E. Hassles With Taking Out the Garbage: Aggravating Aggresomes. *Traffic* (2002) 3(6):388–96. doi: 10.1034/j.1600-0854.2002.30602.x
50. Park Y, Park J, Kim YK. Crosstalk Between Translation and the Aggresome-Autophagy Pathway. *Autophagy* (2018) 14(6):1079–81. doi: 10.1080/15548627.2017.1358849
51. Markossian KA, Kurganov BI. Protein Folding, Misfolding, and Aggregation. Formation of Inclusion Bodies and Aggresomes. *Biochem (Mosc)* (2004) 69(9):971–84. doi: 10.1023/b:biry.0000043539.07961.4c
52. Amengual JE, Johannet P, Lombardo M, Zullo K, Hoehn D, Bhagat G, et al. Dual Targeting of Protein Degradation Pathways With the Selective HDAC6 Inhibitor ACY-1215 and Bortezomib Is Synergistic in Lymphoma. *Clin Cancer Res* (2015) 21(20):4663–75. doi: 10.1158/1078-0432.CCR-14-3068
53. Mishima Y, Santo L, Eda H, Cirstea D, Nemani N, Yee AJ, et al. Ricolinostat (ACY-1215) Induced Inhibition of Aggresome Formation Accelerates Carfilzomib-Induced Multiple Myeloma Cell Death. *Br J Haematol* (2015) 169(3):423–34. doi: 10.1111/bjh.13315
54. Hideshima T, Bradner JE, Wong J, Chauhan D, Richardson P, Schreiber SL, et al. Small-Molecule Inhibition of Proteasome and Aggresome Function Induces Synergistic Antitumor Activity in Multiple Myeloma. *Proc Natl Acad Sci USA* (2005) 102(24):8567–72. doi: 10.1073/pnas.0503221102
55. Watanabe S, Inami H, Oiwa K, Murata Y, Sakai S, Komine O, et al. Aggresome Formation and Liquid-Liquid Phase Separation Independently Induce Cytoplasmic Aggregation of TAR DNA-Binding Protein 43. *Cell Death Dis* (2020) 11(10):909. doi: 10.1038/s41419-020-03116-2
56. Mazzetti S, De Leonardis M, Gagliardi G, Calogero AM, Basellini MJ, Madaschi L, et al. Phospho-HDAC6 Gathers Into Protein Aggregates in Parkinson's Disease and Atypical Parkinsonisms. *Front Neurosci* (2020) 14:624. doi: 10.3389/fnins.2020.00624
57. Hao R, Nanduri P, Rao Y, Panichelli RS, Ito A, Yoshida M, et al. Proteasomes Activate Aggresome Disassembly and Clearance by Producing Unanchored Ubiquitin Chains. *Mol Cell* (2013) 51(6):819–28. doi: 10.1016/j.molcel.2013.08.016
58. Hilverling A, Szego EM, Dinter E, Cozma D, Saridaki T, Falkenburger BH. Maturing Autophagosomes are Transported Towards the Cell Periphery. *Cell Mol Neurobiol* (2021). doi: 10.1007/s10571-021-01116-0
59. Lee JY, Kawaguchi Y, Li M, Kapur M, Choi SJ, Kim HJ, et al. Uncoupling of Protein Aggregation and Neurodegeneration in a Mouse Amyotrophic Lateral Sclerosis Model. *Neurodegener Dis* (2015) 15(6):339–49. doi: 10.1159/000437208
60. Iwata A, Riley BE, Johnston JA, Kopito RR. HDAC6 and Microtubules Are Required for Autophagic Degradation of Aggregated Huntingtin. *J Biol Chem* (2005) 280(48):40282–92. doi: 10.1074/jbc.M508786200
61. Mizushima N, Yoshimori T. How to Interpret LC3 Immunoblotting. *Autophagy* (2007) 3(6):542–5. doi: 10.4161/auto.4600
62. Tanida I, Ueno T, Kominami E. LC3 and Autophagy. *Methods Mol Biol* (2008) 445:77–88. doi: 10.1007/978-1-59745-157-4_4
63. Kabeya Y, Mizushima N, Yamamoto A, Oshitani-Okamoto S, Ohsumi Y, Yoshimori T. LC3, GABARAP and GATE16 Localize to Autophagosomal Membrane Depending on Form-II Formation. *J Cell Sci* (2004) 117(Pt 13):2805–12. doi: 10.1242/jcs.01131
64. Huang R, Liu W. Identifying an Essential Role of Nuclear LC3 for Autophagy. *Autophagy* (2015) 11(5):852–3. doi: 10.1080/15548627.2015.1038016
65. Liu KP, Zhou D, Ouyang DY, Xu LH, Wang Y, Wang LX, et al. LC3B-II Deacetylation by Histone Deacetylase 6 is Involved in Serum-Starvation-Induced Autophagic Degradation. *Biochem Biophys Res Commun* (2013) 441(4):970–5. doi: 10.1016/j.bbrc.2013.11.007
66. Brush MH, Guardiola A, Connor JH, Yao TP, Shenolikar S. Deactylase Inhibitors Disrupt Cellular Complexes Containing Protein Phosphatases and Deacetylases. *J Biol Chem* (2004) 279(9):7685–91. doi: 10.1074/jbc.M310997200
67. Zhang Y, Li N, Caron C, Matthias G, Hess D, Khochbin S, et al. HDAC-6 Interacts With and Deacetylates Tubulin and Microtubules *In Vivo*. *EMBO J* (2003) 22(5):1168–79. doi: 10.1093/emboj/cdg115

68. Matsuyama A, Shimazu T, Sumida Y, Saito A, Yoshimatsu Y, Seigneurin-Berny D, et al. *In Vivo* Destabilization of Dynamic Microtubules by HDAC6-Mediated Deacetylation. *EMBO J* (2002) 21(24):6820–31. doi: 10.1093/emboj/cdf682
69. Mackeh R, Perdiz D, Lorin S, Codogno P, Pous C. Autophagy and Microtubules - New Story, Old Players. *J Cell Sci* (2013) 126(Pt 5):1071–80. doi: 10.1242/jcs.115626
70. Kruppa AJ, Kendrick-Jones J, Buss F. Myosins, Actin and Autophagy. *Traffic* (2016) 17(8):878–90. doi: 10.1111/tra.12410
71. Kast DJ, Dominguez R. The Cytoskeleton-Autophagy Connection. *Curr Biol* (2017) 27(8):R318–R26. doi: 10.1016/j.cub.2017.02.061
72. Hubbert C, Guardiola A, Shao R, Kawaguchi Y, Ito A, Nixon A, et al. HDAC6 is a Microtubule-Associated Deacetylase. *Nature* (2002) 417 (6887):455–8. doi: 10.1038/417455a
73. Wloga D, Joachimiak E, Fabczak H. Tubulin Post-Translational Modifications and Microtubule Dynamics. *Int J Mol Sci* (2017) 18 (10):2207. doi: 10.3390/ijms18102207
74. Janke C, Magiera MM. The Tubulin Code and its Role in Controlling Microtubule Properties and Functions. *Nat Rev Mol Cell Biol* (2020) 21 (6):307–26. doi: 10.1038/s41580-020-0214-3
75. Kochl R, Hu XW, Chan EY, Tooze SA. Microtubules Facilitate Autophagosome Formation and Fusion of Autophagosomes With Endosomes. *Traffic* (2006) 7(2):129–45. doi: 10.1111/j.1600-0854.2005.00368.x
76. Geeraert C, Ratier A, Pfisterer SG, Perdiz D, Cantaloube I, Rouault A, et al. Starvation-Induced Hyperacetylation of Tubulin is Required for the Stimulation of Autophagy by Nutrient Deprivation. *J Biol Chem* (2010) 285(31):24184–94. doi: 10.1074/jbc.M109.091553
77. Jahreiss L, Menzies FM, Rubinsztein DC. The Itinerary of Autophagosomes: From Peripheral Formation to Kiss-and-Run Fusion With Lysosomes. *Traffic* (2008) 9(4):574–87. doi: 10.1111/j.1600-0854.2008.00701.x
78. Nowosad A, Creff J, Jeannot P, Culerrier R, Codogno P, Manenti S, et al. P27 Controls Autophagic Vesicle Trafficking in Glucose-Deprived Cells via the Regulation of ATAT1-Mediated Microtubule Acetylation. *Cell Death Dis* (2021) 12(5):481. doi: 10.1038/s41419-021-03759-9
79. Xie R, Nguyen S, McKeehan WL, Liu L. Acetylated Microtubules are Required for Fusion of Autophagosomes With Lysosomes. *BMC Cell Biol* (2010) 11:89. doi: 10.1186/1471-2121-11-89
80. Hać A, Pierzynowska K, Herman-Antosiewicz A. S6K1 Is Indispensible for Stress-Induced Microtubule Acetylation and Autophagic Flux. *Cells* (2021) 10(4):929. doi: 10.3390/cells10040929
81. Yang L, Zhao L, Cui L, Huang Y, Ye J, Zhang Q, et al. Decreased Alpha-Tubulin Acetylation Induced by an Acidic Environment Impairs Autophagosome Formation and Leads to Rat Cardiomyocyte Injury. *J Mol Cell Cardiol* (2019) 127:143–53. doi: 10.1016/j.yjmcc.2018.12.011
82. Gomez-Suaga P, Paillusson S, Miller CCJ. ER-Mitochondria Signaling Regulates Autophagy. *Autophagy* (2017) 13(7):1250–1. doi: 10.1080/15548627.2017.1317913
83. Friedman JR, Webster BM, Mastronarde DN, Verhey KJ, Voeltz GK. ER Sliding Dynamics and ER-Mitochondrial Contacts Occur on Acetylated Microtubules. *J Cell Biol* (2010) 190(3):363–75. doi: 10.1083/jcb.200911024
84. Liang T, Qi C, Lai Y, Xie J, Wang H, Zhang L, et al. HDAC6-Mediated Alpha-Tubulin Deacetylation Suppresses Autophagy and Enhances Motility of Podocytes in Diabetic Nephropathy. *J Cell Mol Med* (2020) 24(19):11558–72. doi: 10.1111/jcmm.15772
85. Li Z, Liu X, Ma J, Zhang T, Gao X, Liu L. hnRNPK Modulates Selective Quality-Control Autophagy by Downregulating the Expression of HDAC6 in 293 Cells. *Int J Oncol* (2018) 53(5):2200–12. doi: 10.3892/ijo.2018.4517
86. Chen Q, Yue F, Li W, Zou J, Xu T, Huang C, et al. Potassium Bisperoxo(1,10-Phenanthroline)Oxovanadate (Bpv(Phen)) Induces Apoptosis and Pyroptosis and Disrupts the P62-HDAC6 Protein Interaction to Suppress the Acetylated Microtubule-Dependent Degradation of Autophagosomes. *J Biol Chem* (2015) 290(43):26051–8. doi: 10.1074/jbc.M115.653568
87. Haraszti T, Clemen AE, Spatz JP. Biomimetic F-Actin Cortex Models. *Chemphyschem* (2009) 10(16):2777–86. doi: 10.1002/cphc.200900581
88. Wang R, Tan J, Chen T, Han H, Tian R, Tan Y, et al. ATP13A2 Facilitates HDAC6 Recruitment to Lysosome to Promote Autophagosome-Lysosome Fusion. *J Cell Biol* (2019) 218(1):267–84. doi: 10.1083/jcb.201804165
89. Bravo-San Pedro JM, Kroemer G, Galluzzi L. Autophagy and Mitophagy in Cardiovascular Disease. *Circ Res* (2017) 120(11):1812–24. doi: 10.1161/CIRCRESAHA.117.311082
90. Galluzzi L, Baehrecke EH, Ballabio A, Boya P, Bravo-San Pedro JM, Cecconi F, et al. Molecular Definitions of Autophagy and Related Processes. *EMBO J* (2017) 36(13):1811–36. doi: 10.15252/embj.201796697
91. Lee JY, Nagano Y, Taylor JP, Lim KL, Yao TP. Disease-Causing Mutations in Parkin Impair Mitochondrial Ubiquitination, Aggregation, and HDAC6-Dependent Mitophagy. *J Cell Biol* (2010) 189(4):671–9. doi: 10.1083/jcb.201001039
92. Radomski N, Kagebein D, Liebler-Tenorio E, Karger A, Rufer E, Tews BA, et al. Mito-Xenophagic Killing of Bacteria is Coordinated by a Metabolic Switch in Dendritic Cells. *Sci Rep* (2017) 7(1):3923. doi: 10.1038/s41598-017-04142-5
93. Moreno-Gonzalo O, Ramirez-Huesca M, Blas-Rus N, Cibrian D, Saiz ML, Jorge I, et al. HDAC6 Controls Innate Immune and Autophagy Responses to TLR-Mediated Signalling by the Intracellular Bacteria Listeria Monocytogenes. *PloS Pathog* (2017) 13(12):e1006799. doi: 10.1371/journal.ppat.1006799
94. Stoner MW, Thapa D, Zhang M, Gibson GA, Calderon MJ, St Croix CM, et al. Alpha-Lipoic Acid Promotes Alpha-Tubulin Hyperacetylation and Blocks the Turnover of Mitochondria Through Mitophagy. *Biochem J* (2016) 473(12):1821–30. doi: 10.1042/BCJ20160281
95. Guedes-Dias P, de Proenca J, Soares TR, Leitao-Rocha A, Pinho BR, Duchen MR, et al. HDAC6 Inhibition Induces Mitochondrial Fusion, Autophagic Flux and Reduces Diffuse Mutant Huntingtin in Striatal Neurons. *Biochim Biophys Acta* (2015) 1852(11):2484–93. doi: 10.1016/j.bbadis.2015.08.012
96. Islam MA, Sooro MA, Zhang P. Autophagic Regulation of P62 is Critical for Cancer Therapy. *Int J Mol Sci* (2018) 19(5):1405. doi: 10.3390/ijms19051405
97. Cao Y, Luo Y, Zou J, Ouyang J, Cai Z, Zeng X, et al. Autophagy and its Role in Gastric Cancer. *Clin Chim Acta* (2019) 489:10–20. doi: 10.1016/j.cca.2018.11.028
98. Zheng Q, Su H, Ranek MJ, Wang X. Autophagy and P62 in Cardiac Proteinopathy. *Circ Res* (2011) 109(3):296–308. doi: 10.1161/CIRCRESAHA.111.244707
99. Pankiv S, Clausen TH, Lamark T, Brech A, Bruun JA, Outzen H, et al. P62/SQSTM1 Binds Directly to Atg8/LC3 to Facilitate Degradation of Ubiquitinated Protein Aggregates by Autophagy. *J Biol Chem* (2007) 282 (33):24131–45. doi: 10.1074/jbc.M702824200
100. Lee Y, Weihl CC. Regulation of SQSTM1/p62 via UBA Domain Ubiquitination and its Role in Disease. *Autophagy* (2017) 13(9):1615–6. doi: 10.1080/15548627.2017.1339845
101. Lin X, Li S, Zhao Y, Ma X, Zhang K, He X, et al. Interaction Domains of P62: A Bridge Between P62 and Selective Autophagy. *DNA Cell Biol* (2013) 32 (5):220–7. doi: 10.1089/dna.2012.1915
102. Jeong SJ, Zhang X, Rodriguez-Velez A, Evans TD, Razani B. P62/SQSTM1 and Selective Autophagy in Cardiometabolic Diseases. *Antioxid Redox Signal* (2019) 31(6):458–71. doi: 10.1089/ars.2018.7649
103. Yan J, Seibenhener ML, Calderilla-Barbosa L, Diaz-Meco MT, Moscat J, Jiang J, et al. SQSTM1/p62 Interacts With HDAC6 and Regulates Deacetylase Activity. *PloS One* (2013) 8(9):e76016. doi: 10.1371/journal.pone.0076016
104. Galindo-Moreno M, Giraldez S, Saez C, Japon MA, Tortolero M, Romero F. Both P62/SQSTM1-HDAC6-Dependent Autophagy and the Aggresome Pathway Mediate CDK1 Degradation in Human Breast Cancer. *Sci Rep* (2017) 7(1):10078. doi: 10.1038/s41598-017-10506-8
105. Nakashima H, Nguyen T, Goins WF, Chiocca EA. Interferon-Stimulated Gene 15 (ISG15) and ISG15-Linked Proteins Can Associate With Members of the Selective Autophagic Process, Histone Deacetylase 6 (HDAC6) and SQSTM1/P62. *J Biol Chem* (2015) 290(3):1485–95. doi: 10.1074/jbc.M114.593871
106. Zheng Y, Zhu G, Tang Y, Yan J, Han S, Yin J, et al. HDAC6, A Novel Cargo for Autophagic Clearance of Stress Granules, Mediates the Repression of the Type I Interferon Response During Coxsackievirus A16 Infection. *Front Microbiol* (2020) 11:78. doi: 10.3389/fmicb.2020.00078
107. Yan Y, Wang H, Wei C, Xiang Y, Liang X, Phang CW, et al. HDAC6 Regulates Lipid Droplet Turnover in Response to Nutrient Deprivation via P62-Mediated Selective Autophagy. *J Genet Genomics* (2019) 46(4):221–9. doi: 10.1016/j.jgg.2019.03.008

108. Li W, Dai Y, Shi B, Yue F, Zou J, Xu G, et al. LRPPRC Sustains Yap-P27-Mediated Cell Ploidy and P62-HDAC6-Mediated Autophagy Maturation and Suppresses Genome Instability and Hepatocellular Carcinomas. *Oncogene* (2020) 39(19):3879–92. doi: 10.1038/s41388-020-1257-9
109. Jiang X, Huang Y, Liang X, Jiang F, He Y, Li T, et al. Metastatic Prostate Cancer-Associated P62 Inhibits Autophagy Flux and Promotes Epithelial to Mesenchymal Transition by Sustaining the Level of HDAC6. *Prostate* (2018) 78(6):426–34. doi: 10.1002/pros.23487
110. Kelley N, Jeltema D, Duan Y, He Y. NLRP3 Inflammasome: An Overview of Mechanisms of Activation and Regulation. *Int J Mol Sci* (2019) 20(13):3328. doi: 10.3390/ijms20133328
111. Hughes MM, O'Neill LAJ. Metabolic Regulation of NLRP3. *Immunol Rev* (2018) 281(1):88–98. doi: 10.1111/imr.12608
112. Pellegrini C, Antonioli L, Lopez-Castejon G, Blandizzi C, Fornai M. Canonical and Non-Canonical Activation of NLRP3 Inflammasome at the Crossroad Between Immune Tolerance and Intestinal Inflammation. *Front Immunol* (2017) 8:36. doi: 10.3389/fimmu.2017.00036
113. Swanson KV, Deng M, Ting JP. NLRP3 Inflammasome: Molecular Activation and Regulation to Therapeutics. *Nat Rev Immunol* (2019) 19 (8):477–89. doi: 10.1038/s41577-019-0165-0
114. Dalbeth N, Choi HK, Joosten LAB, Khanna PP, Matsuo H, Perez-Ruiz F, et al. Gout. *Nat Rev Dis Primers* (2019) 5(1):69. doi: 10.1038/s41572-019-0115-y
115. Danielski LG, Giustina AD, Bonfante S, Barichello T, Petronilho F. NLRP3 Inflammasome and Its Role in Sepsis Development. *Inflammation* (2020) 43 (1):24–31. doi: 10.1007/s10753-019-01124-9
116. Irrera N, Russo M, Pallio G, Bitto A, Mannino F, Minutoli L, et al. The Role of NLRP3 Inflammasome in the Pathogenesis of Traumatic Brain Injury. *Int J Mol Sci* (2020) 21(17):6204. doi: 10.3390/ijms21176204
117. Hwang I, Lee E, Jeon SA, Yu JW. Histone Deacetylase 6 Negatively Regulates NLRP3 Inflammasome Activation. *Biochem Biophys Res Commun* (2015) 467(4):973–8. doi: 10.1016/j.bbrc.2015.10.033
118. Chen LF, Mu Y, Greene WC. Acetylation of RelA at Discrete Sites Regulates Distinct Nuclear Functions of NF-kappaB. *EMBO J* (2002) 21(23):6539–48. doi: 10.1093/emboj/cdf660
119. Kiernan R, Brès V, Ng RW, Coudart MP, El Messaoudi S, Sardet C, et al. Post-Activation Turn-Off of NF-Kappa B-Dependent Transcription is Regulated by Acetylation of P65. *J Biol Chem* (2003) 278(4):2758–66. doi: 10.1074/jbc.M209572200
120. Jia YJ, Liu ZB, Wang WG, Sun CB, Wei P, Yang YL, et al. HDAC6 Regulates microRNA-27b That Suppresses Proliferation, Promotes Apoptosis and Target MET in Diffuse Large B-Cell Lymphoma. *Leukemia* (2018) 32 (3):703–11. doi: 10.1038/leu.2017.299
121. Yang Q, Li S, Zhou Z, Fu M, Yang X, Hao K, et al. HDAC6 Inhibitor Cay10603 Inhibits High Glucose-Induced Oxidative Stress, Inflammation and Apoptosis in Retinal Pigment Epithelial Cells via Regulating NF-kappaB and NLRP3 Inflammasome Pathway. *Gen Physiol Biophys* (2020) 39(2):169–77. doi: 10.4149/gpb_2019058
122. Liu L, Zhou X, Shetty S, Hou G, Wang Q, Fu J. HDAC6 Inhibition Blocks Inflammatory Signaling and Caspase-1 Activation in LPS-Induced Acute Lung Injury. *Toxicol Appl Pharmacol* (2019) 370:178–83. doi: 10.1016/j.taap.2019.03.017
123. Youn GS, Lee KW, Choi SY, Park J. Overexpression of HDAC6 Induces Pro-Inflammatory Responses by Regulating ROS-MAPK-NF-Kappab/AP-1 Signaling Pathways in Macrophages. *Free Radic Biol Med* (2016) 97:14–23. doi: 10.1016/j.freeradbiomed.2016.05.014
124. Nauseef WM. The Phagocyte NOX2 NADPH Oxidase in Microbial Killing and Cell Signaling. *Curr Opin Immunol* (2019) 60:130–40. doi: 10.1016/j.coi.2019.05.006
125. Buvelot H, Jaquet V, Krause KH. Mammalian NADPH Oxidases. *Methods Mol Biol* (2019) 1982:17–36. doi: 10.1007/978-1-4939-9424-3_2
126. Kleniewska P, Piechota A, Skibska B, Gorąca A. The NADPH Oxidase Family and its Inhibitors. *Archivum Immunol Ther Exp* (2012) 60(4):277–94. doi: 10.1007/s00005-012-0176-z
127. Wang J, Zhao L, Wei Z, Zhang X, Wang Y, Li F, et al. Inhibition of Histone Deacetylase Reduces Lipopolysaccharide-Induced-Inflammation in Primary Mammary Epithelial Cells by Regulating ROS-NF-Small Ka, CyrillicB Signaling Pathways. *Int Immunopharmacol* (2018) 56:230–4. doi: 10.1016/j.intimp.2018.01.039
128. Jo H, Jang HY, Youn GS, Kim D, Lee CY, Jang JH, et al. Hindsiipropane B Alleviates HIV-1 Tat-Induced Inflammatory Responses by Suppressing HDAC6-NADPH Oxidase-ROS Axis in Astrocytes. *BMB Rep* (2018) 51 (8):394–9. doi: 10.5483/bmbrep.2018.51.8.061
129. Youn GS, Cho H, Kim D, Choi SY, Park J. Crosstalk Between HDAC6 and Nox2-Based NADPH Oxidase Mediates HIV-1 Tat-Induced Pro-Inflammatory Responses in Astrocytes. *Redox Biol* (2017) 12:978–86. doi: 10.1016/j.redox.2017.05.001
130. Yazdi AS, Ghoreschi K. The Interleukin-1 Family. *Adv Exp Med Biol* (2016) 941:21–9. doi: 10.1007/978-94-024-0921-5_2
131. Lopez-Castejon G, Brough D. Understanding the Mechanism of IL-1beta Secretion. *Cytokine Growth Factor Rev* (2011) 22(4):189–95. doi: 10.1016/j.cytogfr.2011.10.001
132. Minutoli L, Puzzolo D, Rinaldi M, Irrera N, Marini H, Arcoraci V, et al. ROS-Mediated NLRP3 Inflammasome Activation in Brain, Heart, Kidney, and Testis Ischemia/Reperfusion Injury. *Oxid Med Cell Longev* (2016) 2016:2183026. doi: 10.1155/2016/2183026
133. Abais JM, Xia M, Zhang Y, Boini KM, Li PL. Redox Regulation of NLRP3 Inflammasomes: ROS as Trigger or Effector? *Antioxid Redox Signal* (2015) 22 (13):1111–29. doi: 10.1089/ars.2014.5994
134. Sho T, Xu J. Role and Mechanism of ROS Scavengers in Alleviating NLRP3-Mediated Inflammation. *Biotechnol Appl Biochem* (2019) 66(1):4–13. doi: 10.1002/bab.1700
135. Bae JY, Park HH. Crystal Structure of NALP3 Protein Pyrin Domain (PYD) and its Implications in Inflammasome Assembly. *J Biol Chem* (2011) 286 (45):39528–36. doi: 10.1074/jbc.M111.278812
136. Cao Z, Lindsay JG. The Peroxiredoxin Family: An Unfolding Story. *Subcell Biochem* (2017) 83:127–47. doi: 10.1007/978-3-319-46503-6_5
137. Jian W, Wei X, Chen L, Wang Z, Sun Y, Zhu S, et al. Inhibition of HDAC6 Increases Acetylation of Peroxiredoxin1/2 and Ameliorates 6-OHDA Induced Dopaminergic Injury. *Neurosci Lett* (2017) 658:114–20. doi: 10.1016/j.neulet.2017.08.029
138. Chen Q, Wang Y, Jiao F, Cao P, Shi C, Pei M, et al. HDAC6 Inhibitor ACY1215 Inhibits the Activation of NLRP3 Inflammasome in Acute Liver Failure by Regulating the ATM/F-Actin Signalling Pathway. *J Cell Mol Med* (2021) 25(15):7218–28. doi: 10.1111/jcmm.16751
139. Samir P, Kesavardhana S, Patmore DM, Gingras S, Malireddi RKS, Karki R, et al. DDX3X Acts as a Live-or-Die Checkpoint in Stressed Cells by Regulating NLRP3 Inflammasome. *Nature* (2019) 573(7775):590–4. doi: 10.1038/s41586-019-1551-2
140. Burger D, Fickentscher C, de Moerloose P, Brandt KJ. F-Actin Dampens NLRP3 Inflammasome Activity via Flightless-I and LRRFIP2. *Sci Rep* (2016) 6:29834. doi: 10.1038/srep29834
141. Wang Y, Li X, Chen Q, Jiao F, Shi C, Pei M, et al. Histone Deacetylase 6 Regulates the Activation of M1 Macrophages by the Glycolytic Pathway During Acute Liver Failure. *J Inflammation Res* (2021) 14:1473–85. doi: 10.2147/jir.s302391
142. Man SM, Kanneganti TD. Regulation of Inflammasome Activation. *Immunol Rev* (2015) 265(1):6–21. doi: 10.1111/imr.12296
143. Guan K, Wei C, Zheng Z, Song T, Wu F, Zhang Y, et al. MAVS Promotes Inflammasome Activation by Targeting ASC for K63-Linked Ubiquitination via the E3 Ligase Traf3. *J Immunol (Baltimore Md 1950)* (2015) 194 (10):4880–90. doi: 10.4049/jimmunol.1402851
144. Duong BH, Onizawa M, Oses-Prieto JA, Advincula R, Burlingame A, Malynn BA, et al. A20 Restricts Ubiquitination of Pro-Interleukin-1β Protein Complexes and Suppresses NLRP3 Inflammasome Activity. *Immunity* (2015) 42(1):55–67. doi: 10.1016/j.immuni.2014.12.031
145. Saitoh T, Fujita N, Jang MH, Uematsu S, Yang BG, Satoh T, et al. Loss of the Autophagy Protein Atg16L1 Enhances Endotoxin-Induced IL-1beta Production. *Nature* (2008) 456(7219):264–8. doi: 10.1038/nature07383
146. Nakahira K, Haspel JA, Rathinam VA, Lee SJ, Dolinay T, Lam HC, et al. Autophagy Proteins Regulate Innate Immune Responses by Inhibiting the Release of Mitochondrial DNA Mediated by the NALP3 Inflammasome. *Nat Immunol* (2011) 12(3):222–30. doi: 10.1038/ni.1980
147. Biasizzo M, Kopitar-Jerala N. Interplay Between NLRP3 Inflammasome and Autophagy. *Front Immunol* (2020) 11:591803. doi: 10.3389/fimmu.2020.591803
148. Zhou R, Yazdi AS, Menu P, Tschopp J. A Role for Mitochondria in NLRP3 Inflammasome Activation. *Nature* (2011) 469(7329):221–5. doi: 10.1038/nature09663

149. Shi CS, Shenderov K, Huang NN, Kabat J, Abu-Asab M, Fitzgerald KA, et al. Activation of Autophagy by Inflammatory Signals Limits IL-1β Production by Targeting Ubiquitinated Inflammasomes for Destruction. *Nat Immunol* (2012) 13(3):255–63. doi: 10.1038/ni.2215
150. Harris J, Hartman M, Roche C, Zeng SG, O'Shea A, Sharp FA, et al. Autophagy Controls IL-1beta Secretion by Targeting Pro-IL-1beta for Degradation. *J Biol Chem* (2011) 286(11):9587–97. doi: 10.1074/jbc.M110.202911
151. Deng Q, Wang Y, Zhang Y, Li M, Li D, Huang X, et al. Pseudomonas Aeruginosa Triggers Macrophage Autophagy To Escape Intracellular Killing by Activation of NLRP3 Inflammasome. *Infect Immun* (2016) 84(1):56–66. doi: 10.1128/iai.00945-15
152. Allaeys I, Marceau F, Poubelle PE. NLRP3 Promotes Autophagy of Urate Crystals Phagocytized by Human Osteoblasts. *Arthritis Res Ther* (2013) 15 (6):R176. doi: 10.1186/ar4365
153. Yu J, Nagasu H, Murakami T, Hoang H, Broderick L, Hoffman HM, et al. Inflammasome Activation Leads to Caspase-1-Dependent Mitochondrial Damage and Block of Mitophagy. *Proc Natl Acad Sci USA* (2014) 111 (43):15514–9. doi: 10.1073/pnas.1414859111
154. Jabir MS, Ritchie ND, Li D, Bayes HK, Tourlomousis P, Puleston D, et al. Caspase-1 Cleavage of the TLR Adaptor TRIF Inhibits Autophagy and β-Interferon Production During Pseudomonas Aeruginosa Infection. *Cell Host Microbe* (2014) 15(2):214–27. doi: 10.1016/j.chom.2014.01.010
155. Han X, Sun S, Sun Y, Song Q, Zhu J, Song N, et al. Small Molecule-Driven NLRP3 Inflammation Inhibition via Interplay Between Ubiquitination and Autophagy: Implications for Parkinson Disease. *Autophagy* (2019) 15 (11):1860–81. doi: 10.1080/15548627.2019.1596481
156. Zhan Y, Wang H, Zhang L, Pei F, Chen Z. HDAC6 Regulates the Fusion of Autophagosome and Lysosome to Involve in Odontoblast Differentiation. *Front Cell Dev Biol* (2020) 8:605609. doi: 10.3389/fcell.2020.605609
157. Shimada K, Crother TR, Karlin J, Dagvadorj J, Chiba N, Chen S, et al. Oxidized Mitochondrial DNA Activates NLRP3 Inflammasome During Apoptosis. *Immunity* (2012) 36(3):401–14. doi: 10.1016/j.immuni.2012.01.009
158. Wu X, Gong L, Xie L, Gu W, Wang X, Liu Z, et al. NLRP3 Deficiency Protects Against Intermittent Hypoxia-Induced Neuroinflammation and Mitochondrial ROS by Promoting the PINK1-Parkin Pathway of Mitophagy in a Murine Model of Sleep Apnea. *Front Immunol* (2021) 12:628168. doi: 10.3389/fimmu.2021.628168
159. Xu Y, Tang Y, Lu J, Zhang W, Zhu Y, Zhang S, et al. PINK1-Mediated Mitophagy Protects Against Hepatic Ischemia/Reperfusion Injury by Restraining NLRP3 Inflammasome Activation. *Free Radic Biol Med* (2020) 160:871–86. doi: 10.1016/j.freeradbiomed.2020.09.015
160. Ye JS, Chen L, Lu YY, Lei SQ, Peng M, Xia ZY. Honokiol-Mediated Mitophagy Ameliorates Postoperative Cognitive Impairment Induced by Surgery/Sevoflurane via Inhibiting the Activation of NLRP3 Inflammasome in the Hippocampus. *Oxid Med Cell Longev* (2019) 2019:8639618. doi: 10.1155/2019/8639618
161. Lin Q, Li S, Jiang N, Shao X, Zhang M, Jin H, et al. PINK1-Parkin Pathway of Mitophagy Protects Against Contrast-Induced Acute Kidney Injury via Decreasing Mitochondrial ROS and NLRP3 Inflammasome Activation. *Redox Biol* (2019) 26:101254. doi: 10.1016/j.redox.2019.101254
162. Cao S, Shrestha S, Li J, Yu X, Chen J, Yan F, et al. Melatonin-Mediated Mitophagy Protects Against Early Brain Injury After Subarachnoid Hemorrhage Through Inhibition of NLRP3 Inflammasome Activation. *Sci Rep* (2017) 7(1):2417. doi: 10.1038/s41598-017-02679-z
163. Tu Y, Hershman DL, Bhalla K, Fiskus W, Pellegrino CM, Andreopoulou E, et al. A Phase I-II Study of the Histone Deacetylase Inhibitor Vorinostat Plus Sequential Weekly Paclitaxel and Doxorubicin-Cyclophosphamide in Locally Advanced Breast Cancer. *Breast Cancer Res Treat* (2014) 146 (1):145–52. doi: 10.1007/s10549-014-3008-5
164. Dai Y, Chen S, Wang L, Pei XY, Kramer LB, Dent P, et al. Bortezomib Interacts Synergistically With Belinostat in Human Acute Myeloid Leukaemia and Acute Lymphoblastic Leukaemia Cells in Association With Perturbations in NF-kappaB and Bim. *Br J Haematol* (2011) 153(2):222–35. doi: 10.1111/j.1365-2141.2011.08591.x
165. Yee AJ, Bensinger WI, Supko JG, Voorhees PM, Berdeja JG, Richardson PG, et al. Ricolinostat Plus Lenalidomide, and Dexamethasone in Relapsed or Refractory Multiple Myeloma: A Multicentre Phase 1b Trial. *Lancet Oncol* (2016) 17(11):1569–78. doi: 10.1016/s1470-2045(16)30375-8
166. Vogl DT, Raje N, Jagannath S, Richardson P, Hari P, Orlowski R, et al. Ricolinostat, the First Selective Histone Deacetylase 6 Inhibitor, in Combination With Bortezomib and Dexamethasone for Relapsed or Refractory Multiple Myeloma. *Clin Cancer Res* (2017) 23(13):3307–15. doi: 10.1158/1078-0432.CCR-16-2526

Conflict of Interest: The authors declare that the research was conducted in the absence of any commercial or financial relationships that could be construed as a potential conflict of interest.

Publisher's Note: All claims expressed in this article are solely those of the authors and do not necessarily represent those of their affiliated organizations, or those of the publisher, the editors and the reviewers. Any product that may be evaluated in this article, or claim that may be made by its manufacturer, is not guaranteed or endorsed by the publisher.

frontiers in Immunology

REVIEW
published: 04 November 2021
doi: 10.3389/fimmu.2021.761946

Peptidylarginine Deiminase 2 in Host Immunity: Current Insights and Perspectives

Zhenyu Wu[1,2], *Patrick Li*[1,3], *Yuzi Tian*[1,4], *Wenlu Ouyang*[1,2], *Jessie Wai-Yan Ho*[5], *Hasan B. Alam*[5] *and Yongqing Li*[1*]

[1] Department of Surgery, University of Michigan Hospital, Ann Arbor, MI, United States, [2] Department of Infectious Diseases, Xiangya 2nd Hospital, Central South University, Changsha, China, [3] Department of Internal Medicine, New York University (NYU) Langone Health, New York, NY, United States, [4] Department of Rheumatology, Xiangya Hospital, Central South University, Changsha, China, [5] Department of Surgery, Feinberg School of Medicine, Northwestern University, Chicago, IL, United States

OPEN ACCESS

Edited by:
Markus H. Hoffmann,
University of Erlangen Nuremberg, Germany

Reviewed by:
Sanja Arandjelovic,
University of Virginia, United States
Bo Sun,
Brigham and Women's Hospital and Harvard Medical School, United States

***Correspondence:**
Yongqing Li
yqli@med.umich.edu

Specialty section:
This article was submitted to Inflammation, a section of the journal Frontiers in Immunology

Received: 20 August 2021
Accepted: 20 October 2021
Published: 04 November 2021

Citation:
Wu Z, Li P, Tian Y, Ouyang W, Ho JW-Y, Alam HB and Li Y (2021) Peptidylarginine Deiminase 2 in Host Immunity: Current Insights and Perspectives. Front. Immunol. 12:761946. doi: 10.3389/fimmu.2021.761946

Peptidylarginine deiminases (PADs) are a group of enzymes that catalyze post-translational modifications of proteins by converting arginine residues into citrullines. Among the five members of the PAD family, PAD2 and PAD4 are the most frequently studied because of their abundant expression in immune cells. An increasing number of studies have identified PAD2 as an essential factor in the pathogenesis of many diseases. The successes of preclinical research targeting PAD2 highlights the therapeutic potential of PAD2 inhibition, particularly in sepsis and autoimmune diseases. However, the underlying mechanisms by which PAD2 mediates host immunity remain largely unknown. In this review, we will discuss the role of PAD2 in different types of cell death signaling pathways and the related immune disorders contrasted with functions of PAD4, providing novel therapeutic strategies for PAD2-associated pathology.

Keywords: PAD2, autoimmune diseases, sepsis, NETosis, pyroptosis

HIGHLIGHTS

- Peptidylarginine deiminase (PAD) enzymes catalyze the conversion of arginine residues to citrulline, regulating activity of host immunity.
- PAD2 plays an important yet different role in immune cells than its isozyme PAD4. Although PAD4 is previously identified to be the key regulator in the formation of neutrophil extracellular traps (NETosis), PAD2 also takes part in NETosis in the absence of PAD4.
- *Pad2* deficiency decreases macrophage pyroptosis while *Pad4* deficiency increases pyroptosis.
- PAD2, differing from the other PAD family members, citrullinates arginine 1810 (Cit1810) in repeat 31 of the carboxyl-terminal domain of the largest subunit of RNA polymerase II, which enables the efficient transcription of highly expressed genes needed for cell cycle progression, metabolism, and cell proliferation.

INTRODUCTION

Peptidylarginine deiminases (PADs) are a group of enzymes that catalyze post-translational modification of proteins by converting arginine residues into citrullines (**Figure 1A**) (1, 2). The PAD family consists of five members: PAD1, PAD2, PAD3, PAD4, and PAD6 (3). As the most widely expressed member, PAD2 can be found in many tissues and organs, including brain (4), spinal cord (4), spleen (5), pancreas (6), skeletal muscles (7), secretory glands, and immune cells (8, 9). By citrullinating proteins, PAD2 regulates a number of cellular processes such as gene transcription (10, 11), antigen generation (12), extracellular trap formation (also termed ETosis) (13, 14), and pyroptosis (15).

ETosis is a described cell death that results in the release of a complex lattice of chromatin containing DNA, histones, and other associated proteins (16–18). These extracellular chromatin webs can entrap and kill microbial organisms. Originally, this phenomenon was described in neutrophils, termed NETosis (Neutrophil Extracellular Traps). However, researchers later found that this mechanism also exists in other cell types such as macrophages, eosinophils, and mast cells (19). Thus, some researchers recommend that the mechanism of this cell death be generalized as "ETosis" (20–22), while others prefer using NETosis or macrophage ETosis (METosis) for the death of specific cell sources.

Similar to the structure of PAD4 (23), the N-terminal of PAD2 consists of two immunoglobulin-like domains, IgG domain 1 (residues 1-115) and IgG domain 2 (residues 116-295), and a catalytic domain, the C-terminal (residues 296-665) (24). There are six calcium-binding sites in PAD2 (Ca1-6).

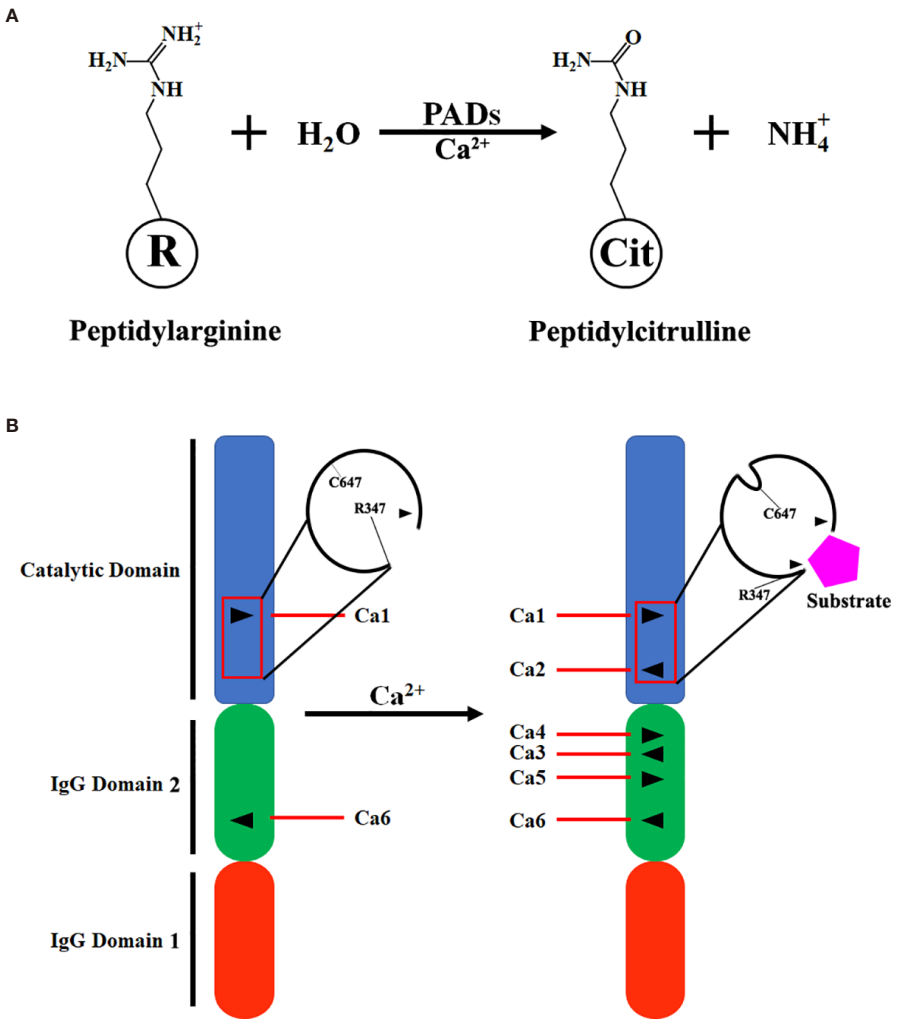

FIGURE 1 | Scheme of citrullination and PAD2 structure. **(A)** A simplified equation describing that PAD2 catalyzes the citrullination of a peptidylarginine residue in the presence of calcium ions (Ca^{2+}). **(B)** Transition of inactivated PAD2 to activated PAD2. Ca1 and Ca6 in PAD2 protein are permanently occupied by Ca^{2+}; when the levels of Ca^{2+} in cytoplasm are elevated, Ca2, Ca3, Ca4 and Ca5 are filled with Ca^{2+} for PAD2 activation. Ca1, Ca2, Ca3, Ca4, Ca5, and Ca6, Calcium-binding sites 1, 2, 3, 4, 5, and 6; IgG, immunoglobin; PAD, peptidylarginine deiminase.

Ca1 and Ca6 are occupied by calcium in both inactivated and activated PAD2. During the activation of PAD2, calcium ions bind to sites Ca3-5. Afterwards, calcium binds to Ca2, which causes conformational changes at the active site. R347 moves out of the active site, and C647 moves in. As such, a pocket-like structure is generated for substrate binding (**Figure 1B**). Then, where does the calcium come from for PAD2 activation? A previous study revealed that adenosine triphosphate (ATP)-induced PAD2 activation can be dramatically diminished in mast cells cultured in calcium-free media, suggesting that calcium needed for PAD2 activation mainly comes from the extracellular space (25). Zheng et al. also demonstrated that Annexin A5 (ANXA5) can bind to the plasma membrane to facilitate calcium influx and further contribute to PAD2 activation (26). Thus, sufficient extracellular calcium is required for the activation of PAD2.

The substrates of PAD2 are quite diverse *in vivo*, including cell structural proteins (27, 28), immunomodulating molecules (29, 30), and histones (31). For instance, vimentin, which is an important part of the cytoskeleton in skeletal muscles and macrophages, is a PAD2 substrate (28). Another crucial protein for cell structure, actin, can also be citrullinated by PAD2 (27). PAD2 can mediate thrombotic activities *via* citrullinating antithrombin (32) and fibrinogen (33). PAD2-catalyzed citrullination of certain immunomodulating cytokines, such as the chemokine (C-X-C motif) ligand (CXCL) 10 (34), interleukin (IL)-8 (29), and CXCL12 (30) is associated with an altered immune response. Additionally, PAD2 can translocate into nuclei and citrullinate histones, regulating gene transcription (10, 26).

Citrullination can change the net charge and increase the hydrophobicity of proteins, which subsequently alters the structures and functions of the proteins (35–39). The effects of citrullination are variable and debated. Hojo-Nakashima et al. revealed that PAD2 is beneficial as it catalyzes vimentin citrullination in THP-1 cells (a human monocytic cell line) to promote the differentiation and maturation of macrophages (40). By contrast, vimentin citrullinated by PAD2 is identified as an autoantigen in rheumatoid arthritis (RA), exhibiting the potentially detrimental role of PAD2 (32). Apart from vimentin, a large number of proteins are found to trigger autoimmune responses following PAD2-mediated citrullination (32). Interestingly, dysregulation of PAD2 activity has been implicated in many diseases such as RA (41), multiple sclerosis (MS) (42), and neurodegenerative disorders (43). Moreover, previous studies revealed that PAD2-catalyzed citrullination is an essential process during various modes of immune cell death, such as ETosis (13, 14) and pyroptosis (15). These modalities of immune cell death may play a major role in the pathogenesis of sepsis and other inflammatory diseases (44, 45). Consequently, it is critical to understand the role of PAD2 in host immunity and related diseases. In the following sections, the mechanisms *via* which PAD2 mediate cellular processes, regulate immune response, and cause diseases will be reviewed and discussed. Understanding the mechanisms of host immunity regulated by PAD2 may ultimately allow for design of novel therapeutic strategies for a multitude of immune disorders.

PAD2 EXPRESSION IN IMMUNE CELLS

PAD2 in Macrophages

Macrophages are immune cells which exhibit relatively rich PAD2 expression (9). Macrophages play an important role both in innate and adaptive immunity. Phagocytosis and pyroptosis are two major pathways involved in the pathogen clearance by innate immunity (46–50). Macrophages contribute to adaptive immunity by presenting the antigens of pathogens to T cells (51–53). PAD2 can affect these immune actions through regulating the differentiation of macrophages (9, 40). Macrophages are derived from monocytes in circulation. Interestingly, although PAD2 mRNA can be detected in monocytes, it is not translated into PAD2 proteins until the initiation of differentiation (9). Moreover, a previous study revealed that the levels of PAD2 mRNA and proteins exhibit concomitant increases in THP-1 cells during the differentiation into macrophages (40). Nonetheless, the underlying mechanisms through which PAD2 mediate monocyte differentiation remain elusive.

PAD2 also mediates the activation of pyroptosis (**Figure 2**), another important signaling pathway associated with anti-pathogen activities in macrophages (15). Pyroptosis is an inflammatory form of macrophage death induced by infection or chemical stimulation and mediated by Caspase-1 and/or Caspase-11 (54). Prior to the activation of Caspase-1, the stimulating signals are sensed by pattern recognition receptors, including NOD-like receptors and AIM2-like receptors, and initiate the assembly of inflammasomes (55–57). During the formation of inflammasomes, a quick increase of protein citrullination can be observed in macrophages (15). Specifically, ASC (apoptosis-associated speck-like protein containing a CARD), a critical component of inflammasomes, is also citrullinated. After PAD2 and PAD4 are dually suppressed by Cl-amidine, a pan-PAD inhibitor (58), the citrullination of ASC is reduced (15). Additionally, the activation of NLRP3 inflammasomes is also dampened, which subsequently diminishes macrophage pyroptosis. In agreement with these findings, our most recent experiments revealed that the knockout of *Pad2* in macrophages can decrease Caspase-1 mediated pyroptosis induced by *Pseudomonas aeruginosa* sepsis (PA-sepsis) (59). In contrast, *Pad4* depletion in the macrophages can increase Caspase-1 mediated pyroptosis in the mouse model of PA-sepsis (59). Therefore, PAD2-mediated ASC citrullination is probably a significant step during inflammasome assembly, which then regulates the activation of Caspase-1 and pyroptosis. Nonetheless, since little effort has been taken to explore the association between PAD2 and pyroptosis, the underlying mechanisms *via* which PAD2 affects Caspase-1 activation remain to be elucidated.

Aside from pyroptosis, macrophages are also reported to undergo another form of cell death termed METosis (**Figure 2**) (13), which describes the release of extracellular trap-like structures from macrophages (20, 60). Similar to NETs, Macrophage ETs (METs) are found in response to various microorganisms (61). METs are capable of trapping and

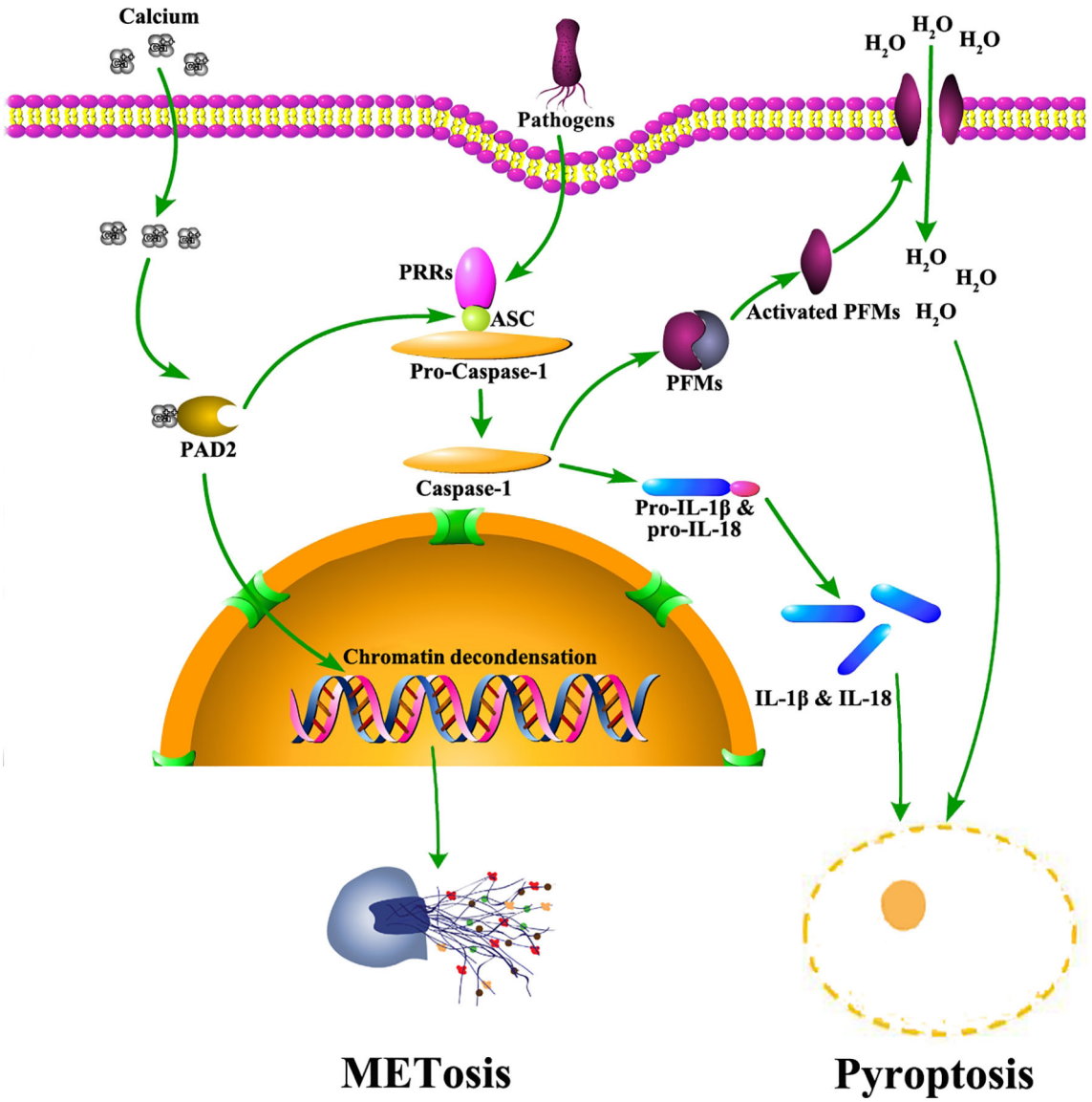

FIGURE 2 | The role of PAD2 in METosis and pyroptosis in macrophages. Pathogens trigger calcium influx into cytoplasm of macrophages. Subsequently, PAD2 is activated due to elevated levels of calcium. Activated PAD2 translocates into the nucleus to induce histone citrullination and chromatin decondensation, leading to METosis. Also, PAD2 mediates pyroptosis *via* citrullinating ASC. Citrullinated ASC participates in the assembly of inflammasomes which activate Caspase-1. Caspase-1 facilitates the maturation of IL-1β and IL-18 *via* cleaving their precursors. Meanwhile, Caspase-1 cleaves and activates PFMs which insert into plasma membrane to create pores allowing massive water to flux in. As a result, macrophages swell and rupture to accomplish pyroptosis, releasing mature IL-1β and IL-18. ASC: apoptosis-associated speck-like protein containing a CARD domain; IL, interleukin; METosis, macrophage death with release of macrophage extracellular traps; PAD2, type 2 peptidylarginine deiminase; PFMs, pore forming molecules; PRR, pattern recognition receptor.

immobilizing microbes to assist in microbial clearance (20). Several studies demonstrated that histone hypercitrullination catalyzed by PADs is an essential step during METosis (13, 62). Due to the alterations in net charges and structures, hypercitrullinated histones render chromatins more susceptible to decondensation (63). Most prior studies conclude that the process of citrullination is driven by PAD4, but a study by Mohanan et al. identified PAD2 as a major mediator in tumor necrosis factor (TNF)-α induced MET release from Raw264.7 macrophages (13). Therefore, further work is needed to clarify the association between PAD2 and METosis.

PAD2 in Neutrophils

Overall, PAD2 seems to have minimal effects on neutrophils due to low expression. The distribution of PAD2 and PAD4 are different in neutrophils. Unlike in macrophages, the PAD that is

predominantly expressed in neutrophils is PAD4 (64–66). PAD4 exists in granules, plasma membrane, and nucleus, while PAD2 is mainly detected in granules (64). Like macrophages, neutrophils can form NETs to defend against microbial infection (65, 67–69). NETosis also requires PAD-catalyzed histone hypercitrullination, which induces chromatin decondensation (63). In contrast to METosis, the citrullinating process in neutrophils is believed to be entirely mediated by PAD4 (65). However, our recent study found that selective inhibition of PAD2 can significantly decrease the generation of Citrullinated histone H3 (CitH3) in lipopolysaccharide (LPS)-stimulated neutrophils (70). The result suggests that PAD2 may also play a role in citrullinating actions within neutrophils. Furthermore, the extracellular release of PAD2 from neutrophils may still be able to citrullinate histone H3 and fibrinogen (64).

PAD2 in T Cells

There are two major subtypes of T cells which are CD4+ T cells and CD8+ T cells (71). CD8+ T cells directly kill microbe-infected cells or tumor cells (72), while CD4+ T cells usually act indirectly to regulate immune response, thus coined "helper T cells" (Th) (73). The relationship between CD8+ T cells and PAD2 is not well studied, while several studies revealed that PAD2 can modulate the polarization and functions of CD4+ T cells (11, 74, 75).

The expression of PAD2 in naïve CD4+ T cells is much lower than that in memory CD4+ T cells, indicating that PAD2 may have effects on the differentiation of CD4+ T cells (74). Actually, the fate of differentiating CD4+ T cells is decided by two key transcription factors, GATA3 and RORγT (76). PAD2 can directly citrullinate these two transcription factors, which changes their DNA binding ability to modulate gene expression (11). PAD2 inhibition decreases the differentiation of Th17 cells but promotes the differentiation of Th2 cells from naïve CD4+ T cells (11). Reversely, PAD2 overexpression in human peripheral blood mononuclear cells reduces Th2 cell polarization and increases Th17 cell polarization (77). Meanwhile, PAD2 regulates the functions of CD4+ T cells (11). PAD2 deficiency enhances cytokine production in Th2 cells but suppress cytokine generation in Th17 cells. Interestingly, although PAD2 is not associated with Th1 polarization, PAD2 inhibition can impair interferon-γ production in Th1 cells (11).

In addition to directly altering the functions and polarization of CD4+ T cells, PAD2 can affect T cell activities by citrullinating certain chemotaxins (i.e., CXCL10 and CXCL11) that mediate the chemotaxis of T cells (34). T cells exhibit lower sensitivity to citrullinated CXCL10 and CXCL11. Therefore, fewer T cells will be attracted to inflammation sites, resulting in attenuated inflammatory response.

PAD2 in B Cells

B cells are a subset of immune cells, which are responsible for antibody production and antigen presentation (78). The expression of PAD2 is low in B cells (79). Nonetheless, PAD2 is probably required for the transition of B cells to plasma cells, as the knockout of *Pad2* can cause a significant reduction in bone marrow plasma cells in a mouse model of TNF- α induced arthritis (80). Consequently, IgG produced by plasma cells is also decreased in *Pad2*$^{-/-}$ mice, which is associated with alleviated severity of TNF-α induced arthritis (80). This may indicate that PAD2 is required for the development of plasma cells. However, given that PAD2-citrullinated proteins are antigens for B cells, another explanation may also be established: *Pad2* knockout reduces the generation of citrullinated proteins, thus resulting in decreased activation of B cells. Hence, further work is needed to clarify the role of PAD2 in B cells.

PAD2 in Other Immune Cells

PAD2 can also interact with other cells to modulate immune response. For example, ATP upregulates the expression of Adamts-9, Rab6b, and TNFRII through activation of PAD2 in mast cells, contributing to the pathogenesis of RA (25). PAD2 and PAD4 inhibition by Cl-amidine also hampers functional maturation of dendritic cells induced by toll-like receptor agonists (81). As evidenced, there remains a paucity of studies exploring the interplay between PAD2 and immune cells. Further clarifying the mechanisms by which PAD2-mediated citrullination participates in immune activities can continue to advance the field in the future clinical applications of PAD2 guided therapies.

PAD2 IN HOST IMMUNITY

The immunomodulatory effects of PAD2 are mostly exerted by citrullinating key proteins involved in the cell signaling pathways. Thus, PAD2 may display different impacts on host immunity under different circumstances, which is determined by the roles of the citrullinated proteins in these pathways. The involvement of PAD2 in autoimmune diseases reflects its pro-inflammatory activity. The pathogenesis of RA is associated with elevated levels of PAD2-citrullinated proteins in synovial fluid (82). B cells can recognize the citrullinated epitopes and generate autoantibodies against the citrullinated proteins (83–85). In 70% of patients with RA, elevated levels of anti-citrullinated protein antibodies (ACPA) can be detected (86). After treatment with antirheumatic drugs, ACPA levels in circulation are significantly reduced correlated with decreased severity of RA (87, 88). These results suggest that protein citrullination by PAD2 can trigger an intensified inflammatory response in RA patients. Of note, RA patients who develop antibodies against PAD2 tend to suffer from less severe damage in joints and other organs (89). However, PAD2 sometimes exhibits the ability to inhibit inflammatory response. For example, Loos et al. reported that PAD2-mediated citrullination of CXCL10 and CXCL11 can reduce their chemotactic ability and thus result in diminished accumulation of inflammatory cells (34). PAD2 can also citrullinate certain transcription factors to mediate the differentiation of immune cells. The knockout of *Pad2* gene in mice can cause a shift in maturation of Th cells, which increases the differentiation of Th2 cells but decreases the differentiation of Th17 cells, rendering the mice susceptible to allergic airway inflammation (11).

The close association between PAD2 and host immunity is partly due to the relatively abundant expression in immune cells (74, 79). PAD2 functions as an important factor not only in the differentiation of immune cells, but also in several cell death signaling pathways (13, 15, 90, 91). Although PAD4 is identified to be the key regulator in NETosis (63, 92, 93), PAD2 may also play a part in the process as NETosis can still occur in the absence of PAD4 (94). Another type of cell death, pyroptosis, which mostly takes place in macrophages, is found to be regulated by PAD2 and PAD4 (15). Additionally, overexpression of PAD2 in Jurkat cells, which are derived from human T lymphocyte cells, can trigger enhanced apoptosis (91). Collectively, these findings indicate that PAD2 has an intimate relationship with immune cells and host immunity.

Infections

Sepsis

Sepsis is characterized by a dysregulated inflammatory response that may result in multi-organ failure (95). The role of PADs in sepsis has been identified in some previous studies (70, 96–98). However, most of them explored the association between PAD4 and sepsis. This was probably due to the critical effects of PAD4 on NETosis, which is believed to be an important signaling pathway involved in the pathogenesis of sepsis (99). The application of pan-PAD inhibitors, which inhibit the activity of both PAD2 and PAD4, can remarkably improve the survival in mouse models of LPS-induced endotoxemia and cecal ligation and puncture (CLP)-induced sepsis (100–102). Nonetheless, when *Pad4*$^{-/-}$ mice were used to explore the individual effects of PAD4 on sepsis, researchers found that *Pad4*-deficiency did not improve survival nor ameliorate bacteremia (94, 98). Accordingly, we revealed that a selective PAD4 inhibitor does not affect survival in LPS-induced endotoxic shock (70). Therefore, we began to hypothesize that the protective effects were derived from PAD2 inhibition. As expected, the employment of a selective PAD2 inhibitor in the same model of LPS-induced endotoxic shock significantly increased survival (70). Thereafter, our studies further demonstrated that the knockout of *Pad2* can improve survival in CLP-induced sepsis and PA-sepsis (59, 103). Therefore, it can be inferred that PAD2 likely acts as a critical mediator in the pathogenesis of sepsis.

Given the minimal effect of PAD4 on sepsis, it raises questions as to why NETosis is closely related to sepsis and why septic animals can benefit from anti-NET therapies. The pathogenicity of NETs is derived from numerous components such as myeloperoxidase, DNA, and Citrullinated histone H3 (CitH3) (104). Such components are also found in extracellular traps released by other immune cells, such as METs, which are more likely to be mediated by PAD2, as PAD2 is more abundantly expressed in macrophages than PAD4 (61). "Anti-NET therapies" are referred to as the clearance of extracellular DNA or CitH3 (105–107), which also eliminate detrimental molecules from other sources including METs at the same time. In contrast, the knockout of PAD4 can only decrease the molecules coming from NETosis. This possibly explains why PAD4 inhibition is not protective during sepsis. In addition, we discovered that selective inhibition of PAD2 can decrease the release of CitH3 in neutrophils (**Figure 3**) (70). Furthermore, antibody neutralization of circulation CitH3, by a commercially available anti-CitH3 antibody, was not shown to attenuate endotoxemia (105). However, administration of the antibody recognizing CitH3 generated from both PAD2 and PAD4 significantly improved survival (105). These findings display the differing effects of PAD2 and PAD4 inhibition during sepsis.

In a mouse model of CLP-induced lethal sepsis, we have newly demonstrated that PAD2 protein is elevated in serum and lung tissue after CLP (103). In septic patients, serum concentrations of PAD2 are positively correlated to lactate (r=0.5, p=0.04) and procalcitonin (PCT) levels (r=0.67, p=0.003) (108). Since lactate and PCT are considered markers for the prognosis and the severity of sepsis (109, 110), elevated PAD2 levels in serum may also serve as a future clinical biomarker and predictor of outcomes. Circulating CitH3 was also found to be positively correlated with blood PAD2 (r values=0.0452, p<0.001) and PAD4 levels (r value=0.363, p<0.01), respectively (108). The levels of PAD2 in bronchoalveolar lavage fluid (BALF) from patients with sepsis and respiratory distress syndrome (ARDS) are also significantly increased compared with those in a healthy control group (108). Furthermore, the Pad2 gene was found to be over-expressed in cells of the BALF of patients with septic specific ARDS. The consistent findings support the possible usage of PAD2 as a biomarker for sepsis specific ARDS and may serve as a distinguishing factor between sepsis specific ARDS and other non-infectious causes of ARDS. PAD2 can mediate the onset of sepsis by directly regulating pyroptosis. We recently found that PA-sepsis induced pyroptosis in macrophages is dramatically decreased in the absence of PAD2, thereby attenuating acute lung injury and improving survival (59). In the murine CLP-sepsis model, *Pad2* depletion enhances bacterial clearance, attenuates sepsis-induced vascular permeability of lung and kidney, and improves survival (103). Moreover, we found that macrophages stimulated by LPS undergo diminished Caspase-11-dependent pyroptosis in the absence of PAD2, which can explain how *Pad2* knockout improves the outcomes of septic mice (**Figure 3**) (103). These findings have highlighted the detrimental role of PAD2-mediated pyroptosis in the pathogenesis of sepsis (**Figure 3**). PAD2 also catalyzes the generation of CitH3 which is recognized as a "danger" signaling molecule (70, 111, 112). Furthermore, it has been reported that "danger" signaling molecules (i.e., ATP and double strand DNA) can elicit the activation of pyroptosis *via* the Caspase-1 dependent pathway (113, 114). Based on this data, we hypothesize that CitH3 may play a role in activating the pyroptotic pathway and that PAD2 can also modulate pyroptosis in an indirect way. Altogether, PAD2 has the potential as both a biomarker and therapeutic target of sepsis.

Although we have demonstrated the effects of PAD2 activation on sepsis, the mechanisms by which PAD2 activation leads to these downstream effects in sepsis remain poorly understood. A previous study demonstrated that ATP induces PAD2 activity *via* P2X7 receptors (25). While ATP is required for almost all biological reactions as the universal energy source (115), once host cells are damaged, stressed, or infected by pathogens, intracellular ATP can be released to become extracellular ATP which serves as a key

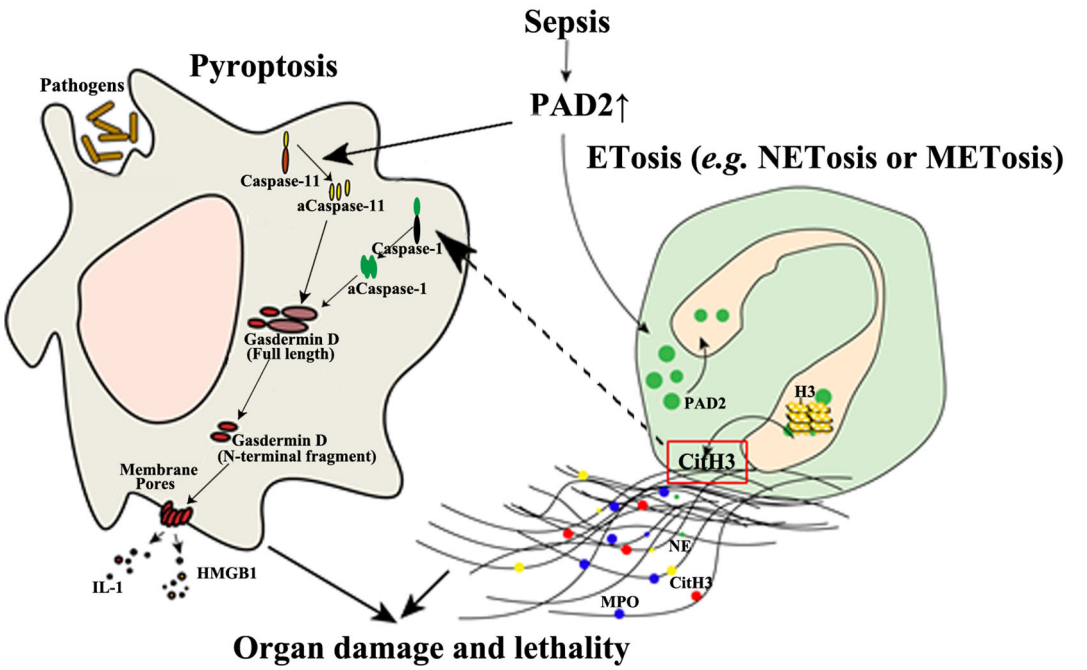

FIGURE 3 | The detrimental effects of PAD2-mediated pyroptosis and ETosis during sepsis. PAD2 facilitates the activation of Caspase-11, a key regulator in non-canonical pyroptosis, and causes macrophage death. In addition, PAD2 can translocate into the nuclei of neutrophils or macrophages and citrullinate histone H3 to induce ETosis. CitH3 generated during this process may further activate the canonical pyroptotic pathway as a danger signal. aCaspase-1/11, activated Caspase-1/11; CitH3, Citrullinated histone H3; ETosis, cell death with release of extracellular traps (ETs); H3, Histone H3; HMGB1, high mobility group box 1; IL, interleukin; M/NETosis, neutrophil/macrophage death with release of extracellular traps; MPO, myeloperoxidase; NE, neutrophil elastase. Lines, pathways already known; Dotted lines, proposed hypothesis for the pathway to elucidated.

"danger" signaling molecule (116–118). Additionally, certain pathogens can also produce and secrete extracellular ATP (119, 120). The extracellular ATP may then bind to P2X7 receptors to induce calcium influx, leading to subsequent PAD2 activation (25). Nonetheless, there is limited evidence supporting that ATP release is responsible for the activation of PAD2 during infections. Thus, further work is required to elucidate the association between infection and PAD2 activity.

Immune Disorders

Rheumatoid Arthritis

The manifestations of RA are characterized by chronic synovitis, systemic inflammation, and the generation of ACPA and rheumatoid factors (121). ACPA recognizes and binds to PAD2/4-citrullinated proteins, including vimentin, keratin, enolase, fibrinogen, and filaggrin (32, 122). ACPA can serve as a useful biomarker with high sensitivity and specificity, and is often a predictor of poor prognosis (123–126).

Among all the citrullinated proteins associated with RA, vimentin is the most frequently studied. Vimentin is an intermediate filament protein that plays a significant role in fixing the position of cytosolic organelles (127). Macrophages, which also express vimentin, are found in high levels in synovial fluid aspirates of RA joints (128). During calcium ionophore-induced macrophage apoptosis, vimentin is found to be citrullinated by PADs (90). Given the low expression of PAD4 in macrophages, PAD2 is likely the predominant PAD in the citrullination of vimentin. The cleavage of vimentin also occurs in the presence of calcium during macrophage pyroptosis (129). Since PAD2 is a calcium-dependent enzyme, it can be inferred that vimentin possibly undergoes citrullination prior to macrophage pyroptotic death. However, the mechanisms which citrullinated vimentin is associated with the pathogenesis of RA are not clear. One explanation is that the host loses its self-tolerance to citrullinated vimentin due to hereditary factors, which leads to production of ACPA (122, 130). As a result, massive ACPA-citrullinated vimentin complexes deposit in the joints, causing activation of complement systems leading to prolonged inflammation (131). Although genetic factors are closely related to the incidence of RA, the effects of environmental factors cannot be neglected (132). For example, a number of RA cases were found to be linked with infection (133). Thus, it is possible that infectious agent-induced macrophage death may be the initial step of RA onset. During the death processes of macrophages, vimentin is citrullinated by PAD2 and released. Meanwhile, more macrophages and other immune cells are attracted to the infected sites due to chemotaxis. Thereafter, citrullinated

vimentin is recognized as an autoantigen which triggers the generation of ACPA. However, this hypothesis cannot explain the pathogenesis of ACPA-negative RA. Therefore, further work is required to understand the complexity of RA.

PAD2 can be detected in synovial fluid from RA patients (134). It was demonstrated that the major sources of PAD2 are inflammatory cells (8). RA patients with higher PAD2 levels in synovial fluid tend to have enhanced disease activity, suggesting that the level of PAD2 in synovial fluid is a potential prognostic indicator (135). Additionally, PAD2 can also be taken as an autoantigen by the host. RA patients who developed autoantibodies against PAD2 are likely to display attenuated joint inflammation and RA-related lung disease (89).

M1 macrophages, which are activated by the classical pathway, can secrete proinflammatory cytokines such as TNF-α and IL-1 and cause joint erosion. While M2 macrophages, which are activated by the alternative pathway, can produce anti-inflammatory cytokines (mainly IL-10 and TGF-β), contributing to vasculogenesis and tissue remodeling and repair, as recently observed in systemic sclerosis. Markers for both macrophage phenotypes may coexist on the same cell (136, 137). Recent studies have revealed that M1/M2 macrophage imbalance strongly contributes to osteoclastogenesis of RA (138). Eghbalzadeh et al. reported that NETs support macrophage polarization toward an M2 phenotype, displaying anti-inflammatory properties. PAD4 deficiency aggravates acute inflammation and increases tissue damage post- acute myocardial infarction, partially due to the lack of NETs (139). It remains largely unknown whether PAD2 affects macrophage polarization.

Multiple Sclerosis

MS is an autoimmune disorder in central nervous system characterized by chronic demyelination of nerve cells (140). Patients with MS usually suffer from loss of sensitivity, changes in sensation, difficulties in coordination or problems with vision (141). The effects of PAD2 on the pathogenesis of MS remain in debate. Researchers revealed that citrullination of myelin basic proteins (MBP) is increased in MS patients (42, 142, 143). Overexpression of PAD2 in mice leads to MBP hypercitrullination and myelin loss in central nervous system (144). Hypercitrullination will not only decrease the stability of MBP, but also put MBP at higher risks of being attacked by T cells (28, 75). Th17 cells, a subtype of T cell, shows enhanced reactivity to citrullinated MBP (75). As mentioned above, PAD2 can facilitate the polarization of CD4+ T cells into Th17 cells (11). Thus, PAD2 plays a critical role in MS pathogenesis. In line with these findings, a study demonstrated that PAD2 inhibition can attenuate disease severity in animal models mimicking MS (145). On the contrary, a study reported that deletion of *Pad2* gene in mice decreased levels of citrullinated MBP but did not reduce the incidence rate of experimental autoimmune encephalomyelitis (146). A recent study discovered that PAD2-mediated citrullination is indispensable during the differentiation and myelination of oligodendrocytes (147). Knockout of *Pad2* in mice will result in motor dysfunction and even decreased myelination in axons (147). Therefore, it is critical to keep a balanced PAD2 level in central nervous system as it maintains the normal structure and functions of nerve cells and further studies should continue to elucidate the role of PAD2 on MS.

Cancers

Currently, PAD2 is implicated in skin tumors (148), breast cancer (10), colorectal cancer (149), and glioblastoma multiforme (150, 151). The intimate relationship between PAD2 and tumors is likely due to the role of PAD2 in modulating gene transcription. PAD2 is the only PAD that citrullinates arginine1810 (Cit1810) in repeat 31 of the carboxyl-terminal domain (CTD) of the largest subunit of RNA polymerase II (RNAP2) (152). Cit1810 is crucial for RNAP2 to overcome the pausing barrier close to the transcription start site, which enables the efficient transcription of highly expressed genes needed for cell cycle progression, metabolism, and cell proliferation (152).

The effects of PAD2 on the development of different tumors are not the same. For example, overexpression of PAD2 has been shown to augment the malignancy of skin tumors (153), while increased PAD2 expression has been linked to improved survival in patients with estrogen receptor (ER)-positive breast cancer (112). However, upregulated PAD2 expression in breast cancer is associated with resistance to tamoxifen treatment (154). These findings make PAD2 a mysterious modulator in tumorigenesis. In the pathogenesis of breast cancer and glioblastoma multiforme, PAD2 modulates gene transcription *via* citrullinating histones (112, 151). In colorectal cancer, however, PAD2 prevents tumor progression by citrullinating β-catenin thus inhibiting the Wnt signaling pathway. PAD2 inhibition will increase the sensitivity of breast cancer cells to tamoxifen (154), while the knockout of *Pad2* will induce great resistance to nitazoxanide in colorectal cancer cells (149). More work is needed to investigate the involvement of PAD2 in other tumors (149).

The therapeutic potential and applications of PAD2 in cancer remains to be further clarified. However, given the role of PAD2 in tumorigenesis and response to chemotherapy, PAD2 will continue to be a biomarker and target of continued interest in the era of personalized cancer care.

CONCLUSIONS AND FUTURE PERSPECTIVES

Citrullination is a posttranslational protein modification catalyzed by PADs and is involved in host immunity. PAD2 has wide-reaching roles through its citrullination of a variety of target proteins. Dysregulated activity of PAD2 is associated with a series of immune disorders including sepsis, RA, MS, and tumor formation (**Figure 4**). In this review, we have summarized PAD2 specific functions on cell death control, transcription

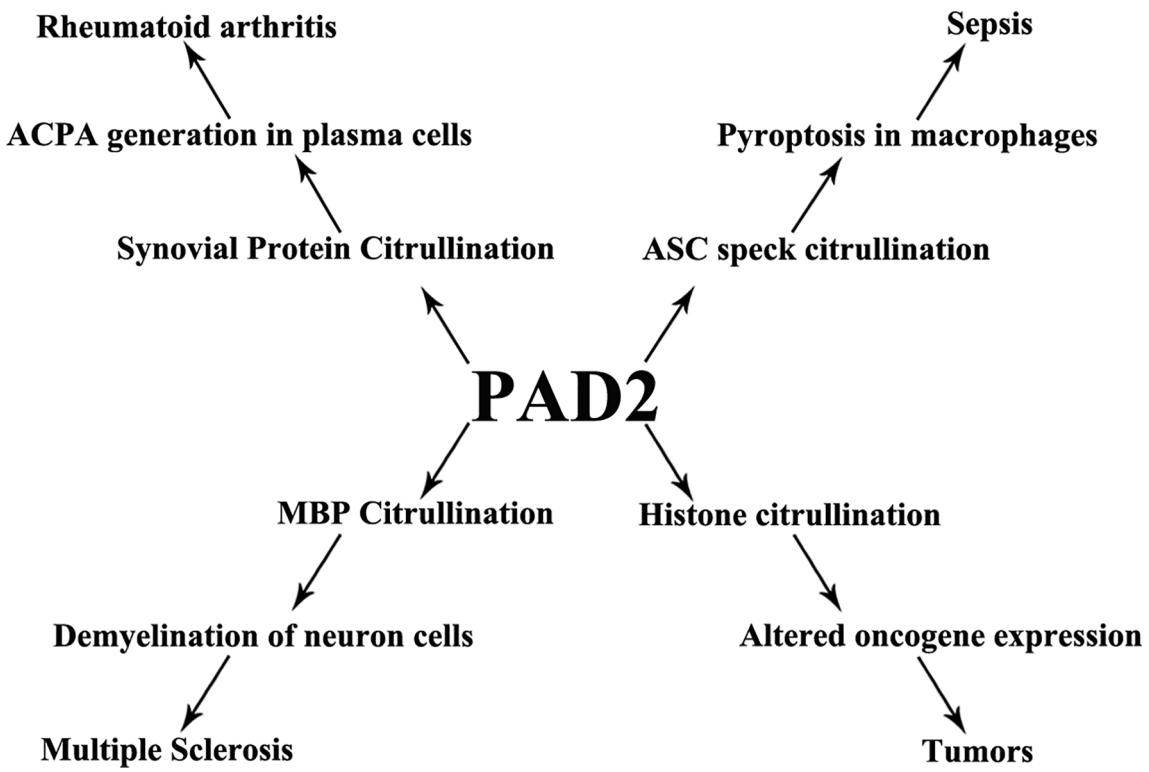

FIGURE 4 | PAD2 and immune disorders. A schematic view showing that PAD2 is associated with a number of diseases and the possible mechanisms underlying pathogenesis. ACPA, anti-citrullinated protein antibodies; ASC, apoptosis-associated speck-like protein containing a CARD domain; MBP, myelin basic protein.

regulation by citrullination of arginine 26 on histone H3 (*e.g.*, sepsis, tumor), and citrullination of vimentin (*e.g.*, RA). We highlight several citrullinated proteins to demonstrate the contributions of PAD2-mediated protein citrullination to RA, sepsis, and cancer within each specific environment. Given that CitH3 is also found to be a biomarker in patients with cancers (155, 156), more epigenetic studies are needed to explore if and how citrullination of histone H3 interferes with transcription factors to regulate RA, sepsis, and cancers. We propose that PAD2 is a promising novel biomarker and therapeutic target for a broad spectrum of diseases including autoimmune and inflammatory diseases, sepsis, MS, and several types of cancer.

AUTHOR CONTRIBUTIONS

ZW and YL drafted the manuscript. PL, YT, WO, JH, HA, and YL made significant revisions to the manuscript. All authors contributed to the article and approved the submitted version.

FUNDING

This work was funded by grants from the National Institute of Health R01 (Grant# RHL155116A) to YL and HA, and the Joint-of-Institute (Grant# U068874) to YL.

REFERENCES

1. Wang S, Wang Y. Peptidylarginine Deiminases in Citrullination, Gene Regulation, Health and Pathogenesis. *Biochim Biophys Acta* (2013) 1829 (10):1126–35. doi: 10.1016/j.bbagrm.2013.07.003
2. Vossenaar ER, Zendman AJ, van Venrooij WJ, Pruijn GJ. PAD, a Growing Family of Citrullinating Enzymes: Genes, Features and Involvement in Disease. *Bioessays* (2003) 25(11):1106–18. doi: 10.1002/bies.10357
3. Chavanas S, Mechin MC, Takahara H, Kawada A, Nachat R, Serre G, et al. Comparative Analysis of the Mouse and Human Peptidylarginine Deiminase Gene Clusters Reveals Highly Conserved non-Coding Segments and a New Human Gene, PADI6. *Gene* (2004) 330:19–27. doi: 10.1016/j.gene.2003.12.038
4. van Beers JJ, Zendman AJ, Raijmakers R, Stammen-Vogelzangs J, Pruijn GJ. Peptidylarginine Deiminase Expression and Activity in PAD2 Knock-Out and PAD4-Low Mice. *Biochimie* (2013) 95(2):299–308. doi: 10.1016/j.biochi.2012.09.029
5. Mohamed BM, Boyle NT, Schinwald A, Murer B, Ward R, Mahfoud OK, et al. Induction of Protein Citrullination and Auto-Antibodies Production in Murine Exposed to Nickel Nanomaterials. *Sci Rep* (2018) 8(1):679. doi: 10.1038/s41598-017-19068-1
6. Takahara H, Tsuchida M, Kusubata M, Akutsu K, Tagami S, Sugawara K. Peptidylarginine Deiminase of the Mouse. Distribution, Properties, and Immunocytochemical Localization. *J Biol Chem* (1989) 264(22):13361–8. doi: 10.1016/S0021-9258(18)51637-9

7. Cherrington BD, Morency E, Struble AM, Coonrod SA, Wakshlag JJ. Potential Role for Peptidylarginine Deiminase 2 (PAD2) in Citrullination of Canine Mammary Epithelial Cell Histones. *PLoS One* (2010) 5(7):e11768. doi: 10.1371/journal.pone.0011768
8. Foulquier C, Sebbag M, Clavel C, Chapuy-Regaud S, Al Badine R, Mechin MC, et al. Peptidyl Arginine Deiminase Type 2 (PAD-2) and PAD-4 But Not PAD-1, PAD-3, and PAD-6 are Expressed in Rheumatoid Arthritis Synovium in Close Association With Tissue Inflammation. *Arthritis Rheum* (2007) 56(11):3541–53. doi: 10.1002/art.22983
9. Vossenaar ER, Radstake TR, van der Heijden A, van Mansum MA, Dieteren C, de Rooij DJ, et al. Expression and Activity of Citrullinating Peptidylarginine Deiminase Enzymes in Monocytes and Macrophages. *Ann Rheum Dis* (2004) 63(4):373–81. doi: 10.1136/ard.2003.012211
10. Cherrington BD, Zhang X, McElwee JL, Morency E, Anguish LJ, Coonrod SA. Potential Role for PAD2 in Gene Regulation in Breast Cancer Cells. *PloS One* (2012) 7(7):e41242. doi: 10.1371/journal.pone.0041242
11. Sun B, Chang HH, Salinger A, Tomita B, Bawadekar M, Holmes CL, et al. Reciprocal Regulation of Th2 and Th17 Cells by PAD2-Mediated Citrullination. *JCI Insight* (2019) 4(22):e129687. doi: 10.1172/jci.insight.129687
12. Arnoux F, Mariot C, Peen E, Lambert NC, Balandraud N, Roudier J, et al. Peptidyl Arginine Deiminase Immunization Induces Anticitrullinated Protein Antibodies in Mice With Particular MHC Types. *Proc Natl Acad Sci U S A* (2017) 114(47):E10169–77. doi: 10.1073/pnas.1713112114
13. Mohanan S, Horibata S, McElwee JL, Dannenberg AJ, Coonrod SA. Identification of Macrophage Extracellular Trap-Like Structures in Mammary Gland Adipose Tissue: A Preliminary Study. *Front Immunol* (2013) 4:67. doi: 10.3389/fimmu.2013.00067
14. Boe DM, Curtis BJ, Chen MM, Ippolito JA, Kovacs EJ. Extracellular Traps and Macrophages: New Roles for the Versatile Phagocyte. *J Leukoc Biol* (2015) 97(6):1023–35. doi: 10.1189/jlb.4RI1014-521R
15. Mishra N, Schwerdtner L, Sams K, Mondal S, Ahmad F, Schmidt RE, et al. Cutting Edge: Protein Arginine Deiminase 2 and 4 Regulate NLRP3 Inflammasome-Dependent IL-1beta Maturation and ASC Speck Formation in Macrophages. *J Immunol* (2019) 203(4):795–800. doi: 10.4049/jimmunol.1800720
16. Amulic B, Hayes G. Neutrophil Extracellular Traps. *Curr Biol* (2011) 21(9): R297–8. doi: 10.1016/j.cub.2011.03.021
17. Liu CL, Tangsombatvisit S, Rosenberg JM, Mandelbaum G, Gillespie EC, Gozani OP, et al. Specific Post-Translational Histone Modifications of Neutrophil Extracellular Traps as Immunogens and Potential Targets of Lupus Autoantibodies. *Arthritis Res Ther* (2012) 14(1):R25. doi: 10.1186/ar3707
18. Saffarzadeh M, Juenemann C, Queisser MA, Lochnit G, Barreto G, Galuska SP, et al. Neutrophil Extracellular Traps Directly Induce Epithelial and Endothelial Cell Death: A Predominant Role of Histones. *PLoS One* (2012) 7 (2):e32366. doi: 10.1371/journal.pone.0032366
19. Aulik NA, Hellenbrand KM, Czuprynski CJ. Mannheimia Haemolytica and its Leukotoxin Cause Macrophage Extracellular Trap Formation by Bovine Macrophages. *Infect Immun* (2012) 80(5):1923–33. doi: 10.1128/IAI.06120-11
20. Loureiro A, Pais C, Sampaio P. Relevance of Macrophage Extracellular Traps in C. Albicans Killing. *Front Immunol* (2019) 10:2767. doi: 10.3389/fimmu.2019.02767
21. Fukuchi M, Miyabe Y, Furutani C, Saga T, Moritoki Y, Yamada T, et al. How to Detect Eosinophil ETosis (EETosis) and Extracellular Traps. *Allergol Int* (2021) 70(1):19–29. doi: 10.1016/j.alit.2020.10.002
22. Nija RJ, Sanju S, Sidharthan N, Mony U. Extracellular Trap by Blood Cells: Clinical Implications. *Tissue Eng Regener Med* (2020) 17(2):141–53. doi: 10.1007/s13770-020-00241-z
23. Arita K, Hashimoto H, Shimizu T, Nakashima K, Yamada M, Sato M. Structural Basis for Ca(2+)-Induced Activation of Human PAD4. *Nat Struct Mol Biol* (2004) 11(8):777–83. doi: 10.1038/nsmb799
24. Slade DJ, Fang P, Dreyton CJ, Zhang Y, Fuhrmann J, Rempel D, et al. Protein Arginine Deiminase 2 Binds Calcium in an Ordered Fashion: Implications for Inhibitor Design. *ACS Chem Biol* (2015) 10(4):1043–53. doi: 10.1021/cb500933j
25. Arandjelovic S, McKenney KR, Leming SS, Mowen KA. ATP Induces Protein Arginine Deiminase 2-Dependent Citrullination in Mast Cells Through the P2X7 Purinergic Receptor. *J Immunol* (2012) 189(8):4112–22. doi: 10.4049/jimmunol.1201098
26. Zheng L, Nagar M, Maurais AJ, Slade DJ, Parelkar SS, Coonrod SA, et al. Calcium Regulates the Nuclear Localization of Protein Arginine Deiminase 2. *Biochemistry* (2019) 58(27):3042–56. doi: 10.1021/acs.biochem.9b00225
27. Darrah E, Rosen A, Giles JT, Andrade F. Peptidylarginine Deiminase 2, 3 and 4 Have Distinct Specificities Against Cellular Substrates: Novel Insights Into Autoantigen Selection in Rheumatoid Arthritis. *Ann Rheum Dis* (2012) 71(1):92–8. doi: 10.1136/ard.2011.151712
28. Alghamdi M, Alasmari D, Assiri A, Mattar E, Aljaddawi AA, Alattas SG, et al. An Overview of the Intrinsic Role of Citrullination in Autoimmune Disorders. *J Immunol Res* (2019) 2019:7592851. doi: 10.1155/2019/7592851
29. Proost P, Loos T, Mortier A, Schutyser E, Gouwy M, Noppen S, et al. Citrullination of CXCL8 by Peptidylarginine Deiminase Alters Receptor Usage, Prevents Proteolysis, and Dampens Tissue Inflammation. *J Exp Med* (2008) 205(9):2085–97. doi: 10.1084/jem.20080305
30. Janssens R, Struyf S, Proost P. The Unique Structural and Functional Features of CXCL12. *Cell Mol Immunol* (2018) 15(4):299–311. doi: 10.1038/cmi.2017.107
31. Zhang X, Bolt M, Guertin MJ, Chen W, Zhang S, Cherrington BD, et al. Peptidylarginine Deiminase 2-Catalyzed Histone H3 Arginine 26 Citrullination Facilitates Estrogen Receptor Alpha Target Gene Activation. *Proc Natl Acad Sci U S A* (2012) 109(33):13331–6. doi: 10.1073/pnas.1203280109
32. Tilvawala R, Nguyen SH, Maurais AJ, Nemmara VV, Nagar M, Salinger AJ, et al. The Rheumatoid Arthritis-Associated Citrullinome. *Cell Chem Biol* (2018) 25(6):691–704.e6. doi: 10.1016/j.chembiol.2018.03.002
33. Damgaard D, Bawadekar M, Senolt L, Stensballe A, Shelef MA, Nielsen CH. Relative Efficiencies of Peptidylarginine Deiminase 2 and 4 in Generating Target Sites for Anti-Citrullinated Protein Antibodies in Fibrinogen, Alpha-Enolase and Histone H3. *PLoS One* (2018) 13(8):e0203214. doi: 10.1371/journal.pone.0203214
34. Loos T, Mortier A, Gouwy M, Ronsse I, Put W, Lenaerts JP, et al. Citrullination of CXCL10 and CXCL11 by Peptidylarginine Deiminase: A Naturally Occurring Posttranslational Modification of Chemokines and New Dimension of Immunoregulation. *Blood* (2008) 112(7):2648–56. doi: 10.1182/blood-2008-04-149039
35. Tarcsa E, Marekov LN, Mei G, Melino G, Lee SC, Steinert PM. Protein Unfolding by Peptidylarginine Deiminase. Substrate Specificity and Structural Relationships of the Natural Substrates Trichohyalin and Filaggrin. *J Biol Chem* (1996) 271 (48):30709–16. doi: 10.1074/jbc.271.48.30709
36. Wang Y, Wysocka J, Sayegh J, Lee YH, Perlin JR, Leonelli L, et al. Human PAD4 Regulates Histone Arginine Methylation Levels via Demethylimination. *Science* (2004) 306(5694):279–83. doi: 10.1126/science.1101400
37. Fert-Bober J, Giles JT, Holewinski RJ, Kirk JA, Uhrigshardt H, Crowgey EL, et al. Citrullination of Myofilament Proteins in Heart Failure. *Cardiovasc Res* (2015) 108(2):232–42. doi: 10.1093/cvr/cvv185
38. Jang B, Jeon YC, Choi JK, Park M, Kim JI, Ishigami A, et al. Peptidylarginine Deiminase Modulates the Physiological Roles of Enolase via Citrullination: Links Between Altered Multifunction of Enolase and Neurodegenerative Diseases. *Biochem J* (2012) 445(2):183–92. doi: 10.1042/BJ20120025
39. Cuthbert GL, Daujat S, Snowden AW, Erdjument-Bromage H, Hagiwara T, Yamada M, et al. Histone Deimination Antagonizes Arginine Methylation. *Cell* (2004) 118(5):545–53. doi: 10.1016/j.cell.2004.08.020
40. Hojo-Nakashima I, Sato R, Nakashima K, Hagiwara T, Yamada M. Dynamic Expression of Peptidylarginine Deiminase 2 in Human Monocytic Leukaemia THP-1 Cells During Macrophage Differentiation. *J Biochem* (2009) 146(4):471–9. doi: 10.1093/jb/mvp097
41. Curran AM, Naik P, Giles JT, Darrah E. PAD Enzymes in Rheumatoid Arthritis: Pathogenic Effectors and Autoimmune Targets. *Nat Rev Rheumatol* (2020) 16(6):301–15. doi: 10.1038/s41584-020-0409-1
42. Calabrese R, Zampieri M, Mechelli R, Annibali V, Guastafierro T, Ciccarone F, et al. Methylation-Dependent PAD2 Upregulation in Multiple Sclerosis Peripheral Blood. *Mult Scler* (2012) 18(3):299–304. doi: 10.1177/1352458511421055
43. Arif M, Kato T. Increased Expression of PAD2 After Repeated Intracerebroventricular Infusions of Soluble Abeta(25-35) in the Alzheimer's Disease Model Rat Brain: Effect of Memantine. *Cell Mol Biol Lett* (2009) 14(4):703–14. doi: 10.2478/s11658-009-0029-x

44. Guimaraes-Costa AB, Nascimento MT, Wardini AB, Pinto-da-Silva LH, Saraiva EM. ETosis: A Microbicidal Mechanism Beyond Cell Death. *J Parasitol Res* (2012) 2012:929743. doi: 10.1155/2012/929743
45. Aglietti RA, Dueber EC. Recent Insights Into the Molecular Mechanisms Underlying Pyroptosis and Gasdermin Family Functions. *Trends Immunol* (2017) 38(4):261–71. doi: 10.1016/j.it.2017.01.003
46. Hirayama D, Iida T, Nakase H. The Phagocytic Function of Macrophage-Enforcing Innate Immunity and Tissue Homeostasis. *Int J Mol Sci* (2017) 19 (1):92. doi: 10.3390/ijms19010092
47. Aderem A, Underhill DM. Mechanisms of Phagocytosis in Macrophages. *Annu Rev Immunol* (1999) 17:593–623. doi: 10.1146/annurev.immunol.17.1.593
48. Miao EA, Leaf IA, Treuting PM, Mao DP, Dors M, Sarkar A, et al. Caspase-1-Induced Pyroptosis is an Innate Immune Effector Mechanism Against Intracellular Bacteria. *Nat Immunol* (2010) 11(12):1136–42. doi: 10.1038/ni.1960
49. Lacey CA, Mitchell WJ, Dadelahi AS, Skyberg JA. Caspase-1 and Caspase-11 Mediate Pyroptosis, Inflammation, and Control of Brucella Joint Infection. *Infect Immun* (2018) 86(9):e00361–18. doi: 10.1128/IAI.00361-18
50. Jorgensen I, Zhang Y, Krantz BA, Miao EA. Pyroptosis Triggers Pore-Induced Intracellular Traps (PITs) That Capture Bacteria and Lead to Their Clearance by Efferocytosis. *J Exp Med* (2016) 213(10):2113–28. doi: 10.1084/jem.20151613
51. Ziegler K, Unanue ER. Identification of a Macrophage Antigen-Processing Event Required for I-Region-Restricted Antigen Presentation to T Lymphocytes. *J Immunol* (1981) 127(5):1869–75.
52. Unanue ER. Antigen-Presenting Function of the Macrophage. *Annu Rev Immunol* (1984) 2:395–428. doi: 10.1146/annurev.iy.02.040184.002143
53. Martinez-Pomares L, Gordon S. Antigen Presentation the Macrophage Way. *Cell* (2007) 131(4):641–3. doi: 10.1016/j.cell.2007.10.046
54. Shi J, Gao W, Shao F. Pyroptosis: Gasdermin-Mediated Programmed Necrotic Cell Death. *Trends Biochem Sci* (2017) 42(4):245–54. doi: 10.1016/j.tibs.2016.10.004
55. Gao J, Peng S, Shan X, Deng G, Shen L, Sun J, et al. Inhibition of AIM2 Inflammasome-Mediated Pyroptosis by Andrographolide Contributes to Amelioration of Radiation-Induced Lung Inflammation and Fibrosis. *Cell Death Dis* (2019) 10(12):957. doi: 10.1038/s41419-019-2195-8
56. Miao EA, Ernst RK, Dors M, Mao DP, Aderem A. Pseudomonas Aeruginosa Activates Caspase 1 Through Ipaf. *Proc Natl Acad Sci U S A* (2008) 105 (7):2562–7. doi: 10.1073/pnas.0712183105
57. Kelley N, Jeltema D, Duan Y, He Y. The NLRP3 Inflammasome: An Overview of Mechanisms of Activation and Regulation. *Int J Mol Sci* (2019) 20(13):3328. doi: 10.3390/ijms20133328
58. Li Y, Liu Z, Liu B, Zhao T, Chong W, Wang Y, et al. Citrullinated Histone H3: A Novel Target for the Treatment of Sepsis. *Surgery* (2014) 156(2):229–34. doi: 10.1016/j.surg.2014.04.009
59. Wu Z, Tian Y, Alam HB, Li P, Duan X, Williams AM, et al. Peptidylarginine Deiminases 2 Mediates Caspase-1-Associated Lethality in Pseudomonas Aeruginosa Pneumonia-Induced Sepsis. *J Infect Dis* (2021) 223(6):1093–102. doi: 10.1093/infdis/jiaa475
60. Okubo K, Kurosawa M, Kamiya M, Urano Y, Suzuki A, Yamamoto K, et al. Macrophage Extracellular Trap Formation Promoted by Platelet Activation is a Key Mediator of Rhabdomyolysis-Induced Acute Kidney Injury. *Nat Med* (2018) 24(2):232–8. doi: 10.1038/nm.4462
61. Doster RS, Rogers LM, Gaddy JA, Aronoff DM. Macrophage Extracellular Traps: A Scoping Review. *J Innate Immun* (2018) 10(1):3–13. doi: 10.1159/000480373
62. Wong KW, Jacobs WRJr. Mycobacterium Tuberculosis Exploits Human Interferon Gamma to Stimulate Macrophage Extracellular Trap Formation and Necrosis. *J Infect Dis* (2013) 208(1):109–19. doi: 10.1093/infdis/jit097
63. Wang Y, Li M, Stadler S, Correll S, Li P, Wang D, et al. Histone Hypercitrullination Mediates Chromatin Decondensation and Neutrophil Extracellular Trap Formation. *J Cell Biol* (2009) 184(2):205–13. doi: 10.1083/jcb.200806072
64. Zhou Y, Chen B, Mittereder N, Chaerkady R, Strain M, An LL, et al. Spontaneous Secretion of the Citrullination Enzyme PAD2 and Cell Surface Exposure of PAD4 by Neutrophils. *Front Immunol* (2017) 8:1200. doi: 10.3389/fimmu.2017.01200
65. Rohrbach AS, Slade DJ, Thompson PR, Mowen KA. Activation of PAD4 in NET Formation. *Front Immunol* (2012) 3:360. doi: 10.3389/fimmu.2012.00360
66. Demers M, Wong SL, Martinod K, Gallant M, Cabral JE, Wang Y, et al. Priming of Neutrophils Toward NETosis Promotes Tumor Growth. *Oncoimmunology* (2016) 5(5):e1134073. doi: 10.1080/2162402X.2015.1134073
67. Schilcher K, Andreoni F, Uchiyama S, Ogawa T, Schuepbach RA, Zinkernagel AS. Increased Neutrophil Extracellular Trap-Mediated Staphylococcus Aureus Clearance Through Inhibition of Nuclease Activity by Clindamycin and Immunoglobulin. *J Infect Dis* (2014) 210(3):473–82. doi: 10.1093/infdis/jiu091
68. Araujo CV, Campbell C, Goncalves-de-Albuquerque CF, Molinaro R, Cody MJ, Yost CC, et al. A PPARgamma AGONIST ENHANCES BACTERIAL CLEARANCE THROUGH NEUTROPHIL EXTRACELLULAR TRAP FORMATION AND IMPROVES SURVIVAL IN SEPSIS. *Shock* (2016) 45 (4):393–403. doi: 10.1097/SHK.0000000000000520
69. Brinkmann V, Reichard U, Goosmann C, Fauler B, Uhlemann Y, Weiss DS, et al. Neutrophil Extracellular Traps Kill Bacteria. *Science* (2004) 303 (5663):1532–5. doi: 10.1126/science.1092385
70. Wu Z, Deng Q, Pan B, Alam HB, Tian Y, Bhatti UF, et al. Inhibition of PAD2 Improves Survival in a Mouse Model of Lethal LPS-Induced Endotoxic Shock. *Inflammation* (2020) 43(4):1436–45. doi: 10.1007/s10753-020-01221-0
71. Golubovskaya V, Wu L. Different Subsets of T Cells, Memory, Effector Functions, and CAR-T Immunotherapy. *Cancers (Basel)* (2016) 8(3):36. doi: 10.3390/cancers8030036
72. Zhang N, Bevan MJ. CD8(+) T Cells: Foot Soldiers of the Immune System. *Immunity* (2011) 35(2):161–8. doi: 10.1016/j.immuni.2011.07.010
73. Tubo NJ, Jenkins MK. CD4+ T Cells: Guardians of the Phagosome. *Clin Microbiol Rev* (2014) 27(2):200–13. doi: 10.1128/CMR.00097-13
74. Liu Y, Lightfoot YL, Seto N, Carmona-Rivera C, Moore E, Goel R, et al. Peptidylarginine Deiminases 2 and 4 Modulate Innate and Adaptive Immune Responses in TLR-7-Dependent Lupus. *JCI Insight* (2018) 3(23): e124729. doi: 10.1172/jci.insight.124729
75. Carrillo-Vico A, Leech MD, Anderton SM. Contribution of Myelin Autoantigen Citrullination to T Cell Autoaggression in the Central Nervous System. *J Immunol* (2010) 184(6):2839–46. doi: 10.4049/jimmunol.0903639
76. Vahedi G, C Poholek A, Hand TW, Laurence A, Kanno Y, O'Shea JJ, et al. Helper T-Cell Identity and Evolution of Differential Transcriptomes and Epigenomes. *Immunol Rev* (2013) 252(1):24–40. doi: 10.1111/imr.12037
77. Chang HH, Liu GY, Dwivedi N, Sun B, Okamoto Y, Kinslow JD, et al. A Molecular Signature of Preclinical Rheumatoid Arthritis Triggered by Dysregulated PTPN22. *JCI Insight* (2016) 1(17):e90045. doi: 10.1172/jci.insight.90045
78. LeBien TW, Tedder TF. B Lymphocytes: How They Develop and Function. *Blood* (2008) 112(5):1570–80. doi: 10.1182/blood-2008-02-078071
79. Ireland JM, Unanue ER. Autophagy in Antigen-Presenting Cells Results in Presentation of Citrullinated Peptides to CD4 T Cells. *J Exp Med* (2011) 208 (13):2625–32. doi: 10.1084/jem.20110640
80. Bawadekar M, Shim D, Johnson CJ, Warner TF, Rebernick R, Damgaard D, et al. Peptidylarginine Deiminase 2 is Required for Tumor Necrosis Factor Alpha-Induced Citrullination and Arthritis, But Not Neutrophil Extracellular Trap Formation. *J Autoimmun* (2017) 80:39–47. doi: 10.1016/j.jaut.2017.01.006
81. Jang B, Kim HW, Kim JS, Kim WS, Lee BR, Kim S, et al. Peptidylarginine Deiminase Inhibition Impairs Toll-Like Receptor Agonist-Induced Functional Maturation of Dendritic Cells, Resulting in the Loss of T Cell-Proliferative Capacity: A Partial Mechanism With Therapeutic Potential in Inflammatory Settings. *J Leukoc Biol* (2015) 97(2):351–62. doi: 10.1189/jlb.3A0314-142RR
82. Vossenaar ER, Nijenhuis S, Helsen MM, van der Heijden A, Senshu T, van den Berg WB, et al. Citrullination of Synovial Proteins in Murine Models of Rheumatoid Arthritis. *Arthritis Rheum* (2003) 48(9):2489–500. doi: 10.1002/art.11229
83. Masson-Bessiere C, Sebbag M, Durieux JJ, Nogueira L, Vincent C, Girbal-Neuhauser E, et al. In the Rheumatoid Pannus, Anti-Filaggrin Autoantibodies are Produced by Local Plasma Cells and Constitute a Higher Proportion of IgG Than in Synovial Fluid and Serum. *Clin Exp Immunol* (2000) 119(3):544–52. doi: 10.1046/j.1365-2249.2000.01171.x
84. Reparon-Schuijt CC, van Esch WJ, van Kooten C, Schellekens GA, de Jong BA, van Venrooij WJ, et al. Secretion of Anti-Citrulline-Containing Peptide Antibody by B Lymphocytes in Rheumatoid Arthritis. *Arthritis Rheum* (2001) 44(1):41–7. doi: 10.1002/1529-0131(200101)44:1<41::AID-ANR6>3.0.CO;2-0
85. Lelieveldt L, Kristyanto H, Pruijn GJM, Scherer HU, Toes REM, Bonger KM. Sequential Prodrug Strategy To Target and Eliminate ACPA-Selective Autoreactive B Cells. *Mol Pharm* (2018) 15(12):5565–73. doi: 10.1021/acs.molpharmaceut.8b00741

86. Schellekens GA, Visser H, de Jong BA, van den Hoogen FH, Hazes JM, Breedveld FC, et al. The Diagnostic Properties of Rheumatoid Arthritis Antibodies Recognizing a Cyclic Citrullinated Peptide. *Arthritis Rheum* (2000) 43(1):155–63. doi: 10.1002/1529-0131(200001)43:1<155::AID-ANR20>3.0.CO;2-3
87. Seegobin SD, Ma MH, Dahanayake C, Cope AP, Scott DL, Lewis CM, et al. ACPA-Positive and ACPA-Negative Rheumatoid Arthritis Differ in Their Requirements for Combination DMARDs and Corticosteroids: Secondary Analysis of a Randomized Controlled Trial. *Arthritis Res Ther* (2014) 16(1): R13. doi: 10.1186/ar4439
88. Ally MM, Hodkinson B, Meyer PW, Musenge E, Tintinger GR, Tikly M, et al. Circulating Anti-Citrullinated Peptide Antibodies, Cytokines and Genotype as Biomarkers of Response to Disease-Modifying Antirheumatic Drug Therapy in Early Rheumatoid Arthritis. *BMC Musculoskelet Disord* (2015) 16:130. doi: 10.1186/s12891-015-0587-1
89. Darrah E, Giles JT, Davis RL, Naik P, Wang H, Konig MF, et al. Autoantibodies to Peptidylarginine Deiminase 2 Are Associated With Less Severe Disease in Rheumatoid Arthritis. *Front Immunol* (2018) 9:2696. doi: 10.3389/fimmu.2018.02696
90. Asaga H, Yamada M, Senshu T. Selective Deimination of Vimentin in Calcium Ionophore-Induced Apoptosis of Mouse Peritoneal Macrophages. *Biochem Biophys Res Commun* (1998) 243(3):641–6. doi: 10.1006/bbrc.1998.8148
91. Hsu PC, Liao YF, Lin CL, Lin WH, Liu GY, Hung HC. Vimentin is Involved in Peptidylarginine Deiminase 2-Induced Apoptosis of Activated Jurkat Cells. *Mol Cells* (2014) 37(5):426–34. doi: 10.14348/molcells.2014.2359
92. Kenny EF, Herzig A, Kruger R, Muth A, Mondal S, Thompson PR, et al. Diverse Stimuli Engage Different Neutrophil Extracellular Trap Pathways. *Elife* (2017) 6:e24437. doi: 10.7554/eLife.24437
93. Thiam HR, Wong SL, Qiu R, Kittisopikul M, Vahabikashi A, Goldman AE, et al. NETosis Proceeds by Cytoskeleton and Endomembrane Disassembly and PAD4-Mediated Chromatin Decondensation and Nuclear Envelope Rupture. *Proc Natl Acad Sci U S A* (2020) 117(13):7326–37. doi: 10.1073/pnas.1909546117
94. Martinod K, Fuchs TA, Zitomersky NL, Wong SL, Demers M, Gallant M, et al. PAD4-Deficiency Does Not Affect Bacteremia in Polymicrobial Sepsis and Ameliorates Endotoxemic Shock. *Blood* (2015) 125(12):1948–56. doi: 10.1182/blood-2014-07-587709
95. Cecconi M, Evans L, Levy M, Rhodes A. Sepsis and Septic Shock. *Lancet* (2018) 392(10141):75–87. doi: 10.1016/S0140-6736(18)30696-2
96. Colon DF, Wanderley CW, Franchin M, Silva CM, Hiroki CH, Castanheira FVS, et al. Neutrophil Extracellular Traps (NETs) Exacerbate Severity of Infant Sepsis. *Crit Care* (2019) 23(1):113. doi: 10.1186/s13054-019-2407-8
97. Biron BM, Chung CS, Chen Y, Wilson Z, Fallon EA, Reichner JS, et al. PAD4 Deficiency Leads to Decreased Organ Dysfunction and Improved Survival in a Dual Insult Model of Hemorrhagic Shock and Sepsis. *J Immunol* (2018) 200(5):1817–28. doi: 10.4049/jimmunol.1700639
98. Claushuis TAM, van der Donk LEH, Luitse AL, van Veen HA, van der Wel NN, van Vught LA, et al. Role of Peptidylarginine Deiminase 4 in Neutrophil Extracellular Trap Formation and Host Defense During Klebsiella Pneumoniae-Induced Pneumonia-Derived Sepsis. *J Immunol* (2018) 201 (4):1241–52. doi: 10.4049/jimmunol.1800314
99. Denning NL, Aziz M, Gurien SD, Wang P. DAMPs and NETs in Sepsis. *Front Immunol* (2019) 10:2536. doi: 10.3389/fimmu.2019.02536
100. Liang Y, Pan B, Alam HB, Deng Q, Wang Y, Chen E, et al. Inhibition of Peptidylarginine Deiminase Alleviates LPS-Induced Pulmonary Dysfunction and Improves Survival in a Mouse Model of Lethal Endotoxemia. *Eur J Pharmacol* (2018) 833:432–40. doi: 10.1016/j.ejphar.2018.07.005
101. Biron BM, Chung CS, O'Brien XM, Chen Y, Reichner JS, Ayala A. Cl-Amidine Prevents Histone 3 Citrullination and Neutrophil Extracellular Trap Formation, and Improves Survival in a Murine Sepsis Model. *J Innate Immun* (2017) 9(1):22–32. doi: 10.1159/000448808
102. Zhao T, Pan B, Alam HB, Liu B, Bronson RT, Deng Q, et al. Protective Effect of Cl-Amidine Against CLP-Induced Lethal Septic Shock in Mice. *Sci Rep* (2016) 6:36696. doi: 10.1038/srep36696
103. Tian Y, Qu S, Alam HB, Williams AM, Wu Z, Deng Q, et al. Peptidylarginine Deiminase 2 has Potential as Both a Biomarker and Therapeutic Target of Sepsis. *JCI Insight* (2020) 5(20):e138873. doi: 10.1172/jci.insight.138873
104. Yipp BG, Kubes P. NETosis: How Vital is it? *Blood* (2013) 122(16):2784–94. doi: 10.1182/blood-2013-04-457671
105. Deng Q, Pan B, Alam HB, Liang Y, Wu Z, Liu B, et al. Citrullinated Histone H3 as a Therapeutic Target for Endotoxic Shock in Mice. *Front Immunol* (2019) 10:2957. doi: 10.3389/fimmu.2019.02957
106. de Jong HK, Koh GC, Achouiti A, van der Meer AJ, Bulder I, Stephan F, et al. Neutrophil Extracellular Traps in the Host Defense Against Sepsis Induced by Burkholderia Pseudomallei (Melioidosis). *Intensive Care Med Exp* (2014) 2(1):21. doi: 10.1186/s40635-014-0021-2
107. Laukova L, Konecna B, Babickova J, Wagnerova A, Meliskova V, Vlkova B, et al. Exogenous Deoxyribonuclease has a Protective Effect in a Mouse Model of Sepsis. *BioMed Pharmacother* (2017) 93:8–16. doi: 10.1016/j.biopha.2017.06.009
108. Tian Y, Russo RM, Li Y, Karmakar M, Liu B, Puskarich MA, et al. Serum Citrullinated Histone H3 Concentrations Differentiate Patients With Septic Verses non-Septic Shock and Correlate With Disease Severity. *Infection* (2021) 49(1):83–93. doi: 10.1007/s15010-020-01528-y
109. Singer M, Deutschman CS, Seymour CW, Shankar-Hari M, Annane D, Bauer M, et al. The Third International Consensus Definitions for Sepsis and Septic Shock (Sepsis-3). *JAMA* (2016) 315(8):801–10. doi: 10.1001/jama.2016.0287
110. Rowland T, Hilliard H, Barlow G. Procalcitonin: Potential Role in Diagnosis and Management of Sepsis. *Adv Clin Chem* (2015) 68:71–86. doi: 10.1016/bs.acc.2014.11.005
111. Dewyer NA, El-Sayed OM, Luke CE, Elfline M, Kittan N, Allen R, et al. Divergent Effects of Tlr9 Deletion in Experimental Late Venous Thrombosis Resolution and Vein Wall Injury. *Thromb Haemost* (2015) 114(5):1028–37. doi: 10.1160/TH14-12-1031
112. Guertin MJ, Zhang X, Anguish L, Kim S, Varticovski L, Lis JT, et al. Targeted H3R26 Deimination Specifically Facilitates Estrogen Receptor Binding by Modifying Nucleosome Structure. *PLoS Genet* (2014) 10(9):e1004613. doi: 10.1371/journal.pgen.1004613
113. Mangan MSJ, Olhava EJ, Roush WR, Seidel HM, Glick GD, Latz E. Targeting the NLRP3 Inflammasome in Inflammatory Diseases. *Nat Rev Drug Discov* (2018) 17(8):588–606. doi: 10.1038/nrd.2018.97
114. Li Q, Cao Y, Dang C, Han B, Han R, Ma H, et al. Inhibition of Double-Strand DNA-Sensing cGAS Ameliorates Brain Injury After Ischemic Stroke. *EMBO Mol Med* (2020) 12(4):e11002.
115. Khakh BS, Burnstock G. The Double Life of ATP. *Sci Am* (2009) 301(6):84–90, 92. doi: 10.1038/scientificamerican1209-84
116. Seror C, Melki MT, Subra F, Raza SQ, Bras M, Saidi H, et al. Extracellular ATP Acts on P2Y2 Purinergic Receptors to Facilitate HIV-1 Infection. *J Exp Med* (2011) 208(9):1823–34. doi: 10.1084/jem.20101805
117. Basu M, Gupta P, Dutta A, Jana K, Ukil A. Increased Host ATP Efflux and its Conversion to Extracellular Adenosine is Crucial for Establishing Leishmania Infection. *J Cell Sci* (2020) 133(7):jcs239939. doi: 10.1242/jcs.239939
118. Gallucci S, Matzinger P. Danger Signals: SOS to the Immune System. *Curr Opin Immunol* (2001) 13(1):114–9. doi: 10.1016/S0952-7915(00)00191-6
119. Nolan LM, Cavaliere R, Turnbull L, Whitchurch CB. Extracellular ATP Inhibits Twitching Motility-Mediated Biofilm Expansion by Pseudomonas Aeruginosa. *BMC Microbiol* (2015) 15:55. doi: 10.1186/s12866-015-0392-x
120. Abbasian B, Shair A, O'Gorman DB, Pena-Diaz AM, Brennan L, Engelbrecht K, et al. Potential Role of Extracellular ATP Released by Bacteria in Bladder Infection and Contractility. *mSphere* (2019) 4(5):e00439–19. doi: 10.1128/mSphere.00439-19
121. Smolen JS, Aletaha D, McInnes IB. Rheumatoid Arthritis. *Lancet* (2016) 388 (10055):2023–38. doi: 10.1016/S0140-6736(16)30173-8
122. Van Steendam K, Tilleman K, Deforce D. The Relevance of Citrullinated Vimentin in the Production of Antibodies Against Citrullinated Proteins and the Pathogenesis of Rheumatoid Arthritis. *Rheumatol (Oxford)* (2011) 50 (5):830–7. doi: 10.1093/rheumatology/keq419
123. Jilani AA, Mackworth-Young CG. The Role of Citrullinated Protein Antibodies in Predicting Erosive Disease in Rheumatoid Arthritis: A Systematic Literature Review and Meta-Analysis. *Int J Rheumatol* (2015) 2015:728610. doi: 10.1155/2015/728610
124. de Vries-Bouwstra JK, Goekoop-Ruiterman YP, Verpoort KN, Schreuder GM, Ewals JA, Terwiel JP, et al. Progression of Joint Damage in Early Rheumatoid Arthritis: Association With HLA-DRB1, Rheumatoid Factor, and Anti-Citrullinated Protein Antibodies in Relation to Different Treatment Strategies. *Arthritis Rheum* (2008) 58(5):1293–8. doi: 10.1002/art.23439

125. Bugatti S, Manzo A, Montecucco C, Caporali R. The Clinical Value of Autoantibodies in Rheumatoid Arthritis. *Front Med (Lausanne)* (2018) 5:339. doi: 10.3389/fmed.2018.00339
126. Vander Cruyssen B, Peene I, Cantaert T, Hoffman IE, De Rycke L, Veys EM, et al. Anti-Citrullinated Protein/Peptide Antibodies (ACPA) in Rheumatoid Arthritis: Specificity and Relation With Rheumatoid Factor. *Autoimmun Rev* (2005) 4(7):468–74. doi: 10.1016/j.autrev.2005.04.018
127. Fuchs E, Weber K. Intermediate Filaments: Structure, Dynamics, Function, and Disease. *Annu Rev Biochem* (1994) 63:345–82. doi: 10.1146/annurev.bi.63.070194.002021
128. Kennedy A, Fearon U, Veale DJ, Godson C. Macrophages in Synovial Inflammation. *Front Immunol* (2011) 2:52. doi: 10.3389/fimmu.2011.00052
129. Davis MA, Fairgrieve MR, Den Hartigh A, Yakovenko O, Duvvuri B, Lood C, et al. Calpain Drives Pyroptotic Vimentin Cleavage, Intermediate Filament Loss, and Cell Rupture That Mediates Immunostimulation. *Proc Natl Acad Sci U S A* (2019) 116(11):5061–70. doi: 10.1073/pnas.1818598116
130. Holers VM. Autoimmunity to Citrullinated Proteins and the Initiation of Rheumatoid Arthritis. *Curr Opin Immunol* (2013) 25(6):728–35. doi: 10.1016/j.coi.2013.09.018
131. Derksen V, Huizinga TWJ, van der Woude D. The Role of Autoantibodies in the Pathophysiology of Rheumatoid Arthritis. *Semin Immunopathol* (2017) 39(4):437–46. doi: 10.1007/s00281-017-0627-z
132. McInnes IB, Schett G. The Pathogenesis of Rheumatoid Arthritis. *N Engl J Med* (2011) 365(23):2205–19. doi: 10.1056/NEJMra1004965
133. Li S, Yu Y, Yue Y, Zhang Z, Su K. Microbial Infection and Rheumatoid Arthritis. *J Clin Cell Immunol* (2013) 4(6):174. doi: 10.4172/2155-9899.1000174
134. Damgaard D, Senolt L, Nielsen MF, Pruijn GJ, Nielsen CH. Demonstration of Extracellular Peptidylarginine Deiminase (PAD) Activity in Synovial Fluid of Patients With Rheumatoid Arthritis Using a Novel Assay for Citrullination of Fibrinogen. *Arthritis Res Ther* (2014) 16(6):498. doi: 10.1186/s13075-014-0498-9
135. Damgaard D, Senolt L, Nielsen CH. Increased Levels of Peptidylarginine Deiminase 2 in Synovial Fluid From Anti-CCP-Positive Rheumatoid Arthritis Patients: Association With Disease Activity and Inflammatory Markers. *Rheumatol (Oxford)* (2016) 55(5):918–27. doi: 10.1093/rheumatology/kev440
136. Trombetta AC, Soldano S, Contini P, Tomatis V, Ruaro B, Paolino S, et al. A Circulating Cell Population Showing Both M1 and M2 Monocyte/Macrophage Surface Markers Characterizes Systemic Sclerosis Patients With Lung Involvement. *Respir Res* (2018) 19(1):186. doi: 10.1186/s12931-018-0891-z
137. Cutolo M, Trombetta AC, Soldano S. Monocyte and Macrophage Phenotypes: A Look Beyond Systemic Sclerosis. Response to: 'M1/M2 Polarisation State of M-CSF Blood-Derived Macrophages in Systemic Sclerosis' by Lescoat et al. *Ann Rheum Dis* (2019) 78(11):e128. doi: 10.1136/annrheumdis-2018-214371
138. Fukui S, Iwamoto N, Takatani A, Igawa T, Shimizu T, Umeda M, et al. M1 and M2 Monocytes in Rheumatoid Arthritis: A Contribution of Imbalance of M1/M2 Monocytes to Osteoclastogenesis. *Front Immunol* (2017) 8:1958. doi: 10.3389/fimmu.2017.01958
139. Eghbalzadeh K, Georgi L, Louis T, Zhao H, Keser U, Weber C, et al. Compromised Anti-Inflammatory Action of Neutrophil Extracellular Traps in PAD4-Deficient Mice Contributes to Aggravated Acute Inflammation After Myocardial Infarction. *Front Immunol* (2019) 10:2313. doi: 10.3389/fimmu.2019.02313
140. Katz Sand I. Classification, Diagnosis, and Differential Diagnosis of Multiple Sclerosis. *Curr Opin Neurol* (2015) 28(3):193–205. doi: 10.1097/WCO.0000000000000206
141. Oh J, Vidal-Jordana A, Montalban X. Multiple Sclerosis: Clinical Aspects. *Curr Opin Neurol* (2018) 31(6):752–9. doi: 10.1097/WCO.0000000000000622
142. Wood DD, Ackerley CA, Brand B, Zhang L, Raijmakers R, Mastronardi FG, et al. Myelin Localization of Peptidylarginine Deiminases 2 and 4: Comparison of PAD2 and PAD4 Activities. *Lab Invest* (2008) 88(4):354–64. doi: 10.1038/labinvest.3700748
143. Yang L, Tan D, Piao H. Myelin Basic Protein Citrullination in Multiple Sclerosis: A Potential Therapeutic Target for the Pathology. *Neurochem Res* (2016) 41(8):1845–56. doi: 10.1007/s11064-016-1920-2
144. Musse AA, Li Z, Ackerley CA, Bienzle D, Lei H, Poma R, et al. Peptidylarginine Deiminase 2 (PAD2) Overexpression in Transgenic Mice Leads to Myelin Loss in the Central Nervous System. *Dis Model Mech* (2008) 1(4-5):229–40. doi: 10.1242/dmm.000729
145. Tejeda EJC, Bello AM, Wasilewski E, Koebel A, Dunn S, Kotra LP. Noncovalent Protein Arginine Deiminase (PAD) Inhibitors Are Efficacious in Animal Models of Multiple Sclerosis. *J Med Chem* (2017) 60(21):8876–87. doi: 10.1021/acs.jmedchem.7b01102
146. Raijmakers R, Vogelzangs J, Raats J, Panzenbeck M, Corby M, Jiang H, et al. Experimental Autoimmune Encephalomyelitis Induction in Peptidylarginine Deiminase 2 Knockout Mice. *J Comp Neurol* (2006) 498(2):217–26. doi: 10.1002/cne.21055
147. Falcao AM, Meijer M, Scaglione A, Rinwa P, Agirre E, Liang J, et al. PAD2-Mediated Citrullination Contributes to Efficient Oligodendrocyte Differentiation and Myelination. *Cell Rep* (2019) 27(4):1090–102.e10. doi: 10.1016/j.celrep.2019.03.108
148. Mohanan S, Horibata S, Anguish LJ, Mukai C, Sams K, McElwee JL, et al. PAD2 Overexpression in Transgenic Mice Augments Malignancy and Tumor-Associated Inflammation in Chemically Initiated Skin Tumors. *Cell Tissue Res* (2017) 370(2):275–83. doi: 10.1007/s00441-017-2669-x
149. Qu Y, Olsen JR, Yuan X, Cheng PF, Levesque MP, Brokstad KA, et al. Small Molecule Promotes Beta-Catenin Citrullination and Inhibits Wnt Signaling in Cancer. *Nat Chem Biol* (2018) 14(1):94–101. doi: 10.1038/nchembio.2510
150. Uysal-Onganer P, MacLatchy A, Mahmoud R, Kraev I, Thompson PR, Inal JM, et al. Peptidylarginine Deiminase Isozyme-Specific PAD2, PAD3 and PAD4 Inhibitors Differentially Modulate Extracellular Vesicle Signatures and Cell Invasion in Two Glioblastoma Multiforme Cell Lines. *Int J Mol Sci* (2020) 21(4):1495. doi: 10.3390/ijms21041495
151. Kosgodage US, Uysal-Onganer P, MacLatchy A, Kraev I, Chatterton NP, Nicholas AP, et al. Peptidylarginine Deiminases Post-Translationally Deiminate Prohibitin and Modulate Extracellular Vesicle Release and MicroRNAs in Glioblastoma Multiforme. *Int J Mol Sci* (2018) 20(1):103. doi: 10.3390/ijms20010103
152. Sharma P, Lioutas A, Fernandez-Fuentes N, Quilez J, Carbonell-Caballero J, Wright RHG, et al. Arginine Citrullination at the C-Terminal Domain Controls RNA Polymerase II Transcription. *Mol Cell* (2019) 73(1):84–96.e7. doi: 10.1016/j.molcel.2018.10.016
153. McElwee JL, Mohanan S, Horibata S, Sams KL, Anguish LJ, McLean D, et al. PAD2 Overexpression in Transgenic Mice Promotes Spontaneous Skin Neoplasia. *Cancer Res* (2014) 74(21):6306–17. doi: 10.1158/0008-5472.CAN-14-0749
154. Li F, Miao L, Xue T, Qin H, Mondal S, Thompson PR, et al. Inhibiting PAD2 Enhances the Anti-Tumor Effect of Docetaxel in Tamoxifen-Resistant Breast Cancer Cells. *J Exp Clin Cancer Res* (2019) 38(1):414. doi: 10.1186/s13046-019-1404-8
155. Grilz E, Mauracher LM, Posch F, Konigsbrugge O, Zochbauer-Muller S, Marosi C, et al. Citrullinated Histone H3, a Biomarker for Neutrophil Extracellular Trap Formation, Predicts the Risk of Mortality in Patients With Cancer. *Br J Haematol* (2019) 186(2):311–20. doi: 10.1111/bjh.15906
156. Thalin C, Lundstrom S, Seignez C, Daleskog M, Lundstrom A, Henriksson P, et al. Citrullinated Histone H3 as a Novel Prognostic Blood Marker in Patients With Advanced Cancer. *PLoS One* (2018) 13(1):e0191231. doi: 10.1371/journal.pone.0191231

Conflict of Interest: The authors declare that the research was conducted in the absence of any commercial or financial relationships that could be construed as a potential conflict of interest.

Publisher's Note: All claims expressed in this article are solely those of the authors and do not necessarily represent those of their affiliated organizations, or those of the publisher, the editors and the reviewers. Any product that may be evaluated in this article, or claim that may be made by its manufacturer, is not guaranteed or endorsed by the publisher.

frontiers in Immunology

ORIGINAL RESEARCH
published: 17 November 2021
doi: 10.3389/fimmu.2021.766391

Circulating CitH3 Is a Reliable Diagnostic and Prognostic Biomarker of Septic Patients in Acute Pancreatitis

Baihong Pan, Yaozhen Li, Yu Liu, Wei Wang, Gengwen Huang* and Yang Ouyang**

Department of General Surgery, Xiangya Hospital, Central South University, Changsha, China

OPEN ACCESS

Edited by:
Wei Chong,
The First Affiliated Hospital of China Medical University, China

Reviewed by:
Weiqin Li,
Nanjing General Hospital of Nanjing Military Command, China
Jan Rossaint,
University of Münster, Germany

***Correspondence:**
Baihong Pan
pbh1990s@126.com
Gengwen Huang
gengwenhuang@outlook.com
Yang Ouyang
oyyking@126.com

Specialty section:
This article was submitted to Inflammation, a section of the journal Frontiers in Immunology

Received: *29 August 2021*
Accepted: *25 October 2021*
Published: *17 November 2021*

Citation:
Pan B, Li Y, Liu Y, Wang W, Huang G and Ouyang Y (2021) Circulating CitH3 Is a Reliable Diagnostic and Prognostic Biomarker of Septic Patients in Acute Pancreatitis. Front. Immunol. 12:766391. doi: 10.3389/fimmu.2021.766391

Purpose: Acute pancreatitis (AP) is an inflammatory disease. AP starts with sterile inflammation and is often complicated with critical local or systemic infection or sepsis in severe cases. Septic AP activates peptidyl arginine deiminase (PAD) and citrullinates histone H3 (CitH3), leading to neutrophil extracellular trap (NET) formation. Investigating the role of NETs and underlying mechanisms in septic AP may facilitate developing diagnostic and therapeutic approaches. In this study, we sought to identify the expression of CitH3 in septic AP patients and to analyze the correlation of CitH3 concentration with NET components as well as clinical outcomes.

Methods: Seventy AP patients with or without sepsis (40 septic cases, 30 nonseptic cases) and 30 healthy volunteers were recruited in this study. Concentration of NET components (CitH3 and double-strain DNA) and key enzymes (PAD2/4) were measured. Clinical and laboratory characteristics of patients were recorded and analyzed.

Results: Levels of CitH3 were elevated significantly in septic AP patients compared with those in nonseptic AP and healthy volunteers. The area under the curve (AUC, 95% confidence interval) for diagnosing septic AP was 0.93 (0.86–1.003), and the cutoff was 43.05 pg/ml. Among septic AP cases ($n = 40$), the concentration of CitH3 was significantly increased in those who did not survive or were admitted to the intensive care unit, when compared with that in those who survived or did not require intensive care unit. Association analysis revealed that CitH3 concentration was positively correlated with PAD2, PAD4, dsDNA concentration, and Sequential Organ Failure Assessment scores.

Conclusion: CitH3 concentration increased in septic AP patients and was closely correlated with disease severity and clinical outcomes. CitH3 may potentially be a diagnostic and prognostic biomarker of septic AP.

Keywords: acute pancreatitis, sepsis, citrullinated histone H3, peptidyl arginine deiminase, diagnosis, prognosis

1 INTRODUCTION

Acute pancreatitis (AP) is an inflammatory disease caused by digestive enzyme activation and self digestion (1). AP causes local or systemic sterile inflammation at early stages; however, up to 40%–70% of AP patients develop pancreatitis-related infection during the late stage or sepsis in severe cases (2). Sepsis is the leading cause of death in AP; thus, early diagnosis of septic AP and prompt initiation of treatments are the key to improving outcomes (3). Microbe culture is the gold standard to distinguish septic pancreatitis from sterile pancreatitis (4, 5), but the test is time consuming and can be unreliable because of false-positive and false-negative results. Identification of reliable circulating biomarkers to diagnose sepsis is therefore highly desirable. Procalcitonin (PCT) has been recognized as a promising sepsis biomarker and is widely used in the clinic (6). However, diagnostic efficacy of PCT is compromised significantly because of its nonspecificity (7). Therefore, novel strategies to identify key pathological signal pathways and improve the rapid diagnosis of septic AP are desperately needed.

Neutrophil extracellular traps (NETs) play a key role in the pathophysiology of septic AP. AP recruits and activates neutrophils, releasing nuclear and cytosolic components such as DNA, histones, and antimicrobial enzymes (8). This process is called NETosis (9). NETs combat infection in septic AP patients by trapping and killing invading microbes. However, recent studies revealed that NETs may also be involved in the pathogenesis of AP through inducing trypsin activation and promoting systemic inflammatory responses and tissue damage (10–13). Moritz et al. have reported in *Nature Communications* that NETs aggregate and occlude pancreatic ducts, driving pancreatitis. Excessive NETs exacerbate sepsis (14), while blockade of NETosis has been proven to ameliorate AP and improve outcomes (15–17).

Previous studies have proven that peptidylarginine deiminase (PAD) activation and downstream citrullination of histone H3 (CitH3) triggers NET formation (18, 19). Among PAD isoforms, PAD2/4 are mainly expressed in immune cells and are involved in the signaling pathway of infectious NETosis. Studies have shown that inhibition of PAD2 or PAD4 significantly decreases sepsis-induced NET formation (20, 21). PAD2/4 activation and CitH3 generation stimulate sepsis-specific gene expression and signaling transduction (22). We have proven that serum levels of CitH3 are increased significantly in both cecal ligation and puncture (CLP) and lipopolysaccharide (LPS)-induced septic mice but not in sterile inflammatory mice, and CitH3 may thus be a reliable diagnostic biomarker of sepsis (23, 24). Moreover, high levels of CitH3 in blood worsen sepsis, while clearance of CitH3 by anti-CitH3 antibodies can significantly improve survival of septic animals (25, 26) through attenuation of sepsis-induced acute lung injury and inflammatory cytokine cascade.

Investigating the pathogenic role of PADs and CitH3 in septic AP patients will facilitate the development of novel diagnostic biomarkers and therapeutic targets. In this study, we sought to measure the concentration of CitH3, to identify the correlation of CitH3 with PAD2/4, and to analyze the potential relationship between CitH3 levels and disease severity and outcomes.

2 MATERIAL AND METHODS

2.1 Enrollment of Study Objects

Forty septic AP patients (SP), 30 noninfectious AP patients (NIP), and 30 healthy volunteers (HV) who were admitted into Xiangya Hospital, Central South University were enrolled in this study. Patients in the SP group were adults who were diagnosed with AP (3) and met the consensus definition for sepsis: confirmed infection (positive microbe culture of peripheral blood or peripancreatic tissue); two or more systemic inflammatory response criteria; and organ dysfunction (27). NIP adult controls were diagnosed with AP for less than 72 h without any sign of infection (fever, radiological sign of peripancreas infection, and negative microbe culture). HV were ambulatory age- and sex-matched adults who had no chronic medical problems or any medications. All procedures were approved by the Institute Review Board of Xiangya Hospital, Central South University. Patients were informed, and consent forms were obtained for research purposes. Clinical data were collected at the time of confirmation of septic or noninfectious AP. Sixty-day survival rates were determined through follow-up study.

2.2 Blood Sample Analysis

Blood samples from the SP group were collected at the time when AP patients met the sepsis criteria. Blood samples from the NIP group were collected when AP was confirmed for less than 72 h without signs of infection. Samples were processed by trained researchers and were stored at −80°C until the time of assay.

Quantification of CitH3 was performed by an enzyme-linked immunosorbent assay (ELISA) that we developed previously (23). In brief, anti-CitH3 monoclonal antibody raised by CitH3 peptides (R2+R8+R17+R26, 30 amino acids) (25) was coated onto 96-well plates as capture antibody and was then blocked by protein-free blocking buffer (Thermo Scientific, Rockford, IL, USA). Blood samples or CitH3 peptide (R2+R8+R17+R26) were incubated in the wells for 2 h, followed by incubation with rabbit anti-CitH3 polyclonal antibody (Abcam, Cambridge, MA, USA). Next, 96-well plates were probed with antirabbit horseradish peroxidase (HRP)-conjugated IgG (Jackson Immuno-Research, West Grove, PA, USA). 3,3′,5,5′-Tetramethylbenzidine (TMB, Thermo Fisheer Scientific, Waltham, MA, USA) was added into wells and incubated for 20 min at room temperature in the dark before adding stop solution (R&D Systems Inc., Minneapolis, MN, USA).

PAD2 and PAD4 were measured using commercial ELISA kits (PAD2, #501450, Cayman Chemical, Ann Arbor, MI, USA; PAD4, #501460, Cayman Chemical). NET-associated double-stranded DNA (dsDNA) was quantified by a PicoGreen assay kit (Invitrogen, San Diego, CA, USA). All procedures were performed in accordance with the manufacturer's instructions.

2.3 Clinical and Laboratory Data Collection

Clinical and laboratory data including age, sex, hospital stay, intensive care unit (ICU) stay, lactate, and PCT were obtained during hospitalization. Sequential organ failure assessment (SOFA) score and its components were recorded based on laboratory results at the same time as blood sample collection (27).

2.4 Statistical Analysis

Categorical values were presented as numbers (percentages), and continuous variables were presented as means (standard deviations) or medians (interquartile ranges). One-way analysis followed by Bonferroni's multiple comparison test was performed for comparison between three or more groups. The Mann-Whitney *U* test was performed for comparisons between two groups. Receiver operating characteristic curves (ROC) were used to identify the diagnostic and prognostic efficacy of CitH3 and PCT. Optimal cutoff values were determined when the Youden index (sensitivity + specificity − 1) was maximized. Correlation between CitH3 and PAD2, PAD4, dsDNA, and SOFA scores were determined by Pearson's regression model. Analyses were performed with GraphPad Prism 7 (GraphPad Software Inc., La Jolla, CA, USA). $p < 0.05$ was defined as statistically significant.

3 RESULTS

3.1 Baseline Characteristics

A total of 100 individuals were enrolled in this study, including 40 septic AP patients, 30 noninfectious AP patients and 30 healthy volunteers (SP, NIP, and HV groups, respectively) from Xiangya Hospital, Central South University. Baseline characteristics are presented in **Table 1** (**Supplementary Materials**).

No significant difference in age and sex were observed between SP, NIP, and HV groups. However, patients in the SP group experienced increased levels of lactate, prolonged hospital and ICU stay, and decreased survival rate. Furthermore, patients in the SP group experienced higher SOFA score (total, respiratory, renal, cardiovascular, neurologic, hepatic, and coagulation SOFA), which suggested that the SP group suffered more severe multiple organ failure.

3.2 Serum CitH3 as a Diagnostic Biomarker of Septic AP Patients

As mentioned, severe AP patients often are complicated with local or systemic infection at late stages. On set of sepsis usually indicates poor outcome. Thus, early diagnosis of sepsis in AP patients is of significant value. In this study, levels of CitH3 were dramatically increased in SP patients compared with both HV and NIP groups (**Figure 1A**) [median (interquartile range): SP 127.3 pg/ml (82.4–210.2), NIP 27.5 pg/ml (21–33.5), HV 26 pg/ml (22.5–35.5); $p < 0.0001$ for SP vs. NIP, $p = 0.001$ for SP vs. HV]. No significant difference was observed between HV and NIP groups. This suggests that CitH3 may distinguish septic AP cases from nonseptic AP cases.

Clinically, PCT is a widely used biomarker for diagnosing infection. Comparison study of PCT and CitH3 were conducted to evaluate the diagnostic value of CitH3. As shown in **Figure 1B**, no significant change in PCT concentration was observed among HV, NIP, and SP groups. Furthermore, ROC curve analysis was conducted in both PCT and CitH3. When comparing HV and SP groups (**Figure 1C**), the areas under the curves (AUCs) and 95% confidence interval (CI) for CitH3 and PCT were 0.94 (0.86–1.02) and 0.92 (0.84–0.99), respectively ($p < 0.0001$). When comparing NIP and SP groups (**Figure 1D**), AUCs (95% CI) for CitH3 and PCT were 0.93 (0.86–1.003) and 0.50 (0.36–0.64), respectively ($p < 0.0001$). This suggests that CitH3 exerts better diagnostic power compared with PCT, especially in distinguishing septic AP patients from noninfectious AP suffers.

Based on the Youden index, CitH3 concentration above 43.05 pg/ml was suggestive of sepsis in AP patients compared with that in HV and NIP patients (**Figure 1E**).

3.3 Serum CitH3 as a Prognostic Biomarker of Septic AP Patients

Survival rate, admittance to the ICU, and SOFA score are the hallmarks of prognosis. All SP AP patients were subgrouped into survival ($n = 33$) and death ($n = 7$) groups or non-ICU ($n = 31$) and ICU ($n = 9$) groups.

3.3.1 Survival Group vs. Death Group

Levels of CitH3 were also increased dramatically in dead cases compared with those in the survival group (**Figure 2A**) ($p = 0.0024$). ROC curve analysis revealed that the AUC (95% CI) was 0.85 (69.29–101.3) when comparing survival and death groups (**Figure 2B**). The cutoff value was 120.1 pg/ml, which suggested that SP patients with CitH3 above 120.1 pg/ml may experience poorer outcome than those with CitH3 lower than 120.1 pg/ml (**Figure 2E**).

3.3.2 Non-ICU Group vs. ICU Group

Levels of CitH3 were also increased dramatically in cases who were admitted to the ICU compared with those in cases who did not require intensive care (**Figure 2C**) ($p = 0.0006$) (**Figure 2E**). ROC curve analysis showed that the AUC (95% CI) was 0.86 (73.55–98.14) when comparing non-ICU and ICU groups (**Figure 2D**). The cutoff value was 129.1 pg/ml, suggesting that septic AP patients with CitH3 above 129.1 pg/ml may suffer a higher possibility of being admitted to the ICU than those with CitH3 lower than 129.1 pg/ml (**Figure 2E**).

3.3.3 SOFA Score

Total SOFA score comprises respiratory, cardiovascular, renal, coagulation, hepatic, and neurologic scores and is a widely used tool for quick assessment of organ dysfunction (28). The higher the score, the more severe the organ dysfunction. Positive correlations were found between CitH3 concentration and total SOFA score ($r = 0.599$, $p < 0.0001$), respiratory SOFA score ($r = 0.569$, $p < 0.0001$), renal SOFA score ($r = 0.437$, $p = 0.0048$), coagulation SOFA score ($r = 0.614$, $p < 0.0001$), and hepatic SOFA score ($r = 0.334$, $p = 0.035$) (**Figures 3A–E**). No obvious correlation was observed between CitH3 concentration and

TABLE 1 | Baseline demographics and clinical characteristics for septic AP patients and noninfectious AP patients.

Variables	SP (*n* = 40)	NIP (*n* = 30)	HV (*n* = 30)	*p*-value
Age (mean (SD))	47.3 (12.37)	55.8 (10.76)	50.9	>0.05
Female (*n* (%))	8 (20)	8 (26.7)	9 (30)	>0.05
PCT (ng/ml, median (IQR))	0.43 (0.17–0.99)	0.27 (0.2–0.8)	0 (0–0.08)	>0.05
Lactate (mmol/L, median (IQR))	2 (1.8–2.4)	1.6 (1.3–1.9)		<0.05
CitH3 (pg/ml, median (IQR))	127.3 (82.4–210.2)	27.5 (21–33.5)	26.5 (20.5–39.75)	<0.05
PAD2 (ng/ml, median (IQR))	3.03 (2.1–3.68)	0.32 (0.21–0.49)	0.16 (0.1–0.26)	<0.05
PAD4 (ng/ml, median (IQR))	3.11 (2.53–4.71)	0.28 (0.14–0.51)	0.12 (0.07–0.21)	<0.05
dsDNA (ng/ml, median (IQR))	913.5 (812–1063)	257 (232.5–294)	89 (65–100)	<0.05
Survivals (*n* (%))	33 (82.5)	30 (100)		<0.05
Length of hospital stay (day, median (IQR))	28.5 (20.8–57)	13.5 (11.3–16.8)		<0.05
Length of ICU stay (day, median (IQR))	4 (1–7.25)	0 (0–0)		<0.05
Total SOFA score (median (IQR))	5 (3–8)	1 (1–2)		<0.05
Respiratory SOFA (median (IQR))	2 (2–3)	1 (1–2)		<0.05
Renal SOFA (median (IQR))	1 (0–3)	0 (0–0)		<0.05
Cardiovascular SOFA (median (IQR))	0 (0–0)	0 (0–0)		<0.05
Neurologic SOFA (median (IQR))	0 (0–0)	0 (0–0)		<0.05
Hepatic SOFA (median (IQR))	1 (0–1)	0 (0–0)		<0.05
Coagulation SOFA (median (IQR))	0 (0–1)	0 (0–0)		<0.05

Categorical variables are shown as number (%). For continuous variables, normally distributed values are shown as mean (SD) while not normally distributed are shown as median (interquartile range Q1/Q3). AP, acute pancreatitis; PCT, procalcitonin; CitH3, citrullinated histone H3; PAD2/4, peptidylarginine deiminase 2/4; ICU, intensive care unit; SOFA, sequential organ failure assessment.

cardiovascular SOFA score (r = 0.225, p = 0.1677), and neurologic SOFA score (r = 0.092, p = 0.57) (**Figures 3F, G**).

3.4 Correlation of Serum CitH3 With NETosis Pathway Components

As mentioned above, CitH3 mainly originates from NETosis. PAD2/4 activation followed by CitH3 and dsDNA complex release is the key mechanism. As shown in **Figures 4A, C, E**, concentration of PAD2, PAD4, and dsDNA were significantly increased in the SP group compared with those in the NIP group and HV groups ($p < 0.05$). Correlation analysis revealed that that serum CitH3 concentration was positively correlated with PAD2, PAD4, and dsDNA [(r = 0.5756, p = 0.0001), (r = 0.3935, p = 0.012), (r = 0.5591, p = 0.0002), respectively] (**Figures 4B, D, E**). These data strongly suggest that elevated serum CitH3 may be released by netting neutrophils in septic AP patients.

4 DISCUSSION

Sepsis is a severe complication in the late stage of AP and accounts for majority of fatal AP cases. Thus, early diagnosis of septic AP and prompt initiation of treatments are essential for improving prognosis. We have previously shown that serum CitH3 is a reliable diagnostic biomarker for sepsis in a murine model (23), and clearance of CitH3 by enzymatic inhibition or antibody neutralization improves survival in septic mice (21, 25). The goal of the current study was to identify whether the diagnostic efficacy of CitH3 for sepsis was conserved in humans. Furthermore, we planned to determine whether the elevated CitH3 concentration in humans is originated from NETosis, because this has been confirmed many times in rodent models. In this study, we found that (1) circulating CitH3 was increased dramatically in septic AP but not in sterile AP or healthy subjects; (2) concentration of CitH3 was positively correlated with PAD2/PAD4 expression and serum dsDNA concentration; (3) serum levels of CitH3 correlated positively with disease severity and clinical outcomes. Therefore, CitH3 may represent a diagnostic and prognostic biomarker of septic AP, mediating the pathogenesis of sepsis in AP.

Neutrophils are the most abundant leukocytes and have been confirmed as the frontline of host immune defense. Classical mechanisms of killing invasive microbes include phagocytosis, degranulation, and reactive oxygen species. Recently, however, a novel antimicrobe strategy—NETosis—was discovered by Brinkmann et al. (9). When stimulated by invading microbes, neutrophils release NETs, a net-like structure consisting of DNA, histones (particularly CitH3), and granule proteins inside neutrophils. NET can trap pathogens by histones and various antipathogen proteinases. Excessive NET formation, however, has been shown to be related to tissue damage, organ dysfunction, and poor outcome in different diseases. Studies have suggested that NETs mediate pathogenesis of AP, and clearance of NETs alleviates pancreatic injury and exerts protective effects (8, 12). Our data further supported these findings. We found that NET components such as CitH3 and dsDNA were increased significantly in septic AP and were closely correlated with disease severity. Furthermore, the positive association between CitH3 and PAD2/4 revealed that elevated CitH3 may be caused by NETosis in septic AP patients.

NETosis is generally associated with activation of PADs and histone citrullination. It has been well documented that only PAD2 and PAD4 isoforms are expressed in immune cells and can translocate into the nucleus to citrullinate histones, while the crucial role of PAD4 in NETosis has been illustrated by plenty of researchers (18, 29, 30). However, whether PAD2 can promote NETosis remains unclear. Recently, Li et al. (31, 32) published two papers suggesting that PAD2 also participates in

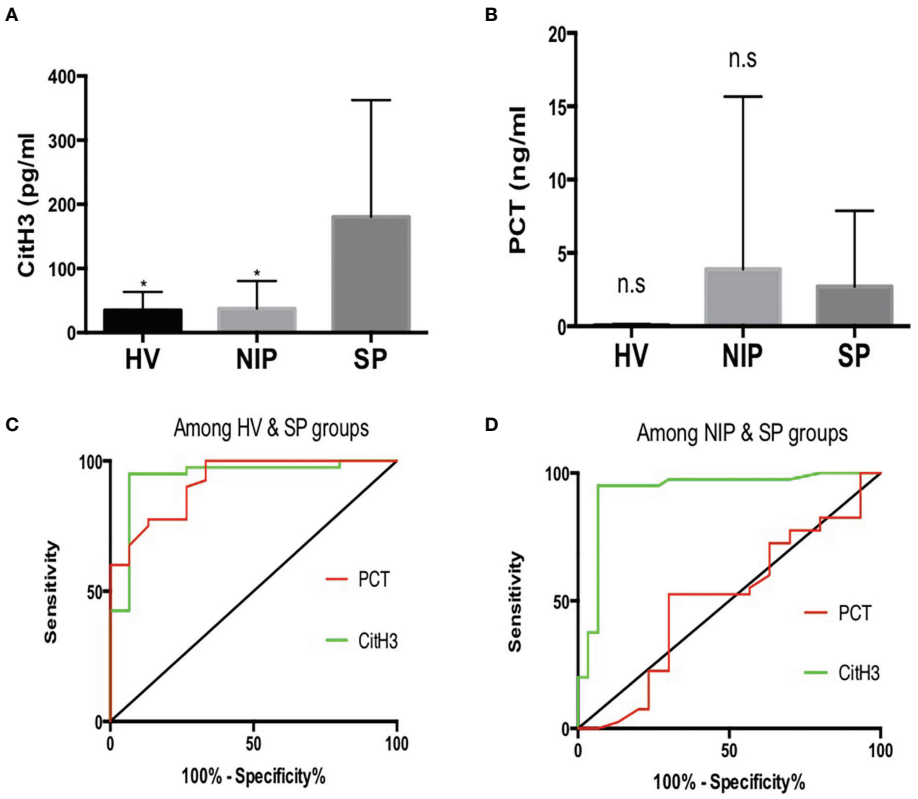

E

Groups	HV vs SP	NIP vs SP
CitH3		
AUC (95% CI)	0.94 (0.86-1.02)	0.93 (0.86-1.003)
Cut-off value (pg/ml)	43.05	43.05
Sensitivity % (95% CI)	95 (83.08-99.39)	95 (83.08-99.39)
Specificity % (95% CI)	93.33 (68.05-99.83)	93.33 (77.93-99.18)
PCT		
AUC (95% CI)	0.92 (0.84-0.99)	0.50 (0.36-0.64)
p	< 0.05	< 0.05

FIGURE 1 | All CitH3 concentration is elevated in septic AP patients and may be a reliable diagnostic biomarker of sepsis in AP. Blood samples from SP, NIP, and HV groups were collected. CitH3 and PCT concentration were measured by ELISA kit. CitH3 concentration was increased significantly in the SP group compared with that in the HV and NIP groups **(A)**. No significant differences in PCT concentration were identified among SP, NIP, and HV groups **(B)**. Receiver operating characteristic curves analysis of CitH3 and PCT to diagnose septic AP compared with that of the HV **(C)** and NIP group **(D)**. Detailed information of receiver operating characteristic curve analysis is presented in the table **(E)**. *$p < 0.05$; ns, non-significant.

NETosis and PAD2 blockade significantly improves survival of septic mice. In the present study, we also found that increased levels of CitH3 positively correlated with PAD2 concentration ($r = 0.5756$). Furthermore, concentration of CitH3 positively correlates with the severity of septic AP. Collectively, we believe that PAD2/4 activation leads to excessive CitH3/NETs release in septic AP patients, thus deteriorating the outcomes.

The most crucial characteristic of a diagnostic biomarker is specificity. As previously described, nonspecificity to sepsis is the

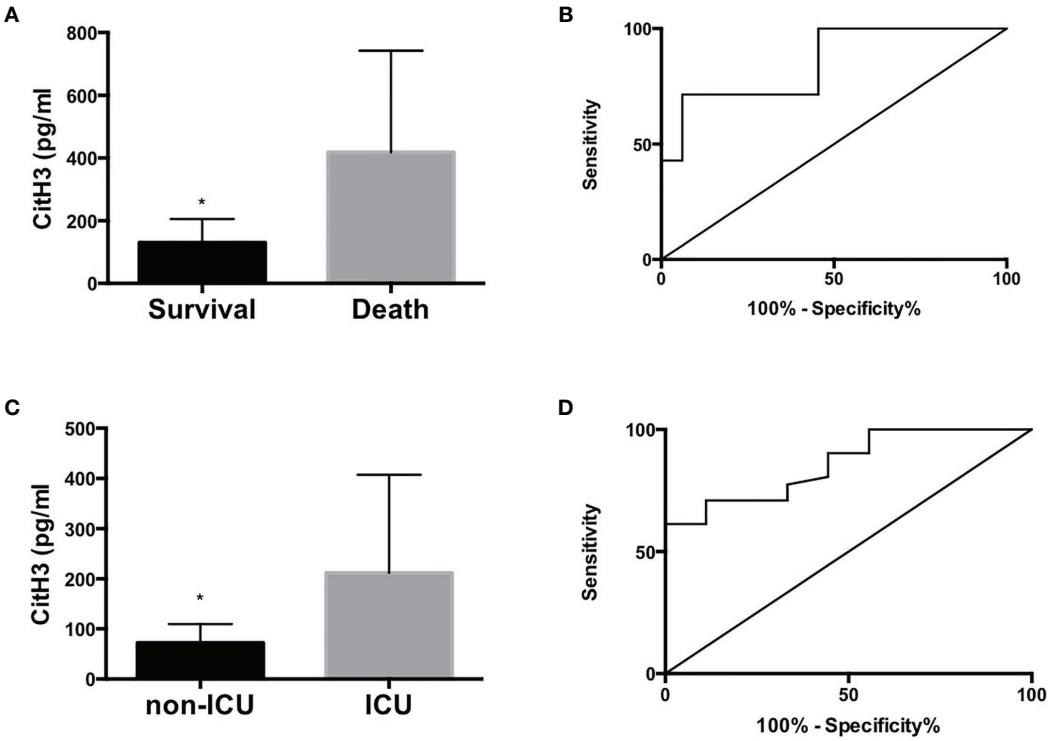

E

Groups	Survival vs Death	Non-ICU vs ICU
CitH3		
AUC (95% CI)	0.85 (69.29-101.3)	0.86 (73.55-98.14)
Cut-off value (pg/ml)	120.1	129.1
Sensitivity % (95% CI)	100 (59.04-100)	61.29 (42.19-78.15)
Specificity % (95% CI)	54.55 (36.35-71.89)	100 (66.37-100)
p	< 0.05	< 0.05

FIGURE 2 | All CitH3 may be a promising prognostic biomarker in septic AP patients. AP patients were subgrouped into survival and death groups **(A)** or ICU (cases admitted into ICU) and non-ICU (cases not admitted into ICU) groups **(C)**. Concentration of CitH3 was measured by ELISA. Levels of CitH3 were increased significantly in the death group and ICU group compared with those in survival group and non-ICU group, respectively. Receiver operating characteristic curve analysis of CitH3 to distinguish survival and death cases **(B)** and cases admitted or not into ICU **(D)**. The detailed information of receiver operating characteristic curve analysis is presented in the table **(E)**. *$p < 0.05$.

major weakness of PCT (7). In this study, we also found that PCT was not specific to sepsis. The concentration of PCT increased not only in the SP group but also in the NIP group without a statistically significant difference (**Figure 1B**). Based on our data, CitH3 may be a more reliable diagnostic biomarker of sepsis compared with PCT. Lactate is widely measured in clinical situations and is a helpful indicator of disease severity and outcome. However, lactate is a response to various acute diseases (myocardial infarction, trauma, shock, etc.) and fails to be specific to sepsis. As shown in **Table 1**, patients in both SP and NIP groups experienced increased lactate concentrations.

This study has several limitations. For most cases, concentration of CitH3 was only identified at the time of diagnosis. Periodical measurement of CitH3 levels may be

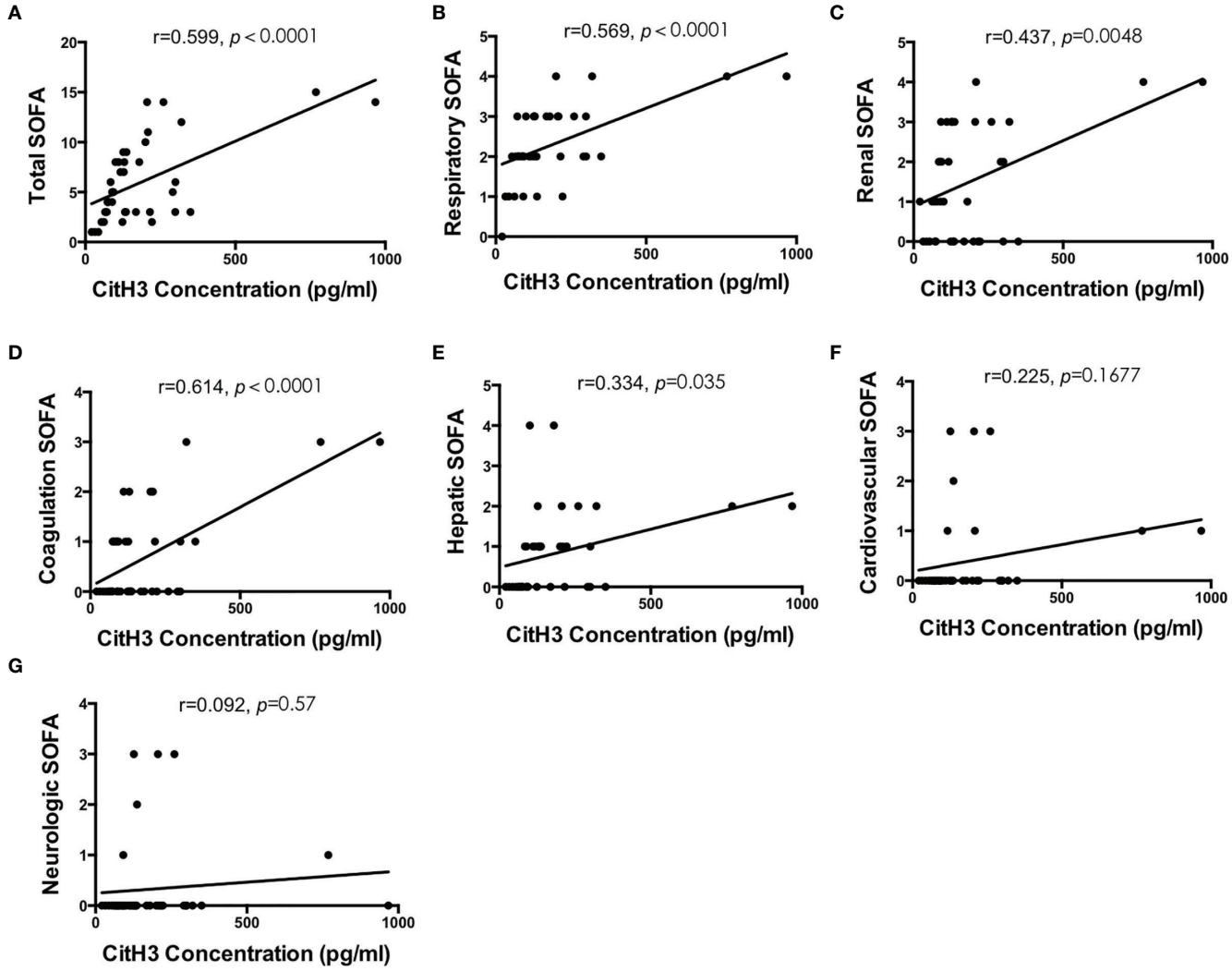

FIGURE 3 | Blood concentration of CitH3 is positively correlated with SOFA score. Association between CitH3 concentration and total SOFA **(A)**, respiratory SOFA **(B)**, renal SOFA **(C)**, coagulation SOFA **(D)**, hepatic SOFA **(E)**, cardiovascular SOFA **(F)**, and neurologic SOFA **(G)** score was determined by *Pearson's regression* analysis.

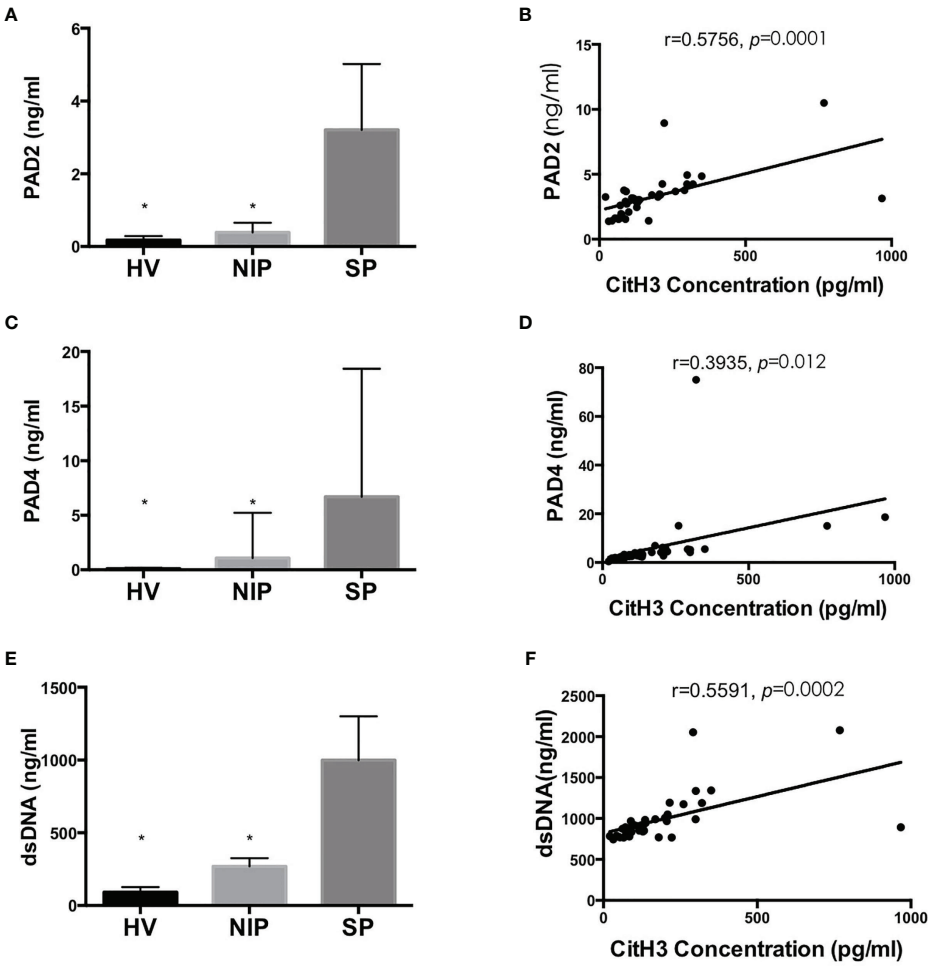

FIGURE 4 | Blood concentration of PAD2/4 and dsDNA is increased significantly in SP group and is positively correlated with CitH3 concentration. Levels of PAD2 **(A)**, PAD4 **(C)**, and dsDNA **(E)** were using commercialized kits. Association between CitH3 concentration and PAD2 **(B)**, PAD4 **(D)**, and dsDNA **(F)** were determined by *Pearson's regression* analysis $*p < 0.05$.

more informative of clinical course and responses to treatments. Tracking of CitH3 changes during hospitalization may more accurately reflect the diagnostic efficacy of CitH3. Additionally, this study only showed clinical data and no animal models were involved. More detailed experiments using animal models to illustrate the presence of NETs may be more convincing. Future studies should be performed to determine whether PAD2/4-CitH3 pathway could be a therapeutic target for septic AP.

In conclusion, this clinical study demonstrates that serum CitH3 increases in septic but not in sterile AP patients. Increased levels of CitH3 are closely correlated with disease severity and clinical outcomes. Association study of CitH3 and PAD2/4 further revealed that circulating CitH3 may originate from septic AP-induced NETs. Overall, serum CitH3 may be a reliable diagnostic and prognostic biomarker of septic AP. Understanding the mechanistic role of the PAD-CitH3 pathway in the pathogenesis of septic AP may facilitate the development of novel diagnostic and therapeutic approaches.

DATA AVAILABILITY STATEMENT

The original contributions presented in the study are included in the article/**Supplementary Material**. Further inquiries can be directed to the corresponding authors.

ETHICS STATEMENT

The studies involving human participants were reviewed and approved by the Institute Review Board of Xiangya Hospital, Central South University. The patients/participants provided their written informed consent to participate in this study.

AUTHOR CONTRIBUTIONS

BP, GH, and YO designed the study. BP, YZL, and YL performed the experiments and interpreted the data. BP wrote the

manuscript, which was critically revised by WW and YO. BP and YO acquired the funding. All authors contributed to the article and approved the submitted version.

FUNDING

This work was funded by grants from Young Research Funding of Xiangya Hospital, Central South University (2019Q10) and the National and Science Foundation of Hunan Province (2020JJ4902).

SUPPLEMENTARY MATERIAL

The Supplementary Material for this article can be found online at: https://www.frontiersin.org/articles/10.3389/fimmu.2021.766391/full#supplementary-material

REFERENCES

1. Frey CF, Zhou H, Harvey DJ, White RH. The Incidence and Case-Fatality Rates of Acute Biliary, Alcoholic, and Idiopathic Pancreatitis in California, 1994-2001. *Pancreas* (2006) 33(4):336–44. doi: 10.1097/01.mpa.0000236727.16370.99
2. Susak YM, Dirda OO, Fedorchuk OG, Tkachenko OA, Skivka LM. Infectious Complications of Acute Pancreatitis Is Associated With Peripheral Blood Phagocyte Functional Exhaustion. *Digestive Dis Sci* (2021) 66(1):121–30. doi: 10.1007/s10620-020-06172-y
3. Frossard JL, Steer ML, Pastor CM. Acute Pancreatitis. *Lancet* (2008) 371 (9607):143–52. doi: 10.1016/S0140-6736(08)60107-5
4. Leppkes M, Maueroder C, Hirth S, Nowecki S, Gunther C, Billmeier U, et al. Externalized Decondensed Neutrophil Chromatin Occludes Pancreatic Ducts and Drives Pancreatitis. *Nat Commun* (2016) 7:10973. doi: 10.1038/ncomms10973
5. Werner J, Feuerbach S, Uhl W, Buchler MW. Management of Acute Pancreatitis: From Surgery to Interventional Intensive Care. *Gut* (2005) 54 (3):426–36. doi: 10.1136/gut.2003.035907
6. Stearns-Kurosawa DJ, Osuchowski MF, Valentine C, Kurosawa S, Remick DG. The Pathogenesis of Sepsis. *Annu Rev Pathol: Mech Dis* (2011) 6:19–48. doi: 10.1146/annurev-pathol-011110-130327
7. Kibe S, Adams K, Barlow G. Diagnostic and Prognostic Biomarkers of Sepsis in Critical Care. *J Antimicrobial Chemotherapy* (2011) 66:Ii33–40. doi: 10.1093/jac/dkq523
8. Madhi R, Rahman M, Taha D, Morgelin M, Thorlacius H. Targeting Peptidylarginine Deiminase Reduces Neutrophil Extracellular Trap Formation and Tissue Injury in Severe Acute Pancreatitis. *J Cell Physiol* (2019) 234(7):11850–60. doi: 10.1002/jcp.27874
9. Brinkmann V, Reichard U, Goosmann C, Fauler B, Uhlemann Y, Weiss DS, et al. Neutrophil Extracellular Traps Kill Bacteria. *Science* (2004) 303 (5663):1532–5. doi: 10.1126/science.1092385
10. Merza M, Hartman H, Rahman M, Hwaiz R, Zhang E, Renstrom E, et al. Neutrophil Extracellular Traps Induce Trypsin ActivationInflammation, and Tissue Damage in Mice With Severe Acute Pancreatitis. *Gastroenterology* (2015) 149(7):1920–31.e8. doi: 10.1053/j.gastro.2015.08.026
11. Bilyy R, Fedorov V, Vovk V, Leppkes M, Dumych T, Chopyak V, et al. Neutrophil Extracellular Traps Form a Barrier Between Necrotic and Viable Areas in Acute Abdominal Inflammation. *Front Immunol* (2016) 7:424. doi: 10.3389/fimmu.2016.00424
12. Korhonen JT, Dudeja V, Dawra R, Kubes P, Saluja A. Neutrophil Extracellular Traps Provide a Grip on the Enigmatic Pathogenesis of Acute Pancreatitis. *Gastroenterology* (2015) 149(7):1682–5. doi: 10.1053/j.gastro.2015.10.027
13. Yang ZW, Meng XX, Xu P. Central Role of Neutrophil in the Pathogenesis of Severe Acute Pancreatitis. *J Cell Mol Med* (2015) 19(11):2513–20. doi: 10.1111/jcmm.12639
14. Clark SR, Ma AC, Tavener SA, McDonald B, Goodarzi Z, Kelly MM, et al. Platelet TLR4 Activates Neutrophil Extracellular Traps to Ensnare Bacteria in Septic Blood. *Nat Med* (2007) 13(4):463–9. doi: 10.1038/nm1565
15. Murthy P, Singhi AD, Ross MA, Loughran P, Paragomi P, Papachristou GI, et al. Enhanced Neutrophil Extracellular Trap Formation in Acute Pancreatitis Contributes to Disease Severity and Is Reduced by Chloroquine. *Front Immunol* (2019) 10:28. doi: 10.3389/fimmu.2019.00028
16. Wu Z, Lu G, Zhang L, Ke L, Yuan C, Ma N, et al. Protectin D1 Decreases Pancreatitis Severity in Mice by Inhibiting Neutrophil Extracellular Trap Formation. *Int Immunopharmacol* (2021) 94:107486. doi: 10.1016/j.intimp.2021.107486
17. Hu J, Kang HX, Chen H, Yao JQ, Yi XL, Tang WF, et al. Targeting Neutrophil Extracellular Traps in Severe Acute Pancreatitis Treatment. *Ther Adv Gastroenterol* (2020) 13:1756284820974913. doi: 10.1177/1756284820974913
18. Wang Y, Li M, Stadler S, Correll S, Li P, Wang D, et al. Histone Hypercitrullination Mediates Chromatin Decondensation and Neutrophil Extracellular Trap Formation. *J Cell Biol* (2009) 184(2):205–13. doi: 10.1083/jcb.200806072
19. Neeli I, Khan SN, Radic M. Histone Deimination as a Response to Inflammatory Stimuli in Neutrophils. *J Immunol* (2008) 180(3):1895–902. doi: 10.4049/jimmunol.180.3.1895
20. Liang Y, Pan B, Alam HB, Deng Q, Wang Y, Chen E, et al. Inhibition of Peptidylarginine Deiminase Alleviates LPS-Induced Pulmonary Dysfunction and Improves Survival in a Mouse Model of Lethal Endotoxemia. *Eur J Pharmacol* (2018) 833:432–40. doi: 10.1016/j.ejphar.2018.07.005
21. Zhao T, Pan B, Alam HB, Liu B, Bronson RT, Deng Q, et al. Protective Effect of Cl-Amidine Against CLP-Induced Lethal Septic Shock in Mice. *Sci Rep* (2016) 6:36696. doi: 10.1038/srep36696
22. Clancy KW, Russell AM, Subramanian V, Nguyen H, Qian Y, Campbell RM, et al. Citrullination/Methylation Crosstalk on Histone H3 Regulates ER-Target Gene Transcription. *ACS Chem Biol* (2017) 12(6):1691–702. doi: 10.1021/acschembio.7b00241
23. Pan B, Alam HB, Chong W, Mobley J, Liu B, Deng Q, et al. CitH3: A Reliable Blood Biomarker for Diagnosis and Treatment of Endotoxic Shock. *Sci Rep* (2017) 7(1):8972. doi: 10.1038/s41598-017-09337-4
24. Park Y, Ryu B, Deng Q, Pan B, Song Y, Tian Y, et al. An Integrated Plasmo-Photoelectronic Nanostructure Biosensor Detects an Infection Biomarker Accompanying Cell Death in Neutrophils. *Small* (2020) 16(1):e1905611. doi: 10.1002/smll.201905611
25. Deng Q, Pan B, Alam HB, Liang Y, Wu Z, Liu B, et al. Citrullinated Histone H3 as a Therapeutic Target for Endotoxic Shock in Mice. *Front Immunol* (2019) 10:2957. doi: 10.3389/fimmu.2019.02957
26. Li Y, Liu Z, Liu B, Zhao T, Chong W, Wang Y, et al. Citrullinated Histone H3: A Novel Target for the Treatment of Sepsis. *Surgery* (2014) 156(2):229–34. doi: 10.1016/j.surg.2014.04.009
27. Singer M, Deutschman CS, Seymour CW, Shankar-Hari M, Annane D, Bauer M, et al. The Third International Consensus Definitions for Sepsis and Septic Shock (Sepsis-3). *JAMA* (2016) 315(8):801–10. doi: 10.1001/jama.2016.0287
28. Vincent JL, de Mendonca A, Cantraine F, Moreno R, Takala J, Suter PM, et al. Use of the SOFA Score to Assess the Incidence of Organ Dysfunction/Failure in Intensive Care Units: Results of a Multicenter, Prospective Study. Working Group on "Sepsis-Related Problems" of the European Society of Intensive Care Medicine. *Crit Care Med* (1998) 26(11):1793–800. doi: 10.1097/00003246-199811000-00016
29. Li P, Li M, Lindberg MR, Kennett MJ, Xiong N, Wang Y. PAD4 is Essential for Antibacterial Innate Immunity Mediated by Neutrophil Extracellular Traps. *J Exp Med* (2010) 207(9):1853–62. doi: 10.1084/jem.20100239
30. Rohrbach AS, Slade DJ, Thompson PR, Mowen KA. Activation of PAD4 in NET Formation. *Front Immunol* (2012) 3:360. doi: 10.3389/fimmu.2012.00360
31. Tian Y, Qu S, Alam HB, Williams AM, Wu Z, Deng Q, et al. Peptidylarginine Deiminase 2 has Potential as Both a Biomarker and Therapeutic Target of Sepsis. *JCI Insight* (2020) 5(20):e138873. doi: 10.1172/jci.insight.138873

32. Wu Z, Deng Q, Pan B, Alam HB, Tian Y, Bhatti UF, et al. Inhibition of PAD2 Improves Survival in a Mouse Model of Lethal LPS-Induced Endotoxic Shock. *Inflammation* (2020) 43(4):1436–45. doi: 10.1007/s10753-020-01221-0

Conflict of Interest: The authors declare that the research was conducted in the absence of any commercial or financial relationships that could be construed as a potential conflict of interest.

Publisher's Note: All claims expressed in this article are solely those of the authors and do not necessarily represent those of their affiliated organizations, or those of the publisher, the editors and the reviewers. Any product that may be evaluated in this article, or claim that may be made by its manufacturer, is not guaranteed or endorsed by the publisher.

frontiers in Immunology

ORIGINAL RESEARCH
published: 25 November 2021
doi: 10.3389/fimmu.2021.700933

miR-221-5p-Mediated Downregulation of JNK2 Aggravates Acute Lung Injury

Jing Yang[1], Hanh Chi Do-Umehara[1†], Qiao Zhang[2], Huashan Wang[1], Changchun Hou[1], Huali Dong[1], Edith A. Perez[1], Marc A. Sala[2], Kishore R. Anekalla[2], James M. Walter[2], Shuwen Liu[3,4], Richard G. Wunderink[2,5], G.R. Scott Budinger[2] and Jing Liu[1]*

[1] Department of Surgery, College of Medicine and University of Illinois Cancer Center, University of Illinois at Chicago, Chicago, IL, United States, [2] Division of Pulmonary and Critical Care Medicine, Department of Medicine, Feinberg School of Medicine, Northwestern University, Chicago, IL, United States, [3] Guangdong Provincial Key Laboratory of New Drug Screening, School of Pharmaceutical Sciences, Southern Medical University, Guangzhou, China, [4] State Key Laboratory of Organ Failure Research, Southern Medical University, Guangzhou, China, [5] Simpson Querrey Institute for Epigenetics, Feinberg School of Medicine, Northwestern University, Chicago, IL, United States

Sepsis and acute lung injury (ALI) are linked to mitochondrial dysfunction; however, the underlying mechanism remains elusive. We previously reported that c-Jun N-terminal protein kinase 2 (JNK2) promotes stress-induced mitophagy by targeting small mitochondrial alternative reading frame (smARF) for ubiquitin-mediated proteasomal degradation, thereby preventing mitochondrial dysfunction and restraining inflammasome activation. Here we report that loss of JNK2 exacerbates lung inflammation and injury during sepsis and ALI in mice. JNK2 is downregulated in mice with endotoxic shock or ALI, concomitantly correlated inversely with disease severity. Small RNA sequencing revealed that miR-221-5p, which contains seed sequence matching to JNK2 mRNA 3' untranslated region (3'UTR), is upregulated in response to lipopolysaccharide, with dynamically inverse correlation with JNK2 mRNA levels. miR-221-5p targets the 3'UTR of JNK2 mRNA leading to its downregulation. Accordingly, miR-221-5p exacerbates lung inflammation and injury during sepsis in mice by targeting JNK2. Importantly, in patients with pneumonia in medical intensive care unit, JNK2 mRNA levels in alveolar macrophages flow sorted from non-bronchoscopic broncholaveolar lavage (BAL) fluid were inversely correlated strongly and significantly with the percentage of neutrophils, neutrophil and white blood cell counts in BAL fluid. Our data suggest that miR-221-5p targets JNK2 and thereby aggravates lung inflammation and injury during sepsis.

Keywords: JNK2, sepsis, lung inflammation and injury, micro RNA (miRNA), smARF, ubiquitination and degradation, mitochondrial dysfunction

OPEN ACCESS

Edited by:
Yongqing Li,
University of Michigan, United States

Reviewed by:
Hagir Suliman,
Duke University, United States
Fen Liu,
The First Affiliated Hospital of Nanchang University, China

****Correspondence:***
Jing Liu
jinglius@uic.edu

†Present address:
Hanh Chi Do-Umehara, Division of Pulmonary and Critical Care Medicine, Department of Medicine, Feinberg School of Medicine, Northwestern University, Chicago, IL, United States

Specialty section:
This article was submitted to Inflammation, a section of the journal Frontiers in Immunology

Received: *27 April 2021*
Accepted: *13 September 2021*
Published: *25 November 2021*

Citation:
Yang J, Do-Umehara HC, Zhang Q, Wang H, Hou C, Dong H, Perez EA, Sala MA, Anekalla KR, Walter JM, Liu S, Wunderink RG, Budinger GRS and Liu J (2021) miR-221-5p-Mediated Downregulation of JNK2 Aggravates Acute Lung Injury. Front. Immunol. 12:700933. doi: 10.3389/fimmu.2021.700933

INTRODUCTION

Severe sepsis, a constellation of clinical signs of systemic inflammation combined with multiple organ dysfunction, is an important cause of death in the United States and the most common cause of death in medical ICUs (1–4). While improved primary source controls, which are primarily driven by early pathogen identification, appropriate antibiotic and organ supportive therapy, have reduced the incidence of multiple organ dysfunction and mortality from sepsis, the underlying pathobiology of sepsis remains poorly understood, and specific therapies to treat patients with sepsis are not available.

Acute lung injury (ALI) or acute respiratory distress syndrome (ARDS) secondary to sepsis is one of the leading causes of death in sepsis. ARDS, the most severe form of ALI, is a clinical syndrome defined by the acute onset of arterial hypoxemia refractory to low flow oxygen therapy and bilateral infiltrates on radiography (5–10). It is estimated that the incidence of ARDS is about 78.9/100,000 in the United States with a mortality rate of 40% (5–10). Even in those who survive ARDS, there is evidence that their long-term quality of life is unfavorably affected (5–10). Despite improvements in processes of care, including mechanical ventilation, fluid management, and other supportive care measures, the mortality from ARDS remains high (5–10), and specific and effective therapies are not available (5–10).

Sepsis and ARDS are linked to mitochondrial dysfunction, and mitochondrial defects have been extensively described in human subjects with sepsis- or severe pneumonia-associated ARDS as well as in animal models of ARDS (11–15). An established body of literature supports an association between mitochondrial damage and dysfunction and sepsis severity in murine models and in patients with sepsis (11, 12, 16–19). However, how sepsis and ARDS are linked to mitochondrial impair is not understood on the molecular level. Mitochondrial autophagy (mitophagy) is a selective form of autophagy that removes damaged mitochondria, thereby serving as an important mechanism of mitochondrial quality control (20, 21). Defective mitophagy results in accumulation of damaged mitochondria, which produce excessive mitochondrial reactive oxygen species (ROS) and release mitochondrial damage-associated molecular patterns (DAMPs) including damaged mitochondrial DNA (mtDNA) fragments into the cytoplasm (intracellular) and circulation (extracellular) that activate toll-like receptor 9 (TLR9) and the NLR family pyrin domain containing 3 (NLRP3) (previously known as NACHT, LRR and PYD domains-containing protein 3 [NALP3] and cryopyrin) inflammasome leading to excessive reactive species generation and exaggerated immune response (20–26). Accumulating evidence demonstrate dysregulated mitophagy in epithelial type II cells (AT2) and alveolar macrophages (AMs) in sepsis and severe acute lung injury (ALI)/ARDS in human subjects and animal models (27–30). Pharmacological and genetic manipulation of proteins involved in mitophagy has been reported to influence the outcomes in animal models of sepsis and ARDS (27–29, 31). However, the mechanisms underlying the deregulation of mitophagy and their functional significance in sepsis-induced ARDS remain largely unknown.

The c-Jun N-terminal protein kinase (JNK) is activated by environmental stresses to coordinate a host of fundamental cellular responses (32–35). JNK has two ubiquitously expressed isoforms, JNK1 and JNK2, which are highly homologous to each other (32–35). We and others have reported that JNK1 is the main JNK isoform activated by canonical JNK agonists while JNK2 activity is negligible and therefore most of the studies have been focused on JNK1 while the biological functions of JNK2 have been largely overlooked (35). We recently reported that JNK2 promotes stress-induced mitophagy independently of its kinase activity by targeting small mitochondrial ARF (smARF) for ubiquitin-mediated proteasomal degradation, thereby preventing mitochondrial dysfunction and restraining inflammasome activation (36). smARF is a short isoform of the tumor suppressor ARF that is translated from an internal initiation site Met45 and localizes exclusively to mitochondria (37–40). We reported that the loss of JNK2 led to accumulation of smARF, which in turn induced mitochondrial depolarization and excessive mitophagic and autophagic activity, resulting in lysosomal degradation of the mitophagy adaptor proteins, including p62 in the steady state. The depletion of p62 and other key components in the mitophagy machinery prevented the cells from mounting appropriate mitophagy in response to subsequent stress, leading to inflammasome hyperactivation and increased mortality during endotoxin shock (36). Here we report that the microRNA (miRNA) miR-221-5p targets JNK2 and thereby aggravates lung inflammation and injury during sepsis. Together with our previous report that JNK2 prevents mitochondrial dysfunction, our study might provide a potential mechanism for the well-documented association between mitochondrial dysfunction and sepsis.

RESULTS

Loss of JNK2, but Not JNK1, Aggravates Lung Inflammation and Injury in Mouse Model of LPS-Induced Acute Lung Injury

Sepsis is often associated with multiple organ dysfunction caused by dysregulation of host response to infection (1–4). The lung is among the most vulnerable and critical organs during sepsis, with acute lung injury (ALI) or ARDS being a common sepsis-induced inflammatory disorder (5–10). LPS, a component of Gram-negative bacterial endotoxin, is the main cause of ALI. We previously reported that loss of JNK2 rendered mice more susceptible to endotoxin-induced septic shock (36). We sought to determine the effect of JNK1 or JNK2 deficiency on lung inflammation and injury in mouse model of LPS-induced ALI. Wild-type, JNK1 KO or JNK2 KO mice were treated intratracheally with LPS, and we observed that the protein content was higher in the bronchoalveolar lavage (BAL) fluid of LPS-treated JNK2 KO mice compared to that in LPS-treated wild-type mice (**Figure 1A**), while it was not different between LPS-treated wild-type and JNK1 KO mice (**Supplementary Figure 1A**). The production of the potent inflammatory cytokine, MCP-1 (monocyte chemoattractant protein 1), was drastically augmented in the BAL

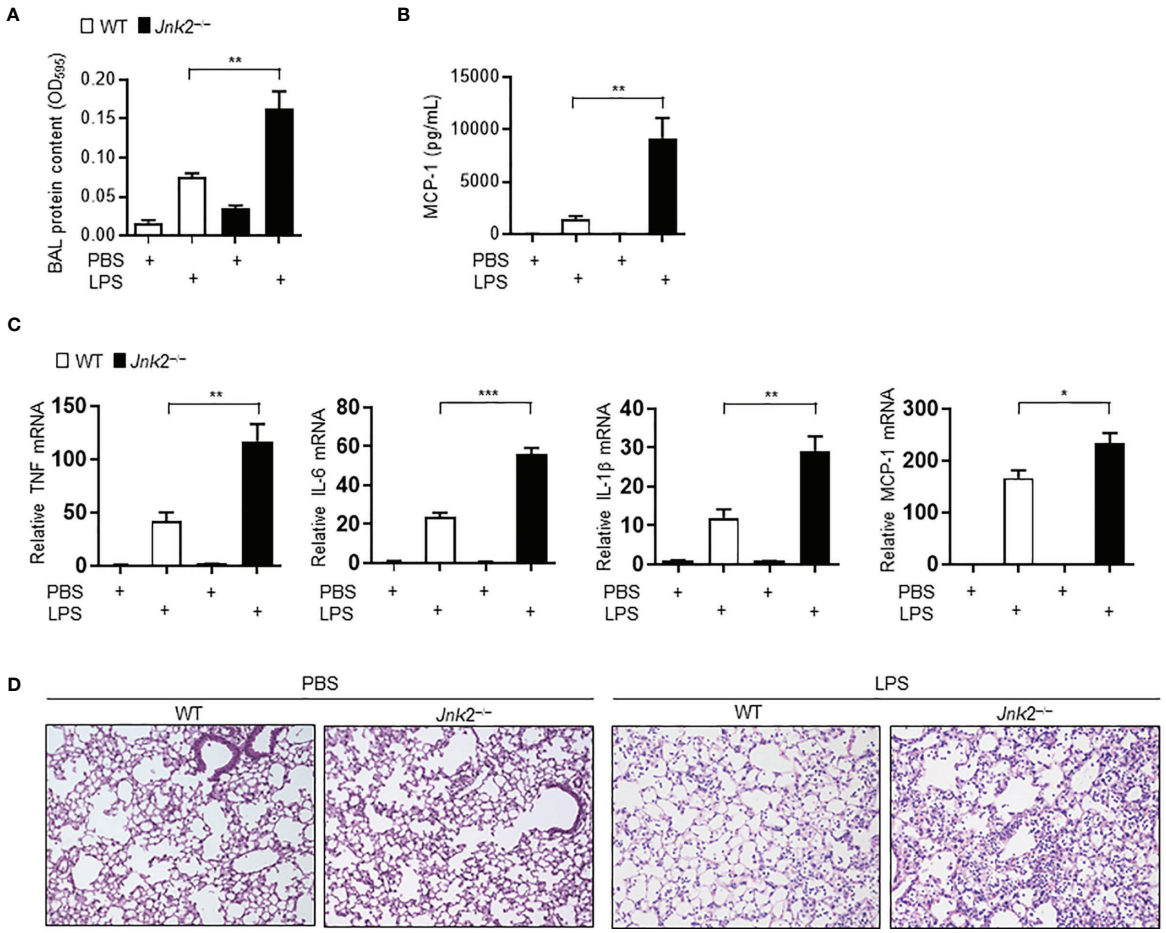

FIGURE 1 | Loss of JNK2 aggravates lung inflammation and injury in mouse model of LPS-induced acute lung injury. Wild-type and JNK2 KO mice were subjected to i.t. LPS-induced ALI. Two days later, mice were harvested. **(A, B)** Protein content **(A)** and production of MCP-1 **(B)** in the BAL fluid. PBS: N=3-6. LPS: N=5-6. **(C)** mRNA expressions of inflammatory cytokines in whole lung homogenates as indicated. N=4. **(D)** Sectional lung histology from PBS- or LPS-treated wild-type and JNK2 KO mice. Data are presented as means ± sem. $^{*}p < 0.05$; $^{**}p < 0.01$; $^{***}p < 0.001$.

fluid of LPS-treated JNK2 KO mice compared to LPS-treated wild-type mice (**Figure 1B**), while it was not different between LPS-treated wild-type and JNK1 KO (**Supplementary Figure 1B**). The mRNA expressions of inflammatory cytokines in the lung, including tumor necrosis factor (TNF), interleukin 6 (IL-6), IL-1β, and monocyte chemoattractant protein-1 (MCP-1), were also enhanced in LPS-treated JNK2 KO mice compared to LPS-treated wild-type mice (**Figure 1C**). On the other hand, there were no statistically significant differences in the production of TNF, interferon gamma (IFN-γ), IL-12p70, IL-6, or IL-10 in the BAL fluid of LPS-treated wild-type and JNK1 KO mice (**Supplementary Figure 1B**). Lung histology showed that the lungs from LPS-treated JNK2 KO had increased lung inflammation and injury, including increased inflammatory cell infiltration and thickening of the alveolar septa, as compared to LPS-treated wild-type mice (**Figure 1D**). Together, these data suggest that loss of JNK2, but not JNK1, exacerbates LPS-induced lung inflammation and injury in mice.

Loss of JNK2 Worsens Lung Inflammation and Injury During *Pseudomonas* Pneumonia

To further validate our conclusion that JNK2 deficiency exacerbates LPS-induced lung inflammation and injury, wild-type or JNK2 KO mice were intranasally infected with *Pseudomonas aeruginosa* (*P. aeruginosa*; strain PA103), a Gram-negative bacterium that produces the major virulence factor LPS. JNK2 KO mice had higher mortality compared to wild-type mice in response to PA103 infection (mice that did not die within 72 h recovered and survived; **Figure 2A**). The cell count and protein content were higher in the BAL fluid of PA103-treated JNK2 KO mice compared to that in PA103-treated wild-type mice (**Figure 2B**). Neutrophils are the major subset of infiltrating inflammatory cells in the lung in murine *Pseudomonas aeruginosa* pneumonia. We observed that neutrophil count in the BAL fluid was higher in PA103-treated JNK2 KO mice compared to PA103-treated wild-type

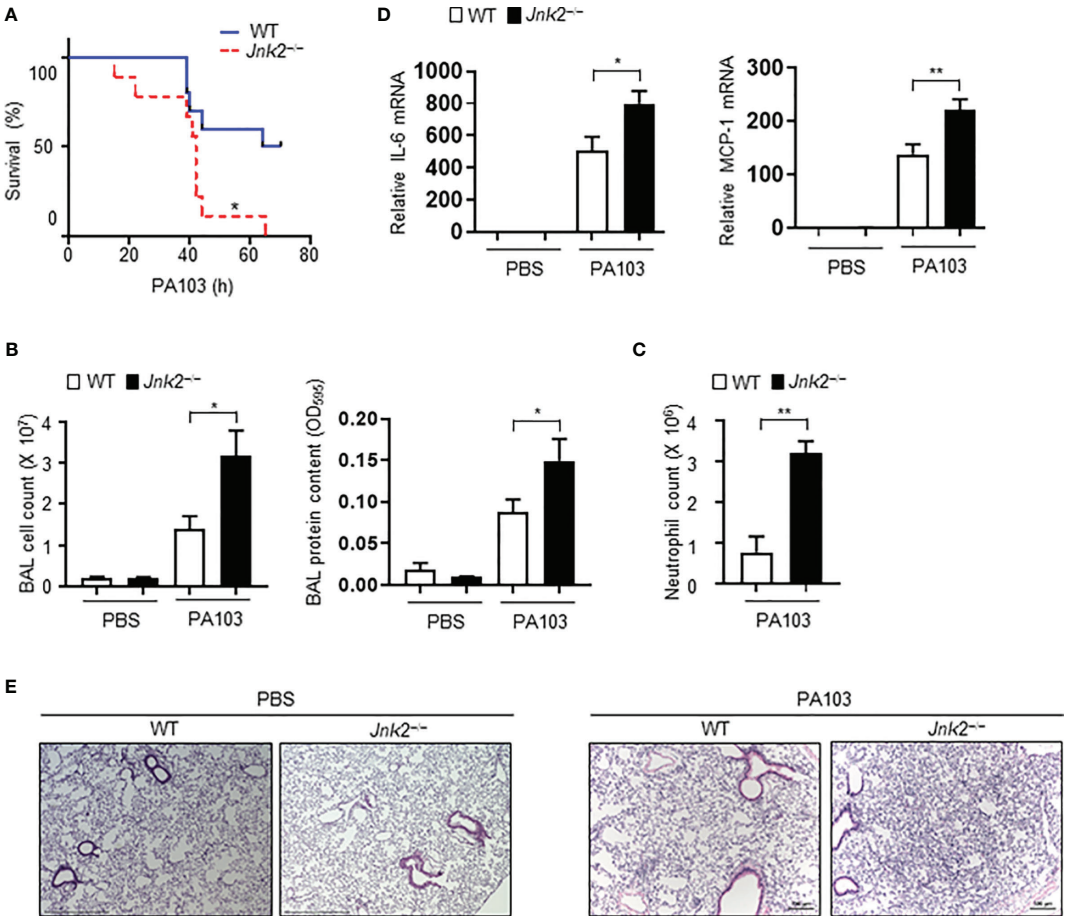

FIGURE 2 | Loss of JNK2 worsens lung inflammation and injury during *pseudomonas* pneumonia. Wild-type and JNK2 KO mice were subjected to i.n. *pseudomonas aeruginosa* (strain PA103)-induced pneumonia. **(A)** Mortality of PA103-treated wild-type and JNK2 KO mice. N=9-10. **(B–E)** Cell count and protein content **(B)** and neutrophil count **(C)** in BAL fluid, and mRNA expressions of inflammatory cytokines from whole lung homogenates **(D)**, or sectional lung histology **(E)** from PBS- or PA103-treated mice. In **(B)**, PBS: N=3-8; PA103: N=13-14. In **(C)**, N=3-4. In **(D)**, PBS: N=3; PA103: N=4-5. Data are presented as means ± sem. $^{*}p < 0.05$; $^{**}p < 0.01$.

mice (**Figure 2C**). mRNA levels of inflammatory cytokines, including IL-6 and MCP-1, were higher in PA103-treated JNK2 KO mice compared to PA103-treated wild-type mice (**Figure 2D**). Accordingly, histological examination revealed increased lung inflammation and injury, including increased inflammatory cell infiltration and thickening of the alveolar septa, in PA103-treated JNK2 KO mice compared to PA103-treated wild-type mice (**Figure 2E**). These data further support our conclusion that loss of JNK2 worsens lung inflammation and injury.

JNK2 Deficiency Aggravates Lung Inflammation and Injury in Cecal Ligation and Puncture-Induced Sepsis

Cecal ligation and puncture (CLP) is a widely used animal model of sepsis. We investigated whether JNK2 deficiency affects CLP-associated lung inflammation and injury. Indeed, lung histology showed increased lung inflammation and injury in CLP-treated JNK2 KO mice compared to CLP-treated wild-type mice, including increased inflammatory cell infiltration and thickening of the alveolar septa (**Figure 3A**). CLP-treated JNK2 KO mice also had increased expression of inflammatory cytokines, including MCP-1 and keratinocytes-derived chemokine (KC) in the lung compared to CLP-treated wild-type mice (**Figure 3B**). These data suggest that JNK2 deletion worsens CLP-associated lung inflammation and injury.

JNK2 mRNA Levels Are Negatively Correlated With Disease Severity During Sepsis

We were wondering whether JNK2 expression is subjected to regulation during endotoxin-induced septic shock. We observed that in mild endotoxic shock induced by intraperitoneal (i.p.) LPS (lower dose 12 mg/kg, which is non-lethal dose), JNK2 mRNA and protein levels in the lung were first decreased at 8-12 h after LPS treatment, and then increased and returned to

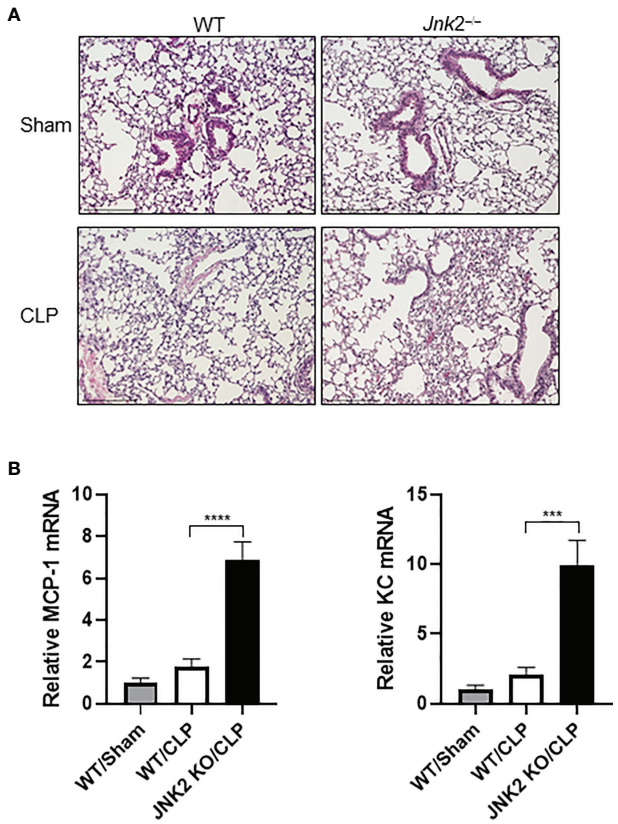

FIGURE 3 | JNK2 deficiency augments lung inflammation and injury in CLP-induced sepsis. **(A)** Sectional lung histology of sham- or CLP-treated wild-type and JNK2 KO mice. **(B)** mRNA expressions of MCP-1 and KC from whole lung homogenates of sham-treated wild type mice or CLP-treated wild-type and JNK2 KO mice. N=3. Data are presented as means ± sem. ***$p < 0.001$; ****$p < 0.0001$.

baseline levels after 24 h (**Figures 4A, B**). Similar results were obtained in the other organs including liver, heart, and colon (**Figure 4A**). However, in severe septic shock (higher dose LPS 35mg/kg, which is lethal dose), JNK2 remained at lower levels and did not increase back at 24 h after the treatment (**Figures 4C, D**). We did not observe statistically significant decrease in JNK1 expression in the lung, colon, or liver under the same conditions (**Supplementary Figures 2A–C**). In contrast, JNK1 mRNA levels in the colon were modesty increased after LPS treatment (**Supplementary Figure 2B**). These data indicate the specific downregulation of JNK2 during septic shock.

JNK2 mRNA Levels Are Negatively Correlated With Lung Injury Severity During *Pseudomonas* Pneumonia

We observed that in response to intranasal *P. aeruginosa*, JNK2 mRNA levels in the wild-type mouse lungs were decreased at 4 h (**Figure 5A**), correlated with a robust induction of pro-inflammatory cytokines, including IL-6, TNF, and MCP-1 (**Figure 5B**), as well as lung inflammation and injury (**Figure 5C**). JNK2 mRNA levels were then increased at 16 h, returned to basal levels at 72 h, and were higher than baseline levels at day 7 (**Figure 5A**), correlated with a gradual decrease in pro-inflammatory cytokine expression (**Figure 5B**) and recovery from lung injury (**Figure 5C**). These data suggest that JNK2 mRNA levels are negatively correlated with lung injury severity during *pseudomonas* pneumonia.

JNK2 mRNA Levels Are Also Negatively Correlated With Lung Injury Severity in LPS-Induced ALI Model

Similar to *P. aeruginosa*-induced ALI model, JNK2 mRNA levels in the wild-type mouse lungs were also decreased at 4 h after intratracheal LPS treatment (**Figure 6A**), correlated with a robust induction of pro-inflammatory cytokines, including MCP-1, IL-6, TNF, and IL-1β (**Figure 6A**). JNK2 mRNA levels were then increased at 8 h, and returned to basal levels after 16 h (**Figure 6A**), correlated with a gradual decrease in pro-inflammatory cytokine expression (**Figure 6A**). To identify the lung cell types in which JNK2 is downregulated by LPS, we isolated primary alveolar type 2 (AT2) cells and alveolar macrophages (AMs) by flow sorting as we previously reported (41) from PBS- and intratracheal LPS-treated mice (**Figure 6B**; left panel). We observed that JNK2 is downregulated in both AT2 cells and AMs by LPS (**Figure 6B**; middle and right panels).

Small RNA Sequencing Revealed That miR-221-5p Is Upregulated in Response to LPS *In Vitro*, Resulting in JNK2 Downregulation

To investigate the mechanism by which JNK2 is downregulated by LPS, murine macrophage RAW 264.7 cells were treated with LPS (10 ng/ml) or *P.* aeruginosa (PA103, 20 multiplicity of infection). We observed that the mRNA levels of JNK2, but not JNK1, were decreased at 2-6 h after LPS treatment, then started to increase at 8 h and returned to baseline levels at 12 h in RAW 264.7 cells (**Figure 7A** and **Supplementary Figure 3A**). JNK2 mRNA levels were also reduced at 2-6 h after PA103 treatment in RAW 264.7 cells (**Figure 7B**). In human macrophages differentiated from human monocytic cell line THP-1 stimulated with phorbol-12-myristate-13-acetate (42), the mRNA levels of JNK2, but not JNK1, were also decreased at 4-6 h after LPS treatment, and then increased at 8 h, which were negatively associated with the induction of IL-6 dynamically (**Figure 7C** and **Supplementary Figures 3B, C**). To determine whether LPS-induced downregulation of JNK2 was due to reduced mRNA stability, RAW 264.7 cells were treated with LPS in the presence of RNA synthesis inhibitor actinomycin D (2 μM). LPS resulted in accelerated mRNA degradation rate of JNK2, but not JNK1, in the presence of actinomycin D (**Supplementary Figure 3D**). MicroRNAs (miRNAs) are small noncoding RNAs that interact with 3′-untranslated region (3'UTR) of target mRNAs leading to mRNA degradation and/or translational repression. Small RNA sequencing of LPS-treated RAW 264.7 cells revealed differentially expressed miRNAs by LPS (**Figure 7D** and

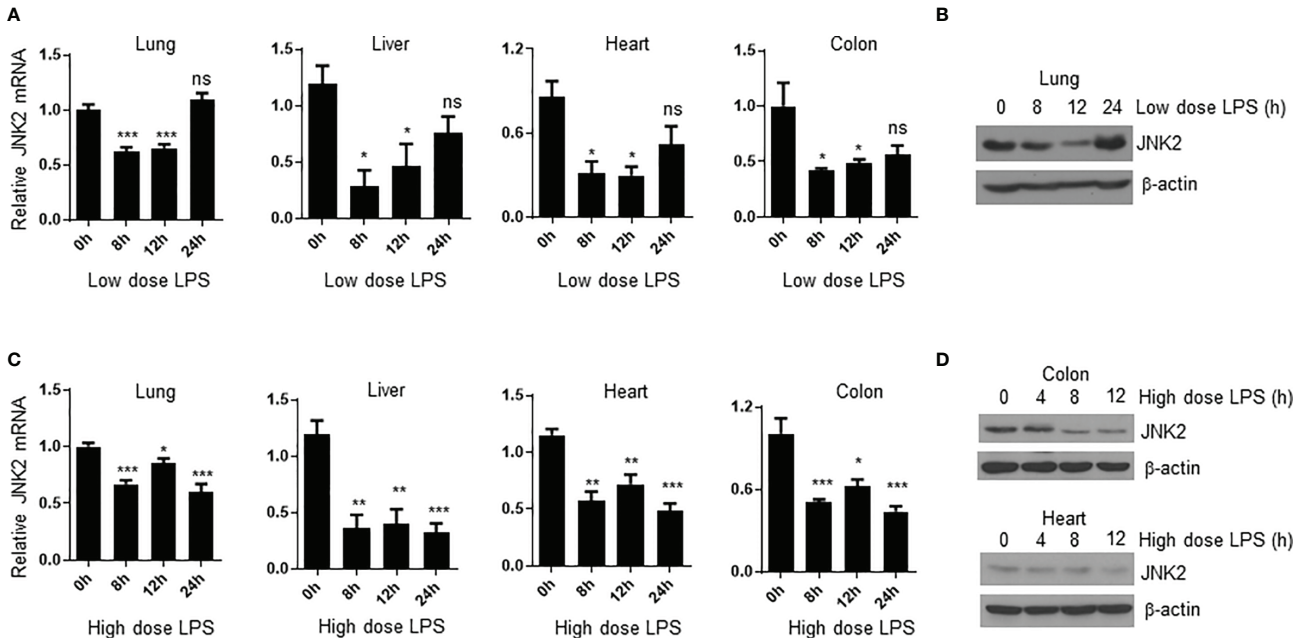

FIGURE 4 | JNK2 mRNA levels are negatively correlated with disease severity during sepsis. **(A)** JNK2 mRNA expression in different organs of wild-type mice treated with low dose LPS for different times as indicated. **(B)** JNK2 protein expression in whole lung homogenates of wild-type mice treated with low dose LPS for different times as indicated. **(C)** JNK2 mRNA expression in different organs of wild-type mice treated with high dose LPS for different times as indicated. **(D)** JNK2 protein expression in whole colon or heart homogenates of wild-type mice treated with high dose LPS for different times as indicated. In **(A, C)**, N=3-6. Data are presented as means ± sem. $^{*}p < 0.05$; $^{**}p < 0.01$; $^{***}p < 0.001$; ns, not significant.

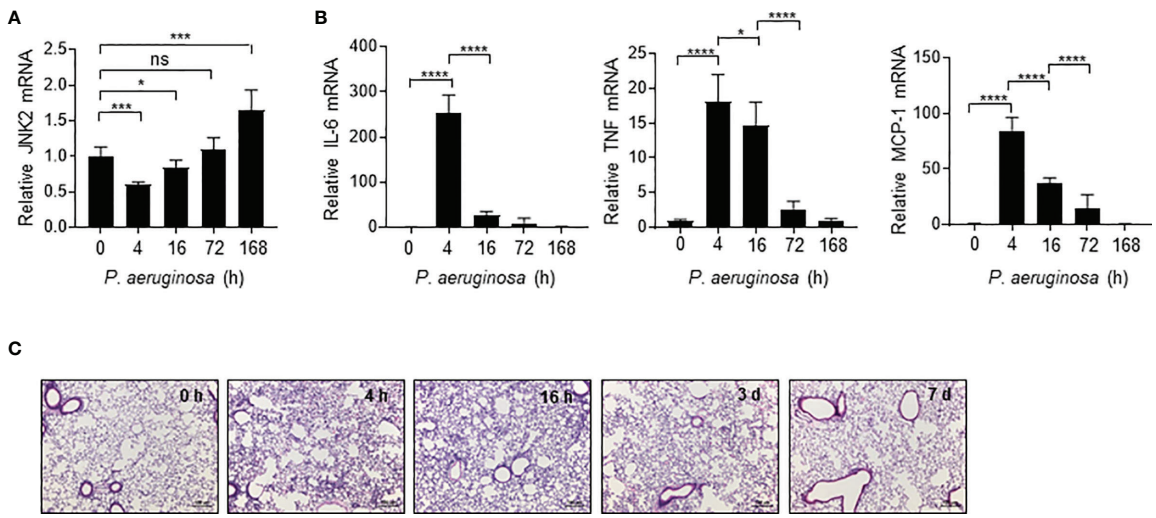

FIGURE 5 | JNK2 mRNA levels are negatively correlated with lung injury severity during *pseudomonas* pneumonia. mRNA expressions of JNK2 **(A)** or inflammatory cytokines **(B)** in whole lung homogenates or lung histology by H&E staining **(C)** from wild-type mice treated with i.n. *pseudomonas aeruginosa* (strain PA103) for different times as indicated. N=3-6. Data are presented as means ± sem. $^{*}p < 0.05$; $^{***}p < 0.001$; $^{****}p < 0.0001$; ns, not significant.

Supplementary Tables 1, 2). Among them, miR-221-5p contains seed sequence matching to JNK2 but not JNK1 mRNA 3'UTR (**Figure 7E**), and importantly, it is induced by LPS with dynamically inverse correlation with JNK2 mRNA levels in LPS-treated RAW 264.7 cells (comparing **Figure 7F** and **Figure 7A**). Furthermore, miR-221-5p mimics, which are chemically modified double-stranded RNA molecules designed to mimic endogenous miRNAs, resulted in downregulation of

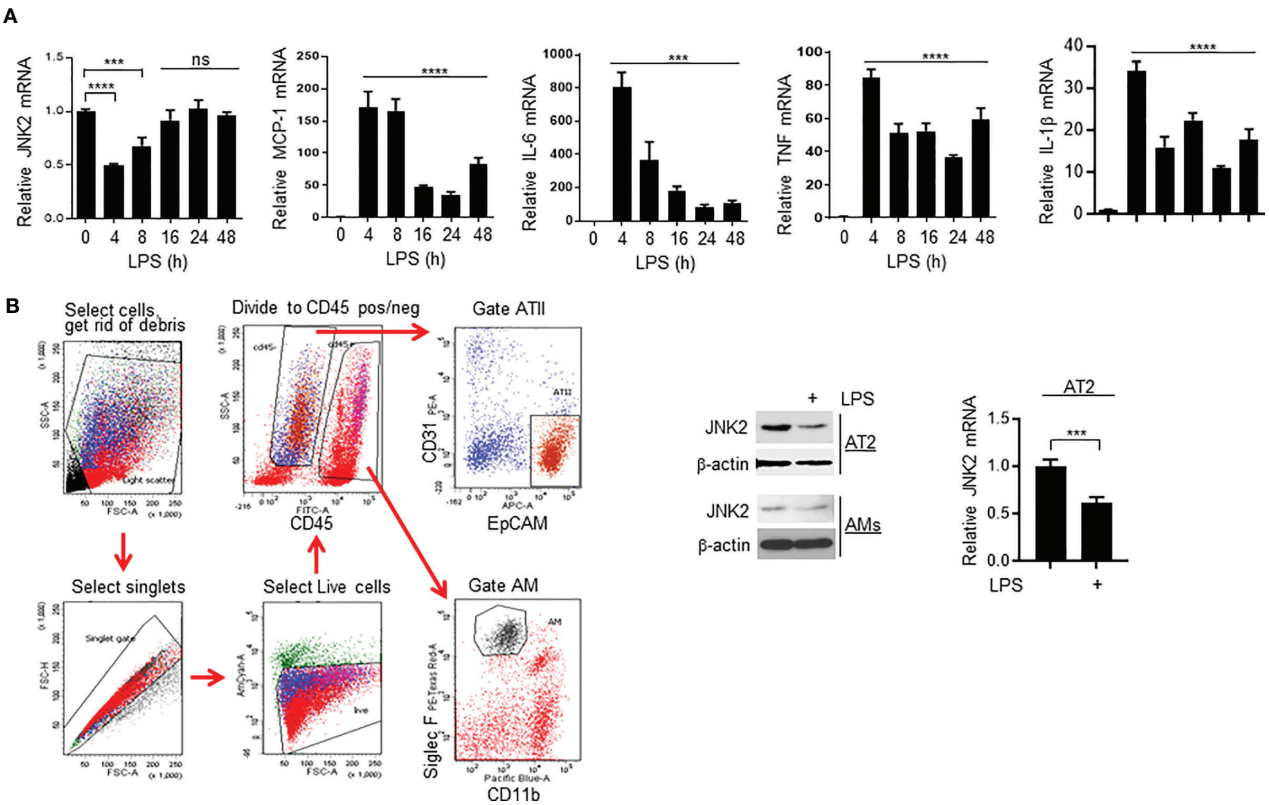

FIGURE 6 | JNK2 mRNA levels are also negatively correlated with lung injury severity in LPS-induced ALI model. **(A)** mRNA expressions of JNK2 or inflammatory cytokines in whole lung homogenates of wild-type mice treated with i.t. LPS. **(B)** Left panel, gating strategy to flow sort AT2 cells and AMs from PBS-treated mouse lung. Middle panel, JNK2 protein expression in AT2 cells and AMs flow-sorted from PBS- or LPS-treated whole lung homogenates. Right panel, JNK2 mRNA level in AT2 cells flow-sorted from PBS- or LPS-treated mouse lung. N=3-6. Data are presented as means ± sem. ***$p < 0.001$; ****$p < 0.0001$; ns, not significant.

JNK2 mRNA (**Figure 7G**, left panel). In contrast, miR-221-5p inhibitors, which are chemically-enhanced RNA oligonucleotides designed to bind and to sequester the complimentary, mature microRNA strand, resulted in upregulation of JNK2 mRNA (**Figure 7G**, right panel). To investigate the *in vivo* relevance of miR-221-5p-mediated downregulation of JNK2, miR-221-5p inhibitor or inhibitor control was delivered intratracheally into the mouse lung. As expected, JNK2 mRNA levels were markedly increased by miR-221-5p inhibitor as compared to inhibitor negative control (**Figure 7H**). These data suggest that miR-221-5p downregulates JNK2. To further evaluate whether miR-221-5p is functional in targeting JNK2 3'UTR, we performed JNK2 3′ UTR Luciferase Reporter Assay. Transfection of miR-221-5p mimics inhibited while transfection of miR-221-5p inhibitors enhanced the luciferase reporter gene expression, which is controlled by JNK2 3′UTR in the promoter region (**Figure 7I**). miRNA-mediated silencing requires the interaction of the target mRNA with the miRNA and Argonaute (Ago) proteins, forming a miRNA-associated ribonucleoprotein complexes (RNPs), which is the core of the RNA-induced silencing complex (RISC) (43). Ago2 RNA immunoprecipitation (RIP) revealed the association of JNK2 mRNA with Ago2 in the presence of miR-221-5p mimics (**Figure 7J**). These data collectively suggest that miR-221-5p targets JNK2 mRNA.

miR-221-5p Exacerbates Sepsis-Induced Lung Inflammation and Injury by Targeting JNK2 mRNA

To determine the role of miR-221-5p in sepsis-induced lung inflammation and injury, we intratracheally delivered miR-221-5p inhibitor or inhibitor control, or miR-221-5p mimic or mimic control into the mouse lung, followed by CLP treatment. miR-221-5p inhibitor decreased the expression of CLP-induced inflammatory cytokines MCP-1 and KC (**Figure 8A**), and attenuated lung inflammation and injury (**Figure 8B**). In contrast, miR-221-5p mimic augmented the expression of CLP-induced MCP-1 and KC, and exacerbated lung inflammation and injury (**Figures 8C, D** and **Supplementary Figure 4A**), which was rescued by overexpression of exogenous JNK2 (**Figures 8C, D** and **Supplementary Figure 4B**). Additionally, overexpression of exogenous JNK2 by adenoviral delivery in the mouse lung resulted in attenuation of CLP-induced lung inflammation and injury as compared to empty adenovirus (Ad/null)-treated mice

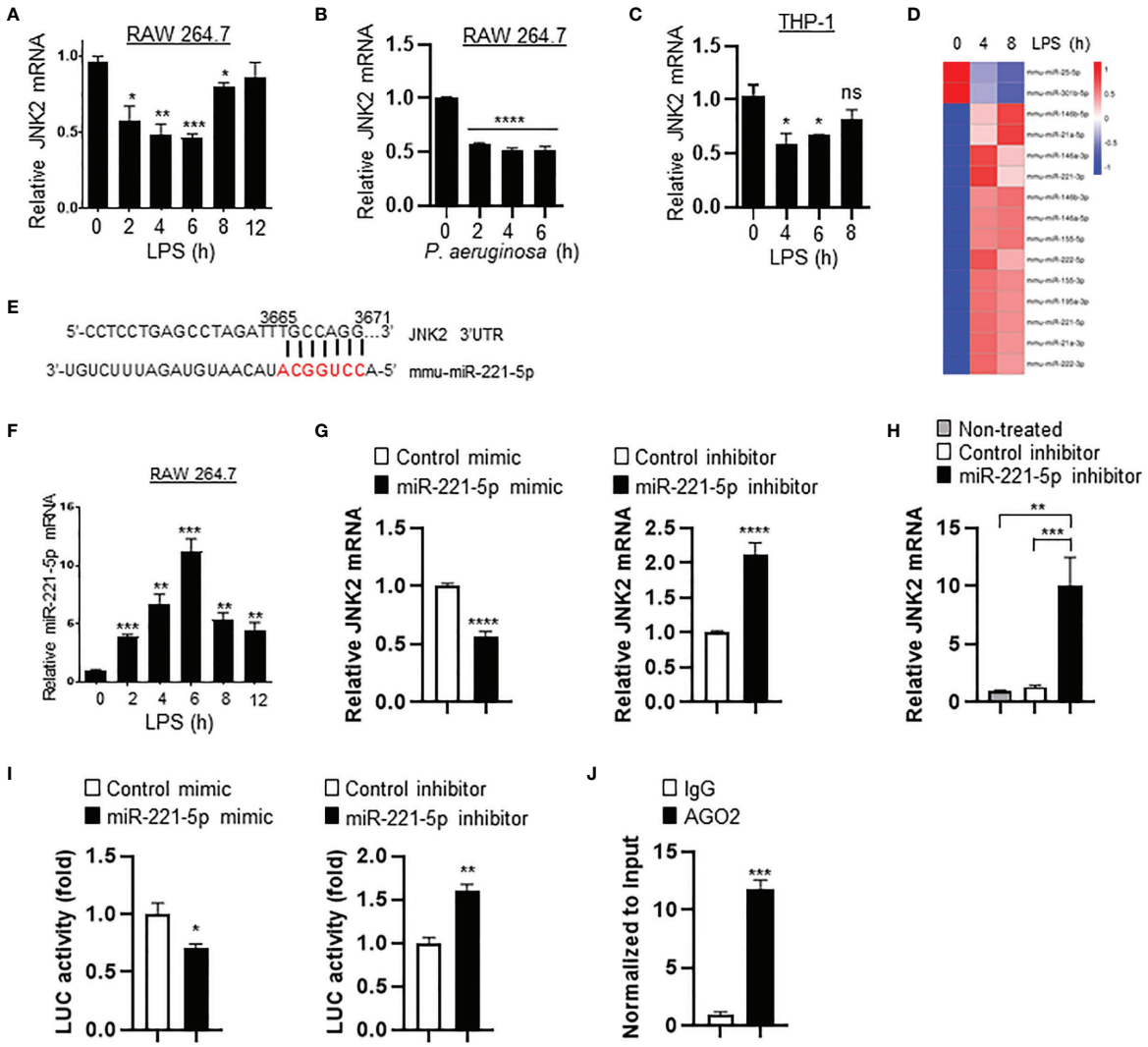

FIGURE 7 | Small RNA sequencing revealed that miR-221-5p is upregulated in response to LPS *in vitro*, resulting in JNK2 downregulation. mRNA expressions of JNK2 in LPS- **(A)** or PA103-treated **(B)** RAW 264.7 cells, or LPS-treated THP-1 cells (PMA-differentiated) **(C)** as indicated. **(D)** Heatmap of differential expressed miRNAs in RAW 264.7 cells treated with LPS for 0, 4, and 8h. **(E)** Seed sequence of miR-221-5p matching to JNK2 mRNA 3'UTR. **(F)** Levels of miR-221-5p in RAW 264.7 cells treated with LPS for different times. **(G)** JNK2 mRNA levels in mouse lung epithelial cells (MLE-12) treated with mimic control or miR-221-5p mimic (left panel), or inhibitor control or miR-221-5p inhibitor (right panel). **(H)** JNK2 mRNA levels in whole lung homogenates of mice intratracheally treated without or with miRNA inhibitor control or miR-221-5p inhibitor. **(I)** JNK2 3'UTR luciferase activity in the presence of miR-221-5p mimic (left panel; normalized to control mimic) or miR-221-5p inhibitor (right panel; normalized to control inhibitor). **(J)** JNK2 mRNA in the RNA-protein complex using Ago2 or control IgG for IP in the presence of miR-221-5p mimic (normalized to input). Data are presented as means ± sem. $^{*}p < 0.05$; $^{**}p < 0.01$; $^{***}p < 0.001$; $^{****}p < 0.0001$; ns, not significant.

(**Figures 8C, D**). We previously reported that JNK2 promotes stress-induced mitophagy thereby preventing mitochondrial dysfunction and restraining the NLRP3 inflammasome activation (36). Activation of the NLRP3 inflammation results in the cleavage of pro-caspase 1 into active caspase 1, which in turn triggers the activation and release of interleukin1 (IL1) family proteins. We observed that miR-221-5p mimic increased the production of active, cleaved caspase 1 in LPS-primed, ATP-stimulated RAW 264.7 cells, as demonstrated by elevated levels of cleaved caspase 1 p10 and decreased levels of pro-caspase 1 proteins (**Figure 8E**). Again, overexpression of exogenous JNK2 rescued the effect of miR-221-5p mimic (**Figure 8E** and **Supplementary Figure 4C**). These data together suggest that miR-221-5p exacerbates sepsis-induced lung inflammation and injury by targeting JNK2 mRNA.

JNK2 Levels in Alveolar Macrophages From Patients With Pneumonia Are Inversely Correlated With The Percentage Of Neutrophils, Neutrophil Count, and White Blood Cell Count in the BAL Fluid

We have developed protocols to reliably identify and isolate AMs by flow cytometry from non-bronchoscopic bronchoalveolar lavage

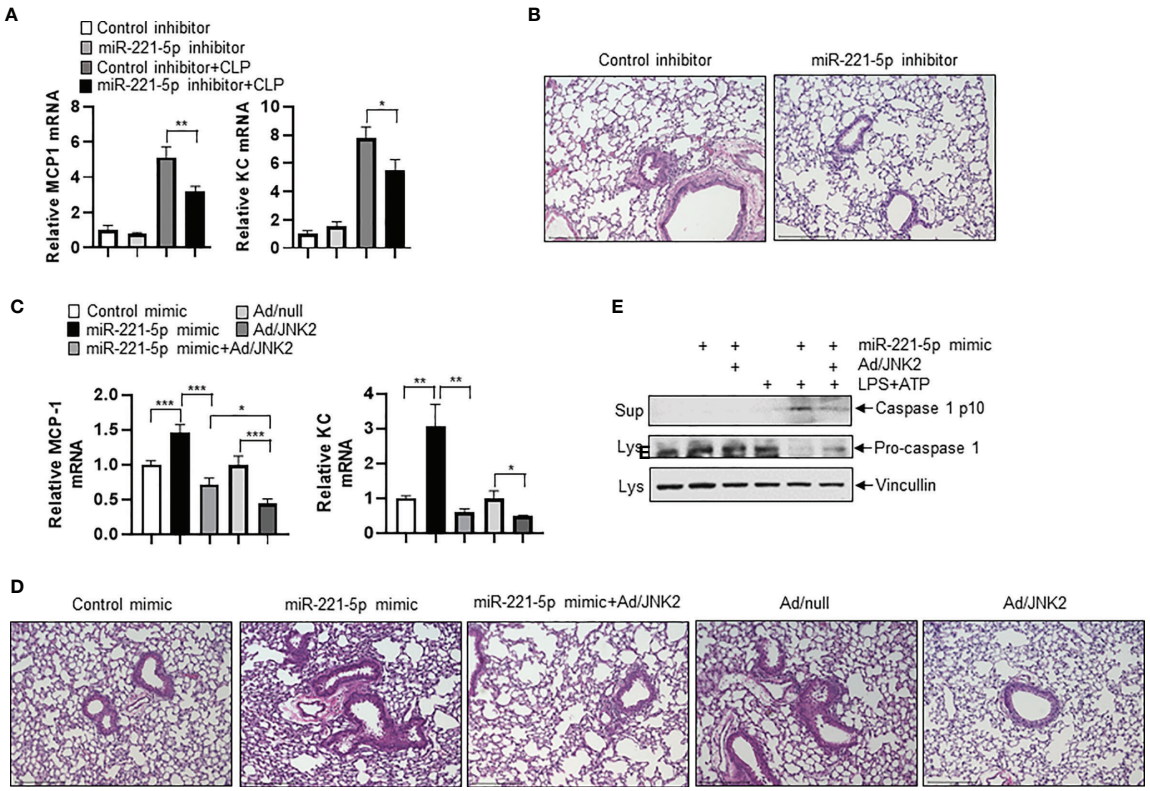

FIGURE 8 | miR-221-5p exacerbates sepsis-induced lung inflammation and injury by targeting JNK2 mRNA. **(A, B)** mRNA levels of MCP-1 and KC in lung tissues **(A)**, or lung histology by H&E staining **(B)** from mice treated intratracheally with control inhibitor or miR-221-5p inhibitor, followed by sham or CLP treatment. N=4. **(C, D)** mRNA levels of MCP-1 and KC in lung tissues **(C)**, or lung histology by H&E staining **(D)** from mice treated intratracheally with control mimic, or miR-221-5p mimic, or miR-221-5p mimic with Ad/JNK2, or Ad/null, or Ad/JNK2, followed by CLP treatment. N=3-5. **(E)** Western blot of Caspase 1 p10 in the supernatant and Pro-caspase 1 in the cell lysates of RAW 264.7 cells transfected with control mimic or miR-221-5p mimic in the absence or presence of Ad/JNK2 infection, followed by treatment with LPS (10 ng/ml) for 16 h and then ATP (2mM) for 1 h. Data are presented as means ± sem. $^{*}p < 0.05$; $^{**}p < 0.01$; $^{***}p < 0.001$.

(NBBAL) samples collected from mechanically ventilated patients with pneumonia (**Supplementary Figure 5A**) (44). This fluid was obtained as part of an Institutional Review Board-approved protocol to obtain an aliquot of lavage fluid from every NBBAL that is performed in the MICU. Flow-sorted AMs from 20 samples were obtained and high-quality RNA was extracted (**Supplementary Figure 5B**). RNA sequencing (RNA-Seq) was performed on these samples and high-quality transcriptomic data was obtained as measured by multiple variables (**Supplementary Figure 5C**). RNA-seq revealed that JNK2 mRNA levels in these AMs were inversely correlated strongly with the percentage of neutrophils, neutrophil count, and white blood cell (WBC) count in the BAL fluid of the patients with pneumonia (**Figures 9A–C**). Note, patient demographics and clinical characteristics were shown in **Supplementary Figure 5D**.

DISCUSSION

We and others have reported that JNK1 is the main JNK isoform activated by canonical JNK agonists while JNK2 activity is negligible and therefore most of the studies have been focused on JNK1 while the biological functions of JNK2 have been largely overlooked (35). Although there is well-established relationship between JNK and mitochondrial dysfunction and also the broad influence of JNK under conditions of stress and inflammation, those studies have been focused on JNK1 while the role of JNK2 is largely unknown (36). In contrast to JNK1, here we identified a protective role of JNK2 in ARDS. As JNK has many vital functions, specific targeting JNK2 without affecting the overall JNK activity (attributable to JNK1) highlights therapeutic potential. We also demonstrated that miR-221-5p targets JNK2 mRNA. As miRNAs are generally only about 22 nucleotides in length and can be released into different body fluids where they are remarkably stable, they offer potentials as biomarkers and drug therapies.

We show that JNK2 but not JNK1 mRNA levels are inversely correlated with lung injury severity in different mouse models of ALI induced by LPS, *Pseudomonas* pneumonia, or septic shock. Importantly, JNK2 mRNA levels in AMs from the BAL fluid of patients with pneumonia were inversely correlated strongly and significantly with the percentage of neutrophils, neutrophil and white blood cell counts in the BAL fluid. These data indicate that

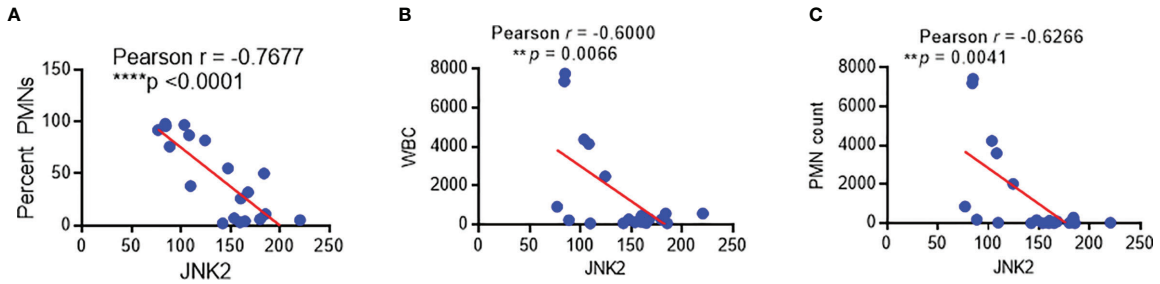

FIGURE 9 | JNK2 levels in alveolar macrophages from patients with pneumonia are inversely correlated with the percentage of neutrophils, neutrophil count, and white blood cell count in the BAL fluid. Correlation of JNK2 mRNA levels (analyzed by RNA-seq) in AMs with neutrophil percentage **(A)**, WBC count **(B)** and neutrophil count **(C)** in the BAL fluid of patients with pneumonia. N=20 subjects. $^{**}p < 0.01$; $^{****}p < 0.0001$.

JNK2 might serve as a marker of sepsis severity and prognosis in the ICU.

An established body of literature supports an association between mitochondrial dysfunction and sepsis and ARDS severity in murine models and in patients with sepsis and ARDS. However, the underlying mechanism remains elusive. Several mechanisms have been proposed. For example, sepsis results in tissue hypoxia, which in turn affects oxidative phosphorylation. Abundant reactive species such as nitric oxide and superoxide are generated during sepsis, which affect mitochondrial respiration. Sepsis-induced hormonal changes also have impact on mitochondrial function. Genes encoding mitochondrial proteins have been reported to be downregulated during sepsis. Dysregulation of mitophagy and mitochondrial biogenesis are also proposed to explain the mitochondrial dysfunction in sepsis (29, 45–47). We previously reported that loss of JNK2 results in defective mitophagy, leading to mitochondrial dysfunction and robust inflammatory response. In the present study, we demonstrate that JNK2 is downregulated in ALI or septic shock, with dynamically inverse correlation with disease severity. Furthermore, JNK2 mRNA levels are also negatively correlated with neutrophil percentage in the BAL fluid of patients with pneumonia. Therefore, our study might provide a potential mechanism to explain the well-documented association between mitochondria dysfunction and sepsis/ARDS.

"Cytokine storm" refers to a prevalent hypothesis to explain the multiple organ dysfunction that develops with sepsis even after effective primary source control is achieved. According to this hypothesis, elevated levels of pro-inflammatory cytokines nonspecifically activate circulating and tissue-resident immune cells, which damage tissues and induce the release of more cytokines, creating a positive feedback loop that culminates in tissue damage and immune exhaustion (48, 49). While substantial evidence for this hypothesis can be found in patients with sepsis and animal models of sepsis, targeting this pathway with anti-cytokine therapy has been largely unsuccessful (48, 50). The newly emergent concept of "disease/tissue tolerance" refers to a complementary hypothesis to explain multiple organ dysfunction in sepsis (51–55). Tolerance is a host defense strategy that reduces the negative impact of infection on host fitness. Tolerance decreases the host susceptibility to tissue damage, or other fitness costs, caused by the pathogens or by the immune response against them, without directly affecting pathogen burden. According to this hypothesis, cells in different tissues can activate cell autonomous processes to maintain their function and survive even in an inflammatory milieu without affecting the severity of inflammation or pathogen burden. According to this model, the development of multiple organ dysfunction in sepsis represents a failure of tissue tolerance. The molecular basis for tissue tolerance is poorly understood, however, autophagy pathways and mitochondrial homeostasis have been implicated. For example, in mouse models of sepsis induced by cecal ligation and puncture (CLP), *Klebsiella pneumoniae*, or systemic LPS administration, a gain of tissue tolerance through activation of autophagy was found to be critical for host protection from sepsis (16, 55). The specific cellular basis for autophagy-mediated protection is not clear, however, a role in the removal of damaged mitochondria is suggested (17), and deregulated mitophagy has been recently recognized as a feature of severe sepsis and has been suggested to result in both enhanced inflammatory cytokine release and reduced tissue tolerance (54, 55). However, the signaling mechanisms that deregulate mitophagy to impair tissue tolerance during sepsis are unknown. Future studies are needed to investigate whether JNK2 servers as the molecular cue here.

MATERIALS AND METHODS

Mice

Jnk1$^{-/-}$ and *Jnk2*$^{-/-}$ mice on the C57BL/6 background were kindly provided by Michael Karin (UCSD). The animal care and experiments were performed in compliance with the institutional and US National Institutes of Health guidelines and were approved by the Northwestern University Animal Care and Use Committee and the University of Illinois at Chicago Animal Care Committee. For the mortality studies, when mice became moribund (hunched posture, lack of curiosity, little or no response to stimuli and not moving when touched), a clinically irreversible condition that leads to inevitable death, according to the guidelines for the selection of humane endpoints in rodent studies at Northwestern University and University of Illinois at Chicago, they were sacrificed.

Reagents

LPS (L2630), β-actin antibody (AC-15), and actinomycin D were from Sigma-Aldrich. ATP was from ENZO Life Sciences. JNK2 antibody was from Cell Signaling Technology (Cat # 4672). AGO2 antibody was from abcam (ab186733). Mouse miRIDIAN miR-221-5p mimic, miRIDIAN miRNA mimic negative control, miRIDIAN mouse miR-221-5p hairpin inhibitor, and miRIDIAN miNA hairpin inhibitor negative control were from Horizon Discovery. Ad/JNK2 was generated by ViraQuest, Inc. by cloning pCDNA3 Flag Jnk2a2 (Addgene, Item ID 13755) into the pVQAd CMV K-NpA vector. Ad/null was from ViraQuest, Inc. miR-221-5p inhibitor and inhibitor control, and miR-221-5p mimic and mimic control were from Horizon Discovery.

LPS-Induced Lung Inflammation and Injury Model

Mice (male, 6–8 weeks of age) were given intratracheal instillation of LPS (6 mg per kg body weight) as we previously reported (56). After 48 h, the BAL fluid was collected for cell counts and protein quantification. Lungs were fixed, embedded in paraffin, and analyzed by staining with hematoxylin and eosin. In some experiments, lung tissues were collected for qRT-PCR of genes at different times after LPS treatment as indicated.

Mouse Model of Acute Pneumonia

Mice (male, 6–8 weeks of age) were inoculated intranasally with *P. aeruginosa* (strain PA103, 2×10^5 colony-forming units per mouse) as described as we previously reported (56). For survival experiments, mice were monitored every 8 h for up to 7 d. At 16 h after infection, the BAL fluid was collected for cell counts and protein quantification. Lungs were fixed, embedded in paraffin, and analyzed by staining with hematoxylin and eosin. In some experiments, lung tissues were collected for qRT-PCR of genes at different times after the infection as indicated.

CLP-Induced Sepsis Model

CLP was performed as previously described (57). Briefly, mice were anesthetized with isoflurane, and a 1-cm midline abdominal incision was made. The cecum was then exposed, ligated and punctured with a 21-gauge needle. A small amount of cecal content was extruded from the perforation sites. The cecum was returned to the peritoneal cavity and the peritoneum is closed. Sham-operated mice were treated with cecal exposure without ligation and puncture. Mice were harvested at 24 h.

Small RNA Sequencing

RAW 264.7 cells treated with LPS for 0, 4, and 8 h were subjected to small RNA-seq, which was performed by Novogene. Briefly, RNA integrity was assessed using Agilent Bioanalyzer 2100 system (Agilent Technologies, CA, USA), and RNA concentration was measured using Qubit® 2.0 Flurometer (Life Technologies, CA, USA). Sequencing libraries were generated using NEBNext®Multiplex Small RNA Library Prep Set for Illumina® (NEB, USA.) following the manufacturer's instructions and index codes were added to attribute sequences to each sample. DNA fragments corresponding to 140~160bp (the length of small noncoding RNA plus the 3' and 5' adaptors) were recovered and the library quality was assessed using the Agilent Bioanalyzer 2100 system with DNA High Sensitivity Chips. The clustering of the index-coded samples was performed on a cBot Cluster Generation System using TruSeq SR Cluster Kit v3-cBot-HS (Illumia) according to the manufacturer's instructions. After cluster generation, the library preparations were sequenced on an Illumina Hiseq 2500/2000platform and 50bp single-end reads were generated. The small RNA tags were mapped to reference sequence by Bowtie without mismatch to analyze their expression and distribution on the reference. miRNA expression levels were measured by TPM (transcript per million) using the normalization formula: Normalized expression = mapped read count/Total reads*1000000. Differential expression analysis of two conditions was performed using the DEGseq R package. P-value was adjusted using qvalue. qvalue<0.01 and |log2(foldchange)|>1 was set as the threshold for significantly differential expression by default.

Lung Histology by Hematoxylin and Eosin Stain

Hematoxylin and Eosin (H&E) Staining was performed by the Research Histology Core at University of Illinois at Chicago (UIC). Briefly, 5-micron paraffin sections were deparaffinized and rehydrated. The sections were then stained in Mayers Hematoxylin for 1 minute, followed by wash with 4-5 changes of Tap water, 1X PBS for 1 minute, and 3 changes of distilled water. Slides were counterstained in Alcoholic-Eosin for 1 minute, and then dehydrated through 3 changes of 95% EtOH and 2 changes of 100% EtOH 1 minute each, followed by 3 changes of Xylene 1 minute each change and then mount and coverslip. Nuclei were stained blue while cytoplasm was stained pink.

Analysis of Cytokines and Chemokines

The concentration of cytokines and chemokines in the BAL fluid were quantified by a cytometric bead array kit for mouse proinflammatory cytokines and chemokines (CBA; BD Biosciences).

Adenovirus Infection

Mice were infected intratracheally with 1×10^9 plaque-forming units of adenovirus per mouse. Cells were infected with adenovirus at a multiplicity of infection of 50.

Intratracheal Delivery of miRNA Mimic or Inhibitor

miRNA mimic or inhibitor (1.25 μL of 0.4 nmol/μL) were mixed with 1.25 μL of invivofectamine-complexation buffer (cat# IVF3001, ThermoFisher), followed by addition of 2.5 μL of invivofectamine (pre-equilibrated to room temperature). The mixture was then vortexed vigorously for 2 s, and incubated at 50°C for 30 min, followed by addition of 45 μL of 1x PBS pH 7.4. The miRNA mimic or inhibitor solution was maintained at room temperature during the procedure. At 2 h, mice were harvested or underwent sham or CLP treatment.

JNK2 3′UTR Luciferase Reporter Assay

JNK2 3'UTR reporter construct (LightSwitch™ 3'UTR GoClone®, Product code 32012, Active Motif Inc.), which expresses the luciferase reporter gene fused to the 3′UTR of JNK2, was transfected into HEK293 cells (ATCC) together with miR-221 mimic or mimic control (40 nM), or miR-221 inhibitor or inhibitor control (40 nM). At 48 h, luciferase activity was measured using LightSwitch™ Luciferase Assay Kit (Active Motif Inc.) according to the manufacturer's instructions.

Ago2 RNA Immunoprecipitation

Ago2 RIP was performed using Ago2 antibody for immunoprecipitation (IP) as described in: https://www.abcam.com/epigenetics/rna-immunoprecipitation-rip-protocol. JNK2 mRNA was detected by reverse transcriptase followed by qPCR using the following primers: 5'- AGTGATTGA TCCAGACAAGCG-3' and 5'-GCGGGGTCATACCA AACAGTA-3', and was normalized to input.

Quantitative PCR

Quantitative PCR (qPCR) was performed using iQ™ SYBR® Green Supermix (BIO-RAD) on a CFX Connect™ Real-Time PCR Dection System (BIO-RAD). mRNA expression of a particular gene was normalized to hypoxanthine-guanine phosphoribosyltransferse (HPRT) for mouse genes. Primer sequences were listed in **Supplementary Table 3**. For qRT-PCR, total RNA was extracted using TRIzol® (Thermo Fisher Scientific), followed by cDNA synthesis using M-MuLV Reverse Transcriptase according to the manufacturer's instructions.

miRNA Quantification by RT-qPCR

MiR-221-5p was quantified using stem-loop quantitative reverse transcription PCR (RT-qPCR). Briefly, RNA was extracted with miRNeasy Micro Kit (QIAGEN; Cat # 217084), followed by reverse transcription using stem-loop RT primers (Primer sequences were listed in **Supplementary Table 4**). The RT product was amplified by qPCR using miR-221-5p specific forward primer and the universal reverse primer (Primer sequences were listed in **Supplementary Table 4**).

RNA-Seq of Alveolar Macrophages Isolated from BAL Fluid of Patients With Pneumonia

RNA-seq was performed in flow-sorted AMs from BAL fluid of patients as described as we reported (41).

Fluorescence-Activated Cell Sorting

The lungs were digested with dispase (Corning) and 0.1 mg/mL DNase I. Red blood cells were removed using 1x BD Pharm Lyse solution (BD Biosciences). Cells were washed in MACS buffer (Miltenyi Biotech) and counted using a Countess automated cell counter (Invitrogen). For isolation of AT2 cells and AMs, single cell suspension was incubated in 0.5μg Fc Block (BD Biosciences) for 10 minutes at 4°C, followed by staining with FITC conjugated anti-mouse CD45 (eBioscience), APC conjugated anti-mouse EpCAM (eBioscience), PE conjugated anti-mouse CD31 (eBioscience), PE-CF594 conjugated anti-mouse SiglecF (BD Biosciences) and efluor450 conjugated anti-mouse CD11b (eBioscience). The FACS experiments were performed using a BD FACSAria SORP 5-Laser instrument (BD Immunocytometry Systems) equipped with 355nm, 405nm, 488nm, 561nm and 640nm excitation lasers located at the Northwestern University Flow Cytometry Core Facility. All data collection and sorting were performed using BD FACS Diva software (BD Biosciences) and data analyses were performed using FlowJo software (Tree Star, Ashland, OR). Fluorescence minus one (FMO) controls were used for gating analyses to distinguish positively from negatively staining cell populations. Compensation was performed using single color controls prepared from BD Comp Beads (BD Biosciences). Compensation matrices were calculated and applied using FlowJo software (Tree Star). Biexponential transformation was adjusted manually when necessary. For simultaneous isolation of AT2 and other myeloid cells, after blocking, cells were incubated with Biotin conjugated anti-mouse CD45 antibody for 10 minutes at room temperature. Cells then were separated using MagniSort Streptavidin Positive selection beads (eBioscience) according to the manufacturer's instructions. AT2 cells will be isolated from the CD45 negative fraction by flow sorting using FITC conjugated anti-mouse CD45 (eBioscience), APC conjugated anti-mouse EpCAM (eBioscience) and PE conjugated anti-mouse CD31 (eBioscience). The myeloid cell populations will be isolated from the CD45 positive fraction by flow sorting using FITC conjugated anti-mouse CD45 (eBioscience), PerCPCy5.5 conjugated anti-mouse MHC II (BioLegend), eFluor450 conjugated anti-mouse Ly6C (eBioscience), APC conjugated anti-mouse CD24 (eBioscience), Alexa700 conjugated anti-mouse Ly6G (BD Biosciences), APCCy7 conjugated anti-mouse CD11b (BioLegend), PE conjugated anti-mouse CD64 (BioLegend), PE-CF594 conjugated anti-mouse SiglecF (BD Biosciences) and PECy7 conjugated anti-mouse CD11c (eBioscience) (58).

Patients

Inclusion criteria: Mechanically ventilated adult patients aged 18 years or older in the ICU in whom a NBBAL was performed to investigate suspected pneumonia. Exclusion: NBBALs with > 12% bronchial epithelial cell, patients who were neutropenic, and who had bronchiectasis or cystic fibrosis. A non-bronchoscopic BAL (NBBAL) is a routine procedure performed in our medical intensive care unit (MICU) to sample the distal airspace in mechanically ventilated patients with suspected infection. During this bedside procedure, respiratory therapists (RT) advance a 16-French catheter *via* the patient's endotracheal tube into the distal airways, where non-bacteriostatic saline is instilled and then withdrawn. The major difference between a traditional bronchoscopic BAL and a NBBAL is that an NBBAL is not performed under direct visualization. Rather, the NBBAL scope is introduced into either the left or right lung and advanced until resistance is encountered. NBBAL is routinely used in our MICU as it is inexpensive and can be performed by RTs without direct physician oversight facilitating timely alveolar sampling for

patients admitted to the intensive care unit or who develop new acute lung pathology at night. The study protocol was approved by the Northwestern University Institutional Review Board (44).

Statistical Analysis

Data were analyzed by an unpaired Student's *t*-test, with the assumption of normal distribution of data and equal sample variance.

DATA AVAILABILITY STATEMENT

The raw data supporting the conclusions of this article will be made available by the authors, without undue reservation.

ETHICS STATEMENT

The animal study was reviewed and approved by Northwestern University Animal Care and Use Committee and the University of Illinois at Chicago Animal Care Committee.

AUTHOR CONTRIBUTIONS

JY, HD-U, QZ, HW, CH, HD, EP, and MS performed experiments. KA and JW performed RNA-seq analysis of AMs flow-sorted from BAL fluid of patients. SL, RW, and GB provided reagents and suggestions. JL contributed to manuscript preparation, hypothesis generation, and experimental design. All authors contributed to the article and approved the submitted version.

FUNDING

JL is supported by the US National Institutes of Health (HL141459 to JL).

SUPPLEMENTARY MATERIAL

The Supplementary Material for this article can be found online at: https://www.frontiersin.org/articles/10.3389/fimmu.2021.700933/full#supplementary-material

REFERENCES

1. Mayr FB, Yende S, Angus DC. Epidemiology of Severe Sepsis. *Virulence* (2014) 5(1):4–11. doi: 10.4161/viru.27372
2. Martin GS, Mannino DM, Eaton S, Moss M. The Epidemiology of Sepsis in the United States From 1979 Through 2000. *N Engl J Med* (2003) 348 (16):1546–54. doi: 10.1056/NEJMoa022139
3. Ulloa L, Tracey KJ. The "Cytokine Profile": A Code for Sepsis. *Trends Mol Med* (2005) 11(2):56–63. doi: 10.1016/j.molmed.2004.12.007
4. Rittirsch D, Flierl MA, Ward PA. Harmful Molecular Mechanisms in Sepsis. *Nat Rev Immunol* (2008) 8(10):776–87. doi: 10.1038/nri2402
5. Ware LB, Matthay MA. The Acute Respiratory Distress Syndrome. *N Engl J Med* (2000) 342(18):1334–49. doi: 10.1056/NEJM200005043421806
6. Eisner MD, Thompson T, Hudson LD, Luce JM, Hayden D, Schoenfeld D, et al. Efficacy of Low Tidal Volume Ventilation in Patients With Different Clinical Risk Factors for Acute Lung Injury and the Acute Respiratory Distress Syndrome. *Am J Respir Crit Care Med* (2001) 164(2):231–6. doi: 10.1164/ajrccm.164.2.2011093
7. Rubenfeld GD, Caldwell E, Peabody E, Weaver J, Martin DP, Neff M, et al. Incidence and Outcomes of Acute Lung Injury. *N Engl J Med* (2005) 353 (16):1685–93. doi: 10.1056/NEJMoa050333
8. Herridge MS, Tansey CM, Matte A, Tomlinson G, Diaz-Granados N, Cooper A, et al. Functional Disability 5 Years After Acute Respiratory Distress Syndrome. *N Engl J Med* (2011) 364(14):1293–304. doi: 10.1056/NEJMoa1011802
9. Angus DC, Linde-Zwirble WT, Lidicker J, Clermont G, Carcillo J, Pinsky MR. Epidemiology of Severe Sepsis in the United States: Analysis of Incidence, Outcome, and Associated Costs of Care. *Crit Care Med* (2001) 29(7):1303–10. doi: 10.1097/00003246-200107000-00002
10. Alberti C, Brun-Buisson C, Burchardi H, Martin C, Goodman S, Artigas A, et al. Epidemiology of Sepsis and Infection in ICU Patients From an International Multicentre Cohort Study. *Intensive Care Med* (2002) 28 (2):108–21. doi: 10.1007/s00134-001-1143-z
11. Brealey D, Brand M, Hargreaves I, Heales S, Land J, Smolenski R, et al. Association Between Mitochondrial Dysfunction and Severity and Outcome of Septic Shock. *Lancet* (2002) 360(9328):219–23. doi: 10.1016/S0140-6736(02)09459-X
12. Protti A, Singer M. Bench-To-Bedside Review: Potential Strategies to Protect or Reverse Mitochondrial Dysfunction in Sepsis-Induced Organ Failure. *Crit Care* (2006) 10(5):228.
13. Singer M. Mitochondrial Function in Sepsis: Acute Phase Versus Multiple Organ Failure. *Crit Care Med* (2007) 35(9 Suppl):S441–8. doi: 10.1097/01.CCM.0000278049.48333.78
14. Harrois A, Huet O, Duranteau J. Alterations of Mitochondrial Function in Sepsis and Critical Illness. *Curr Opin Anaesthesiol* (2009) 22(2):143–9. doi: 10.1097/ACO.0b013e328328d1cc
15. Dada LA, Sznajder JI. Mitochondrial Ca(2)+ and ROS Take Center Stage to Orchestrate TNF-Alpha-Mediated Inflammatory Responses. *J Clin Invest* (2011) 121(5):1683–5. doi: 10.1172/JCI57748
16. Russell JA, Walley KR. Update in Sepsis 2012. *Am J Respir Crit Care Med* (2013) 187(12):1303–7. doi: 10.1164/rccm.201303-0567UP
17. Morse D. Carbon Monoxide, a Modern "Pharmakon" for Sepsis. *Am J Respir Crit Care Med* (2012) 185(8):800–1. doi: 10.1164/rccm.201202-0224ED
18. Nakahira K, Kyung SY, Rogers AJ, Gazourian L, Youn S, Massaro AF, et al. Circulating Mitochondrial DNA in Patients in the ICU as a Marker of Mortality: Derivation and Validation. *PloS Med* (2013) 10(12):e1001577; discussion e1001577. doi: 10.1371/journal.pmed.1001577
19. MacGarvey NC, Suliman HB, Bartz RR, Fu P, Withers CM, Welty-Wolf KE, et al. Activation of Mitochondrial Biogenesis by Heme Oxygenase-1-Mediated NF-E2-Related Factor-2 Induction Rescues Mice From Lethal Staphylococcus Aureus Sepsis. *Am J Respir Crit Care Med* (2012) 185(8):851–61. doi: 10.1164/rccm.201106-1152OC
20. Youle RJ, Narendra DP. Mechanisms of Mitophagy. *Nat Rev Mol Cell Biol* (2011) 12(1):9–14. doi: 10.1038/nrm3028
21. Ding WX, Yin XM. Mitophagy: Mechanisms, Pathophysiological Roles, and Analysis. *Biol Chem* (2012) 393(7):547–64. doi: 10.1515/hsz-2012-0119
22. Wilson JG, Liu KD, Zhuo H, Caballero L, McMillan M, Fang X, et al. Mesenchymal Stem (Stromal) Cells for Treatment of ARDS: A Phase 1 Clinical Trial. *Lancet Respir Med* (2015) 3(1):24–32. doi: 10.1016/S2213-2600(14)70291-7
23. Lupfer C, Thomas PG, Anand PK, Vogel P, Milasta S, Martinez J, et al. Receptor Interacting Protein Kinase 2-Mediated Mitophagy Regulates Inflammasome Activation During Virus Infection. *Nat Immunol* (2013) 14 (5):480–8. doi: 10.1038/ni.2563
24. Zhou R, Yazdi AS, Menu P, Tschopp J. A Role for Mitochondria in NLRP3 Inflammasome Activation. *Nature* (2011) 469(7329):221–5. doi: 10.1038/nature09663
25. Nakahira K, Haspel JA, Rathinam VA, Lee SJ, Dolinay T, Lam HC, et al. Autophagy Proteins Regulate Innate Immune Responses by Inhibiting the Release of Mitochondrial DNA Mediated by the NALP3 Inflammasome. *Nat Immunol* (2011) 12(3):222–30. doi: 10.1038/ni.1980
26. Schumacker PT, Gillespie MN, Nakahira K, Choi AM, Crouser ED, Piantadosi CA, et al. Mitochondria in Lung Biology and Pathology: More Than Just a Powerhouse. *Am J Physiol Lung Cell Mol Physiol* (2014) 306(11):L962–74. doi: 10.1152/ajplung.00073.2014

27. Aggarwal S, Mannam P, Zhang J. Differential Regulation of Autophagy and Mitophagy in Pulmonary Diseases. *Am J Physiol Lung Cell Mol Physiol* (2016) 311(2):L433–52. doi: 10.1152/ajplung.00128.2016
28. Ryter SW, Choi AM. Autophagy in Lung Disease Pathogenesis and Therapeutics. *Redox Biol* (2015) 4:215–25. doi: 10.1016/j.redox.2014.12.010
29. Mannam P, Shinn AS, Srivastava A, Neamu RF, Walker WE, Bohanon M, et al. MKK3 Regulates Mitochondrial Biogenesis and Mitophagy in Sepsis-Induced Lung Injury. *Am J Physiol Lung Cell Mol Physiol* (2014) 306(7):L604–19. doi: 10.1152/ajplung.00272.2013
30. Suliman HB, Kraft B, Bartz R, Chen L, Welty-Wolf KE, Piantadosi CA. Mitochondrial Quality Control in Alveolar Epithelial Cells Damaged by S. Aureus Pneumonia in Mice. *Am J Physiol Lung Cell Mol Physiol* (2017) 313(4):L699–709.
31. Zhang Y, Sauler M, Shinn AS, Gong H, Haslip M, Shan P, et al. Endothelial PINK1 Mediates the Protective Effects of NLRP3 Deficiency During Lethal Oxidant Injury. *J Immunol* (2014) 192(11):5296–304. doi: 10.4049/jimmunol.1400653
32. Hibi M, Lin A, Smeal T, Minden A, Karin M. Identification of an Oncoprotein- and UV-Responsive Protein Kinase That Binds and Potentiates the C-Jun Activation Domain. *Genes Dev* (1993) 7(11):2135–48. doi: 10.1101/gad.7.11.2135
33. Chang L, Karin M. Mammalian MAP Kinase Signalling Cascades. *Nature* (2001) 410(6824):37–40. doi: 10.1038/35065000
34. Davis RJ. Signal Transduction by the JNK Group of MAP Kinases. *Cell* (2000) 103(2):239–52. doi: 10.1016/S0092-8674(00)00116-1
35. Liu J, Minemoto Y, Lin A. C-Jun N-Terminal Protein Kinase 1 (JNK1), But Not JNK2, Is Essential for Tumor Necrosis Factor Alpha-Induced C-Jun Kinase Activation and Apoptosis. *Mol Cell Biol* (2004) 24(24):10844–56. doi: 10.1128/MCB.24.24.10844-10856.2004
36. Zhang Q, Kuang H, Chen C, Yan J, Do-Umehara HC, Liu XY, et al. The Kinase Jnk2 Promotes Stress-Induced Mitophagy by Targeting the Small Mitochondrial Form of the Tumor Suppressor ARF for Degradation. *Nat Immunol* (2015) 16(5):458–66. doi: 10.1038/ni.3130
37. Reef S, Zalckvar E, Shifman O, Bialik S, Sabanay H, Oren M, et al. A Short Mitochondrial Form of P19arf Induces Autophagy and Caspase-Independent Cell Death. *Mol Cell* (2006) 22(4):463–75. doi: 10.1016/j.molcel.2006.04.014
38. Grenier K, Kontogiannea M, Fon EA. Short Mitochondrial ARF Triggers Parkin/PINK1-Dependent Mitophagy. *J Biol Chem* (2014) 289(43):29519–30. doi: 10.1074/jbc.M114.607150
39. Reef S, Kimchi A. A smARF Way to Die: A Novel Short Isoform of P19arf Is Linked to Autophagic Cell Death. *Autophagy* (2006) 2(4):328–30. doi: 10.4161/auto.3107
40. Reef S, Shifman O, Oren M, Kimchi A. The Autophagic Inducer smARF Interacts With and Is Stabilized by the Mitochondrial P32 Protein. *Oncogene* (2007) 26(46):6677–83. doi: 10.1038/sj.onc.1210485
41. Do-Umehara HC, Chen C, Zhang Q, Misharin AV, Abdala-Valencia H, Casalino-Matsuda SM, et al. Epithelial Cell-Specific Loss of Function of Miz1 Causes a Spontaneous COPD-Like Phenotype and Up-Regulates Ace2 Expression in Mice. *Sci Adv* (2020) 6(33):eabb7238. doi: 10.1126/sciadv.abb7238
42. Herbst RS, Heymach JV, Lippman SM. Lung Cancer. *N Engl J Med* (2008) 359 (13):1367–80. doi: 10.1056/NEJMra0802714
43. Wang Y, Juranek S, Li H, Sheng G, Tuschl T, Patel DJ. Structure of an Argonaute Silencing Complex With a Seed-Containing Guide DNA and Target RNA Duplex. *Nature* (2008) 456(7224):921–6. doi: 10.1038/nature07666
44. Walter JM, Ren Z, Yacoub T, Reyfman PA, Shah RD, Abdala-Valencia H, et al. Multidimensional Assessment of the Host Response in Mechanically Ventilated Patients With Suspected Pneumonia. *Am J Respir Crit Care Med* (2019) 199(10):1225–37. doi: 10.1164/rccm.201804-0650OC
45. Lelubre C, Vincent JL. Mechanisms and Treatment of Organ Failure in Sepsis. *Nat Rev Nephrol* (2018) 14(7):417–27. doi: 10.1038/s41581-018-0005-7
46. Kim MJ, Bae SH, Ryu JC, Kwon Y, Oh JH, Kwon J, et al. SESN2/sestrin2 Suppresses Sepsis by Inducing Mitophagy and Inhibiting NLRP3 Activation in Macrophages. *Autophagy* (2016) 12(8):1272–91. doi: 10.1080/15548627.2016.1183081
47. Cloonan SM, Choi AM. Mitochondria in Lung Disease. *J Clin Invest* (2016) 126(3):809–20. doi: 10.1172/JCI81113
48. Hotchkiss RS, Karl IE. The Pathophysiology and Treatment of Sepsis. *N Engl J Med* (2003) 348(2):138–50. doi: 10.1056/NEJMra021333
49. Angus DC, van der Poll T. Severe Sepsis and Septic Shock. *N Engl J Med* (2013) 369(9):840–51. doi: 10.1056/NEJMra1208623
50. Russell JA. Management of Sepsis. *N Engl J Med* (2006) 355(16):1699–713. doi: 10.1056/NEJMra043632
51. Medzhitov R, Schneider DS, Soares MP. Disease Tolerance as a Defense Strategy. *Science* (2012) 335(6071):936–41. doi: 10.1126/science.1214935
52. Ayres JS, Schneider DS. Tolerance of Infections. *Annu Rev Immunol* (2012) 30:271–94. doi: 10.1146/annurev-immunol-020711-075030
53. Schneider DS, Ayres JS. Two Ways to Survive Infection: What Resistance and Tolerance can Teach Us About Treating Infectious Diseases. *Nat Rev Immunol* (2008) 8(11):889–95. doi: 10.1038/nri2432
54. Medzhitov R. Septic Shock: On the Importance of Being Tolerant. *Immunity* (2013) 39(5):799–800. doi: 10.1016/j.immuni.2013.10.012
55. Figueiredo N, Chora A, Raquel H, Pejanovic N, Pereira P, Hartleben B, et al. Anthracyclines Induce DNA Damage Response-Mediated Protection Against Severe Sepsis. *Immunity* (2013) 39(5):874–84. doi: 10.1016/j.immuni.2013.08.039
56. Do-Umehara HC, Chen C, Urich D, Zhou L, Qiu J, Jang S, et al. Suppression of Inflammation and Acute Lung Injury by Miz1 via Repression of C/EBP-δ. *Nat Immunol* (2013) 14(5):461–9. doi: 10.1038/ni.2566
57. Rittirsch D, Huber-Lang MS, Flierl MA, Ward PA. Immunodesign of Experimental Sepsis by Cecal Ligation and Puncture. *Nat Protoc* (2009) 4 (1):31–6. doi: 10.1038/nprot.2008.214
58. Misharin AV, Morales-Nebreda L, Mutlu GM, Budinger GR, Perlman H. Flow Cytometric Analysis of Macrophages and Dendritic Cell Subsets in the Mouse Lung. *Am J Respir Cell Mol Biol* (2013) 49(4):503–10. doi: 10.1165/rcmb.2013-0086MA

Conflict of Interest: The authors declare that the research was conducted in the absence of any commercial or financial relationships that could be construed as a potential conflict of interest.

frontiers in Immunology

ORIGINAL RESEARCH
published: 07 December 2021
doi: 10.3389/fimmu.2021.761345

Citrullinated Histone H3 Mediates Sepsis-Induced Lung Injury Through Activating Caspase-1 Dependent Inflammasome Pathway

Yuzi Tian[1,2,3,4], Patrick Li[2,5], Zhenyu Wu[2,6], Qiufang Deng[2], Baihong Pan[2], Kathleen A. Stringer[7,8], Hasan B. Alam[2,9], Theodore J. Standiford[8] and Yongqing Li[2]**

[1] Department of Rheumatology and Immunology, Xiangya Hospital, Central South University, Changsha, China, [2] Department of Surgery, University of Michigan Health System, Ann Arbor, MI, United States, [3] National Clinical Research Center for Geriatric Disorders, Xiangya Hospital, Central South University, Changsha, China, [4] Provincial Clinical Research Center for Rheumatic and Immunologic Diseases, Xiangya Hospital, Central South University, Changsha, China, [5] Department of Internal Medicine, New York University (NYU) Langone Health, New York, NY, United States, [6] Department of Infectious Disease, Second Xiangya Hospital, Central South University, Changsha, China, [7] Department of Clinical Pharmacy, College of Pharmacy, University of Michigan, Ann Arbor, MI, United States, [8] Division of Pulmonary and Critical Care Medicine, University of Michigan Medical Center, Ann Arbor, MI, United States, [9] Department of Surgery, Feinberg School of Medicine, Northwestern University, Chicago, IL, United States

OPEN ACCESS

Edited by:
Krishna Rajarathnam, University of Texas Medical Branch at Galveston, United States

Reviewed by:
Mingfang Lu, Fudan University, China
Krzysztof Guzik, Jagiellonian University, Poland

***Correspondence:**
Yongqing Li
yqli@med.umich.edu
Theodore J. Standiford
tstandif@med.umich.edu

Specialty section:
This article was submitted to Inflammation, a section of the journal Frontiers in Immunology

Received: *19 August 2021*
Accepted: *17 November 2021*
Published: *07 December 2021*

Citation:
Tian Y, Li P, Wu Z, Deng Q, Pan B, Stringer KA, Alam HB, Standiford TJ and Li Y (2021) Citrullinated Histone H3 Mediates Sepsis-Induced Lung Injury Through Activating Caspase-1 Dependent Inflammasome Pathway. Front. Immunol. 12:761345. doi: 10.3389/fimmu.2021.761345

Sepsis is a life-threatening organ dysfunction caused by dysregulated host response to infection that often results in acute lung injury (ALI)/acute respiratory distress syndrome (ARDS). An emerging mechanism of sepsis-induced ARDS involves neutrophils/macrophages undergoing cell death, releasing nuclear histones to cause tissue damage that exacerbates pulmonary injury. While published studies focus on unmodified histones, little is known about the role of citrullinated histone H3 (CitH3) in the pathogenesis of sepsis and ALI. In this study, we found that levels of CitH3 were elevated in the patients with sepsis-induced ARDS and correlated to PaO2/FiO2 in septic patients. Systematic administration of CitH3 peptide in mice provoked Caspase-1 activation in the lung tissue and caused ALI. Neutralization of CitH3 with monoclonal antibody improved survival and attenuated ALI in a mouse sepsis model. Furthermore, we demonstrated that CitH3 induces ALI through activating Caspase-1 dependent inflammasome in bone marrow derived macrophages and bone marrow derived dendritic cells. Our study suggests that CitH3 is an important mediator of inflammation and mortality during sepsis-induced ALI.

Keywords: citrullinated histone H3 (CitH3), sepsis, acute lung injury, Caspase-1 (CASP1), inflammasome

INTRODUCTION

Sepsis is a serious clinical problem with high morbidity and mortality (1–3). The ultimate cause of death in sepsis patients is multiple organ dysfunction. Acute lung injury (ALI), which is clinically manifest as acute respiratory distress syndrome (ARDS), represents the major devastating complication of sepsis (2, 4–7). Despite progress in the understanding of the pathophysiology of

sepsis and organ dysfunction, the treatment relies largely on supportive care (8, 9). Therefore, researches to define the pathogenic mechanisms in sepsis and sepsis-induced ARDS are urgently needed to identify novel therapeutic targets.

One of the main pathophysiological events in of sepsis-induced ARDS is uncontrolled inflammation induced by cytokines and other inflammatory mediators. For example, host-derived danger-associated molecular patterns (DAMPs) like kidney mitochondrial, particularly cell-free mtDNA, developed during ALI/ARDS could act as a critical activator of the innate immune system and inflammation (10–12). Activation of the inflammasome pathway is one of the innate immune defenses triggered during ALI/ARDS (13). Upon sign of cellular 'danger', the signaling platform sensor protein recruits adaptor protein and effector protein to constitute a functional inflammasome. Generally, NLR Family Pyrin Domain Containing 3 (NLRP3) and Absent in Melanoma 2 (AIM2) are the most well-studied inflammasomes in ALI, with both pathways leading to the activation of effector protein Caspase-1 and the maturation of pro-inflammatory cytokines interleukin (IL)-1β and IL-18 (14–16). Elevated IL-1β and IL-18 play prominent roles in promoting inflammation in the lung. For example, elevated levels of circulating IL-18 are associated with a poor long-term prognosis in patients with sepsis-induced ARDS (17). In several different rodent models, IL-18/IL-1β neutralization or IL-1R signaling antagonism reduced lung injury (17–21).

A variety of danger signals are capable of activating inflammasomes. These include pathogen-associated molecular patterns (PAMPs) (22) and DAMPs, such as histone, adenosine triphosphate (ATP) and uric-acid crystals. Histones are important structural elements of the nucleosomes, which regulate gene expression and facilitate the formation of dense chromatin compaction (23). However, circulating histones have been found to be potent inflammasome activators (24). During sterile inflammatory liver injury, histones activate the NLRP3 inflammasome in Kupffer cells (25). In sepsis, extracellular histones mediate multiple organ dysfunction, such as cardiomyopathy (26) and ALI (27), through activating the NLRP3 inflammasome.

Citrullinated histone H3 (CitH3) is the post-translational modified form of histone H3. It is catalyzed by calcium-dependent enzymes peptidyl arginine deiminase 2 (PAD2) and peptidyl arginine deiminase 4 (PAD4). CitH3 has been recently found to be related to the severity of illness in patients with sepsis (28), and may represent a potential therapeutic target for endotoxic shock (29). However, the role of CitH3 in sepsis-induced ARDS is not yet clear. In this study, the expression of CitH3 in septic ARDS patients and septic ALI mouse model was determined. We then explored the effect of CitH3 peptide or neutralizing CitH3 administration in septic mouse model on lung injury and Caspase-1 activation in lung tissue. Finally, the direct effect of CitH3 on Caspase-1 activation in bone marrow derived macrophages (BMDMs) and bone marrow derived dendritic cells (BMDCs) *in vitro* was assessed.

MATERIALS AND METHODS

Human Subjects

Three types of human samples were used in our study: 1) plasma from healthy controls and sepsis-induced ARDS patients, 2) bronchoalveolar lavage fluid (BALF) from healthy controls and sepsis-induced ARDS patients, 3) serum from sepsis patients who were then divided into sepsis patients with ARDS and sepsis patients without ARDS based on PaO2/FiO2 ratio.

Plasma and BALF samples were collected from sepsis-induced ARDS patients and healthy control subjects enrolled in the Acute Lung Injury Specialized Center of Clinically Oriented Research (SCCOR) as a part of a randomized trial of granulocyte-macrophage colony-stimulating factor administration (clinicaltrials.gov NCT00201409) conducted at the University of Michigan (30). Samples from only the placebo arm of the study were utilized. Healthy volunteers were asymptomatic, ambulatory non-smokers under 60 years of age, who had no known chronic medical conditions and were taking no medications. Serum samples and clinical data were collected from patients with sepsis during a consecutive enrollment observation cohort study conduct at the University of Michigan (28). Bronchoalveolar lavage fluid (BALF) was collected and processed by standard techniques. The sample preparation and patient information acquisition have been previously described (31). Human studies were approved by the University of Michigan Institutional Review Board (HUM00056630, IRB#2003-0430 and IRB#2003-0829). Written informed consents were obtained from all participants or their legal proxy for medical decision making before study inclusion.

Mice

Experiments were performed using 8-15 weeks old C57B/6J male mice purchased from Jackson Laboratories. All animals were housed under specific pathogen-free conditions with free access to food and water. Animal studies were performed within the National Institutes of Health guidelines and were approved by the University of Michigan Animal Care and Use Committee (PRO00008861).

CitH3 and H3 Peptides Synthesis

The CitH3 and H3 peptides were generated by New England Peptide Inc (Gardner, MA, USA). The sequence for H3 and Cit H3 peptides are "[H2N-ARTKQTARKSTGGKAPRKQ LATKAARKSAP-amide" and "[H2N-A(Cit)TKQTA(Cit)KSTG GKAP(Cit)KQLATKAA(Cit)KSAP-amide", separately. The purity for both of them is ≥95% measured by HPLC. These peptides have been described in our recent publication (29, 32).

Mouse Models of Acute Lung Injury

Acute lung injury in murine models were induced through two methods: 1) Cecum ligation and puncture (CLP) polymicrobial sepsis model or 2) administration of CitH3 peptide. Briefly, the peritoneal cavity was opened under inhaled isoflurane anesthesia. The cecum was exposed, ligated below the ileocecal

valve using a 5-0 silk suture at 75% percent from the tip, and punctured through and through with a 21-gauge needle. For antibody neutralization experiments, our in-house developed CitH3 monoclonal antibody (26) with four citrulline residues (20mg/kg) or mouse immunoglobulin G (IgG) (20mg/kg) were intravenously injected 4 h after CLP. In the CitH3 peptide challenge model, the CitH3 peptide with four citrulline residues [A(Cit)TKQTA(Cit) KSTGGKAP(Cit) KQLATKAA (Cit)KSAP] (16.5 mg/kg) or vehicle was intravenously administered. For all the animal studies, mice were monitored for 10 days, or sacrificed at specific time points to harvest lung tissue, BALF and serum samples for mechanistic studies.

Lung Injury Analysis

The harvested lung tissues were fixed in 4% paraformaldehyde, embedded in paraffin, and sliced into 5 μm sections. Hematoxylin and Eosin (H&E) staining was performed for histology detection. The ALI scoring was conducted by a pathologist blinded to the experiment groups. ALI was classified into 6 categories based on the parameters of 1) neutrophils, 2) septal hemorrhage and congestion, 3) septal mononuclear cell/lymphocyte infiltration, 4) alveolar hemorrhage, 5) alveolar macrophages, and 6) alveolar edema. The severity of each category was graded from 0 (minimal) to 3 (maximal) and the total score was calculated by adding the scores in each of these categories (28).

BMDMs and BMDCs Isolation

BMDMs and BMDCs were isolated from WT mice using well-established protocols (33). In brief, bone marrow cells were flushed from the femur and tibia using 60 mL of Hank's Balanced Salt Solution, and then incubated with specific completed medium. BMDMs were incubated with Iscove's Modified Dulbecco's Medium (IMDM) supplemented with 20% L929 cell culture medium, penicillin, streptomycin, 2-mercaptoethanol, glutamine, and 10% heat-inactivated fetal calf serum (FBS) (Gibco, Thermo Fisher Scientific). BMDCs were incubated with RPMI-1640 supplemented with 20 ng/ml rmGM-CSF (Biolegend #576302), penicillin, streptomycin, and 10% FBS. The medium was refreshed on day 3. Cells were harvested on day 7 for use in subsequent experiments.

Cell Culture and Treatment

BMDMs and BMDCs were plated in a 12-well plate at the density of 106/ml in the above-mentioned complete medium. The next day, cells were treated with 30 μg/ml CitH3 (Cayman chemical, #17926) or H3 (Cayman chemical, #10263) protein dissolved in opti-MEM medium for 5 h. Cell-free supernatant was reserved for ELISA. Cell lysates were analyzed by Western blot with antibodies against Caspase-1 and β-actin.

Western Blotting

Murine cell and tissue lysates were prepared with radioimmunoprecipitation assay (RIPA) buffer. Protein lysates were separated by sodium dodecyl-sulfate polyacrylamide gel electrophoresis (SDS-PAGE) and transferred to nitrocellulose membranes (Bio-Rad, Hercules, CA). Membranes were probed with anti-CitH3 (Abcam #ab5103, 1:1000 dilution), anti-Caspase-1 (Abcam # ab179515, 1:1000 dilution), anti-IL-1 β (R&D system, # AF-401-NA, 1:1000 dilution) and anti- β -actin (Cell Signaling Technology, #3700, 1:1000 dilution) antibodies, followed by HRP-conjugated anti-rabbit secondary antibody (Invitrogen, #G-21234) or Dylight 800-conjugated anti-mouse secondary antibody (Cell Signaling Technology, #5257S). Images were visualized with ChemiDoc™ Touch Imaging System (Bio-Rad) and analyzed with Image Lab (Bio-Rad).

Enzyme-Linked Immunosorbent Assay (ELISA)

Concentrations of CitH3 were measured by an in-house developed ELISA as previously described (32). Levels of IL-1 β, IL-18 and TNF-α in cell supernatant and BALF were measured by the ELISA core in the University of Michigan using the core-developed sandwich ELISA (34, 35).

Statistical Analyses

For the human data, the Pearson-D'Agostino normality test was first applied. Since none of the comparisons passed the normality test, the non-parametric Mann-Whitney U test was used to compare differences between the two groups.

For mouse *in vivo* and *in vitro* studies, parametric tests were used because the sample size was too small for normality testing. The unpaired two-sided t test was used to compare differences between two groups, and the one-way analysis of variances (ANOVA) followed by Bonferroni's multiple comparisons test was used to compare multiple groups. The survival curve was analyzed by log-rank test.

A p-value less than 0.05 was considered significant for all experiments. Statistical analyses were conducted, and figures generated, using Prism software (GraphPad, San Diego, CA).

RESULTS

CitH3 Is Increased in Septic ARDS Patients and CLP-Induced Animal Model of Sepsis

Sepsis is a common predisposing factor for ARDS. We measured the levels of CitH3 in the plasma and BALF from patients with sepsis-induced ARDS. Compared with healthy volunteers, patients with sepsis-induced ARDS had significantly higher CitH3 concentrations within 7 days of ARDS onset. The elevations of CitH3 were found in both the circulation (**Figure 1A**) and in alveolar space (**Figure 1B**). At the same time, we divided septic patients into two groups based on the PaO2/FiO2 index, and septic patients with PaO2/FiO2 < 300 mmHg showed significantly higher levels of circulating CitH3 (**Figure 1C**). Previously, we have repeatedly showed that CLP induced ALI in the murine model (35, 36). To see the coherence between human sepsis-ARDS and murine sepsis-ALI, the levels of CitH3 were measured in mouse serum and BLAF. Consistent with the results of human ARDS patients, the concentrations of CitH3 were elevated in both serum (**Figure 1D**) and lung tissues

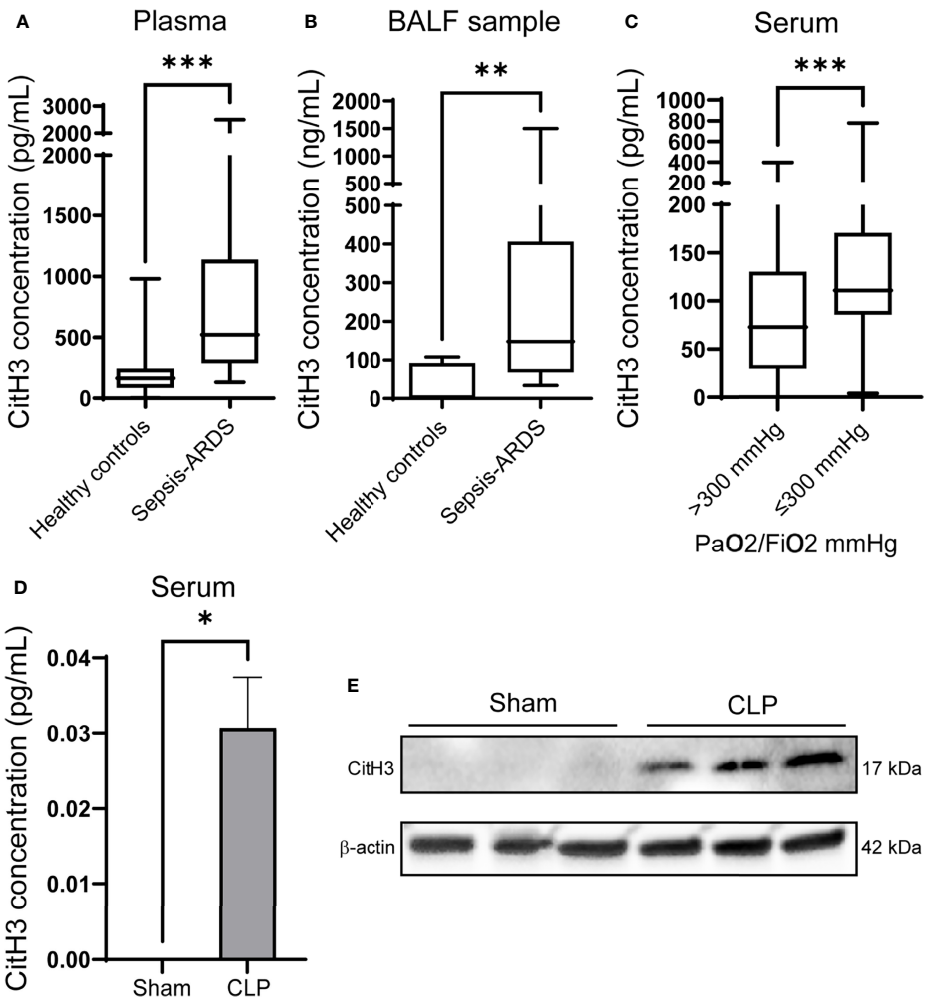

FIGURE 1 | CitH3 is increased in septic ARDS patients and CLP-induced animal model of sepsis. Levels of CitH3 in **(A)** plasma and **(B)** BALF from healthy controls and patients with sepsis-induced ARDS (n = 19 *vs* 13 for plasma samples; n = 7 *vs* 11 for BALF samples). **(C)** Circulating CitH3 in septic patients with PaO2/Fi02 > 300 mmHg (n=90) and ≤300 mmHg (n = 44). **(D)** Levels of serum CitH3 in sham and CLP-induced sepsis-ALI mouse model at 12 hours (n = 3/group). **(E)** Western blot results show the expression of CitH3 in mouse lung tissue with or without CLP (n = 3/group). Nonnormality data are expressed as minimal to maximal value with quantile range **(A–C)**. Data in D are expressed as mean ± SEM. *P < 0.05, **P < 0.01, ***P <0.001. SEM, standard error of the mean.

(**Figure 1E**) of the CLP-induced ALI. Together, our results suggest that CitH3 may be involved in the development of ALI/ARDS.

Systemic Administration of CitH3 Peptide in Mice Leads to Its Accumulation in Lung Tissues and Induces Expression of Endogenous CitH3 Protein

To determine the effect of the CitH3 on lung injury responses *in vivo*, mice were systemically challenged with CitH3 peptide through tail vein injection. The distribution of CitH3 peptide was examined by ELISA afterward. At baseline, the concentration of CitH3 was not detected (<20 pg/ml) in the serum. However, CitH3 was enriched at a high concentration in the serum at 7 h and decreased by 24 h (**Figure 2A**). A similar trend of CitH3 was also found in mouse BALF (**Figure 2B**). Since ELISA was not able to distinguish the signal of exogenous Cith3 peptide from endogenous CitH3 protein, Western blot was performed. We showed the level of CitH3 protein (17 kDa) was also increased in the lung tissue after CitH3 peptide (3.5 kDa) treatment (**Figure 2C**). The results indicate CitH3 peptide injection leads to accumulation and expression of CitH3 in lung tissues.

Systemic Administration of CitH3 Peptide in Mice Induces Caspase-1 Activation and Lung Injury

The histology of lung tissue was examined in mice with CitH3 peptide treatment. Compared with the vehicle group, mice treated with CitH3 showed pathological features of ALI, manifested as more inflammatory infiltration, alveolar

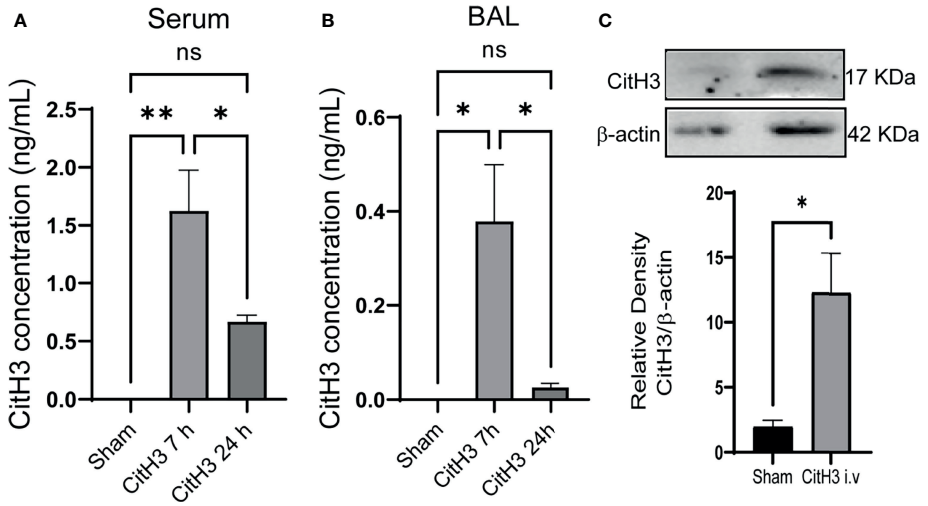

FIGURE 2 | Intravenous injection of Cith3 in mouse induces its accumulation in lung tissue. Levels of CitH3 in **(A)** serum (n = 3, 4, 4 for each group) and **(B)** BALF (n = 3, 5, 5 for each group) in mouse after i.v. injection of CitH3 peptide at 0 h, 7 h and 24 h. **(C)** Representative Western blot images and densitometry quantification of expression of CitH3 protein in mouse lung tissue with or without CitH3 peptide challenging (n = 3/group) at 24 h. Data are expressed as mean ± SEM. *P < 0.05, **P < 0.01. i.v., intravenous; ns, not significant; SEM, standard error of the mean.

hemorrhage, pulmonary congestion, edema, and thickening of the alveolar wall (**Figure 3A**). We hypothesized that extracellular CitH3 mediated ALI through activating Caspase-1 dependent inflammasome. Caspase-1 activation and cytokine release were examined. The activation of Caspase-1 in the lung tissue of the CitH3 treatment group was significantly increased (**Figure 3B**), and the release of IL-1β, IL-18 and TNF-α in BALF was also observed (**Figures 3C–E**).

CitH3 Activates Caspase-1 Dependent Inflammasomes in BMDMs and BMDCs

To further verify the activation effects of CitH3 protein on Caspase-1 dependent inflammasomes, we used CitH3 protein to stimulate BMDMs and BMDCs *in vitro*. The CitH3 protein induced robust Caspase-1 activation in both BMDMs and BMDCs, which was manifested by increased Caspase-1 cleavage (**Figures 4A, B**) and IL-1 β and IL-18 secretion (**Figures 4C, D**). It has been reported that histone H3 protein activates Caspase-1 dependent inflammasomes, such as NLRP3, and triggers sterile inflammation. In this study, CitH3 protein was more effective than H3 peptide in inducing the activation of Caspase-1 and elevation of IL-1β and IL-18. It is worth noting that TNF-α, an important transcription regulator of the inflammasome (37), was also significantly up-regulated after treatment with the CitH3 protein in BMDMs and BMDCs (**Figures 4C–D**).

Neutralization of CitH3 Decreases Mortality and Lung Injury in Sepsis-Induced ALI Model

We further showed that neutralizing CitH3 by intravenous injection of CitH3 antibody significantly increased the survival rate of CLP-induced septic mice, compared with the IgG group (**Figure 5A**). As expected, the lung injury was also attenuated in the CitH3 antibody treatment group (**Figure 5B**). CLP augmented significant Caspase-1 activation in the lung tissue, and treatment with CitH3 antibody attenuated this effect as assessed by pro-Caspase-1 and pro-IL-1β cleavage (**Figure 5C**).

DISCUSSION

In the current study, we have demonstrated for the first time that the expression of CitH3 was increased in the serum and BALF of the patients with sepsis-induced ARDS. In addition, the CitH3 levels in the septic patients with PaO2/FiO2 ≤ 300 were significantly higher than that of sepsis patients with PaO2/FiO2>300. Systematic administration of CitH3 peptide in mice provokes Caspase-1 activation in the lung tissue and causes acute lung injury, which may be mediated by CitH3-induced Caspase-1 activation in BMDMs and BMDCs. Neutralization of CitH3 with a monoclonal antibody in the CLP-induced sepsis model improves survival and attenuates acute lung injury as well as pro-Caspase-1 cleavage in the lung tissue.

Extracellular histone H3 has previously been identified as a potential mediator of sepsis and sepsis-induced organ injury (27, 38, 39). However, histone H3 could undergo various post-translational modifications (PTM) under stress before being released, such as phosphorylation, acetylation, methylation, ubiquitination and citrullination. These PTMs are recognized as important mechanisms for regulating gene expression, but few studies have focused on the effects of these modified histones on sepsis and ALI after they are released from the cell. CitH3 is a key

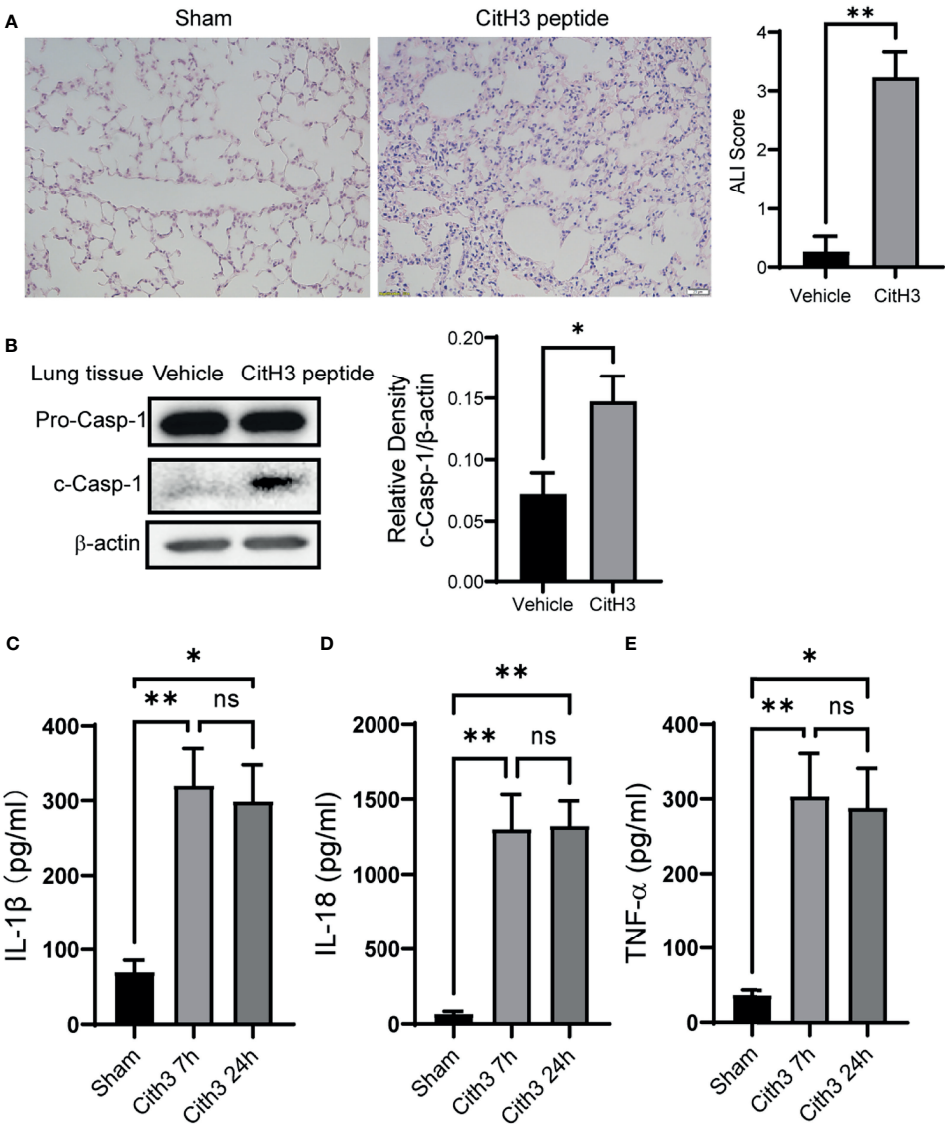

FIGURE 3 | Intravenous injection of CitH3 induces Caspase-1 activation in lung tissue. **(A)** Representative histology images of murine lungs and ALI score following H&E staining in Sham and CitH3 treatment group. **(B)** Representative Western blot images and densitometry quantification of activation of Caspase-1 in mouse lung tissue with or without CitH3 peptide challenging (n = 3/group). Concentrations of **(C)** IL-1β, **(D)** IL-18, and **(E)** TNF-α in the BALF in mouse after i.v. injection of CitH3 peptide at 0 h, 7 h, and 24 h (n = 4/group). Data are expressed as mean ± SEM. *P < 0.05, **P < 0.01. i.v., intravenous; ns, not significant, SEM, standard error of the mean.

component released from cells during the formation of neutrophil extracellular traps (NETs), which is a form of neutrophil death triggered by stimuli such as microbial, DAMPs and other noxious agents. In 2011, our team first identified CitH3, the post-translational form of H3, as a potential serum protein biomarker in a lethal model of lipopolysaccharides (LPS)-induced shock (40). Over the last decade, we have made significant progress in establishing CitH3 as a reliable biomarker for septic patients and the concentrations of CitH3 in blood correlated with disease severity (28). Moreover, we demonstrated chemical interventions that inhibit CitH3 are beneficial in mouse models of both endotoxic and septic shock. Targeting CitH3 is a potential therapeutic strategy for the mouse model of endotoxic shock (29). Consistent with our findings, Tsung et al. found that CitH3 was elevated in lung tissue of murine ALI model as part of component of NETs released during ALI (41). Besides, Yuan's team found that CitH3 caused endothelial barrier dysfunction (42). And histone H3 citrullination has been reported to reduce antibacterial activity and exacerbates proteolytic degradation of histone H3 (43). The current study revealed an association between extracellular CitH3 and the severity of sepsis-ALI and possible mechanisms involved, identifying CitH3 as a potentially viable therapeutic target to reduce the severity and consequences of sepsis-ALI.

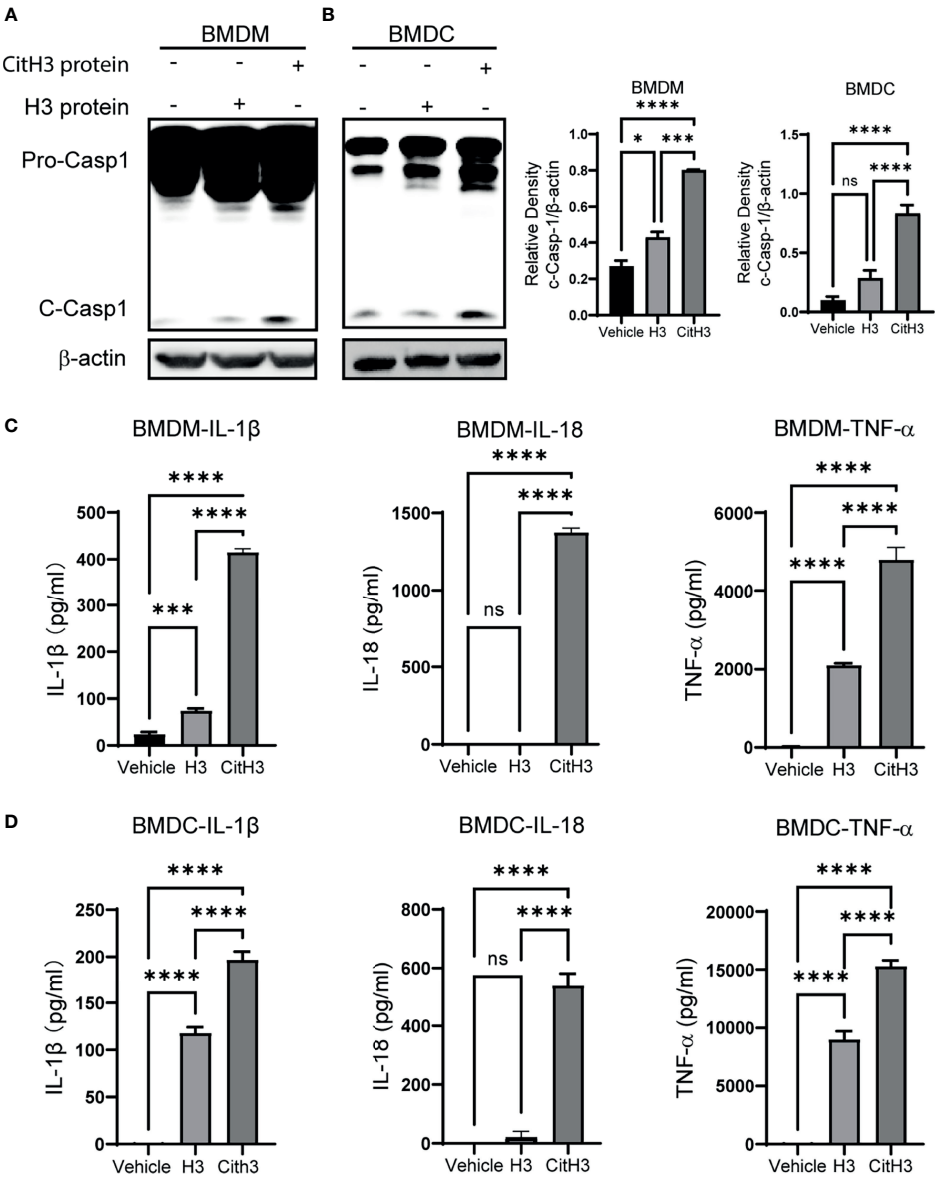

FIGURE 4 | CitH3 induces activation of Caspase-1 in BMDMs and BMDCs. BMDMs and BMDCs were isolated from WT mice. Representative Western blot images and densitometry quantification of activation of Caspase-1 in **(A)** BMDMs (n = 3) and **(B)** BMDCs (n = 5) after treatment with vehicle, H3 or CitH3 for 5 h. Concentrations of IL-1β, IL-18 and TNF-α in the supernatant of **(C)** BMDMs (n = 4/group) and **(D)** BMDCs (n = 5/group) after treatment with vehicle, H3 or CitH3 for 5 h. Results are representative of more than 3 independent experiments. Data are expressed as mean ± SEM. *P < 0.05, ***P < 0.001, ****P < 0.0001. ns, not significant; SEM, standard error of the mean.

While this study focused on sepsis-ALI/ARDS, we found that the levels of CitH3 were elevated in both the alveolar space and in the circulation of septic patients, suggesting that CitH3 may not only play a role in local inflammatory response but also the systemic inflammatory changes seen in sepsis. However, after challenging mice with CitH3 peptide, the lung tissue showed the most significant elevation of endogenous CitH3 protein compared to other tissues (**Supplemental Figure 1**), which indicates that CitH3 may preferentially localize in the lung. That is in accordance with the fact that lung is a highly vulnerable organ in sepsis. It is tempting to speculate that circulating CitH3 peptide that accumulates in lung tissue after tail vein injection may directly or indirectly activate neutrophils or other immune cells, and ultimately lead to the passive or active release of CitH3 protein.

As with sepsis-ALI/ARDS, we suspect NETs are the important source of CitH3. Systematic inflammation and infection induce neutrophils to migrate to the lung tissue and release the NETs to sequester bacteria, which is a mechanism for pathogen inactivation proposed previously. NETs, which contain

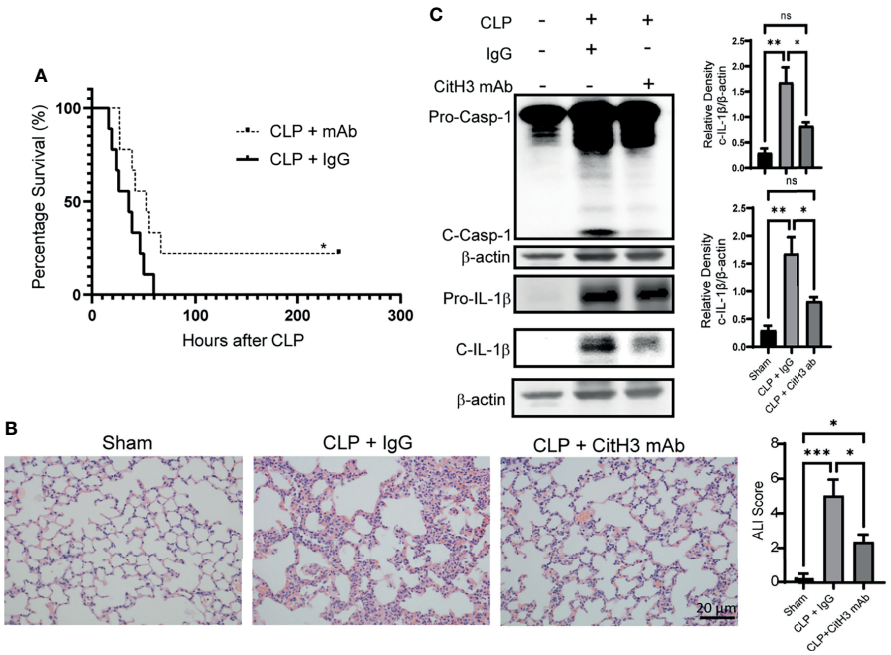

FIGURE 5 | Neutralization of CitH3 in murine CLP model decreases mortality and Caspase-1 induced lung injury. WT mice were subject to CLP model and then intravenously (4h after CLP) treated with 20 mg/kg IgG or CitH3 monoclonal antibody. **(A)** The survival curve of mice with or without CitH3 monoclonal antibody in CLP model (n = 9/group). **(B)** Representative histology images of murine lungs and ALI score following H&E staining in Sham, CLP with IgG or CitH3 monoclonal antibody treatment group at 24 h. **(C)** Representative Western blot images and densitometry quantification of activation of Caspase-1 (n = 3/group) and cleavage of IL-1β (n = 4/group) in the lung tissues of Sham, CLP with IgG or CitH3 monoclonal antibody treatment group at 24 h. Data are expressed as mean ± SEM. *P < 0.05, **P < 0.01, ***P <0.001. ns, not significant; SEM, standard error of the mean.

a complex of chromatin fibers mixed with granule-derived antimicrobial peptides and enzymes, trap and kill bacteria (44–46). While NETs can help to target and trap bacteria, the released CitH3 aggravates pulmonary inflammation in lung by activating Caspase-1 dependent inflammasomes in BMDMs and BMDCs, which may further exacerbate lung injury.

Caspase-1 mediated inflammasome activation in macrophages and dendritic cells plays an important role in ALI (47). In the present study, CitH3 induced Caspase-1 activation in both BMDMs and BMDCs. Of note, to activate Caspase-1 *in vitro*, it normally requires PAMPs like LPS priming process to induce production of pro-Caspase-1, pro-IL-1β and pro-IL-18. However, CitH3 treatment not only can induce Caspase-1 activation, but also could induce significant elevation of pro-Caspase-1 and pro-IL-1β itself (**Supplemental Figure 2**). We observed that incubation of BMDMs and BMDCs with CitH3 protein can also release large amounts of TNF-α in the supernatant. TNF-α was found to activate selectively the NLRP3 inflammasome without the requirement for a priming signal through the TNF receptor–Caspase-8–Caspase-1 pathway (48, 49). Besides, it was reported that TNF-α is an important transcriptional regulator of inflammasome components (50). Tnf–/– BMDCs and mice showed a marked reduction expression of inflammasome components, including pro-Caspase-1, pro-IL-1b and pro-IL-18 (37). Thus, we suspect that CitH3 protein could trigger both NF-Kβ and Caspase-1 pathway activation. The TNF-α released from BMDMs and BMDCs by CitH3 treatment could activate TNF receptor–Caspase-8–Caspase-1 pathway directly or induce the expression of pro-Caspase-1, pro-IL-1β and pro-IL-18. At the same time, CitH3 activates the inflammasome, leading to the cleavage of pro-Caspase-1, pro-IL-1β and pro-IL-18.

The lungs are populated by macrophages, which are equipped with a set of pattern recognition receptors (PRRs), including Toll-like receptors (TLR) and scavenger receptors, readily respond to DAMPs. Several studies have shown that inflammation caused by TLR activation by endogenous ligands participates in the development of ALI/ARDS (51, 52). In contrast to the homeostatic apoptosis, highly pro-inflammatory necrotic types of cell death, such as necroptosis and pyroptosis tend to trigger an inflammatory response during ALI/ARDS. In this current study, CitH3 peptide also induced cell death after treatment in BMDMs (**Supplemental Figure 3**). Therefore, in addition to releasing IL-1β and TNF-α, CitH3 may also exaggerate ALI by releasing DAMPs into the lung tissue through Caspase-1 mediated pyroptosis pathway. In contrast to the IL-1β release and Caspase-1 cleavage, the H3 treatment group showed comparable cell death to the CitH3 treatment group (**Supplemental Figure 3**). This indicates that CitH3 and/or H3 may activate multiple cell death pathways besides Caspase-1 mediated cell death. Actually, the high concentration of TNF-α released after treatment with CitH3 and H3 can also induced other lytic cell death like necroptosis (53). Interestingly, a recent study showed that

prolonged exposure of myeloid cells to DAMPs like oxLDLs can induce cell to switch between cell death pathways (54). CitH3 and H3 may also activate different cell death pathways simultaneously or undergo a transition between different cell death pathways. Altogether, the DMAPs released by CitH3 induced cell death may also be an important effector mechanism of CitH3.

CitH3 is catalyzed by PAD2 and PAD4, two enzymes present in both neutrophils and macrophages. We used citrullinated histone H3 (R2/R8/R17/R26) peptide to develop the CitH3 mAb antibody used in this study. This CitH3 mAb recognizes epitopes on CitH3 that are specific for both PAD4 (R2/R8/R17) (55) and PAD2 (R26) (56). Therefore, it can more effectively sequester CitH3 generated by both PAD2 and PAD4 as compared with the commercial CitH3 antibody bound only to the epitope of R2/R8/R17 (29), which makes it a potentially effective agent for treating sepsis-ALI in animal models.

This study has several limitations. We only identified the role for CitH3 in a murine CLP model of sepsis-induced ALI, whereas its role in other ALI models (such as pneumonia-ALI) requires further study. In addition, our study showed that CitH3 mediates lung injury through Caspase-1 dependent inflammasome pathway. However, multiple inflammasomes such as NLRP3, AIM2, and pyrin, could lead to activation of Caspase-1. Both AIM2 and NLRP3 have been reported to participate in the pathogenesis of ALI/ARDS (57, 58). It is unclear whether CitH3 induced Caspase-1 cleavage due to the activation of NLRP3 or other inflammasomes, or a combination of multiple different ones. Moreover, our *in vitro* experiments demonstrated that CitH3 significantly induced more Caspase-1 activation compared to H3. Even so, it is still important to determine whether such effect could be extended to all *in vivo* studies. Further investigations are required to have a better understanding of the precise mechanisms in the future.

In conclusion, we have shown that CitH3 is associated with relevant clinical outcomes in sepsis-ARDS in patients and in murine models of lung injury. CitH3 induces Caspase-1 dependent inflammasome activation in BMDMs and BMDCs *in vitro*, and leads to acute lung injury *in vivo*. Moreover, we demonstrated that treatment of septic mice with CitH3 monoclonal antibody significantly improves survival and sepsis-ALI in a murine model of CLP-induced septic shock, likely due to inhibition of CitH3 activated Caspase-1 dependent inflammasome pathway. Blockade of the CitH3-Caspase-1 pathway may represent a promising therapeutic target for septic shock and sepsis-induced ALI.

DATA AVAILABILITY STATEMENT

The raw data supporting the conclusions of this article will be made available by the authors, without undue reservation.

ETHICS STATEMENT

The studies involving human participants were reviewed and approved by University of Michigan Institutional Review Board. The patients/participants provided their written informed consent to participate in this study. The animal study was reviewed and approved by University of Michigan Animal Care and Use Committee.

AUTHOR CONTRIBUTIONS

YL, TS, HA, YT, and PL contributed to the concept and design of the study. KS and TS provided the clinical data and samples. YT, ZW, QD, and BP contributed to the performance of the assays. YT performed all the statistical analysis and wrote the manuscript. YL, TS, and KS contributed to the revision of manuscript. All authors contributed to the article and approved the submitted version.

FUNDING

This work was funded by grants from the National Institute of Health R01 (R01HL155116) to YL and HA and the Joint-of-Institute (Grant# U068874) to YL.

SUPPLEMENTARY MATERIAL

The Supplementary Material for this article can be found online at: https://www.frontiersin.org/articles/10.3389/fimmu.2021.761345/full#supplementary-material

REFERENCES

1. Ferrer R, Artigas A, Suarez D, Palencia E, Levy MM, Arenzana A, et al. Effectiveness of Treatments for Severe Sepsis: A Prospective, Multicenter, Observational Study. *Am J Respir Crit Care Med* (2009) 180(9):861–6. doi: 10.1164/rccm.200812-1912OC
2. Husak L, Marcuzzi A, Herring J, Wen E, Yin L, Capan DD, et al. National Analysis of Sepsis Hospitalizations and Factors Contributing to Sepsis in-Hospital Mortality in Canada. *Healthc Q* (2010) 13 Spec No:35–41. doi: 10.12927/hcq.2010.21963
3. Angus DC, van der Poll T. Severe Sepsis and Septic Shock. *N Engl J Med* (2013) 369(21):2063. doi: 10.1056/NEJMra1208623
4. Ware LB, Matthay MA. The Acute Respiratory Distress Syndrome. *N Engl J Med* (2000) 342(18):1334–49. doi: 10.1056/NEJM200005043421806
5. Angus DC, Linde-Zwirble WT, Lidicker J, Clermont G, Carcillo J, Pinsky MR. Epidemiology of Severe Sepsis in the United States: Analysis of Incidence, Outcome, and Associated Costs of Care. *Crit Care Med* (2001) 29(7):1303–10. doi: 10.1097/00003246-200107000-00002
6. Hotchkiss RS, Karl IE. The Pathophysiology and Treatment of Sepsis. *N Engl J Med* (2003) 348(2):138–50. doi: 10.1056/NEJMra021333
7. Sandrock CE, Albertson TE. Controversies in the Treatment of Sepsis. *Semin Respir Crit Care Med* (2010) 31(1):66–78. doi: 10.1055/s-0029-1246290
8. Stearns-Kurosawa DJ, Osuchowski MF, Valentine C, Kurosawa S, Remick DG. The Pathogenesis of Sepsis. *Annu Rev Pathol* (2011) 6:19–48. doi: 10.1146/annurev-pathol-011110-130327
9. King EG, Bauzá GJ, Mella and D.G. Remick JR. Pathophysiologic Mechanisms in Septic Shock. *Lab Invest* (2014) 94(1):4–12. doi: 10.1038/labinvest.2013.110

10. Hernández-Beeftink T, Guillen-Guio B, Rodríguez-Pérez H, Marcelino-Rodríguez I, Lorenzo-Salazar JM, Corrales A, et al. Whole-Blood Mitochondrial DNA Copies Are Associated With the Prognosis of Acute Respiratory Distress Syndrome After Sepsis. *Front Immunol* (2021) 12:737369. doi: 10.3389/fimmu.2021.737369
11. Varon J, Englert JA. Kidney-Lung Cross Talk During ARDS: Mitochondrial DAMPs Join the Conversation. *Am J Physiol Lung Cell Mol Physiol* (2021) 320 (5):L819–20. doi: 10.1152/ajplung.00093.2021
12. Hepokoski M, Wang J, Li K, Li Y, Gupta P, Mai T, et al. Altered Lung Metabolism and Mitochondrial DAMPs in Lung Injury Due to Acute Kidney Injury. *Am J Physiol Lung Cell Mol Physiol* (2021) 320(5):L821–31. doi: 10.1152/ajplung.00578.2020
13. Schroder K, Tschopp J. The Inflammasomes. *Cell* (2010) 140(6):821–32. doi: 10.1016/j.cell.2010.01.040
14. Martinon F, Burns K, Tschopp J. The Inflammasome: A Molecular Platform Triggering Activation of Inflammatory Caspases and Processing of proIL-Beta. *Mol Cell* (2002) 10(2):417–26. doi: 10.1016/S1097-2765(02)00599-3
15. Davis BK, Wen H, Ting JP. The Inflammasome NLRs in Immunity, Inflammation, and Associated Diseases. *Annu Rev Immunol* (2011) 29:707–35. doi: 10.1146/annurev-immunol-031210-101405
16. De Nardo D, Latz E. NLRP3 Inflammasomes Link Inflammation and Metabolic Disease. *Trends Immunol* (2011) 32(8):373–9. doi: 10.1016/j.it.2011.05.004
17. Dolinay T, Kim YS, Howrylak J, Hunninghake GM, An CH, Fredenburgh L, et al. Inflammasome-Regulated Cytokines Are Critical Mediators of Acute Lung Injury. *Am J Respir Crit Care Med* (2012) 185(11):1225–34. doi: 10.1164/rccm.201201-0003OC
18. Jordan JA, Guo RF, Yun EC, Sarma V, Warner RL, Crouch LD, et al. Role of IL-18 in Acute Lung Inflammation. *J Immunol* (2001) 167(12):7060–8. doi: 10.4049/jimmunol.167.12.7060
19. Kuipers MT, Aslami H, Janczy JR, van der Sluijs KF, Vlaar AP, Wolthuis EK, et al. Ventilator-Induced Lung Injury Is Mediated by the NLRP3 Inflammasome. *Anesthesiology* (2012) 116(5):1104–15. doi: 10.1097/ALN.0b013e3182518bc0
20. Cohen TS, Prince AS. Activation of Inflammasome Signaling Mediates Pathology of Acute P. Aeruginosa Pneumonia. *J Clin Invest* (2013) 123 (4):1630–7. doi: 10.1172/JCI66142
21. Wu J, Yan Z, Schwartz DE, Yu J, Malik AB, Hu G. Activation of NLRP3 Inflammasome in Alveolar Macrophages Contributes to Mechanical Stretch-Induced Lung Inflammation and Injury. *J Immunol* (2013) 190(7):3590–9. doi: 10.4049/jimmunol.1200860
22. Franchi L, Muñoz-Planillo R, Reimer T, Eigenbrod T, Núñez G. Inflammasomes as Microbial Sensors. *Eur J Immunol* (2010) 40(3):611–5. doi: 10.1002/eji.200940180
23. Venkatesh S, Workman JL. Histone Exchange, Chromatin Structure and the Regulation of Transcription. *Nat Rev Mol Cell Biol* (2015) 16(3):178–89. doi: 10.1038/nrm3941
24. Allam R, Darisipudi MN, Tschopp J, Anders HJ. Histones Trigger Sterile Inflammation by Activating the NLRP3 Inflammasome. *Eur J Immunol* (2013) 43(12):3336–42. doi: 10.1002/eji.201243224
25. Huang H, Chen HW, Evankovich J, Yan W, Rosborough BR, Nace GW, et al. Histones Activate the NLRP3 Inflammasome in Kupffer Cells During Sterile Inflammatory Liver Injury. *J Immunol* (2013) 191(5):2665–79. doi: 10.4049/jimmunol.1202733
26. Kalbitz M, Grailer JJ, Fattahi F, Jajou L, Herron TJ, Campbell KF, et al. Role of Extracellular Histones in the Cardiomyopathy of Sepsis. *FASEB J* (2015) 29 (5):2185–93. doi: 10.1096/fj.14-268730
27. Grailer JJ, Canning BA, Kalbitz M, Haggadone MD, Dhond RM, Andjelkovic AV, et al. Critical Role for the NLRP3 Inflammasome During Acute Lung Injury. *J Immunol* (2014) 192(12):5974–83. doi: 10.4049/jimmunol.1400368
28. Tian Y, Russo RM, Li Y, Karmakar M, Liu B, Puskarich MA, et al. Serum Citrullinated Histone H3 Concentrations Differentiate Patients With Septic Verses Non-Septic Shock and Correlate With Disease Severity. *Infection* (2021) 49(1):83–93. doi: 10.1007/s15010-020-01528-y
29. Deng Q, Pan B, Alam HB, Liang Y, Wu Z, Liu B, et al. Citrullinated Histone H3 as a Therapeutic Target for Endotoxic Shock in Mice. *Front Immunol* (2019) 10:2957. doi: 10.3389/fimmu.2019.02957
30. Paine R3rd, Standiford TJ, Dechert RE, Moss M, Martin GS, Rosenberg AL, et al. A Randomized Trial of Recombinant Human Granulocyte-Macrophage Colony Stimulating Factor for Patients With Acute Lung Injury. *Crit Care Med* (2012) 40(1):90–7. doi: 10.1097/CCM.0b013e31822d7bf0
31. Kovach MA, Singer B, Martinez-Colon G, Newstead MW, Zeng X, Mancuso P, et al. IL-36γ Is a Crucial Proximal Component of Protective Type-1-Mediated Lung Mucosal Immunity in Gram-Positive and -Negative Bacterial Pneumonia. *Mucosal Immunol* (2017) 10(5):1320–34. doi: 10.1038/mi.2016.130
32. Pan B, Alam HB, Chong W, Mobley J, Liu B, Deng Q, et al. CitH3: A Reliable Blood Biomarker for Diagnosis and Treatment of Endotoxic Shock. *Sci Rep* (2017) 7(1):8972. doi: 10.1038/s41598-017-09337-4
33. He Y, Zeng MY, Yang D, Motro B, Núñez G. NEK7 Is an Essential Mediator of NLRP3 Activation Downstream of Potassium Efflux. *Nature* (2016) 530 (7590):354–7. doi: 10.1038/nature16959
34. Magupalli VG, Negro R, Tian Y, Hauenstein AV, Di Caprio G, Skillern W, et al. HDAC6 Mediates an Aggresome-Like Mechanism for NLRP3 and Pyrin Inflammasome Activation. *Science* (2020) 369(6510):eaas8995. doi: 10.1126/science.aas8995
35. Tian Y, Qu S, Alam HB, Williams AM, Wu Z, Deng Q, et al. Peptidylarginine Deiminase 2 has Potential as Both a Biomarker and Therapeutic Target of Sepsis. *JCI Insight* (2020) 5(20):e138873. doi: 10.1172/jci.insight.138873
36. Deng Q, Zhao T, Pan B, Dennahy IS, Duan X, Williams AM, et al. Protective Effect of Tubastatin A in CLP-Induced Lethal Sepsis. *Inflammation* (2018) 41 (6):2101–9. doi: 10.1007/s10753-018-0853-0
37. McGeough MD, Wree A, Inzaugarat ME, Haimovich A, Johnson CD, Peña CA, et al. TNF Regulates Transcription of NLRP3 Inflammasome Components and Inflammatory Molecules in Cryopyrinopathies. *J Clin Invest* (2017) 127(12):4488–97. doi: 10.1172/JCI90699
38. Xu J, Zhang X, Pelayo R, Monestier M, Ammollo CT, Semeraro F, et al. Extracellular Histones Are Major Mediators of Death in Sepsis. *Nat Med* (2009) 15(11):1318–21. doi: 10.1038/nm.2053
39. Lv X, Wen T, Song J, Xie D, Wu L, Jiang X, et al. Extracellular Histones Are Clinically Relevant Mediators in the Pathogenesis of Acute Respiratory Distress Syndrome. *Respir Res* (2017) 18(1):165. doi: 10.1186/s12931-017-0651-5
40. Li Y, Liu B, Fukudome EY, Lu J, Chong W, Jin G, et al. Identification of Citrullinated Histone H3 as a Potential Serum Protein Biomarker in a Lethal Model of Lipopolysaccharide-Induced Shock. *Surgery* (2011) 150(3):442–51. doi: 10.1016/j.surg.2011.07.003
41. Liu S, Su X, Pan P, Zhang L, Hu Y, Tan H, et al. Neutrophil Extracellular Traps Are Indirectly Triggered by Lipopolysaccharide and Contribute to Acute Lung Injury. *Sci Rep* (2016) 6(1):1–8. doi: 10.1038/srep37252
42. Meegan JE, Yang X, Beard RSJr., Jannaway M, Chatterjee V, Taylor-Clark TE, et al. Citrullinated Histone 3 Causes Endothelial Barrier Dysfunction. *Biochem Biophys Res Commun* (2018) 503(3):1498–502. doi: 10.1016/j.bbrc.2018.07.069
43. Tanner L, Bhongir RKV, Karlsson CAQ, Le S, Ljungberg JK, Andersson P, et al. Citrullination of Extracellular Histone H3.1 Reduces Antibacterial Activity and Exacerbates Its Proteolytic Degradation. *J Cyst Fibros* (2021) 20(2):346–55. doi: 10.1016/j.jcf.2020.07.010
44. Williams AE, Chambers RC. The Mercurial Nature of Neutrophils: Still an Enigma in ARDS? *Am J Physiol Lung Cell Mol Physiol* (2014) 306(3):L217–30. doi: 10.1152/ajplung.00311.2013
45. Standiford TJ, Ward PA. Therapeutic Targeting of Acute Lung Injury and Acute Respiratory Distress Syndrome. *Transl Res* (2016) 167(1):183–91. doi: 10.1016/j.trsl.2015.04.015
46. Twaddell SH, Baines KJ, Grainge C, Gibson PG. The Emerging Role of Neutrophil Extracellular Traps in Respiratory Disease. *Chest* (2019) 156 (4):774–82. doi: 10.1016/j.chest.2019.06.012
47. Peukert K, Fox M, Schulz S, Feuerborn C, Frede S, Putensen C, et al. Inhibition of Caspase-1 With Tetracycline Ameliorates Acute Lung Injury. *Am J Respir Crit Care Med* (2021) 204(1):53–63. doi: 10.1164/rccm.202005-1916OC
48. Gaidt MM, Ebert TS, Chauhan D, Schmidt T, Schmid-Burgk JL, Rapino F, et al. Human Monocytes Engage an Alternative Inflammasome Pathway. *Immunity* (2016) 44(4):833–46. doi: 10.1016/j.immuni.2016.01.012
49. Verma D, Fekri SZ, Sigurdardottir G, Bivik Eding C, Sandin C, Enerbäck C. Enhanced Inflammasome Activity in Patients With Psoriasis Promotes

Systemic Inflammation. *J Invest Dermatol* (2021) 141(3):586–95.e5. doi: 10.1016/j.jid.2020.07.012
50. Sharma D, Malik A, Guy C, Vogel P, Kanneganti TD. TNF/TNFR Axis Promotes Pyrin Inflammasome Activation and Distinctly Modulates Pyrin Inflammasomopathy. *J Clin Invest* (2019) 129(1):150–62. doi: 10.1172/JCI121372
51. Tolle LB, Standiford TJ. Danger-Associated Molecular Patterns (DAMPs) in Acute Lung Injury. *J Pathol* (2013) 229(2):145–56. doi: 10.1002/path.4124
52. Land WG. Role of DAMPs in Respiratory Virus-Induced Acute Respiratory Distress Syndrome—With a Preliminary Reference to SARS-CoV-2 Pneumonia. *Genes Immun* (2021) p:1–20. doi: 10.1038/s41435-021-00140-w
53. Trimova G, Yamagata K, Iwata S, Hirata S, Zhang T, Uemura F, et al. Tumour Necrosis Factor Alpha Promotes Secretion of 14-3-3η by Inducing Necroptosis in Macrophages. *Arthritis Res Ther* (2020) 22(1):1–11. doi: 10.1186/s13075-020-2110-9
54. Nogieć A, Bzowska M, Demczuk A, Varol and K. Guzik C. Phenotype and Response to PAMPs of Human Monocyte-Derived Foam Cells Obtained by Long-Term Culture in the Presence of oxLDLs. *Front Immunol* (2020) 11:1592. doi: 10.3389/fimmu.2020.01592
55. Wang Y, Wysocka J, Sayegh J, Lee YH, Perlin JR, Leonelli L, et al. Human PAD4 Regulates Histone Arginine Methylation Levels via Demethylimination. *Science* (2004) 306(5694):279–83. doi: 10.1126/science.1101400
56. Zhang X, Bolt M, Guertin MJ, Chen W, Zhang S, Cherrington BD, et al. Peptidylarginine Deiminase 2-Catalyzed Histone H3 Arginine 26 Citrullination Facilitates Estrogen Receptor α Target Gene Activation. *Proc Natl Acad Sci USA* (2012) 109(33):13331–6. doi: 10.1073/pnas.1203280109
57. Wu G, Zhu Q, Zeng J, Gu X, Miao Y, Xu W, et al. Extracellular Mitochondrial DNA Promote NLRP3 Inflammasome Activation and Induce Acute Lung Injury Through TLR9 and NF-κb. *J Thorac Dis* (2019) 11(11):4816–28. doi: 10.21037/jtd.2019.10.26
58. Wang J, Li R, Peng Z, Hu B, Rao X, Li J. HMGB1 Participates in LPS–induced Acute Lung Injury by Activating the AIM2 Inflammasome in Macrophages and Inducing Polarization of M1 Macrophages via TLR2, TLR4, and RAGE/Nf–κb Signaling Pathways. *Int J Mol Med* (2020) 45(1):61–80. doi: 10.3892/ijmm.2019.4402

Conflict of Interest: The authors declare that the research was conducted in the absence of any commercial or financial relationships that could be construed as a potential conflict of interest.

Publisher's Note: All claims expressed in this article are solely those of the authors and do not necessarily represent those of their affiliated organizations, or those of the publisher, the editors and the reviewers. Any product that may be evaluated in this article, or claim that may be made by its manufacturer, is not guaranteed or endorsed by the publisher.

frontiers in Immunology

ORIGINAL RESEARCH
published: 06 January 2022
doi: 10.3389/fimmu.2021.786666

Lactylated Histone H3K18 as a Potential Biomarker for the Diagnosis and Predicting the Severity of Septic Shock

Xin Chu[1†], Chenyi Di[1†], Panpan Chang[2], Lina Li[3], Zhe Feng[1], Shirou Xiao[1], Xiaoyu Yan[1], Xiaodong Xu[4], Hexin Li[5], Ruomei Qi[6], Huan Gong[6], Yanyang Zhao[6], Fei Xiao[5] and Zhigang Chang[1]*

[1] Department of Surgical Intensive Care Medicine, Beijing Hospital, National Center of Gerontology, Institute of Geriatric Medicine, Chinese Academy of Medical Sciences, Beijing, China, [2] Trauma Center, Department of Orthopaedics and Traumatology, Peking University People's Hospital, Beijing, China, [3] School of Traditional Chinese Medicine, Beijing University of Chinese Medicine, Beijing, China, [4] Department of Haematology, Beijing Hospital, National Center of Gerontology, Institute of Geriatric Medicine, Chinese Academy of Medical Sciences, Beijing, China, [5] Clinical Biobank, Beijing Hospital, National Center of Gerontology, Institute of Geriatric Medicine, Chinese Academy of Medical Sciences, Beijing, China, [6] The Key Laboratory of Geriatrics, Beijing Institute of Geriatrics, Institute of Geriatric Medicine, Chinese Academy of Medical Sciences, Beijing Hospital/National Center of Gerontology of National Health Commission, Beijing, China

OPEN ACCESS

Edited by:
Wei Chong,
The First Affiliated Hospital of China Medical University, China

Reviewed by:
Christine Uta Vohwinkel, University of Colorado Denver, United States
Xianjin Du, Wuhan University, China

***Correspondence:**
Zhigang Chang
zhigangchang@hotmail.com

[†]*These authors have contributed equally to this work*

Specialty section:
This article was submitted to Inflammation, a section of the journal Frontiers in Immunology

Received: *30 September 2021*
Accepted: *16 December 2021*
Published: *06 January 2022*

Citation:
Chu X, Di C, Chang P, Li L, Feng Z, Xiao S, Yan X, Xu X, Li H, Qi R, Gong H, Zhao Y, Xiao F and Chang Z (2022) Lactylated Histone H3K18 as a Potential Biomarker for the Diagnosis and Predicting the Severity of Septic Shock. Front. Immunol. 12:786666. doi: 10.3389/fimmu.2021.786666

Objective: To date, there are no studies regarding the lactylation profile and its role in critically ill patients. Thus, we aimed to examine expression of histone H3 lysine 18 (H3K18) lactylation and its role in patients with septic shock.

Methods: Thirteen healthy volunteers and 35 critically ill patients from the Department of Surgical Intensive Care Medicine, Beijing Hospital were enrolled in our study. Baseline information and clinical outcomes were obtained prospectively. Lactylation levels of all proteins and H3K18 from peripheral blood mononuclear (PBMC) were determined by western blotting and serum levels of inflammatory cytokines by flow cytometry. Arginase-1 (*Arg1*) and Krüppel-like factor-4 (*Klf4*) mRNA expression was evaluated by quantitative real-time PCR (qRT-PCR).

Results: Lactylation was found to be an all-protein post-translational modification and was detected in PBMCs from both healthy volunteers and critically ill patients, with a significantly higher relative density in shock patients (t=2.172, P=0.045). H3K18la was expressed in all subjects, including healthy volunteers, with the highest level in septic shock patients (compared with non-septic shock patients, critically ill without shock patients and healthy volunteers P=0.033, 0.000 and 0.000, respectively). Furthermore, H3K18la protein expression correlated positively with APACHE II scores, SOFA scores on day 1, ICU stay, mechanical ventilation time and serum lactate (ρ=0.42, 0.63, 0.39, 0.51 and 0.48, respectively, ρ=0.012, 0.000, 0.019, 0.003 and 0.003, respectively). When we matched patients with septic shock and with non-septic shock according to severity, we found higher H3K18la levels in the former group (t=-2.208, P =0.040). Moreover, H3K18la exhibited a close correlation with procalcitonin levels (ρ=0.71, P=0.010). Patients with high H3K18la expression showed higher IL-2, IL-5, IL-6, IL-8, IL-10, IL-17, IFN-α levels

(ρ=0.33, 0.37, 0.62, 0.55, 0.65, 0.49 and 0.374 respectively, P=0.024, 0.011, 0.000, 0.000, 0.000 and 0.000 respectively). H3K18la expression also displayed a positive correlation with the level of *Arg1* mRNA (ρ=0.561, P=0.005).

Conclusions: Lactylation is an all-protein post-translational modification occurring in both healthy subjects and critically ill patients. H3K18la may reflect the severity of critical illness and the presence of infection. H3K18la might mediate inflammatory cytokine expression and *Arg1* overexpression and stimulate the anti-inflammatory function of macrophages in sepsis.

Keywords: septic shock, critical illness, histone, lactylation, H3K18

INTRODUCTION

Sepsis, currently defined as a dysregulated immune response to infection, is a systemic inflammatory response induced by infection that can develop into septic shock and even life-threatening organ dysfunction (1, 2). Sepsis represents a major intensive care problem, with incidence rates of up to 535 cases per 100,000 person-years and rising (3). Furthermore, in-hospital mortality due to sepsis remains high at 25-30% (4, 5), and hospital mortality for septic shock ranges from 40 to 60% (6–8). Overall, patients with sepsis and septic shock experience a sharp decline in health-related quality of life during ICU stays and increased rates of death in long-term care (9–11). Despite significant improvements in the diagnosis and management of sepsis, it remains a challenging clinical entity due to its variable aetiology and presentation, and diagnosis is often documented only after clinical deterioration during a hospital stay (12, 13). Differential diagnosis is also difficult in patients with circulatory shock, especially when accompanied by other conditions, such as cardiac injury and hypovolemia and trauma, or in the absence of archetypal signs of infection, e.g., in young infants, the elderly, and the immunocompromised (14–17).

Sepsis initiates a complex immunologic response that dysregulates the homoeostatic balance between pro- and anti-inflammatory processes, and prognosis might be quite different with similar injuries. Recent evidence from the fields of microbiology and immunology, as well as a small number of human sepsis studies, suggests that epigenetic regulation may play a central role in the pathogenesis of this heterogeneous response (18). Indeed, widespread genetic reprogramming leads to disruption of fundamental cellular processes, resulting in endothelial dysfunction, mitochondrial and metabolic derangement, immune failure, and cardiovascular collapse (19), and such events include DNA methylation, histone modifications, and transcriptional regulation by noncoding RNAs (19–21). Histones are subject to a variety of covalent modifications, including methylation, citrullination, acetylation, and phosphorylation, that alter their relationship to each other and to DNA (19). A survival advantage is associated with attenuation of local and systemic proinflammatory cytokines, protection against distant organ injury, enhanced bacterial clearance and phagocytosis, and inhibition of immune cell apoptosis (22, 23). Previous studies found that modifications of histone acetylation and citrullination significantly improve survival, attenuate "cytokine storms" and sepsis-associated coagulopathy, and decrease bone marrow atrophy in a lethal mouse septic model (22–28).

Recently, Zhang *et al.* reported that under biological stress, such as hypoxia, lipopolysaccharides or bacterial infection (such as *Escherichia coli, Acinetobacter baumannii* and *Pseudomonas aeruginosa*), macrophages induce a new post-translational modification (PTM), namely, histone lactylation (29), the discovery of which advances research in this field. The authors found that histones were lactylated in M1 macrophages when exposed to hypoxia, lipopolysaccharide/IFN-γ or bacteria. Increased histone H3 lysine 18 lactylation (H3K18la) induces expression of homeostatic genes involved in healing, including *Arg1*. A previous study showed that p300 [also known as lysine-acetyltransferase (KAT3B)] specifically acetylates histone H3K18 and H3K27 (30). During bacterial and adenovirus infection, H3K18 acetylation is significantly reduced through SIRT2 and CBP/p300 (31). Hence, it is reasonable to hypothesize that the reduction in H3K18 acetylation that occurs in infection may in turn increase H3K18 lactylation (same site of modification) *via* p300, and both may be a promising pair of H3K18 modifications that correlate with sepsis and septic shock.

However, to our knowledge, no clinical study has explored lactylation levels in humans or the relationship between histone lactylation and inflammatory levels during sepsis. Indeed, studies to date have investigated interactions at the cellular level, whereas the expression profile of protein lactylation in humans remains to be investigated; for example, lactylation of histones, which are the major nuclear proteins, has not been examined. In this study, we explored lactylation of all proteins in critically ill patients and further evaluated expression of H3K18la in circulating peripheral blood mononuclear cells (PBMCs) to assess its role in patients with septic shock and in those with non-septic shock. The underlying mechanisms and physiological relevance were further detected through comparisons of inflammatory cytokines and macrophage function biomarkers from the same patients.

METHODS

Study Design and Participants

This historical cohort study was approved by the institutional ethics board of Beijing Hospital (2018BJYYEC-197-02). Patients admitted to the Department of Surgical Intensive Care Medicine

of Beijing Hospital from August 22, 2018, to June 21, 2021, were enrolled. All participants were over 16 years old and signed informed consent; the patients were in the ICU for over 24 hours. Septic shock patients were screened at ICU admission according to the third international consensus definition for sepsis and septic shock (sepsis-3) (2). The definition of septic shock was as follows: vasopressors required to maintain mean artery pressure (MAP)≥ 65 mmHg and serum lactate level ≥ 2 mmol/L despite adequate fluid resuscitation.

Non-septic shock patients included those with haemorrhagic shock, cardiogenic shock, and obstructive shock (pulmonary embolism). The definition of shock includes (32) patients with signs of hypoperfusion and low blood pressure. Tissue hypoperfusion manifests as follows: 1. the skin is cold, clammy and blue, pale or discoloured; 2. altered mental status is present and characterized by obtundation, disorientation and confusion; and 3. urine output is decreased to <0.5 ml/kg/h. Low blood pressure was defined as a systolic blood pressure (SBP) of <90 mmHg, maintenance of a mean artery pressure (MAP) of <65 mmHg, or a decrease of >40 mmHg from baseline.

Critically ill patients without shock were those who did not meet the criteria for shock but were admitted to the ICU for high-risk critical care and intensive treatment, such as major surgery and senior patients with comorbidities.

After enrolment, the following baseline information was collected: age, sex, comorbidities, Sequential Organ Failure Assessment (SOFA) score (ICU admission day one to day three), Acute Physiology and Chronic Health Evaluation II (APACHE II) score within 24 hours, duration of mechanical ventilation, length of ICU stay, length of hospital stay, and 28-day mortality. The following laboratory indicators based from the same collection date were also assessed: serum lactate, white blood cell count (WBC), neutrophil count, neutrophil percentage, lymphocyte count, lymphocyte percentage, monocyte count, monocyte percentage, procalcitonin (PCT) level, and C-reactive protein (CRP) level.

Blood Samples

Blood samples (5-10 ml) were collected from all participants (ICU patients and healthy volunteers) in Ethylenediaminetetraacetic acid (EDTA)-containing and serum-separating tubes for peripheral blood mononuclear cell (PBMC) isolation and serum separation, respectively. Blood samples were collected within 24 hours after admission.

PBMC Isolation and Serum Separation

Under sterile conditions, blood samples in EDTA-containing tubes were centrifuged at 3000 rpm for 5 minutes at 20°C. The supernatant was aspirated into cryopreservation tubes and diluted 1:1 with phosphate-buffered saline (PBS) pH-7.2 in a 50-ml tube. The diluted blood samples were layered on top of 15 ml Lymphoprep™ (STEMCELL Technologies Cat# 07851) in a 50-ml tube and centrifuged at 500 x g for 20 minutes at 20°C. Most of the upper layer was aspirated, leaving the white buffy coat at the interphase; the buffy coat was carefully transferred to a new 50-ml tube, which was filled with PBS, mixed and centrifuged at 500 x g for 7 minutes at 20°C. The supernatant was completely removed, and if the precipitate at the bottom of the tubes had red impurities, red blood cell buffer (Solarbio Cat#R1010) was added for 5 minutes; a sufficient amount of PBS was added, and the tube was centrifuged at 500 x g for 7 minutes at 20°C. After removing the supernatant, the PBMCs were harvested and resuspended in 2 ml cryoprotective agent (serum: DMSO = 9:1) and stored at -80°C.

Under sterile conditions, blood samples in serum-separating tubes were centrifuged at 3000 rpm for 10 minutes at 4°C. The supernatant was aspirated into cryopreservation tubes and stored at -80°C.

Multiple Microsphere Immunofluorescence Assay

Twelve serum cytokines (IL-1β, IL-2, IL-4, IL-5, IL-6, IL-8, IL-10, IL-12p70, IL-17, IFN-α, IFN-γ, TNF-α) were assessed using the multiple microsphere immunofluorescence assay with flow cytometry (cytokines kit, RAISECARE; BD FACS Canto II flow cytometer). The calibration tubes were filled with 25 µl calibration product sample in matrix B, and 25 µl serum sample in buffer was added. The samples were fully mixed with 25 µl of capture microsphere antibodies; then, 25 µl of detection antibodies was added to all tubes, which were shielded from light at room temperature with shaking at 400-500 r/min for incubation. Two hours later, 25 µl SA-PE was added to all tubes, and the tubes were shielded from light at room temperature with shaking at 400-5500 r/min for incubation. Half an hour later, 500 µl of 1× wash buffer was added to the tubes, which were vortexed for several seconds and centrifuged at 500 x g for 5 minutes. After decanting the liquid, 300 µl 1× wash buffer was added to the tubes, which were vortexed for several seconds, and the 12 cytokines indicated above were detected by flow cytometry. At least 1100 microspheres for each sample were collected to ensure the accuracy of the data, which were analysed using LEGENDplex8.0 analysis software.

RNA Extraction and qRT-PCR

Total RNA was extracted using the guanidine isothiocyanate-phenol-chloroform method (RNAiso Plus, TaKaRa Bio Code No. 9109). The RNA yield was determined by a Thermo Nanodrop 2000C (A260/A280). The quality of the RNA was assessed by agarose gel electrophoresis. Qualified samples were denatured at 65°C for 5 minutes, and reverse transcription of cDNA was conducted with reverse transcription reagents. A DNase step was included to remove residual genomic DNA. The primers used were designed with Primer 5.0 to assemble the upstream and downstream regions of target genes. cDNA and primers were added to a qRT-PCR system (TransStart® Tip Green qPCR SuperMix, AQ141-02; restriction enzymes, Thermo Fisher). The real-time PCR mixture contained 5 µl 2×PCR mix, 0.5 µl primer F (10 µM), 0.5 µL primer R (10 µM), 1 µl template and 3 µl ddH_2O at a final volume of 10 µl. Reactions were performed in a Roche LightCycler 480 II (Mannheim, Germany) under the following conditions: 95°C for 5 min; 45 cycles of PCR amplification consisting of denaturation at 95°C for 10 sec, annealing at 60°C for 30 sec, and 72°C for 10 sec; and melting curve analysis including 95°C for 5 sec, 65°C for 1 min and 97°C

for 1 sec. The samples were cooled at 4°C for 30 sec, and fluorescence was measured. GAPDH was used as an internal control, and expression data were normalized using the delta-delta CT method.

The primers used in qRT-PCR were as follows:

5'-GCTGTGGATGGAAATTCGCC-3'/5'-CTTCTGGCAGTGTGGGTCAT-3'(*Klf4*),

5'-GGGTTGACTGACTGGAGAGC-3'/5'-CGTGGCTGTCCCTTTGAGAA-3'(*Arg1*),

5'-TGACTTCAACAGCGACACCCA-3'/5'-CACCCTGTTGCTGTAGCCAAA3'(*Gapdh*).

Histone Extraction and Western Blotting

Western Blotting With a Pan Anti-Lactyl-Lysine Antibody

Whole-cell lysates were prepared with lysis buffer (1% SDS, 1% protease inhibitors, 3 μM TSA, 50 mM NAM) and sonication. The lysis mixture was centrifuged at 12000 x g for 10 minutes at 4°C to remove cell debris, and the supernatant was transferred to new tubes. Protein concentrations were determined using a Thermo Scientific™ Pierce™ BCA Protein Assay Kit (Cat#23227). Sodium dodecyl sulfate-polyacrylamide gel electrophoresis (SDS-PAGE) was performed. Based on protein concentration results, 15 μg total protein was mixed with 5 μl 4× loading buffer and 2% SDS to a final volume of 20 μl and separated on an SDS-12% polyacrylamide gel at 15 mA/gel for approximately 15 minutes for stacking and at 35 mA/gel for resolution. Staining was performed using Coomassie Blue (R-250) for 2 hours at room temperature, and the gel was then decolorized. For western blotting, anti-lactyl-lysine antibody (PTM-1401RM; Lot: K111421; 1:1000 dilution in Life Technologies™ Antibody Diluent Reagent Solution cat# 003218) was used as the primary antibody and incubated overnight at 4°C. The secondary antibody was goat anti-rabbit IgG (H+L) (Thermo Pierce, Peroxidase Conjugated, 31460) diluted 1:10,000 in TBS-T with 5% milk at room temperature for 2 hours. Bands were detected quantitatively using VILBER Fusion Solo S.

Histone Extraction

Total histone proteins were extracted using an EpiQuik Total Histone Extraction Kit (Cat# OP-0006-100): Tubes with PBMCs were centrifuged at 1000 rpm for 5 mins at 4°C and resuspended in Diluted 1X Prelysis Buffer at 10^7 cells/ml. The tubes were kept on ice for 10 minutes with gentle stirring and centrifuged at 10,000 rpm for 1 min at 4°C. After removing the supernatant, the cells were resuspended in three-fold volumes (approximately 200 μl/10^7 cells) of lysis buffer and incubated on ice for 30 minutes. After centrifugation at 12,000 rpm for 5 minutes at 4°C, the supernatant (containing acid-soluble proteins) was transferred to new cryopreservation tubes, with 0.3 volumes of balance-DTT buffer added immediately. Protein concentrations were determined using a Thermo Scientific™ Pierce™ BCA Protein Assay Kit (Cat#23227). The isolated histones were stored at −80°C until use.

Western Blotting With an Anti-H3k18la Antibody

Histones extracted from PBMCs were assessed for protein concentration using a Thermo Scientific™ Pierce™ BCA Protein Assay Kit (Cat#23227). Based on the protein concentration results, 15 μg total protein was combined with 5 μl 5× loading buffer and 2% SDS to a final volume of 20 μl and separated on a 5% laminated glue + 15% separation gel at 80 V/gel for stacking and 120 V/gel for resolution. Wet transfer to a 0.2-μm PVDF membrane (Immobilon™-P^{SQ} membrane) was performed at 200 mA for 3 hours. The membranes were soaked in blocking buffer (5% skimmed milk) for 2 hours. Primary antibodies were applied overnight at 4°C [anti-lactyl-histone H3 (Lys18) rabbit mAb (PTM-1406RM; Lot: K111421; 1:1000 dilution in Life Technologies™ Antibody Diluent Reagent Solution cat# 003218) and anti-histone H3 antibody Nuclear Marker and ChIP Grade (ab1791) (1:1000 dilution in Life Technologies™ Antibody Diluent Reagent Solution)]. The secondary antibody [goat anti-rabbit IgG H&L (HRP) (ab6721)] diluted 1:3000 in TBS-T with 5% milk was added and incubated at room temperature for 2 hours. The bands detected were quantitatively analysed using VILBER Fusion Solo S.

Statistical Analysis

Normally distributed data were compared using Student's *t*-test or one-way analysis of variance (one-way ANOVA), and the results are shown as the mean ± SD; Pearson correlation was applied. Nonnormally distributed data were analysed using the non parametric Mann-Whitney *U* test, and the results are expressed as the median and interquartile range (IQR); Spearman correlation was applied. Categorical variables were compared with the chi-square or Fisher's exact test, and the results are shown as numbers and percentages. The diagnostic value was determined by receiver operating characteristic (ROC) curve analysis. True positive rate (sensitivity) is plotted against the false positive rate (1-specificity) at different classification thresholds. The area under the ROC curve (AUC) gives an index of the performance of the classifier. Higher values of AUC correspond to a good prediction of the model. $P<0.05$ was considered statistically significant. IBM SPSS 22.0 software was used for all statistical analyses.

RESULTS

Baseline Characteristics

The study population included 24 patients with different kinds of shock (including 13 with septic shock, 7 with haemorrhagic shock, 2 with obstructive shock, and 2 with cardiogenic shock), 11 critically ill patients without shock, and 13 healthy volunteers. The mean age and percentage of males were 65.77 years old and 69.2% for the septic shock group and 72.82 years old and 45.5% for the non-septic shock group, 64.27 years old and 45.5% for the critically ill without shock group, and 26.00 years old and 38.5% for the healthy volunteer group, respectively. There were no significant differences in sex or age among the three groups (septic shock, non-septic shock and critically ill without shock) (P=0.517; P=0.433). There was also no significant difference in

comorbidities among the three groups (more details in **Table 1**). Compared to the group of critically ill patients without shock, patients in the shock groups (septic shock and non-septic shock) had higher SOFA and APACHE II scores (P=0.001; P=0.000) and longer ICU stays and mechanical ventilation times (P=0.000; P=0.009); however, there were no significant differences in hospital stay between these two groups (P=0.295). One patient in the septic shock group and 2 in the non-septic shock group died during the study period.

Level of All-Protein Lysine Lactylation

To obtain a primary overall picture of lactylation in the study subjects, a preliminary analysis was performed by collecting clinical information and blood samples from 4 non-septic shock patients, 6 septic shock patients and 8 healthy volunteers, and levels of all-protein lactylation in PBMCs were determined by western blotting. As shown in **Figures 1A, B**, lactylation was an all-protein post-translational modification found in both healthy and shock patients. A difference in expression between the two groups was clearly detectable, as indicated by differences in corresponding band densities. In the all-protein range, shock patients had higher levels of lactylation than healthy volunteers (t=2.172, P=0.045) (more details are given in **Figure 1C**), whereas differences between septic and non-septic shock patients were not obvious (Z=-1.066, P=0.286). Internal reference proteins were not available, as they might also be modified. In our study, equal amounts of 15 μg protein were added to each lane such that WB results would be comparable between participants.

Level of H3K18 Lactylation in ICU Patients and Healthy Volunteers

H3K18la was expressed in all subjects, including the volunteers (**Figure 2**). The mean level of H3K18la relative density in patients was 0.65, 0.45, and 0.32 in the septic shock, non-septic shock, and critically ill without groups, respectively, and 0.21 in healthy volunteers. Among all ICU patients, H3K18la was highest in those with septic shock (compared with non-septic shock patients, P=0.033; compared with critically ill without shock patients, P=0.000). Non-septic shock patients also had a higher H3K18la relative density than healthy volunteers (P=0.005). However, no significant differences were found between the critically ill patients without shock and non-septic shock (P=0.265) or between the critically ill patients without shock and healthy volunteers (P=0.390) (more details are given in **Figure 2**).

TABLE 1 | Baseline characteristic of ICU patients and healthy volunteers.

Baseline Characteristics	ALL (n = 48)	Septic Shock (n = 13)	Non-septic Shock (n = 11)	Critically ill without Shock (n = 11)	Healthy Volunteers (n = 13)	*P* value in the first three groups	*P* value in four groups
	Mean ± SD/Median (IQR)						
Age (years)	62.00 (28.00-77.75)	65.77 ± 16.65	72.82 ± 12.45	64.27 ± 19.43	26.00 (24.50-28.00)	0.433	0.000
Sex [male (%)]	24 (50.00)	9 (69.23)	5 (45.45)	5 (45.45)	5 (38.46)	0.517	0.518
Comorbidities [n](%)							
Chronic Pulmonary Disease	3 (6.25)	1 (7.69)	0 (0.00)	2 (18.18)	0 (0.00)	0.497	0.287
Chronic Kidney Disease	3 (6.25)	1 (7.69)	0 (0.00)	2 (18.18)	0 (0.00)	0.497	0.287
Cardiovascular Disease	10 (20.83)	3 (23.08)	4 (36.36)	3 (27.27)	0 (0.00)	0.894	0.101
Hepatopathy	3 (6.25)	2 (15.38)	1 (9.09)	0 (0.00)	0 (0.00)	0.760	0.486
Diabetes	10 (20.83)	4 (30.77)	2 (18.18)	4 (36.36)	0 (0.00)	0.724	0.083
Hypertension	18 (37.50)	7 (53.85)	4 (36.36)	7 (63.64)	0 (0.00)	0.409	0.002
Hyperlipidemia	3 (6.25)	0 (0.00)	1 (9.09)	2 (18.18)	0 (0.00)	0.279	0.122
Malignant Tumor	15 (31.25)	4 (30.77)	5 (45.45)	6 (54.55)	0 (0.00)	0.576	0.011
APACHE II score	21.00 (16.00-24.00)	28.85 ± 11.02	19.82 ± 4.92	15.18 ± 5.98	–	0.001	–
SOFA score on day 1	7.00 (5.00-10.00)	11.08 ± 3.52	7.46 ± 2.07	4.00 (3.00-7.00)	–	0.000	–
Length of ICU stay (days)	7.00 (3.00-19.00)	20.00 (10.00-56.00)	5.00 (3.00-10.00)	2.00 (1.00-4.00)	–	0.000	–
Length of Hospital stay (days)	24.00 (16.00-47.00)	47.15 ± 34.57	31.82 ± 24.14	21.00 (17.00-32.00)	–	0.295	–
Mechanical ventilation percentage	2 (4.17)	0 (0.00)	0 (0.00)	2 (18.18)	–	0.185	–
Mechanical ventilation time	2.00 (1.00-12.00)	5.00 (2.75-73.00)	2.00 (1.25-10.50)	1.00 (1.00-1.50)	–	0.009	–
28-days mortality	3 (6.25)	1 (7.69)	2 (18.18)	0 (0.00)	–	0.497	–

ICU, intensive care unit; IQR, inter quartile range; APACHE Ⅱ score, acute physiology and chronic health evaluation Ⅱ score; SOFA, sequential organ failure assessment; P values were calculated by Mann-Whitney U test, Students' t-test or one-way analysis of variance (one-way ANOVA), and χ^2 test or Fisher's exact test, as appropriate. P values below 0.05 indicates statistical significance.

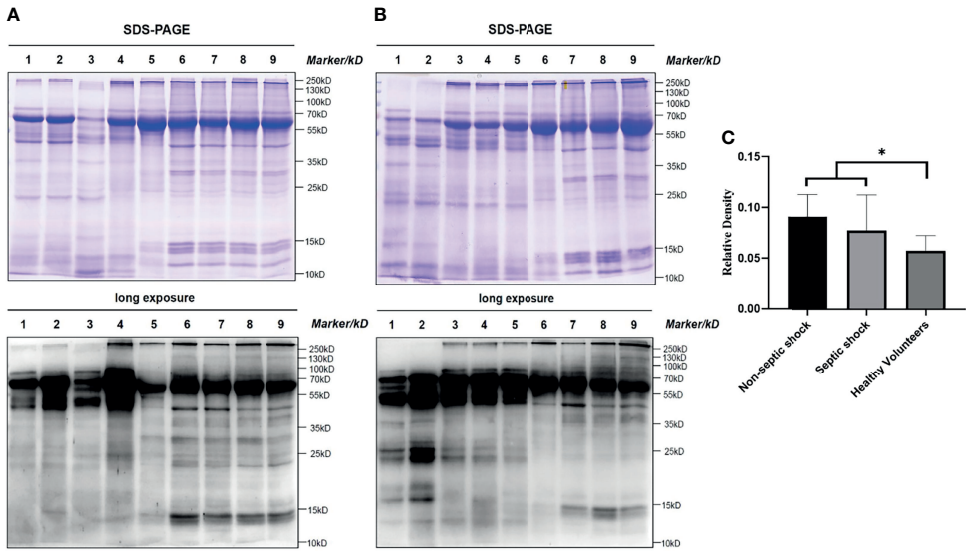

FIGURE 1 | All protein lactyl-lysine lactylation in different groups. Lactylation is an all-protein-posttranslational modification found in both healthy and shock patients. The difference was significant between shock patients and healthy volunteers (Students' t= 2.172, P=0.045). **(A)** and **(B)**: Bands 1-2: non-septic shock patients; bands 3-5: septic shock patients; bands 6-9: healthy volunteers; **(C)**: Relative density: (lane greyscale value of the anti-lactyl-lysine antibody)/(lane greyscale of SDS–PAGE × 15 μg). *P < 0.05.

H3K18 Lactylation Correlation With Severity and Prognosis

There was a positive correlation between H3K18la and the APACHE II score, SOFA score on day 1, ICU stay and mechanical ventilation time (Spearman correlation coefficients 0.42, 0.63, 0.39, 0.51, respectively; P=0.012, 0.000, 0.019, and 0.007, respectively) (more details are given in **Figure 3**).

As depicted in **Figure 4**, expression of H3K18la exhibited a positive correlation with the serum level of lactate (Spearman correlation coefficient 0.48; P=0.003).

H3K18 Lactylation Correlation With Infection

As the level of H3K18la correlates with the severity as described above, conclusions should not be drawn simply by comparing relative density in septic shock and non-septic shock patients. As shown in **Supplemental Table 1**, clinical parameters indicating severity and prognosis such as APACHE II, SOFA score on day 1, and ICU stay were significantly different between the septic shock and non-septic shock patients.

To study the role of H3K18la in relation to infection, we matched patients with septic shock and with non-septic shock (haemorrhagic shock, cardiogenic shock and obstructive shock) according to severity and examined prognostic indicators (APACHE II, SOFA, length of ICU stay, and serum lactate). Pairwise comparison of the adjusted median/mean was conducted while taking into account the above parameters. After we removed 3 patients with severe septic shock and 1 non-septic shock patient, there were no significant differences in APACHE II, SOFA score on day 1, ICU stay or serum lactate between the septic shock and non-septic shock patients (P =0.141, 0.052, 0.052, and 0.353, respectively; more details are given in **Supplemental Table 2**). We retested H3K18la between septic and non-septic shock patients, and the results still showed a significant difference (t=-2.208, P =0.040), suggesting that H3K18la is associated with infection. We conducted ROC curve analysis to find out the diagnostic cut-off value of H3K18la in differentiating septic shock patients from non-septic shock patients. A cut-off level of H3K18la relative density over 0.4683 is optimal to make a differential diagnosis, with an 84.6% sensitivity and 63.6% specificity, respectively (more details in **Supplementary Figure 1**).

H3K18la Lactylation Correlation With Laboratory Parameters of Infection

We further analysed the link between H3K18la expression and inflammatory parameters, including PCT, CRP, WBC, neutrophil count, neutrophil percentage, lymphocyte count, lymphocyte percentage, monocyte count and monocyte percentage, as depicted in **Figure 5**. H3K18la displayed a positive correlation with PCT (Spearman correlation coefficient=0.71, P=0.010) but a negative one with the monocyte percentage (Pearson correlation coefficient=-0.36, P=0.041).

H3K18 Lactylation Correlation With Inflammatory Cytokines

Expression of inflammatory cytokines, including IL-1β, IL-2, IL-4, IL-5, IL-6, IL-8, IL-10, IL-12p70, IL-17, IFN-α, IFN-γ, and TNF-α, was assessed by flow cytometry in all subjects, including healthy volunteers. We further analysed the relationship between H3K18la expression and levels of inflammatory cytokines. As indicated in **Figure 6**, H3K18la exhibited a close positive

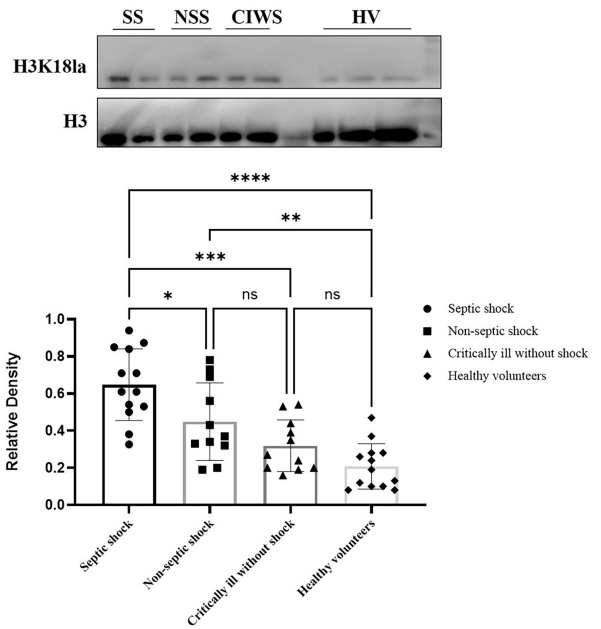

FIGURE 2 | Expression of H3K18 lactylation in ICU patients and healthy volunteers. H3K18la was expressed in all subjects, including the volunteers. The mean level of the H3K18la were significantly different among the four groups of septic shock, non-septic shock, critically ill without shock; and healthy volunteers (Welch ANOVA F=16.158, *P*<0.001). The differences were also significant between the septic shock group and the non-septic group, critically ill without shock group and healthy volunteers (Tukey *post hoc* test *P*=0.033, 0.000 and 0.000, respectively). There is no significant difference between the critically ill without shock group and the healthy volunteers (Tukey *post hoc* test *P*=0.390), or between the non-septic shock group and the critically ill without shock group (Tukey *post hoc* test *P*=0.265). Compared with healthy volunteers, patients in the non-septic shock group have higher H3K18la (Tukey *post hoc* test *P*=0.005). SS, septic shock; NSS, non-septic shock; CIWS, critically ill without shock; HV, healthy volunteers. *P < 0.05, **P < 0.01, ***P < 0.001, ****P < 0.0001, NS, not significant.

correlation with IL-6 and IL-10 (Spearman correlation coefficient=0.62 and 0.65, *P*=0.000 and 0.000) and a weak positive correlation with IL-2, IL-5, IL-8, IL-17 and IFN-α (more details in **Figure 6**).

H3K18 Lactylation Correlation With Markers of Macrophage Function

As illustrated in **Figure 7**, H3K18la had a positive correlation with *Arg1* mRNA expression (Spearman correlation coefficient=0.56, *P*=0.005) but no correlation with that of *Klf4* (Spearman correlation coefficient=-0.06, *P*=0.779).

DISCUSSION

In our study, we first found that lactylation, a newly identified protein post-translational modification, exists differentially in peripheral blood samples of healthy volunteers and critically ill patients. To our knowledge, this is also the first clinical study exploring the relationship between H3K18la and septic shock. Importantly, our study is the first to indicate that H3K18la correlates significantly with the severity and prognosis of critically ill patients and can differentiate septic shock from non-septic shock.

Lactate, one of the most crucial intermediates of carbohydrate and nonessential amino acid metabolism, has long been mistakenly considered metabolic waste (29). Emerging evidence suggests that lactate is more likely to be a "stress signal", an autocrine, paracrine and endocrine factor. In acidosis, exogenous lactate infusion has an alkalotic effect (33). As the major gluconeogenesis precursor, lactate serves as fuel (34) and an anti-inflammatory agent in traumatic brain injury (35), acute pancreatitis (36), hepatitis (36), myocardial infarction, cardiac surgery, acute heart failure (37, 38), burns (39) and sepsis (40, 41). In addition, accumulation of lactate

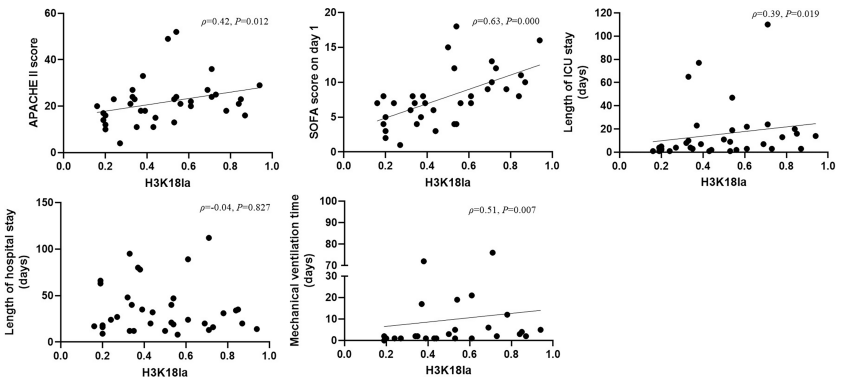

FIGURE 3 | H3K18 lactylation correlation with severity and prognosis. H3K18la has a positive correlation with the APACHE II score, SOFA score on Day 1, length of ICU stay and mechanical ventilation time (Spearman correlation coefficient 0.42, 0.63, 0.39 and 0.51, respectively; *P*=0.012, 0.000, 0.019 and 0.007, respectively). H3K18la, relative density of H3K18 lactylation in western blotting. ICU, intensive care unit; IQR, inter quartile range; APACHE II score, acute physiology and chronic health evaluation II score; SOFA, sequential organ failure assessment. *P* values below 0.05 indicate statistical significance.

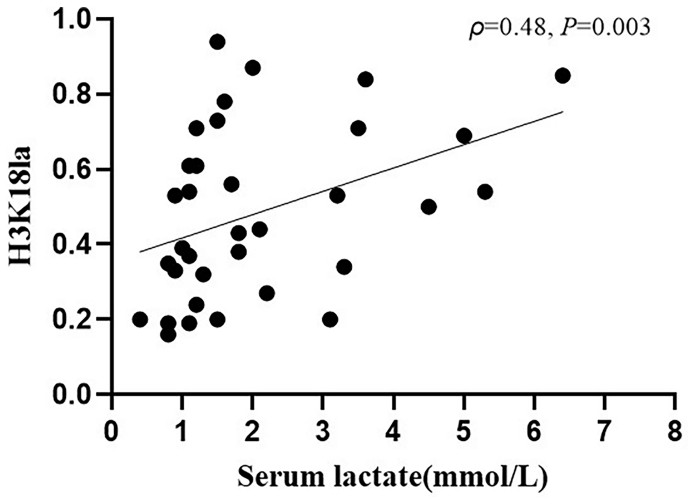

FIGURE 4 | H3K18la lactylation correlation with serum lactate in ICU patients. H3K18la had a positive correlation with serum lactate (Spearman correlation coefficient 0.48; *P*=0.003). H3K18la: The relative density of H3K18 lactylation in western blotting. Serum lactate: Serum lactate level at blood sample date. *P* values below 0.05 indicate statistical significance.

helps cancer cells escape immunity and has an inhibitory effect on immune killing (42–46). Following the first report of lactylation in *Nature* in 2019, a series of studies found that macrophages take up extracellular lactate to promote self-protein lactylation under both physiological and pathophysiological conditions (29, 47–50), which further explains the immunological function of lactate at the molecular level.

In our study, we first performed a small-sample-size preliminary experiment and found that lactylation is an all-protein post-translational modification that is present in healthy and ill subjects. We found that lactylation is universally present in humans and on nearly all proteins of various sizes, not only in the range of histones. Additionally, we observed a clearly detectable difference between shock patients and healthy volunteers. Nevertheless, protein degradation could not be avoided. The earliest frozen samples we used were from 2018, and we did not extract histone proteins. We sought to obtain a primary overall picture of lactylation in subjects; the pan anti-lactyl-lysine results could only show an overall expression profile in critically ill patients and healthy volunteers and indicate rough differences in all-protein lactylation.

To date, studies using a pan anti-lactyl-lysine antibody have not found direct evidence demonstrating which histone is lactylated and induces macrophage phenotypic alterations.

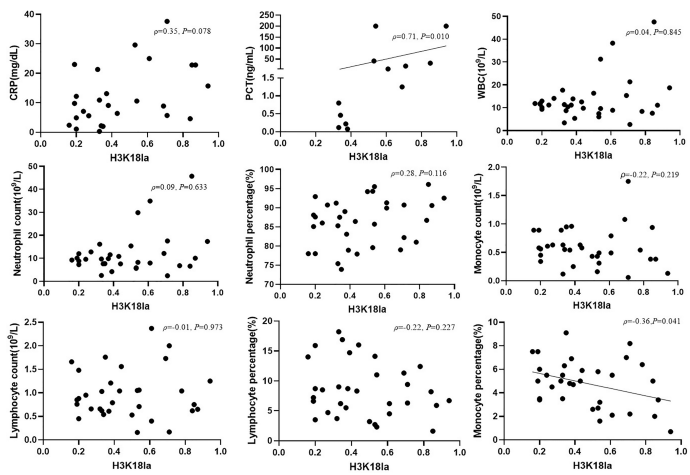

FIGURE 5 | H3K18la lactylation correlation with infectious laboratory parameters. Protein expression of H3K18la has a positive correlation with the serum level of PCT (Spearman correlation coefficient 0.71, *P*=0.010) and has a negative correlation with monocyte percentage (Pearson correlation coefficient -0.36, *P*=0.041). PCT, procalcitonin; CRP, C-reactive protein; WBC, white blood count. *P* values below 0.05 indicate statistical significance.

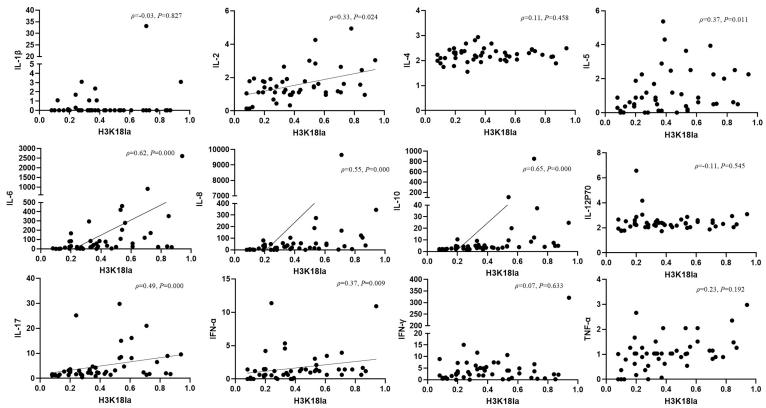

FIGURE 6 | H3K18 lactylation correlation with inflammatory cytokines. Protein level of H3K18la has a positive correlation with the serum levels of IL-2, IL-5, IL-6, IL-8, IL-10, IL-17, IFN-α (Spearman correlation coefficient 0.32, 0.37, 0.62, 0.55,0.65, 0.49 and 0.37 respectively; *P*=0.024, 0.011, 0.000, 0.000, 0.000, 0.000 and 0.009, respectively). H3K18la, relative density of H3K18 lactylation in western blotting. IL, interleukin, IFN, interferon, TNF-tumour necrosis factor. Serum levels of cytokines were assessed using a multiple microsphere immunofluorescence assay with flow cytometry. *P* values below 0.05 indicate statistical significance.

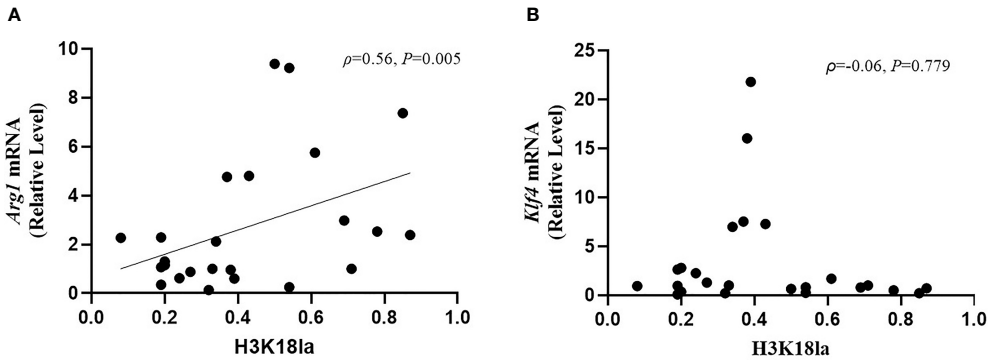

FIGURE 7 | H3K18 lactylation correlation with markers of macrophages function. The protein level of H3K18la had a positive correlation with *Arg1* mRNA expression (Spearman correlation coefficient=0.56, *P*=0.005) but no correlation with *Klf4* mRNA expression (Spearman correlation coefficient=-0.06, *P*=0.779). H3K18la, relative density of H3K18 lactylation in western blotting. qRT-PCR was used to detect *Arg1* **(A)** and *Klf4* **(B)** mRNA expression. GAPDH was used as an internal control.

In 2019, Zhang *et al.* reported that histone lactylation occurs in M1 macrophages exposed to hypoxia, lipopolysaccharide/IFN-γ or bacteria. Increased histone lactylation (H3K18la) induces expression of homeostatic genes involved in healing, including *Arg1*, and is associated with the M2-like phenotype (29). After an extensive literature review, we selected H3K18 as a modification site for detecting lactylation levels in our participants. H3K18la displayed a positive correlation with serum lactate (Spearman correlation coefficient 0.48; *P*=0.003, **Figure 4**). However, as indicated in **Figure 4**, several patients with normal levels of serum lactate (< 2 mmol/l) had a relatively high level of H3K18la, which suggests that H3K18 lactylation might be independent of serum lactate. Our study also shows that H3K18la exhibits a positive correlation with the APACHE II score, SOFA score on day 1, ICU stay and mechanical ventilation time, suggesting that H3K18la may constitute as a prominent independent biomarker that reflects the severity and prognosis of critically ill patients.

Several studies have revealed that lactylation may correlate with the release of inflammatory factors during sepsis (49, 50). p300 (also known as KAT3B), a classic acetyltransferase that specifically acetylates histone H3K18 and H3K27 (30), also catalyses protein lactylation (29), and the study by Eskandarian *et al.* found H3K18 acetylation to be significantly reduced during bacterial and adenovirus infection through SIRT2 and CBP/p300 (31). Overall, it is reasonable to hypothesize that the reduction in H3K18 acetylation in infection may in turn promote H3K18 lactylation (same site of modification) *via* p300. To further explore the role of H3K18la in sepsis, we divided patients with shock into subgroups of septic shock and non-septic shock, and the results showed that the former had the highest level of H3K18la (see details in **Figure 2**). As the clinical outcome of the patients in the septic shock group was worse than that of those in the non-septic shock group (see details in **Supplemental Table 1**), we further conducted pairwise

comparisons of adjusted medians/means by taking into account the APACHE II score, SOFA score, ICU stay and lactate level (see details in **Supplemental Table 2**). We re-assessed the H3K18la level between the septic and non-septic shock patients, and the results still showed a significant difference (t=-2.208, P=0.040), suggesting that H3K18la is involved in the pathophysiologic process of sepsis-induced shock.

Sepsis and septic shock had been associated with multiple biomarkers of inflammation, such as PCT (51, 52), CRP (53), Soluble CD14 subtype (54), and soluble urokinase-type plasminogen activator receptor(suPAR) (55), etc. However, there is no single golden standard diagnostic biomarker to differentiate septic shock patients from non-septic shock patients (2, 56). In our study, we also found an optimal cut-off value of H3K18la relative density (0.4683) to make a diagnosis of septic shock, with an 84.6% sensitivity and 63.6% specificity. Further studies with larger sample size are needed to verify our findings. To further confirm the relationship between H3K18la with infection, we compared expression of H3K18la with clinical biomarkers of infection, including WBC, neutrophil count, neutrophil percentage, lymphocyte count, lymphocyte percentage, monocyte count, monocyte percentage, PCT and CRP levels. The results showed that H3K18la correlates closely with PCT (Spearman correlation coefficient=0.711, P=0.010). It is well known that serum levels of PCT are increased in bacterial infection but that levels remain unchanged or only moderately increase in a non-infection condition (57, 58). Combined with our findings, it is reasonable to infer an important relationship between H3K18la and infection.

Regardless, our study did not detect a direct relationship of H3K18la with WBC and CRP. Indeed, the value of leucocytosis in the diagnosis of infection and sepsis remains low, as it is influenced by many non-infectious factors, such as myocardial infarction, catecholamines, and corticosteroids (29), and may also markedly decline in the setting of severe infection (59). Previous studies have reported that PCT has better sensitivity than CRP for differentiating bacterial infections from nonbacterial infections (60, 61), and it has been reported that trauma patients experience various degrees of stress that elicit an inflammatory response, which causes an elevation in PCT concentrations, even in the absence of infection (62). Our study only included one traumatic-haemorrhagic patient, a female aged 81, whose PCT was 0.22 ng/ml, which was within the normal value (<0.5 ng/ml).

Regarding mechanisms of H3K18la in infection, we assessed expression of cytokines and genes that are critical in infection. Zhang *et al.* (29) performed RNA-seq analysis at 0, 4, 8, 16 and 24 h after challenge with LPS and IFN-γ; 1,223 genes specifically marked by increased H3K18la were more likely to be activated or reactivated at later time points (16 or 24 h) during M1 polarization, correlating well with the induction of intracellular lactate and histone Kla levels at these later time points (29). In our study, H3K18la correlated with inflammation-related cytokines, and patients with high H3K18la had higher IL-10 and IL-6 levels (more details are given in **Figure 6**). In the pathophysiology of sepsis, the proinflammatory cytokine IL-6 is known to play a pivotal role and is an overproduced cytokine that causes hypercytokaemia (63). IL-10 signalling activates the Jak-STAT pathway (64) and PI3K-Akt-GSK pathway, a process that suppresses expression of various inflammatory genes (65). IL-10 drives the molecular pathway that enhances immunosuppression during late sepsis (66), which correlates with mortality in patients with infection (67). The results of our analysis of circulating cytokines in patients showed that in addition to proinflammatory cytokines (such as IL-6), concentrations of the potent anti-inflammatory cytokine IL-10 were increased. Combined with the significant relationship with IL-10, H3K18la might not only differentiate patients with sepsis but also indicate prognosis. On the other hand, IL-10 enhances the phenotype of M2 macrophages in synergy with IL-4, which consequently induces expression of anti-inflammatory genes, including *Arg1* (68, 69).

Arg1 and *Klf4* levels increase in macrophages during type 2 immune responses and wound repair (29, 47). Macrophages stimulated by interferon-γ (IFN-γ) and interleukin-4 (IL-4) and IL-10 induce *Arg1* to produce increased amounts of iNOS, inhibiting efficient clearance of bacteria (70). At later time points after infection, H3K18la-mediated anti-inflammatory (such as IL-10 and *Arg1*) overexpression may be related to late death (71). Our results are consistent with current advances involving cellular and molecular findings.

Finally, there are several limitations to this study. First, the clinical findings could not provide direct evidence demonstrating the participation of lactate-induced H3K18la in the regulation of IL-10 in sepsis. Therefore, the effect of sepsis-derived lactylation on the initiation and progression of sepsis remains an open and interesting question. Second, this was a one-centre, small-sample-size, historical cohort study, and several biases were inevitable. Limited by the sample size, the conclusions must be viewed as preliminary and treated with caution, and further studies with larger sample sizes are needed to verify our findings. Lactylation might be a potentially very important mechanism during various biological stresses. As yet, the key enzymes (write, read and erase multiple histone modification), the correlation with acetylation and other modifications, the site-specific gene functions, signalling receptors and pathways remain mostly undefined. In the future, multi-center, large sample size studies are needed to confirm its expression profile in different disease specific patterns, while much more basic researches are needed regarding its mechanisms.

In conclusion, lactylation is an all-protein posttranslational modification that exists in healthy and ill patients. H3K18la may reflect the severity of critical illness as well as the existence of infection. H3K18la correlates positively with inflammatory cytokine production. H3K18la-mediated anti-inflammatory effects, such as IL-10 overexpression, may play an important role in the anti-inflammatory function of macrophages as well as *Arg1* expression in sepsis.

DATA AVAILABILITY STATEMENT

The datasets presented in this study can be found in online repositories. The names of the repository/repositories and accession number(s) can be found in the article/**Supplementary Material**.

ETHICS STATEMENT

The studies involving human participants were reviewed and approved by the institutional ethics board of Beijing Hospital (2018BJYYEC-197-02). Written informed consent to participate in this study was provided by the participants' legal guardian/ next of kin.

AUTHOR CONTRIBUTIONS

XC and ZC contributed to the conception of the study, data interpretation and drafted the manuscript. CD, PC, LL, ZF, SX, XY, XX, HL, RQ, HG, YZ, and FX contributed to data collection and critically revised the manuscript for important intellectual content. All authors contributed to the article and approved the submitted version.

FUNDING

This work was supported by the Beijing Hospital New-star Plan of Science and Technology (BJ-2018-134) and Fundamental Research Funds for the Central Universities (3332018173).

SUPPLEMENTARY MATERIAL

The Supplementary Material for this article can be found online at: https://www.frontiersin.org/articles/10.3389/fimmu.2021.786666/full#supplementary-material

Supplementary Figure 1 | ROC curve of H3K18la for diagnosis septic shock patients from non-septic shock patients. The area under the ROC curve (AUC) was 0.755 (P = 0.034). The cut-off value of H3K18la was 0.4683, with sensitivity of 84.6% and specificity of 63.6%. ROC, receiver operating characteristic.

REFERENCES

1. Cecconi M, Evans L, Levy M, Rhodes A. Sepsis and Septic Shock. *Lancet* (2018) 392:75–87. doi: 10.1016/s0140-6736(18)30696-2
2. Singer M, Deutschman CS, Seymour CW, Shankar-Hari M, Annane D, Bauer M, et al. The Third International Consensus Definitions for Sepsis and Septic Shock (Sepsis-3). *Jama* (2016) 315:801–10. doi: 10.1001/jama.2016.0287
3. Walkey AJ, Lagu T, Lindenauer PK. Trends in Sepsis and Infection Sources in the United States. A Population-Based Study. *Ann Am Thorac Soc* (2015) 12:216–20. doi: 10.1513/AnnalsATS.201411-498BC
4. Fleischmann C, Scherag A, Adhikari NK, Hartog CS, Tsaganos T, Schlattmann P, et al. Assessment of Global Incidence and Mortality of Hospital-Treated Sepsis. Current Estimates and Limitations. *Am J Respir Crit Care Med* (2016) 193:259–72. doi: 10.1164/rccm.201504-0781OC
5. Cohen J, Vincent JL, Adhikari NK, Machado FR, Angus DC, Calandra T, et al. Sepsis: A Roadmap for Future Research. *Lancet Infect Dis* (2015) 15:581–614. doi: 10.1016/s1473-3099(15)70112-x
6. Martin GS, Mannino DM, Eaton S, Moss M. The Epidemiology of Sepsis in the United States From 1979 Through 2000. *N Engl J Med* (2003) 348:1546–54. doi: 10.1056/NEJMoa022139
7. Vincent JL, Marshall JC, Namendys-Silva SA, François B, Martin-Loeches I, Lipman J, et al. Assessment of the Worldwide Burden of Critical Illness: The Intensive Care Over Nations (ICON) Audit. *Lancet Respir Med* (2014) 2:380–6. doi: 10.1016/s2213-2600(14)70061-x
8. Vincent JL, Sakr Y, Sprung CL, Ranieri VM, Reinhart K, Gerlach H, et al. Sepsis in European Intensive Care Units: Results of the SOAP Study. *Crit Care Med* (2006) 34:344–53. doi: 10.1097/01.ccm.0000194725.48928.3a
9. Hofhuis JG, Spronk PE, van Stel HF, Schrijvers AJ, Rommes JH, Bakker J. The Impact of Severe Sepsis on Health-Related Quality of Life: A Long-Term Follow-Up Study. *Anesth Analg* (2008) 107:1957–64. doi: 10.1213/ane.0b013e318187bbd8
10. Nesseler N, Defontaine A, Launey Y, Morcet J, Mallédant Y, Seguin P, et al. Long-Term Mortality and Quality of Life After Septic Shock: A Follow-Up Observational Study. *Intensive Care Med* (2013) 39:881–8. doi: 10.1007/s00134-013-2815-1
11. Wang HE, Szychowski JM, Griffin R, Safford MM, Shapiro NI, Howard G. Long-Term Mortality After Community-Acquired Sepsis: A Longitudinal Population-Based Cohort Study. *BMJ Open* (2014) 4:e004283. doi: 10.1136/bmjopen-2013-004283
12. Kaukonen KM, Bailey M, Pilcher D, Cooper DJ, Bellomo R. Systemic Inflammatory Response Syndrome Criteria in Defining Severe Sepsis. *N Engl J Med* (2015) 372:1629–38. doi: 10.1056/NEJMoa1415236
13. Martínez-Paz P, Aragón-Camino M, Gómez-Sánchez E, Lorenzo-López M, Gómez-Pesquera E, Fadrique-Fuentes A, et al. Distinguishing Septic Shock From non-Septic Shock in Postsurgical Patients Using Gene Expression. *J Infect* (2021) 83:147–55. doi: 10.1016/j.jinf.2021.05.039
14. Clifford KM, Dy-Boarman EA, Haase KK, Maxvill K, Pass SE, Alvarez CA. Challenges With Diagnosing and Managing Sepsis in Older Adults. *Expert Rev Anti Infect Ther* (2016) 14:231–41. doi: 10.1586/14787210.2016.1135052
15. Henning DJ, Carey JR, Oedorf K, Day DE, Redfield CS, Huguenel CJ, et al. The Absence of Fever Is Associated With Higher Mortality and Decreased Antibiotic and IV Fluid Administration in Emergency Department Patients With Suspected Septic Shock. *Crit Care Med* (2017) 45:e575–82. doi: 10.1097/ccm.0000000000002311
16. Warnock C, Totterdell P, Tod AM, Mead R, Gynn JL, Hancock B. The Role of Temperature in the Detection and Diagnosis of Neutropenic Sepsis in Adult Solid Tumour Cancer Patients Receiving Chemotherapy. *Eur J Oncol Nurs* (2018) 37:12–8. doi: 10.1016/j.ejon.2018.10.001
17. Young PJ, Bellomo R. Fever in Sepsis: Is it Cool to be Hot? *Crit Care* (2014) 18:109. doi: 10.1186/cc13726
18. Binnie A, et al. Epigenetics of Sepsis. *Crit Care Med* (2020) 48:745–56. doi: 10.1097/ccm.0000000000004247
19. Ince C, Mayeux PR, Nguyen T, Gomez H, Kellum JA, Ospina-Tascón GA, et al. THE ENDOTHELIUM IN SEPSIS. *Shock* (2016) 45:259–70. doi: 10.1097/shk.0000000000000473
20. Cross D, Drury R, Hill J, Pollard AJ. Epigenetics in Sepsis: Understanding Its Role in Endothelial Dysfunction, Immunosuppression, and Potential Therapeutics. *Front Immunol* (2019) 10:1363. doi: 10.3389/fimmu.2019.01363
21. Goldberg AD, Allis CD, Bernstein E. Epigenetics: A Landscape Takes Shape. *Cell* (2007) 128:635–8. doi: 10.1016/j.cell.2007.02.006
22. Li Y, Zhao T, Liu B, Halaweish I, Mazitschek R, Duan X, et al. Inhibition of Histone Deacetylase 6 Improves Long-Term Survival in a Lethal Septic Model. *J Trauma Acute Care Surg* (2015) 78:378–85. doi: 10.1097/ta.0000000000000510
23. Williams AM, Dennahy IS, Bhatti UF, Biesterveld BE, Graham NJ, Li Y, et al. Histone Deacetylase Inhibitors: A Novel Strategy in Trauma and Sepsis. *Shock* (2019) 52:300–6. doi: 10.1097/shk.0000000000001308
24. Zhao T, Li Y, Liu B, Bronson RT, Halaweish I, Alam HB. Histone Deacetylase III as a Potential Therapeutic Target for the Treatment of Lethal Sepsis. *J Trauma Acute Care Surg* (2014) 77:913–919; discussion 919. doi: 10.1097/ta.0000000000000347
25. Williams AM, Dennahy IS, Bhatti UF, Biesterveld BE, Graham NJ, Li Y, et al. Histone Deacetylase Inhibition Attenuates Cardiomyocyte Hypoxia-Reoxygenation Injury. *Curr Mol Med* (2018) 18:711–8. doi: 10.2174/1566524019666190208102729
26. Siddiqui AZ, Bhatti UF, Deng Q, Biesterveld BE, Tian Y, Wu Z, et al. Cl-Amidine Improves Survival and Attenuates Kidney Injury in a Rabbit Model of Endotoxic Shock. *Surg Infect (Larchmt)* (2021) 22:421–6. doi: 10.1089/sur.2020.189
27. Liang Y, Pan B, Alam HB, Deng Q, Wang Y, Chen E, et al. Inhibition of Peptidylarginine Deiminase Alleviates LPS-Induced Pulmonary Dysfunction

and Improves Survival in a Mouse Model of Lethal Endotoxemia. *Eur J Pharmacol* (2018) 833:432–40. doi: 10.1016/j.ejphar.2018.07.005
28. Li Y, Liu Z, Liu B, Zhao T, Chong W, Wang Y, et al. Citrullinated Histone H3: A Novel Target for the Treatment of Sepsis. *Surgery* (2014) 156:229–34. doi: 10.1016/j.surg.2014.04.009
29. Zhang D, Tang Z, Huang H, Zhou G, Cui C, Weng Y, et al. Metabolic Regulation of Gene Expression by Histone Lactylation. *Nature* (2019) 574:575–80. doi: 10.1038/s41586-019-1678-1
30. Jin Q, Yu LR, Wang L, Zhang Z, Kasper LH, Lee JE, et al. Distinct Roles of GCN5/PCAF-Mediated H3K9ac and CBP/p300-Mediated H3K18/27ac in Nuclear Receptor Transactivation. *EMBO J* (2011) 30:249–62. doi: 10.1038/emboj.2010.318
31. Eskandarian HA, Impens F, Nahori MA, Soubigou G, Coppée JY, Cossart P, et al. A Role for SIRT2-Dependent Histone H3K18 Deacetylation in Bacterial Infection. *Science* (2013) 341:1238858. doi: 10.1126/science.1238858
32. Cecconi M, De Backer D, Antonelli M, Beale R, Bakker J, Hofer C, et al. Consensus on Circulatory Shock and Hemodynamic Monitoring. Task Force of the European Society of Intensive Care Medicine. *Intensive Care Med* (2014) 40:1795–815. doi: 10.1007/s00134-014-3525-z
33. Brooks GA. Lactate as a Fulcrum of Metabolism. *Redox Biol* (2020) 35:101454. doi: 10.1016/j.redox.2020.101454
34. Hui S, Ghergurovich JM, Morscher RJ, Jang C, Teng X, Lu W, et al. Glucose Feeds the TCA Cycle *via* Circulating Lactate. *Nature* (2017) 551:115–8. doi: 10.1038/nature24057
35. Glenn TC, Martin NA, Horning MA, McArthur DL, Hovda DA, Vespa P, et al. Lactate: Brain Fuel in Human Traumatic Brain Injury: A Comparison With Normal Healthy Control Subjects. *J Neurotrauma* (2015) 32:820–32. doi: 10.1089/neu.2014.3483
36. Hoque R, Farooq A, Ghani A, Gorelick F, Mehal WZ. Lactate Reduces Liver and Pancreatic Injury in Toll-Like Receptor- and Inflammasome-Mediated Inflammation *via* GPR81-Mediated Suppression of Innate Immunity. *Gastroenterology* (2014) 146:1763–74. doi: 10.1053/j.gastro.2014.03.014
37. Bergman BC, Tsvetkova T, Lowes B, Wolfel EE. Myocardial Glucose and Lactate Metabolism During Rest and Atrial Pacing in Humans. *J Physiol* (2009) 587:2087–99. doi: 10.1113/jphysiol.2008.168286
38. Shapiro NI, Howell MD, Talmor D, Nathanson LA, Lisbon A, Wolfe RE, et al. Serum Lactate as a Predictor of Mortality in Emergency Department Patients With Infection. *Ann Emerg Med* (2005) 45:524–8. doi: 10.1016/j.annemergmed.2004.12.006
39. Spitzer JJ. Gluconeogenesis in the Burned Patient. *J Trauma* (1979) 19:899–900.
40. Garcia CK, Brown MS, Pathak RK, Goldstein JL. cDNA Cloning of MCT2, A Second Monocarboxylate Transporter Expressed in Different Cells Than MCT1. *J Biol Chem* (1995) 270:1843–9. doi: 10.1074/jbc.270.4.1843
41. Marik P, Bellomo R. A Rational Approach to Fluid Therapy in Sepsis. *Br J Anaesth* (2016) 116:339–49. doi: 10.1093/bja/aev349
42. Colegio OR, Chu NQ, Szabo AL, Chu T, Rhebergen AM, Jairam V, et al. Functional Polarization of Tumour-Associated Macrophages by Tumour-Derived Lactic Acid. *Nature* (2014) 513:559–63. doi: 10.1038/nature13490
43. Peng M, Yin N, Chhangawala S, Xu K, Leslie CS, Li MO. Aerobic Glycolysis Promotes T Helper 1 Cell Differentiation Through an Epigenetic Mechanism. *Science* (2016) 354:481–4. doi: 10.1126/science.aaf6284
44. de la Cruz-López KG, Castro-Muñoz LJ, Reyes-Hernández DO, García-Carrancá A, Manzo-Merino J. Lactate in the Regulation of Tumor Microenvironment and Therapeutic Approaches. *Front Oncol* (2019) 9:1143. doi: 10.3389/fonc.2019.01143
45. Rabinowitz JD, Enerbäck S. Lactate: The Ugly Duckling of Energy Metabolism. *Nat Metab* (2020) 2:566–71. doi: 10.1038/s42255-020-0243-4
46. Watson MJ, Vignali PDA, Mullett SJ, Overacre-Delgoffe AE, Peralta RM, Grebinoski S, et al. Metabolic Support of Tumour-Infiltrating Regulatory T Cells by Lactic Acid. *Nature* (2021) 591:645–51. doi: 10.1038/s41586-020-03045-2
47. Irizarry-Caro RA, McDaniel MM, Overcast GR, Jain VG, Troutman TD, Pasare C. TLR Signaling Adapter BCAP Regulates Inflammatory to Reparatory Macrophage Transition by Promoting Histone Lactylation. *Proc Natl Acad Sci USA* (2020) 117:30628–38. doi: 10.1073/pnas.2009778117
48. Cui H, Xie N, Banerjee S, Ge J, Jiang D, Dey T, et al. Lung Myofibroblasts Promote Macrophage Profibrotic Activity Through Lactate-Induced Histone Lactylation. *Am J Respir Cell Mol Biol* (2021) 64:115–25. doi: 10.1165/rcmb.2020-0360OC
49. Dichtl S, Lindenthal L, Zeitler L, Behnke K, Schlösser D, Strobl B, et al. Lactate and IL6 Define Separable Paths of Inflammatory Metabolic Adaptation. *Sci Adv* (2021) 7(26):eabg3505. doi: 10.1126/sciadv.abg3505
50. Yang K, Fan M, Wang X, Xu J, Wang Y, Tu F, et al. Lactate Promotes Macrophage HMGB1 Lactylation, Acetylation, and Exosomal Release in Polymicrobial Sepsis. *Cell Death Differ* (2021). doi: 10.1038/s41418-021-00841-9
51. Kopterides P, Siempos II, Tsangaris I, Tsantes A, Armaganidis A. Procalcitonin-Guided Algorithms of Antibiotic Therapy in the Intensive Care Unit: A Systematic Review and Meta-Analysis of Randomized Controlled Trials. *Crit Care Med* (2010) 38:2229–41. doi: 10.1097/CCM.0b013e3181f17bf9
52. Anand D, Das S, Bhargava S, Srivastava LM, Garg A, Tyagi N, et al. Procalcitonin as a Rapid Diagnostic Biomarker to Differentiate Between Culture-Negative Bacterial Sepsis and Systemic Inflammatory Response Syndrome: A Prospective, Observational, Cohort Study. *J Crit Care* (2015) 30:218.e217–212. doi: 10.1016/j.jcrc.2014.08.017
53. Opal SM, Wittebole X. Biomarkers of Infection and Sepsis. *Crit Care Clin* (2020) 36:11–22. doi: 10.1016/j.ccc.2019.08.002
54. Wu J, Hu L, Zhang G, Wu F, He T. Accuracy of Presepsin in Sepsis Diagnosis: A Systematic Review and Meta-Analysis. *PloS One* (2015) 10:e0133057. doi: 10.1371/journal.pone.0133057
55. Henriquez-Camacho C, Losa J. Biomarkers for Sepsis. *BioMed Res Int* (2014) 2014:547818. doi: 10.1155/2014/547818
56. Hotchkiss RS, Moldawer LL, Opal SM, Reinhart K, Turnbull IR, Vincent JL. Sepsis and Septic Shock. *Nat Rev Dis Primers* (2016) 2:16045. doi: 10.1038/nrdp.2016.45
57. Kollef MH, Sherman G, Ward S, Fraser VJ. Inadequate Antimicrobial Treatment of Infections: A Risk Factor for Hospital Mortality Among Critically Ill Patients. *Chest* (1999) 115:462–74. doi: 10.1378/chest.115.2.462
58. Ugarte H, Silva E, Mercan D, De Mendonça A, Vincent JL. Procalcitonin Used as a Marker of Infection in the Intensive Care Unit. *Crit Care Med* (1999) 27:498–504. doi: 10.1097/00003246-199903000-00024
59. Murray CK, Hoffmaster RM, Schmit DR, Hospenthal DR, Ward JA, Cancio LC, et al. Evaluation of White Blood Cell Count, Neutrophil Percentage, and Elevated Temperature as Predictors of Bloodstream Infection in Burn Patients. *Arch Surg* (2007) 142:639–42. doi: 10.1001/archsurg.142.7.639
60. Simon L, Gauvin F, Amre DK, Saint-Louis P, Lacroix J. Serum Procalcitonin and C-Reactive Protein Levels as Markers of Bacterial Infection: A Systematic Review and Meta-Analysis. *Clin Infect Dis* (2004) 39:206–17. doi: 10.1086/421997
61. Huang X, Wang J, Li H. Diagnostic and Prognostic Values of Serum Procalcitonin and C-Reactive Protein in Patients of Bacterial Sepsis. *Zhonghua Yi Xue Za Zhi* (2014) 94:2106–9. doi: 10.3760/cma.j.issn.0376-2491.2014.27.007
62. AlRawahi AN, AlHinai FA, Doig CJ, Ball CG, Dixon E, Xiao Z, et al. The Prognostic Value of Serum Procalcitonin Measurements in Critically Injured Patients: A Systematic Review. *Crit Care* (2019) 23:390. doi: 10.1186/s13054-019-2669-1
63. Nakamura M, Oda S, Sadahiro T, Watanabe E, Abe R, Nakada T-A, et al. Correlation Between High Blood IL-6 Level, Hyperglycemia, and Glucose Control in Septic Patients. *Crit Care (London England)* (2012) 16:R58–8. doi: 10.1186/cc11301
64. Carey AJ, Tan CK, Ulett GC. Infection-Induced IL-10 and JAK-STAT: A Review of the Molecular Circuitry Controlling Immune Hyperactivity in Response to Pathogenic Microbes. *Jakstat* (2012) 1:159–67. doi: 10.4161/jkst.19918
65. Antoniv TT, Ivashkiv LB. Interleukin-10-Induced Gene Expression and Suppressive Function Are Selectively Modulated by the PI3K-Akt-GSK3 Pathway. *Immunology* (2011) 132:567–77. doi: 10.1111/j.1365-2567.2010.03402.x
66. Bah I, Kumbhare A, Nguyen L, McCall CE, El Gazzar M. IL-10 Induces an Immune Repressor Pathway in Sepsis by Promoting S100A9 Nuclear Localization and MDSC Development. *Cell Immunol* (2018) 332:32–8. doi: 10.1016/j.cellimm.2018.07.003

67. van Dissel JT, van Langevelde P, Westendorp RG, Kwappenberg K, Frölich M. Anti-Inflammatory Cytokine Profile and Mortality in Febrile Patients. *Lancet* (1998) 351:950–3. doi: 10.1016/s0140-6736(05)60606-x
68. Krishnamurthy P, Rajasingh J, Lambers E, Qin G, Losordo DW, Kishore R. IL-10 Inhibits Inflammation and Attenuates Left Ventricular Remodeling After Myocardial Infarction *via* Activation of STAT3 and Suppression of HuR. *Circ Res* (2009) 104:e9–18. doi: 10.1161/circresaha.108.188243
69. Makita N, Hizukuri Y, Yamashiro K, Murakawa M, Hayashi Y. IL-10 Enhances the Phenotype of M2 Macrophages Induced by IL-4 and Confers the Ability to Increase Eosinophil Migration. *Int Immunol* (2015) 27:131–41. doi: 10.1093/intimm/dxu090
70. Brigo N, Pfeifhofer-Obermair C, Tymoszuk P, Demetz E, Engl S, Barros-Pinkelnig M, et al. Cytokine-Mediated Regulation of ARG1 in Macrophages and Its Impact on the Control of Salmonella Enterica Serovar Typhimurium Infection. *Cells* (2021) 10(7):1823. doi: 10.3390/cells10071823
71. Hotchkiss RS, Monneret G, Payen D. Immunosuppression in Sepsis: A Novel Understanding of the Disorder and a New Therapeutic Approach. *Lancet Infect Dis* (2013) 13:260–8. doi: 10.1016/s1473-3099(13)70001-x

Conflict of Interest: The authors declare that the research was conducted in the absence of any commercial or financial relationships that could be construed as a potential conflict of interest.

frontiers in Immunology

ORIGINAL RESEARCH
published: 31 January 2022
doi: 10.3389/fimmu.2021.789141

GPR174 mRNA Acts as a Novel Prognostic Biomarker for Patients With Sepsis *via* Regulating the Inflammatory Response

Jianli Wang[1†], *Yanyan Hu*[1†], *Zhongshu Kuang*[1†], *Yao Chen*[1], *Lingyu Xing*[1], *Wei Wei*[1], *Mingming Xue*[1], *Sucheng Mu*[1], *Chaoyang Tong*[1*], *Yilin Yang*[1*] *and Zhenju Song*[1,2,3*]

[1] *Department of Emergency Medicine, Zhongshan Hospital, Fudan University, Shanghai, China,* [2] *Shanghai Key Laboratory of Lung Inflammation and Injury, Shanghai, China,* [3] *Shanghai Institute of Infectious Disease and Biosecurity, School of Public Health, Fudan University, Shanghai, China*

Previous studies indicated that G-protein coupled receptor 174 (GPR174) is involved in the dysregulated immune response of sepsis, however, the clinical value and effects of GPR174 in septic patients are still unknown. This study is aimed to evaluate the potential value of GPR174 as a prognostic biomarker for sepsis and explore the pathological function of GPR174 in cecal ligation and puncture (CLP)-induced septic mice. In this prospective longitudinal study, the expressions of peripheral *GPR174* mRNA were measured in 101 septic patients, 104 non-septic ICU controls, and 46 healthy volunteers at Day 1, 7 after ICU (Intensive Care Unit) admission, respectively. Then, the clinical values of GPR174 for the diagnosis, severity assessment, and prognosis of sepsis were analyzed. Moreover, the expressions of *GPR174* mRNA in CLP-induced septic mice were detected, and *Gpr174*-knockout (KO) mice were used to explore its effects on inflammation. The results showed that the levels of *GPR174* mRNA were significantly decreased in septic patients compared with non-septic ICU and healthy controls. In addition, the expressions of *GPR174* mRNA were correlated with the lymphocyte (Lym) counts, C-reactive protein (CRP), and APACHE II and SOFA scores. The levels of *GPR174* mRNA at Day 7 had a high AUC in predicting the death of sepsis (0.83). Further, we divided the septic patients into the higher and lower *GPR174* mRNA expression groups by the ROC cut-off point, and the lower group was significantly associated with poor survival rate (P = 0.00139). Similarly, the expressions of peripheral *Gpr174* mRNA in CLP-induced septic mice were also significantly decreased, and recovered after 72 h. Intriguingly, *Gpr174*-deficient could successfully improve the outcome with less multi-organ damage, which was mainly due to an increased level of IL-10, and decreased levels of IL-1β and TNF-α. Further, RNA-seq showed that *Gpr174* deficiency significantly induced a phenotypic shift toward multiple immune response pathways in septic mice. In summary, our results indicated that the expressions of *GPR174* mRNA were associated with the severity of sepsis, suggesting that GPR174 could be a potential

OPEN ACCESS

Edited by:
Wei Chong,
The First Affiliated Hospital of China Medical University, China

Reviewed by:
Andreas Limmer,
Essen University Hospital, Germany
Yong Ming Yao,
First Affiliated Hospital of Chinese PLA General Hospital, China

***Correspondence:**
Zhenju Song
song.zhenju@zs-hospital.sh.cn
Yilin Yang
yang.yilin@zs-hospital.sh.cn
Chaoyang Tong
tong.chaoyang@zs-hospital.sh.cn

[†]*These authors have contributed equally to this work and share first authorship*

Specialty section:
This article was submitted to Inflammation, a section of the journal Frontiers in Immunology

Received: *04 October 2021*
Accepted: *08 December 2021*
Published: *31 January 2022*

Citation:
Wang J, Hu Y, Kuang Z, Chen Y, Xing L, Wei W, Xue M, Mu S, Tong C, Yang Y and Song Z (2022) GPR174 mRNA Acts as a Novel Prognostic Biomarker for Patients With Sepsis via Regulating the Inflammatory Response. Front. Immunol. 12:789141. doi: 10.3389/fimmu.2021.789141

prognosis biomarker for sepsis. In addition, GPR174 plays an important role in the development of sepsis by regulating the inflammatory response.

Keywords: GPR174, sepsis, biomarker, prognosis, immune response

INTRODUCTION

Sepsis is a life-threatening organ dysfunction that is caused by a dysregulated host response to infection (Sepsis-3) (1). In 2017, a WHO resolution recognized sepsis as a global health priority with an unacceptably high mortality rate of 30 to 50% (2). It is well known that systemic inflammatory response syndrome accompanied by a hyper-inflammatory state leads to multiple organ dysfunction syndromes (MODS) or death (3). With further studies of immune response and pathological mechanism of sepsis, several markers have been found and evaluated for early recognition, diagnosis, and management of sepsis (4–6). However, finding novel diagnostic and targeted therapeutic biomarkers is still pivotal for septic patients due to the unsatisfactory specificity and sensitivity of the currently available biomarkers (7).

G protein-coupled receptors (GPCRs) are a group of cell surface receptors that detect extracellular molecules and activate cellular responses (8). GPCRs have been considered as one of the largest families of validated drug targets, which involve almost overall physiological functions and pathological processes. Approximately 34% of Food and Drug Administration (FDA)-approved drugs target this family (9). GPR174 is activated by lysophosphatidylserine (LysoPS), a lipid mediator known to induce rapid degranulation of mast cells, suppress proliferation of T lymphocytes, and enhance macrophage phagocytosis of apoptotic neutrophils (10, 11). GPR174 has been reported to play an important role in regulating the functions of regulatory T cells and activating B cells (12, 13). *In vitro*, overexpressed GPR174 effectively inhibited the proliferation of CHO cells stimulated by LysoPS (14). In a mice model of experimental autoimmune encephalomyelitis (EAE), the deficiency of *Gpr174* resulted in immunological tolerance to IFN-γ-dependent lesion by constraining regulatory T cells' development and function (15). In angiotensin II (Ang II)-treated mice, GPR174 could inhibit retinopathy by reducing inflammation (16). In addition, a genome-wide association study (GWAS) in the Chinese population implied that GPR174 variation could be a risk factor for Graves's disease (17).

Our previous studies indicated that lack of *Gpr174* significantly decreased the concentrations of proinflammatory cytokines, such as tumor necrosis factor-α (TNF-α), interleukin-1β (IL-1β) in lipopolysaccharide (LPS)-induced septic mice (18), which suggested that GPR174 might be considered as a potential biomarker for the patients with sepsis. However, the clinical values of GPR174 for the diagnosis, severity, and prognosis of sepsis have yet to be investigated. Thus, we conducted a prospective, non-interventional cohort study to assess the association between the levels of *GPR174* mRNA and the severity and mortality of septic patients. Further, we explored the potential effects and mechanism of GPR174 on the host immune responses in CLP-induced mice.

MATERIALS AND METHODS

Septic Patients and Controls

A prospective study was carried out in the emergency intensive care unit (ICU) of Zhongshan Hospital, Fudan University, Shanghai, China. From December 2017 to September 2019, 101 septic patients who met the clinical criteria for sepsis-3 were enrolled (1). There were 104 non-septic patients in the ICU (poly-trauma, cerebral trauma, intracranial hemorrhage, cerebrovascular accidents, and hypertensive emergencies) recruited as non-septic ICU controls. Furthermore, septic patients were divided into survival group and non-survival group according to the survival of 90 days.

Exclusion criteria included age below 18 years, pregnancy, severe chronic respiratory disease, severe chronic liver disease (defined as Child-Pugh score > 10), malignancy, immune disease, using high-dose immunosuppressive therapy, and AIDS patients. In addition, 46 age- and gender-matched healthy volunteers with no medical problems were obtained from the medical examination center of Zhongshan Hospital, Fudan University, China. The flowchart of this study is shown in **Supplementary Figure 1**.

Patients' characteristics (age, gender, and previous health status), as well as clinical data including Sequential Organ Failure Assessment (SOFA) and Acute Physiology and Chronic Health Evaluation II (APACHE II) scores, source of primary infection, and ICU mortality, were obtained after ICU admission. The characteristics of patients, mechanical ventilation, and vasopressor treatment are shown in **Table 1**. This study was approved by the Ethics Committee Study Board of Zhongshan Hospital, Fudan University, Shanghai, China (number: B2014-082). Written informed consent was obtained from patients, the next of kin, or guardians on the behalf of the participants before enrollment according to the Declaration of Helsinki.

Mice

Gpr174 knock-out (*Gpr174*-KO) mice generated by a homologous recombination method were provided by Shanghai Southern Model Biotechnology Co. Ltd. (Shanghai, China). Age- and gender-matched C57BL/6 mice were obtained from Fudan University, Shanghai, China. Mice were housed under a specific pathogen-free condition with a 12 h-light/12 h-dark cycle, 22 ± 2°C. Animal experiments were approved by the Ethics Committee of Laboratory Animal Science, Fudan University, China (number 201804001Z).

TABLE 1 | Baseline characteristics of patients at ICU admission.

Variables	Non-septic ICU Controls	Septic Patients	*P*. value
n	104	101	
Demographics			
Age, year, mean ± S.D.	61.6 ± 18.9	61.5 ± 16.7	0.937
Male, sex, n (%)	58 (55.8)	55 (54.5)	0.85
Patients' outcomes			
90-d mortality, n (%)	2 (1.9)	26 (25.7)	<0.001
Severity of disease			
SOFA score, median (IQR)	1 (0 - 3)	4 (2 - 7)	<0.001
APACHE II score, media (IQR)	7 (4 - 11)	12 (7 - 19)	<0.001
Primary site of infections			
Pneumonia, n (%)		62 (61.4)	
Urinary tract infections, n (%)		10 (9.9)	
Intra-abdominal infections, n (%)		18 (17.8)	
Blood, n (%)		8 (7.9)	
Others, n (%)		3 (3.0)	
Invasive ventilation, n (%)	3 (2.9)	30 (29.7)	<0.001
Non-invasive ventilation, n (%)	6 (5.7)	23 (22.8)	<0.001
CRRT, n (%)	0 (0)	2 (1.98)	0.143
Vasopressors, n (%)	1 (0.96)	22 (27)	<0.001
Laboratory parameters			
CRP, mg/L, median (IQR)	47.8 (17.2, 100.1)	86.9 (26.1, 150.4)	0.010
PCT, ng/mL, median (IQR)	0.2 (0.1, 1.3)	0.8 (0.2, 8.9)	<0.001
WBC, $*10^9$/L, median (IQR)	8.4 (6.0, 11.5)	10.8 (7.1, 15.5)	0.001
Neu, $*10^9$/L, median (IQR)	6.3 (3.9, 9.3)	9.3 (5.7, 13.5)	<0.001
Lym, $*10^9$/L, median (IQR)	1.1 (0.8, 1.7)	0.9 (0.5, 1.3)	<0.001
IL-2R, U/mL, median (IQR)	842 (530, 1325)	1116 (694, 1851)	0.001
IL-6, pg/mL, median (IQR)	16.1 (7.8, 52.1)	29.8 (10.2, 89.1)	0.015
IL-8, pg/mL, median (IQR)	21.0 (13.3, 40.0)	44.0 (24.0, 82.0)	<0.001
IL-10, pg/mL, median (IQR)	5.0 (5.0, 8.5)	8.6 (5.0, 17.8)	<0.001

ICU, Intensive Care Unit; SOFA, sequential organ failure assessment; APACHE, acute physiology and chronic health evaluation; CRP, C-reactive protein; PCT, procalcitonin; WBC, white blood cells; Neu, neutrophil; Lym, Lymphocyte.

CLP-Induced Septic Mouse Model

The CLP-induced septic mouse model was established as described previously (19). In short, mice were anesthetized with 1% pentobarbital (i.p. 10 ml/kg of body weight). After that, the cecum was ligated in half, and a 21-gauge needle was used to puncture the stump once to squeeze out a small number of feces. The cecum was placed back into a normal intraabdominal position, and the abdominal incision was closed by applying sample running sutures. Then, pre-warmed normal saline (50 ml/kg of body weight) was injected subcutaneously. Sham-operated control mice underwent the same surgical procedures without puncture or ligation. The survival rate was monitored daily for 1 week.

Quantitative Polymerase Chain Reaction

The expressions of *GPR174* mRNA in peripheral blood of all samples were tested by quantitative PCR on Day 1 (D1) and Day 7 (D7) after ICU admission. Peripheral blood mononuclear cells (PBMC) were isolated from fresh anticoagulant blood by Ficoll lymphocyte separation solution (Lymphoprep, Axis-Shield, UK). The total RNAs from all enrolled subjects and mice were extracted using TRIzol reagent (Life Technologies, Carlsbad, CA) and then 10 μg of RNA samples were reverse-transcribed into cDNA with Prime Script™ reagent kit (Takara, Dalian, China) following the manufacturer's instructions. Quantitative PCR was performed with SYBR® Premix Ex Taq™ II (Takara, Dalian, China) on a 7500 Real-time PCR system (Applied Biosystems, Carlsbad, CA), according to the manufacturer's instructions.

Primers used were as follows:

human-GPR174 sense 5'-ATCATCTGCCTTGCCTGT GTACTC, antisense 5'-CGCCAATGGTCATCATAACAACGG; human-GAPDH sense 5'-AAGGTCGGAGTCAACGGATT, antisense 5'- CTCCTGGAAGATGGTGATGG; mouse-Gpr174 sense 5'- TTGGTCTGCATCAGTGTGCGAAG, antisense 5'-CAGGCAGGCAAGGCAGATGATC; mouse-Gapdh sense 5'-GGAGAGTGTTTCCTCGTCCC, antisense 5'-ACTGT GCCGTTGAATTTGCC; mouse-Cfh sense; 5'- GTATCAA AACGGATTGTGACGT, antisense 5'- TAACACATGTCACA GTGTCTGA; mouse-Oas1g sense 5'- TAAGAAACAGCTGTA CGAGGTT, antisense 5'- CCAGATGAGGATGGTGTAGATT; mouse-Spp1 sense 5'- AAACACACAGACTTGAGCATTC, antisense 5'- TTAGGGTCTAGGACTAGCTTGT.

Cytokine's Measurement

Blood samples of septic and ICU non-septic patients and mice were centrifuged (3500 rpm, 15 min, room temperature) after collection. The serum was immediately frozen in liquid nitrogen (LN2) and stored at -80°C for further use. The levels of IL-1β, IL-2R, IL-6, IL-8, and IL-10 were measured by ELISA kit (R&D Systems, Inc., Minneapolis, MN) according to the manufacturer's

protocol. Serum concentrations of CRP and PCT were measured by IMMAGE800 analyzer (Beckman Coulter, Inc. CA) and VIDAS B.R.A.H.M.S PCT analyzer (Biomerieux, Lyon, France). Routine blood tests and blood gas analysis were conducted in the clinical laboratory of Zhongshan Hospital, Fudan University, Shanghai, China.

Hematoxylin and Eosin Stain

Tissues (lung, liver) were excised at 0 h, 12 h, 24 h, 72 h, and 1 and 2 weeks after CLP, washed with DPBS, fixed with 4% formalin buffer, and paraffin embedded. There were 4-6 μm sections cut and placed on glass slides, deparaffinized in xylene, and rehydrated in a series of alcohol solutions. Sections were then washed in distilled water, and stained with H&E for histopathological examination.

RNA-Sequencing

Total RNA was digested by DNase I (Qiagene) and separated by Dynabeads® mRNA DIRECT™ Kit (Life Technologies). The isolated mRNAs were used for mRNA-seq libraries with a KAPA Stranded mRNA-Seq Kit according to the manufacturer's instructions. Libraries were sequenced on the Hiseq Xten system (Illumina) with a reading length of 150 base pairs (bps). Differentially expressed genes (DEGs) between *Gpr174*-KO and Wild type (WT) mice were identified using the Bioconductor package RUVSeq (version 1.0.0, http://www.bioconductor.org). Hierarchical cluster analysis of the DEGs was carried out by the "hclust" function of the "stats" package in R software (https://www.r-project.org/). The heatmap for this cluster analysis of the DE genes was drawn with heatmap.2 function in the "gplots" package. Gene ontology analysis (GO analysis) performed by Blast2GO software (version 4) was used to provide a further understanding of these results.

Statistical Analysis

Normal distribution data were expressed as means and standard deviations (S.D.) with Student's t-test or ANOVA test. Non-normal distribution continuous data were expressed as medians with the 25th and 75th quartiles applying Mann-Whitney U test or Kruskal-Wallis test followed by Dunn's multiple comparisons post-test. Categorical data were expressed as frequency and percentage. Non-parametric Spearman's rank correlation coefficient was performed to test correlations between two parameters. For analyzing the independent predictors of 90-day mortality, binary logistic regression was used to determine the discriminative power of *GPR174* mRNA for 90-day mortality. Receiver-operating characteristic (ROC) curves were constructed and the area under the curve (AUC) was determined with a 95% confidence interval (CI). The bootstrap and Venkatraman's test were used for comparing the AUC using the "pROC" package in R (20). Kaplan-Meier curves of disease-free survival were plotted and compared by Cox regression analysis in the groups layering by ROC cut-off point. For murine survival studies, Kaplan-Meier analyses followed by log-rank tests were performed. All statistical analyses were done using SPSS 16.0, R 4.0.2, and GraphPad Prism version 5.01 (GraphPad Software, San Diego, CA). P values less than 0.05 were considered statistically significant.

RESULTS

Baseline Characteristics of Septic and Non-Septic ICU Patients

The demographic and clinical characteristics of septic patients and non-septic ICU controls are presented in **Table 1**. No age effects were observed between septic patients and non-septic ICU controls (61.5 vs. 61.6, *P*=0.937). The 90-day mortality was 25.7% in septic patients, while 2% in non-septic ICU controls. After ICU admission (Day 1), septic patients had significantly higher APACHE II and SOFA scores than non-septic ICU controls. Non-survival septic patients also had significantly higher APACHE II and SOFA scores, and the utilization rate of mechanical ventilation and vasoactive agents than survivors (**Table 2**). The levels of serum PCT, IL-2R, IL-6, and the counts of WBC, neutrophil, and lymphocyte were also significantly higher in septic patients than that in non-septic ICU controls (**Table 1**). However, there was no difference between non-survivors and survivors in sepsis patients at Day 1 (D1) for these inflammatory markers (**Table 2**).

The Levels of Relative Expressions of *GPR174* mRNA in Septic and Non-Septic ICU Patients

The relative expressions of *GPR174* mRNA in septic patients at D1 were significantly lower than that in non-septic ICU controls and healthy volunteers (**Figure 1A**). The levels of *GPR174* mRNA had no significant difference between survivors and non-survivors in patients with sepsis at D1 (**Figure 1B**). However, lower expressions of serum *GPR174* mRNA were observed in non-survivors compared to survivors at Day 7 after admission (D7) (**Figure 1B**). Interestingly, with the recovery of sepsis, the concentration of *GPR174* mRNA in septic patients returned to the level of healthy subjects (**Figure 1C**).

The Correlations of *GPR174* mRNA With APACHE II and SOFA Scores, and Inflammatory Cytokines in Septic Patients

Our results showed that *GPR174* mRNA levels were significant negative correlations with APACHE II and SOFA scores (**Figure 2**). As for other biomarkers, a significant negative correlation was observed between *GPR174* mRNA and CRP, while there is a positive correlation for the count of Lym at D7 (**Figure 3**). However, no significant correlations were found among the levels of *GPR174* mRNA and PCT, IL-2R, IL-6, IL8, IL-10, and the count of Neu, WBC at D7.

Then, we detected the individual change of those markers from D1 to D7 both in survivors and non-survivors in sepsis. Interestingly, *GPR174* mRNA showed remarkable differences both in the non-survivor and survivor groups (ascending in the survivors and descending in non-survivors, respectively),

TABLE 2 | Baseline characteristics of survivors and non-survivors in septic patients at ICU admission.

Parameter	Survivors	Non-survivors	*P* value
n	75	26	
Demographics			
Age, year, mean ± S.D.	60 ± 2.03	65 ± 2.94	0.182
Male, sex, *n*	37 (49.3)	18 (69.2)	0.11
Severity of disease			
SOFA score, median (IQR)	2 (1, 4)	7 (4, 9)	0.001
APACHE II score, media (IQR)	7 (5, 13)	16 (13, 24)	<0.001
Primary site of infections			
Pneumonia, *n* (%)	37 (49.3)	25 (96.1)	<0.001
Urinary tract infections, *n* (%)	10 (13.3)		<0.001
Intra-abdominal infections, *n* (%)	18 (24)		<0.001
Blood, *n* (%)	8 (10.6)		<0.001
Others, *n* (%)	2 (2.7)	1 (3.8)	0.093
Invasive ventilation, *n* (%)	12 (16)	18 (69)	<0.001
Non-invasive ventilation, *n* (%)	17 (22.7)	6 (23.1)	0.999
CRRT, *n* (%)	0	2 (7.7)	0.064
Vasopressors, *n* (%)	9 (12)	13 (50)	<0.001
Laboratory parameters			
CRP, mg/L, median (IQR)	55.5 (18.3, 114.5)	90 (31.8, 133.9)	0.699
PCT, ng/mL, median (IQR).	0.4 (0.1, 2.3)	1.4 (0.2, 9.9)	0.643
WBC, $*10^9$/L, median (IQR)	8.8 (6.5, 12.5)	12.0 (9.1, 20.0)	0.322
Neu, $*10^9$/L, median (IQR)	6.8 (4.5, 10.3)	10.2 (6.8, 17.8)	0.184
Lym, $*10^9$/L, median (IQR)	1.0 (0.7, 1.5)	0.6 (0.4, 1.2)	0.104
IL-2R, U/mL, median (IQR)	938 (571, 1483)	1059 (854. 2166)	0.732
IL-6, pg/mL, median (IQR)	21.0 (8.1, 66.0)	47.0 (14.3, 129.0)	0.559
IL-8, pg/mL, median (IQR)	27.0 (15.0, 57.8)	62.0 (22.0, 87.0)	0.473
IL-10, pg/mL, median (IQR)	5.7 (5.0, 11.6)	7.8 (5.4, 12.5)	0.573

ICU, Intensive Care Unit; SOFA, sequential organ failure assessment; APACHE, acute physiology and chronic health evaluation; CRP, C-reactive protein; PCT, procalcitonin; WBC, white blood cells; Neu, neutrophil; Lym, Lymphocyte.

while other biomarkers did not show such results, even for APACHE II and SOFA scores (**Supplementary Figure 2**).

The Correlations of GPR*174* mRNA With 90-Day Mortality in Patients With Sepsis

Using binary logistic regression analysis adjusted by age and gender, both *GPR174* mRNA (OR = 0.004, $P = 0.003$) and CRP (OR = 1.010, $P = 0.031$) at D7 were found to be independent predictors of 90-day mortality in patients with sepsis (**Table 3**).

We further investigated the prognostic value of *GPR174* mRNA in sepsis with the ROC analysis. The area under the ROC curve (AUC) of *GPR174* mRNA at D7 was higher than that at D1 (0.83 vs. 0.60; $P < 0.001$). Furthermore, *via* comparing the AUC of *GPR174* mRNA with APACHE II score, SOFA score, CRP, PCT at D7, we found that the AUC of *GPR174* mRNA was higher than that of PCT (0.83 vs. 0.66; $P = 0.05$). However, there was no difference when compared with CRP (AUC = 0.72, $P = 0.21$), APACHE II score (AUC = 0.88; $P = 0.704$), and SOFA score (AUC = 0.92; $P = 0.26$) (**Figure 4**).

The Clinical Value of *GPR174* mRNA at Day 7 in Predicting the 90-Day Mortality

The samples were divided into higher and lower *GPR174* mRNA groups according to ROC cut-off point and the K-M survival curve was obtained by Cox regression analysis. At D1, the cut-off level for *GPR174* mRNA is 0.071, and the sensitivity and specificity were 0.880 and 0.338, respectively. At D7, the cut-off level for *GPR174* mRNA is 0.101, and the sensitivity and specificity were 0.890 and 0.720, respectively. The Kaplan-Meier curves showed that no significant difference was found between the two groups at D1 [HR = 0.756, 95% CI = (0.291, 1.966), $P = 0.566$], while the mortality of the lower *GPR174* mRNA group at D7 was significantly higher than that of the higher *GPR174* mRNA group [HR = 0.224, 95% CI = (0.090, 0.561), $P = 0.001$] (**Figure 5**).

The Dynamic Changes of *Gpr174* mRNA in Mice After CLP-Induced Sepsis

To further study the expression of *Gpr174* mRNA in sepsis, a CLP-induced septic mice model (n = 20 per group) was used to test the expression of *Gpr174* mRNA in PBMC and spleen. Compared to control mice with sham surgery, the levels of *Gpr174* mRNA in PBMC significantly decreased in septic mice, then met an ascending inflection point at 72 h (**Supplementary Figure 3A**), while it continuously decreased in the spleen (**Supplementary Figure 3B**).

The pathological injury of the liver and lung after CLP was confirmed by H&E staining (n = 5 per group). The results showed that clear polygonal hepatic lobules with obvious hepatic cords and sinuses were seen in the liver in the sham surgery group. However, the boundaries of some hepatic lobules were not clear after CLP, and hepatic cord disorder could be seen in hepatic lobules. The damage was most severe at 72 h, which was characterized by cell edema, infiltration of inflammatory

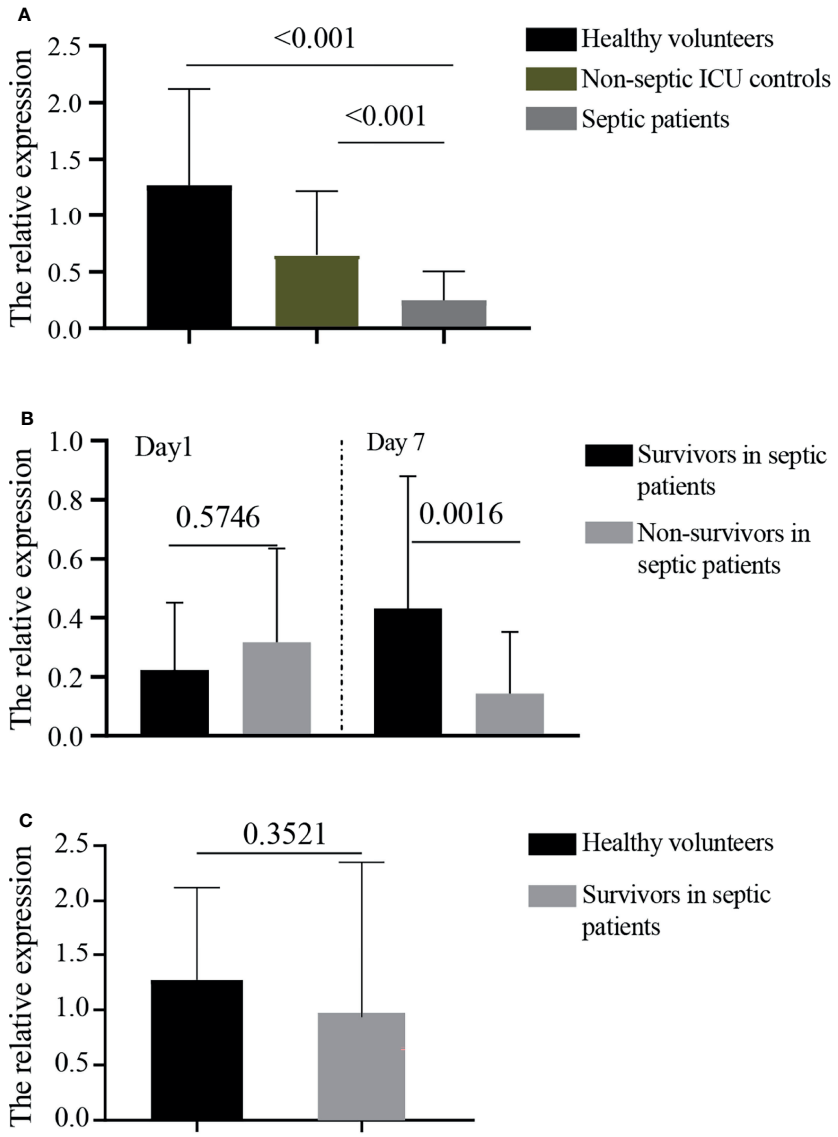

FIGURE 1 | The relative expressions of GPR174 mRNA in patients. **(A)** The concentrations of serum *GPR174* mRNA were measured by quantitative PCR from 101 septic patients, 104 non-septic ICU controls, and 46 healthy volunteers. **(B)** The concentrations of *GPR174* mRNA were measured from survivors and non-survivors in septic patients at Day 1 and Day 7 after ICU admission. **(C)** The levels of *GPR174* mRNA in sepsis survivors at discharge were compared with healthy volunteers. *P* values less than 0.05 were considered statistically significant.

cells, and hepatic sinus congestion (**Supplementary Figure 3C**). As for lung tissues, the alveolar cavity was clearly visible in the sham surgery group, while most of the alveolar cavity showed exudation and edema. Severe inflammatory cells infiltration was observed at 72 h after CLP (**Supplementary Figure 3D**).

Gpr174-Deficiency Alleviated Mortality and Inflammatory Response in CLP-Induced Septic Mice

Compared with sham mice, the mortality rate of *Gpr174*-KO septic mice was dramatically decreased from 55% to 25% (n = 20 per group) (**Supplementary Figure 4A**). In addition, *Gpr174*-deficiency significantly alleviated the pathology scores of lung and liver, respectively. H&E staining showed that inflammatory cell infiltration and edema of lung tissue were less severe in *Gpr174*-KO + CLP mice compared to WT + CLP mice (**Supplementary Figure 4B**). Moreover, the hepatic cells edema was less in *Gpr174*-KO + CLP mice than that in WT + CLP mice (**Supplementary Figure 4C**).

To evaluate the effect of GPR174 on the dysregulated systemic inflammation, the serum levels of IL-1β, TNF-α, and IL-10 were examined at 24 h after the CLP challenge (n = 5 per group). The results showed that the levels of IL-1β and TNF-α were significantly decreased in *Gpr174*-KO+CLP mice than in the

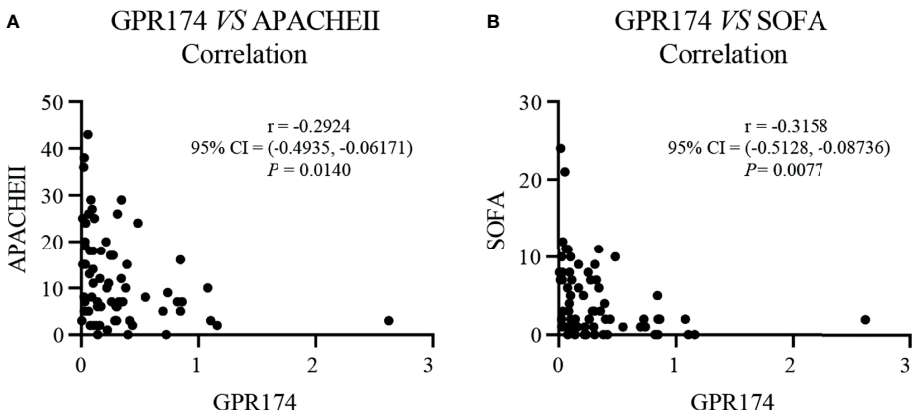

FIGURE 2 | The levels of *GPR174* mRNA were correlated with disease severity in septic patients. **(A)** Correlation of the relative expression of *GPR174* mRNA with APACHE II score in patients with sepsis. **(B)** Correlation of the expression of *GPR174* mRNA with SOFA score in patients with sepsis. Dots represent individual participants. *P* values less than 0.05 were considered statistically significant.

WT+CLP mice, and the levels of IL-10 were significantly increased (**Supplementary Figure 5**).

Then, RNA-seq was used to explore the mechanism of GPR174 in the pathogenesis of sepsis. A total of 10,389 genes were identified compared between *Gpr174*-KO mice and WT mice at 24 h after the CLP challenge (n = 3 per group). *Gpr174*-KO+CLP mice and WT+CLP mice were well separated by cluster PCA analysis (**Figure 6A**). We defined the identified genes as differentially expressed genes (DEPs) if there was a log2FC in excess of 1.5 or less than -1.5, FDR < 0.05. A total of 360 genes changed significantly as shown in the heatmap (**Figure 6B**). GO analysis and Kyoto Encyclopedia of Genes and Genomes (KEGG) pathway enrichment analysis were performed to provide a further understanding of these results. A similar differential effect was observed in the molecular and immunologic pathways that were impacted between *Gpr174*-KO+CLP mice and WT+CLP mice. Further validation of the findings was carried out by qPCR. Intriguingly, we found that representative potential mediators of the immune response, including dendritic cell-specific transmembrane protein and macrophage mannose receptor 1 were highly upregulated, while interleukin-12 subunit alpha and Sialoadhesin were downregulated (**Figure 6C**).

DISCUSSION

Early diagnosis and intervention are important for improving the prognosis of sepsis. Although several serum biomarkers, APACHE II and SOFA scores were applied to diagnose and assess the illness severity of sepsis in clinical practice (21), there were no ideal targeted biomarkers to predict the initiate and progress of sepsis. Recently, GPR174, a seven-transmembrane G protein-coupled receptor, was identified to be mainly expressed on immune cells such as T/B cells (22) and reported as a risk factor for subcutaneous metastases (23), Graves' disease (24), and autoimmune Addison's disease (25). To explore the effects of GPR174 in sepsis, we conducted a series of animal studies and found that GPR174 could regulate the anti-inflammatory response by negatively regulating Treg and B cell functions and attenuating the tissue injury (18, 26). However, the association between GPR174 and severity, mortality of septic patients was still unknown.

In this prospective observational study, we found that the relative expression of *GPR174* mRNA was significantly lower in septic patients than that in non-septic ICU controls and healthy volunteers at D1, which indicated that GPR174 might be a novel biomarker for early diagnosis of sepsis. Moreover, decreased relative expression of serum *GPR174* mRNA was related to the illness severity of sepsis. Importantly, both logistic regression and Cox regression analysis showed that GPR174 was an independent predictor of 90-day mortality in septic patients. Similarly, declining expression of *GPR174* mRNA was found in CLP-induced septic mice. All these results suggested that decreasing *GPR174* mRNA was associated with increased mortality in sepsis. We further carried out the change of the markers on individuals dynamically, including *GPR174* mRNA, APACHE II and SOFA scores, CRP, and PCT. Interestingly, only *GPR174* mRNA showed remarkable differences both in the non-survivor and survivor groups (ascending in the survivors and descending in non-survivors, respectively), which indicated that GPR174 might be a sensitivity prognostic biomarker in sepsis.

During severe infection, the body could eliminate pathogens *via* activating inflammatory reaction, which in turn leads to tissue damage due to uncontrolled cytokine storm (27–29). In view of the role of GPR174 in immune response, we focused on the relationship between GPR174 and immune indicators such as IL-2R, IL-6, IL-8, IL-10, and the counts of WBC, neutrophil, and lymphocyte in septic patients. *GPR174* mRNA had a positive correlation with the counts of lymphocytes. In addition, transcriptomic results showed a shift in *Gpr174*-KO mice, involving T cell homeostasis after the CLP challenge.

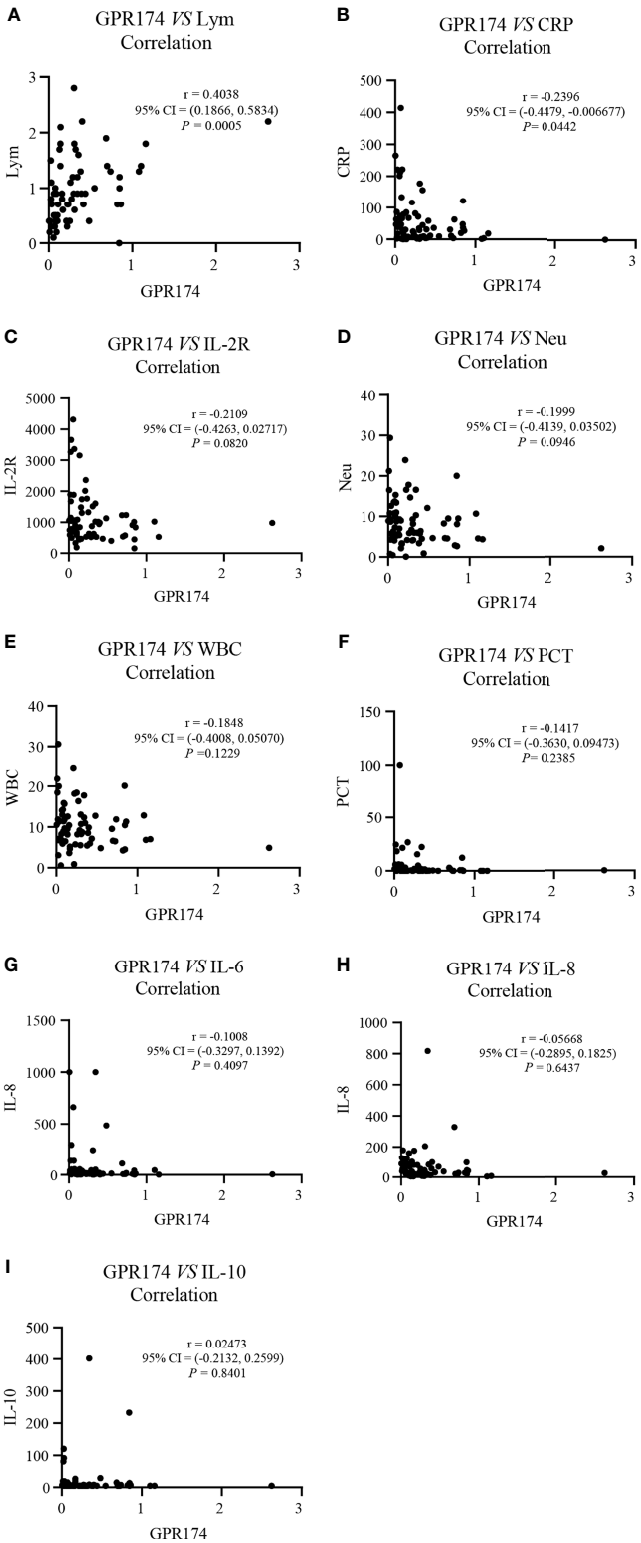

FIGURE 3 | The expression of *GPR174* mRNA correlated with laboratory parameters in septic patients. **(A–I)** Correlation of the expression of *GPR174* mRNA with the counts of WBC, Neu, and Lym, CRP, IL-2R, PCT, IL-6, IL-8, and IL-10 in patients with sepsis, respectively. Dots represent individual participants. *P* values less than 0.05 were considered statistically significant.

TABLE 3 | Independent factors predicting 90-day mortality in septic patients.

Variable	B	OR	95% CI	*P* value
On the day of admission (Day1)				
GPR174	1.321	3.748	0.623-22.536	0.149
CRP	0.000	1.000	0.995-1.005	0.864
PCT	-0.003	0.997	0.979-1.017	0.792
At Day 7 after admission (Day7)				
GPR174	-5.557	0.004	0.001-0.150	0.003
CRP	0.010	1.010	1.001-1.020	0.031
PCT	0.079	1.082	0.969-1.209	0.162

Adjusted by age and gender.
OR, odds ratio; 95% CI, 95% confidence interval CRP, C-reactive protein; PCT, procalcitonin.

Meanwhile, the lack of *GPR174* had significantly decreased the serum concentrations of proinflammatory cytokines (IL-1β and TNF-α) after the CLP challenge in mice, while increased the serum concentration of anti-inflammatory cytokines (IL-10). Following re-exposure to LPS, macrophages exhibit an immunosuppressive state known as LPS tolerance, which is characterized by repressed proinflammatory cytokine production. Recently, Chiara Porta et al. reported that LPS-tolerant

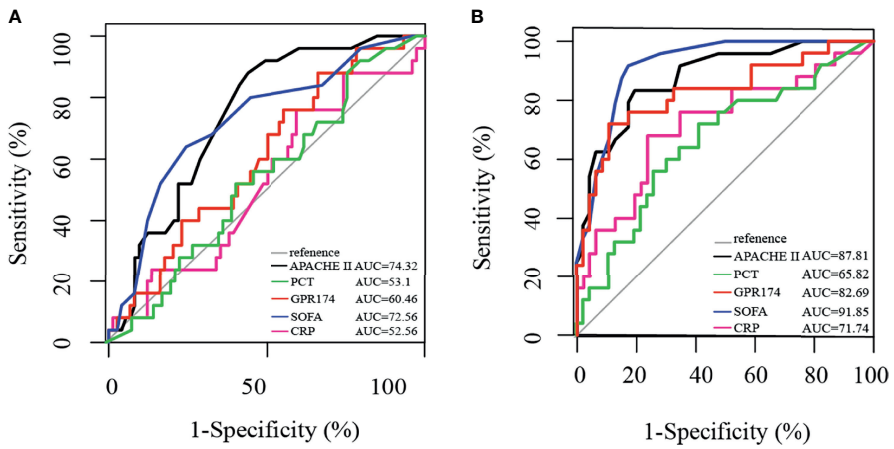

FIGURE 4 | Receiving operating characteristic (ROC) curve for predicting 90-day mortality in septic patients. **(A)** ROC of APACHE II score, PCT, *GPR174* mRNA, SOFA score, and CRP for mortality at ICU admission. **(B)** ROC of APACHE II score, PCT, *GPR174* mRNA, SOFA score, and CRP for mortality at Day 7 after ICU admission.

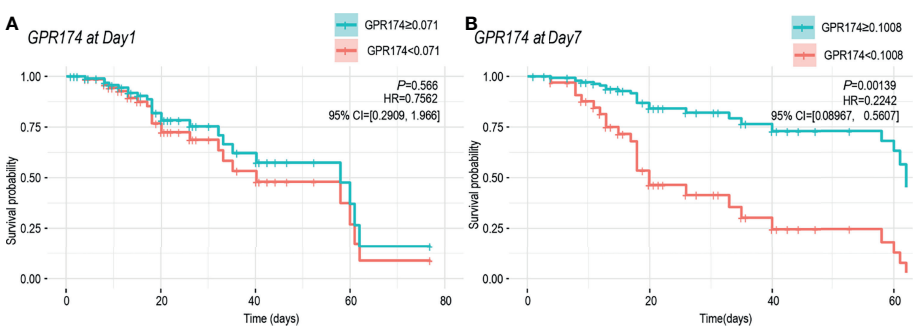

FIGURE 5 | Cox regression model for survival analysis. **(A)** K-M survival curve of the *GPR174* mRNA expression at ICU admission. Patients were divided into higher and lower *GPR174* mRNA groups according to the cut-off level of 0.071. **(B)** K-M survival curve of the *GPR174* mRNA expression at D7 after ICU admission. Patients were divided into higher and lower *GPR174* mRNA groups according to the cut-off level of 0.1008. HR: Hazard Ratio. 95% CI: 95% confidence interval.

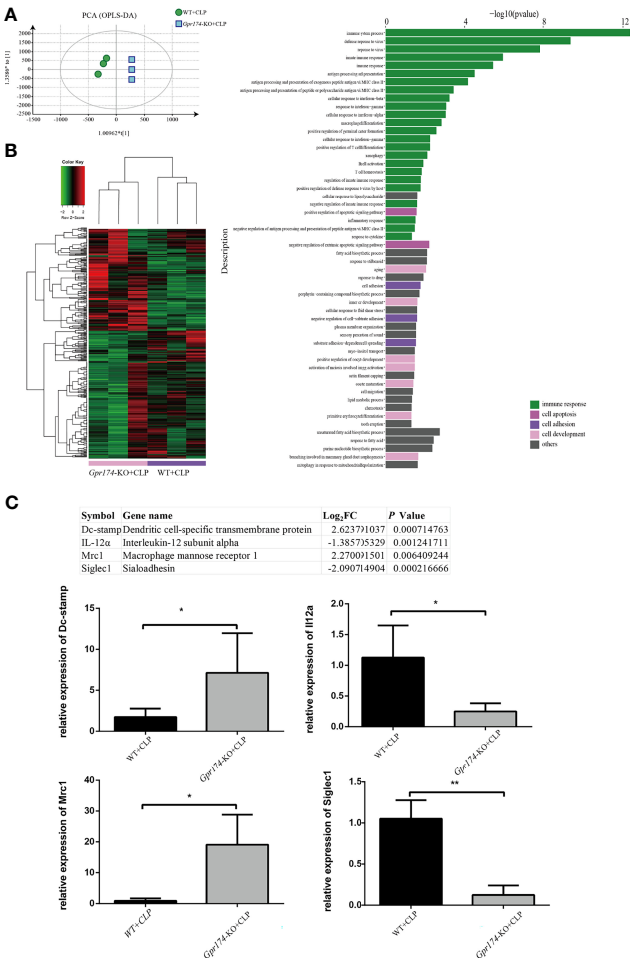

Symbol	Gene name	Log_2FC	*P* Value
Dc-stamp	Dendritic cell-specific transmembrane protein	2.623771037	0.000714763
IL-12α	Interleukin-12 subunit alpha	-1.385735329	0.001241711
Mrc1	Macrophage mannose receptor 1	2.270091501	0.006409244
Siglec1	Sialoadhesin	-2.090714904	0.000216666

FIGURE 6 | Distinct transcriptional signature in spleen after CLP treated between Gpr174-KO and wild type mice (n = 3 per group). **(A)** Sample correlation was computed by PCA analysis. Percentages in PCA analysis axis indicated the proportional variance explained by PC. **(B)** Differentially expression genes (DEG) were expressed by heatmap with normalized raw z-scores (left) and pyramid plot with -log_{10} (*P* value) demonstrated the involved pathways form DES genes (right). **(C)** qPCR verification of most differentially expressed genes (n = 3-6). Representative genes from the table were verified by qPCR. Values are mean with SEM, *P < 0.05, **P < 0.01.

macrophages have the phenotype of M2-polarized cells (30). M2 macrophages produce anti-inflammatory cytokines/chemokines such as IL-10, TGF-β, and CCL18 (AMAC-1). IL-10 has been shown to be expressed in LPS-resistant macrophages and limits excessive inflammatory reactions in response to endotoxin (31). Here, we previously reported a *Gpr174*-efficiently Treg that could promote polarization of macrophages toward anti-inflammatory M2 macrophages by IL-10 and cell-contact pathway both *in vitro* and *in vivo* (18). These all indicated that the GPR174 might be involved in LPS tolerance.

Other potential mechanisms in sepsis include the decreased expression of a broad array of downregulation of numerous positive costimulatory molecules, and upregulation of inhibitory receptors/ligands (32–34). Specifically, transcripts of Dc-stamp, which is involved in regulating dendritic cell antigen presentation activity and played a role in the maintenance of immune self-tolerance (35), were highly upregulated in *Gpr174*-KO mice. Macrophage mannose receptor 1 (Mrc1), known as a phagocytic receptor for bacteria, fungi, and other pathogens (36, 37), was also upregulated in *Gpr174*-KO mice. On the other hand, Interleukin-12 subunit alpha (IL-12α), acting as a growth factor of activated T and NK cells, had obviously decreased in the present transcriptomic results (38). Similarly, Sialoadhesin (Siglec1), which depending on the IFN/JAK/STAT1 signaling pathway (39), had obviously decreased in *Gpr174*-KO mouse vs. wild-type mouse after CLP injury. These results revealed and supported the potential role of GPR174 on immunoregulation, however, the specific mechanism remains to be studied.

Several limitations should be addressed in the current study. First, the small sample size did not allow in-depth analysis of the relationships between GPR174 and disease severity, as well as mortality, so a larger multicenter study is required in the future.

Second, further studies are needed to explore the exact function and mechanism of GPR174 in the host immune response during sepsis.

In conclusion, our results first showed that the expression of *GPR174* mRNA is associated with disease severity and mortality in sepsis. Monitoring the levels of *GPR174* mRNA could be effective in the identification of septic patients at high risk of death. Further studies are needed to explore the regulating mechanism of GPR174 on immune cells during sepsis.

DATA AVAILABILITY STATEMENT

The datasets presented in this study can be found in online repositories. The names of the repository/repositories and accession number(s) can be found below: https://www.ncbi.nlm.nih.gov/, BioProject ID: PRJNA771765.

ETHICS STATEMENT

The studies involving human participants were reviewed and approved by the Ethics Committee Study Board of Zhongshan Hospital, Fudan University, Shanghai, China. The patients/participants provided their written informed consent to participate in this study. The animal study was reviewed and approved by the Ethics Committee Study Board of Zhongshan Hospital, Fudan University, Shanghai, China.

AUTHOR CONTRIBUTIONS

ZS, YY, and CT conceived and designed the experiments. YH and ZK collected the samples and clinical data. JW performed the animal experiments. YC and LX performed the statistical analysis. WW and MX contributed reagents/materials/analysis tools. SM helped to draft and revise the manuscript. All authors contributed to the article and approved the submitted version.

FUNDING

This work was supported by Shanghai Municipal Health Bureau (Grant No. ZXYXZ-201906, Grant No. GWV-10.2-XD04), Science and Technology of Shanghai Committee (Grant No. 20Y11900100, Grant No. 21MC1930400, Grant No.20DZ 2261200), and National Natural Science Foundation of China (Grant No. 82072214).

ACKNOWLEDGMENTS

The authors gratefully acknowledged the nurses and staff of the EICU of Zhongshan Hospital, Fudan University, China.

SUPPLEMENTARY MATERIAL

The Supplementary Material for this article can be found online at: https://www.frontiersin.org/articles/10.3389/fimmu.2021.789141/full#supplementary-material

Supplementary Figure 1 | Study flowchart.

Supplementary Figure 2 | The trend of the markers on individuals from D1 to D7 in septic patients. The individual trend of GPR174 mRNA, APACHE II score, SOFA score, CRP, IL-2R, PCT, IL-6, IL-8, and IL-10, the counts of Neu, Lym, and WBC were tested both in non-survivor and survivor of septic patients, respectively. Dots represent individual participants. P values less than 0.05 were considered statistically significant.

Supplementary Figure 3 | The changes of Gpr174 mRNA and injury of vital organs in CLP-induced septic mouse. **(A)** Levels of *Gpr174* mRNA in PBMC were tested by quantitative PCR, which were collected at 0 h, 12 h, 24 h, 72 h, 1 w, 2 w in CLP-induced sepsis. **(B)** Levels of *Gpr174* mRNA in the spleen were tested by quantitative PCR collected at 0 h, 12 h, 24 h, 72 h, 1 w, 2 w in CLP-induced sepsis. **(C)** Representative examples of hematoxylin and eosin (H&E)-stained liver tissues from mice at 0 h, 12 h, 24 h, 1 w, 2 w after CLP (n = 5 per group). Hepatic cord disorder (shown by the black arrow) could be seen in hepatic lobules in septic mice. **(D)** Representative examples of H&E-stained lung tissues from mice at 0 h, 12 h, 24 h, 1 w, 2 w after CLP (n = 5 per group). Alveolar cavity showed exudation, edema, and hemorrhage by the black arrow. **(E, F)** Histological scores of the liver and lung in CLP-induced septic mice (n = 5 per group). *P <0.05; **P <0.01.

Supplementary Figure 4 | The effect of *Gpr174* deficiency on CLP-induced sepsis (n = 20 per group). **(A)** Survival rates were monitored for 1 w in *Gpr174*-KO mice compared with wild type (WT) after CLP-induced sepsis (n = 20 per group). **(B)** Representative H&E staining examples and histological scores for lung tissues at 24 h after CLP-induced sepsis. **(C)** Representative H&E staining examples and histological scores for liver tissues at 24 h after CLP (n = 5 per group). $^{*}P < 0.05$; $^{**}P < 0.01$.

Supplementary Figure 5 | *Gpr174* regulated the production of pro- and anti-inflammatory cytokines in CLP-induced septic mice (n = 5 per group). Cytokines in blood from septic mice were determined by ELISA at 24 h after CLP. **(A, C)** IL-1β and TNF-α levels were downregulated in *Gpr174*-KO + CLP mice. **(B)** IL-10 was upregulated compared to WT + CLP group. $^{*}P < 0.05$; $^{**}P < 0.01$.

REFERENCES

1. Singer M, Deutschman CS, Seymour CW, Shankar-Hari M, Annane D, Bauer M, et al. The Third International Consensus Definitions for Sepsis and Septic Shock (Sepsis-3). *JAMA* (2016) 315:801–10. doi: 10.1001/jama.2016.0287
2. Reinhart K, Daniels R, Kissoon N, Machado FR, Schachter RD, Finfer S. Recognizing Sepsis as a Global Health Priority- a WHO Resolution. *N Engl J Med* (2017) 377:414–7. doi: 10.1056/NEJMp1707170
3. van der Poll T, Van de Veerdonk FL, Scicluna BP, Netea MG. The Immunopathology of Sepsis and Potential Therapeutic Targets. *Nat Rev Immunol* (2017) 17(7):407–20. doi: 10.1038/nri.2017.36
4. Liu Q, Yao Y-M. Inflammatory Response and Immune Regulation of High Mobility Group Box-1 Protein in Treatment of Sepsis. *World J Emerg Med* (2010) 1(2):93–8.
5. Blaurock-Möller N, Gröger M, Siwczak F, Dinger J, Schmerler D, Mosig AS, et al. CAAP48, A New Sepsis Biomarker, Induces Hepatic Dysfunction in an Invitroliver-on-Chip Model. *Front Immunol* (2019) 10:273. doi: 10.3389/fimmu.2019.00273
6. Liu S, Wang X, She F, Zhang W, Liu H, Zhao X, et al. Effects of Neutrophil-To-Lymphocyte Ratio Combined With Interleukin-6 in Predicting 28-Day Mortality in Patients With Sepsis. *Front Immunol* (2021) 12:639735. doi: 10.3389/fimmu.2021.639735
7. Zhu T, Su Q, Wang C, Shen L, Chen H, Feng S, et al. SDF4 Is a Prognostic Factor for 28-Days Mortality in Patients With Sepsis *via* Negatively

Regulating ER Stress. *Front Immunol* (2021) 12:659193. doi: 10.3389/fimmu.2021.659193
8. Trzaskowski B, Latek D, Yuan S, Ghoshdastider U, Debinski A, Filipek S, et al. Action of Molecular Switches in GPCRs–theoretical and Experimental Studies. *Curr Med Chem* (2012) 19(8):1090–109. doi: 10.2174/092986712799320556
9. Wettschureck N, Offermanns S. Mammalian G Proteins and Their Cell Type Specific Functions. *Physiol Rev* (2005) 85(4):1159–204. doi: 10.1152/physrev.00003.2005
10. Garcia-Marcos M. Complementary Biosensors Reveal Different G-Protein Signaling Modes Triggered by GPCRs and Non-Receptor Activators. *Elife* (2021) 10:e65620. doi: 10.7554/eLife.65620
11. Inoue A, Ishiguro J, Kitamura H, Arima N, Okutani M, Shuto A, et al. TGF-Alpha Shedding Assay: An Accurate and Versatile Method Fordetecting GPCR Activation. *Nat Methods* (2012) 9:1021–9. doi: 10.1038/nmeth.2172
12. Konkel JE, Zhang D, Zanvit P, Chia C, Zangarle-Murray T, Jin W, et al. Transforming Growth Factor-β Signaling in Regulatory T Cells Controls T Helper-17 Cells and Tissue-Specific Immune Responses. *Immunity* (2017) 46 (4):660–74. doi: 10.1016/j.immuni.2017.03.015
13. Zhao R, Chen X, Ma W, Zhang J, Guo J, Zhong X, et al. A GPR174–CCL21 Module Imparts Sexual Dimorphism to Humoral Immunity. *Nature* (2020) 577(7790):416–20. doi: 10.1038/s41586-019-1873-0
14. Sugita K, Yamamura C, Tabata K, Fujita N. Expression of Orphan G-Protein Coupled Receptor GPR174 in CHO Cells Induced Morphological Changes and Proliferation Delay *via* Increasing Intracellular cAMP. *Biochem Biophys Res Commun* (2013) 430(1):190–5. doi: 10.1016/j.bbrc.2012.11.046
15. Barnes MJ, Li CM, Xu Y, An J, Huang Y, Cyster JG. The Lysophosphatidylserine Receptor GPR174 Constrains Regulatory T Cell Development and Function. *J Exp Med* (2015) 212:1011–20. doi: 10.1084/jem.20141827
16. Yue J, Zhao X. GPR174 Suppression Attenuates Retinopathy in Angiotensin II (Ang II)-Treated Mice by Reducing Inflammation *via* PI3K/AKT Signaling. *BioMed Pharmacother* (2020) 122:109701. doi: 10.1016/j.biopha.2019.109701
17. Chu X, Shen M, Xie F, Miao XJ, Shou WH, Liu L, et al. An X Chromosome-Wide Association Analysis Identifies Variants in GPR174 as a Risk Factor for Graves' Disease. *J Med Genet* (2013) 50:479–85. doi: 10.1136/jmedgenet-2013-101595
18. Qiu D, Chu X, Hua L, Yang Y, Li K, Han Y, et al. Gpr174-Deficient Regulatory T Cells Decrease Cytokine Storm in Septic Mice. *Cell Death Dis* (2019) 10 (3):233–47. doi: 10.1038/s41419-019-1462-z
19. Rittirsch D, Huber-Lang MS, Flierl MA, Ward PA. Immunodesign of Experimental Sepsis by Cecal Ligation and Puncture. *Nat Protoc* (2009) 4:31–6. doi: 10.1038/nprot.2008.214
20. Robin X, Turck N, Hainard A, Tiberti N, Lisacek F, Sanchez JC, et al. pROC: An Open-Source Package for R and S+ to Analyze and Compare ROC Curves. *BMC Bioinf* (2021) 7:77. doi: 10.1186/1471-2105-12-77
21. Sandroni C, Nolan J, Cavallaro F, Antonelli M. In-Hospital Cardiac Arrest: Incidence, Prognosis and Possible Measures to Improve Survival. *Intensive Care Med* (2007) 33(2):237–45. doi: 10.1007/s00134-006-0326-z
22. Makide K, Uwamizu A, Shinjo Y, Ishiguro J, Okutani M, Inoue A, et al. Novel Lysophosphoplipid Receptors: Their Structure and Function. *J Lipid Res* (2014) 55(10):1986–95. doi: 10.1194/jlr.R046920
23. Qin Y, Verdegaal EME, Siderius M, Bebelman JP, Smit MJ, Leurs R, et al. Quantitative Expression Profiling of G-Protein-Coupled Receptors (GPCRs) in Metastatic Melanoma: The Constitutively Active Orphan GPCR GPR18 as Novel Drug Target. *Pigment Cell Melanoma Res* (2011) 24(1):207–18. doi: 10.1111/j.1755-148X.2010.00781.x
24. Zhao S, Xue L, Liu W, Gu ZH, Pan CM, Yang SY, et al. Robust Evidence for Five New Graves' Disease Risk Loci From a Staged Genome-Wide Association Analysis. *Hum Mol Genet* (2013) 22(16):3347–62. doi: 10.1093/hmg/ddt183
25. Napier C, Mitchell AL, Gan E, Wilson I, Pearce SH. Role of the X-Linked Gene GPR174 in Autoimmune Addison's Disease. *J Clin Endocrinol Metab* (2015) 100(1):187–90. doi: 10.1210/jc.2014-2694
26. Zhu M, Li C, Song Z, Mu S, Wang J, Wei W, et al. The Increased Marginal Zone B Cells Attenuates Early Inflammatory Responses During Sepsis in Gpr174 Deficient Mice. *Int Immunopharmacol* (2020) 81:106034. doi: 10.1016/j.intimp.2019.106034
27. Sewnath ME, Olszyna DP, Birjmohun R, ten Kate FJ, Gouma DJ, van Der Poll T, et al. IL-10-Deficient Mice Demonstrate Multiple Organ Failure and Increased Mortality During Escherichia Coli Peritonitis Despite an Accelerated Bacterial Clearance. *J Immunol* (2001) 166:6323–31. doi: 10.4049/jimmunol.166.10.6323
28. Matsukawa A, Takeda K, Kudo S, Maeda T, Kagayama M, Akira S. Aberrant Inflammation and Lethality to Septic Peritonitis in Mice Lacking STAT3 in Macrophages and Neutrophils. *J Immunol* (2003) 171:6198–205. doi: 10.4049/jimmunol.171.11.6198
29. Liu G, Burns S, Huang G, Boyd K, Proia RL, Flavell RA, et al. The Receptor S1P1 Overrides Regulatory T Cell-Mediated Immune Suppression Through Akt-mTOR. *Nat Immunol* (2009) 10:769–77. doi: 10.1038/ni.1743
30. Porta C, Rimoldi M, Raes G, Brys L, Ghezzi P, Di Liberto D, et al. Tolerance and M2 (Alternative) Macrophage Polarization Are Related Processes Orchestrated by P50 Nuclear Factor kappaB. *Proc Natl Acad Sci USA* (2009) 106(35):14978–83. doi: 10.1073/pnas.0809784106
31. Grütz G. New Insights Into the Molecular Mechanism of Interleukin-10-Mediated Immunosuppression. *J Leukoc Biol* (2005) 77(1):3–15. doi: 10.1189/jlb.0904484
32. Davenport EE, Burnham KL, Radhakrishnan J, Humburg P, Hutton P, Mills TC, et al. Genomic Landscape of the Individual Host Response and Outcomes in Sepsis: A Prospective Cohort Study. *Lancet Respir* (2016) 4:259–71. doi: 10.1016/S2213-2600(16)00046-1
33. Thampy LK, Remy KE, Walton AH, Hong Z, Liu K, Liu R, et al. Restoration of T Cell Function in Multi-Drug Resistant Bacterial Sepsis After Interleukin-7, Anti-PD-L1, and OX-40 Administration. *PloS One* (2018) 13:e0199497. doi: 10.1371/journal.pone.0199497
34. Dobin A, Davis CA, Schlesinger F, Drenkow J, Zaleski C, Jha S, et al. STAR: Ultrafast Universal RNA-Seq Aligner. *Bioinformatics* (2013) 29:15–21. doi: 10.1093/bioinformatics/bts635
35. Cardoso CC, Pereira AC, de Sales Marques C, Moraes MO. Leprosy Susceptibility: Genetic Variations Regulate Innate and Adaptive Immunity, and Disease Outcome. *Future Microbiol* (2011) 6(5):533–49. doi: 10.2217/fmb.11.39
36. Gaudet P, Livstone MS, Lewis SE, Thomas PD. Phylogenetic-Based Propagation of Functional Annotations Within the Gene Ontology Consortium. *Brief Bioinform* (2011) 12(5):449–62. doi: 10.1093/bib/bbr042
37. Zhou Y, Do DC, Ishmael FT, Squadrito ML, Tang HM, Tang HL, et al. Mannose Receptor Modulates Macrophage Polarization and Allergic Inflammation Through miR-511-3p. *Allergy Clin Immunol* (2018) 141 (1):350–64. doi: 10.1016/j.jaci.2017.04.049
38. Ruffell B, Chang-Strachan D, Chan V, Rosenbusch A, Ho CM, Pryer N, et al. Macrophage IL-10 Blocks CD8+ T Cell-Dependent Responses to Chemotherapy by Suppressing IL-12 Expression in Intratumoral Dendritic Cells. *Cancer Cell* (2014) 26(5):623–37. doi: 10.1016/j.ccell.2014.09.006
39. Zheng Q, Hou J, Zhou Y, Yang Y, Xie B, Cao X. Siglec1 Suppresses Antiviral Innate Immune Response by Inducing TBK1 Degradation *via* the Ubiquitin Ligase TRIM27. *Cell Res* (2015) 25(10):1121–36. doi: 10.1038/cr.2015.108

Conflict of Interest: The authors declare that the research was conducted in the absence of any commercial or financial relationships that could be construed as a potential conflict of interest.

Publisher's Note: All claims expressed in this article are solely those of the authors and do not necessarily represent those of their affiliated organizations, or those of the publisher, the editors and the reviewers. Any product that may be evaluated in this article, or claim that may be made by its manufacturer, is not guaranteed or endorsed by the publisher.

Advantages of publishing in Frontiers

OPEN ACCESS
Articles are free to read for greatest visibility and readership

FAST PUBLICATION
Around 90 days from submission to decision

HIGH QUALITY PEER-REVIEW
Rigorous, collaborative, and constructive peer-review

TRANSPARENT PEER-REVIEW
Editors and reviewers acknowledged by name on published articles

Frontiers
Avenue du Tribunal-Fédéral 34
1005 Lausanne | Switzerland

Visit us: www.frontiersin.org
Contact us: frontiersin.org/about/contact

REPRODUCIBILITY OF RESEARCH
Support open data and methods to enhance research reproducibility

DIGITAL PUBLISHING
Articles designed for optimal readership across devices

FOLLOW US
@frontiersin

IMPACT METRICS
Advanced article metrics track visibility across digital media

EXTENSIVE PROMOTION
Marketing and promotion of impactful research

LOOP RESEARCH NETWORK
Our network increases your article's readership